Functional characterisation of the interplay between Ndc1, Nup53 and Nup155 in nuclear pore complex biogenesis

Dissertation

der Mathematisch-Naturwissenschaftlichen Fakultät

der Eberhard Karls Universität Tübingen

zur Erlangung des Grades eines

Doktors der Naturwissenschaften

(Dr. rer. nat.)

vorgelegt von

Nathalie Eisenhardt, geb. Widmann

aus Leonberg (Baden-Württemberg)

Tübingen

2013

Tag der mündlichen Qualifikation:	05.02.2014
Dekan:	Prof. Dr. Wolfgang Rosenstiel
1. Berichterstatter:	PD Dr. Wolfram Antonin
2. Berichterstatter:	Prof. Dr. Gerd Jürgens

Acknowledgement

First and foremost, I would like to express my sincere gratitude to my PhD supervisor PD Dr. Wolfram Antonin for giving me the opportunity to work in his lab on such a challenging and exciting project. I am very grateful for his continuous guidance and support as well as for his patience throughout the course of my PhD. In particular, I would like to thank him for having always an open door and for all the time he spent discussing ideas and experiments with me. I cannot appreciate enough his valuable scientific and professional advice from which I learned a lot.

I would also like to thank all members of my PhD advisory committee: Prof. Dr. Gerd Jürgens, Prof. Dr. Ralf Sommer and Dr. Yvonne Grömping. Thanks for all the fruitful discussions, the scientific input and the encouragement. This significantly contributed to the success of my PhD. Further, I am very grateful to Prof. Dr. Gerd Jürgens for the evaluation of this thesis.

A great working atmosphere made my everyday lab-life much more enjoyable. Thanks to all former and current lab-mates, Ruchika Sachdev, Josef Redolfi, Gandhi Theerthagiri, Michael Lorenz, Benjamin Vollmer, Katharina Schellhaus, Adriana Magalska, Allana Schooley, Paola DeMagistris, Daniel Moreno, Susanne Astrinidis, Cornelia Sieverding, Cathrin Gramminger, Nathanael Cottam and Kathrin Werner for their great support, scientific discussions and fruitful collaborations and to our amazing Hiwis Franziska Hoppe and particularly Tobias Strittmatter for their technical support. My special thanks go to Josef for starting the work on transmembrane nucleoporins. Ruchika and Vikash, I would like to express my heartfelt gratitude to you for being more than lab-mates. I am very greatful for having friends who always supported me, professionally and personally. Thanks for exchanging scientific ideas, for listening to all my sorrows and for sharing unforgettable moments.

Many people from FML and the Max Planck Institute for Developmental Biology greatly contributed to making all kinds of experiments possible. I would like to thank Dr. Heinz Schwarz, Dr. Matthias Flötenmeyer and Jürgen Berger for their help with TEM and Dr. Antonia Failla and Dr. Christian Liebig for teaching me confocal microscopy. Moreover, I would like to thank Nadine Weiss for being an excellent animal caretaker and all technical staff of the institute.

I am also grateful for having received a scholarship throughout my PhD studies from the Max-Planck-Society providing financial support.

Zum Schluss möchte ich noch meinen besonderen Dank an meine Familie ausdrücken, die immer an mich geglaubt, mich unterstützt hat und für mich da war. Vor allem den Dank, der meinem Mann Patrick gebührt, kann man nicht in Worte fassen. Ohne dich wäre all dies nicht möglich gewesen.

Table of contents

Summary

In eukaryotic cells, the nucleus is enclosed by the two continuous membranes of the nuclear envelope establishing a physical barrier that spatially separates the nucleoplasm from the cytoplasm. To accommodate bidirectional transport across this barrier nuclear pore complexes (NPCs) form highly selective transport channels. These huge protein complexes coat the pore membrane region, which arises of the fusion of both nuclear envelope membranes.

NPCs are constituted by the concerted assembly of hundreds of polypeptides from roughly 30 different proteins termed nucleoporins. Out of these, only three nucleoporins are stably integrated into the pore membrane to anchor the NPCs via transmembrane domains. Although accuracy of NPC assembly is essential to ensure cell viability and proliferation a detailed understanding of the complex NPC biogenesis is lacking.

NPCs are assembled at two different phases of the metazoan cell cycle. At the end of every cell division NPCs have to re-assemble concomitantly with the re-forming nuclear envelope around the segregated daughter chromosomes. Additionally, NPCs are formed *de novo* during interphase into an intact nuclear envelope, which is also the exclusive assembly mode in organisms undergoing a closed mitosis as *Saccharomyces cerevisiae*. Particularly, how NPCs integrate both, in the growing nuclear envelope at the end of mitosis and the closed nuclear envelope during interphase, is by far and largely unknown.

During my PhD work, I functionally characterised the transmembrane nucleoporin Ndc1, which is the only conserved integral membrane nucleoporin, in NPC assembly at the end of mitosis. Ndc1 is part of a crucial and conserved interaction network at the pore membrane where it interacts with Nup53 and Nup155, two nucleoporins belonging to the structural Nup93 complex. All three proteins are required for NPC assembly in yeast and metazoans but their specific roles as well as the role of their interactions were undetermined. By a detailed biochemical and cell biological analysis using purified recombinant proteins and *in vitro* nuclear assembly reactions, I reveal that the direct interaction of Ndc1 and Nup53 is essential for metazoan NPC formation at the end of mitosis. Ndc1 influences the membrane deformation activity

of Nup53. This membrane deforming capability is specifically required for NPC assembly during interphase. As the Ndc1-Nup53 interaction and the membrane deformation function of Nup53 are also conserved in yeast this suggests that the interaction might be conserved functionally and also needed during interphasic NPC assembly.

Nup53 is the central player of the Nup93 complex linking most complex members with each other and the pore membrane. However, it has been unresolved whether the interaction with Nup155 has an important role for NPC assembly. I demonstrate that the functional complex of Nup53 and Nup155 is required to recruit downstream nucleoporins via Nup93, another essential NPC protein, to nascent NPCs at the end of mitosis.

Altogether, this study identifies the first elementary function of the conserved transmembrane nucleoporin Ndc1 and highlights new mechanistic details of the step-wise process of NPC assembly at the end of mitosis. Consequently, this new knowledge adds to a deeper understanding of the precise order and function of the early events during NPC biogenesis.

Zusammenfassung

In Eukaryonten wird der Zellkern von einer Kernhülle, die aus zwei kontinuierlichen Membranen besteht, umschlossen. Diese Membranen bilden eine physikalische Barriere, welche das Zytoplasma vom Nukleoplasma räumlich trennt. Um Stofftransport in beide Richtungen über diese Barriere hinweg zu ermöglichen, formen Kernporenkomplexe äußerst selektive Transportkanäle. Diese riesigen Proteinkomplexe ummanteln den Bereich der Porenmembran, die durch die Verbindung der beiden Membranen entsteht.

Kernporenkomplexe bestehen aus hunderten Polypeptiden von insgesamt etwa 30 verschiedenen Proteinen, sogenannten Nukleoporinen, die in einem diffizilen und fein aufeinander abgestimmten Prozess zusammengebaut werden. Von diesen Nukleoporinen sind nur drei fest in die Porenmembran integriert, welche die Kernporenkomplexe mittels Transmembrandomänen verankern. Obwohl der präzise Zusammenbau der Kernporen für das Überleben und die Proliferation von Zellen essentiell ist, fehlt bislang noch ein detailliertes Verständnis der komplexen Biogenese der Kernporenkomplexe.

Bei Vielzellern entstehen Kernporenkomplexe in zwei unterschiedlichen Phasen des Zellzyklus. Am Ende jeder Zellteilung müssen Kernporenkomplexe gleichzeitig mit der Kernhülle wieder aufgebaut werden, um die segregierten Tochter-Chromosomen zu umschließen. Darüber hinaus werden Kernporenkomplexe während der Interphase *de novo* in die intakte Kernhülle eingebaut. Diese Art des Kernporenbaus stellt auch den einzig möglichen Mechanismus bei Organismen wie *Saccharomyces cerevisiae* dar, die eine geschlossene Mitose vollziehen. Bislang ist es noch völlig unverstanden, wie Kernporenkomplexe sowohl in die wieder entstehende, wachsende Kernhülle am Ende der Mitose als auch in die geschlossene Kernhülle während der Interphase eingebaut werden.

Im Rahmen meiner Doktorarbeit charakterisierte ich die Funktion des Transmembran-Nukleoporins Ndc1 beim Kernporenaufbau am Ende der Mitose, welches als einziges integrales Protein der Porenmembran konserviert ist. Ndc1 ist Teil eines wichtigen, konservierten Interaktionsnetzwerks an der Porenmembran, wo es mit den zwei Nukleoporinen Nup53 und Nup155, die zum strukturgebenden

Nup93-Komplex gehören, interagiert. Alle drei Proteine sind für den Kernporenbau sowohl in Hefe als auch in Mehrzellern zwingend erforderlich, aber ihre genaue Rolle sowie die Funktionen ihrer Interaktionen waren bislang unbekannt. Durch detaillierte zellbiologische und biochemische Untersuchungen mit aufgereinigten rekombinanten Proteinen und einem *in vitro* System, das den Kernporenaufbau nachstellt, zeige ich, dass die direkte Interaktion von Ndc1 und Nup53 bei Mehrzellern essentiell für den Kernporenaufbau am Ende der Mitose ist. Ndc1 moduliert die membran-verformende Aktivität von Nup53. Diese membran-verformende Aktivität ist für den Kernporenaufbau während der Interphase relevant und zwingend erforderlich. Die Tatsache, dass die Ndc1-Nup53-Interaktion und die membran-verformende Eigenschaft von Nup53 auch in Hefe konserviert sind, legt den Schluss nahe, dass die Interaktion auch funktionell konserviert und daher für den interphasischen Kernporenaufbau essentiell sein könnte.

Nup53 ist der zentrale Baustein des Nup93-Komplexes, da er die meisten Proteine des Komplexes untereinander und mit der Porenmembran vernetzt. Trotzdem war es bislang unerforscht, ob seine Interaktion mit Nup155 eine bedeutende Rolle beim Kernporenaufbau spielt. Ich weise nach, dass ein funktioneller Komplex aus Nup53 und Nup155 am Ende der Mitose erforderlich ist, um im weiteren Prozess des Kernporenaufbaus benötigte Nukleoporine über Nup93, ein weiteres essentielles Nukleoporin für den Kernporenbau, an die intermediären Kernporenkomplexe zu rekrutieren.

Insgesamt demonstriert diese Arbeit erstmals eine elementar wichtige Funktion des konservierten Transmembran-Nukleoporins Ndc1 und beleuchtet neue mechanistische Details des schrittweisen Aufbaus von Kernporenkomplexen am Ende der Mitose. Durch das neu gewonnene Wissen wird ein tieferes Verständnis des exakten mechanistischen Ablaufs und der Rolle einiger wichtiger, initialer Schritte der Biogenese von Kernporenkomplexen ermöglicht.

1. Introduction

1.1. Internal organisation of eukaryotic cells

The biological kingdom consists of two fundamentally different types of cells: prokaryotic and eukaryotic cells. As already implied by their names, the major structural difference is the existence of membrane-enclosed sub-cellular organelles. The acquisition of intrinsic membranes in eukaryotes provides the possibility to spatially organise complex vital functions into distinct compartments and ensures proper functionality of high genetic and cellular complexity.

Eukaryotes possess numerous membrane-delimited organelles with a unique set of proteins as the nucleus, the endoplasmic reticulum (ER), the Golgi apparatus, mitochondria, lysosomes, endosomes or vacuoles (Alberts, 2007). Of all organelles, the nucleus is the most prominent one and the determining attribute of eukaryotic cells. Its main function is to protect, organise and regulate the genetic material, which is physically separated from the rest of the cell by a double membrane layer: the nuclear envelope.

1.2. The nuclear envelope

The nuclear envelope forms a double-membrane barrier that separates the nucleoplasm and the cytoplasm in eukaryotic cells. Even though membrane-enclosure of eukaryotic DNA is essential for cell viability the nuclear envelope is not a static structure but rather undergoes a lot of structural changes during the cell cycle.

1.2.1. Topology of the nuclear envelope

The nuclear envelope consists of two parallel and continuous membrane sheets: the inner nuclear membrane (INM) and the outer nuclear membrane (ONM, Figure 1, Watson, 1955). The ONM is also continuous with the ER and shares most but not all integral membrane proteins with it (for review see Hetzer et al, 2005) whereas the INM harbours a unique group of embedded proteins (Schirmer & Gerace, 2005). The retention of these proteins in the INM is achieved by specific interactions with the

underlying nuclear lamina, which is a meshwork of intermediate filaments that stabilises and structures the nucleus, chromatin or each other (Foisner & Gerace, 1993, or see Burke & Stewart, 2002; Worman & Courvalin, 2000 for review).

The INM and ONM are fused at multiple sites, the so called pore membranes, where the lipid bilayer is highly curved and decorated with nuclear pore complexes (NPCs). NPCs are embedded in the pore membranes and mediate the molecular exchange between the nucleus and the cytosol (for review see Antonin et al, 2008; Wente & Rout, 2010).

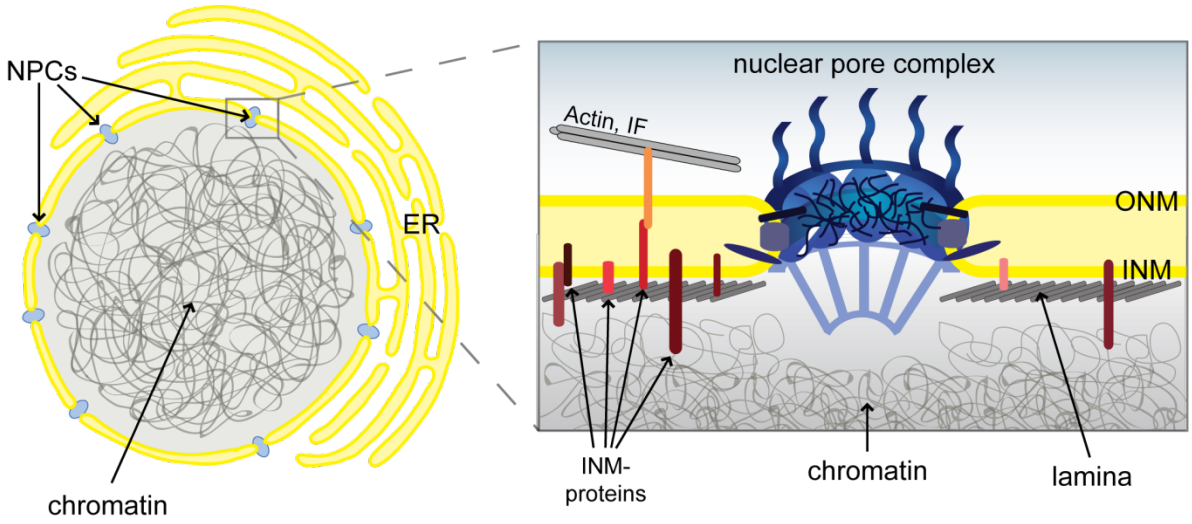

Figure 1: The nuclear envelope.

The nuclear envelope is formed by two parallel membrane sheets, the inner nuclear membrane (INM) and the outer nuclear membrane (ONM), which are fused at the sites where nuclear pore complexes (NPCs) incorporate. The ONM is continuous with the endoplasmic reticulum (ER). The INM is attached to the underlying lamina. INM-proteins interact with the chromatin and the lamina. Protein bridges between integral membrane proteins connect both membrane layers with each other as well as the cytoskeleton in the cytoplasm formed by Actin or intermediate filaments (IF) and the nuclear lamina. (Based on Hetzer, 2010).

The two membrane leaflets of the nuclear envelope are additionally connected by protein bridges across their perinuclear space. KASH-proteins of the ONM, which do not enrich in the ER, provide a link between the cytoskeleton in the cytoplasm and the chromatin and its overlying lamina in the nucleus by establishing interactions with proteins of the SUN-family residing in the INM (for review see Burke, 2012; Starr &

Fridolfsson, 2010). These protein interactions probably ensure the separation of the INM and the ONM at an even distance of approximately 50 nm (Voeltz & Prinz, 2007).

1.2.2. Nuclear envelope biogenesis

The nuclear envelope is a highly dynamic membrane system undergoing structural changes throughout the cell cycle (Figure 2). Most dramatically, during open mitosis of metazoans the membranes of the nuclear envelope, including NPCs, have to be dismantled to allow chromatin capturing by the mitotic spindle (for review see Kutay & Hetzer, 2008). The nuclear envelope membranes and their integral protein components are re-distributed into the mitotic ER (Daigle et al, 2001; Ellenberg et al, 1997; Yang et al, 1997) and peripherally associated factors like most NPC components are mixed with the cytosolic content of the cell. At the end of mitosis, the nuclear envelope has to re-form around the segregated chromosomes in the newly emerging daughter cells. Nuclear envelope re-formation starts during the late stages of anaphase (Daigle et al, 2001; Ellenberg et al, 1997; Haraguchi et al, 2000). It depends on the attraction of several chromatin-binding INM-proteins and maybe also of transmembrane nucleoporins to the decondensing chromatin (Anderson et al, 2009; Ulbert et al, 2006). At first, ER-tubules probably make initial contacts with the chromatin followed by subsequent recruitment of more membranes and an expansion into a flattened membrane sheet (Anderson & Hetzer, 2007; Puhka et al, 2007). However, an alternative model suggests that nuclear envelope membranes re-form from ER sheets (Lu et al, 2011; Poteryaev et al, 2005). The speed of chromatin-mediated nuclear envelope re-formation seems limited by the abundance of INM-proteins and membrane-shaping proteins of the tubular ER, the Reticulons (Rtn) and DP1. The depletion of individual INM-proteins delays the process of nuclear envelope formation and *vice versa*, their artificial over-expression accelerates the process (Anderson et al, 2009). In contrast, reduction of Rtn-levels, which are usually found in highly curved membranes of the ER (Hu et al, 2008; Voeltz et al, 2006), speeds-up nuclear envelope formation after mitosis whereas their over-expression delays the process (Anderson & Hetzer, 2008). Finally, the re-formed nuclear envelope has to seal around the newly formed NPCs, which were assembled

concomitantly, to re-establish the nuclear compartment. However, how these final steps occur, is not resolved yet (for review see Guttinger et al, 2009; Schooley et al, 2012).

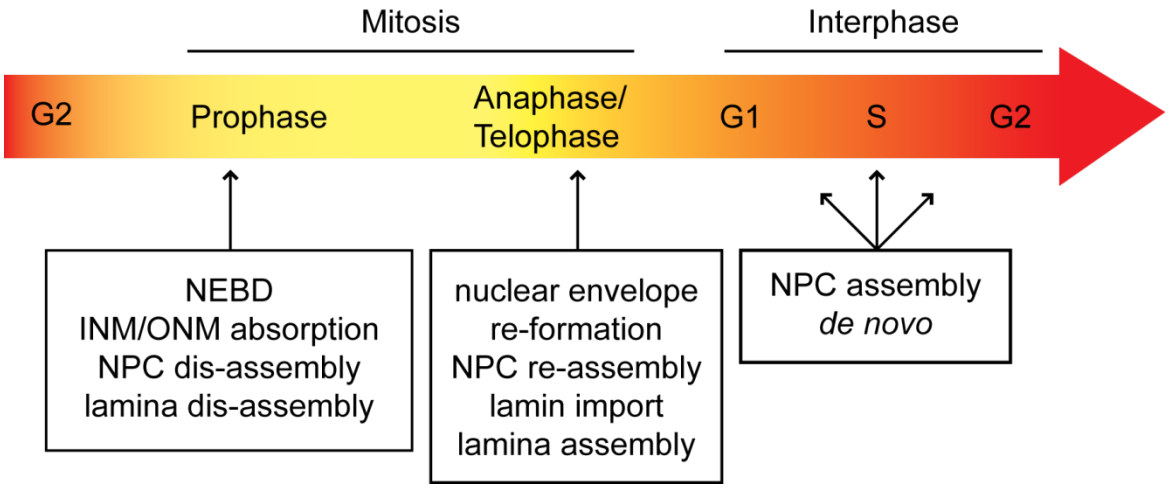

Figure 2: Nuclear envelope dynamics through the cell cycle.

The nuclear envelope is highly dynamic undergoing a lot of structural changes during the cell cycle. In prophase at the beginning of mitosis, the nuclear envelope breaks down (NEBD) resulting in absorption of the inner nuclear membrane (INM) and the outer nuclear membrane (ONM) by the endoplasmic reticulum. Concomitantly, nuclear pore complexes (NPCs) dis-assemble as well as the nuclear lamina. At the end of mitosis starting in late anaphase, the nuclear envelope and NPCs re-form. Lamins are then imported into the nucleus to re-build the nuclear lamina. During interphase of the cell cycle (G1, S and G2-phase) newly formed NPCs are assembled and integrated into the closed nuclear envelope. (Modified from Hetzer et al, 2005).

Also in organisms undergoing a closed mitosis, where spindle microtubules directly form inside the nucleus or can pass the nuclear membranes (De Souza et al, 2004; Finley & Berman, 2005; Ribeiro et al, 2002), the nuclear envelope still undergoes massive structural changes. One example for membrane remodelling is nuclear growth during interphase. Nuclear growth requires membrane expansion due to lipid feeding from the ER and the targeting of integral membrane proteins as well as insertion of newly synthesised NPCs (Anderson & Hetzer, 2007; D'Angelo et al, 2006; Maul et al, 1971).

1.3. Nuclear pore complexes

In order to allow molecular exchange between the cytoplasm and the nucleus across the nuclear envelope barrier, nuclear pore complexes (NPCs) are inserted in the pore membrane to act as transport channels. NPCs enable the relatively free diffusion of small molecules and facilitate selective transport of various cargoes including proteins, RNAs, ribonucleoprotein complexes, ribosomal subunits or viral particles (for review see Macara, 2001; Wente & Rout, 2010). NPCs are huge macromolecular assemblies with an estimated mass between approximately 40 and 120 MDa depending on the organism (Cronshaw et al, 2002; Reichelt et al, 1990; Rout et al, 2000). Despite these differences in mass, the overall architecture, composition and function of NPCs is highly conserved and is described in detail in the following paragraphs.

1.3.1. NPC composition and architecture

The structure and composition of these giant proteinaceous complexes has been intensively analysed by biochemical approaches, electron microscopy and more recently also by cryo-electron tomography and revealed that NPCs consist of only about 30 different proteins termed nucleoporins (Nups, Table 1) that assemble in an eight-fold rotational symmetry (Alber et al, 2007; Beck et al, 2004; Beck et al, 2007; Cronshaw et al, 2002; Frenkiel-Krispin et al, 2010; Maimon et al, 2012; Rout et al, 2000; Yang et al, 1998). As each nucleoporin is present in multiple copies, the fully assembled NPC is made up by approximately 500-1000 single protein molecules. Based on their localisation within the NPC, nucleoporins can be mainly classified into structural nucleoporins forming the stable core scaffold of the NPC and barrier nucleoporins of the central channel mediating transport and size-exclusion functions of the pore (Alber et al, 2007). The core scaffold consists of integral membrane proteins of the pore membrane domain, nucleoporins forming the cytoplasmic and nucleoplasmic rings and nucleoporins constituting the spoke ring structure (Figure 3). The spoke ring structure is in close contact with the pore membrane and sandwiched between the cytoplasmic and nucleoplasmic rings. The nuclear basket and the cytoplasmic filaments extend the NPC core vertically and are attached to the

nucleoplasmic and cytoplasmic rings, respectively. The barrier nucleoporins frame the central channel of the pore and are characterised by a high content of phenylalanine-glycine (FG) repeats that are responsible for their interactions with transport receptors (Isgro & Schulten, 2005; Radu et al, 1995; Strawn et al, 2004).

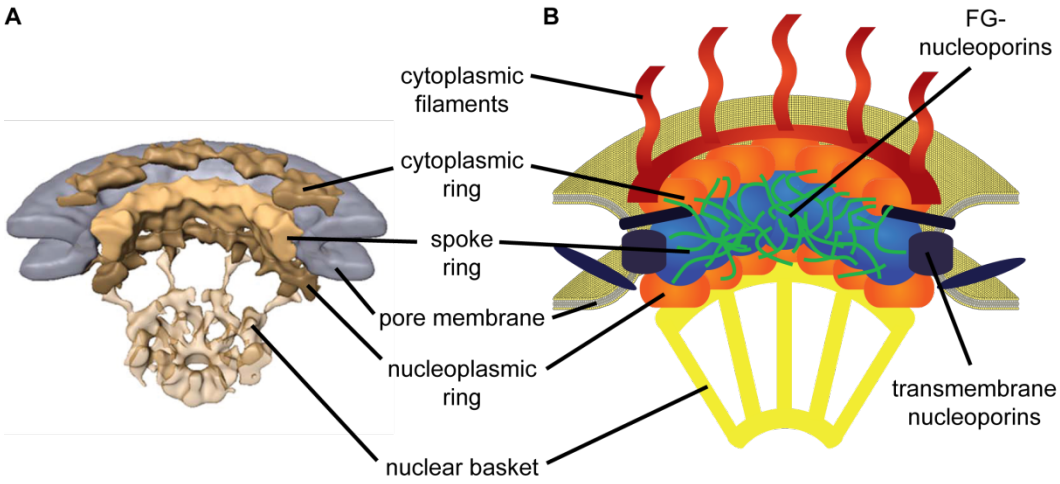

Figure 3: Overall structure and composition of NPCs.

A: 3D-model of the nuclear pore complex (NPC) from *Dictiostylium* reconstructed from cryo-electron tomography. (Adapted from Beck et al, 2007).

B: Schematic illustration of the different parts of the NPC, into which nucleoporins can be grouped: spoke ring (blue), cyto- and nucleoplasmic rings (orange), cytoplasmic filaments (red), nuclear basket (yellow) and FG-nucleoporins (green) of the central channel. (Based on Antonin et al, 2008; Brohawn et al, 2009; Hoelz et al, 2011).

1.3.1.1. The Nup107/160 complex

The cytoplasmic and nucleoplasmic rings of the core scaffold are formed by the evolutionary conserved heptameric Nup84 complex in yeast and by the Nup107/160 complex in vertebrates consisting of nine complex members (Belgareh et al, 2001; DeGrasse et al, 2009; Liu et al, 2009; Loiodice et al, 2004; Mans et al, 2004; Neumann et al, 2010; Siniossoglou et al, 1996; Vasu et al, 2001, Table 1). These members are Nup133, Nup96, Sec13, Nup107, Nup85, Seh1, Nup160, Nup37 and Nup43. Sometimes Elys/Mel28 is accounted as tenth member of this complex. The homologues yeast complex contains Nup84, Nup120, Nup85, Nup145C, Sec13, Seh1 and Nup133 (Lutzmann et al, 2002; Lutzmann et al, 2005). Up to date, it is the best characterised subcomplex of the NPC particularly in structural terms and

biochemically. Its components assemble stoichiometrically and adopt a Y-shaped architecture (Lutzmann et al, 2002; Siniossoglou et al, 2000; Siniossoglou et al, 1996). Structural analyses of the components of the yeast Nup84 complex revealed fold similarities with the coat complex proteins of clathrin, COPI and COPII coated vesicles (Brohawn et al, 2008; Devos et al, 2004). Even the overall arrangement of the Nup84 heptamer and the clathrin triskelion look identical (Kampmann & Blobel, 2009). Hence, it seems likely that nucleoporins of the yeast Nup84 or vertebrate Nup107/160 complex and vesicle coats evolved from a 'protocoatamer' ancestor, which had an important role in the evolution of eukaryotes (Devos et al, 2004; Devos et al, 2006). However, it is not clear whether these proteins fulfil similar roles in stabilising a highly curved membrane. In comparison to the NPC, vesicle coats show some drastic differences. On the one hand, their composition is simpler (for review see McMahon & Mills, 2004; Stagg et al, 2007). On the other hand, vesicle coats completely enclose a positively curved membrane surface without direct contact to the membrane. In the NPC, the coat can only be laterally continuous within the plane of the pore but not towards the nucleoplasmic and cytoplasmic edges (Brohawn et al, 2009; Onischenko & Weis, 2011). However, in the plane of the pore the membrane has a negative curvature (Antonin & Mattaj, 2005). Hence, it is speculated that additional factors are involved to stabilise the unique membrane arrangement of the NPC. Putative candidates could either be members of the Nup93 complex or transmembrane nucleoporins. Indeed some interactions with members of these complexes have been identified (Lutzmann et al, 2005; Mitchell et al, 2010) but whether these interactions could correspond to binding to adaptor proteins as for vesicle coats is unknown.

	Xenopus laevis	*S. cerevisiae*
cyto-/nucleoplasmic ring	Nup107	Nup84
	Nup160	Nup120
	Nup133	Nup133
Nup107/Nup160 complex	Nup96	Nup145C
	Nup85	Nup75
Nup84 complex	Nup43	-
	Nup37	-
	Sec13	Sec13
	Seh1	Seh1
	Mel28/Elys	-
spoke ring	Nup93	Nic96
	Nup53	Nup53/Nup59
Nup93 complex	Nup155	Nup157/Nup170
	Nup188	Nup188
Nic96 complex	Nup205	Nup192
transmembrane nucleoporins	Ndc1	Ndc1
	Pom121	-
	Gp210	-
	-	Pom34
	-	Pom152
FG-nucleoporins of the central channel	Nup62	Nsp1
	Nup58/Nup45	Nup49
	Nup54	Nup57
	Nup98	Nup116/Nup100/Nup145N
	Rae1	Gle2
nuclear basket	Nup153	Nup1/Nup60
	Nup50	Nup2
	Tpr	Mlp1/Mlp2
cytoplasmic filaments	Nup358	-
	Nup214	Nup159
	Nlp1	Nup42
	Nup88	Nup82
	Aladin	-

Table 1: Molecular NPC composition in *Xenopus* and *S. cervisiae*.

All known nucleoporins of *Xenopus leavis* and *S. cerevisiae* are listed. The nucleoporins are arranged according to their conservation and the respective NPC part they constitute and colour-coded according to Figure 3B.

1.3.1.2. The Nup93 complex

The Nup93 complex is also well conserved among eukaryotes (DeGrasse et al, 2009; Mans et al, 2004; Neumann et al, 2010) and forms the inner or spoke ring of the NPC consisting of five proteins: Nup53, which is also called Nup35 (Cronshaw et al, 2002), Nup155, Nup188, Nup205 and the eponymous Nup93. In yeast the corresponding complex is termed Nic96 complex and has seven members due to gene duplication events for Nup53 and Nup155, which are therefore orthologous to Nup53 and Nup59 and Nup157 and Nup170, respectively. The detailed positioning and arrangement of these nucleoporins within their complex is not determined yet. However, biochemical studies identified multiple interactions within the complex as well as to nucleoporins of all other structural complexes, including membrane embedded nucleoporins, and the central channel. These findings emphasise an important bridging function of the Nup93 complex within NPCs. Hence, these nucleoporins are also often called adaptor or linker nucleoporins.

Both, Nup53 and Nup155 make contacts with the pore membrane. Nup53 and the yeast homologues Nup53 and Nup59 interact with the transmembrane nucleoporin Ndc1 via a region in their C-terminus (Hawryluk-Gara et al, 2008; Hawryluk-Gara et al, 2005; Mansfeld et al, 2006; Onischenko et al, 2009; Patel & Rexach, 2008; Uetz et al, 2000). In yeast these interactions between Nup53 or Nup59 and Ndc1 are mutually exclusive. Moreover, Nup53 has also a direct membrane binding ability (Patel & Rexach, 2008; Vollmer et al, 2012). In the *Xenopus* Nup53 protein two independent membrane interaction sites were identified: one is located in the N-terminal part of the protein and one at the C-terminal end (Figure 4, Vollmer et al, 2012). Additionally, Nup53 can also self-interact resulting in Nup53-dimers, which interact via a central RNA-recognition motif (RRM, Handa et al, 2006; Vollmer et al, 2012). This domain represents an unusual RRM-domain. Normally, these domains mediate direct RNA-binding of monomeric proteins (Birney et al, 1993). In the case of Nup53, two conserved hydrophobic residues were identified that substitute for two otherwise positively charged amino acids in the RRM-fold, which would usually be involved in binding the negatively charged nucleic acid in canonical RRM-domains: F172 and W203 (Handa et al, 2006; Vollmer et al, 2012). Additional Nup53 interaction partners in the Nup93 complex are Nup155, which binds to the C-terminal half of the protein, and Nup93 for which the N-terminal half mediates the interaction

(Amlacher et al, 2011; Fahrenkrog et al, 2000; Hawryluk-Gara et al, 2008; Hawryluk-Gara et al, 2005; Lusk et al, 2002; Onischenko et al, 2009; Sachdev et al, 2012; Uetz et al, 2000). The Nup93 interaction thereby stabilises the interaction of Nup53 with Nup155 (Sachdev et al, 2012). Due to this huge number of interactions with other complex members, which are also seen in yeast, Nup53 seems to be the central factor of the Nup93 complex.

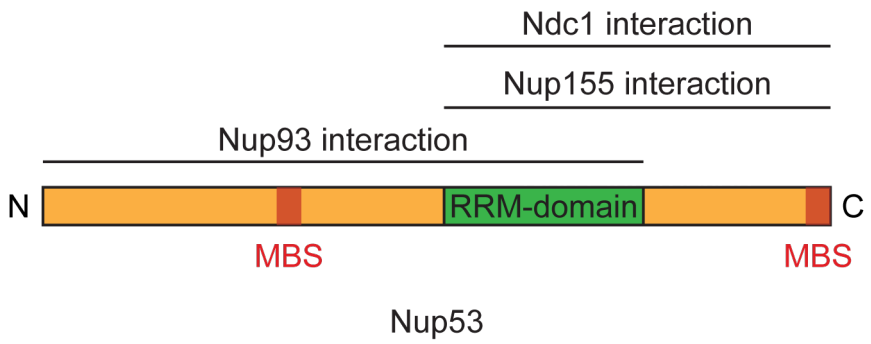

Figure 4: Schematic overview of *Xenopus* Nup53 architecture.

Nup53 consists of an N-terminal region, that contains a membrane binding site (MBS, red), a central RRM-domain (green), which mediates homo-dimerisation, and a C-terminal part, which contains a distal membrane binding and deformation site (MBS, red). It can interact with Nup93 via the N-terminal half as well as with Nup155 and Ndc1 via its C-terminal half. (Adapted from Eisenhardt et al, 2013).

Nup155 also interacts with the pore membrane but indirectly via binding to transmembrane proteins. The vertebrate protein interacts with Ndc1 and Pom121 and one of the yeast counterparts, Nup170, interacts with Pom152 (Makio et al, 2009; Mitchell et al, 2010; Yavuz et al, 2010).

The two biggest complex members, Nup188 and Nup192, are linked via Nup93 or Nic96 and form two mutually exclusive subcomplexes in yeast and metazoans (Amlacher et al, 2011; Kosova et al, 1999; Nehrbass et al, 1996; Theerthagiri et al, 2010). Finally, Nup93 and Nic96 connect the entire complex to the central channel of the pore by interactions with Nup62 in vertebrates or the Nsp1 protein in yeast (Grandi et al, 1993; Grandi et al, 1995).

Despite the multiple interactions linking all Nup93 complex members in a complex interaction network, the Nup93 complex seems no rigid block tethered to the pore membrane. Surprisingly, due to flexible linker motifs mediating most of the

interactions the complex might rather possess some structural variability which could enable local deformations like dilatation or shrinkage in order to flexibly adopt for certain demands like transport (Amlacher et al, 2011).

1.3.1.3. Transmembrane Nucleoporins

Transmembrane nucleoporins are the third group of nucleoporins forming the structural NPC core. Although NPCs are located on and associated with membranes this group consists of only three to four nucleoprins that are stably anchored in the lipid bilayer. In vertebrates, three integral pore membrane proteins have been identified: Gp210, Pom121 and Ndc1 (Greber et al, 1990; Mansfeld et al, 2006; Soderqvist & Hallberg, 1994; Stavru et al, 2006). In yeast there are four proteins known that embed in the pore membrane region: Pom33, Pom34, Pom152 and Ndc1 (Chadrin et al, 2010; Chial et al, 1998; Miao et al, 2006; Wozniak et al, 1994). Surprisingly, the transmembrane nucleoporins are poorly conserved in evolution and Ndc1 is the only protein that is present in almost all eukaryotes (DeGrasse et al, 2009; Neumann et al, 2010). In yeast, Ndc1, which is also called cut11, is also an essential component of the spindle pole body, where it is required for spindle pole body insertion into the nuclear envelope (West et al, 1998; Winey et al, 1993). Ndc1 interacts with Nup53 and Nup155 of the Nup93 complex (see also section 1.3.1.1) both in yeast and metazoans (Hawryluk-Gara et al, 2008; Mansfeld et al, 2006; Onischenko et al, 2009). In yeast, it is also part of a protein complex with the integral membrane nucleoporins Pom152 and Pom34 (Onischenko et al, 2009). Moreover, Ndc1 interacts with Nup155 and Aladin in metazoans (Kind et al, 2009; Mitchell et al, 2010; Yamazumi et al, 2009).

Pom121 and GP210 as well as Pom152 are single spanning transmembrane proteins (Soderqvist & Hallberg, 1994; Tcheperegine et al, 1999; Wozniak & Blobel, 1992) whereas Pom34 passes the pore membrane twice (Miao et al, 2006) and Pom33 as well as Ndc1 contain even six predicted transmembrane helices (Chadrin et al, 2010; Lau et al, 2006; Mansfeld et al, 2006; Stavru et al, 2006, Figure 5). The transmembrane regions are extended towards the pore side of the membrane for Pom121 and Ndc1 as well as for Pom34 whereas Gp210 and Pom152 contain big

luminal domains protruding in the perinuclear space (Tcheperegine et al, 1999; Wozniak et al, 1989; Wozniak et al, 1994). Hence, it was speculated that Pom152 and Gp210 could be involved in stabilising intermediate structures of the nuclear envelope or contribute to fusion events of the INM and ONM which might be required for NPC formation (Devos et al, 2006). However, data indicate that Gp210 seems rather involved in nuclear envelope disassembly (Galy et al, 2008; Onischenko et al, 2007) and might also not be expressed universally in all tissues (Olsson et al, 2004). It is therefore still debated which of the transmembrane nucleoporins are important for NPC assembly and what could be their specific functions in this process.

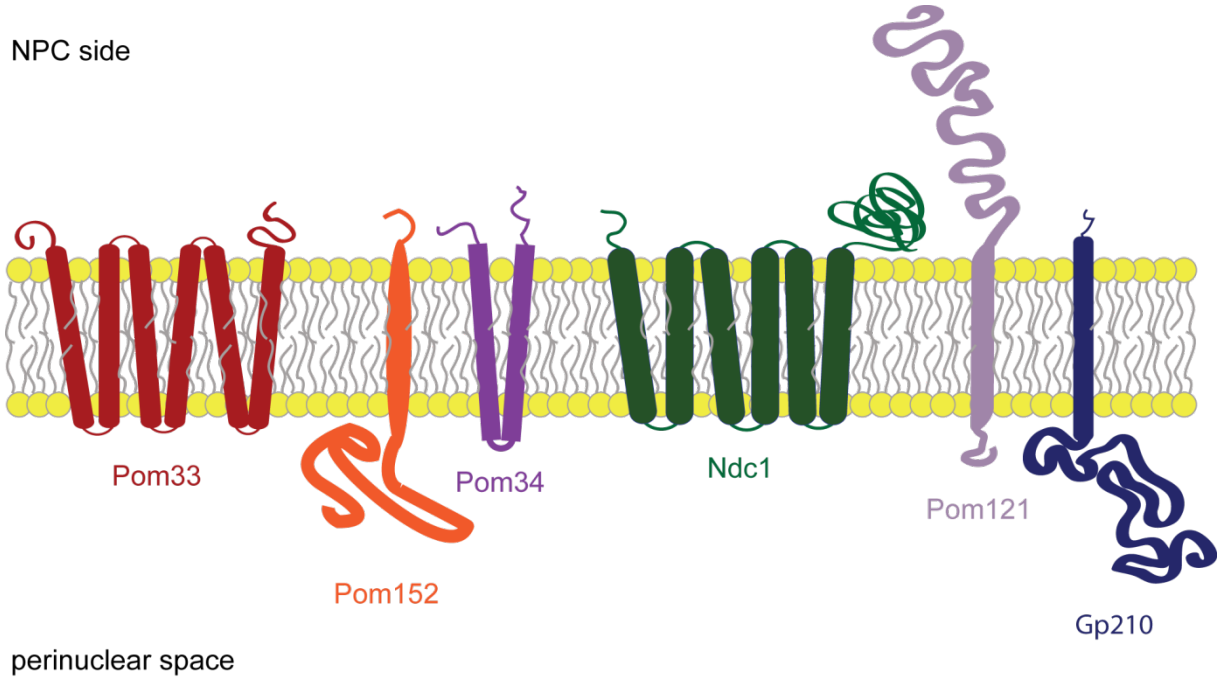

Figure 5: Scheme of topology of the different transmembrane nucleoporins in yeast and metazoans.

Yeast cells contain four different transmembrane nucleoporins: Pom33 (red), Pom152 (orange), Pom34 (purple), and Ndc1 (green), whereas in metazoans three proteins are known: Ndc1, Pom121 (lilac) and Gp210 (blue). The yeast Pom152 and the metazoan Pom121 and Gp210 are single transmembrane-spanning nucleoporins. Pom34 has two transmembrane domains and Ndc1 and Pom33 contain six predicted transmembrane regions.

1.3.2. NPC assembly

NPCs are giant multi-protein complexes playing essential roles for cell survival and proliferation. They have to undergo a highly regulated and coordinated biogenesis. With every cell division in cells executing an open mitosis NPCs have to disassemble at the beginning and re-assemble at the end of mitosis. Additionally, NPC formation occurs during interphase of the metazoan cell cycle, when cells double their number of pores (Maul et al, 1971). Here, NPCs have to be integrated into an intact nuclear envelope. Similarly, in some organisms that undergo a closed or semi-closed mitosis with only partial disassembly of their NPCs new NPCs also need to integrate into the existing nuclear envelope (De Souza et al, 2004; Winey et al, 1997). The interphasic assembly of NPCs into an intact nuclear envelope is not restricted to dividing cells but also occurs during cell differentiation or in response to the metabolic activity. Recently, some evidence accumulated that both types of NPC assembly might occur via different mechanisms (Doucet et al, 2010; Dultz & Ellenberg, 2010). However, detailed mechanistic knowledge of the interphasic NPC assembly mode is so far lacking.

1.3.2.1. Step-wise NPC assembly at the end of mitosis

The NPC assembly process at the end of mitosis has been intensively studied for many years by *in vivo* and *in vitro* approaches applying biochemical methods as well as light and electron microscopy techniques. Many mechanistic details that have been revealed for this process are based on a cell free system derived from *Xenopus laevis* egg extracts by which nuclei can be reconstituted *in vitro* (Lohka & Masui, 1983; Newmeyer et al, 1986b; Sheehan et al, 1988; Vigers & Lohka, 1991; Wilson & Newport, 1988). It turned out that NPC assembly at the end of an open mitosis is a highly ordered, step-wise process that starts on chromatin in early anaphase (Belgareh et al, 2001; Bodoor et al, 1999; Dultz et al, 2008; Theisen et al, 2008).

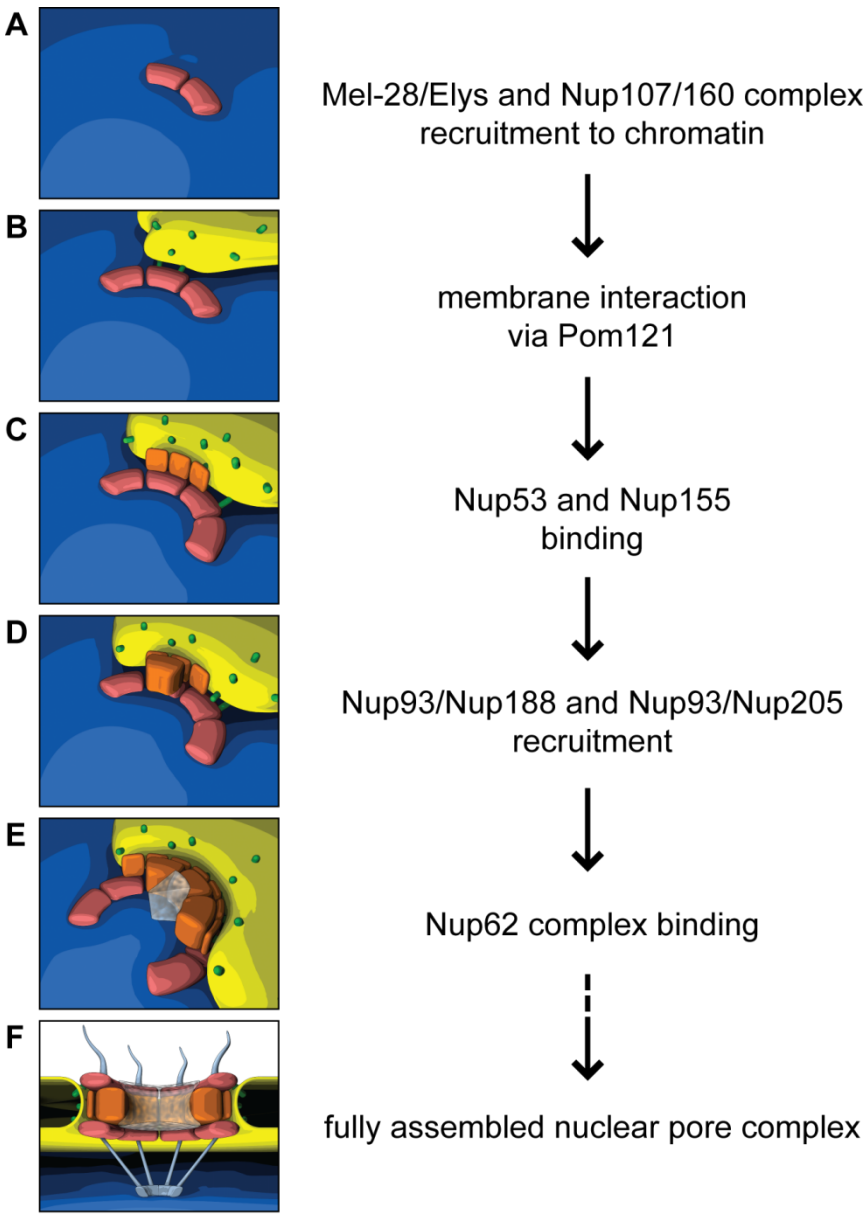

Figure 6: Step-wise NPC assembly at the end of mitosis.

A: Nuclear pore complex (NPC) assembly after cell division starts by the recruitment of the Nup107/160 complex (red) to decondensing chromatin (blue) via the DNA-binding protein Mel28/Elys (red).

B: Nuclear precursor membranes (yellow) associate next via the integral membrane nucleoporin Pom121 (green).

C: Afterwards, the first members of the Nup93 complex (orange), Nup53 and Nup155, are recruited, which can interact with transmembrane nucleoporins.

D: This step is followed by the association of the residual Nup93 complex members via Nup93 interaction with Nup53 and Nup155.

E: Nup93 also recruits the FG-containing Nup62 (light blue). FG-containing nucleoporins form the central channel of the NPC establishing size-exclusion and barrier functions.

F: Finally, components of the nuclear basket and cytoplasmic filaments are recruited in less defined steps resulting in completion of the assembly process. (Adapted from Schooley et al, 2012).

Initially, the DNA-binding nucleoporin Mel28/Elys, which binds chromatin via its AT-hook, recruits the Nup107/160 complex (Franz et al, 2007; Galy et al, 2006; Gillespie et al, 2007; Rasala et al, 2006; Rasala et al, 2008, Figure 6). Both, Mel28/Elys and the Nup107/160 complex, which constitute the 'seeds' of NPC assembly (Rotem et al, 2009), are essential for NPC assembly as their immunodepletion from *Xenopus* egg extracts results in the formation of nuclei enclosed by a nuclear envelope without NPCs (Franz et al, 2007; Harel et al, 2003; Walther et al, 2003). Next, small fractions of Nup50 and Nup153 join the NPC assembly sides on the chromatin (Dultz et al, 2008). As all following steps in NPC assembly depend on the presence of membranes (Rotem et al, 2009), nuclear envelope precursor membranes associate next with the seeded pre-pore structures on the chromatin. Membrane recruitment to the NPC assembly sides is mediated by the binding of the transmembrane nucleoporin Pom121 to the Nup107/160 complex (Antonin et al, 2005; Mitchell et al, 2010; Yavuz et al, 2010). Together with Pom121, Ndc1 joins as both components reside in the same membrane vesicle pool in *Xenopus* egg extracts and were detected at the nuclear envelope at similar times (Antonin et al, 2005; Dultz et al, 2008). Pom121 and Ndc1 are both essential for NPC formation *in vitro* and *in vivo* (Antonin et al, 2005; Mansfeld et al, 2006; Mitchell et al, 2010; Stavru et al, 2006). If these transmembrane nucleoporins are depleted in the *Xenopus* system, nuclear envelope and NPC formation is blocked and nuclear envelope precursor vesicles attach to chromatin without fusion. In cells, their RNAi-mediated down-regulation also results in drastic NPC defects (Antonin et al, 2005; Funakoshi et al, 2007; Stavru et al, 2006). Next, Nup53 appears at the intermediate NPC structures. As revealed recently, its direct membrane binding ability is required for the recruitment (Vollmer et al, 2012). Nup53 can interact with Ndc1 but whether this interaction contributes to NPC assembly is unclear. Yet, it seems that Nup53 can locate to NPC assembly sides independent of Ndc1 (Hawryluk-Gara et al, 2008; Vollmer et al, 2012). Nup155 associates next or maybe also simultaneously with Nup53 to the assembling NPCs. It can directly interact with both transmembrane nucleoporins Ndc1 and Pom121 as well as with Nup53 (Hawryluk-Gara et al, 2008; Hawryluk-Gara et al, 2005; Mitchell et al, 2010). The interaction of Nup53 and Nup155 is strengthened *in vitro* by Nup93, which is therefore most likely recruited after Nup53 and Nup155 (Sachdev et al, 2012). Nup93 is probably joining in two discrete subcomplexes with its mutually exclusive interaction partners Nup188 and Nup205 (Amlacher et al, 2011;

Theerthagiri et al, 2010). The completion of the Nup93 complex finalises the formation of the structural backbone of the NPC. Afterwards, barrier nucleoporins are recruited, for which Nup93 is the essential player. Nup62 is joining the NPC core as first FG-containing nucleoporin via direct binding to Nup93 simultaneously with the FG-nucleoporin Nup98 (Dultz et al, 2008; Sachdev et al, 2012). This step renders the forming NPCs transport and size-exclusion competent (Galy et al, 2003; Hulsmann et al, 2012; Laurell et al, 2011). Finally, as last steps, for which detailed kinetic analyses are lacking, Gp210 and peripheral nucleoporins of the nucleoplasmic and cytoplasmic filaments are recruited to finish the NPC assembly process (Bodoor et al, 1999; Dultz et al, 2008; Hase & Cordes, 2003).

1.3.2.2. NPC assembly during interphase

In contrast to NPC assembly at the end of mitosis, interphasic assembly is much less understood. Also, whether the underlying mechanisms are similar or substantially different is unresolved. At least, most of the protein interactions within NPCs are conserved in yeast and metazoans suggesting a similar order of recruitment of the individual nucleoporins and subcomplexes could occur (Patel & Rexach, 2008). However, depending on the cell cycle phase, the overall time for NPC assembly as well as the initiating factors seem different. Interphasic NPC assembly is significantly slower (Dultz & Ellenberg, 2010) and independent of Mel28/Elys (Doucet & Hetzer, 2010). Instead, Pom121 and Nup133, which contains a membrane curvature sensing amphipathic lipid packing sensor (ALPS) motif (Drin et al, 2007), are required early in interphasic assembly (Doucet & Hetzer, 2010). As NPC formation into an intact nuclear envelope requires the fusion of the INM and ONM, it was postulated that Nup133 could stabilise the intermediate fusion pore. Moreover, Rtns have been implicated in interphasic NPC assembly, which could also stabilise positive membrane curvature (Dawson et al, 2009). Recently, a membrane deformation function of Nup53 was identified, which is specifically required during interphase assembly (Vollmer et al, 2012). Altogether, this hints towards a particular need of membrane curvature stabilising proteins for interphasic NPC assembly and the specific requirement of membrane associated factors. Another integral membrane protein of the INM, Sun1, which forms a bridge across the perinuclear space by

interaction with KASH-proteins, is also involved in the interphasic assembly mode (Talamas & Hetzer, 2011). Genetic studies in yeast identified an intricate protein interaction network on the pore membrane between transmembrane and membrane associated nucleoporins of the Nup93 complex (Onischenko et al, 2009). In double-depletions of the Nup155 homologues Nup157 and Nup170, NPC intermediates at the INM were observed (Makio et al, 2009). Over-expression of yeast Nup53 causes aberrant membrane structures, which contain Ndc1, Pom152 and Nup170 (Marelli et al, 2001). Hence, Nup53 and Nup155 could be important for interphasic NPC assembly. However, the proof of their exact function is still lacking and the mechanistic details of NPC assembly during interphase of the cell cycle remain open.

1.3.2.3. Reconstitution of nuclear envelope and NPC assembly *in vitro*

A unique system to study nuclear envelope and NPC assembly *in vitro* is derived from cell-free extracts from amphibian eggs of *Xenopus laevis* (Lohka & Maller, 1985). As the *Xenopus* oocyte is a very large cell it contains a stockpile of all cellular components including nuclear envelope and NPC precursors making it an ideal source of material for *in vitro* nuclear reconstitution reactions. These egg extracts can be prepared in different cell cycle stages. To study NPC assembly at the end of mitosis, so called interphasic egg extracts are generated from eggs physiologically arrested in metaphase of meiosis II, which transit into S-phase (interphase) during the preparation due to an increase in intracellular calcium (Murray, 1991). These extracts are further purified into a cytosolic and a membrane-containing fraction (Vigers & Lohka, 1991). Upon incubation of cytosol and membranes with demembranated sperm chromatin, functional nuclei form in the presence of an energy regenerating system, which are able to replicate their DNA or for nucleo-cytoplasmic transport (Blow & Laskey, 1986; Newmeyer et al, 1986a). These nuclei contain a decondensed chromatin that is enclosed by a continuous nuclear envelope, in which NPCs are faithfully embedded (Macaulay & Forbes, 1996). During this reaction, the binding of membrane vesicles to the surface of the chromatin template can be observed after a few minutes (Figure 7). After approximately 50 minutes these membranes then fuse into a closed nuclear envelope. This step is followed by further decondensation of the membrane-enclosed chromatin leading to nuclear

expansion. Finally, a spherical, fully functional nucleus is formed. These nuclei can be analysed for their molecular composition or functionality by various techniques, e.g. immunofluorescence can be used to proof integration of NPCs and individual nucleoporins in the nuclear envelope.

The cell-free reconstitution system based on *Xenopus* egg extracts endows multiple advantageous. As the reaction occurs in a test tube complex cellular processes can be broken down into individual steps, which can be studied in detail independent of cellular vitality. Moreover, these extracts can easily be manipulated biochemically by adding or removing individual factors to study their specific role. In this regard, multiple factors required for nuclear envelope and NPC formation have been identified and characterised in detail (Finlay & Forbes, 1990; Finlay et al, 1991; Franz et al, 2005; Franz et al, 2007; Grandi et al, 1997; Harel et al, 2003; Powers et al, 1995; Theerthagiri et al, 2010; Walther et al, 2003; Walther et al, 2001; Walther et al, 2002). These studies can even be extended to integral membrane proteins, which are usually difficult to analyse *in vitro* (Antonin et al, 2005; Mansfeld et al, 2006). Hence, the *Xenopus* system provides a unique versatile tool faithfully mimicking physiological cellular nuclei and is especially potent to unravel molecular details of NPC assembly and function.

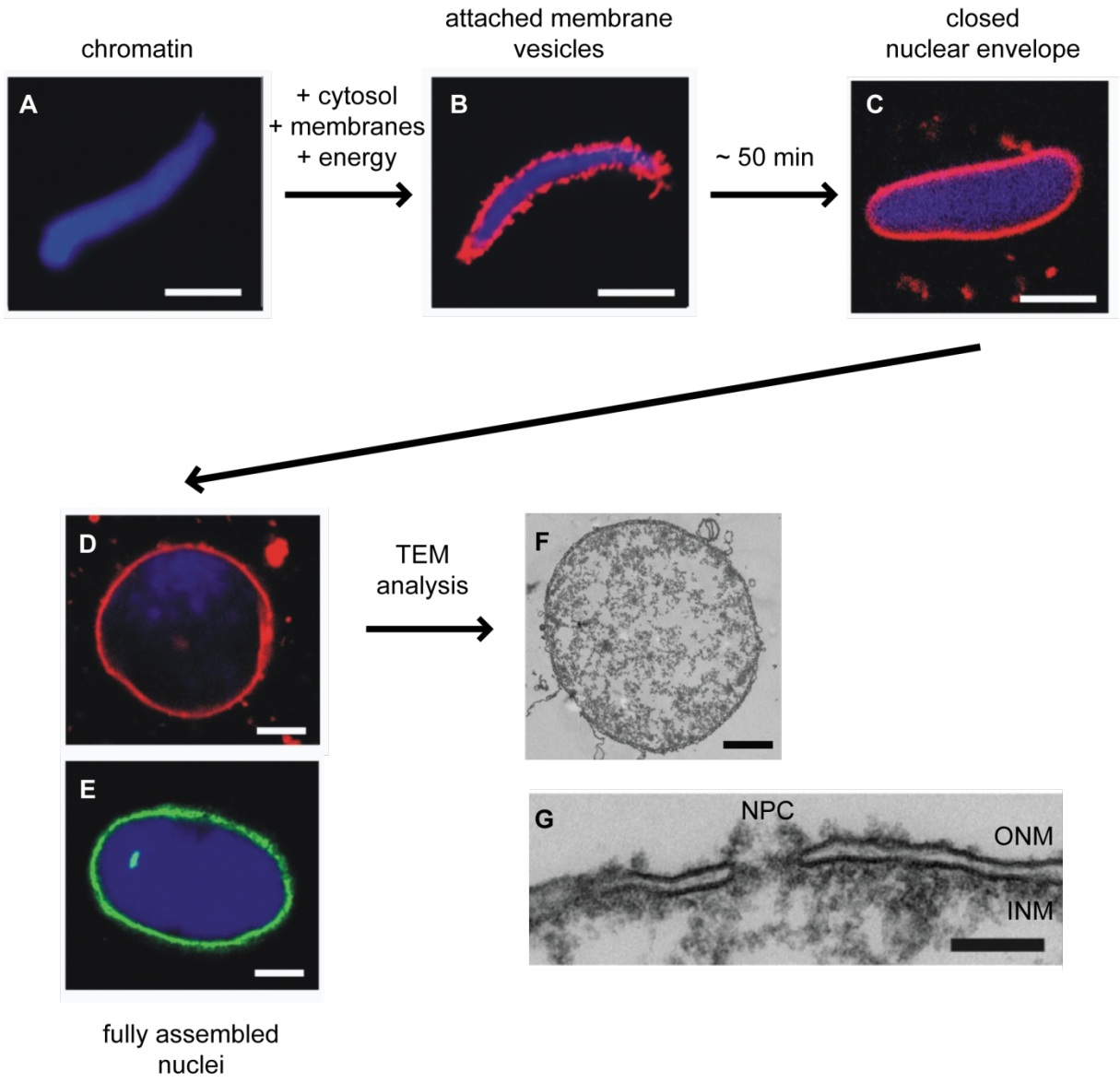

Figure 7: *In vitro* nuclear assembly reactions.

Upon incubation of demembranated sperm chromatin (A) with cytosol and membranes derived from *Xenopus laevis* egg extracts, nuclei form *in vitro* in an energy-dependent reaction. Chromatin can be stained with DAPI (blue), membranes with the lipophilic dye $DiIC_{18}$ (red). Membrane vesicles first attach to chromatin (B) and fuse after about 50 min into a closed nuclear envelope (C). Finally, the chromatin decondenses completely and the nuclei round up (D). Nuclear pore complexes (NPCs, green) can be detected by immunofluorescence (E). By transmission electron microscopy (Rotem et al) analysis the closed nuclear envelope is clearly seen (F) and NPCs appear as electron dense structures located at the fusion sites of the inner (INM) and outer nuclear membrane (ONM, G). Bars are 10 µm, and for G 100 nm.

1.3.3. Nuclear functions of NPCs

The main function of the NPC is to facilitate selective nucleo-cytoplasmic transport while at the same time establishing a diffusion barrier. Apart from its transport functions, NPCs and NPC components are also involved in several other essential nuclear functions during mitosis or interphase like chromatin organisation, gene regulation or aging (D'Angelo & Hetzer, 2006).

NPCs comprise a main central channel of approximately 30-40 nm in width and additional peripheral channels with a diameter of ~10 nm (Beck et al, 2007; Hinshaw et al, 1992). The central channel is responsible for forming the permeability barrier of the pore, which excludes molecules bigger than 40 kDa and 5 nm from passive diffusion (Feldherr & Akin, 1990; Keminer & Peters, 1999; Mohr et al, 2009). This diffusion barrier is formed by FG-repeat containing nucleoporins, which form a mesh-like hydrogel via interactions of natively unfolded regions (Denning et al, 2003; Frey et al, 2006; Hulsmann et al, 2012; Strawn et al, 2004). Moreover, FG-nucleoporins provide multiple binding sites for interactions with transport receptors to execute active, selective transport (Isgro & Schulten, 2005; Stewart et al, 2001; Strawn et al, 2004).

1.3.3.1. Transport of soluble proteins

The general requirements for selective transport of soluble cargoes through NPCs are the presence of a transport signal in the cargo protein, a transport receptor and energy. The signal sequence is either a nuclear localisation signal (NLS) for nuclear import, which is usually a stretch of basic amino acids (Goldfarb et al, 1986), or a nuclear export sequence (NES), which is typically a stretch of hydrophobic amino acids (Guttler & Gorlich, 2011). Canonical transport has been intensively studies and is mediated by transport receptors belonging to the karyopherin family (for review see Aitchison & Rout, 2012; Fried & Kutay, 2003; Strom & Weis, 2001; Terry et al, 2007; Wente & Rout, 2010). These transport receptors are also known as importins and exportins and their most prominent member is importin β (Gorlich et al, 1994; Strom & Weis, 2001). Their function depends on the interaction with the small GTPase Ran, which dictates the directionality of the transport based on its concentration gradient

(Izaurralde et al, 1997; Melchior et al, 1993; Moore & Blobel, 1993). In the nucleus, Ran is primarily present in the GTP-bound form. This is due to the chromosomal localisation of RCC1, which is the GTP-exchange factor for Ran. In contrast, the predominant form in the cytoplasm is Ran-GDP as the Ran-GTP-activating protein, which activates GTP-hydrolysis, is bound to the cytoplasmic filaments of the NPC.

To facilitate nuclear import, import receptors bind the NLS on their cargo either directly or via adaptor proteins like importin α (Gorlich et al, 1995; Radu et al, 1995). To translocate the complex through NPCs, import receptors cooperatively interact with the FG-repeats of nucleoporins flanking the central channel of the pore (Isgro & Schulten, 2005; Stewart et al, 2001; Strawn et al, 2004). In the nucleus, binding of Ran-GTP stimulates release of the cargo (and the adaptor) resulting in the termination of the import (Moroianu et al, 1996). Finally, the karyopherin recycles back to the cytoplasm, where GTP-hydrolysis of Ran drives dissociation of the karyopherin-Ran complex and frees the receptor for the next round of import (Floer et al, 1997). Nuclear export occurs in an analogous mirrored mechanism. In this process, Ran-GTP stimulates cargo binding to the export receptor in the nucleus. After transport to the cytoplasm, cargo release is triggered by GTP-hydrolysis (Moroianu & Blobel, 1995). To complete the cycle, the export receptor is then transported back to the nucleus, where it is available for binding a new cargo.

Although active transport across the NPC has to overcome the permeability barrier of the pore, the translocation process itself does not require energy. The only energy-consuming step is the hydrolysis of Ran-GTP which is required for termination of the transport and directionality (Englmeier et al, 1999; Ribbeck et al, 1999; Schwoebel et al, 1998). This makes the translocation process through the NPC highly efficient with a capacity of up to 500 translocation events per second (Ribbeck & Gorlich, 2001).

1.3.3.2. Transport of integral membrane proteins

Apart from soluble proteins, also membrane-integrated proteins of the INM have to be transported through NPCs to reach their final destination. However, in comparison to transport of soluble cargoes this transport mechanism is far less studied. At the moment there are several modes postulated by which transport of INM-proteins could

occur (for review see Katta et al, 2013; Zuleger et al, 2012). One scenario is the diffusion-retention model, which assumes that proteins can freely diffuse from the ER and ONM to the INM by using the peripheral channels of the NPC. In the INM proteins are then retained via stable interactions with lamins and chromatin. This model is supported by the size-limitation of the nucleoplasmic domain to 60 kDa, which might be determined by the width of the channels (Soullam & Worman, 1995). However, some INM-proteins require energy to translocate through NPCs (Ohba et al, 2004). Moreover, the existence of NLS-like motifs in several INM-proteins also questioned the diffusion-retention model and lead to the postulation of a receptor-mediated import similar to soluble cargoes (Furukawa et al, 1995; King et al, 2006; Soullam & Worman, 1993; Turgay et al, 2010). However, trimeric complexes comprising the INM-protein, importin β and its adaptor importin α would exceed the available space within the peripheral channels. One solution for this problem was the discovery of a smaller importin α protein, which can facilitate INM-transport independent of importin β (Braunagel et al, 2007; Rexach, 2006; Saksena et al, 2006). Taken together, it seems that several modes of transport of INM-proteins exist: lateral diffusion along the continuous membranes of the ONM and INM, transport factor- and signal sequence dependent transport. So far it is not understood whether all mechanisms exist in parallel as redundant targeting mechanisms. Hence, further studies on the transport of INM-proteins are needed in the future to unravel the precise molecular details.

2. Aim of the thesis

The aim of my PhD project was to characterise the role of the transmembrane nucleoporin Ndc1 in NPC assembly in mechanistic detail. Although Ndc1 is the only conserved integral membrane protein of the NPC of crucial function in NPC assembly in yeast and metazoans, its exact role was not elucidated yet. One explanation was the lack of a potent recombinant *in vitro* system when I started the project. Hence, my first goal was to set-up conditions to purify Ndc1, including its transmembrane regions, from bacteria and to use the recombinant factor in the *Xenopus laevis* egg extract system.

Ndc1 was known to interact with Nup53, another essential nucleoporin for NPC formation. This interaction is evolutionary conserved suggesting an important functionality. Hence, analysing this interaction by a detailed biochemical mapping on both proteins was an auspicious starting point to unravel Ndc1's function. During the course of my PhD work, a membrane-binding and deformation ability was discovered for Nup53 in our laboratory that overlaps with the Ndc1 interaction site assigned in my analysis. As the membrane binding function is required for NPC assembly, it was necessary to dissect these different features. Therefore, I generated a mutant of Nup53, which is solely impaired in the Ndc1 interaction but retained all other functions of the protein. By investigating different fragments and mutants of Ndc1 and Nup53 compromised in the interaction for their functionality in NPC assembly I characterised the individual contribution of the Ndc1 interaction to NPC assembly.

Nup53 is an interaction knob within NPCs, combining different modes of interactions and connecting different essential factors for NPC assembly. Elucidating the role of the Ndc1-Nup53 interaction revealed a deeper understanding of the complex functions of Nup53. However, to complete the picture about the Nup53-dependent steps in NPC assembly the interaction with Nup155, which is also crucial for NPC assembly, had to be dissected from all other features of Nup53. Therefore, I extended my studies on this question. Again, a detailed biochemical analysis provided the basis by narrowing down the interaction region and enabled the generation of a specific Nup53 point mutant deficient for Nup155 interaction. To investigate the role of the Nup53-Nup155 interaction for NPC assembly this mutant was then employed in the *Xenopus* system and analysed in detail.

3. List of publications included in the thesis

All results described in this thesis have been published in one of the following articles:

1) Theerthagiri G, **Eisenhardt N**, Schwarz H, Antonin W.
   The nucleoporin Nup188 controls passage of membrane proteins across the nuclear pore complex.
   J Cell Biol. 2010 Jun 28;189(7):1129-42. doi: 10.1083/jcb.200912045.

2) Vollmer B, Schooley A, Sachdev R, **Eisenhardt N**, Schneider AM, Sieverding C, Madlung J, Gerken U, Macek B, Antonin W.
   Dimerization and direct membrane interaction of Nup53 contribute to nuclear pore complex assembly.
   EMBO J. 2012 Oct 17;31(20):4072-84. doi: 10.1038/emboj.2012.256.

3) **Eisenhardt N**, Redolfi J, Antonin W.
   Interaction of Nup53 with Ndc1 and Nup155 is required for nuclear pore complex assembly.
   J Cell Sci. 2014 Feb 15;127(Pt 4):908-21. doi: 10.1242/jcs.141739. Epub 2013 Dec 20.

4) **Eisenhardt N**, Schooley A, Antonin W.
   Xenopus in vitro assays to analyze the function of transmembrane nucleoporins and targeting of inner nuclear membrane proteins.
   Methods in Cell Biol. 2014;122:193-218. doi: 10.1016/B978-0-12-417160-2.00009-6. *in press*

4. Personal contribution to publications done in teamwork

1) Theerthagiri G, **Eisenhardt N**, Schwarz H, Antonin W.
   The nucleoporin Nup188 controls passage of membrane proteins across the nuclear pore complex.
   J Cell Biol. 2010 Jun 28;189(7):1129-42. doi: 10.1083/jcb.200912045.

In this publication, I am the second author and contributed to the assay used to study transport of integral membrane proteins to the INM described in Figure 5. For this, I established the methods to express and purify the recombinant reporter proteins from *Escherichia coli* (*E. coli*) and to reconstitute them into proteoliposomes by gelfiltration which can easily fuse with endogenous membranes in nuclear assembly reactions. All recombinant integral membrane proteins used in this study were expressed, purified and reconstituted by me (Figure 5, 6, S4 and S5). Additionally, I read the first draft of the manuscript critically and gave helpful input to complete the paper for publication to GT and WA, who wrote the manuscript together.

TG designed and performed all experiments under the supervision of WA except TEM staining of depleted nuclei (Figure S2C), which was done by HS, and analysed the data together with WA.

2) Vollmer B, Schooley A, Sachdev R, **Eisenhardt N**, Schneider AM, Sieverding C, Madlung J, Gerken U, Macek B, Antonin W.
   Dimerization and direct membrane interaction of Nup53 contribute to nuclear pore complex assembly.
   EMBO J. 2012 Oct 17;31(20):4072-84. doi: 10.1038/emboj.2012.256.

As fourth author in this publication, I established the techniques to prepare liposomes by rehydration of a dried lipid film and subsequent extrusion used in this study together with BV (Figure 6 and S7). Furthermore, I performed GST-pulldown experiments to analyse the interactions of Nup53 with Ndc1 and Nup155 (Figure S1B), including expression and purification of the GST-bait proteins. By discussing the first draft of the manuscript with BV I was also involved in finalising the paper.

BV established methods for Nup53 protein purification, liposome floatation and tubulation and designed and performed all liposome and nuclear assembly experiments under the supervision of WA. He also prepared all the figures for the manuscript. Together with WA, BV analysed the data and wrote the manuscript. AS analysed nuclei of the interphasic NPC assembly assay quantitatively for their NPC content (Figure 5B). RS did GST-pulldown experiments for Nup93 and Nup205 (Figure S1A) and discovered the highly phosphorylated state of Nup53 during mitosis (Figure S3A). AMS did analytical size-exclusion of the Nup53 RRM-mutant (Figure 2A). CS cloned all protein constructs and prepared *Xenopus* egg extracts. JM and BM did mass spectra analyses for mitotic specific phosphorylations on Nup53 (Figure S3B). UG performed light scattering measurements of liposome radii (Figure S4). WA supervised the study.

3) **Eisenhardt N**, Redolfi J, Antonin W.
   Interaction of Nup53 with Ndc1 and Nup155 is required for nuclear pore complex assembly.
   J Cell Sci. 2014 Feb 15;127(Pt 4):908-21. doi: 10.1242/jcs.141739. Epub 2013 Dec 20.

As first author of this publication, I designed the study under the supervision of WA. To recombinantly express and purify full-length Ndc1 protein (i.e. with all six transmembrane regions), I refined the methods developed by JR. For the interaction of Nup53 and Ndc1, I engineered the GST-pulldown assay. All experiments using recombinant proteins, including expression and purification of all recombinant factors, were done by me. Data analyses were carried out by WA and me. With support from WA, I wrote the manuscript and I designed and prepared all figures.

4) **Eisenhardt N**, Schooley A, Antonin W.
Xenopus in vitro assays to analyze the function of transmembrane nucleoporins and targeting of inner nuclear membrane proteins.
Methods in Cell Biol. 2014;122:193-218. doi: 10.1016/B978-0-12-417160-2.00009-6. *in press*

In this method paper, in which I am listed as first author, I describe the assays in detail, which I established in our lab to analyse recombinant integral membrane proteins in NPC assembly or to study the transport of proteins of the INM through NPCs. As already mentioned above, these methods served as important tools in two publications (Eisenhardt et al, 2013; Theerthagiri et al, 2010).

WA described the methods for the preparation of egg extracts cytosol and membranes and the depletion of transmembrane nucleoporins from these extracts as well as the assay to measure transport of integral membrane proteins to the INM.

AS refined the methods for preparing cytosol and membrane fractions from *Xenopus* egg extracts and for the analysis of reconstituted nuclei by immunofluorescence.

The manuscript was assembled and finalised for submission by me.

5. Results

This chapter summarises the results of my PhD work, which were all included in one of the publications listed in section 3. For details, please refer to the original articles in the appendix as indicated in the text.

5.1. Establishing expression and purification of integral nuclear envelope proteins and their application in *Xenopus* egg extracts

The main goal of my PhD project was to functionally characterise the transmembrane nucleoporin Ndc1 in NPC assembly. In order to do this, I wanted to work with recombinant proteins purified from a bacterial host. As an integral membrane protein, Ndc1 is physiologically embedded in a lipid environment, which might influence its functionality. Hence, in order to functionally purify Ndc1, I first had to establish techniques to purify it from *Escherichia coli* (*E. coli*) and to reconstitute the purified factor into a membrane environment. By fusion of the Ndc1 sequence to a MISTIC-tag, which directs the integral membrane protein to the *E. coli* membranes during translation (Kefala et al, 2007; Roosild et al, 2005), I was able to enhance the expression yield to suitable concentrations for purification. To provide a membranous environment, I reconstituted purified Ndc1 into detergent solubilised *Xenopus* membranes by size-exclusion chromatography (Antonin et al, 2005, see section 5.1.2). These reconstituted membrane vesicles delivered fully functional Ndc1 proteins in nuclear assembly reactions (Figure 2 in Eisenhardt et al, 2013). Alternatively, integral membrane proteins can be similarly reconstituted in proteoliposomes using any artificial lipid mixture. Such proteoliposomes can be added to preformed nuclei in nuclear assembly reactions containing endogenous membranes, where they fuse spontaneously with the ER and ONM. As I was able to generally assign these purification and reconstitution techniques on the purification of other integral membrane proteins of the nuclear envelope these techniques provided the basis to develop a novel approach to analyse transport of proteins of the INM across NPCs (Theerthagiri et al, 2010). Taken together, this demonstrates that the conditions, which I established to purify recombinant integral membrane proteins, are well suited to obtain functional proteins. Moreover, reconstituted *Xenopus* membrane

vesicles and proteoliposomes provide a useful tool to apply recombinant integral membrane proteins to nuclear assembly reaction *in vitro*.

5.2. Ndc1 is essential for NPC assembly and regulates Nup53's membrane deformation function

The transmembrane nucleoporin Ndc1 was known to play an essential role in metazoan NPC assembly at the end of mitosis (Mansfeld et al, 2006; Stavru et al, 2006). However, why Ndc1 is required for NPC assembly was unresolved when I started the work of this thesis. After having established experimental conditions in our laboratory to express recombinant integral nuclear membrane proteins in *E. coli* as well as to purify them and to work with them *in vitro* (see section 5.1) I was able to investigate Ndc1's specific function in NPC assembly in more detail.

5.2.1. Different domains of Ndc1 contribute to NPC assembly

To characterise the role of Ndc1 in NPC assembly, I immunodepleted the endogenous protein from *Xenopus* membranes using a specific Ndc1-antibody (Mansfeld et al, 2006). By reconstitution of either full-length recombinant Ndc1 or two different Ndc1-fragments into the immunodepleted membranes I analysed which region of Ndc1 is required for nuclear envelope and NPC formation (Figure 2 in Eisenhardt et al, 2013). The Ndc1-fragments either spanned the predicted six transmembrane regions of the N-terminal half of the protein (amino acids 1-301, Lau et al, 2006; Stavru et al, 2006) or comprised the last transmembrane region and the subsequent C-terminal half, which folds into a globular domain (amino acids 234-660, Mansfeld et al, 2006). Although both recombinant protein fragments localised to the nuclear envelope, none of the fragments was able to rescue the block in nuclear envelope and NPC formation known to be caused by Ndc1-depletion (Mansfeld et al, 2006). This demonstrates that both parts of Ndc1 are crucial for NPC assembly.

5.2.2. Ndc1 interacts with Nup53 in *Xenopus* egg extracts

The observation that several regions in Ndc1 are required for nuclear envelope and NPC assembly raised the question what could be the role of the different parts. Ndc1 extracted from nuclei of rat cells interacts with human Nup53 (Hawryluk-Gara et al, 2008; Mansfeld et al, 2006). Hence, I tested whether this interaction is conserved in the *Xenopus* proteins (Figure S1B in Vollmer et al, 2012). In GST-pulldown experiments with *Xenopus* egg extract cytosol I observed the binding of Ndc1 to Nup53 indicating the conservation of this interaction. As the Ndc1 interaction site overlaps with the C-terminal membrane binding and deformation site in Nup53, I tested Nup53 constructs that were impaired for membrane interaction either by removing the last amino acid, a hydrophobic Tryptophane, or by introducing two point mutations into the RRM-domain, which inhibits dimerisation and in turn membrane interaction, for Ndc1 binding. Both constructs were able to interact with Ndc1 (Vollmer et al, 2012). These experiments therefore show that Ndc1 interaction and direct membrane binding of Nup53 occur independently.

5.2.3. The transmembrane domain of Ndc1 binds directly to Nup53's C-terminus

In yeast, Ndc1 and Nup53 interact directly (Onischenko et al, 2009). Hence, I determined whether this interaction is also direct in *Xenopus* and which part of Ndc1 binds to Nup53 (Figure 1 in Eisenhardt et al, 2013). For this, I established a GST-pulldown assay with recombinantly expressed Ndc1 full-length protein or Ndc1-fragments. To avoid the use of detergent, which could interfere with protein-protein interactions, I generated vesiculated *E.coli* membranes harbouring the over-expressed Ndc1 protein. Recombinant full-length Ndc1 interacted with Nup53 in this assay, suggesting a direct interaction of Ndc1 and Nup53. Also the N-terminal half of Ndc1 comprising the transmembrane helices bound to Nup53 whereas the C-terminal half did not interact. This observation was also confirmed by co-immunoprecipitation experiments in HeLa cells. Hence, the N-terminal transmembrane domain of Ndc1 provides the binding region for Nup53.

Next, I used this assay to map the Ndc1 interaction site on Nup53 more closly. Although Nup53 dimerisation via its RRM-domain is not needed for Ndc1 interaction (Vollmer et al, 2012) the RRM-domain itself has some contribution to Ndc1-binding (Figure S1 in Eisenhardt et al, 2013). Altogether, the N-terminal half of Ndc1 interacts with a region located within the C-terminal half of Nup53 upstream of the membrane binding site.

5.2.4. The transmembrane part of Ndc1 is dispensable for NPC assembly if Nup53 lacks the Ndc1 interaction site

Based on the observations that Ndc1's N-terminal half is needed for NPC assembly (see section 5.2.1) and the fact that this region mediates interaction with Nup53 (see section 5.2.3), I wondered whether the interaction of Ndc1 and Nup53 is crucial for NPC assembly. To test this, I performed co-depletion experiments, in which I specifically removed endogenous Nup53 from the cytosol of *Xenopus* egg extracts and Ndc1 from the membrane fraction (Figure 3 in Eisenhardt et al, 2013). Consistent with the individual depletions of Ndc1 and Nup53 (Hawryluk-Gara et al, 2008; Mansfeld et al, 2006; Vollmer et al, 2012), co-depletion of both proteins caused a block in nuclear envelope and NPC formation, which I could rescue by adding-back both factors as recombinant proteins. However, when I added different combinations of full-length proteins or fragments of Ndc1 and Nup53 back to the reaction, a truncated Nup53-fragment, which lacks the last eight amino acids and is therefore unable to interact with Ndc1 (Vollmer et al, 2012), was sufficient to rescue the co-depletion phenotype together with the C-terminal part of Ndc1 but not in combination with the N-terminal Ndc1-fragment. Hence, the N-terminal half of Ndc1, which provides the Nup53 interaction region, is dispensable if Nup53 is missing the Ndc1 interaction site. The C-terminal half of Ndc1 seems to fulfil another essential function in NPC assembly, which is independent of Nup53. Strikingly, in the context of full-length Nup53, only the C-terminal fragment of Ndc1 was insufficient for NPC assembly and full-length Ndc1 was required to form NPCs.

5.2.5. The Ndc1-Nup53 interaction is crucial for NPC assembly due to Nup53's membrane deformation activity

Although the N-terminal half of Ndc1 was dispensable for forming a closed nuclear envelope and NPCs in the presence of a truncated Nup53 protein, both parts of Ndc1 were required in the context of full-length Nup53 (see sections 5.2.1 and 5.2.4). Thus, I assumed that the interaction between Nup53's C-terminus and Ndc1's N-terminus fulfils a specific yet unknown function. As the last eight amino acids of Nup53 combine two different features, namely interaction with Ndc1 as well as membrane binding and deformation (Vollmer et al, 2012), the difference between full-length Nup53 and the truncated form was not only manifested in the ability to bind Ndc1. Thus, the two different functions of Nup53's C-terminus needed to be dissected to understand the role of the Ndc1-Nup53 interaction in NPC assembly. Therefore, I generated a Nup53 deletion construct that was impaired for Ndc1 interaction but retained all other functions, including membrane binding and deformation (Figure 4 and S2 in Eisenhardt et al, 2013). This Nup53 deletion construct, solely impaired for Ndc1 interaction, was then analysed in detail in NPC assembly (Figure 5 in Eisenhardt et al, 2013). In the presence of the deletion construct, nuclear envelope and NPC formation was blocked indicating that the interaction of Ndc1 and Nup53 is indeed required for NPC assembly. As the interaction was dispensable when Nup53 was additionally defective for membrane interaction and deformation via its C-terminus, I then removed the last amino acid from the deletion construct, which renders Nup53 unable to deform membranes (Vollmer et al, 2012). Consistently with the shorter truncation lacking the last eight amino acids (see section 5.2.4), this construct supported formation of a closed nuclear envelope and NPCs. In contrast, affecting the N-terminal membrane binding site, which does not deform membranes, did not result in a NPC formation-rescue. This illustrates that the Ndc1-Nup53 interaction is required due to Nup53's membrane deformation ability.

Moreover, this Nup53 deletion construct, which is impaired for Ndc1 interaction but still able to bind to its other interaction partners Nup155 and Nup93 (Hawryluk-Gara et al, 2008; Hawryluk-Gara et al, 2005; Vollmer et al, 2012), had also a dominant negative effect on nuclear envelope and NPC assembly in the presence of endogenous Nup53 (Figure 5E in Eisenhardt et al, 2013). Consistent with previous

observations, this dominant-negative effect was dependent on Nup53's ability to bind and deform membranes. In summary, these results demonstrate that the interaction of Ndc1 and Nup53 is crucial for NPC assembly and might be required to modulate Nup53's membrane deformation ability.

5.3. The Nup53-Nup155 interaction recruits Nup155 to assembling NPCs and is crucial for NPC assembly

Nup53 is known to interact with Nup155 in yeast and metazoans (Amlacher et al, 2011; Hawryluk-Gara et al, 2008; Hawryluk-Gara et al, 2005; Marelli et al, 1998; Onischenko et al, 2009; Sachdev et al, 2012; Uetz et al, 2000; Vollmer et al, 2012). As both interaction partners are essential for NPC assembly (Franz et al, 2005; Hawryluk-Gara et al, 2008; Vollmer et al, 2012) it was assumed that their interaction might also be crucial for NPC formation. In order to decipher all the diverse functions and interactions of Nup53 and their contribution to NPC assembly I also wanted to investigate the role of the Nup53-Nup155 interaction. For this, I first mapped the interaction site more closely on Nup53 to be able to dissect Nup155 interaction from all other features which Nup53 inherits, and then tested the role of this interaction in NPC assembly.

5.3.1. Nup53 binds Nup155 via a region upstream of the Ndc1 interaction site

The Nup53-Nup155 interaction site was previously mapped to a region within the C-terminal half of human Nup53 without the last 26 amino acids by using rat liver cell extracts (Hawryluk-Gara et al, 2008). Based on this result I started to analyse the interaction in the *Xenopus* proteins using GST-pulldown experiments (Figure S1B in Vollmer et al, 2012). The corresponding C-terminal half of *Xenopus* Nup53 comprising the RRM-domain and the subsequent C-terminus interacts with Nup155, also if the C-terminal end is truncated of the last eight amino acids but not if the RRM-domain alone was tested. Furthermore, a Nup53 construct that was impaired for dimerisation due to mutations in the RRM-domain (F172E/W203E) showed a weaker binding to Nup155. This illustrates that the Nup53-Nup155 interaction is

conserved in *Xenopus* and is located upstream of the Ndc1 interaction and C-terminal membrane binding site.

As dimerisation via the RRM-domain, which is crucial for Nup53's membrane binding, influences the binding of Nup53 to Nup155, the interaction site had to be mapped more precisely to be able to generate a Nup53 construct that is specifically impaired in Nup155 interaction (Figure 6 in Eisenhardt et al, 2013). For this, I chose an experimental set-up, in which both interaction partners are used as recombinantly expressed proteins, which has already been employed in a previous study (Sachdev et al, 2012). C-terminal removal of the last 25 amino acids from Nup53 did not affect the interaction with Nup155 but when the N-terminal RRM-domain was removed from the Nup53-bait construct the interaction with Nup155 was impaired. These experiments indicate that the region on Nup53 mediating the Nup155 interaction contains the RRM-domain as well as a stretch of the subsequent part. Based on sequence conservation across species, I designed a point mutant of Nup53 by exchanging a Lysine residue at position 262, which located within the identified region, to an uncharged Alanine. This mutant was specifically impaired in the Nup155 interaction without affecting Ndc1 binding (Figure 6D, E and S3 in Eisenhardt et al, 2013).

5.3.2. NPC assembly is blocked if Nup53 is unable to interact with Nup155

Finally, I investigated the effect of this mutant on NPC assembly to decipher the role of the Nup53-Nup155 interaction (Figure 7 in Eisenhardt et al, 2013). The mutant Nup53 construct defective in Nup155 binding was unable to promote nuclear envelope and NPC assembly and Nup155 as well as other nucleoporins of the Nup93 complex remained absent from the chromatin template. This demonstrates that the interaction of Nup53 and Nup155 is essential for nuclear envelope and NPC assembly to recruit the other members of the Nup93 complex to the forming NPCs.

6. Discussion

This thesis describes for the first time an essential function of the conserved transmembrane nucleoporin Ndc1 in NPC assembly identified by biochemical and cell biological *in vitro* analyses. I showed that the direct interaction of Ndc1 and Nup53 is required for NPC assembly as long as Nup53 can deform membranes. This implies that this interaction is necessary to regulate Nup53's membrane deformation activity, which influences NPC formation at the end of mitosis. Moreover, I reveal the crucial requirement of the Nup53-Nup155 interaction for NPC assembly. With this study I add new molecular details to the understanding of the step-wise NPC assembly process at the end of mitosis and the embedding of NPCs into the nuclear envelope.

6.1. Advantages of recombinant integral membrane proteins of the nuclear envelope for *in vitro* studies

The nuclear envelope consists of a continuous membrane system of the ONM, pore membrane region and the INM and contains probably hundreds of integral membrane proteins (Dreger et al, 2001; Korfali et al, 2010; Schirmer et al, 2003; Wilkie et al, 2011). Although especially INM-proteins are involved in diverse vital functions like chromatin organisation, gene expression or DNA metabolism (Dauer & Worman, 2009; Heessen & Fornerod, 2007; Reddy et al, 2008), most of these transmembrane proteins are still uncharacterised. In the NPC, crucial roles have been assigned to Ndc1 and Pom121 for NPC assembly (Antonin et al, 2005; Doucet et al, 2010; Mansfeld et al, 2006; Mitchell et al, 2010; Shaulov et al, 2011; Stavru et al, 2006; Talamas & Hetzer, 2011) yet without elucidating their specific requirement in detail. One reason for this is that it is challenging to purify and work with integral membrane proteins *in vitro*. However, to assign the specific role of a protein in detail purified components are highly advantageous. Firstly, effects coming from co-purified cellular factors (i.e. other eukaryotic proteins) can be excluded. Secondly, fragments and mutants can be used to map specific regions required for functionality. So far, most studies have either been performed *in vivo* or with fragments only comprising the soluble region neglecting the membrane-integrated part of the protein and its

function. In the rare cases, where full-length proteins were applied, the factors were purified from eukaryotic hosts. These protein preparations are difficult and time consuming and hence not suitable to study much different protein constructs. To generate mutants and fragments of the entire protein of interest in a faster and cheaper way, expression and purification from *E. coli* was the system of choice. Over-expression of an integral membrane protein is often toxic for *E. coli* or results in cytoplasmic aggregates (for review see Drew et al, 2003). Fusion of the MISTIC-sequence from *B. subtilis*, which inserts the eukaryotic protein into the bacterial membrane during translation (Kefala et al, 2007; Roosild et al, 2005), to the eukaryotic transmembrane protein was the solution to overcome these problems and to obtain a sufficient yield of functional recombinant membrane proteins from the bacterial host. With this technique, also fragments of the transmembrane region of the protein could be studied *in vitro*. This possibility resulted in enlightening the requirement of the transmembrane region of Ndc1 for fine-tuning of Nup53's membrane deformation activity.

The possibility of adding fusion tags to recombinant proteins also permits easy direct detection of the protein or detection by immunofluorescence, especially if there is no specific antibody available or to distinguish the recombinant and the endogenous factors. For example, using an EGFP-tag in my experiments enabled the detection of the N-terminal Ndc1-fragment (Figure 2 and 3 in Eisenhardt et al, 2013).

Recombinant nuclear membrane proteins can be conveniently added to *Xenopus* egg extracts after reconstitution into membrane vesicles. A physiological membrane environment is crucial for functionality of many membrane proteins (Eytan, 1982). Besides, the detergent used for solubilisation of the recombinant factor from the membrane has to be replaced. As *in vitro* nuclear assembly reactions require the presence of multiple proteins and different types of membrane vesicles (Antonin et al, 2005; Drummond et al, 1999; Salpingidou et al, 2008; Ulbert et al, 2006; Vigers & Lohka, 1991) the presence of endogenous *Xenopus* membranes is mandatory. If an integral membrane compound of the nuclear envelope has to be additionally added to the reaction, reconstitution into artificial liposomes is a convenient way to deliver the exogenous recombinant protein via spontaneous fusion of the proteoliposomes with cellular membranes (Theerthagiri et al, 2010). To replace an endogenous factor

by a recombinant fragment or mutant, the purified protein can be reconstituted into detergent solubilised *Xenopus* membranes (Antonin et al, 2005).

As the protein expression, purification and reconstitution methods did not only work for Ndc1 but could be generally extended on other integral membrane proteins of the nuclear envelope, these techniques provided the opportunity to develop a novel assay to study the transport of INM-proteins through NPCs (Theerthagiri et al, 2010). Similarly, many INM-proteins of unknown function could be characterised in the future based on these techniques, especially if the transmembrane domains execute essential functions.

6.2. The Ndc1-Nup53 interaction plays a crucial role for NPC assembly

Previous studies suggested that the interaction of Nup53 and Ndc1 is dispensable for NPC formation at the end of mitosis (Hawryluk-Gara et al, 2008; Vollmer et al, 2012). These assumptions were based on the observation that Nup53 constructs lacking 8 or 26 amino acids of their C-termini were able to promote NPC assembly *in vitro* although they were unable to interact with Ndc1. My studies reveal that these reports neglected the C-terminal membrane deformation activity of Nup53 that was additionally impaired by the truncations. Only the careful dissection of the different features of Nup53 allowed a better understanding of its multiple important roles in NPC assembly and highlighted the requirement of the Ndc1-Nup53 interaction for metazoan NPC assembly at the end of mitosis.

6.2.1. The nucleoporins Ndc1 and Nup53 and their interaction are conserved features among eukaryotes

Ndc1 and Nup53 were known as conserved crucial factors for NPC assembly in yeast and vertebrates (Hawryluk-Gara et al, 2008; Hawryluk-Gara et al, 2005; Madrid et al, 2006; Mans et al, 2004; Mansfeld et al, 2006; Marelli et al, 1998; Onischenko et al, 2009; Rodenas et al, 2009; Stavru et al, 2006; Vollmer et al, 2012). Analogously to the yeast orthologues (Onischenko et al, 2009), I show that *Xenopus* Ndc1 and Nup53 also interact directly pointing towards strict conservations not only of the two

proteins but also of the role of their interaction. The mapping of the interaction site on Nup53 localised the binding region to the C-terminal end close but upstream of the C-terminal membrane binding and deformation site, for which the last amino acid is compulsory (Vollmer et al, 2012). In yeast, both Nup53 homologues also interact with Ndc1 via regions in their C-terminal part (Onischenko et al, 2009). Interestingly, these proteins also show membrane deformation activities (Vollmer et al, 2012), which are probably mediated by the C-terminal ends that are predicted to form amphipathic alpha-helices (Marelli et al, 2001; Patel & Rexach, 2008; Vollmer et al, 2012). The C-terminus of Nup53 is highly conserved among eukaryotes (Vollmer et al, 2012, Figure 8). Hence, the functional role of the Ndc1-Nup53 interaction to regulate membrane deformation of Nup53 in order to allow for NPC assembly might most likely be conserved. Interestingly, Ndc1 is dispensable in *A. nidulans* (DeGrasse et al, 2009; Liu et al, 2009; Neumann et al, 2010). However, also no obvious Nup53 homologue was found in this fungus. This is in line with my data that indicates that the Ndc1-Nup53 interaction is only required if Nup53 has a membrane deforming activity but dispensable if Nup53 is unable to deform membranes. Thus, highlighting the fact that Ndc1 interaction is not needed if Nup53 is absent from the organism. Surprisingly, *Amoebozoa* also miss obvious Ndc1 homologues although Nup53 was identified (Neumann et al, 2010). In these organisms, Nup53 could either be regulated by other proteins or be inactive for membrane deformation. Indeed, the sequence conservation within the C-terminus of *Dictyostelium discoideum* is not very high to the yeast and metazoan proteins. Especially the last amino acid, a Tryptophane, which is essential for membrane binding and tubulation in *Xenopus* (Vollmer et al, 2012), is not conserved. Hence, whether Nup53 has also a membrane-deformation activity in these organisms has to be revealed firstly.

In *Xenopus*, the C-terminal half of Ndc1 showed an additional essential role for NPC assembly. As Ndc1 is dispensable in *A. nidulans* it might be that the C-terminal role of Ndc1 is not conserved in this species and specific to higher eukaryotes, where it is known to interact with Nup155 and Aladin (Kind et al, 2009; Mitchell et al, 2010; Yamazumi et al, 2009). Interestingly, in yeast no interaction between Nup155 and Ndc1 was identified (Onischenko et al, 2009). Instead, the Nup155 orthologue Nup170 binds to the integral membrane nucleoporin Pom152. This interaction could act redundantly in functional terms to localise the Nup155-homologue to the pore

membrane. Alternatively, it could be possible that *A. nidulans* possesses another different nucleoporin acting redundantly to Ndc1's C-terminal part.

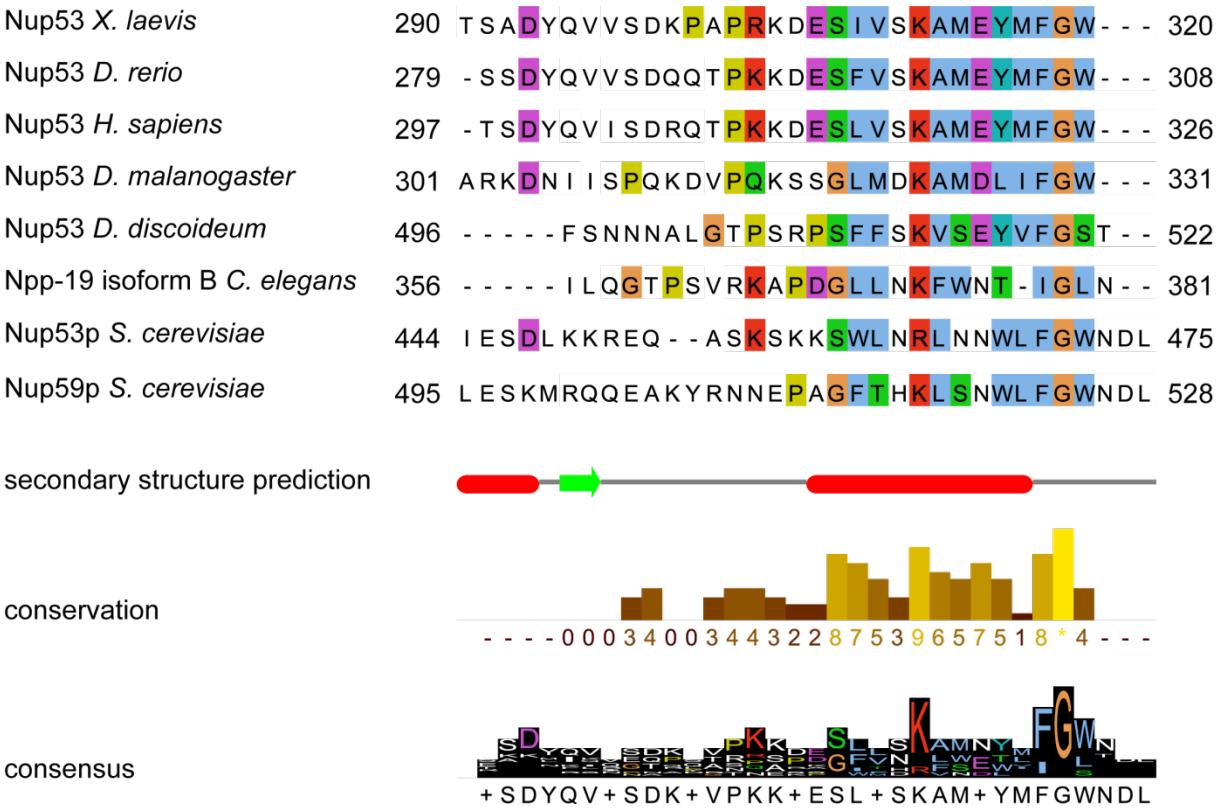

Figure 8: The C-terminus of Nup53 is highly conserved in metazoans and yeast.

Multiple sequence alignment of the last 31 amino acids of *Xenopus laevis* Nup53 with Nup53 from *zebrafish*, *human*, *Drosophila*, *Dictyostelium discoideum*, *C. elegans* and the two *S. cerevisiae* homologues Nup53p and Nup59p by clustal omega algorithm (Sievers et al, 2011). Conserved hydrophobic amino acids (AILMFWV) and Cysteine (C) are coloured in blue, positively charged amino acids (RK) in red, negatively charged amino acids (DE) in magenta, uncharged polar amino acids (NQST) in green, Histidine and Tyrosine (HY) in cyan, and Proline (P) in yellow if present in at least 60% of the sequences. If the Cysteine (C) conservation is more than 80%, it is coloured pink. The smallest amino acid Glycine (G) is always coloured orange, independent of the conservation. Secondary structure is predicted by JNETHMM using the Jalview software (Waterhouse et al, 2009). Red cylinders indicate predicted α-helixes, green arrows β-barrels. The conservation and consensus sequence are shown by histograms.

I identified the N-terminal transmembrane region as the Nup53 interaction site in Ndc1. In other species, the Nup53 binding region on Ndc1 is unresolved so far. The transmembrane regions in Ndc1 are well conserved although overall the conservation of some regions within the C-terminal part of Ndc1 is higher (Mansfeld et al, 2006; Stavru et al, 2006, Figure 9).

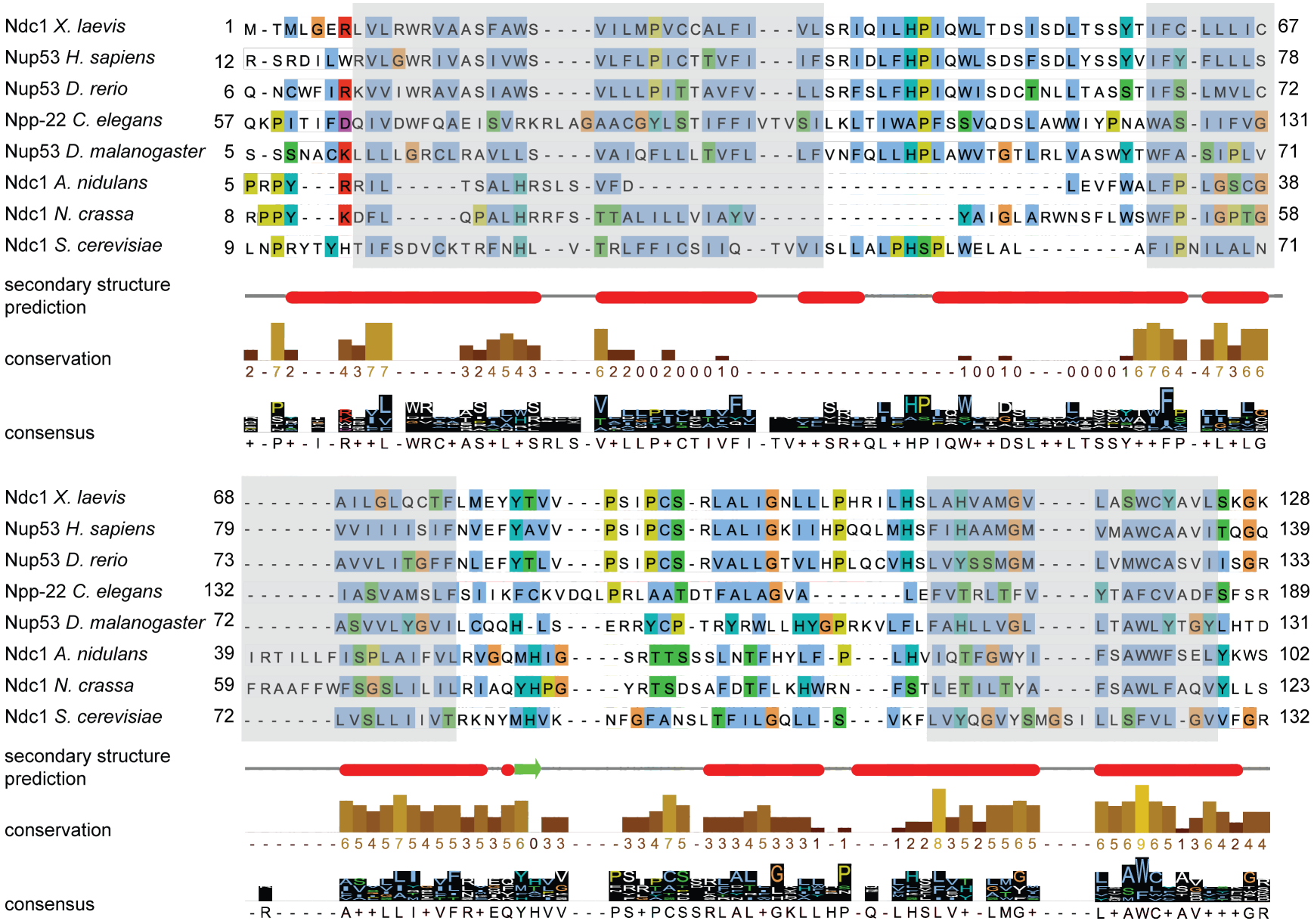
Ndc1 X. laevis
Nup53 H. sapiens
Nup53 D. rerio
Npp-22 C. elegans
Nup53 D. malanogaster
Ndc1 A. nidulans
Ndc1 N. crassa
Ndc1 S. cerevisiae
secondary structure prediction
conservation
consensus

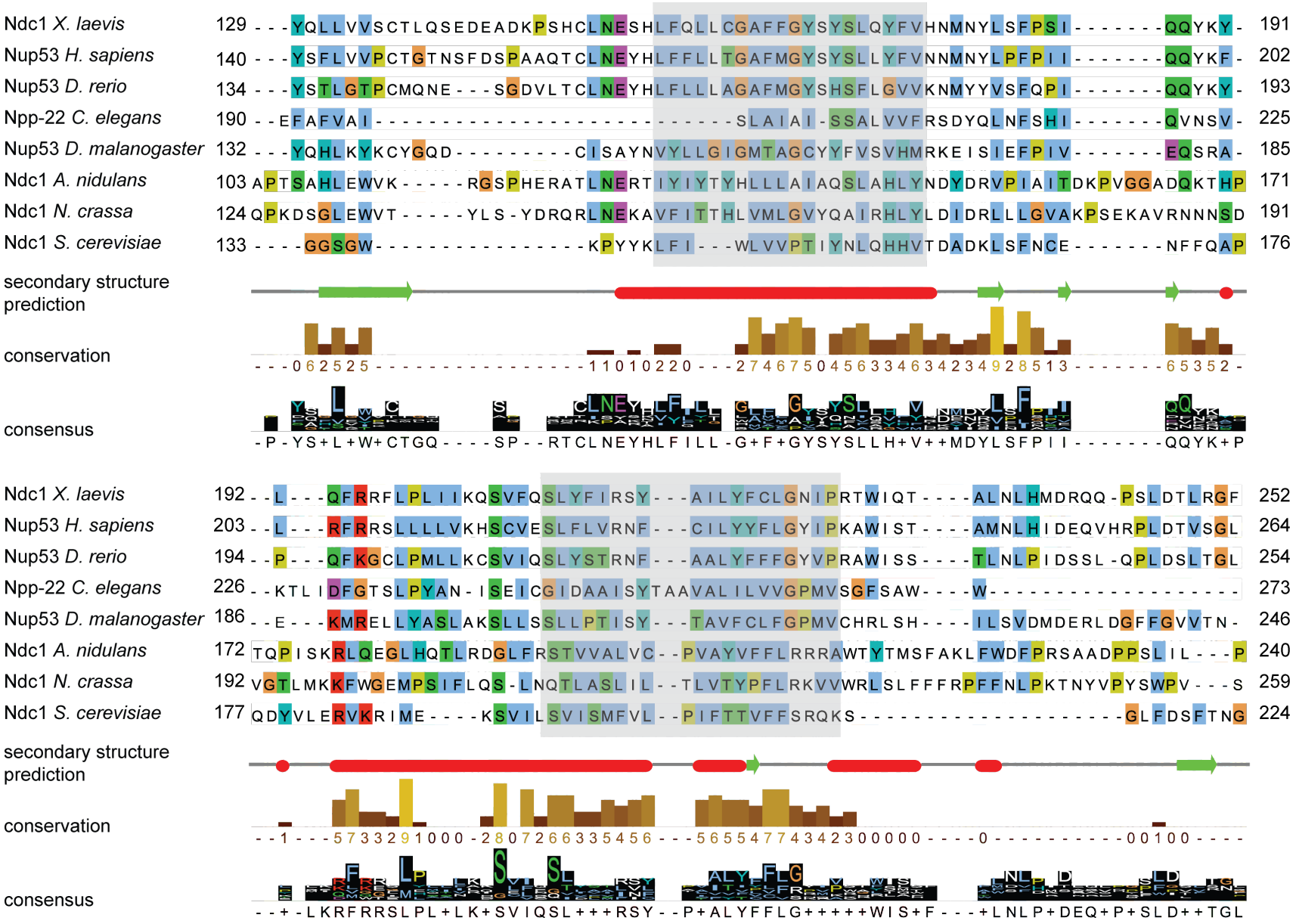
Ndc1 X. laevis 129 - - - YQLLVVSCTLQSEDEADKPSHCLNESHLFQLLCGAFFGYSYSLQYFVHNMNYLSFPSI - - - - - - - QQYKY - 191
Nup53 H. sapiens 140 - - - YSFLVVPCTGTNSFDSPAAQTCLNEYHLFFLLTGAFMGYSYSLLYFVNNMNYLPFPII - - - - - - - QQYKF - 202
Nup53 D. rerio 134 - - - YSTLGTPCMQNE - - - SGDVLTCLNEYHLFLLLAGAFMGYSHSFLGVVKNMYYVSFQPI - - - - - - - QQYKY - 193
Npp-22 C. elegans 190 - - EFAFVAI - SLAIAI - SSALVVFRSDYQLNFSHI - - - - - - - QVNSV - 225
Nup53 D. malanogaster 132 - - - YQHLKYKCYGQD - - - - - - - - - CISAYNVYLLGIGMTAGCYYFVSVHMRKEISIEFPIV - - - - - - - EQSRA - 185
Ndc1 A. nidulans 103 APTSAHLEWVK - - - - - RGSPHERATLNERTIYIYTYHLLLAIAQSLAHLYNDYDRVPIAITDKPVGGADQKTHP 171
Ndc1 N. crassa 124 QPKDSGLEWVT - - - - - YLS - YDRQRLNEKAVFITTHLVMLGVYQAAIRHLYLDIDRLLLGVAKPSEKAVRNNNSD 191
Ndc1 S. cerevisiae 133 - - - - GGSGW - - - - - - - - - - - - - - - - KPYYKLFI - - - WLVVPTIYNLQHHVTDADKLSFNCE - - - - - - - NFFQAP 176
secondary structure prediction
conservation
- - - 0 6 2 5 2 5 - - - - - - - - - - - - - - - - 1 1 0 1 0 2 2 0 - - - 2 7 4 6 7 5 0 4 5 6 3 3 4 6 3 4 2 3 4 9 2 8 5 1 3 - - - - - - - 6 5 3 5 2 -
consensus
- P - YS + L + W + CTGQ - - - - SP - - RTCLNEYHLF ILL - G + F + GYSYSLLH + V + + MDYLSFPII - - - - - - - QQYK + P
Ndc1 X. laevis 192 - - L - - - QFRRFLPLII KQSVFQSLYFIRSY - - - AILYFCLGNIPRTWIQT - - - - ALNLHMDRQQ - PSLDTLRGF 252
Nup53 H. sapiens 203 - - L - - - RFRRSLLLLV KHSCVESLFLVRNF - - - CILYYFLGYIPKAWIST - - - - AMNLHIDEQVHRPLDTVSGL 264
Nup53 D. rerio 194 - - P - - - QFKGCLPMLL KCSVIQSLYSTRNF - - - AALYFFFGYVPRAWISS - - - - TLNLPIDSSL - QPLDSLTGL 254
Npp-22 C. elegans 226 - - KTLIDFGTSLPYAN - ISEICGIDAAISYTAAVALILVVGPMVSGFSAW - - - - W - - - - - - - - - - - - - - - - - - 273
Nup53 D. malanogaster 186 - - E - - - KMRELLYASLAKSLLSSLLPTISY - - - TAVFCLFGPMVCHRLSH - - - - ILSVDMDERLDGFFGVVTN - 246
Ndc1 A. nidulans 172 TQPISKRLQEGLHQTLRDGLFRSTVVALVC - - PVAYVFFLRRRAWTYTMSFAKLFWDFPRSAADPPSLIL - - - P 240
Ndc1 N. crassa 192 VGTLMKKFWGEMPSIFLQS - LNQTLASLIL - - TLVTYPFLRKVVWRLSLFFFRPFFNLPKTNYVPYSWPV - - - S 259
Ndc1 S. cerevisiae 177 QDYVLERVKRIME - - - - KSVILSVISMFVL - - PIFTTVFFSRQKS - GLFDSFTNG 224
secondary structure prediction
conservation
- - 1 - - - 5 7 3 3 2 9 1 0 0 0 - 2 8 0 7 2 6 6 3 3 5 4 5 6 - - - 5 6 5 5 4 7 7 4 3 4 2 3 0 0 0 0 0 - - - - 0 - - - - - - - - - - 0 0 1 0 0 - - - -
consensus
- - + - LKRFRRSLPL + LK + SVIQSL + + + RSY - - P + ALYFFLG + + + + + WIS + F - - - + LNLP + DEQ + P + SLD + + TGL

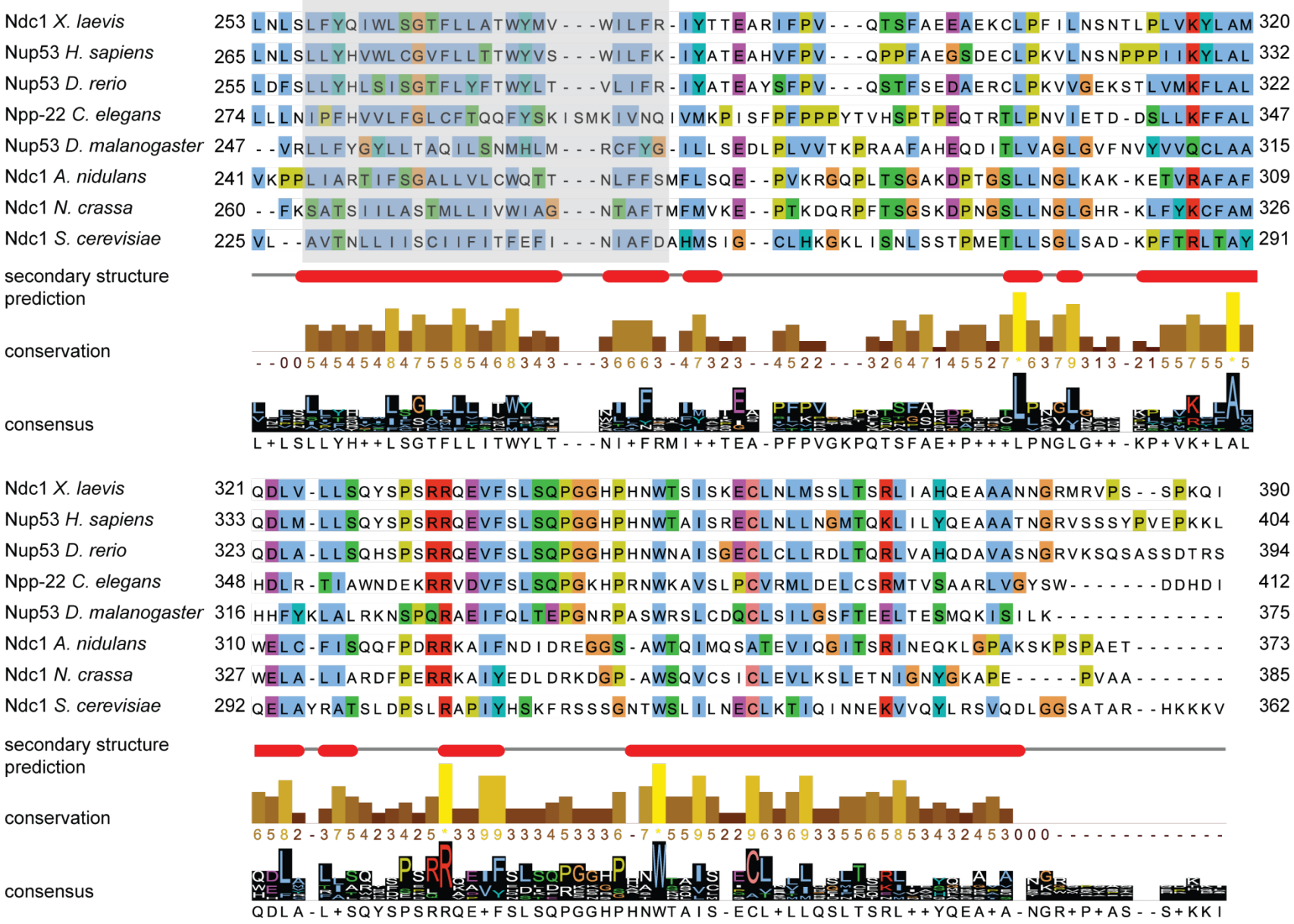
Ndc1 X. laevis 253 LNLSLFYQIWLSGTFLLATWYMV---WILFR-IYTTEARIFPV---QTSFAEEAEKCLPFILNSNTLPLVKYLAM 320
Nup53 H. sapiens 265 LNLSLLYHVWLCGVFLLTTWYVS---WILFK-IYATEAHVFPV---QPPFAEGSDECLPKVLNSNPPPIIKYLAL 332
Nup53 D. rerio 255 LDFSLLYHLSISGTFLYFTWYLT---VLIFR-IYATEAYSFPV---QSTFSEDAERCLPKVVGEKSTLVMKFLAL 322
Npp-22 C. elegans 274 LLLNIPFHVVLFGLCFTQQFYSKISMKIVNQIVMKPISFPFPPPYTVHSPTPEQTRTLPNVIETD-DSLLKFFAL 347
Nup53 D. malanogaster 247 --VRLLFYGYLLTAQILSNMHLM---RCFYG-ILLSEDLPLVVTKPRAAFAHEQDITLVAGLGVFNVYVVQCLAA 315
Ndc1 A. nidulans 241 VKPPLIARTIFSGALLVLCWQTT---NLFFSMFLSQE--PVKRGQPLTSGAKDPTGSLLNGLKAK-KETVRAFAF 309
Ndc1 N. crassa 260 --FKSATSIILASTMLLIVWIAG---NTAFTMFMVKE--PTKDQRPFTSGSKDPNGSLLNGLGHR-KLFYKCFAM 326
Ndc1 S. cerevisiae 225 VL--AVTNLLIISCIIFITFEFI---NIAFDAHMSIG--CLHKGKLISNLSSTPMETLLSGLSAD-KPFTRLTAY 291
secondary structure prediction
conservation
--005454548475585468343---36663-47323--4522---32647145527*63793 13-2155755*5
consensus
L+LSLLYH++LSGTFLLITWYLT---NI+FRMI++TEA-PFPVGKPQTSFAE+P+++LPNGLG++-KP+VK+LAL
Ndc1 X. laevis 321 QDLV-LLSQYSPSRRQEVFSLSQPGGHPHNWTSISKECLNLMSSLTSRLIAHQEAAANNGRMRVPS--SPKQI 390
Nup53 H. sapiens 333 QDLM-LLSQYSPSRRQEVFSLSQPGGHPHNWTAISRECLNLLNGMTQKLILYQEAAATNGRVSSSYPVEPKKL 404
Nup53 D. rerio 323 QDLA-LLSQHSPSRRQEVFSLSQPGGHPHNWNAISGECLCLLRDLTQRLVAHQDAVASNGRVKSQSASSDTRS 394
Npp-22 C. elegans 348 HDLR-TIAWNDEKRRVDVFSLSQPGKHPRNWKAVSLPCVRMLDELCSRMTVSAARLVGYSW-------DDHDI 412
Nup53 D. malanogaster 316 HHFYKLALRKNSPQRAEIFQLTEPGNRPASWRSLCDQCLSILGSFTEELTESMQKISILK------------ 375
Ndc1 A. nidulans 310 WELC-FISQQFPDRRKAIFNDIDREGGS-AWTQIMQSATEVIQGITSRINEQKLGPAKSKPSPAET------- 373
Ndc1 N. crassa 327 WELA-LIARDFPERRKAIYEDLDRKDGP-AWSQVCSICLEVLKSLETNIGNYGKAPE-----PVAA------- 385
Ndc1 S. cerevisiae 292 QELAYRATSLDPSLRAPIYHSKFRSSSGNTWSLILNECLKTIQINNEKVVQYLRSVQDLGGSATAR--HKKKV 362
secondary structure prediction
conservation
6582-375423425*33993333453336-7*55952296369335565853432453000------------
consensus
QDLA-L+SQYSPSRRQE+FSLSQPGGHPHNWTAIS-ECL+LLQSLTSRL++YQEA+A-NGR+P+AS--S+KKI

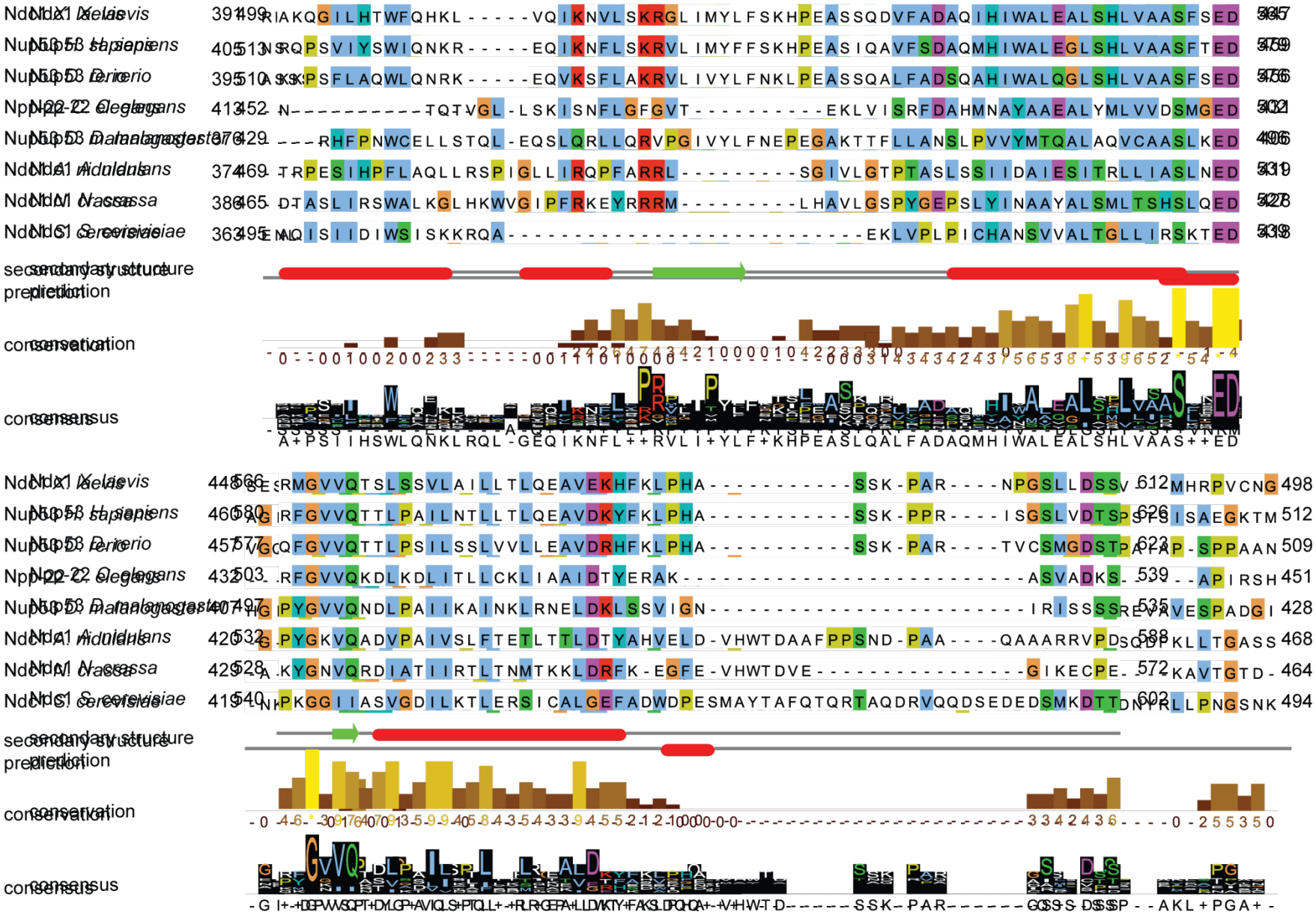
secondary structure prediction
conservation
consensus
secondary structure prediction
conservation
consensus

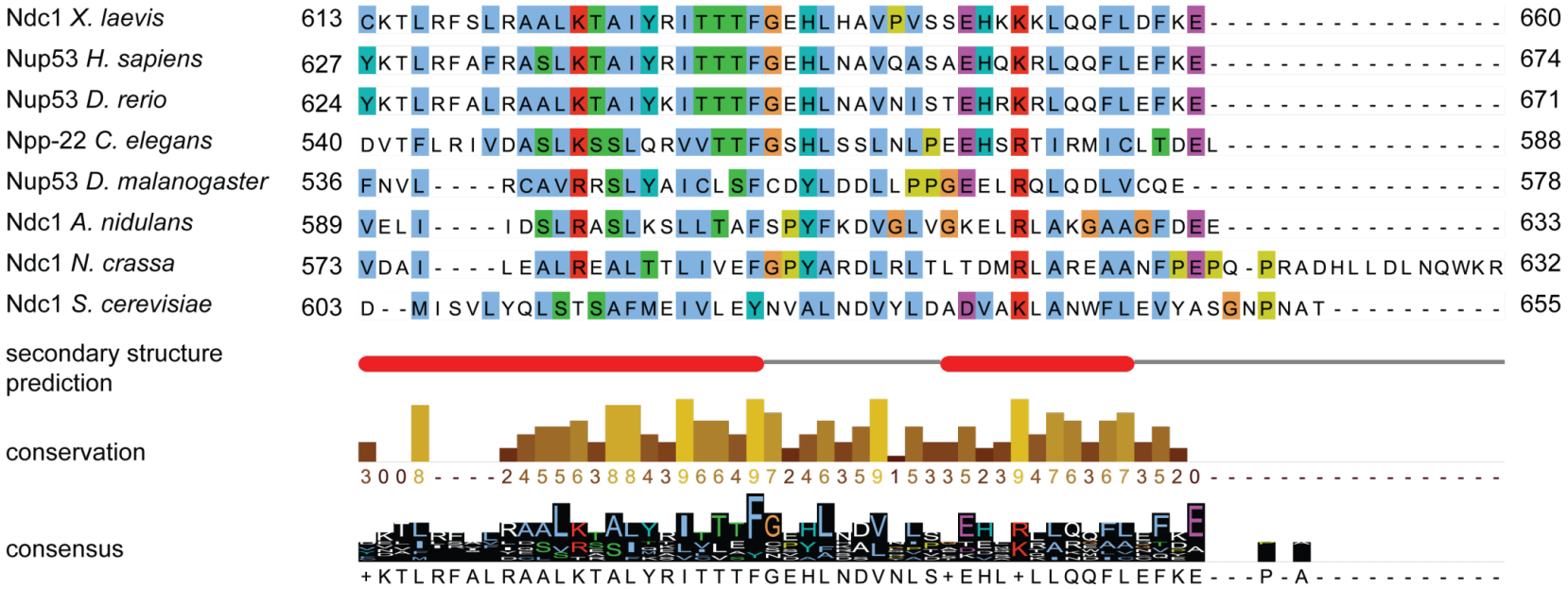

Figure 9: Multiple sequence alignment of Ndc1.

Xenopus laevis Ndc1 sequence was aligned with *human*, *zebrafish*, *C. elegans*, *Drosophila*, *A. nidulans*, *N. crassa* and *S. cerevisiae* Ndc1 using the clustal omega algorithm (Sievers et al, 2011). Amino acid colouring corresponds to clustal omega colouring with AILMFWV and C coloured in blue, RK in red, NQST in green ED in magenta, HY in cyan, and P in yellow if present in at least 60% (see Figure 8). G is always orange and C pink if present at least 80%. To predict secondary structure elements JNETHMM using the Jalview software was used (Waterhouse et al, 2009). Predicted α-helixes are indicated by red cylinders, β-barrels by green arrows. The conservation and consensus sequence are depicted in histograms. Grey boxes indicate the predicted transmembrane regions according to Lau et al, 2006; Mansfeld et al, 2006; Stavru et al, 2006.

Hence, the C-terminal region was previously assumed to mediate protein interaction with Nup53 (Mansfeld et al, 2006). However, it failed to bind to human Nup53 (Mitchell et al, 2010). This result corresponds with our mapping analysis and indicates that the Nup53 binding region is probably also located in the N-terminal half for human Ndc1. Especially as the interacting region in Nup53 is a membrane binding region, it makes sense that the part of Ndc1 responsible for the interaction locates close to a membrane. Altogether, Ndc1, Nup53 and their interaction are well conserved among different species both as protein sequences and functionally.

6.2.2. Possible mechanisms for how Nup53's membrane deformation ability could be regulated by Ndc1

As the binding sites on both, Ndc1 and Nup53, are most likely embedded in the nuclear pore membrane, the interaction of these proteins could take place within the lipid-bilayer, where Nup53 either interacts with lipids and Ndc1 or where Ndc1 prevents or weakens the interaction of Nup53 with the membrane. It seems more likely that Nup53 is able to interact with both, lipids and Ndc1. Pulldown experiments with Nup53 constructs containing an intact RRM-domain showed more background binding and therefore recruited more Ndc1 in total than RRM-mutants, which was probably due to additional interactions with the membrane of the vesicles via the membrane binding site (Figure 1 in Eisenhardt et al, 2013, and unpublished data). I was able to separate Ndc1 binding from Nup53's membrane interaction by the deletion of a small stretch of eight amino acids. As my data demonstrate, the Ndc1-Nup53 interaction is crucial for NPC assembly whenever Nup53 possesses the ability to deform membranes and thus the interaction most likely inhibits or counteracts membrane bending of Nup53. How could this be achieved mechanistically? The C-term of Nup53 is supposed to adopt an amphipathic alpha-helical structure (Marelli et al, 1998), which could intercalate into one leaflet of the pore membrane resulting in displacement of the lipid headgroups and a rearrangement of the hydrophobic lipid alkyl chains. This process induces a positive curving on the membrane as it is known for other proteins containing amphipathic alpha-helices, e.g. Arf-proteins (Amor et al, 1994; Antonny et al, 1997; Drin et al, 2007). For most of these instances, the protein only folds into the amphipathic helix once it is in contact with the membrane (Cornell

& Taneva, 2006; Drin et al, 2007). This might also be the case for Nup53. Thus, the Ndc1 interaction could insulate Nup53 either from its interaction with the lipid environment avoiding the folding of the C-terminal region into an amphipathic alpha-helix (Figure 10A) or Ndc1 itself could bind the amphipathic helix of Nup53, which in turn cannot intercalate into the membrane any more (Figure 10B). Alternatively, the interaction with Ndc1 in the nuclear pore membrane might induce a conformational change on Nup53 thereby inhibiting its membrane deformation activity as the amphipathic helix might no longer be accessible for intercalation into the membrane (Figure 10C). Without Ndc1, Nup53 would then be constitutively active for membrane deformation via its amphipathic alpha-helix, which might result in a block of NPC assembly (see also section 6.2.3). Another possible scenario could be that Ndc1 itself also influences the membrane shape and thereby counteracts the curvature induced by Nup53 (Figure 10D). Integral membrane proteins can induce local membrane curvature due to their intrinsic three-dimensional shape. However, in this regard only a few integral membrane proteins have been identified so far and all of them support positive membrane curvature (Mackinnon, 2004; Unwin, 2005). But as the structure of only a minority of the transmembrane proteins is solved, inducing negative membrane bending might be a possible mechanism in general. Actually, the C-terminal membrane binding and deformation site of Nup53 is dispensable for NPC formation at the end of mitosis as membrane interaction can be probably achieved via the N-terminal membrane binding site, which seems to act partially redundantly (Vollmer et al, 2012). However, Ndc1 seems to only modify membrane deformation without affecting the membrane binding capability of Nup53's C-terminal end as a Nup53 protein construct with an intact C-terminus but an impaired N-terminal membrane binding site can still support NPC assembly at the end of mitosis (Vollmer et al, 2012). This would favour a model of sequential interactions. Nup53 could initially interact with the pore membrane via its C-terminal membrane binding site and the Ndc1 interaction manifests after the initial membrane contact, which then either results in insulation or antagonises the curvature. Altogether, there are several possibilities conceivable by which Ndc1 regulates membrane deformation of Nup53. But why might it be important for postmitotic NPC assembly to inhibit membrane deforming activities?

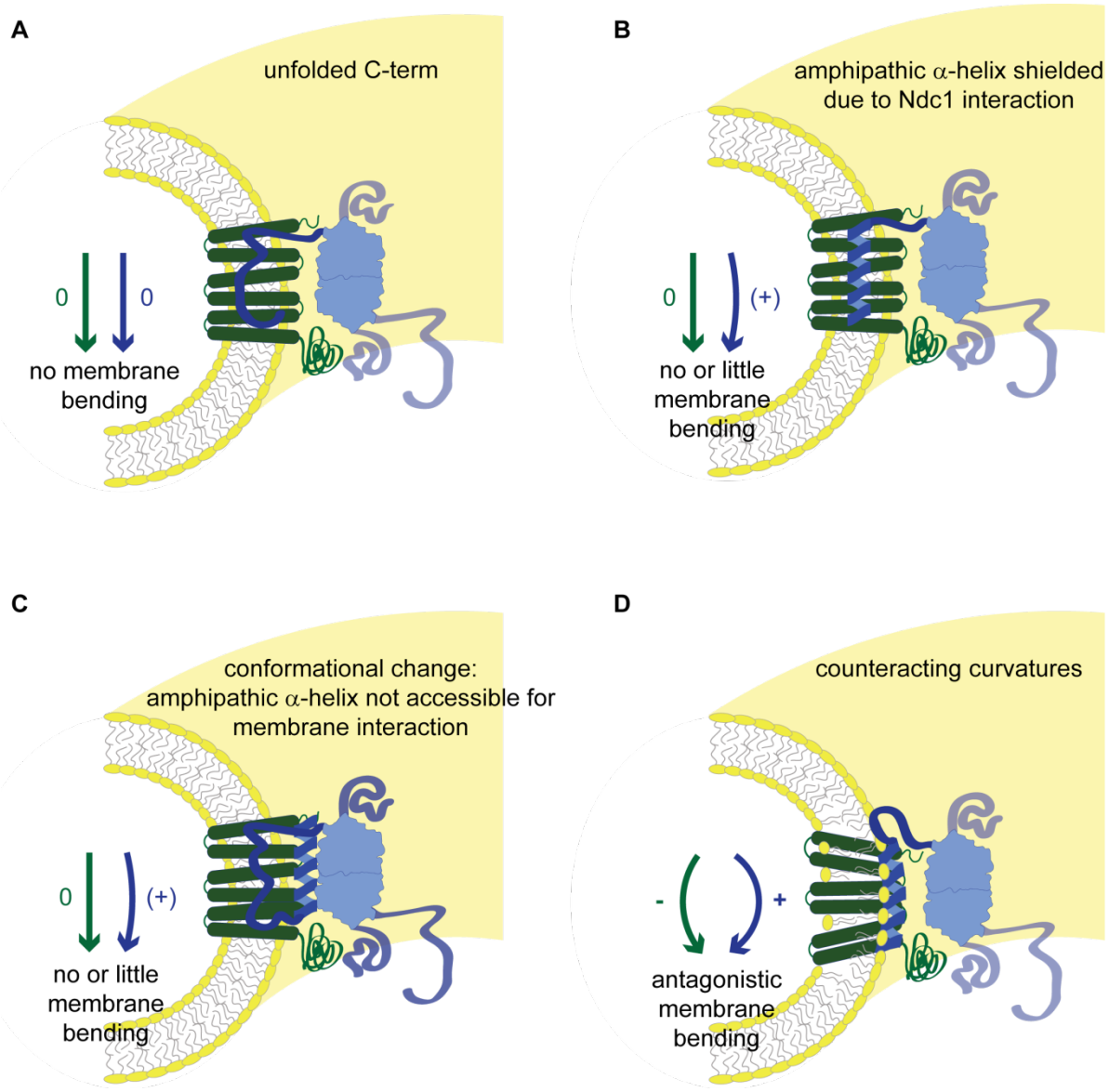

Figure 10: Ndc1 regulates the membrane deformation activity of Nup53's C-term.

The transmembrane regions of Ndc1 (green) and the C-term of Nup53 (blue) interact within the lipid bilayer of the pore membrane. This interaction reduces, inhibits or counteracts the membrane deformation capability of Nup53. The C-terminal part of Nup53 could be prevented from folding into the amphipathic helix due to the interaction (A) or the amphipathic helix could interact with Ndc1 and thus not integrate into the membrane leaflet (B). The interaction with Ndc1 could also induce a conformational change on Nup53 burying the amphipathic helix in the interaction surface and preventing its access to the membrane (C). Alternatively, Ndc1 might induce an antagonistic curvature on the membrane (D). For the sake of simplicity, only one C-terminal end of the Nup53-dimer is shown to interact with Ndc1 or the membrane. Other interactions (also membrane binding by Nup53's N-termini) are also neglected.

6.2.3. Why could membrane deformation be inhibitory for NPC assembly and needs to be modulated?

At the end of mitosis, the nuclear envelope re-forms from mitotic ER (for review see Antonin et al, 2008; Prunuske & Ullman, 2006; Schooley et al, 2012). In order to enclose the decondensing chromatin by a double membrane layer, two parallel flat membrane sheets are required. Although it is unresolved whether the nuclear envelope is formed from tubular ER (Anderson & Hetzer, 2007; Puhka et al, 2007) or extended ER cisternae (Lu et al, 2011; Poteryaev et al, 2005) in any case the ER membranes have to extend laterally and finally seal into a closed nuclear envelope with its typical membrane arrangement (Antonin & Mattaj, 2005): a saddle-like shape with a positive membrane curvature along the membrane surface of the double-layer and a negative curvature within the plane of the pore (Figure 11). This shape is fundamentally different from the membrane shapes present in the ER, which always show high positive curvature either in two dimensions as it is the case for ER tubes or one dimension at the edges of ER sheets (Shibata et al, 2010, Figure 11A). Both, in tubular ER and ER sheets the highly curved surfaces are covered with the membrane shaping proteins of the Rtn-family and DP1 (Shibata et al, 2010; Voeltz et al, 2006). These proteins are important for initial stages of nuclear envelope formation at the end of mitosis (Anderson & Hetzer, 2007) and were found along the highly curved leading edges of nuclear membranes when growing around the chromatin at the end of mitosis (Lu & Kirchhausen, 2012). However, eventually they need to be displaced from the emerging nuclear envelope during its re-formation process (Anderson & Hetzer, 2008). The displacement of membrane tubulating proteins determines the speed of nuclear envelope re-formation as in cells over-expression of Rtn delayed this process and a reduction of Rtn-levels accelerated nuclear envelope growth (Anderson & Hetzer, 2008). The reason for this might be that Rtns and DP1 inhibit negative curvature generation. Nup53 induces membrane deformation via its C-terminal membrane binding site similar to Rtns *in vitro*. On liposomes, Nup53 and Rtn4 both induce tubulation (Hu et al, 2008; Vollmer et al, 2012) suggesting a positive membrane curving ability. Hence, Nup53 could also be inhibitory for the final pore membrane arrangement when it is active for membrane deformation. Here, Ndc1 might come into play and inactivates Nup53's membrane curving when localised in the pore membrane. As opposite directed membrane

curvatures could energetically balance each other (Terasaki et al, 2013) it might even be that the co-existing negative and positive curvature in the pore membrane do not need active deformation but can be adopted passively. NPCs could serve as scaffolds that stabilise and maintain the membrane curvatures of the pore. Especially components of the Nup107/160 complex would be prime candidates to act as such a coat as several members show structural similarities to vesicle coat proteins (Brohawn et al, 2008; Devos et al, 2004; Mans et al, 2004). Hence, active deformation of the membranes might even be counter-productive and is – in the case of Nup53 – therefore avoided by the presence of Ndc1.

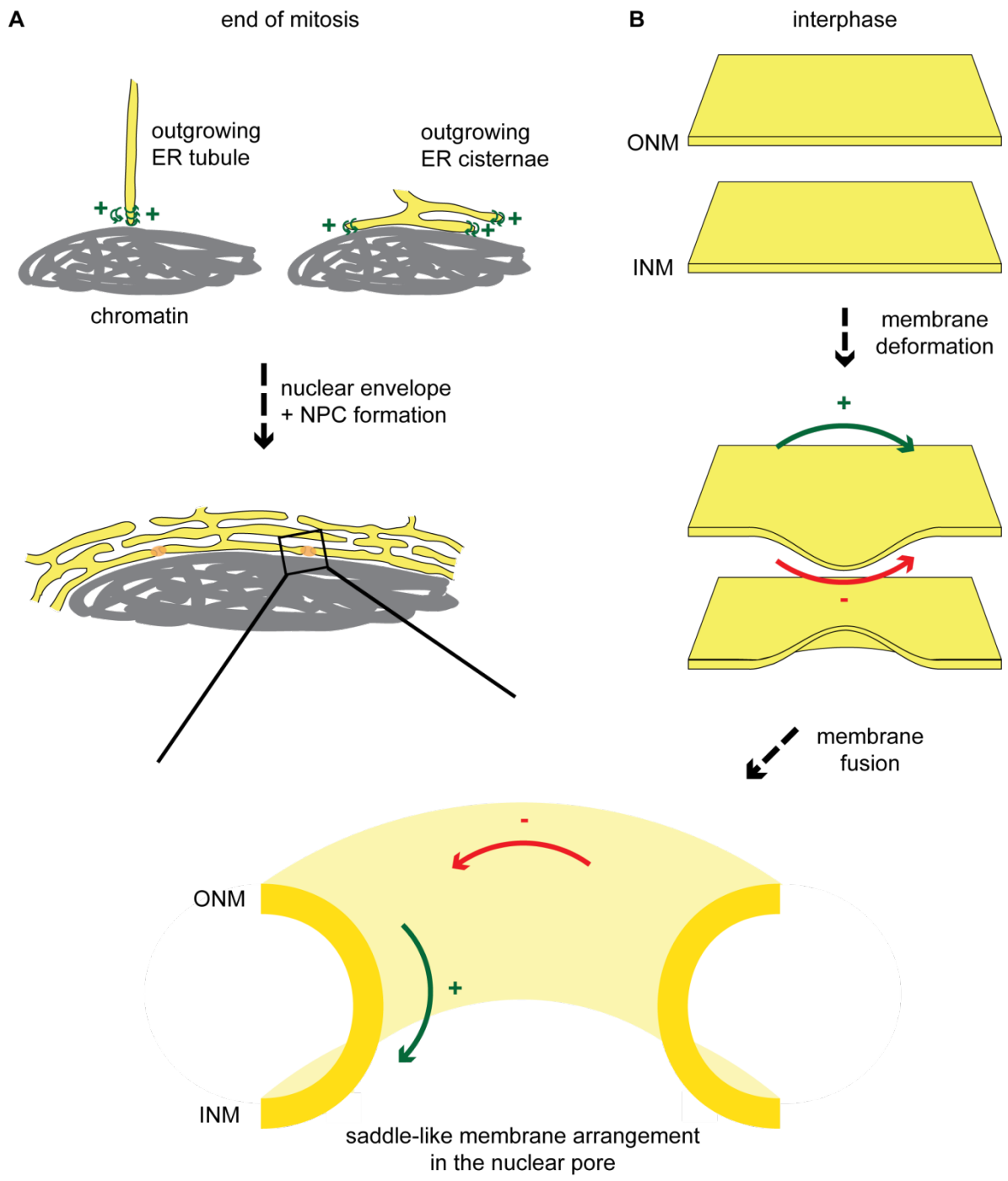

Figure 11: Membrane curvatures during NPC assembly at the end of mitosis and in interphase.

At the end of mitosis the nuclear envelope re-forms from the mitotic endoplasmic reticulum (ER) either by outgrowing tubules or from ER cisternae (A). ER tubules and the edges of ER cisternae show high positive membrane curvature (+, green arrows). Finally, a closed nuclear envelope is formed, which has a unique saddle-like shape with coexisting positive (+, green arrow) and negative curvature (-, red arrow). During interphase, NPCs are inserted into the pore membrane, which results from fusion of the inner (INM) and outer nuclear membranes (ONM, B). During initial membrane deformation and the fusion process regions of high positive (+, green arrow) and negative membrane curvature occur (-, red arrow).

6.2.4. The Ndc1-Nup53 interaction could be important during interphasic NPC assembly

Interestingly, the membrane deformation activity of Nup53 plays a crucial role during NPC assembly in interphase, when new NPCs are embedded into an intact nuclear envelope (Vollmer et al, 2012). However, the process of interphasic NPC assembly is comparatively less studied and might be substantially different from NPC formation and insertion at the end of mitosis (Doucet et al, 2010; Dultz & Ellenberg, 2010). The role of Ndc1 in this NPC assembly mode is currently unknown. Also the time-points when Ndc1 and Nup53 are recruited to the sites of interphasic NPC formation are unresolved. As Ndc1, Nup53 and their interaction are conserved in yeast (see section 6.2.1), which undergo a closed mitosis, it is likely that the interaction of Ndc1 and Nup53 also has a crucial role when NPCs are embedded into a pre-existing nuclear envelope. It was recently reported that Rtn1 and the DP1 homologue Yop1, membrane bending proteins of the ER, are important for yeast NPC assembly (Dawson et al, 2009) and their co-depletion results in NPC clustering. Rtn4, the metazoan Rtn1 homologue, seems also required for NPC assembly during interphase as antibody inhibition in the *Xenopus* system caused a block in interphasic NPC formation (Dawson et al, 2009). Collectively, these observations suggest that membrane deformation is required for NPC formation in the presence of a closed nuclear envelope. Whether the membrane deforming proteins of the ER and Nup53 act in concert or are needed during different stages of this NPC assembly mode is unknown and both scenarios are possible. It is likely that membrane deforming proteins are only transiently needed and be involved in initial steps of interphasic NPC formation. Indeed, Rtns are mainly absent from planar nuclear membranes during interphase (Kiseleva et al, 2007; Voeltz et al, 2006). During later steps in NPC assembly when the membranes are already dented towards each other (Figure 11B) they might be displaced from the nuclear envelope. Either Nup53 could functionally substitute for these proteins or if the membrane curvature does not need further deformation but instead stabilisation also other NPC components, as the Nup107/160 complex, could fulfil this scaffolding function (see section 6.2.3). Indeed, Nup133, which contains a membrane curvature sensing ALPS motif, has an important early role during interphasic NPC assembly (Doucet & Hetzer, 2010; Drin et al, 2007). Membrane curving could also be important to catalyse membrane

fusion. Yeast cells co-depleted of Rtn1 and Yop1 showed some NPC-like structures that did not fully span the pore membrane (Dawson et al, 2009). These could represent an intermediate state of NPC assembly without fusion of the INM and ONM into a pore. However, it is unknown whether the membrane bending proteins might be important for juxtaposing the two nuclear envelope membranes in order to support their fusion. Actually, if the INM and the ONM are dented towards each other in a fusion intermediate, negative curvature needs to be generated at most positions of the membrane (Antonin, 2009). Interestingly, Ndc1 can interact with both, Rtn1 and Yop1 in yeast (Casey et al, 2012). Hence, it is possible that Ndc1 plays also a regulatory role for these membrane shaping proteins. Positive curvature inducing proteins might thus be selectively inhibited by Ndc1 at regions where they would be counter-active.

It might be also envisioned that Nup53 is recruited early during interphasic NPC assembly and might be involved in the approximation of the two membranes of the nuclear envelope enabling their final fusion into a pore (Vollmer et al, 2012, Figure 11B). Ndc1 could join the assembly sites later when the nuclear membranes do not need further deformation by Nup53 and inhibit its C-terminal membrane deformation activity. The conservation of the Ndc1-Nup53 interaction in yeast suggests that Ndc1 also needs to modulate Nup53's membrane deformation activity at some time-point during interphasic assembly. This might be an interesting topic for future studies. However, the final arrangement of the pore membrane with *de novo* embedded NPCs will be identical to re-assembled NPCs with co-existing positive and negative membrane curvatures (see section 6.2.3). The Ndc1-Nup53 interaction would then allow for this saddle-like structure in interphasic NPC formation for which active membrane bending might be inhibitory.

6.3. Nup53 is a crucial factor for downstream NPC assembly and localises Nup155 to nascent pores

Nup53 was already known to be a crucial factor for metazoan NPC assembly for several years (Hawryluk-Gara et al, 2008; Rodenas et al, 2009). By detailed *in vitro* analyses its multiple roles are recently emerging to which my thesis also contributes.

As my data elucidates, Nup53 is a key factor to recruit the other Nup93 complex members via Nup155 to nascent pores during NPC assembly at the end of mitosis (Eisenhardt et al, 2013). Hence, the interaction of Nup53 and Nup155 is necessary for NPC assembly. This knowledge adds an important detail to our mechanistic understanding of the step-wise process of NPC formation and their membrane integration after cell division.

Nup155 is present in all eukaryotic supergroups and probably existed in the last eukaryotic common ancestor (DeGrasse et al, 2009; Mans et al, 2004; Neumann et al, 2010) pointing towards a fundamental role in NPC assembly and function. Both, metazoan and yeast Nup155 proteins are essential for NPC assembly (Franz et al, 2005; Kiger et al, 1999; Makio et al, 2009; Mitchell et al, 2010). In yeast and metazoans, Nup155 is part of an intricate interaction network at the pore membrane (Amlacher et al, 2011; Hawryluk-Gara et al, 2005; Makio et al, 2009; Mitchell et al, 2010; Onischenko et al, 2009; Sachdev et al, 2012; Uetz et al, 2000). The conservation of this entire set of interactions between integral membrane nucleoporins, Nup53 and Nup155 suggests also an important functional role of these interactions (Figure 12).

So far, it was unresolved how Nup155 is recruited to assembling NPCs at the end of mitosis and which of the aforementioned interactions is important for this. As the Nup155 interaction site localises close to the RRM-domain of Nup53, which is crucial for Nup53's interaction with membranes (Vollmer et al, 2012), it was impossible in previous studies to dissect the relevance of RRM-mediated membrane binding and Nup155 interaction for NPC assembly (Hawryluk-Gara et al, 2008; Rodenas et al, 2009; Vollmer et al, 2012). My studies show that Nup53 is indeed the crucial factor for Nup155 recruitment and this interaction is required for NPC formation. As the C-terminal half of Ndc1 shows also an important function for NPC formation it cannot be ruled out that the Ndc1-Nup155 interaction is also crucial for NPC assembly (Mitchell et al, 2010). Although Nup155 could also be recruited by Pom121 (Mitchell et al, 2010; Yavuz et al, 2010) it does not localise to chromatin substrates if the interaction with Nup53 is disrupted. In this case also all other members of the Nup93 complex remain absent. This shows that one important function of Nup155 is the recruitment of downstream nucleoporins in the NPC assembly process, namely Nup93, to allow for progression and completion of NPC formation. Out of all possible interactions

committed by Nup155, the interaction with Nup53 is therefore essential to ensure its correct localisation and function at nascent nuclear pores.

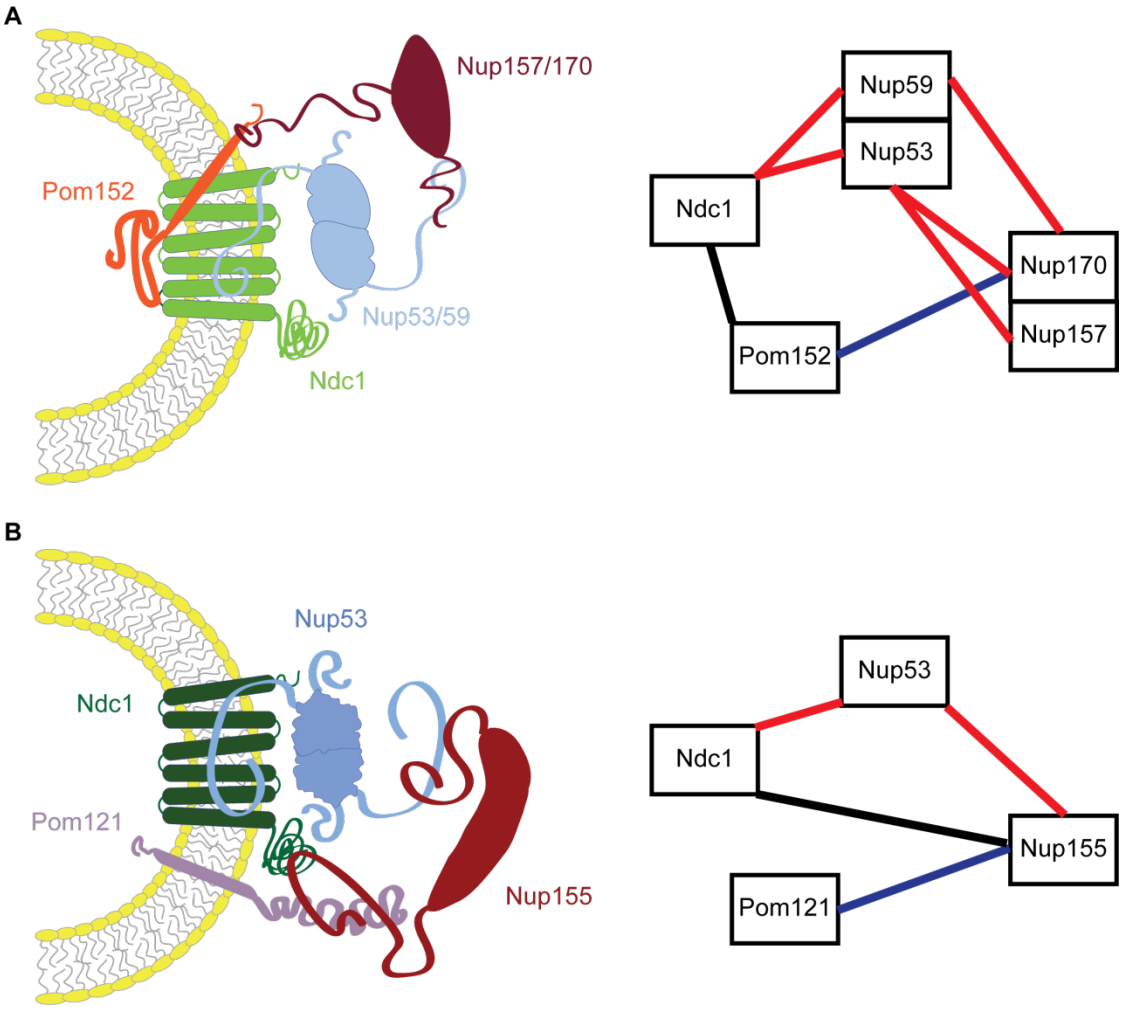

Figure 12: Conserved interaction network of integral membrane nucleoporins, Nup53 and Nup155.

A: In yeast, the two Nup155 homologues Nup157 and Nup170 (dark red) both interact with Nup53 (blue). Nup170 also interacts with Nup59, a Nup53 homologue, and the integral membrane nucleoporin Pom152 (orange). Pom152 interacts with the integral membrane nucleoporin Ndc1 (green), which also binds to Nup53 and Nup59. The red connection lines indicate conserved interactions in yeast and Xenopus. The blue line between Pom152 and Nup170 depicts an interaction similar to Pom121 and Nup155 in metazoans indirectly connecting Nup155 or its orthologue with the pore membrane although the transmembrane nucleoporins Pom121 and Pom152 are structurally not conserved.

B: In *Xenopus*, Nup155 (red) also interacts with Nup53 (blue) and two integral membrane nucleoporins, Pom121 (violet) and Ndc1 (green). Ndc1 also interacts with Nup53 as in yeast. Red lines depict conserved interactions and the blue line a functionally similar interaction to yeast indirectly connecting Nup155 with an integral membrane nucleoporin of the pore membrane.

For the sake of simplicity correct stoichiometry is ignored and only one C-terminal end of Nup53/59 is shown to interact with Ndc1 or Nup155/157/170.

6.4. The order and function of Ndc1, Nup53 and Nup155 in metazoan NPC assembly at the end of mitosis

NPC re-assembly at the end of metazoan mitosis starts on chromatin as the seeding-point for NPC formation (Rasala et al, 2008; Rotem et al, 2009; Walther et al, 2003) and progresses sequentially by the ordered recruitment of individual nucleoporins or nucleoporin subcomplexes (Bodoor et al, 1999; Dultz et al, 2008). Many individual steps of this process have been identified by live cell imaging or by *in vitro* reconstitution experiments with *Xenopus* egg extracts.

The components of the Nup93 complex are recruited after nuclear envelope precursor membranes have been retracted to the assembly sites on chromatin, where Mel28/Elys and members of the Nup107/160 complex are already present (Dultz et al, 2008, Figure 13). Nup53 is the first member of the Nup93 complex appearing at the nascent pores (Eisenhardt et al, 2013; Vollmer et al, 2012). Its recruitment depends primarily on direct membrane interaction (Vollmer et al, 2012). Ndc1, which resides in the nuclear envelope precursor membranes, seems dispensable for localising Nup53 to the assembling NPCs as Nup53 truncations incapable of the Ndc1 interaction show proper localisation to chromatin templates (Hawryluk-Gara et al, 2008; Vollmer et al, 2012). However, in the absence of Ndc1 upon depletion, Nup53 recruitment was reduced (Eisenhardt et al, 2013). Hence, Ndc1 alone is insufficient to recruit full-length Nup53 to NPC assembly sites but contributes in some way. Nup53 might initially bind to the nuclear precursor membranes via one or both of its membrane interaction sites and Ndc1 might strengthen or stabilise this interaction. Without Ndc1, Nup53 would probably tubulate the membranes resulting in a block in NPC formation (see section 6.2.3). The lack of recruitment of downstream factors could then favour the dissociation of Nup53 from the membranes. Once Nup53 is properly recruited and the interaction with Ndc1 is established, Nup155 is localised to assembling NPCs via direct interaction with Nup53 (Eisenhardt et al, 2013). Recent data indicate that this interaction is stabilised by Nup93, which associates next with the nascent pores (Sachdev et al, 2012). Nup93 is probably joining the NPC assembly sites in two distinct complexes with either Nup188 or Nup205 (Amlacher et al, 2011; Theerthagiri et al, 2010). These complexes are only recruited after the Nup53-Nup155 interaction has been established. Additional interactions of Nup155 with the transmembrane nucleoporins

Ndc1 and Pom121 (Mitchell et al, 2010; Yavuz et al, 2010) might also be required for NPC assembly progression but the role of these interactions remains unknown for now. As Nup53 is directly interacting with nuclear membranes it might shuttle Nup155 into close proximity to the membranes and therein embedded proteins supporting the establishment of Nup155's interaction network. Finally, the recruitment of the Nup93 complex is followed by recruitment of the Nup62 complex via Nup93 (Sachdev et al, 2012) and the concomitant association of Nup98 (Dultz et al, 2008). Eventually, other FG-repeat containing nucleoporins are recruited to complete NPC assembly and construct fully functional pores within the nuclear envelope.

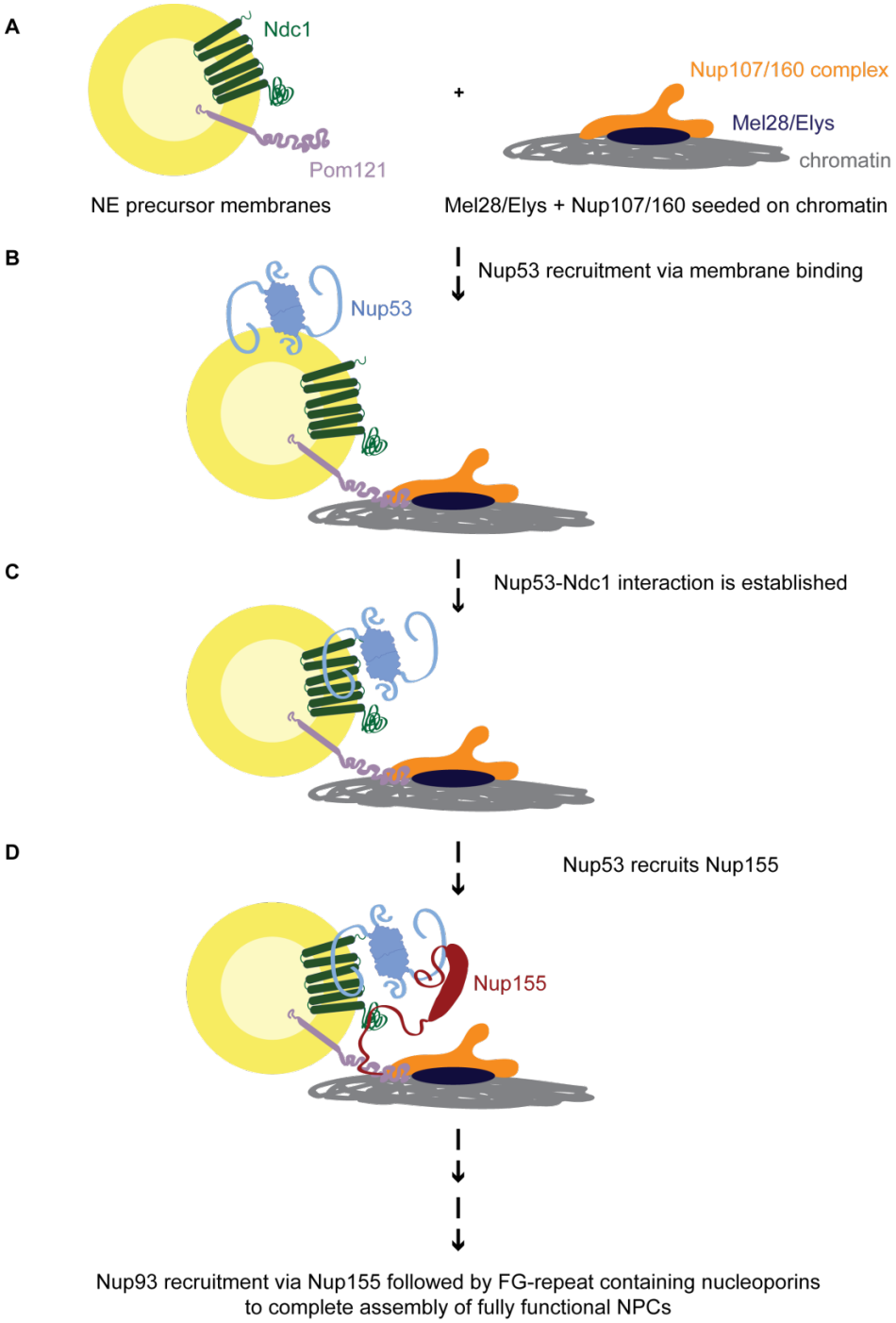

Figure 13: Ordered NPC assembly at the end of mitosis.

After nuclear envelope precursor membranes containing the transmembrane nucleoporins Ndc1 (green) and Pom121 (violet) have been recruited to chromatin, on which Mel28/Elys (dark blue) and Nup107/160 complex members (orange) are bound (A), Nup53 (blue) joins the nascent pores by direct membrane binding (B). Nup53's C-terminal end interacts with Ndc1 in the pore (C) and this interaction is required for nuclear pore complex (NPC) assembly progression. Next, Nup53 recruits Nup155 (red) to the immature NPCs (D). The Nup53-Nup155 interaction is essential to recruit Nup93 and afterwards FG-repeat containing nucleoporins, including the Nup62 complex to complete NPC assembly.

For the sake of simplicity correct stoichiometry is ignored and only one C-terminal end of the Nup53-dimer is shown to interact with Ndc1 or with Nup155.

References

Aitchison JD, Rout MP (2012) The yeast nuclear pore complex and transport through it. *Genetics* **190:** 855-883

Alber F, Dokudovskaya S, Veenhoff LM, Zhang W, Kipper J, Devos D, Suprapto A, Karni-Schmidt O, Williams R, Chait BT, Sali A, Rout MP (2007) The molecular architecture of the nuclear pore complex. *Nature* **450:** 695-701

Amlacher S, Sarges P, Flemming D, van Noort V, Kunze R, Devos DP, Arumugam M, Bork P, Hurt E (2011) Insight into structure and assembly of the nuclear pore complex by utilizing the genome of a eukaryotic thermophile. *Cell* **146:** 277-289

Amor JC, Harrison DH, Kahn RA, Ringe D (1994) Structure of the human ADP-ribosylation factor 1 complexed with GDP. *Nature* **372:** 704-708

Anderson DJ, Hetzer MW (2007) Nuclear envelope formation by chromatin-mediated reorganization of the endoplasmic reticulum. *Nat Cell Biol* **9:** 1160-1166

Anderson DJ, Hetzer MW (2008) Reshaping of the endoplasmic reticulum limits the rate for nuclear envelope formation. *J Cell Biol* **182:** 911-924

Anderson DJ, Vargas JD, Hsiao JP, Hetzer MW (2009) Recruitment of functionally distinct membrane proteins to chromatin mediates nuclear envelope formation in vivo. *J Cell Biol* **186:** 183-191

Antonin W (2009) Nuclear envelope: membrane bending for pore formation? *Curr Biol* **19:** R410-412

Antonin W, Ellenberg J, Dultz E (2008) Nuclear pore complex assembly through the cell cycle: Regulation and membrane organization. *FEBS Lett* **582:** 2004-2016

Antonin W, Franz C, Haselmann U, Antony C, Mattaj IW (2005) The integral membrane nucleoporin pom121 functionally links nuclear pore complex assembly and nuclear envelope formation. *Mol Cell* **17:** 83-92

Antonin W, Mattaj IW (2005) Nuclear pore complexes: round the bend? *Nat Cell Biol* **7:** 10-12

Antonny B, Huber I, Paris S, Chabre M, Cassel D (1997) Activation of ADP-ribosylation factor 1 GTPase-activating protein by phosphatidylcholine-derived diacylglycerols. *J Biol Chem* **272:** 30848-30851

Beck M, Forster F, Ecke M, Plitzko JM, Melchior F, Gerisch G, Baumeister W, Medalia O (2004) Nuclear pore complex structure and dynamics revealed by cryoelectron tomography. *Science* **306:** 1387-1390

Beck M, Lucic V, Forster F, Baumeister W, Medalia O (2007) Snapshots of nuclear pore complexes in action captured by cryo-electron tomography. *Nature* **449:** 611-615

Belgareh N, Rabut G, Bai SW, van Overbeek M, Beaudouin J, Daigle N, Zatsepina OV, Pasteau F, Labas V, Fromont-Racine M, Ellenberg J, Doye V (2001) An evolutionarily conserved NPC subcomplex, which redistributes in part to kinetochores in mammalian cells. *J Cell Biol* **154:** 1147-1160

Birney E, Kumar S, Krainer AR (1993) Analysis of the RNA-recognition motif and RS and RGG domains: conservation in metazoan pre-mRNA splicing factors. *Nucleic Acids Res* **21:** 5803-5816

Blow JJ, Laskey RA (1986) Initiation of DNA replication in nuclei and purified DNA by a cell-free extract of Xenopus eggs. *Cell* **47:** 577-587

Bodoor K, Shaikh S, Salina D, Raharjo WH, Bastos R, Lohka M, Burke B (1999) Sequential recruitment of NPC proteins to the nuclear periphery at the end of mitosis. *J Cell Sci* **112:** 2253-2264.

Braunagel SC, Williamson ST, Ding Q, Wu X, Summers MD (2007) Early sorting of inner nuclear membrane proteins is conserved. *Proc Natl Acad Sci U S A* **104:** 9307-9312

Brohawn SG, Leksa NC, Spear ED, Rajashankar KR, Schwartz TU (2008) Structural evidence for common ancestry of the nuclear pore complex and vesicle coats. *Science* **322:** 1369-1373

Brohawn SG, Partridge JR, Whittle JR, Schwartz TU (2009) The nuclear pore complex has entered the atomic age. *Structure* **17:** 1156-1168

Bruce Alberts AJ, Julian Lewis, Martin Raff, Keith Roberts, Peter Walter (2007) *Molecular Biology of the Cell*, 5 edn. New York: Garland Science.

Burke B (2012) It takes KASH to hitch to the SUN. *Cell* **149:** 961-963

Burke B, Stewart CL (2002) Life at the edge: the nuclear envelope and human disease. *Nat Rev Mol Cell Biol* **3:** 575-585

Casey AK, Dawson TR, Chen J, Friederichs JM, Jaspersen SL, Wente SR (2012) Integrity and function of the Saccharomyces cerevisiae spindle pole body depends on connections between the membrane proteins Ndc1, Rtn1, and Yop1. *Genetics* **192:** 441-455

Chadrin A, Hess B, San Roman M, Gatti X, Lombard B, Loew D, Barral Y, Palancade B, Doye V (2010) Pom33, a novel transmembrane nucleoporin required for proper nuclear pore complex distribution. *J Cell Biol* **189:** 795-811

Chial HJ, Rout MP, Giddings TH, Winey M (1998) Saccharomyces cerevisiae Ndc1p is a shared component of nuclear pore complexes and spindle pole bodies. *J Cell Biol* **143:** 1789-1800.

Cornell RB, Taneva SG (2006) Amphipathic helices as mediators of the membrane interaction of amphitropic proteins, and as modulators of bilayer physical properties. *Current protein & peptide science* **7:** 539-552

Cronshaw JM, Krutchinsky AN, Zhang W, Chait BT, Matunis MJ (2002) Proteomic analysis of the mammalian nuclear pore complex. *J Cell Biol* **158:** 915-927.

D'Angelo MA, Anderson DJ, Richard E, Hetzer MW (2006) Nuclear pores form de novo from both sides of the nuclear envelope. *Science* **312:** 440-443

D'Angelo MA, Hetzer MW (2006) The role of the nuclear envelope in cellular organization. *Cellular and molecular life sciences : CMLS* **63:** 316-332

Daigle N, Beaudouin J, Hartnell L, Imreh G, Hallberg E, Lippincott-Schwartz J, Ellenberg J (2001) Nuclear pore complexes form immobile networks and have a very low turnover in live mammalian cells. *J Cell Biol* **154:** 71-84.

Dauer WT, Worman HJ (2009) The nuclear envelope as a signaling node in development and disease. *Dev Cell* **17:** 626-638

Dawson TR, Lazarus MD, Hetzer MW, Wente SR (2009) ER membrane-bending proteins are necessary for de novo nuclear pore formation. *J Cell Biol* **184:** 659-675

De Souza CP, Osmani AH, Hashmi SB, Osmani SA (2004) Partial nuclear pore complex disassembly during closed mitosis in Aspergillus nidulans. *Curr Biol* **14:** 1973-1984

DeGrasse JA, DuBois KN, Devos D, Siegel TN, Sali A, Field MC, Rout MP, Chait BT (2009) Evidence for a shared nuclear pore complex architecture that is conserved from the last common eukaryotic ancestor. *Mol Cell Proteomics* **8:** 2119-2130

Denning DP, Patel SS, Uversky V, Fink AL, Rexach M (2003) Disorder in the nuclear pore complex: the FG repeat regions of nucleoporins are natively unfolded. *Proc Natl Acad Sci U S A* **100:** 2450-2455

Devos D, Dokudovskaya S, Alber F, Williams R, Chait BT, Sali A, Rout MP (2004) Components of coated vesicles and nuclear pore complexes share a common molecular architecture. *PLoS Biol* **2:** e380

Devos D, Dokudovskaya S, Williams R, Alber F, Eswar N, Chait BT, Rout MP, Sali A (2006) Simple fold composition and modular architecture of the nuclear pore complex. *Proc Natl Acad Sci U S A* **103:** 2172-2177

Doucet CM, Hetzer MW (2010) Nuclear pore biogenesis into an intact nuclear envelope. *Chromosoma* **119:** 469-477

Doucet CM, Talamas JA, Hetzer MW (2010) Cell cycle-dependent differences in nuclear pore complex assembly in metazoa. *Cell* **141:** 1030-1041

Dreger M, Bengtsson L, Schoneberg T, Otto H, Hucho F (2001) Nuclear envelope proteomics: novel integral membrane proteins of the inner nuclear membrane. *Proc Natl Acad Sci U S A* **98:** 11943-11948

Drew D, Froderberg L, Baars L, de Gier JW (2003) Assembly and overexpression of membrane proteins in Escherichia coli. *Biochim Biophys Acta* **1610:** 3-10

Drin G, Casella JF, Gautier R, Boehmer T, Schwartz TU, Antonny B (2007) A general amphipathic alpha-helical motif for sensing membrane curvature. *Nat Struct Mol Biol* **14:** 138-146

Drummond S, Ferrigno P, Lyon C, Murphy J, Goldberg M, Allen T, Smythe C, Hutchison CJ (1999) Temporal differences in the appearance of NEP-B78 and an LBR-like protein during Xenopus nuclear envelope reassembly reflect the ordered recruitment of functionally discrete vesicle types. *J Cell Biol* **144:** 225-240.

Dultz E, Ellenberg J (2010) Live imaging of single nuclear pores reveals unique assembly kinetics and mechanism in interphase. *J Cell Biol* **191:** 15-22

Dultz E, Zanin E, Wurzenberger C, Braun M, Rabut G, Sironi L, Ellenberg J (2008) Systematic kinetic analysis of mitotic dis- and reassembly of the nuclear pore in living cells. *J Cell Biol* **180:** 857-865

Eisenhardt N, Redolfi J, Antonin W. (2014) Interaction of Nup53 with Ndc1 and Nup155 is required for nuclear pore complex assembly. *J Cell Sci*. **127**: 908-21.

Ellenberg J, Siggia ED, Moreira JE, Smith CL, Presley JF, Worman HJ, Lippincott-Schwartz J (1997) Nuclear membrane dynamics and reassembly in living cells: targeting of an inner nuclear membrane protein in interphase and mitosis. *J Cell Biol* **138:** 1193-1206.

Englmeier L, Olivo JC, Mattaj IW (1999) Receptor-mediated substrate translocation through the nuclear pore complex without nucleotide triphosphate hydrolysis. *Curr Biol* **9:** 30-41.

Eytan GD (1982) Use of liposomes for reconstitution of biological functions. *Biochim Biophys Acta* **694:** 185-202

Fahrenkrog B, Hubner W, Mandinova A, Pante N, Keller W, Aebi U (2000) The yeast nucleoporin Nup53p specifically interacts with Nic96p and is directly involved in nuclear protein import. *Mol Biol Cell* **11:** 3885-3896

Feldherr CM, Akin D (1990) The permeability of the nuclear envelope in dividing and nondividing cell cultures. *J Cell Biol* **111:** 1-8

Finlay DR, Forbes DJ (1990) Reconstitution of biochemically altered nuclear pores: transport can be eliminated and restored. *Cell* **60:** 17-29

Finlay DR, Meier E, Bradley P, Horecka J, Forbes DJ (1991) A complex of nuclear pore proteins required for pore function. *J Cell Biol* **114:** 169-183

Finley KR, Berman J (2005) Microtubules in Candida albicans hyphae drive nuclear dynamics and connect cell cycle progression to morphogenesis. *Eukaryotic cell* **4:** 1697-1711

Floer M, Blobel G, Rexach M (1997) Disassembly of RanGTP-karyopherin beta complex, an intermediate in nuclear protein import. *J Biol Chem* **272:** 19538-19546

Foisner R, Gerace L (1993) Integral membrane proteins of the nuclear envelope interact with lamins and chromosomes, and binding is modulated by mitotic phosphorylation. *Cell* **73:** 1267-1279.

Franz C, Askjaer P, Antonin W, Iglesias CL, Haselmann U, Schelder M, de Marco A, Wilm M, Antony C, Mattaj IW (2005) Nup155 regulates nuclear envelope and nuclear pore complex formation in nematodes and vertebrates. *EMBO J* **24:** 3519-3531

Franz C, Walczak R, Yavuz S, Santarella R, Gentzel M, Askjaer P, Galy V, Hetzer M, Mattaj IW, Antonin W (2007) MEL-28/ELYS is required for the recruitment of nucleoporins to chromatin and postmitotic nuclear pore complex assembly. *EMBO Rep* **8:** 165-172

Frenkiel-Krispin D, Maco B, Aebi U, Medalia O (2010) Structural analysis of a metazoan nuclear pore complex reveals a fused concentric ring architecture. *J Mol Biol* **395:** 578-586

Frey S, Richter RP, Gorlich D (2006) FG-rich repeats of nuclear pore proteins form a three-dimensional meshwork with hydrogel-like properties. *Science* **314:** 815-817

Fried H, Kutay U (2003) Nucleocytoplasmic transport: taking an inventory. *Cellular and molecular life sciences : CMLS* **60:** 1659-1688

Funakoshi T, Maeshima K, Yahata K, Sugano S, Imamoto F, Imamoto N (2007) Two distinct human POM121 genes: requirement for the formation of nuclear pore complexes. *FEBS Lett* **581:** 4910-4916

Furukawa K, Pante N, Aebi U, Gerace L (1995) Cloning of a cDNA for lamina-associated polypeptide 2 (LAP2) and identification of regions that specify targeting to the nuclear envelope. *EMBO J* **14:** 1626-1636

Galy V, Antonin W, Jaedicke A, Sachse M, Santarella R, Haselmann U, Mattaj I (2008) A role for gp210 in mitotic nuclear-envelope breakdown. *J Cell Sci* **121:** 317-328

Galy V, Askjaer P, Franz C, López-Iglesias C, Mattaj IW (2006) MEL-28, a novel nuclear envelope and kinetochore protein essential for zygotic nuclear envelope assembly in C. elegans. *Curr Biol*

Galy V, Mattaj IW, Askjaer P (2003) Caenorhabditis elegans nucleoporins Nup93 and Nup205 determine the limit of nuclear pore complex size exclusion in vivo. *Mol Biol Cell* **14:** 5104-5115

Gillespie PJ, Khoudoli GA, Stewart G, Swedlow JR, Blow JJ (2007) ELYS/MEL-28 chromatin association coordinates nuclear pore complex assembly and replication licensing. *Curr Biol* **17:** 1657-1662

Goldfarb DS, Gariepy J, Schoolnik G, Kornberg RD (1986) Synthetic peptides as nuclear localization signals. *Nature* **322:** 641-644

Gorlich D, Prehn S, Laskey RA, Hartmann E (1994) Isolation of a protein that is essential for the first step of nuclear protein import. *Cell* **79:** 767-778

Gorlich D, Vogel F, Mills AD, Hartmann E, Laskey RA (1995) Distinct functions for the two importin subunits in nuclear protein import. *Nature* **377:** 246-248

Grandi P, Dang T, Pane N, Shevchenko A, Mann M, Forbes D, Hurt E (1997) Nup93, a vertebrate homologue of yeast Nic96p, forms a complex with a novel 205-kDa protein and is required for correct nuclear pore assembly. *Mol Biol Cell* **8:** 2017-2038

Grandi P, Doye V, Hurt EC (1993) Purification of NSP1 reveals complex formation with 'GLFG' nucleoporins and a novel nuclear pore protein NIC96. *EMBO J* **12:** 3061-3071

Grandi P, Schlaich N, Tekotte H, Hurt EC (1995) Functional interaction of Nic96p with a core nucleoporin complex consisting of Nsp1p, Nup49p and a novel protein Nup57p. *EMBO J* **14:** 76-87

Greber UF, Senior A, Gerace L (1990) A major glycoprotein of the nuclear pore complex is a membrane-spanning polypeptide with a large lumenal domain and a small cytoplasmic tail. *EMBO J* **9:** 1495-1502.

Guttinger S, Laurell E, Kutay U (2009) Orchestrating nuclear envelope disassembly and reassembly during mitosis. *Nat Rev Mol Cell Biol* **10:** 178-191

Guttler T, Gorlich D (2011) Ran-dependent nuclear export mediators: a structural perspective. *Embo J* **30:** 3457-3474

Handa N, Kukimoto-Niino M, Akasaka R, Kishishita S, Murayama K, Terada T, Inoue M, Kigawa T, Kose S, Imamoto N, Tanaka A, Hayashizaki Y, Shirouzu M, Yokoyama S (2006) The crystal structure of mouse Nup35 reveals atypical RNP motifs and novel homodimerization of the RRM domain. *J Mol Biol* **363:** 114-124

Haraguchi T, Koujin T, Hayakawa T, Kaneda T, Tsutsumi C, Imamoto N, Akazawa C, Sukegawa J, Yoneda Y, Hiraoka Y (2000) Live fluorescence imaging reveals early recruitment of emerin, LBR, RanBP2, and Nup153 to reforming functional nuclear envelopes. *J Cell Sci* **113 (Pt 5):** 779-794

Harel A, Orjalo AV, Vincent T, Lachish-Zalait A, Vasu S, Shah S, Zimmerman E, Elbaum M, Forbes DJ (2003) Removal of a single pore subcomplex results in vertebrate nuclei devoid of nuclear pores. *Mol Cell* **11:** 853-864.

Hase ME, Cordes VC (2003) Direct interaction with nup153 mediates binding of Tpr to the periphery of the nuclear pore complex. *Mol Biol Cell* **14:** 1923-1940

Hawryluk-Gara LA, Platani M, Santarella R, Wozniak RW, Mattaj IW (2008) Nup53 is required for nuclear envelope and nuclear pore complex assembly. *Mol Biol Cell* **19:** 1753-1762

Hawryluk-Gara LA, Shibuya EK, Wozniak RW (2005) Vertebrate Nup53 interacts with the nuclear lamina and is required for the assembly of a Nup93-containing complex. *Mol Biol Cell* **16:** 2382-2394

Heessen S, Fornerod M (2007) The inner nuclear envelope as a transcription factor resting place. *EMBO Rep* **8:** 914-919

Hetzer M, Walther TC, Mattaj IW (2005) Pushing the Envelope: Structure, Function, and Dynamics of the Nuclear Periphery. *Annu Rev Cell Dev Biol*

Hetzer MW (2010) The nuclear envelope. *Cold Spring Harb Perspect Biol* **2:** a000539

Hinshaw JE, Carragher BO, Milligan RA (1992) Architecture and design of the nuclear pore complex. *Cell* **69:** 1133-1141

Hoelz A, Debler EW, Blobel G (2011) The structure of the nuclear pore complex. *Annu Rev Biochem* **80:** 613-643

Hu J, Shibata Y, Voss C, Shemesh T, Li Z, Coughlin M, Kozlov MM, Rapoport TA, Prinz WA (2008) Membrane proteins of the endoplasmic reticulum induce high-curvature tubules. *Science* **319:** 1247-1250

Hulsmann BB, Labokha AA, Gorlich D (2012) The permeability of reconstituted nuclear pores provides direct evidence for the selective phase model. *Cell* **150:** 738-751

Isgro TA, Schulten K (2005) Binding dynamics of isolated nucleoporin repeat regions to importin-beta. *Structure* **13:** 1869-1879

Izaurralde E, Kutay U, von Kobbe C, Mattaj IW, Gorlich D (1997) The asymmetric distribution of the constituents of the Ran system is essential for transport into and out of the nucleus. *Embo J* **16:** 6535-6547

Kampmann M, Blobel G (2009) Three-dimensional structure and flexibility of a membrane-coating module of the nuclear pore complex. *Nat Struct Mol Biol* **16:** 782-788

Katta SS, Smoyer CJ, Jaspersen SL (2013) Destination: inner nuclear membrane. *Trends Cell Biol*

Kefala G, Kwiatkowski W, Esquivies L, Maslennikov I, Choe S (2007) Application of Mistic to improving the expression and membrane integration of histidine kinase receptors from Escherichia coli. *Journal of structural and functional genomics* **8:** 167-172

Keminer O, Peters R (1999) Permeability of single nuclear pores. *Biophysical journal* **77:** 217-228

Kiger AA, Gigliotti S, Fuller MT (1999) Developmental genetics of the essential Drosophila nucleoporin nup154: allelic differences due to an outward-directed promoter in the P-element 3' end. *Genetics* **153:** 799-812

Kind B, Koehler K, Lorenz M, Huebner A (2009) The nuclear pore complex protein ALADIN is anchored via NDC1 but not via POM121 and GP210 in the nuclear envelope. *Biochem Biophys Res Commun* **390:** 205-210

King MC, Lusk CP, Blobel G (2006) Karyopherin-mediated import of integral inner nuclear membrane proteins. *Nature* **442:** 1003-1007

Kiseleva E, Morozova KN, Voeltz GK, Allen TD, Goldberg MW (2007) Reticulon 4a/NogoA locates to regions of high membrane curvature and may have a role in nuclear envelope growth. *J Struct Biol* **160:** 224-235

Korfali N, Wilkie GS, Swanson SK, Srsen V, Batrakou DG, Fairley EA, Malik P, Zuleger N, Goncharevich A, de Las Heras J, Kelly DA, Kerr AR, Florens L, Schirmer EC (2010) The leukocyte nuclear envelope proteome varies with cell activation and contains novel transmembrane proteins that affect genome architecture. *Mol Cell Proteomics* **9:** 2571-2585

Kosova B, Pante N, Rollenhagen C, Hurt E (1999) Nup192p is a conserved nucleoporin with a preferential location at the inner site of the nuclear membrane. *J Biol Chem* **274:** 22646-22651

Kutay U, Hetzer MW (2008) Reorganization of the nuclear envelope during open mitosis. *Curr Opin Cell Biol* **20:** 669-677

Lau CK, Delmar VA, Forbes DJ (2006) Topology of yeast Ndc1p: predictions for the human NDC1/NET3 homologue. *The anatomical record Part A, Discoveries in molecular, cellular, and evolutionary biology* **288:** 681-694

Laurell E, Beck K, Krupina K, Theerthagiri G, Bodenmiller B, Horvath P, Aebersold R, Antonin W, Kutay U (2011) Phosphorylation of Nup98 by multiple kinases is crucial for NPC disassembly during mitotic entry. *Cell* **144:** 539-550

Liu HL, De Souza CP, Osmani AH, Osmani SA (2009) The three fungal transmembrane nuclear pore complex proteins of Aspergillus nidulans are dispensable in the presence of an intact An-Nup84-120 complex. *Mol Biol Cell* **20:** 616-630

Lohka MJ, Maller JL (1985) Induction of nuclear envelope breakdown, chromosome condensation, and spindle formation in cell-free extracts. *J Cell Biol* **101:** 518-523

Lohka MJ, Masui Y (1983) Formation in vitro of sperm pronuclei and mitotic chromosomes induced by amphibian ooplasmic components. *Science* **220:** 719-721.

Loiodice I, Alves A, Rabut G, Van Overbeek M, Ellenberg J, Sibarita JB, Doye V (2004) The entire Nup107-160 complex, including three new members, is targeted as one entity to kinetochores in mitosis. *Mol Biol Cell* **15:** 3333-3344

Lu L, Kirchhausen T (2012) Visualizing the high curvature regions of post-mitotic nascent nuclear envelope membrane. *Commun Integr Biol* **5:** 16-18

Lu L, Ladinsky MS, Kirchhausen T (2011) Formation of the postmitotic nuclear envelope from extended ER cisternae precedes nuclear pore assembly. *J Cell Biol* **194:** 425-440

Lusk CP, Makhnevych T, Marelli M, Aitchison JD, Wozniak RW (2002) Karyopherins in nuclear pore biogenesis: a role for Kap121p in the assembly of Nup53p into nuclear pore complexes. *J Cell Biol* **159:** 267-278

Lutzmann M, Kunze R, Buerer A, Aebi U, Hurt E (2002) Modular self-assembly of a Y-shaped multiprotein complex from seven nucleoporins. *EMBO J* **21:** 387-397

Lutzmann M, Kunze R, Stangl K, Stelter P, Toth KF, Bottcher B, Hurt E (2005) Reconstitution of Nup157 and Nup145N into the Nup84 complex. *J Biol Chem* **280:** 18442-18451

Macara IG (2001) Transport into and out of the nucleus. *Microbiology and molecular biology reviews : MMBR* **65:** 570-594, table of contents

Macaulay C, Forbes DJ (1996) Assembly of the nuclear pore: biochemically distinct steps revealed with NEM, GTP gamma S, and BAPTA. *J Cell Biol* **132:** 5-20

Mackinnon R (2004) Structural biology. Voltage sensor meets lipid membrane. *Science* **306:** 1304-1305

Madrid AS, Mancuso J, Cande WZ, Weis K (2006) The role of the integral membrane nucleoporins Ndc1p and Pom152p in nuclear pore complex assembly and function. *J Cell Biol* **173:** 361-371

Maimon T, Elad N, Dahan I, Medalia O (2012) The human nuclear pore complex as revealed by cryo-electron tomography. *Structure* **20:** 998-1006

Makio T, Stanton LH, Lin CC, Goldfarb DS, Weis K, Wozniak RW (2009) The nucleoporins Nup170p and Nup157p are essential for nuclear pore complex assembly. *J Cell Biol* **185:** 459-473

Mans BJ, Anantharaman V, Aravind L, Koonin EV (2004) Comparative genomics, evolution and origins of the nuclear envelope and nuclear pore complex. *Cell Cycle* **3:** 1612-1637

Mansfeld J, Guttinger S, Hawryluk-Gara LA, Pante N, Mall M, Galy V, Haselmann U, Muhlhausser P, Wozniak RW, Mattaj IW, Kutay U, Antonin W (2006) The conserved transmembrane nucleoporin NDC1 is required for nuclear pore complex assembly in vertebrate cells. *Mol Cell* **22:** 93-103

Marelli M, Aitchison JD, Wozniak RW (1998) Specific binding of the karyopherin Kap121p to a subunit of the nuclear pore complex containing Nup53p, Nup59p, and Nup170p. *J Cell Biol* **143:** 1813-1830.

Marelli M, Lusk CP, Chan H, Aitchison JD, Wozniak RW (2001) A link between the synthesis of nucleoporins and the biogenesis of the nuclear envelope. *J Cell Biol* **153:** 709-724.

Maul GG, Price JW, Lieberman MW (1971) Formation and distribution of nuclear pore complexes in interphase. *J Cell Biol* **51:** 405-418

McMahon HT, Mills IG (2004) COP and clathrin-coated vesicle budding: different pathways, common approaches. *Curr Opin Cell Biol* **16:** 379-391

Melchior F, Paschal B, Evans J, Gerace L (1993) Inhibition of nuclear protein import by nonhydrolyzable analogues of GTP and identification of the small GTPase Ran/TC4 as an essential transport factor. *J Cell Biol* **123:** 1649-1659

Miao M, Ryan KJ, Wente SR (2006) The integral membrane protein Pom34p functionally links nucleoporin subcomplexes. *Genetics* **172:** 1441-1457

Mitchell JM, Mansfeld J, Capitanio J, Kutay U, Wozniak RW (2010) Pom121 links two essential subcomplexes of the nuclear pore complex core to the membrane. *J Cell Biol* **191:** 505-521

Mohr D, Frey S, Fischer T, Guttler T, Gorlich D (2009) Characterisation of the passive permeability barrier of nuclear pore complexes. *EMBO J* **28:** 2541-2553

Moore MS, Blobel G (1993) The GTP-binding protein Ran/TC4 is required for protein import into the nucleus. *Nature* **365:** 661-663

Moroianu J, Blobel G (1995) Protein export from the nucleus requires the GTPase Ran and GTP hydrolysis. *Proc Natl Acad Sci U S A* **92:** 4318-4322

Moroianu J, Blobel G, Radu A (1996) Nuclear protein import: Ran-GTP dissociates the karyopherin alphabeta heterodimer by displacing alpha from an overlapping binding site on beta. *Proc Natl Acad Sci U S A* **93:** 7059-7062

Murray AW (1991) Cell cycle extracts. *Methods Cell Biol* **36:** 581-605

Nehrbass U, Rout MP, Maguire S, Blobel G, Wozniak RW (1996) The yeast nucleoporin Nup188p interacts genetically and physically with the core structures of the nuclear pore complex. *J Cell Biol* **133:** 1153-1162.

Neumann N, Lundin D, Poole AM (2010) Comparative genomic evidence for a complete nuclear pore complex in the last eukaryotic common ancestor. *PLoS One* **5:** e13241

Newmeyer DD, Finlay DR, Forbes DJ (1986a) In vitro transport of a fluorescent nuclear protein and exclusion of non-nuclear proteins. *J Cell Biol* **103:** 2091-2102

Newmeyer DD, Lucocq JM, Burglin TR, De Robertis EM (1986b) Assembly in vitro of nuclei active in nuclear protein transport: ATP is required for nucleoplasmin accumulation. *Embo J* **5:** 501-510

Ohba T, Schirmer EC, Nishimoto T, Gerace L (2004) Energy- and temperature-dependent transport of integral proteins to the inner nuclear membrane via the nuclear pore. *J Cell Biol* **167:** 1051-1062

Olsson M, Scheele S, Ekblom P (2004) Limited expression of nuclear pore membrane glycoprotein 210 in cell lines and tissues suggests cell-type specific nuclear pores in metazoans. *Exp Cell Res* **292:** 359-370

Onischenko E, Stanton LH, Madrid AS, Kieselbach T, Weis K (2009) Role of the Ndc1 interaction network in yeast nuclear pore complex assembly and maintenance. *J Cell Biol* **185:** 475-491

Onischenko E, Weis K (2011) Nuclear pore complex-a coat specifically tailored for the nuclear envelope. *Curr Opin Cell Biol* **23:** 293-301

Onischenko EA, Crafoord E, Hallberg E (2007) Phosphomimetic mutation of the mitotically phosphorylated serine 1880 compromises the interaction of the transmembrane nucleoporin gp210 with the nuclear pore complex. *Exp Cell Res* **313:** 2744-2751

Patel SS, Rexach MF (2008) Discovering novel interactions at the nuclear pore complex using bead halo: a rapid method for detecting molecular interactions of high and low affinity at equilibrium. *Mol Cell Proteomics* **7:** 121-131

Poteryaev D, Squirrell JM, Campbell JM, White JG, Spang A (2005) Involvement of the actin cytoskeleton and homotypic membrane fusion in ER dynamics in Caenorhabditis elegans. *Mol Biol Cell* **16:** 2139-2153

Powers MA, Macaulay C, Masiarz FR, Forbes DJ (1995) Reconstituted nuclei depleted of a vertebrate GLFG nuclear pore protein, p97, import but are defective in nuclear growth and replication. *J Cell Biol* **128:** 721-736

Prunuske AJ, Ullman KS (2006) The nuclear envelope: form and reformation. *Curr Opin Cell Biol* **18:** 108-116

Puhka M, Vihinen H, Joensuu M, Jokitalo E (2007) Endoplasmic reticulum remains continuous and undergoes sheet-to-tubule transformation during cell division in mammalian cells. *J Cell Biol* **179:** 895-909

Radu A, Blobel G, Moore MS (1995) Identification of a protein complex that is required for nuclear protein import and mediates docking of import substrate to distinct nucleoporins. *Proc Natl Acad Sci U S A* **92:** 1769-1773

Rasala BA, Orjalo AV, Shen Z, Briggs S, Forbes DJ (2006) ELYS is a dual nucleoporin/kinetochore protein required for nuclear pore assembly and proper cell division. *Proc Natl Acad Sci U S A* **103:** 17801-17806

Rasala BA, Ramos C, Harel A, Forbes DJ (2008) Capture of AT-rich chromatin by ELYS recruits POM121 and NDC1 to initiate nuclear pore assembly. *Mol Biol Cell* **19:** 3982-3996

Reddy KL, Zullo JM, Bertolino E, Singh H (2008) Transcriptional repression mediated by repositioning of genes to the nuclear lamina. *Nature* **452:** 243-247

Reichelt R, Holzenburg A, Buhle EL, Jr., Jarnik M, Engel A, Aebi U (1990) Correlation between structure and mass distribution of the nuclear pore complex and of distinct pore complex components. *J Cell Biol* **110:** 883-894.

Rexach MF (2006) A sorting importin on Sec61. *Nat Struct Mol Biol* **13:** 476-478

Ribbeck K, Gorlich D (2001) Kinetic analysis of translocation through nuclear pore complexes. *EMBO J* **20:** 1320-1330

Ribbeck K, Kutay U, Paraskeva E, Gorlich D (1999) The translocation of transportin-cargo complexes through nuclear pores is independent of both Ran and energy. *Curr Biol* **9:** 47-50

Ribeiro KC, Pereira-Neves A, Benchimol M (2002) The mitotic spindle and associated membranes in the closed mitosis of trichomonads. *Biology of the cell / under the auspices of the European Cell Biology Organization* **94:** 157-172

Rodenas E, Klerkx EP, Ayuso C, Audhya A, Askjaer P (2009) Early embryonic requirement for nucleoporin Nup35/NPP-19 in nuclear assembly. *Dev Biol* **327:** 399-409

Roosild TP, Greenwald J, Vega M, Castronovo S, Riek R, Choe S (2005) NMR structure of Mistic, a membrane-integrating protein for membrane protein expression. *Science* **307:** 1317-1321

Rotem A, Gruber R, Shorer H, Shaulov L, Klein E, Harel A (2009) Importin beta regulates the seeding of chromatin with initiation sites for nuclear pore assembly. *Mol Biol Cell* **20:** 4031-4042

Rout MP, Aitchison JD, Suprapto A, Hjertaas K, Zhao Y, Chait BT (2000) The yeast nuclear pore complex: composition, architecture, and transport mechanism. *J Cell Biol* **148:** 635-651.

Sachdev R, Sieverding C, Flotenmeyer M, Antonin W (2012) The C-terminal domain of Nup93 is essential for assembly of the structural backbone of nuclear pore complexes. *Mol Biol Cell* **23:** 740-749

Saksena S, Summers MD, Burks JK, Johnson AE, Braunagel SC (2006) Importin-alpha-16 is a translocon-associated protein involved in sorting membrane proteins to the nuclear envelope. *Nat Struct Mol Biol* **13:** 500-508

Salpingidou G, Rzepecki R, Kiseleva E, Lyon C, Lane B, Fusiek K, Golebiewska A, Drummond S, Allen T, Ellis JA, Smythe C, Goldberg MW, Hutchison CJ (2008) NEP-

A and NEP-B both contribute to nuclear pore formation in Xenopus eggs and oocytes. *J Cell Sci* **121:** 706-716

Schirmer EC, Florens L, Guan T, Yates JR, 3rd, Gerace L (2003) Nuclear membrane proteins with potential disease links found by subtractive proteomics. *Science* **301:** 1380-1382

Schirmer EC, Gerace L (2005) The nuclear membrane proteome: extending the envelope. *Trends Biochem Sci* **30:** 551-558

Schooley A, Vollmer B, Antonin W (2012) Building a nuclear envelope at the end of mitosis: coordinating membrane reorganization, nuclear pore complex assembly, and chromatin de-condensation. *Chromosoma* **121:** 539-554

Schwoebel ED, Talcott B, Cushman I, Moore MS (1998) Ran-dependent signal-mediated nuclear import does not require GTP hydrolysis by Ran. *J Biol Chem* **273:** 35170-35175

Shaulov L, Gruber R, Cohen I, Harel A (2011) A dominant-negative form of POM121 binds chromatin and disrupts the two separate modes of nuclear pore assembly. *J Cell Sci* **124:** 3822-3834

Sheehan MA, Mills AD, Sleeman AM, Laskey RA, Blow JJ (1988) Steps in the assembly of replication-competent nuclei in a cell-free system from Xenopus eggs. *J Cell Biol* **106:** 1-12

Shibata Y, Shemesh T, Prinz WA, Palazzo AF, Kozlov MM, Rapoport TA (2010) Mechanisms determining the morphology of the peripheral ER. *Cell* **143:** 774-788

Sievers F, Wilm A, Dineen D, Gibson TJ, Karplus K, Li W, Lopez R, McWilliam H, Remmert M, Soding J, Thompson JD, Higgins DG (2011) Fast, scalable generation of high-quality protein multiple sequence alignments using Clustal Omega. *Molecular systems biology* **7:** 539

Siniossoglou S, Lutzmann M, Santos-Rosa H, Leonard K, Mueller S, Aebi U, Hurt E (2000) Structure and assembly of the Nup84p complex. *J Cell Biol* **149:** 41-54

Siniossoglou S, Wimmer C, Rieger M, Doye V, Tekotte H, Weise C, Emig S, Segref A, Hurt EC (1996) A novel complex of nucleoporins, which includes Sec13p and a Sec13p homolog, is essential for normal nuclear pores. *Cell* **84:** 265-275

Soderqvist H, Hallberg E (1994) The large C-terminal region of the integral pore membrane protein, POM121, is facing the nuclear pore complex. *Eur J Cell Biol* **64:** 186-191.

Soullam B, Worman HJ (1993) The amino-terminal domain of the lamin B receptor is a nuclear envelope targeting signal. *J Cell Biol* **120:** 1093-1100

Soullam B, Worman HJ (1995) Signals and structural features involved in integral membrane protein targeting to the inner nuclear membrane. *J Cell Biol* **130:** 15-27

Stagg SM, LaPointe P, Balch WE (2007) Structural design of cage and coat scaffolds that direct membrane traffic. *Curr Opin Struct Biol* **17:** 221-228

Starr DA, Fridolfsson HN (2010) Interactions between nuclei and the cytoskeleton are mediated by SUN-KASH nuclear-envelope bridges. *Annu Rev Cell Dev Biol* **26:** 421-444

Stavru F, Hulsmann BB, Spang A, Hartmann E, Cordes VC, Gorlich D (2006) NDC1: a crucial membrane-integral nucleoporin of metazoan nuclear pore complexes. *J Cell Biol* **173:** 509-519

Stewart M, Baker RP, Bayliss R, Clayton L, Grant RP, Littlewood T, Matsuura Y (2001) Molecular mechanism of translocation through nuclear pore complexes during nuclear protein import. *FEBS Lett* **498:** 145-149

Strawn LA, Shen T, Shulga N, Goldfarb DS, Wente SR (2004) Minimal nuclear pore complexes define FG repeat domains essential for transport. *Nat Cell Biol* **6:** 197-206

Strom AC, Weis K (2001) Importin-beta-like nuclear transport receptors. *Genome biology* **2:** REVIEWS3008

Talamas JA, Hetzer MW (2011) POM121 and Sun1 play a role in early steps of interphase NPC assembly. *J Cell Biol* **194:** 27-37

Tcheperegine SE, Marelli M, Wozniak RW (1999) Topology and functional domains of the yeast pore membrane protein Pom152p. *J Biol Chem* **274:** 5252-5258.

Terasaki M, Shemesh T, Kasthuri N, Klemm RW, Schalek R, Hayworth KJ, Hand AR, Yankova M, Huber G, Lichtman JW, Rapoport TA, Kozlov MM (2013) Stacked endoplasmic reticulum sheets are connected by helicoidal membrane motifs. *Cell* **154:** 285-296

Terry LJ, Shows EB, Wente SR (2007) Crossing the nuclear envelope: hierarchical regulation of nucleocytoplasmic transport. *Science* **318:** 1412-1416

Theerthagiri G, Eisenhardt N, Schwarz H, Antonin W (2010) The nucleoporin Nup188 controls passage of membrane proteins across the nuclear pore complex. *J Cell Biol* **189:** 1129-1142

Theisen U, Straube A, Steinberg G (2008) Dynamic Rearrangement of Nucleoporins During Fungal "Open" Mitosis. *Mol Biol Cell*

Turgay Y, Ungricht R, Rothballer A, Kiss A, Csucs G, Horvath P, Kutay U (2010) A classical NLS and the SUN domain contribute to the targeting of SUN2 to the inner nuclear membrane. *EMBO J* **29:** 2262-2275

Uetz P, Giot L, Cagney G, Mansfield TA, Judson RS, Knight JR, Lockshon D, Narayan V, Srinivasan M, Pochart P, Qureshi-Emili A, Li Y, Godwin B, Conover D, Kalbfleisch T, Vijayadamodar G, Yang M, Johnston M, Fields S, Rothberg JM (2000) A comprehensive analysis of protein-protein interactions in Saccharomyces cerevisiae. *Nature* **403:** 623-627

Ulbert S, Platani M, Boue S, Mattaj IW (2006) Direct membrane protein-DNA interactions required early in nuclear envelope assembly. *J Cell Biol* **173:** 469-476

Unwin N (2005) Refined structure of the nicotinic acetylcholine receptor at 4A resolution. *J Mol Biol* **346:** 967-989

Vasu S, Shah S, Orjalo A, Park M, Fischer WH, Forbes DJ (2001) Novel vertebrate nucleoporins Nup133 and Nup160 play a role in mRNA export. *J Cell Biol* **155:** 339-354

Vigers GP, Lohka MJ (1991) A distinct vesicle population targets membranes and pore complexes to the nuclear envelope in Xenopus eggs. *J Cell Biol* **112:** 545-556.

Voeltz GK, Prinz WA (2007) Sheets, ribbons and tubules - how organelles get their shape. *Nat Rev Mol Cell Biol* **8:** 258-264

Voeltz GK, Prinz WA, Shibata Y, Rist JM, Rapoport TA (2006) A class of membrane proteins shaping the tubular endoplasmic reticulum. *Cell* **124:** 573-586

Vollmer B, Schooley A, Sachdev R, Eisenhardt N, Schneider AM, Sieverding C, Madlung J, Gerken U, Macek B, Antonin W (2012) Dimerization and direct membrane interaction of Nup53 contribute to nuclear pore complex assembly. *EMBO J* **31:** 4072-4084

Walther TC, Alves A, Pickersgill H, Loiodice I, Hetzer M, Galy V, Hulsmann BB, Kocher T, Wilm M, Allen T, Mattaj IW, Doye V (2003) The conserved Nup107-160 complex is critical for nuclear pore complex assembly. *Cell* **113:** 195-206.

Walther TC, Fornerod M, Pickersgill H, Goldberg M, Allen TD, Mattaj IW (2001) The nucleoporin Nup153 is required for nuclear pore basket formation, nuclear pore complex anchoring and import of a subset of nuclear proteins. *EMBO J* **20:** 5703-5714.

Walther TC, Pickersgill HS, Cordes VC, Goldberg MW, Allen TD, Mattaj IW, Fornerod M (2002) The cytoplasmic filaments of the nuclear pore complex are dispensable for selective nuclear protein import. *J Cell Biol* **158:** 63-77.

Waterhouse AM, Procter JB, Martin DM, Clamp M, Barton GJ (2009) Jalview Version 2--a multiple sequence alignment editor and analysis workbench. *Bioinformatics (Oxford, England)* **25:** 1189-1191

Watson ML (1955) The nuclear envelope; its structure and relation to cytoplasmic membranes. *The Journal of biophysical and biochemical cytology* **1:** 257-270

Wente SR, Rout MP (2010) The nuclear pore complex and nuclear transport. *Cold Spring Harb Perspect Biol* **2:** a000562

West RR, Vaisberg EV, Ding R, Nurse P, McIntosh JR (1998) cut11(+): A gene required for cell cycle-dependent spindle pole body anchoring in the nuclear envelope and bipolar spindle formation in Schizosaccharomyces pombe. *Mol Biol Cell* **9:** 2839-2855

Wilkie GS, Korfali N, Swanson SK, Malik P, Srsen V, Batrakou DG, de las Heras J, Zuleger N, Kerr AR, Florens L, Schirmer EC (2011) Several novel nuclear envelope transmembrane proteins identified in skeletal muscle have cytoskeletal associations. *Mol Cell Proteomics* **10:** M110 003129

Wilson KL, Newport J (1988) A trypsin-sensitive receptor on membrane vesicles is required for nuclear envelope formation in vitro. *J Cell Biol* **107:** 57-68.

Winey M, Hoyt MA, Chan C, Goetsch L, Botstein D, Byers B (1993) NDC1: a nuclear periphery component required for yeast spindle pole body duplication. *J Cell Biol* **122:** 743-751.

Winey M, Yarar D, Giddings TH, Jr., Mastronarde DN (1997) Nuclear pore complex number and distribution throughout the Saccharomyces cerevisiae cell cycle by

three-dimensional reconstruction from electron micrographs of nuclear envelopes. *Mol Biol Cell* **8:** 2119-2132

Worman HJ, Courvalin JC (2000) The inner nuclear membrane. *J Membr Biol* **177:** 1-11.

Wozniak RW, Bartnik E, Blobel G (1989) Primary structure analysis of an integral membrane glycoprotein of the nuclear pore. *J Cell Biol* **108:** 2083-2092.

Wozniak RW, Blobel G (1992) The single transmembrane segment of gp210 is sufficient for sorting to the pore membrane domain of the nuclear envelope. *J Cell Biol* **119:** 1441-1449.

Wozniak RW, Blobel G, Rout MP (1994) POM152 is an integral protein of the pore membrane domain of the yeast nuclear envelope. *J Cell Biol* **125:** 31-42.

Yamazumi Y, Kamiya A, Nishida A, Nishihara A, Iemura S, Natsume T, Akiyama T (2009) The transmembrane nucleoporin NDC1 is required for targeting of ALADIN to nuclear pore complexes. *Biochem Biophys Res Commun* **389:** 100-104

Yang L, Guan T, Gerace L (1997) Integral membrane proteins of the nuclear envelope are dispersed throughout the endoplasmic reticulum during mitosis. *J Cell Biol* **137:** 1199-1210.

Yang Q, Rout MP, Akey CW (1998) Three-dimensional architecture of the isolated yeast nuclear pore complex: functional and evolutionary implications. *Mol Cell* **1:** 223-234

Yavuz S, Santarella-Mellwig R, Koch B, Jaedicke A, Mattaj IW, Antonin W (2010) NLS-mediated NPC functions of the nucleoporin Pom121. *FEBS Lett* **584:** 3292-3298

Zuleger N, Kerr AR, Schirmer EC (2012) Many mechanisms, one entrance: membrane protein translocation into the nucleus. *Cellular and molecular life sciences : CMLS* **69:** 2205-2216

Abbreviations list

µm	micro meter
3D	three dimensional
A. nidulans	*Aspergillus nidulans*
ALPS	amphipathic lipid packing sensor
B. subtilis	*Bacillus subtilis*
C. elegans	*Caenorhabditis elegans*
D. discoideum	*Dictyostelium discoideum*
D. melanogaster	*Drosophila melanogaster*
D. rerio	*Danio rerio*
DAPI	4′,6-diamidino-2-phenylindole
$DiIC_{18}$	1,1'-dioctadecyl-3,3,3',3'-tetramethylindocarbocyanine perchlorate
DNA	desoxyribonucleic acid
E. coli	*Escherichia coli*
e.g.	*exempli gratia* (latin); for example
ER	endoplasmic reticulum
FG	phenylalanine glycine dipeptide
GST	glutathione S-transferase
H. sapiens	*Homo sapiens*
i.e.	*id est* (latin); that is
IF	intermediate filament
INM	inner nuclear membrane
kDa	kilo dalton
MBS	membrane binding site
MDa	Mega dalton
min	minute
MISTIC	membrane-integrating sequence for translation of integral membrane protein constructs
N. crassa	*Neurospora crassa*
NEBD	nuclear envelope break-down
NES	nuclear export sequence

NLS	nuclear localisation signal
nm	nano meter
NPC	Nuclear pore complex
Nup	nucleoporin
ONM	outer nuclear membrane
RNA	ribonucleic acid
RRM	RNA-recognition motif
Rtn	reticulon
S. cerevisiae	*Saccharomyces cerevisiae*
TEM	transmission electron microscopy
TEV	tobacco etch virus
X. laevis	*Xenopus laevis*
Xenopus	*Xenopus laevis*

Appendix

Original published articles and submitted pre-print manuscripts, which are included in this thesis.

Published June 21, 2010

The nucleoporin Nup188 controls passage of membrane proteins across the nuclear pore complex

Gandhi Theerthagiri,[1] Nathalie Eisenhardt,[1] Heinz Schwarz,[2] and Wolfram Antonin[1]

[1]Friedrich Miescher Laboratory of the Max Planck Society and [2]Max Planck Institute for Developmental Biology, Max Planck Campus Tübingen, 72076 Tübingen, Germany

All transport across the nuclear envelope (NE) is mediated by nuclear pore complexes (NPCs). Despite their enormous size, ~60 MD in vertebrates, they are comprised of only ~30 distinct proteins (nucleoporins or Nups), many of which form subcomplexes that act as building blocks for NPC assembly. One of these evolutionarily conserved subcomplexes, the Nup93 complex, is a major structural component linking the NPC to the membranes of the NE. Using in vitro nuclear assembly assays, we show that two components of the Nup93 complex, Nup188 and Nup205, are dispensable for NPC formation. However, nuclei lacking Nup188 increase in size by several fold compared with wild type. We demonstrate that this phenotype is caused by an accelerated translocation of integral membrane proteins through NPCs, suggesting that Nup188 confines the passage of membrane proteins and is thus crucial for the homeostasis of the different nuclear membranes.

Introduction

The defining attribute of eukaryotes is the compartmentalization of genetic material inside the cell's nucleus. The physical boundary of the nuclear envelope (NE) has allowed eukaryotic cells to separate transcription and translation both spatially and temporally to achieve a level of regulatory complexity unprecedented in prokaryotes. Two lipid bilayers form the NE, the outer nuclear membrane (ONM) and the inner nuclear membrane (INM; for review see Hetzer et al., 2005). The ONM is continuous with the ER and is thought to have a rather similar protein composition (Mattaj, 2004; Lusk et al., 2007). The INM is characterized by a set of integral membrane proteins, although little is currently known as to how this specific protein composition is established and maintained (Mattaj, 2004; Zuleger et al., 2008).

Nuclear pore complexes (NPCs) are incorporated into the NE at sites where the INM and the ONM are fused. They function as gatekeepers of the nucleus, performing the essential cellular role of mediating an enormous exchange of proteins, nucleic acids, and other factors between the nucleoplasm and the cytoplasm. Transport of soluble factors has attracted much interest in previous decades: ions and small metabolites can diffuse through the NPCs; however, molecules >2.5 nm in radius (Mohr et al., 2009) are actively translocated by a large family of transport receptors (for reviews see Weis, 2003; Cook et al., 2007).

In addition to soluble cargoes, membrane-anchored proteins must also reach the nuclear interior. In the interphasic cell, passage through the NPC via the facing pore membrane is the most likely mechanism by which this could occur (Ohba et al., 2004). Transmembrane proteins of the NE are thought to be synthesized in the ER. They might reach the ONM and the cytoplasmic portion of the NPC by diffusion, although the existence of a directed transport mechanism cannot currently be ruled out. As INM proteins pass along the pore membrane, both transmembrane segments and hydrophilic domains encounter elements of the NPC. A recent study in mammalian cells has demonstrated that transport of integral membrane proteins to the INM is energy dependent (Ohba et al., 2004), and in budding yeast, INM targeting has been found to require transport receptors (King et al., 2006).

NPCs are huge assemblies of ~45 MD in budding yeast and 60 MD in vertebrates (for review see Brohawn et al., 2008). They are formed by about 30 different nuclear pore proteins

Correspondence to Wolfram Antonin: wolfram.antonin@tuebingen.mpg.de

Abbreviations used in this paper: INM, inner nuclear membrane; LBR, lamin B receptor; MISTIC, membrane-integrating sequence for translation of integral membrane protein constructs; NE, nuclear envelope; NPC, nuclear pore complex; ONM, outer nuclear membrane; TEV, tobacco etch virus.

© 2010 Theerthagiri et al. This article is distributed under the terms of an Attribution–Noncommercial–Share Alike–No Mirror Sites license for the first six months after the publication date (see http://www.rupress.org/terms). After six months it is available under a Creative Commons License (Attribution–Noncommercial–Share Alike 3.0 Unported license, as described at http://creativecommons.org/licenses/by-nc-sa/3.0/).

Supplemental Material can be found at:
http://jcb.rupress.org/content/suppl/2010/06/16/jcb.200912045.DC1.html

The Rockefeller University Press $30.00
J. Cell Biol. Vol. 189 No. 7 1129–1142
www.jcb.org/cgi/doi/10.1083/jcb.200912045

THE JOURNAL OF CELL BIOLOGY

Downloaded from jcb.rupress.org on December 5, 2013

Published June 21, 2010

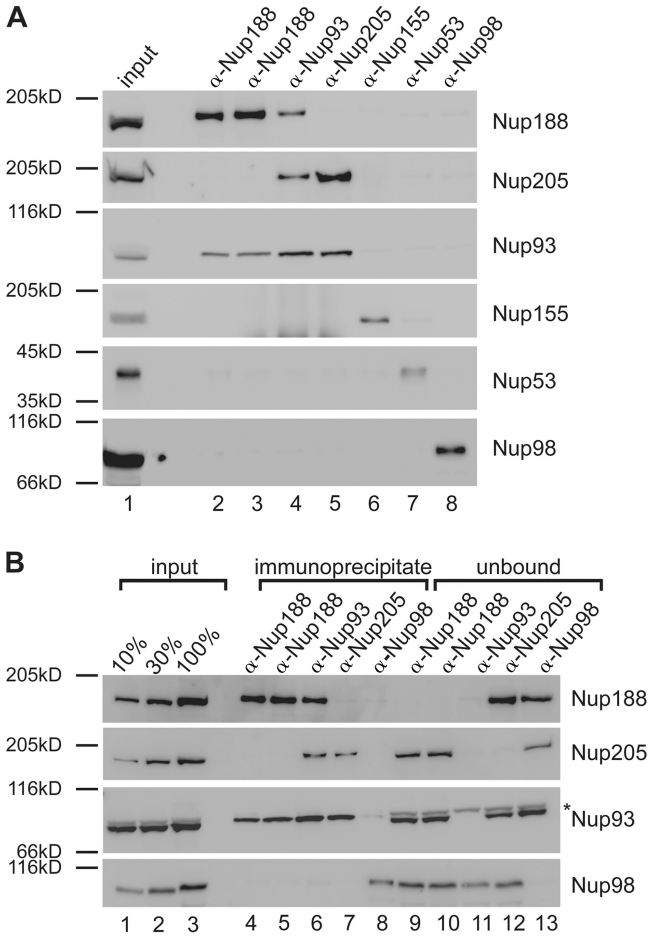

Figure 1. **Nup93 forms two distinct complexes.** (A) Immunoprecipitations were performed from *Xenopus* egg cytosol with antibodies against Nup188 (two antibodies raised in different rabbits), Nup93, Nup205, Nup155, and Nup53 and, as a control, Nup98. The indicated proteins were identified by Western blotting with the respective antisera. 10% of starting material (input) was loaded on the left. (B) Quantitative immunoprecipitations were performed from limited amounts of *Xenopus* egg cytosol with antibodies against Nup188, Nup93, and Nup205 and, as a control, Nup98. Immunoprecipitates and unbound material as well as 10, 30, and 100% of the starting material (input) were analyzed by Western blotting. The Nup93 antibody also recognized a cross-reactivity (asterisk) in the starting and unbound material migrating slightly slower.

referred to as nucleoporins or Nups. Although most, if not all, nucleoporins have now been identified, it is not understood how the individual nucleoporins interact to form this large complex (Antonin et al., 2008; D'Angelo and Hetzer, 2008).

The majority of nucleoporins are organized in discrete subcomplexes each present in multiple copies in the NPC. The best characterized of these is the heptameric Nup84 complex in yeast and the vertebrate counterpart, the nonameric Nup107–Nup160 complex, which is essential for NPC assembly and one of the major structural components of the pore (Fabre and Hurt, 1997; Boehmer et al., 2003; Galy et al., 2003; Harel et al., 2003; Walther et al., 2003). The second major structural unit of the NPC is the Nup93 subcomplex in vertebrates or the Nic96 complex in yeast. In vertebrates, it is comprised of five nucleoporins: Nup205, Nup188, Nup155, Nup93, and Nup53. Both Nup155 and Nup53 have been found to be essential for NE and NPC assembly (Franz et al., 2005; Hawryluk-Gara et al., 2008), and loss of the two budding yeast Nup155 homologues Nup170p and Nup157p blocks NPC assembly (Makio et al., 2009). Interestingly, Nup170p and Nup157p bind to Nup53p and Nup59p, which in turn associate, like the corresponding Nup53 in vertebrates, with the transmembrane nucleoporin Ndc1p (Mansfeld et al., 2006; Onischenko et al., 2007), potentially anchoring the NPC in the membrane of the NE. In vertebrates, the three remaining nucleoporins Nup205, Nup188, and Nup93 are thought to exist in a complex (Meier et al., 1995). Immunodepletion of Nup93 from *Xenopus laevis* extracts followed by in vitro nuclear assembly reactions resulted in nuclei with reduced NPC staining, which suggests that NPC formation is impaired in the absence of Nup93 (Zabel et al., 1996). Similarly, the budding yeast Nup93 homologue Nic96p is required for NPC formation and interacts with both Nup188p and Nup192 (Nehrbass et al., 1996; Zabel et al., 1996; Gomez-Ospina et al., 2000), which in metazoans correspond to Nup188 and Nup205, respectively.

In this study, we characterize vertebrate Nup188 and Nup205. We show that both interact with Nup93 but not with each other and form two distinct complexes that can be functionally distinguished. Depletion of the Nup188–Nup93 complex from *Xenopus* egg extracts produces in vitro assembled nuclei that increase several fold in size compared with control nuclei and that contain NPCs, which allow an elevated flow of INM proteins across the pore membrane. This suggests that Nup188–Nup93 can restrict the passage of membrane proteins from the ONM to the INM and is thus an important factor in the establishment of these two membrane subcompartments of the NE.

Results

Nup93 is part of two different complexes

To understand the protein interaction network of the Nup93 complex, we performed immunoprecipitations using antibodies against each of the five members of the complex from the cytosol of *Xenopus* egg extracts (Fig. 1 A). Antibodies against Nup53 and Nup155 precipitated the respective antigens but not major proportions of other members of the Nup93 complex (Fig. 1 A, lane 6 and 7), as observed previously (Franz et al., 2005; Hawryluk-Gara et al., 2008). Unexpectedly, the three remaining members of the complex did not form a trimeric complex: antibodies against Nup188 from two different rabbits coprecipitated Nup93 but not Nup205 (Fig. 1 A, lane 2 and 3), and antibodies against Nup205 precipitated Nup93 but not Nup188 (Fig. 1 A, lane 5). Consistent with this, antibodies against Nup93 coprecipitated both Nup188 and Nup205 (Fig. 1 A, lane 4). As a negative control, no interactions were seen between Nup98 and Nup205, Nup188, Nup155, Nup93 or Nup53.

To exclude the possibility that the lack of interaction is caused by precipitating only a subpopulation of Nup188 or Nup205, we performed the experiment in a quantitative manner (Fig. 1 B). Even when all Nup188 was immunoprecipitated and therefore removed from the unbound (Fig. 1 B, lane 9 and 10), Nup205 was not detected in the precipitate (Fig. 1 B, lane 4 and 5) and vice versa (Fig. 1 B, lane 7 and 12). Both Nup188 and Nup205 immunoprecipitated ~45% of Nup93 (Fig. S1).

Downloaded from jcb.rupress.org on December 5, 2013

Published June 21, 2010

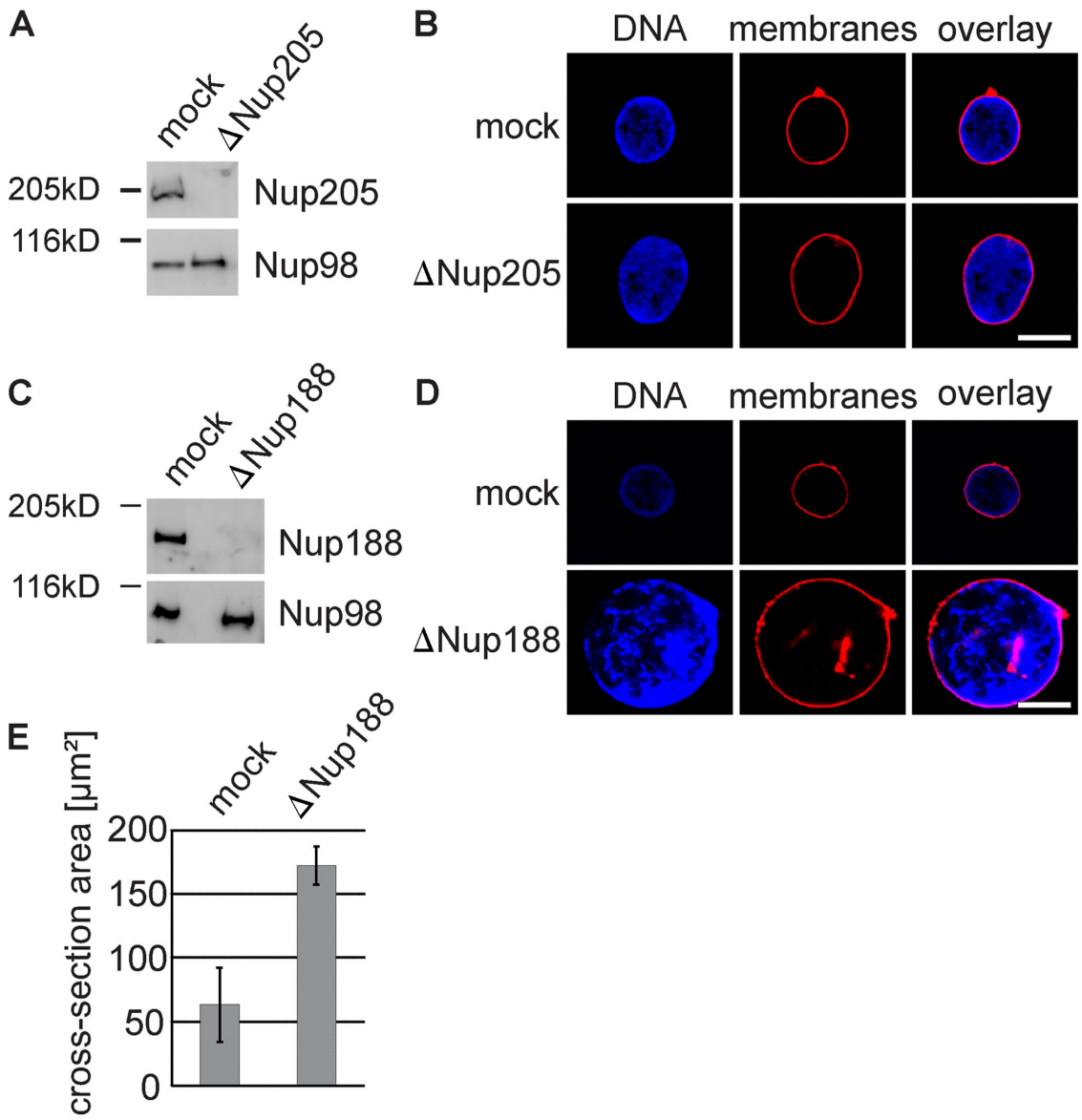

Figure 2. **Removal of Nup188–Nup93 enlarges nuclei.** (A and C) Western blot analysis of mock- and Nup205–Nup93 (A)- or Nup188–Nup93 (C)-depleted extracts. (B and D) Nuclei were assembled in mock- and Nup205–Nup93 (B)- or Nup188–Nup93 (D)-depleted extracts for 90 min, fixed with 4% PFA and 0.5% glutaraldehyde, and analyzed for chromatin and membrane staining (blue, DAPI; red, DiIC18). (E) Quantitation of the cross-sectional area of mock- and Nup188–Nup93-depleted nuclei of experiments performed as in D. More than 100 randomly chosen chromatin substrates were counted per reaction. The mean of three independent experiments is shown, and error bars represent the total variation. Bars, 20 μm.

These data indicate that Nup93 forms two distinct complexes in *Xenopus* egg extracts of approximate equal abundance, one with Nup188 and one with Nup205.

Nuclei lacking Nup188–Nup93 enlarge in size

To understand the functional significance of the two Nup93 complexes for NPC assembly and function, we depleted them separately from *Xenopus* egg extracts using antibodies specific for Nup205 or Nup188. Extracts were efficiently depleted of the respective Nup93 complexes, as determined by Western blotting (Fig. 2, A and C) and immunofluorescence (Fig. 3 A and Fig. S2 A). Nuclei formed in extracts depleted of the Nup205–Nup93 complex for 90 min were normal in appearance, as visualized by the membrane and chromatin stain (Fig. 2 B), and contained NPCs (Fig. S2 A), as determined by mAb414 staining, which recognizes FG repeat–containing nucleoporins, and with Nup93, Nup188, Nup53, and Nup155, the other members of the Nup93 complex (Fig. S2 B). In contrast, nuclei lacking Nup188–Nup93 were much larger than control nuclei (Fig. 2, D and E). These nuclei also contained NPCs (Fig. 3 A), as shown by mAb414 immunofluorescence. We found threefold more NPCs on Nup188–Nup93-depleted (18,480 ± 4,224 NPCs per nucleus) compared with control nuclei (6,137 ± 1,080; see Fig. 7 B). However, the NPC density per membrane area remained approximately constant (8.5 ± 1.2 NPCs/μm^2 in Nup188–Nup93 vs. 9.1 ± 1.2 NPCs/μm^2 in mock depletion). The NPCs contained Nup93 as well as Nup205, Nup53, and Nup155 (Fig. 3 B). Except for their increased size, Nup188–Nup93-depleted nuclei did not exhibit morphological alterations of the nuclear

Downloaded from jcb.rupress.org on December 5, 2013

Published June 21, 2010

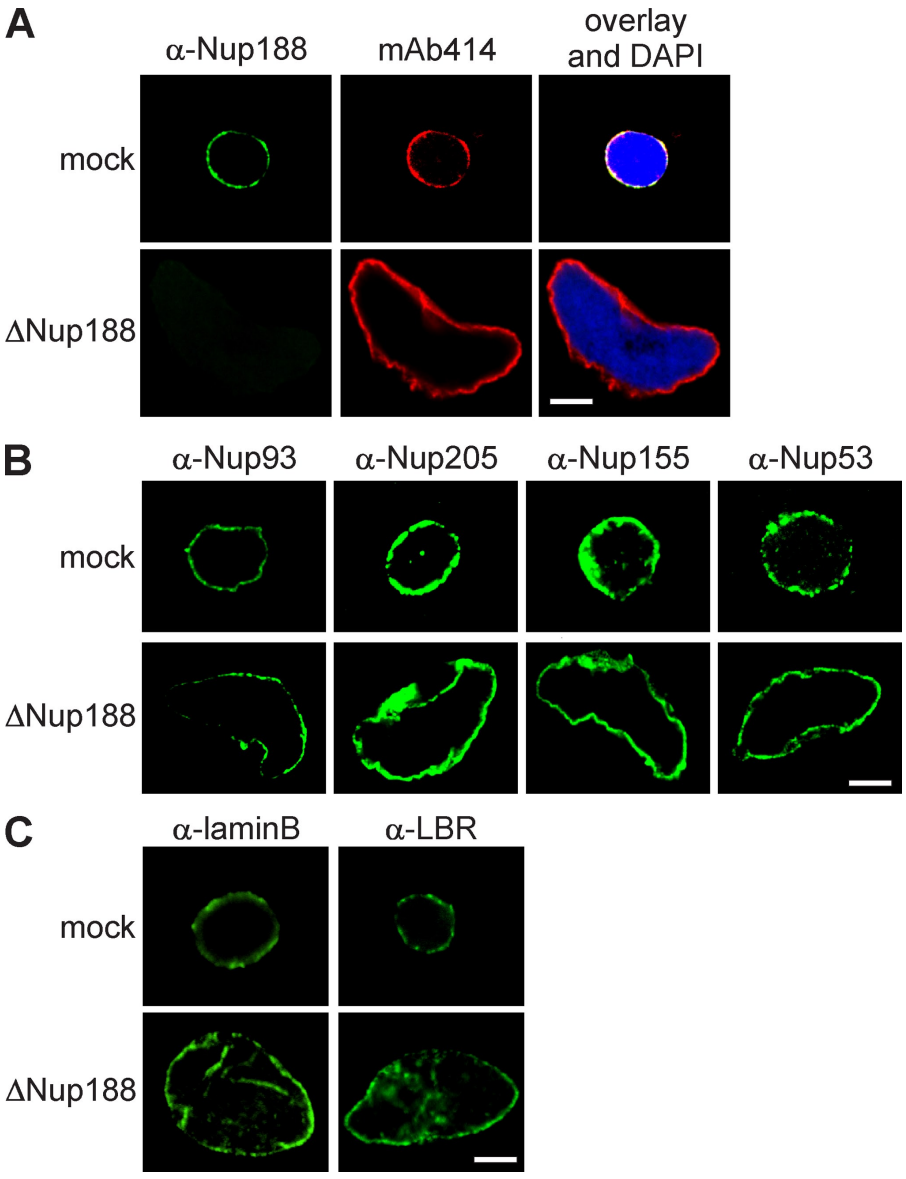

Figure 3. **Nup188–Nup93-depleted nuclei contain NPCs and INM proteins.** (A) Nuclei were assembled in mock- or Nup188–Nup93-depleted extracts for 90 min, fixed with 4% PFA, and analyzed with Nup188-specific antibodies (green) or the monoclonal antibody mAb414, which recognizes FG-repeat nucleoporins (red). Chromatin is stained with DAPI. (B and C) Samples were prepared as in A and analyzed by immunofluorescence with the indicated antibodies. Bars, 20 µm.

membranes or NPCs (Fig. S2 C), as determined by transmission electron microscopy. Also, marker proteins like B-type lamins and lamin B receptor (LBR) localized to the INM (Fig. 3 C). In a time course, chromatin substrates in mock- and Nup188–Nup93-depleted extracts were undistinguishable until a closed NE was formed at 50 min, after which Nup188–Nup93-depleted nuclei grew rapidly in size (Fig. S3). It should be noted that control nuclei also grow after having formed a closed NE as long as reentry into mitosis is blocked; however, they do this at a significantly slower rate.

Nup188–Nup93-depleted nuclei have normal nuclear functions

Given that Nup188–Nup93-depleted nuclei grow to an increased size after a closed NE is formed, we sought to determine which nuclear function is responsible for the observed phenotype. Upon nuclear assembly in *Xenopus* egg extracts, DNA can undergo one round of replication. Replication licensing ensures that replication happens exactly once during each round of the cell cycle (Blow and Sleeman, 1990). We wanted to know whether Nup188–Nup93 depletion impairs replication licensing, causing more than one round of DNA replication, which would in turn lead to increased DNA content in the nuclei. To test this idea, we assembled nuclei in mock- and Nup188–Nup93-depleted extracts in the presence of 16 µM of the DNA polymerase inhibitor aphidicolin. These conditions blocked DNA replication, as confirmed by the failure of DNA to incorporate fluorescently labeled nucleotides (Fig. 4 A). When DNA replication was blocked, the size of Nup188–Nup93-depleted nuclei still enlarged, indicating that the volume increase is not caused by a higher DNA content.

NPCs constitute a diffusion barrier between the cytoplasm and the nucleoplasm for substances >30 kD (Mohr et al., 2009), which can be translocated only by signal-mediated transport. We were wondering whether depletion of Nup188–Nup93 would impair this diffusion barrier, causing an uncontrolled accumulation of material in the nucleus and in turn lead to the observed size increase. Indeed, the yeast homologue Nup188p

Downloaded from jcb.rupress.org on December 5, 2013

Published June 21, 2010

was shown to be important for the diffusion barrier (Shulga et al., 2000). To test the integrity of the diffusion barrier of the NPC, we added fluorescently labeled dextrans of different but defined sizes to in vitro assembled nuclei that were lacking either Nup205 or Nup188 (Fig. 4 B). Both, Nup205–Nup93- and Nup188–Nup93-depleted nuclei were still able to exclude 70-kD dextrans, indicating that the diffusion barrier in these nuclei was intact. Smaller sized 10-kD dextrans could diffuse through the NPC as expected. As a control for an impaired diffusion barrier, nuclei depleted for Nup98 did not exclude the 70-kD dextran. These data indicate that a malfunction of the diffusion barrier of the NPC is unlikely to cause the enlargement of Nup188–Nup93-depleted nuclei.

NPCs mediate signal-dependent import and export across the NE. To check whether these functions are affected by Nup188–Nup93 depletion, we first tested nuclear accumulation of substrates containing an importin α/β– or transportin-based import signal, respectively. Both substrates were fused to an N-terminal EGFP linked to a tobacco etch virus (TEV) protease recognition site. They were added to a nuclear assembly reaction at 50 min, when an NE had formed and Nup188–Nup93- and mock-depleted nuclei were of similar size with approximately the same NPC content (2,737 ± 1,160 NPCs per nucleus in mock-depleted nuclei vs. 2,739 ± 1,437 in Nup188–Nup93-depleted nuclei; see Fig. 7 B). At the indicated time points, a TEV protease fused to a bacterial protein (NusA) was added. NusA increased the size of the protease fusion protein to 90 kD, which prevented its diffusion through the NPC. Nuclear import of the substrates rendered them protease protected and they could thus be quantified by Western blotting. Import kinetics were unchanged upon Nup188–Nup93 depletion for both substrates (Fig. 4 C).

To check for nuclear export, we used an EGFP-fused shuttling substrate with a nuclear import and export signal. The substrate did not accumulate in the nucleus both in mock- and Nup188–Nup93-depleted nuclei, indicating that nuclear export was not impaired (Fig. 4 D). To verify the function of the shuttling substrate, we added leptomycin B, which blocks crm1-mediated nuclear export (Fornerod et al., 1997). As expected, under these conditions, the shuttling substrate accumulated in the nucleus. Interestingly, leptomycin B–treated control nuclei did not increase in size, showing that a block in nuclear export does not phenocopy Nup188–Nup93 depletion. These data show that nuclei lacking Nup188–Nup93 have unchanged nuclear transport capabilities for the tested proteins. Together with the fact that the Nup188–Nup93-depleted nuclei replicate their DNA and grow, both processes requiring nuclear import, it is unlikely that an impairment of nuclear transport of soluble cargoes causes the observed nuclear growth phenotype upon Nup188–Nup93 depletion.

Xenopus egg extracts are largely transcriptionally inactive. Thus, an accumulation of mRNA in the nucleus is unlikely to cause nuclear enlargement. Coherent with this, addition of the transcriptional inhibitors 5,6-dichloro-1-β-D-ribobenzimidazole or actinomycin D did not block nuclear growth of Nup188–Nup93-depleted nuclei (unpublished data).

Nup188–Nup93 restricts transport of membrane proteins through the NPC

Having established that both diffusion and active transport of soluble substrates is unlikely to account for the increase in nuclear size upon Nup188–Nup93 depletion, we focused on the transport of membrane components. As described in the section Nuclei lacking Nup188–Nup93 enlarge in size, nuclei assembled in *Xenopus* egg extracts did enlarge upon further incubation provided that reentry into mitosis was prevented. However, this nuclear growth was much slower in untreated or mock-depleted extracts compared with the Nup188–Nup93-depleted nuclei (Fig. S3 and not depicted). We reasoned that as nuclear growth requires expansion of the NE, it must also involve an acquisition of nuclear membrane components. As the ER is continuous with the ONM, it is easy to envision how membrane components (both lipids and proteins) can be delivered to the ONM. The INM and ONM are connected by the membrane facing the NPC, the pore membrane. Thus, if the INM expands, membrane components need to pass through the NPC via the pore membrane. We speculated that pore membrane passage could limit and restrict nuclear growth and that this restriction might be attenuated upon Nup188–Nup93 depletion. To investigate this, we developed an assay to follow the transport of integral membrane proteins to the INM. BC08, an INM protein with a single C-terminal transmembrane region (Ulbert et al., 2006), was fused to an N-terminal EGFP followed by a recognition site for the TEV protease. The fusion protein was expressed and purified in *Escherichia coli* and reconstituted into liposomes. Liposomes were then added to a nuclear assembly reaction at time points when the NE had already formed around chromatin and under conditions in which they readily fused with the ER (Fig. 5, A and B). The reporter was distributed immediately throughout the membranes of the ER, including the NE, as observed by immunofluorescence (Fig. 5 B). After 30 min, the reporter was enriched at the NE. To distinguish between INM and ONM (including bulk ER) localization, we added the TEV protease fused to NusA, which prevents its diffusion through the NPC. Initially, the reporter was protease sensitive, indicating that it was localized to the ER and the ONM. However, after 30 min, the reporter was protease protected, which is indicative of INM localization. At the same time point, a TEV protease coupled to an NLS-bearing peptide (which is therefore localized to the interior of the nucleus) was able to cleave the reporter. This confirms that the reporter remains cleavable when it is accessible to the protease, and therefore, it is localization to INM that renders it protease protected in this assay. Cleavage of the reporter and its protease protection can be also followed by Western blotting over time, which indicates that about half of the reporter was protease protected after 10 min (Fig. 5 C).

Having established a functional assay for INM translocation, we asked whether the increased size of Nup188–Nup93-depleted nuclei is the result of accelerated membrane delivery to the INM. Nuclei were assembled in Nup188–Nup93- or mock-depleted extracts for 50 min, at which point the NE was closed but the nuclei had not increased in size (Fig. S3, 50-min time points). Liposomes containing the reporter were then added,

Downloaded from jcb.rupress.org on December 5, 2013

Published June 21, 2010

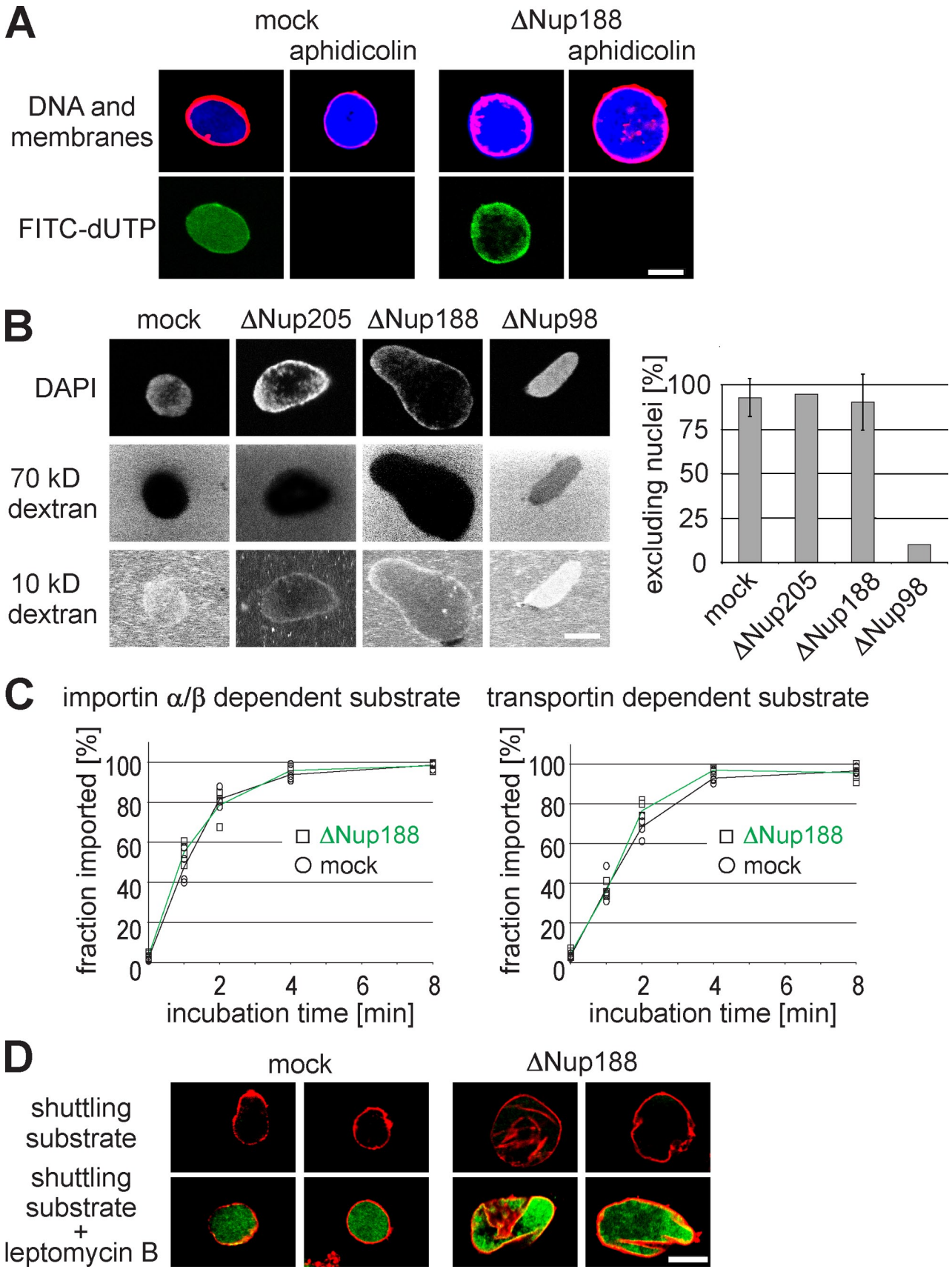

Figure 4. **Nuclear functions are unaffected by Nup188–Nup93 depletion.** (A) Nuclei were assembled in mock- or Nup188–Nup93-depleted extracts. After 50 min, fluorescently labeled dUTP (green in overlay) and, where indicated, aphidicolin were added. After 90 min, replication was analyzed by confocal microscopy. Membranes were stained with DiIC18 (red), and chromatin was stained with DAPI (blue). (B) Nuclei were assembled in mock-,

Downloaded from jcb.rupress.org on December 5, 2013

Published June 21, 2010

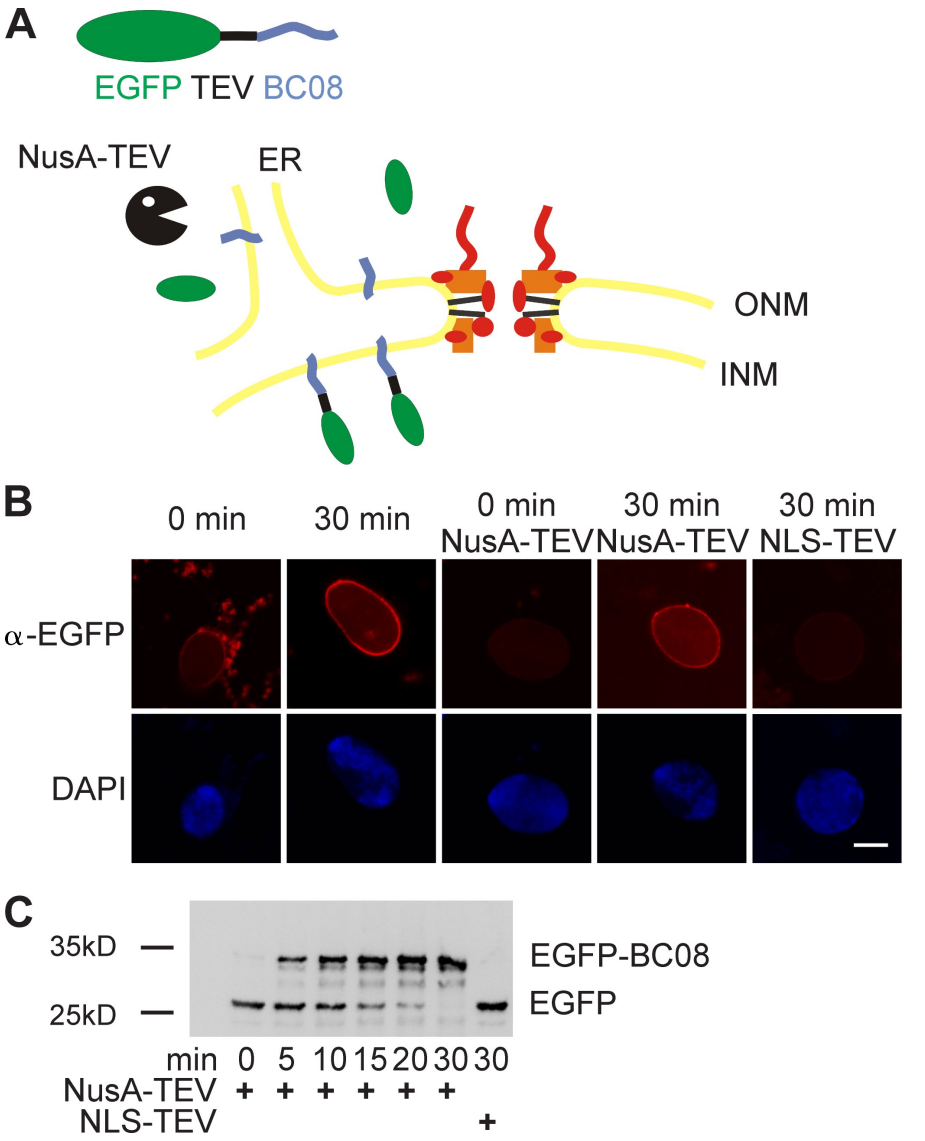

Figure 5. **An assay for the transport of membrane proteins to the INM.** (A) Schematic representation of the assay. The transmembrane-containing INM protein BC08 is fused to an EGFP domain followed by a recognition site for the TEV protease (top). The fusion protein is reconstituted into liposomes that rapidly fuse with the ER and ONM in the nuclear assembly reaction. INM localization of the reporter can be distinguished from ONM and ER localization by the reporter's protection from TEV protease fused with a large NusA domain to prevent its diffusion through the NPC. (B) Nuclei were assembled in *Xenopus* egg extracts. After 50 min, i.e., when a closed NE had formed, proteoliposomes containing the reporter were added. At the indicated time points, buffer, NusA-fused TEV protease, or TEV protease linked to NLS peptides was added. Protease cleavage was stopped after 5 min by fixation, and samples were processed for immunofluorescence and analyzed by confocal microscopy. α-EGFP immunofluorescence is shown in red, and DAPI is shown in blue. (C) Reactions were performed as in B. Protease cleavage was stopped by the addition of SDS sample buffer and boiling. Protease protection of the reporter was analyzed by Western blotting with the position of the uncleaved (EGFP-BC08) and the cleaved reporter with only the EGFP visible indicated. Bar, 20 µm.

and protease protection followed over time. In Nup188–Nup93-depleted nuclei, ∼50% of the reporter was protease protected after 5 min, significantly earlier than in control-treated nuclei (Fig. 6, A and B). Similar results were obtained when a reporter containing the first transmembrane region of the LBR, sufficient for INM targeting (Soullam and Worman, 1995), was used (Fig. S4 A). To confirm that the effect of Nup188–Nup93 depletion was specific, an addback experiment was performed. *Xenopus* Nup93 and mouse Nup188 were cotranslated in vitro (Fig. S4 B) and added to mock- or Nup188–Nup93-depleted extracts. Nuclei assembled in these extracts grew to a similar size as mock-treated extracts (Fig. 6 C and Fig. S4 C) and, importantly, did not show accelerated delivery of the BC08 and LBR reporter to the INM (Fig. 6 B and Fig. S4 A). As the antibody against *Xenopus* Nup188 does not detect the mammalian orthologue by immunofluorescence, nuclei assembled in Nup188–Nup93-depleted extracts supplemented with the recombinant proteins were isolated, and incorporation of recombinant Nup188–Nup93 into the nuclei was confirmed by Western blotting (Fig. 6 D). Notably, addition of neither Nup188 nor Nup93 alone rescued the observed phenotypes, indicating that the complex of Nup188 and Nup93 is indeed required (unpublished data).

Nup205–Nup93-, Nup188–Nup93-, and Nup98-depleted extracts. After 90 min, fluorescently labeled 2-MD (not depicted), 70-kD (middle), and 10-kD (bottom) dextrans were added. DNA was stained with DAPI, and samples were analyzed by confocal microscopy. For quantitation, only nuclei with an intact NE (as judged by the exclusion of 2-MD dextrans; >95% of nuclei in each sample) were analyzed. For mock- and Nup188–Nup93-depleted samples, seven independent experiments were analyzed (error bars show the standard deviation), and for Nup205–Nup93- and Nup98-depleted samples, two independent experiments were analyzed. (C) Nuclei were assembled as in A. After 50 min, i.e., when a closed NE had formed, importin α/β– or transportin-dependent reporter substrates containing a TEV cleavage site were added. To assay the nuclear import kinetics of the reporter, NusA-fused TEV protease was added at the indicated time points. Protease cleavage was stopped after 1 min by the addition of SDS sample buffer and boiling. Lines mark the mean of four independent experiments. (D) Nuclei were assembled as in A, and an EGFP-fused shuttling substrate was added. Nuclear export function was inhibited by the addition of 300 nM leptomycin B. Nuclei were isolated and analyzed by confocal microscopy. Membranes are stained with DiIC18 (red). Bars, 20 µm.

Downloaded from jcb.rupress.org on December 5, 2013

Published June 21, 2010

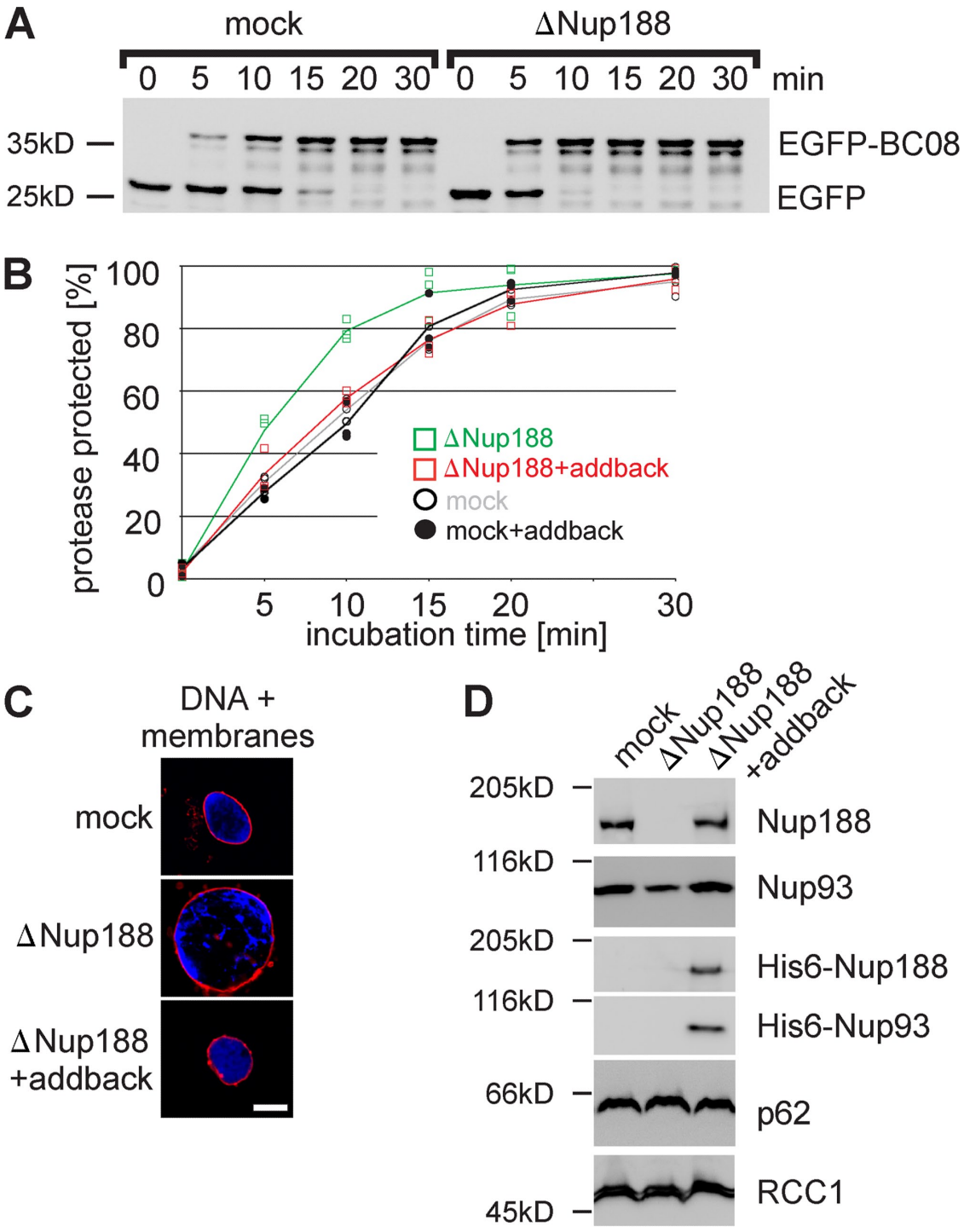

Figure 6. **Nup188–Nup93 depletion causes a faster delivery of integral membrane proteins to the INM.** (A) Nuclei were assembled in mock- or Nup188–Nup93-depleted *Xenopus* egg extracts and analyzed by Western blotting. Positions of the uncleaved (EGFP-BC08) and the cleaved (EGFP) reporter are indicated. (B) Quantification from three independent experiments performed as in A. Squares are from Nup188–Nup93-depleted samples (green without and red with the addition of in vitro translated Nup188–Nup93 [addback]), and circles are from mock-treated samples. Lines mark the mean of three independent experiments. (C) The addition of recombinant Nup188–Nup93 rescues the Nup188–Nup93 depletion phenotype. Nuclei were assembled for 120 min in mock- or Nup188–Nup93-depleted extracts without or with the addition of in vitro translated Nup188–Nup93 (addback), fixed with 4% PFA and 0.5% glutaraldehyde, and analyzed for chromatin and membrane staining (blue, DAPI; red, DiIC18). (D) In vitro translated Nup188–Nup93 is incorporated into in vitro assembled nuclei. Nuclei were assembled for 1 h to ensure approximately equal NPC numbers per nucleus, isolated, and analyzed by Western blotting. In vitro translated Nup188 and Nup93 could be also detected using an anti-His6 antibody (third and fourth row). The nucleoporin p62 was detected with mAb414, and the chromatin-binding protein RCC1 serves as a control for equal loading of nuclei. Bar, 20 µm.

Downloaded from jcb.rupress.org on December 5, 2013

Published June 21, 2010

Collectively, these data indicate that both the increase in nuclear size and the accelerated targeting of integral membrane proteins to the INM are specific for Nup188–Nup93 depletion. Interestingly, nuclei depleted for Nup205–Nup93 showed the same rate of INM targeting of the two reporters as mock controls (Fig. S4 D), which is consistent with the fact that they do not show the nuclear growth phenotype.

As INM proteins reached the nuclear interior significantly faster in Nup188–Nup93-depleted nuclei compared with controls, we wondered whether the effect was specific to proteins destined for the INM or whether the segregation of the INM from the ONM and connected ER was lost in the absence of Nup188–Nup93. To test this idea, we replaced the INM reporter with bona fide ER membrane proteins: SPC18, a membrane-spanning subunit of the signal peptidase complex, or a C-terminal fragment (including the transmembrane region) of the ER-localized chaperone protein calnexin. Both reporters were sensitive to TEV protease cleavage even after 60 min, indicating that they were not localized to the INM (Fig. S5 A). Notably, the cytoplasmic domains for the SPC18 (31 kD)- and calnexin (41 kD)-based reporters fall within the size range of the nucleoplasmic regions of the BC08 and LBR reporters described in the preceding experiments. Therefore, Nup188–Nup93-depleted NPCs continue to act as a diffusion barrier preventing uncontrolled intermixing of INM and ONM (and ER) components.

The nucleoplasmic domains of most INM proteins are limited in size to ~40 kD. It has been shown that increasing this size to 47 kD prevents membrane protein targeting to the INM (Ohba et al., 2004). We tested whether depletion of Nup188–Nup93 would impair the stringency of this size limit. For this, the size of the BC08 reporter was increased to 94 kD and 64 kD by fusing an additional NusA or GST moiety, respectively (Fig. S5 B). In all cases, the reporter did not target to the INM, both in mock- and Nup188–Nup93-depleted nuclei.

Up to now, we have demonstrated that upon Nup188–Nup93 depletion, the passage of INM proteins through the pore is enhanced and that the transfer of membrane components could be rate limiting for nuclear growth. Two possible scenarios can be envisioned. Nup188–Nup93 could restrict the passage of transmembrane or membrane proteins through the pore. Depletion of Nup188–Nup93 might abrogate this restriction, causing an increased flow of membrane components through the pore, leading to an enlargement of the NE in which more NPCs can integrate (Fig. 7 A, top route). Alternatively, Nup188–Nup93 depletion could facilitate NPC formation, giving rise to more NPCs with an overall increased total transport capacity (Fig. 7 A, bottom route). In this scenario, the increase in NE area would be a secondary effect. To distinguish the two possibilities, we blocked de novo NPC assembly into intact NEs by an excess of importin β (D'Angelo et al., 2006), which inhibits the Nup107–Nup160 complex, an essential early component for NPC formation (Harel et al., 2003; Walther et al., 2003; Rasala et al., 2006; Franz et al., 2007). When 2 µM importin β was added to mock- and Nup188–Nup93-depleted extracts after 50 min, i.e., when a closed NE with intact NPCs was formed, the NPC number did not increase in the next 70 min (Fig. 7 B, green bars). Despite approximately the same number of NPCs at the time of importin β addition and a subsequent block in de novo NPC assembly, Nup188–Nup93-depleted nuclei grew within the next 70 min significantly faster than mock-depleted nuclei so that the NPC density at the end of the incubation time was more decreased in Nup188–Nup93-depleted compared with mock-depleted nuclei (2.8 NPCs/µm^2 NE membrane vs. 5.2 NPCs/µm^2; Fig. 7 B, red bars). These data indicate that the accelerated growth of the nuclei and the nuclear membrane expansion upon Nup188–Nup93 depletion cannot only be attributed to an increased NPC number. Importantly, in Nup188–Nup93-depleted nuclei treated with importin β, the EGFP-BC08 reporter was still protease protected significantly earlier than in mock-treated nuclei (Fig. 7 C). Therefore, we could rule out that an increased NPC number was the primary cause of the enhanced translocation of the reporter to the INM. Collectively, this demonstrates that Nup188–Nup93 depletion results in increased passage of proteins destined for the INM across the NPC. This suggests that Nup188–Nup93 is a crucial component within the NPC that restricts the flux of integral membrane proteins and likely other membrane components along the pore membrane.

Discussion

In this study, we have shown that the nucleoporin Nup93 is part of two distinct complexes. It interacts either with Nup205 or -188. Unexpectedly, nuclei depleted of Nup188–Nup93 grew to enormous sizes, a phenotype previously not observed upon depletion of a nucleoporin. Integral membrane proteins and probably other membrane components are delivered faster to the INM upon Nup188–Nup93 depletion. We suggest that this causes rapid expansion of the NE as a primary effect and in turn facilitates increased integration of NPCs. The higher NPC number would have a higher overall transport rate both for soluble cargoes and membrane components, which would then further augment the nuclear growth effect.

Transport of soluble cargo via the NPC has been intensely studied in previous decades (for reviews see Weis, 2003; Cook et al., 2007). However, transmembrane proteins must also access the INM, where several of them bind lamin and/or chromatin. Little is currently known about how transmembrane proteins are delivered to the INM of the interphasic nucleus (Zuleger et al., 2008). Although a scenario can be envisioned in which the ONM and INM periodically fuse to provide transient connections allowing diffusional exchange between these membrane domains, there is at present no evidence supporting this. Alternatively, membrane vesicle budding from the ONM into the perinuclear lumen and subsequent fusion with the INM could also explain how membrane proteins are delivered to the INM. However, aside from the observation that the reverse process occurs during herpesvirus egress from the nucleus (Mettenleiter et al., 2009), there is little proof for this model. A more likely scenario involves transmembrane protein transit from the ONM to the INM via the NPC along the plane of the pore membrane. Indeed, antibodies to the transmembrane nucleoporin gp210 as well as WGA, a lectin which cross-links several nucleoporins, are both able to block the movement of integral membrane

Downloaded from jcb.rupress.org on December 5, 2013

Published June 21, 2010

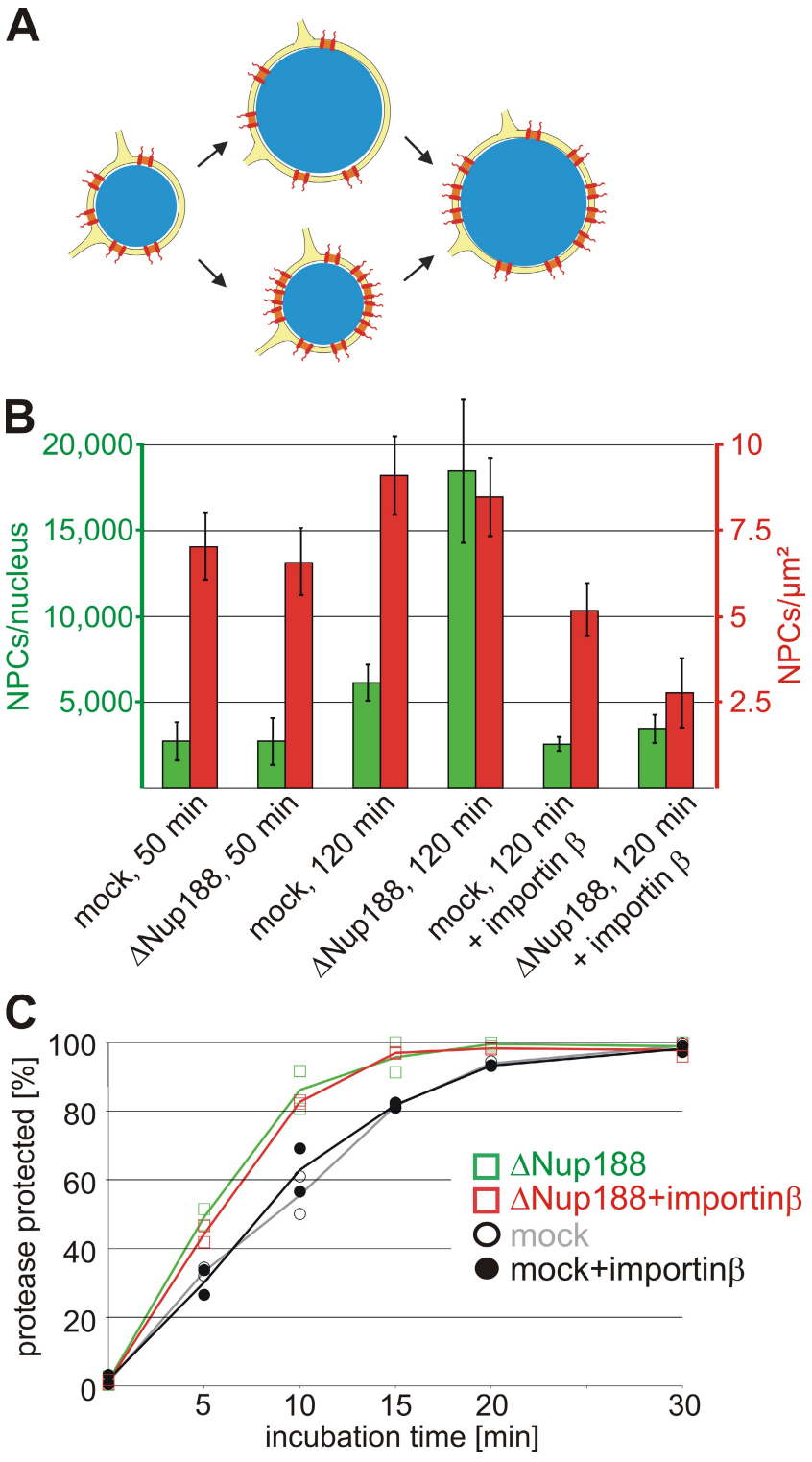

Figure 7. **The nuclear growth phenotype and the faster INM targeting are independent of the increased NPC number upon Nup188–Nup93 depletion.** (A) Two possible scenarios for the relationship of the nuclear membrane expansion and the increase in NPC numbers upon Nup188–Nup93 depletion. In the top route, Nup188–Nup93 depletion causes a faster growth of the NE, which in turn allows more NPCs (red) to be integrated. In the bottom route, NPC assembly increases on Nup188–Nup93-depleted nuclei. The resulting higher total transport capacity of these allows accelerated nuclear volume and envelope expansion. (B) Nuclei were assembled in mock- and Nup188–Nup93-depleted extracts for 50 min and 120 min. Where indicated, de novo NPC assembly was blocked by the addition of 2 µM importin β after 50 min, i.e., after a closed NE had formed, and nuclei were further incubated for 70 min. NPC numbers per nucleus (green bars) and NPC density (red bars) were quantified. (C) Nuclei were assembled in mock- and Nup188–Nup93-depleted extracts for 50 min. Then, where indicated, de novo NPC assembly was blocked by the addition of 2 µM importin β. INM targeting of the reporter was analyzed as in Fig. 6. Squares are from Nup188–Nup93-depleted samples, and circles from mock-treated samples. Lines mark the mean of two independent experiments.

proteins from the ONM to the INM, most likely by sterically occluding the passageways (Ohba et al., 2004). In yeast, deletion of Nup170, one of the Nup155 homologues, causes delocalization of two integral membrane proteins, Heh1p and Heh2p, from the INM (King et al., 2006). Together with the fact that delivery of Heh1p and Heh2p to the INM requires classical transport receptors (importin α and β), these data argue strongly in favor of NPC involvement in the movement of integral membrane proteins from the ONM to the INM. Indeed, when depleting the Nup107–Nup160 complex, which leads to the formation of nuclei without NPCs (Harel et al., 2003; Walther et al., 2003), no INM targeting of the reporter constructs was observed (Fig. S5 C).

In this study, we show that Nup188–Nup93 restricts the passage of integral membrane proteins from the ONM to the INM. Although proteins destined to the INM reach these sites faster in Nup188–Nup93-depleted nuclei, bona fide ER proteins

Downloaded from jcb.rupress.org on December 5, 2013

Published June 21, 2010

are not mislocalized to the INM. In yeast, depletion of Nup188p or the integral membrane nucleoporin Pom152p was found to reduce INM localization of the ubiquitin ligase Doa10p (Deng and Hochstrasser, 2006). Normally, the majority of cellular Doa10p resides in the ER, although it is also found at the INM, where it drives the degradation of intranuclear targets. During excessive nuclear membrane proliferation, Doa10p is enriched at the INM. Under these conditions, deletion of Nup188 causes the redistribution of Doa10p to the ER, probably via enhanced passage through the NPC.

Nucleoporins containing FG-repeat domains contribute to the transport properties of the NPC by establishing a permeability barrier and promoting transport receptor–mediated NPC passage. They are mainly localized to the interior center of the NPC (Rout et al., 2000; Alber et al., 2007). In contrast, Nup188p and Nup170p do not contain FG repeats and are found comparatively more proximal to the pore membrane. Interestingly, depletion of Nup188–Nup93 did not reduce mAb414 staining, which recognizes FG-containing nucleoporins (Fig. 3 A), and did not destroy the diffusion barrier of the NPC or affect nuclear import and export of soluble reporter cargoes (Fig. 4). This suggests that the transport of soluble and membrane proteins requires distinct features within the NPC and uses different pathways within the pore.

It has been proposed that NPCs accommodate not only a large central channel for active and transport receptor–mediated import and export but also eight peripheral channels that mediate passive exchange of metabolites and ions (Hinshaw and Milligan, 2003; Kramer et al., 2007; Naim et al., 2007). Although recent cryoelectron tomography of NPCs from *Dictyostelium discoideum* confirmed the existence of peripheral channels ∼9 nm in diameter (Beck et al., 2007), the idea of separate passageways for soluble factors is in contrast to the prevailing model in which FG-repeat domains form a common barrier for both facilitated and passive exchange (Ribbeck and Görlich, 2001; Rout and Aitchison, 2001). Passive diffusion is sensitive to many of the same ligands and inhibitors that target active transport across the NE. This argues strongly for a single permeability barrier for soluble molecules passing through the NPC either by active transport or passive diffusion (Mohr et al., 2009). Alternatively, the peripheral channels could be important for membrane proteins passing the NPC (Powell and Burke, 1990; Zuleger et al., 2008). Although the nucleoplasmic domains of most INM proteins are limited in size to ∼40 kD and therefore might be small enough to fit in the cavities of the channels, we propose that structural rearrangements within the NPC are necessary to allow for integral membrane passage without disrupting the diffusion barrier. Depletion of Nup188–Nup93 may enhance conformational flexibility within the NPC, resulting in the increased passage of membrane proteins through the NPC that we have observed in this study without affecting the size limit for these proteins.

The metazoan Nup93 complex and the corresponding Nic96 complex in yeast is one of the major building blocks of the NPC. However, compared with the well-characterized Nup107–Nup160 complex, which can be purified from *Xenopus* egg extracts (Vasu et al., 2001; Walther et al., 2003), the association of Nup93 complex components is remarkably less stable. Nup155 and Nup53 can be precipitated mainly as individual proteins, as observed previously (Franz et al., 2005; Hawryluk-Gara et al., 2008). Additionally, Nup205, Nup188, and Nup93 do not exist in a single complex in *Xenopus* egg extracts as previously suggested (Meier et al., 1995). Formerly, immunoprecipitations were performed using antibodies against Nup93, which, as we have shown, actually precipitates two different Nup93-containing complexes. However, the Nup188–Nup93 and the Nup205–Nup93 interactions seem to be rather stable. Interestingly, in the add-back experiment, we could only restore the phenotype if Nup188 and Nup93 were coexpressed and added despite the fact that after Nup188–Nup93 depletion, ∼50% of Nup93 remains in the extracts (most in a complex with Nup205 and a smaller proportion not bound to Nup205; Fig. 1 and Fig. S1), suggesting that Nup93 cannot exchange between the different complexes under the given conditions.

Whereas depletion of Nup155 and Nup53 from *Xenopus* egg extracts prevents NPC and NE formation (Franz et al., 2005; Hawryluk-Gara et al., 2008), extracts depleted of Nup205–Nup93 or Nup188–Nup93 assemble nuclei with seemingly intact NPCs and a closed NE. Currently, we cannot exclude the possibility that the Nup188–Nup93 and Nup205–Nup93 complexes have partially redundant functions during NPC formation. Double depletion of both complexes (with antibodies against Nup205 and Nup188) followed by nuclear assembly reactions was for technical reasons unfeasible, requiring, in total, four rounds of incubation of extracts with antibody beads. Interestingly, depletion of Nup93-containing complexes from *Xenopus* egg extracts with α-Nup93 antibodies blocked NPC assembly (Grandi et al., 1997; unpublished data). However, we cannot exclude the possibility that Nup93 is of functional importance outside of its role in the Nup188–Nup93 and Nup205–Nup93 complexes. Indeed, a subfraction of 5–10% of Nup93 has been shown to interact with the FG repeat–containing nucleoporin p62 (Zabel et al., 1996), as does the yeast homologue Nic96p with Nsp1p (Zabel et al., 1996). This could be a subpopulation distinct from the Nup188–Nup93 and Nup205–Nup93 complexes. Notably, we found that ∼5% of Nup93 cannot be depleted with a combination of antibodies against Nup205 and Nup188 (Fig. S1)

Depletion of neither Nup188–Nup93 nor Nup205–Nup93 impaired the exclusion limit of the NPCs for inert substances (Fig. 4 B). For Nup205–Nup93, this was particularly unexpected as depletion of *Caenorhabditis elegans* Nup205 by RNAi causes failure of nuclear exclusion of 70-kD dextrans (Galy et al., 2003). Interestingly, up to now, no *C. elegans* Nup188 orthologue has been identified. It is possible that the Nup205–Nup93 and Nup188–Nup93 complexes in *Xenopus* have partially redundant functions in establishing the exclusion limit of NPCs. Because of the absence of Nup188 in *C. elegans*, Nup205–Nup93 could still accommodate this function, which is lost upon Nup205 depletion.

In summary, our work establishes that members of the Nup93 complex, which is regarded as one of the structural building blocks of the NPC, can be depleted without blocking NPC formation. Intriguingly, Nup188–Nup93 is rather important for controlling the passage of transmembrane proteins and

Downloaded from jcb.rupress.org on December 5, 2013

Published June 21, 2010

probably other membrane components through the NPC. Thus, in addition to regulating the composition of the nucleoplasm by restricting access of soluble factors to the nuclear interior, NPCs are also important in the establishment of the two membrane subcompartments of the NE.

Materials and methods

Materials

An EST containing the C-terminal region of *Xenopus* Nup188 (GenBank/EMBL/DDBJ accession number BQ725804) was identified by BLAST search using the mouse sequence as bait. ESTs for *Xenopus* Nup98, Nup205, BC08, LBR, and mouse Nup188 were under GenBank/EMBL/DDBJ accession numbers CF286969, CA986989, BC082226, BC124994, BG861579, respectively. *Xenopus* Nup53, NPM2, calnexin, and SPC18 were amplified from a *Xenopus* cDNA.

Leptomycin B and aphidicolin were obtained from Enzo Life Sciences, Inc., and DiIC18 (1,1′-dioctadecyl-3,3,3′,3′-tetramethylindocarbocyanine perchlorate), fluorescently labeled dextrans, and secondary antibodies (Alexa Fluor 488 goat α-rabbit IgG and Cy3 goat α-mouse IgG) were obtained from Invitrogen. Detergents were purchased from EMD, and lipids were purchased from Avanti Polar Lipids, Inc.

Antibodies

For the generation of antibodies, a fragment of *Xenopus* Nup188 corresponding to aa 1573–1731 of the mouse sequence and a fragment of Nup98 (aa 1–185) were expressed as GST fusion proteins and purified using glutathione Sepharose (GE Healthcare). Fragments of *Xenopus* Nup53 (aa 78–310) and LBR (aa 47–216) were cloned into pET28a (EMD), expressed as a His6-tagged fusion, and purified using Ni–nitrilotriacetic acid agarose (QIAGEN). A fragment of *Xenopus* Nup205 (aa 1–283) was fused to NusA as a solubility tag, cloned into pET28a, and expressed as a His6-tagged fusion. Recombinant proteins were dialyzed to PBS and injected into rabbits for antibody production.

Antibodies against Nup155 and RCC1 (Franz et al., 2005) as well as Nup160 and Nup93 (Franz et al., 2007) have been described previously. mAb414 was obtained from Babco, anti–lamin B (X223) was obtained from ImmuQuest, and anti-EGFP and anti-His6 were obtained from Roche.

DNA replication, dextran exclusion, and nuclear transport function

For testing DNA replication, nuclear assembly reactions were incubated with 43.5 µM fluorescein-12-dUTP and, where indicated, 16 µM aphidicolin. Samples were fixed and processed for microscopy as described previously (Franz et al., 2005). All fluorescence microscopy images were recorded on the confocal microscope (FV1000; Olympus; equipped with a photomultiplier [model R7862; Hamamatsu]) with 405-, 488-, and 559-nm laser lines and a 60× NA 1.35 oil immersion objective lens using the Fluoview software (Olympus) at room temperature using Vectashield (Vector Laboratories) as a mounting medium.

For the size exclusion assay, nuclei were assembled for 90 min, at which point 10 µg/ml of 10-kD dextran labeled with Texas red, 30 µg/ml of 70-kD dextran labeled with fluorescein, and 40 µg/ml of 2-MD dextran labeled with tetramethylrhodamine were added. The samples were incubated for 5 min and analyzed by confocal microscopy without fixation and mounting, but otherwise as in the previous paragraph.

TEV protease was fused to a NusA domain, cloned into pET28a, and expressed and purified as a His6-tagged fusion. TEV protease without a NusA domain was expressed and purified as a His6-tagged fusion and cross-linked to NLS peptides as described previously (Vasu et al., 2001).

To test importin α/β– or transportin-dependent nuclear import function, full-length NPM2 (nucleoplasmin) or Nplc-M9-M10 (from Englmeier et al. [1999]), respectively, was fused to an N-terminal EGFP, followed by a TEV recognition site, and cloned into a modified pET28a vector, allowing purification via a C-terminal His6 tag. After Ni–nitrilotriacetic acid chromatography, all substrates were further purified by size exclusion chromatography on a Sepharose 200 column (GE Healthcare). 50-µl nuclear assembly reactions were assembled in the volume ratio as described previously (Franz et al., 2005). 50 min after the addition of membranes, 1 µg of the respective reporter was added. At the indicated time points, 10 µl of the samples was added to 1 µl of 5 µg/µl NusA-TEV protease and incubated for 1 min at 20°C. TEV cleavage was stopped by the addition of SDS sample buffer and immediate incubation at 95°C for 5 min, followed by SDS-PAGE and Western blotting.

For testing nuclear export function, a reporter as well as a control substrate, Nplc-M9-NES and Nplc-M9-M10, respectively (from Englmeier et al. [1999]) were fused to an N-terminal EGFP, cloned into pET28a, and purified as in the previous paragraph. 0.1 mg/ml of the export reporters was added to a nuclear assembly reaction, incubated for 90 min, fixed, and processed for microscopy.

For generation of reporter constructs for INM targeting, full-length BC08, a part of the N terminus of LBR including the first transmembrane region (aa 146–258), and full-length SPC18 (all from *Xenopus*) were fused to an N-terminal MISTIC (membrane-integrating sequence for translation of integral membrane protein constructs) fragment (Roosild et al., 2005), followed by a thrombin cleavage site, an EGFP domain, and a TEV protease cleavage site, and cloned into a modified pET28a vector, allowing purification via a C-terminal His6 tag. For the calnexin reporter construct, the C-terminal region including the transmembrane region of calnexin (aa 485–608) was placed 3′ of the MISTIC fragment and 5′ of the TEV cleavage site and the EGFP domain and integrated into the modified pET28a vector with a C-terminal His6 tag. For the INM targeting constructs with increased nucleoplasmatic sizes, a NusA or GST domain was inserted 5′ of the EGFP moiety in the reporter constructs.

Proteins were expressed in *E. coli* BL21de3, purified in the presence of 1% (wt/vol) cetyltrimethylammonium bromide on magnetic Ni-loaded agarose beads (EMD), and dialyzed for 16 h against PBS containing 1 mM EDTA. The MISTIC fragments were cleaved off using thrombin, and the reporters were reconstituted into liposomes. For this, ∼10 µg of protein was mixed with 20 µl of a lipid mix containing 3 mg/ml cholesterol, 3 mg/ml Na-phosphatidylserine, 3 mg/ml Na-phosphatidylinositol, 6 mg/ml phosphatidylethanolamine, 15 mg/ml phosphatidylcholine (all solubilized in 10% octylglucopyranoside), and 2 µl of 1 mg/ml DiIC18 in DMSO. Detergent was removed by passing the sample over a G-50 column equilibrated in sucrose buffer (10 mM Hepes, 250 mM sucrose, 50 mM KCl, and 2.5 mM $MgCl_2$, pH 7.5). The proteoliposome-containing fraction (identified by the color of the dye) was collected, and the liposomes were pelleted by centrifugation for 30 min at 200,000 *g*. The pellets were resuspended in 40 µl of sucrose buffer. Proteins were correctly oriented within the liposomes with the EGFP unit facing the exterior as judged by their sensitivity to TEV protease cleavage.

45 µl of cytosol supplemented with 1 µl of 20 mg/ml glycogen and 1 µl of energy mix (50 mM ATP, 500 mM creatine phosphate, and 10 mg/ml creatine kinase) was incubated with 7,500 sperm heads as chromatin template. 50 min after the addition of 2.5 µl of membranes, 5 µl of resuspended proteoliposomes was added. At the indicated time points, 10 µl of the samples was added to 1 µl of 5 µg/µl NusA-TEV protease in sucrose buffer and incubated for 5 min at 20°C. The cleavage reaction was stopped by fixation with 4% PFA and processed for microscopy as described previously (Franz et al., 2005). For Western blot analysis, TEV cleavage was stopped by the addition of SDS sample buffer and immediate incubation at 95°C for 5 min, followed by SDS-PAGE and Western blotting.

In vitro translation

For the in vitro translation, we generated a modified pET28a vector containing a stem loop–forming sequence derived from the 5′ untranslated region of gene 10 of the T7 bacteriophage (5′-AGGGAGACCACAACGGUUUCCCU-3′) 5′ of the in vitro transcribed/translated gene. This is known to enhance in vitro transcription (O'Connor and Dahlberg, 2001). As DNA templates, full-length mouse Nup188 and *Xenopus* Nup93 were cloned into this vector and used in the PURExpress in vitro synthesis kit (New England Biolabs, Inc.) according to the manufacturer's instructions, extending the incubation time to 4 h.

Miscellaneous

Generation of affinity resins for protein depletion, preparation of sperm heads and floated membranes, nuclear assembly reactions, and transmission electron microscopy were performed as described previously (Franz et al., 2005) except that tannic acid was omitted to increase the visibility of NPCs. For depletions, high speed extracts were incubated twice with a 1:1 bead to cytosol ratio for 40 min (Franz et al., 2007). Prelabeled membranes were prepared as in Antonin et al. [2005] using DiIC18, and immunoprecipitations were performed as in Franz et al. [2007]. NPCs from at least 50 nuclei from three independent experiments were counted (D'Angelo et al., 2006) using the Imaris 6.1.5 software (Bitplane AG) for 3D reconstruction. In vitro assembled nuclei were isolated as in Baur et al. (2007).

Online supplemental material

Fig. S1 shows the quantification of the relative amounts of the different Nup93 complexes. Fig. S2 shows immunofluorescences of nuclei lacking

Downloaded from jcb.rupress.org on December 5, 2013

Published June 21, 2010

Nup205–Nup93 as well as transmission electron images of mock- and Nup188–Nup93-depleted nuclei. Fig. S3 shows the time course of nuclear assembly in mock- and Nup188–Nup93-depleted extracts. Fig. S4 shows INM targeting assays on nuclei lacking Nup188–Nup93 and Nup205–Nup93 and additional data of the addback experiments. Fig. S5 provides supporting experiments characterizing the INM targeting assay. Online supplemental material is available at http://www.jcb.org/cgi/content/full/jcb.200912045/DC1.

We thank Josef Redolfi and Cornelia Sieverding for excellent technical support, Virgilio Failla for help with NPC quantification, and Elisa Izaurralde, Adriana Magalska, Ruchika Sachdev, Allana Schooley, and Benjamin Vollmer for critical reading of the manuscript.

Submitted: 8 December 2009
Accepted: 26 May 2010

References

Alber, F., S. Dokudovskaya, L.M. Veenhoff, W. Zhang, J. Kipper, D. Devos, A. Suprapto, O. Karni-Schmidt, R. Williams, B.T. Chait, et al. 2007. Determining the architectures of macromolecular assemblies. *Nature*. 450:683–694. doi:10.1038/nature06404

Antonin, W., C. Franz, U. Haselmann, C. Antony, and I.W. Mattaj. 2005. The integral membrane nucleoporin pom121 functionally links nuclear pore complex assembly and nuclear envelope formation. *Mol. Cell*. 17:83–92. doi:10.1016/j.molcel.2004.12.010

Antonin, W., J. Ellenberg, and E. Dultz. 2008. Nuclear pore complex assembly through the cell cycle: regulation and membrane organization. *FEBS Lett.* 582:2004–2016. doi:10.1016/j.febslet.2008.02.067

Baur, T., K. Ramadan, A. Schlundt, J. Kartenbeck, and H.H. Meyer. 2007. NSF- and SNARE-mediated membrane fusion is required for nuclear envelope formation and completion of nuclear pore complex assembly in *Xenopus laevis* egg extracts. *J. Cell Sci.* 120:2895–2903. doi:10.1242/jcs.010181

Beck, M., V. Lucić, F. Förster, W. Baumeister, and O. Medalia. 2007. Snapshots of nuclear pore complexes in action captured by cryo-electron tomography. *Nature*. 449:611–615. doi:10.1038/nature06170

Blow, J.J., and A.M. Sleeman. 1990. Replication of purified DNA in *Xenopus* egg extract is dependent on nuclear assembly. *J. Cell Sci.* 95:383–391.

Boehmer, T., J. Enninga, S. Dales, G. Blobel, and H. Zhong. 2003. Depletion of a single nucleoporin, Nup107, prevents the assembly of a subset of nucleoporins into the nuclear pore complex. *Proc. Natl. Acad. Sci. USA*. 100:981–985. doi:10.1073/pnas.252749899

Brohawn, S.G., N.C. Leksa, E.D. Spear, K.R. Rajashankar, and T.U. Schwartz. 2008. Structural evidence for common ancestry of the nuclear pore complex and vesicle coats. *Science*. 322:1369–1373. doi:10.1126/science.1165886

Cook, A., F. Bono, M. Jinek, and E. Conti. 2007. Structural biology of nucleocytoplasmic transport. *Annu. Rev. Biochem.* 76:647–671. doi:10.1146/annurev.biochem.76.052705.161529

D'Angelo, M.A., and M.W. Hetzer. 2008. Structure, dynamics and function of nuclear pore complexes. *Trends Cell Biol.* 18:456–466. doi:10.1016/j.tcb.2008.07.009

D'Angelo, M.A., D.J. Anderson, E. Richard, and M.W. Hetzer. 2006. Nuclear pores form de novo from both sides of the nuclear envelope. *Science*. 312:440–443. doi:10.1126/science.1124196

Deng, M., and M. Hochstrasser. 2006. Spatially regulated ubiquitin ligation by an ER/nuclear membrane ligase. *Nature*. 443:827–831. doi:10.1038/nature05170

Englmeier, L., J.C. Olivo, and I.W. Mattaj. 1999. Receptor-mediated substrate translocation through the nuclear pore complex without nucleotide triphosphate hydrolysis. *Curr. Biol.* 9:30–41. doi:10.1016/S0960-9822(99)80044-X

Fabre, E., and E. Hurt. 1997. Yeast genetics to dissect the nuclear pore complex and nucleocytoplasmic trafficking. *Annu. Rev. Genet.* 31:277–313. doi:10.1146/annurev.genet.31.1.277

Fornerod, M., M. Ohno, M. Yoshida, and I.W. Mattaj. 1997. CRM1 is an export receptor for leucine-rich nuclear export signals. *Cell*. 90:1051–1060. doi:10.1016/S0092-8674(00)80371-2

Franz, C., P. Askjaer, W. Antonin, C.L. Iglesias, U. Haselmann, M. Schelder, A. de Marco, M. Wilm, C. Antony, and I.W. Mattaj. 2005. Nup155 regulates nuclear envelope and nuclear pore complex formation in nematodes and vertebrates. *EMBO J.* 24:3519–3531. doi:10.1038/sj.emboj.7600825

Franz, C., R. Walczak, S. Yavuz, R. Santarella, M. Gentzel, P. Askjaer, V. Galy, M. Hetzer, I.W. Mattaj, and W. Antonin. 2007. MEL-28/ELYS is required for the recruitment of nucleoporins to chromatin and postmitotic nuclear pore complex assembly. *EMBO Rep.* 8:165–172. doi:10.1038/sj.embor.7400889

Galy, V., I.W. Mattaj, and P. Askjaer. 2003. *Caenorhabditis elegans* nucleoporins Nup93 and Nup205 determine the limit of nuclear pore complex size exclusion in vivo. *Mol. Biol. Cell*. 14:5104–5115. doi:10.1091/mbc.E03-04-0237

Gomez-Ospina, N., G. Morgan, T.H. Giddings Jr., B. Kosova, E. Hurt, and M. Winey. 2000. Yeast nuclear pore complex assembly defects determined by nuclear envelope reconstruction. *J. Struct. Biol.* 132:1–5. doi:10.1006/jsbi.2000.4305

Grandi, P., T. Dang, N. Pané, A. Shevchenko, M. Mann, D. Forbes, and E. Hurt. 1997. Nup93, a vertebrate homologue of yeast Nic96p, forms a complex with a novel 205-kDa protein and is required for correct nuclear pore assembly. *Mol. Biol. Cell*. 8:2017–2038.

Harel, A., A.V. Orjalo, T. Vincent, A. Lachish-Zalait, S. Vasu, S. Shah, E. Zimmerman, M. Elbaum, and D.J. Forbes. 2003. Removal of a single pore subcomplex results in vertebrate nuclei devoid of nuclear pores. *Mol. Cell*. 11:853–864. doi:10.1016/S1097-2765(03)00116-3

Hawryluk-Gara, L.A., M. Platani, R. Santarella, R.W. Wozniak, and I.W. Mattaj. 2008. Nup53 is required for nuclear envelope and nuclear pore complex assembly. *Mol. Biol. Cell*. 19:1753–1762. doi:10.1091/mbc.E07-08-0820

Hetzer, M.W., T.C. Walther, and I.W. Mattaj. 2005. Pushing the envelope: structure, function, and dynamics of the nuclear periphery. *Annu. Rev. Cell Dev. Biol.* 21:347–380. doi:10.1146/annurev.cellbio.21.090704.151152

Hinshaw, J.E., and R.A. Milligan. 2003. Nuclear pore complexes exceeding eightfold rotational symmetry. *J. Struct. Biol.* 141:259–268. doi:10.1016/S1047-8477(02)00626-3

King, M.C., C.P. Lusk, and G. Blobel. 2006. Karyopherin-mediated import of integral inner nuclear membrane proteins. *Nature*. 442:1003–1007. doi:10.1038/nature05075

Kramer, A., Y. Ludwig, V. Shahin, and H. Oberleithner. 2007. A pathway separate from the central channel through the nuclear pore complex for inorganic ions and small macromolecules. *J. Biol. Chem.* 282:31437–31443. doi:10.1074/jbc.M703720200

Lusk, C.P., G. Blobel, and M.C. King. 2007. Highway to the inner nuclear membrane: rules for the road. *Nat. Rev. Mol. Cell Biol.* 8:414–420. doi:10.1038/nrm2165

Makio, T., L.H. Stanton, C.C. Lin, D.S. Goldfarb, K. Weis, and R.W. Wozniak. 2009. The nucleoporins Nup170p and Nup157p are essential for nuclear pore complex assembly. *J. Cell Biol.* 185:459–473. doi:10.1083/jcb.200810029

Mansfeld, J., S. Güttinger, L.A. Hawryluk-Gara, N. Panté, M. Mall, V. Galy, U. Haselmann, P. Mühlhäusser, R.W. Wozniak, I.W. Mattaj, et al. 2006. The conserved transmembrane nucleoporin NDC1 is required for nuclear pore complex assembly in vertebrate cells. *Mol. Cell*. 22:93–103. doi:10.1016/j.molcel.2006.02.015

Mattaj, I.W. 2004. Sorting out the nuclear envelope from the endoplasmic reticulum. *Nat. Rev. Mol. Cell Biol.* 5:65–69. doi:10.1038/nrm1263

Meier, E., B.R. Miller, and D.J. Forbes. 1995. Nuclear pore complex assembly studied with a biochemical assay for annulate lamellae formation. *J. Cell Biol.* 129:1459–1472. doi:10.1083/jcb.129.6.1459

Mettenleiter, T.C., B.G. Klupp, and H. Granzow. 2009. Herpesvirus assembly: an update. *Virus Res.* 143:222–234. doi:10.1016/j.virusres.2009.03.018

Mohr, D., S. Frey, T. Fischer, T. Güttler, and D. Görlich. 2009. Characterisation of the passive permeability barrier of nuclear pore complexes. *EMBO J.* 28:2541–2553. doi:10.1038/emboj.2009.200

Naim, B., V. Brumfeld, R. Kapon, V. Kiss, R. Nevo, and Z. Reich. 2007. Passive and facilitated transport in nuclear pore complexes is largely uncoupled. *J. Biol. Chem.* 282:3881–3888. doi:10.1074/jbc.M608329200

Nehrbass, U., M.P. Rout, S. Maguire, G. Blobel, and R.W. Wozniak. 1996. The yeast nucleoporin Nup188p interacts genetically and physically with the core structures of the nuclear pore complex. *J. Cell Biol.* 133:1153–1162. doi:10.1083/jcb.133.6.1153

O'Connor, M., and A.E. Dahlberg. 2001. Enhancement of translation by the epsilon element is independent of the sequence of the 460 region of 16S rRNA. *Nucleic Acids Res.* 29:1420–1425. doi:10.1093/nar/29.7.1420

Ohba, T., E.C. Schirmer, T. Nishimoto, and L. Gerace. 2004. Energy- and temperature-dependent transport of integral proteins to the inner nuclear membrane via the nuclear pore. *J. Cell Biol.* 167:1051–1062. doi:10.1083/jcb.200409149

Onischenko, E.A., E. Crafoord, and E. Hallberg. 2007. Phosphomimetic mutation of the mitotically phosphorylated serine 1880 compromises the interaction of the transmembrane nucleoporin gp210 with the nuclear pore complex. *Exp. Cell Res.* 313:2744–2751. doi:10.1016/j.yexcr.2007.05.011

Powell, L., and B. Burke. 1990. Internuclear exchange of an inner nuclear membrane protein (p55) in heterokaryons: in vivo evidence for the

Downloaded from jcb.rupress.org on December 5, 2013

Published June 21, 2010

interaction of p55 with the nuclear lamina. *J. Cell Biol.* 111:2225–2234. doi:10.1083/jcb.111.6.2225

Rasala, B.A., A.V. Orjalo, Z. Shen, S. Briggs, and D.J. Forbes. 2006. ELYS is a dual nucleoporin/kinetochore protein required for nuclear pore assembly and proper cell division. *Proc. Natl. Acad. Sci. USA*. 103:17801–17806. doi:10.1073/pnas.0608484103

Ribbeck, K., and D. Görlich. 2001. Kinetic analysis of translocation through nuclear pore complexes. *EMBO J.* 20:1320–1330. doi:10.1093/emboj/20.6.1320

Roosild, T.P., J. Greenwald, M. Vega, S. Castronovo, R. Riek, and S. Choe. 2005. NMR structure of Mistic, a membrane-integrating protein for membrane protein expression. *Science*. 307:1317–1321. doi:10.1126/science.1106392

Rout, M.P., and J.D. Aitchison. 2001. The nuclear pore complex as a transport machine. *J. Biol. Chem.* 276:16593–16596. doi:10.1074/jbc.R100015200

Rout, M.P., J.D. Aitchison, A. Suprapto, K. Hjertaas, Y. Zhao, and B.T. Chait. 2000. The yeast nuclear pore complex: composition, architecture, and transport mechanism. *J. Cell Biol.* 148:635–651. doi:10.1083/jcb.148.4.635

Shulga, N., N. Mosammaparast, R. Wozniak, and D.S. Goldfarb. 2000. Yeast nucleoporins involved in passive nuclear envelope permeability. *J. Cell Biol.* 149:1027–1038. doi:10.1083/jcb.149.5.1027

Soullam, B., and H.J. Worman. 1995. Signals and structural features involved in integral membrane protein targeting to the inner nuclear membrane. *J. Cell Biol.* 130:15–27. doi:10.1083/jcb.130.1.15

Ulbert, S., M. Platani, S. Boue, and I.W. Mattaj. 2006. Direct membrane protein-DNA interactions required early in nuclear envelope assembly. *J. Cell Biol.* 173:469–476. doi:10.1083/jcb.200512078

Vasu, S., S. Shah, A. Orjalo, M. Park, W.H. Fischer, and D.J. Forbes. 2001. Novel vertebrate nucleoporins Nup133 and Nup160 play a role in mRNA export. *J. Cell Biol.* 155:339–354. doi:10.1083/jcb.200108007

Walther, T.C., A. Alves, H. Pickersgill, I. Loïodice, M. Hetzer, V. Galy, B.B. Hülsmann, T. Köcher, M. Wilm, T. Allen, et al. 2003. The conserved Nup107-160 complex is critical for nuclear pore complex assembly. *Cell*. 113:195–206. doi:10.1016/S0092-8674(03)00235-6

Weis, K. 2003. Regulating access to the genome: nucleocytoplasmic transport throughout the cell cycle. *Cell*. 112:441–451. doi:10.1016/S0092-8674(03)00082-5

Zabel, U., V. Doye, H. Tekotte, R. Wepf, P. Grandi, and E.C. Hurt. 1996. Nic96p is required for nuclear pore formation and functionally interacts with a novel nucleoporin, Nup188p. *J. Cell Biol.* 133:1141–1152. doi:10.1083/jcb.133.6.1141

Zuleger, N., N. Korfali, and E.C. Schirmer. 2008. Inner nuclear membrane protein transport is mediated by multiple mechanisms. *Biochem. Soc. Trans.* 36:1373–1377. doi:10.1042/BST0361373

Downloaded from jcb.rupress.org on December 5, 2013

Theerthagiri et al., http://www.jcb.org/cgi/content/full/jcb.200912045/DC1

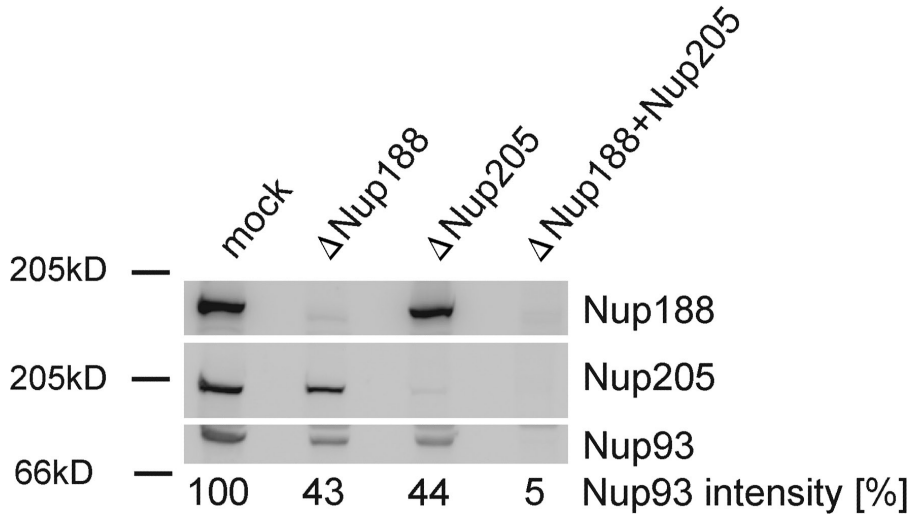

Figure S1. **Quantitation of the different Nup93-containing complexes.** Extracts were passed over a control IgG (mock), α-Nup188, α-Nup205, or a mixed α-Nup188/α-Nup205 matrix. Unbound material was analyzed by Western blotting, and the Nup93 signal was quantified and normalized to the mock control.

THE JOURNAL OF CELL BIOLOGY

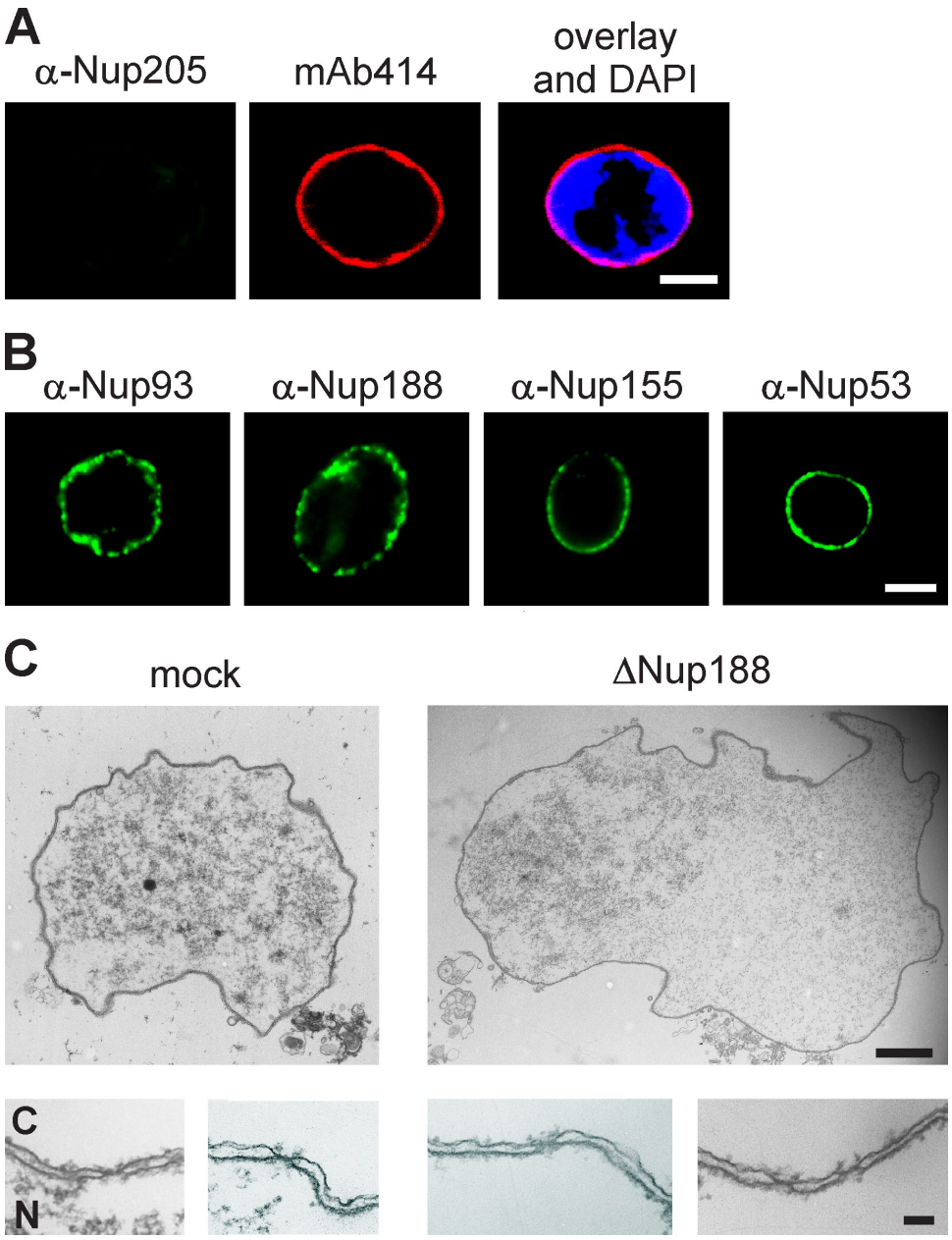

Figure S2. **Immunofluorescences of nuclei lacking Nup205–Nup93 and transmission electron images of mock- and Nup188–Nup93-depleted nuclei.** (A) Nup205–Nup93-depleted nuclei contain NPCs. Nuclei were assembled in Nup205–Nup93-depleted extracts for 90 min, fixed with 4% PFA, and analyzed with Nup205-specific antibodies (green) and the monoclonal antibody mAb414 (red). Chromatin is stained with DAPI. (B) Nup205–Nup93-depleted nuclei contain all other nucleoporins of the subcomplex. Samples were prepared as in A and analyzed by immunofluorescence with the indicated antibodies. (C) Electron microscopy analysis of Nup188–Nup93-depleted nuclei transmission electron microscopy analysis of nuclei assembled in mock- and Nup188–Nup93-depleted extracts. C indicates the cytoplasmic site, and N indicates the nucleoplasmic site of the NE. Bars: (A and B) 20 µm; (C, top) 1 µm; (C, bottom) 100 nm.

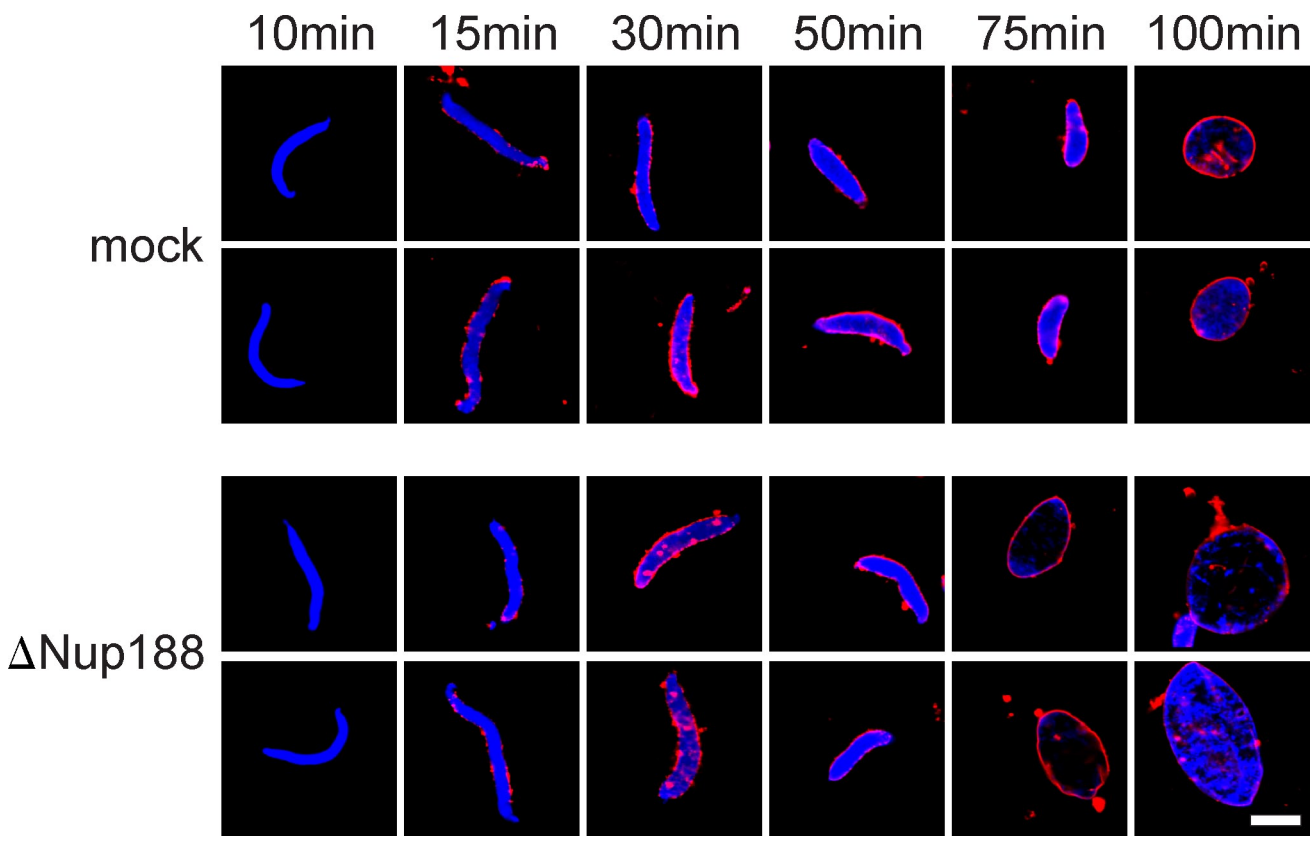

Figure S3. **Time course of nuclear assembly in mock- and Nup188–Nup93-depleted extracts.** Nup188–Nup93-depleted nuclei grow faster after NE closure. Demembranated sperm chromatin was incubated in mock- or Nup188–Nup93-depleted *Xenopus* egg extracts for 10 min. At this time, DiIC18-prelabeled membranes (red in overlay) were added to the reaction. Reactions were stopped at the indicated time points by fixation with 4% PFA and 0.5% glutaraldehyde, chromatin was stained with DAPI (blue), and the samples were analyzed by confocal microscopy. Bar, 20 µm.

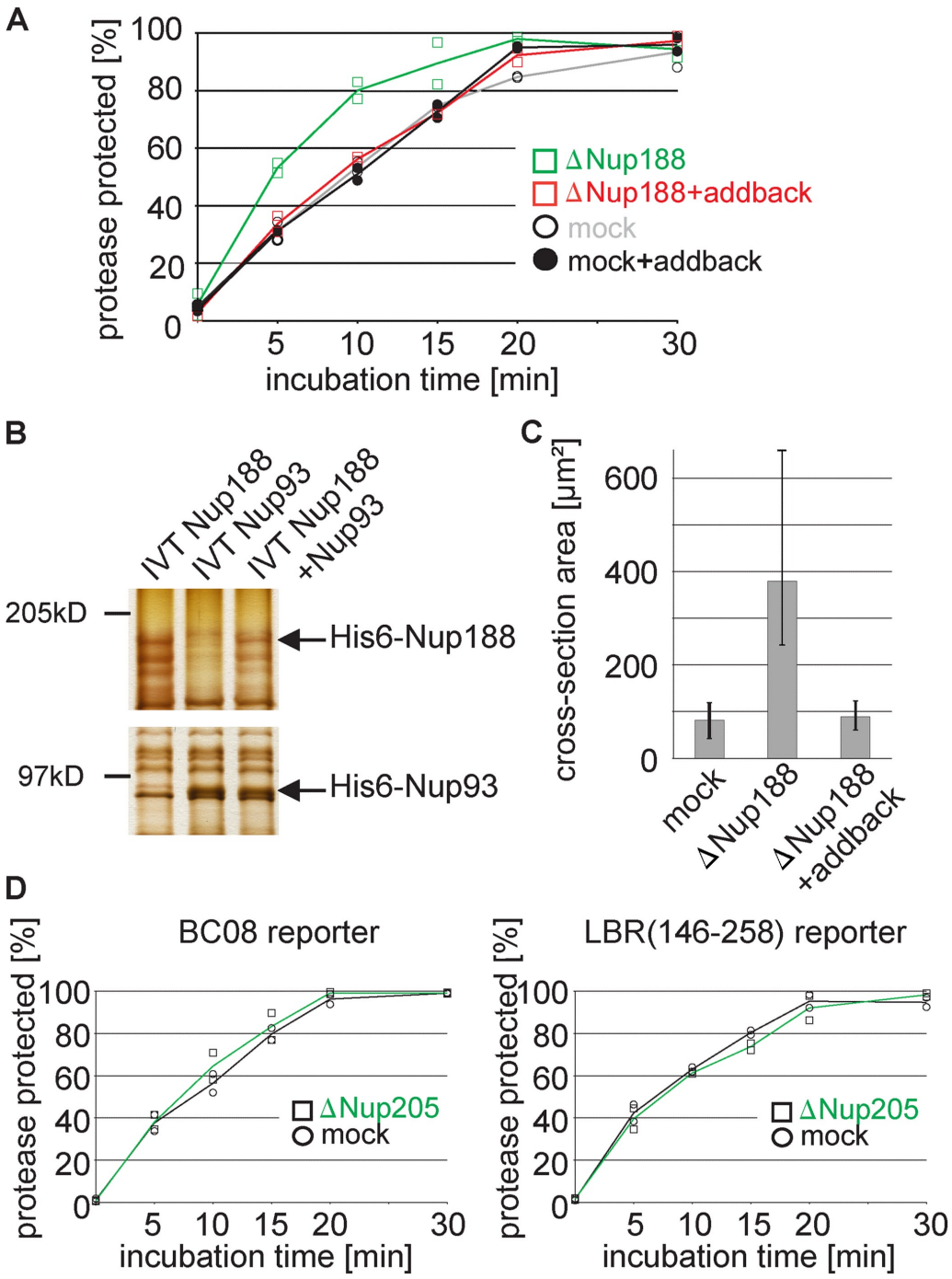

Figure S4. **INM targeting assays on nuclei lacking Nup188–Nup93 and Nup205–Nup93 and additional data of the addback experiments.** (A) Nup188–Nup93 depletion causes a faster delivery of an LBR reporter to the INM. Quantification of INM targeting of an LBR-based transport substrate. Squares are from Nup188–Nup93-depleted samples (green without and red with addition of in vitro translated Nup188–Nup93 [addback]), and circles are from mock-treated samples. Lines mark the mean of two independent experiments. (B) Analysis of the recombinant Nup188–Nup93 used in the addback experiments. In vitro translated (IVT) products of Nup188 alone, Nup93 alone, and combined Nup188–Nup93 were analyzed by SDS-PAGE (8%) and silver stained. Positions of full-length recombinant Nup188 and Nup93 are indicated. (C) The addback restores normal nuclear size in Nup188–Nup93-depleted nuclei. Quantitation of the cross-sectional area of nuclei assembled for 120 min in mock- or Nup188–Nup93– depleted extracts or Nup188–Nup93-depleted extracts supplemented with in vitro translated Nup188–Nup93 (addback). More than 30 randomly chosen chromatin substrates were counted per reaction. The mean of three independent experiments is shown, and error bars represent the total variation. (D) Nup205–Nup93-depleted nuclei show normal INM targeting. Quantification of INM targeting of the BC08- and LBR-based transport substrate from two independent experiments in Nup205–Nup93-depleted nuclei (squares and green line for mean) and mock-depleted nuclei (circles and black line for mean).

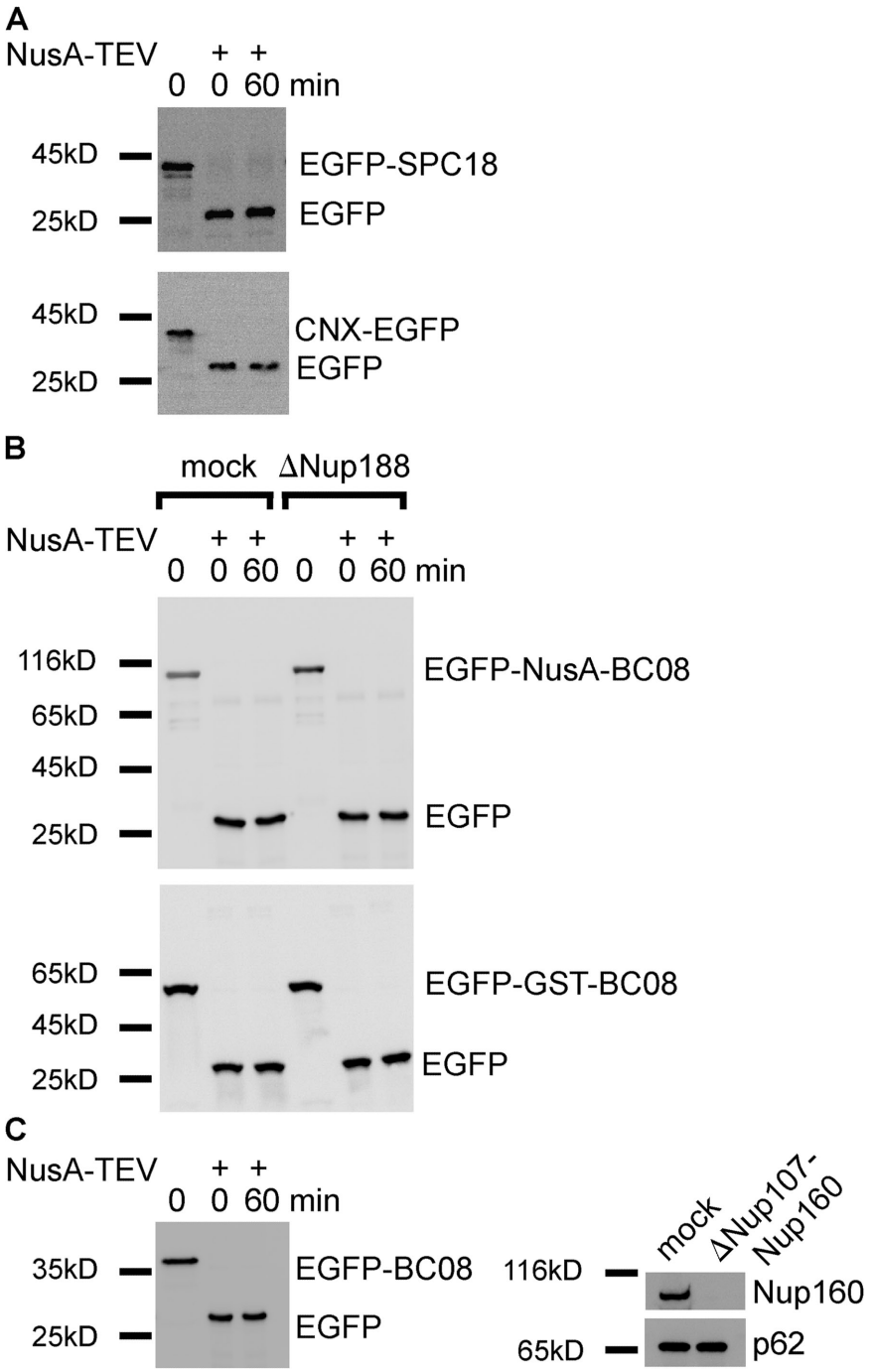

Figure S5. **Supporting experiments characterizing the INM targeting assay.** (A) ER proteins are not mistargeted in Nup188–Nup93-depleted nuclei. Two reporters based on bona fide ER membrane proteins (the signal peptidase subunit SPC18 [top] or a fragment of the transmembrane region and C-terminal part of the ER chaperon calnexin [CNX; bottom]) were used in Nup188–Nup93-depleted extracts. Where indicated, after 0 or 60 min, NusA-TEV protease was added, and samples analyzed by Western blotting. Protease protection was not detected even after 60 min, indicating that substrates did not localize to the INM. (B) Nup188–Nup93-depleted NPCs show normal size exclusion limits for targeting of INM proteins. The nucleoplasmic domain of the BC08 reporter was increased to 94 or 64 kD and used in mock- or Nup188–Nup93-depleted extracts. Where indicated, after 0 or 60 min, NusA-TEV protease was added, and samples were analyzed by Western blotting. Protease protection was not detected even after 60 min, indicating that substrates did not localize to the INM. (C) Nup107–Nup160-depleted nuclei show no INM targeting. The EGFP-BC08 reporter was used in Nup107–Nup160-depleted extracts (Walther et al., 2003). Where indicated, after 0 or 60 min, NusA-TEV protease was added, and samples were analyzed by Western blotting (left). Protease protection was not detected even after 60 min, indicating that substrates did not localize to the INM. Removal of Nup160 upon Nup107–Nup160 depletion is shown on the right. The nucleoporin p62 detected with the antibody mAb414 serves as a loading control.

Reference

Walther, T.C., A. Alves, H. Pickersgill, I. Loïodice, M. Hetzer, V. Galy, B.B. Hülsmann, T. Köcher, M. Wilm, T. Allen, et al. 2003. The conserved Nup107-160 complex is critical for nuclear pore complex assembly. *Cell*. 113:195–206. doi:10.1016/S0092-8674(03)00235-6

The EMBO Journal (2012) 31, 4072–4084 | © 2012 European Molecular Biology Organization | Some Rights Reserved 0261-4189/12
www.embojournal.org

THE EMBO JOURNAL

EMBO open

Dimerization and direct membrane interaction of Nup53 contribute to nuclear pore complex assembly

Benjamin Vollmer[1], Allana Schooley[1], Ruchika Sachdev[1], Nathalie Eisenhardt[1], Anna M Schneider[2], Cornelia Sieverding[1], Johannes Madlung[3], Uwe Gerken[4,5], Boris Macek[3] and Wolfram Antonin[1,*]

[1]Friedrich Miescher Laboratory of the Max Planck Society, Tübingen, Germany, [2]Max Planck Institute for Developmental Biology, Department of Biochemistry, Tübingen, Germany, [3]Proteome Center Tübingen, University of Tübingen, Tübingen, Germany and [4]Institute of Microbiology, University of Hohenheim, Stuttgart, Germany

Nuclear pore complexes (NPCs) fuse the two membranes of the nuclear envelope (NE) to a pore, connecting cytoplasm and nucleoplasm and allowing exchange of macromolecules between these compartments. Most NPC proteins do not contain integral membrane domains and thus it is largely unclear how NPCs are embedded and anchored in the NE. Here, we show that the evolutionary conserved nuclear pore protein Nup53 binds independently of other proteins to membranes, a property that is crucial for NPC assembly and conserved between yeast and vertebrates. The vertebrate protein comprises two membrane binding sites, of which the C-terminal domain has membrane deforming capabilities, and is specifically required for *de novo* NPC assembly and insertion into the intact NE during interphase. Dimerization of Nup53 contributes to its membrane interaction and is crucial for its function in NPC assembly.

The EMBO Journal (2012) **31,** 4072–4084. doi:10.1038/emboj.2012.256; Published online 7 September 2012
Subject Categories: membranes & transport; cell & tissue architecture
Keywords: nuclear envelope formation; nuclear pore complex assembly; nuclear membrane; Nup35; Nup53

Introduction

The defining feature of the eukaryotic cell is the compartmentalization of genetic material inside the nucleus. The spatial and temporal separation of transcription and translation has enabled eukaryotes to achieve a level of regulatory complexity that is unprecedented in prokaryotes. This is accomplished by the nuclear envelope (NE), which serves as the physical barrier between the cytoplasm and the nucleoplasm. Nuclear pore complexes (NPCs) are the exclusive gateways in the NE allowing diffusion of small substances and regulated trafficking of macromolecules up to a size of 15 nm for ribosomal subunits or even 50 nm for Balbiani ring particles (for review, see Wente and Rout, 2010; Hoelz *et al*, 2011; Bilokapic and Schwartz, 2012). NPCs form large pores in the NE, having a diameter of ~130 nm. Unlike other transport channels, NPCs span two lipid bilayers, at sites where the outer and inner membranes of the NE are fused. Therefore, NPCs are assumed to play an important role in deforming these membranes to form a pore as well as in stabilizing this highly curved pore membrane (Antonin *et al*, 2008).

Given the structural complexity and extraordinary transport capabilities of NPCs, it is quite surprising that these huge macromolecular assemblies of 40–60 MDa are only composed of ~30 different proteins. These nucleoporins (Nups) can be roughly categorized into those forming the structure of the pore and those mediating transport through the NPC. The latter class is characterized by a high number of FG repeats. Two evolutionary conserved subcomplexes form the major part of the structural scaffold. The Nup107–160 complex in metazoa, or the corresponding Nup84 complex in yeast, is the best characterized of these owing to an extensive set of genetic, biochemical and structural data. Computational and structural analyses suggest that this complex is related to vesicle coats (Devos *et al*, 2004; Mans *et al*, 2004; Brohawn *et al*, 2008). It is possible that these proteins form a coat-like assembly stabilizing the curved pore membrane of the NPC, which is analogous to clathrin or COPI and II during vesicle formation (Field *et al*, 2011; Onischenko and Weis, 2011). Notably, neither clathrin nor COP coats interact directly with the lipid bilayers. They are rather linked to the deformed membrane via adaptor and integral proteins (McMahon and Mills, 2004). Although three integral membrane proteins are known in the vertebrate NPC, it is unclear how a possible link between the Nup107–160 complex and the membrane is established.

The second major structural and evolutionarily conserved subcomplex of the NPC is the metazoan Nup93 complex, Nic96 in yeast, which might serve as a link to the pore membrane. In vertebrates, it is composed of five nucleoporins: Nup205, Nup188, Nup155, Nup93 and Nup53. Nup53, also referred to as Nup35 (Cronshaw *et al*, 2002), interacts with Nup93 and Nup155 (Hawryluk-Gara *et al*, 2005), corresponding to Nup170 and Nic96 in yeast (Marelli *et al*, 1998; Fahrenkrog *et al*, 2000). Nup155, Nup93 and Nup53 are each indispensable for NPC formation in vertebrates (Franz *et al*, 2005; Hawryluk-Gara *et al*, 2008; Mitchell *et al*, 2010; Sachdev *et al*, 2012). Interestingly, Nup53 and its corresponding yeast homologues Nup53p and Nup59p interact with the transmembrane nucleoporin NDC1, thereby potentially linking the NPC to the pore membrane (Mansfeld *et al*, 2006; Onischenko *et al*, 2009). Although NDC1 is essential in both vertebrates and yeast (Winey *et al*, 1993; West *et al*, 1998; Mansfeld *et al*, 2006; Stavru *et al*, 2006) it is not found in all eukaryotes (Mans *et al*, 2004; DeGrasse *et al*, 2009; Neumann *et al*, 2010), suggesting that in

*Corresponding author. Friedrich Miescher Laboratory of the Max Planck Society, Spemannstraße 39, Tübingen 72076, Germany.
Tel.: +49 70 7160 1836; Fax: +49 70 7160 1801;
E-mail: wolfram.antonin@tuebingen.mpg.de
[5]Present address: Lehrstuhl für Experimentalphysik IV, University of Bayreuth, Universitätsstrasse 30, 95447 Bayreuth, Germany

Received: 16 April 2012; accepted: 21 August 2012; published online: 7 September 2012

 ©2012 European Molecular Biology Organization

some organisms NPCs can form in the absence of a Nup53–NDC1 interaction. Indeed, *Aspergillus nidulans* is viable in the absence of all three known transmembrane nucleoporins (Liu *et al*, 2009). This suggests that there are alternative modes of interaction between the nucleoporins and the pore membrane.

Here, we show that Nup53 binds membranes directly and independently of other proteins. It possesses two membrane interaction regions, which are important for NPC assembly. Although either site is sufficient for NPC assembly at the end of mitosis, the C-terminal membrane binding site of Nup53 is specifically required for NPC assembly during interphase, probably because of its membrane deforming capabilities.

Results

Nup53 is a membrane binding protein

Overexpression of Nup53 in yeast causes expansion of the NE (Marelli *et al*, 2001). Similar membrane proliferation phenotypes have been observed upon overexpression of nuclear membrane binding proteins, such as lamin B (Prufert *et al*, 2004). Yeast Nup53 contains a C-terminal region predicted to form an amphipathic helix (Marelli *et al*, 2001; Patel and Rexach, 2008), which could serve as a membrane binding module. However, Nup53 interacts with the integral pore membrane protein NDC1 in both yeast and metazoa (Mansfeld *et al*, 2006; Onischenko *et al*, 2009) and thus might be linked to the membrane via this interaction. We therefore tested whether Nup53 is able to interact with membranes independently of other proteins.

To assay for membrane binding, we generated liposomes with an average radius of ~150 nm. These liposomes were incubated with different, recombinantly expressed nucleoporins and floated through sucrose cushions. Liposome binding proteins were recovered after centrifugation from the top fraction (Figure 1A). A Nup133 membrane binding fragment (Drin *et al*, 2007) was used as a positive control and found in the liposome containing top fraction (Figure 1A). Similarly, Xenopus Nup53 was found in the top fraction, indicating membrane interaction. In contrast, a fragment of the FG repeat-containing nucleoporin Nup98 did not bind liposomes. Thus, Xenopus Nup53 binds directly to

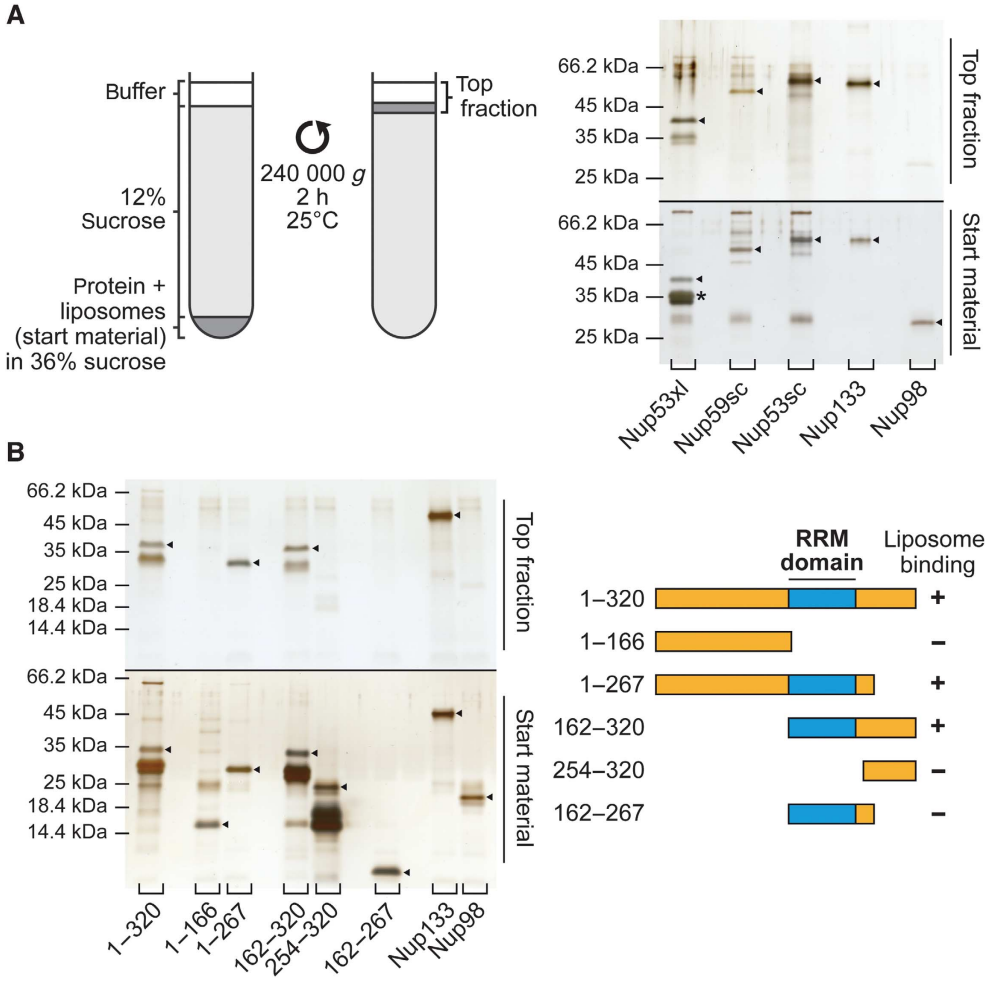

Figure 1 Nup53 directly binds membranes. (**A**) 3 μM recombinant Xenopus Nup53 (Nup53xl), the two yeast orthologues Nup59sc and Nup53sc as well as fragments of Nup133 and Nup98 as positive and negative controls, respectively, were incubated with 6 mg/ml fluorescently labelled liposomes prepared from *E. coli* polar lipids and floated through a sucrose gradient as indicated on the left. Top fractions of the gradient, as well as 3% of the starting material, were analysed by SDS–PAGE and silver staining. Please note that Nup53 is sensitive to C-terminal degradation (*) and that the full-length protein significantly enriched in the liposome bound fraction. (**B**) Full-length (1–320) and different fragments of Xenopus Nup53 as well as fragments of Nup133 and Nup98 were analysed for liposome binding as in (**A**). Only fragments comprising the RRM domain (indicated in blue in the schematic representation) bound liposomes.

©2012 European Molecular Biology Organization

membranes independently of other interacting proteins. To determine whether this feature is conserved during evolution, we tested the two yeast homologues Nup53p and Nup59p, which both bound liposomes (Figure 1A).

We next sought to define the regions of Xenopus Nup53 important for its membrane interaction. Nup53 can be roughly divided into three parts: the N-terminus (amino acid (aa) 1–166), a middle region (aa 166–267) comprising a conserved RNA recognition motif (RRM) domain and the C-terminus (aa 267–320) (Figure 1B). We generated different N- and C-terminal truncations of Nup53 and tested them for liposome binding (Figure 1B). While full-length Nup53 (aa 1–320) bound to liposomes, the N-terminal region of the protein (aa 1–166) showed no binding. Extending this fragment by 100 aa to include the RRM domain rendered the protein capable of membrane binding (aa 1–267). The C-terminal half of Nup53 (aa 162–320), which included the RRM domain, also interacted with liposomes. However, a fragment consisting of only the C-terminal region of Nup53 but lacking the RRM domain (aa 254–320) could not bind liposomes. Surprisingly, a fragment comprising only the RRM domain (aa 162–267) did not bind liposomes showing that the RRM domain is necessary but not sufficient for Nup53 membrane binding.

Nup53 dimerization is necessary for membrane binding and NPC formation

As the RRM domain is crucial for Nup53 membrane interaction we investigated the function of this domain. The crystal structure of the mouse domain suggests that it acts as a dimerization rather than an RNA binding module (Handa *et al*, 2006). We designed a mutant of this domain by exchanging two amino acids (F172E/W203E) in the dimerization surface. Size exclusion chromatography in combination with multi-angle laser light scattering revealed that the resulting fragment was monomeric (Figure 2A).

To confirm that the dimerization occurs also *in vivo*, we performed co-transfection experiments in HeLa cells using HA- and myc-tagged Xenopus Nup53. Either α-HA or α-myc antibodies immunoprecipitated both HA- and myc-tagged wild-type Nup53 indicating that the proteins formed a complex (Figure 2B, lanes 5 and 10). If cells were transfected with either construct separately before they were mixed for protein extraction, then no co-immunoprecipitation was observed (Figure 2B, lanes 9 and 14) demonstrating that complex formation cannot occur under the conditions of the immunoprecipitation. Co-transfections of RRM mutants as well as RRM mutants and wild-type protein did not result in complex formation (Figure 2B, lanes 6–8 and 11–13) indicating that the F172E/W203E exchange inhibited dimerization/oligomerization.

Next, we tested the effect of these mutations on membrane binding. In the context of the full-length protein, these mutations decreased liposome binding by 70% (Figure 2C) suggesting that the dimerization of Nup53 is important for its membrane interaction.

As Nup53 is essential for postmitotic NPC formation (Hawryluk-Gara *et al*, 2008) we examined the relevance of Nup53 membrane binding for this. We employed *Xenopus laevis* egg extracts to study nuclear reformation *in vitro* (Lohka, 1998). With antibodies against Nup53 we depleted the endogenous protein without co-depletion of other nucleoporins including the other members of the Nup93 complex: Nup93, Nup155, Nup205 and Nup188 (Figure 2D). These depleted extracts were incubated with sperm heads serving as chromatin template. In the absence of Nup53, NPC formation was blocked (Figure 2E) as reported (Hawryluk-Gara *et al*, 2008). This was indicated by the absence of immunofluorescent signal on the chromatin surface for mab414, an antibody recognizing several nucleoporins that represent a major subfraction of the NPC. Addition of recombinantly expressed wild-type Nup53 to the depleted extracts at levels similar to the endogenous protein (Figure 2D) restored NPC formation. The recombinant protein was integrated into NPCs as indicated by immunostaining with a Nup53 antibody. In contrast, the dimerization and membrane binding defective Nup53 mutant (1–320 F172E/W203E) was unable to substitute for the endogenous protein in NPC formation (Figure 2E).

Individual depletion of several nucleoporins essential for NPC assembly from Xenopus egg extracts also blocks formation of a closed NE. These nucleoporins include POM121, NDC1, Nup155, Nup93 (Antonin *et al*, 2005; Franz *et al*, 2005; Mansfeld *et al*, 2006; Sachdev *et al*, 2012) and Nup53 (Hawryluk-Gara *et al*, 2008). Upon Nup53 depletion, membrane vesicles bound to the chromatin surface but did not fuse to form a closed NE (Figure 2F; Hawryluk-Gara *et al*, 2008). This phenotype was rescued by the wild-type Nup53 protein, but not by the dimerization defective mutant. Together with the liposome-binding assay, this suggests that Nup53 membrane binding could be important for NPC assembly and formation of a closed NE. However, we cannot exclude that the RRM mutant also affects interaction of Nup53 with other nucleoporins. Indeed, in GST pull-down assays we observed a slight reduction of Nup93, Nup205 and Nup155 binding to Nup53 in the context of the RRM mutant as compared to the wild-type protein (Supplementary Figure S1A). In contrast, NDC1 binding to Nup53 was unaffected by the dimerization mutant (Supplementary Figure S1B).

Nup53 possesses two membrane binding regions

These results reveal a crucial role for Nup53 dimerization via its RRM domain in NE reformation. However, the RRM domain alone did not bind to membranes. We tested different Nup53 truncations for liposome binding to map the membrane interaction sites (Figure 3A; Supplementary Figure S2 shows the purity of all recombinant proteins used in the different liposome experiments). An N-terminal fragment of Nup53 including the RRM domain (aa 1–267) bound to liposomes with only a slightly decreased binding efficiency, 83% of the levels of the full-length protein. Further truncations from the N-terminus revealed a minimal membrane binding region between aa 93 and 107 as indicated by a four-fold decrease in liposome binding upon removal of these 15 amino acids. This region comprises a patch of basic residues, which as in other membrane binding proteins might be important for the interaction with negatively charged lipids. Indeed, changing two residues to negatively charged residues (R105E/K106E) abolished membrane binding (Figure 3A, 83% reduction as compared to the 93–267 fragment).

Interestingly, the N-terminal membrane binding region of Nup53 contains one of two regions that were differentially phosphorylated depending on the cell-cycle stage (Supplementary Figure S3; Supplementary Table S1). Two

 ©2012 European Molecular Biology Organization

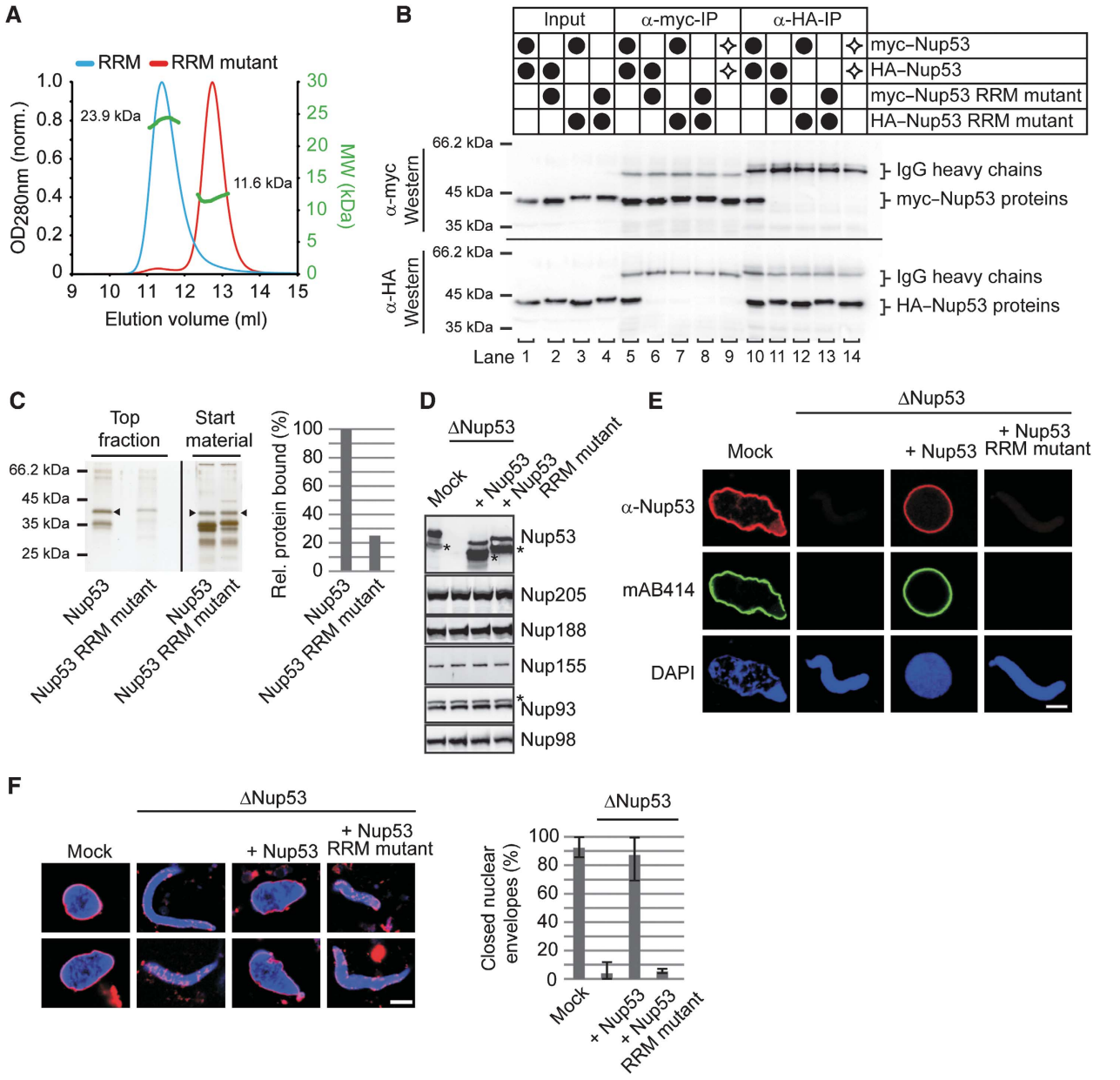

Figure 2 Dimerization of the RRM domain is essential for Nup53 membrane binding and nuclear pore complex formation. (**A**) Size exclusion chromatography on a Superdex75 10/300 GL column followed by multi-angle static laser light scattering of the Xenopus Nup53 RRM domain and the F172E/W203E mutant, which rendered the domain monomeric. The green dots relate to the secondary axis and show the molecular weight of the eluting particles. (**B**) HeLa cells were co-transfected with myc- and HA-tagged Xenopus Nup53 wild-type protein and/or dimerization mutant as indicated (●). Proteins were immunoprecipitated from cell lysates with α-myc or α-HA antibodies, and analysed by western blotting. Ten per cent of the start materials are loaded as input. To exclude complex formation after cell lysis, extracts from single transfected myc–Nup53 and HA–Nup53 cell batches were mixed and processed for immunoprecipitation (✧). Under these conditions, no co-precipitation was observed. (**C**) Full-length Xenopus Nup53 and the respective F172E/W203E mutant (RRM mutant) were analysed for liposome binding as in Figure 1. The right panel shows the quantitation of liposome binding analysed by western blotting and normalized to the levels of the wild-type protein (one out of two independent experiments). (**D**) Western blot analysis of mock, Nup53-depleted (ΔNup53) and Nup53-depleted extracts supplemented with recombinant wild-type protein (Nup53) or the dimerization mutant (Nup53 RRM mutant), respectively. Recombinant proteins were added to approximate endogenous Nup53 levels (judged by the full-length protein, please note for both endogenous and recombinant Nup53 proteins C-terminal degradation products (*)). The recombinant Nup53 migrated slightly faster than the endogenous protein due to absence of eukaryotic post-translational modifications. The Nup93 antibody recognizes a slightly slower migrating cross-reactivity by western blotting (*). (**E**) Nuclei were assembled in mock, Nup53-depleted extracts or Nup53-depleted extracts supplemented with wild-type protein (Nup53) or the dimerization mutant for 120 min, fixed with 4% PFA and analysed with Nup53 antibodies (red) and mAb414 (green). Chromatin was stained with DAPI. Bar: 10 μm. (**F**) Nuclei were assembled as in (**E**), fixed with 2% PFA and 0.5% glutaraldehyde and analysed for chromatin (blue: DAPI) and membrane staining (red: DiIC18, bar: 10 μm). Right panel shows the quantitation of chromatin substrates with a closed nuclear envelope (averages of three independent experiments with >300 randomly chosen chromatin substrates per sample, error bars represent the range).

amino acids identified, Serine 94 and Threonine 100, are phosphorylated during mitosis, most likely by cdk 1 as they possess a consensus site for this kinase (Blethrow *et al*, 2008). To investigate the impact of this modification on membrane binding, we generated mutants mimicking the phosphorylated (S94E/T100E) and the unphosphorylated

©2012 European Molecular Biology Organization

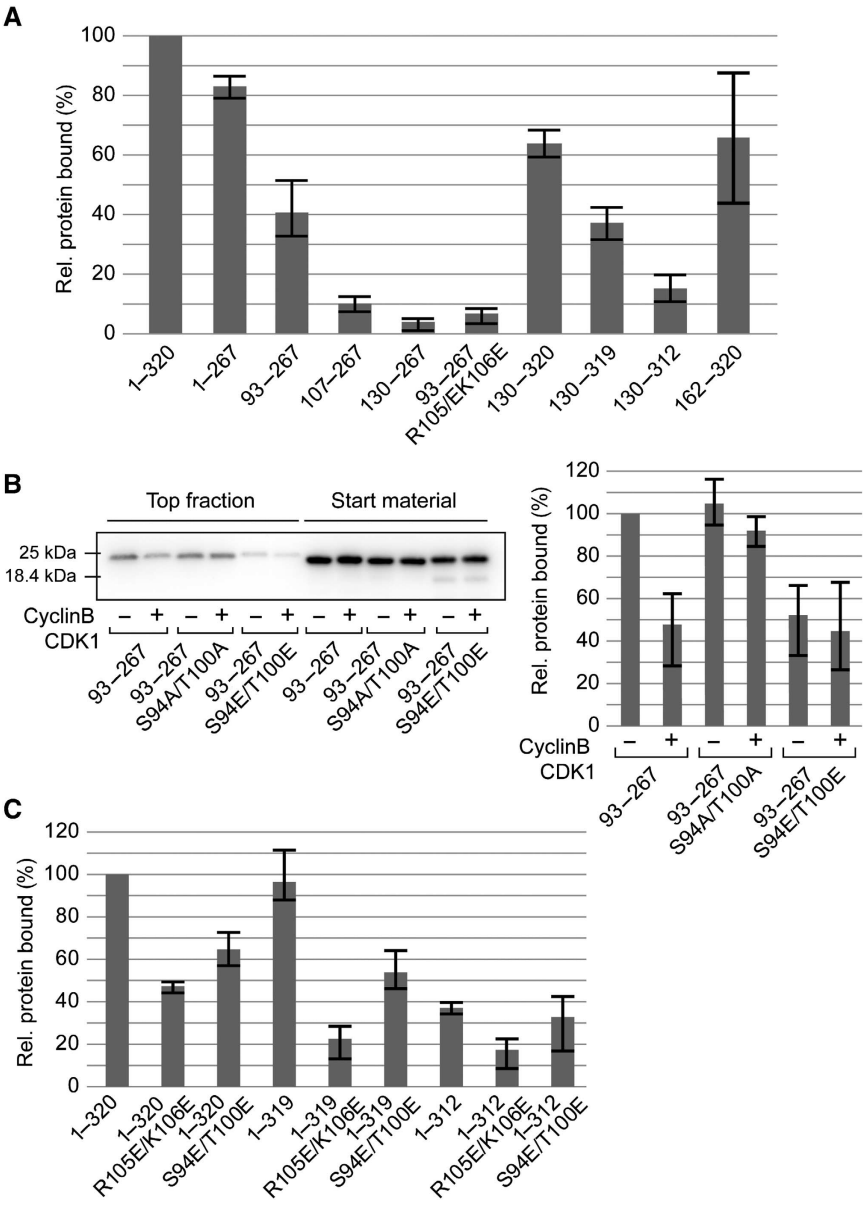

Figure 3 Nup53 possesses two independent membrane binding regions. (**A**) Full-length protein (1–320) and different fragments of Xenopus Nup53 were quantitatively analysed for liposome binding as in Figure 2B (normalized to the full-length protein, three independent experiments). (**B**) A fragment comprising the first membrane binding region and the RRM domain (93–267) as well as a phosphomimetic (93–267 S94E/T100E) and a non-phosphorylatable mutant (93–267 S94A/T100A) was treated with CyclinB/CDK1. Samples were tested for liposome binding as in Figure 1A and analysed by western blotting (left panel) and quantified (right panel: two independent experiments, normalized to liposome binding of wild-type fragment without CDK1 pretreatment). (**C**) Mutants/truncations affecting the N- (1–320 R105E/K106E, 1–320 S94E/T100E), the C-terminal (1–319, 1–312) as well as both (1–319 R105E/K106E, 1–319 S94E/T100E, 1–312 R105E/K106E, 1–312 S94E/T100E) membrane binding sites of Nup53 were quantitatively assayed for liposome binding in the context of full-length protein (normalized to wild-type protein (1–320), average of three independent experiments, error bars represent the range).

(S94A/T100A) state of the protein. The phosphomimetic mutant was impaired in liposome binding (Figure 3B, reduced by 50% compared to the 93–267 fragment) while the S94A/T100A control bound to liposomes with efficiency comparable to the wild type. Furthermore, *in vitro* phosphorylation by CyclinB/CDK1 reduced liposome binding of the wild-type protein by 50%, levels similar to the phosphomimetic mutant (S94E/T100E), but did not affect the S94A/T100A mutant, suggesting that mitotic phosphorylation regulates the membrane binding of Nup53.

The C-terminal part of Nup53 also interacts with membranes, an activity that requires the presence of the RRM domain (Figure 1B). Fragments comprising both regions showed efficient binding to liposomes (aa 130–320 and 162–320) (Figure 3A). The second membrane binding region was mapped to the absolute C-terminus of Nup53 as deletion of the last amino acid reduced liposome binding by 42% (aa 130–319) and removal of the last eight amino acids abolished liposome binding (aa 130–312).

These data suggest that Nup53 possesses two independent membrane binding sites. Consistently, in the context of the full-length protein mutations in the N-terminal site (R105E/K106E as well as S94E/T100E) reduced liposome binding by 50 and 40% (Figure 3C). Deletion of the

 ©2012 European Molecular Biology Organization

C-terminal amino acid had a less prominent effect, but removal of the last eight amino acids reduced liposome binding by 60%. The combination of mutations and truncations affecting both binding sites showed an additive effect supporting the view that each site is individually capable of membrane binding. Our data also suggest that the N-terminal membrane interaction is mediated via a pair of basic amino acids. The N-terminal binding site is additionally dependent on membrane curvature, the fragment binding less efficiently to more highly curved membranes (Supplementary Figure S4). Conversely, the C-terminal membrane binding site is less sensitive to membrane curvature and seems to largely depend on the last amino acid, a hydrophobic tryptophan. This could indicate that the two membrane interaction sites operate via different binding mechanisms. In both cases, the dimerization of Nup53 via the RRM domain is important: mutations in the individual membrane binding fragments (93–267 F172E/W203E and 130–320 F172E/W203E) rendering the RRM domain monomeric reduced their membrane interaction (Supplementary Figure S5).

Nup53 membrane binding is necessary for NPC formation

The Nup53 mutant defective in RRM dimerization, which showed reduced membrane binding, was unable to substitute for the endogenous protein in nuclear assembly (Figure 2). We therefore analysed the contribution of each of the membrane interaction sites to NPC assembly by substituting endogenous Nup53 with constructs defective in the N-terminal membrane interaction site, lacking the C-terminal membrane interaction site, or comprising a combination of both deficient sites (Figure 4A). Surprisingly, mutants of the N-terminal membrane binding site (1–320 R105E/K106E and 1–320 S94E/T100E) supported NPC formation as indicated by mAB414 staining (Figure 4A). They also supported formation of a closed NE (Figure 4A and B). Correspondingly, mutations in the N-terminal binding region did not alter the NE localization of any other nucleoporins (Figure 4D). These nucleoporins include members of the Nup93 complex (Nup93, Nup188, Nup205 and Nup155) as well as the transmembrane nucleoporins NDC1 and POM121. Accordingly, interactions of these mutants with Nup93 and Nup205, which bind the N-terminal part of Nup53 (Fahrenkrog *et al*, 2000; Hawryluk-Gara *et al*, 2008), were unaffected as shown by GST pull downs (Supplementary Figure S1A).

The fragment lacking the C-terminal tryptophan (1–319) also supported NPC assembly and formation of a closed NE. Deletion of this tryptophan did not interfere with Nup53 binding to NDC1 or Nup155 (Supplementary Figure S1B), two binding partners interacting with the C-terminal region. The truncation lacking the last eight C-terminal amino acids (1–312) also allowed for NPC assembly and formation of a closed NE. All tested nucleoporins were located at the NE in these nuclei (Figure 4D). Notably, this truncation did not bind to NDC1 (Supplementary Figure S1B), supporting the view that the Nup53–NDC1 interaction is not required for postmitotic NPC formation (Hawryluk-Gara *et al*, 2008). These observations suggest that a single Nup53 membrane binding region is sufficient for NPC assembly at the end of mitosis.

In contrast to the Nup53 mutants and truncations that abrogate one membrane binding region, mutants affecting both membrane binding sites (1–319 R105E/K106E, 1–319 S94E/T100E, 1–312 R105E/K106E and 1–312 S94E/T100E) did not support NPC assembly and NE reformation (Figure 4A). Under these conditions, MEL28 (also referred to as ELYS) as well as Nup107, which both bind early to chromatin during the NPC assembly process (Galy *et al*, 2006; Rasala *et al*, 2006; Franz *et al*, 2007), as well as the transmembrane nucleoporins, NDC1 and POM121, were detected on the chromatin (Figure 4D). In contrast, Nup205, Nup188, Nup155 and Nup93 were not recruited. However, this lack of recruitment as well as the block in NPC assembly is unlikely to be caused by disrupting Nup53 binding to these interaction partners as the mutations introduced did not affect binding to Nup93, Nup205 and Nup155 in GST pull downs (Supplementary Figure S1A). It is also unlikely that the loss of the Nup53–NDC1 interaction caused this phenotype as the Nup53 fragment 1–312 still allowed for postmitotic NPC assembly but was not able to bind NDC1 (Supplementary Figure S1B). Nup58 representing an FG-containing nucleoporin of the central channel as well as the peripheral nucleoporin Nup88 was also absent on chromatin in the presence of a Nup53 construct that lacked both membrane binding regions (1–312 R105E/K106E) (Figure 4D). These data support the conclusion that the direct Nup53 membrane interaction is important for postmitotic NPC formation.

Interphasic NPC assembly requires the C-terminal membrane binding site of Nup53

Metazoan NPC assembly occurs in two different stages of the cell cycle: at the end of mitosis when NPCs assemble concomitantly with the reforming NE and during interphase when new NPCs are assembled and integrated into the intact NE (Antonin *et al*, 2008; Doucet and Hetzer, 2010). Recent data suggest that there are different requirements for these two possible modes of NPC assembly (Doucet *et al*, 2010). The *in vitro* nuclear assemblies described up to now reflect the situation at the end of mitosis. We therefore assayed whether the mutants that support postmitotic NPC assembly also support NPC formation during interphase. In an experimental set-up developed by the Hetzer laboratory (Dawson *et al*, 2009), nuclei with newly integrated NPCs can be visualized by an influx of dextrans when nucleoporins forming the permeability barrier of newly formed NPCs are depleted. Under these conditions, mutants defective in the N-terminal membrane binding site of Nup53 (1–320 R105E/K106E and 1–320 S94E/T100E) supported interphasic NPC formation (Figure 5A). Conversely, Nup53 truncations affecting the C-terminal membrane binding site did not substitute for the wild-type protein in this mode of NPC assembly. This indicates that, in contrast to postmitotic NPC assembly where both membrane binding regions individually support NPC formation, only the C-terminal membrane binding site of Nup53 is required for interphasic NPC formation.

Interestingly, the Nup53 truncation lacking the C-terminal tryptophan (1–319) did not support interphasic NPC assembly in the dextran influx assay despite the fact that membrane interaction is only slightly reduced (Figure 3C). We confirmed these findings in an independent assay directly counting NPCs identified by mAB414 immunostaining (D'Angelo *et al*, 2006; Theerthagiri *et al*, 2010). NPC numbers were determined on nuclei where NPCs assembled in the postmitotic and interphasic mode and nuclei where interphasic

©2012 European Molecular Biology Organization

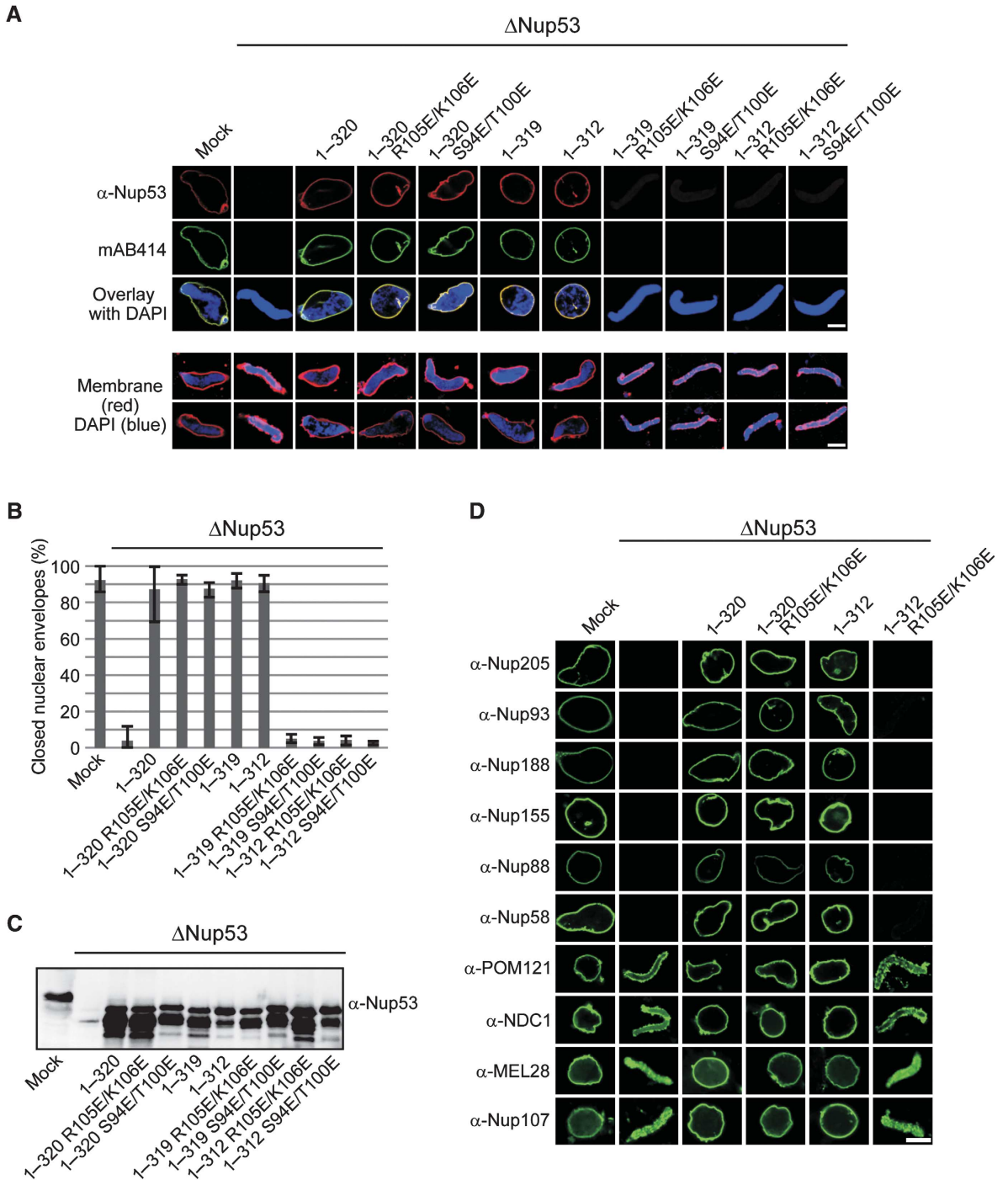

Figure 4 Either of the two membrane binding regions of Nup53 is sufficient for postmitotic NPC assembly. (**A**) Nuclei were assembled in mock, Nup53-depleted extracts or Nup53-depleted extracts supplemented with wild-type Nup53 (1–320), constructs featuring mutations in the N-terminal membrane binding site (1–320 R105E/K106E, 1–320 S94E/T100E), constructs lacking the C-terminal membrane binding site (1–319, 1–312) or both (1–319 R105E/K106E, 1–319 S94E/T100E, 1–312 R105E/K106E, 1–312 S94E/T100E), respectively. Samples were fixed after 120 min with 4% PFA and analysed with Nup53 antibodies (red) and mAb414 (green, upper panel) or with 2% PFA and 0.5% glutaraldehyde and analysed for chromatin (blue: DAPI) and membrane staining (red: DiIC18, lower panel). Bars: 10 μm. (**B**) Quantitation of chromatin substrates with a closed NE was done as in Figure 2F. (**C**) Western blot analysis of extracts used in (**A**) showing the re-addition of the recombinant proteins to approximately endogenous Nup53 levels. (**D**) Nuclei were assembled as in (**A**), fixed with 4% PFA and analysed with respective antibodies. Bar: 10 μm.

NPC formation was specifically blocked by addition of 2 μM importin β (D'Angelo *et al*, 2006; Theerthagiri *et al*, 2010). The NPC numbers of nuclei assembled for 120 min in the presence of recombinant wild-type Nup53 as well as the Nup53 mutant defective in the N-terminal membrane binding site (1–320 R105E/K106E) were reduced by importin β addition after 50 min, i.e., when a closed NE with intact NPC was formed (Figure 5B). In contrast, the Nup53 truncation lacking the C-terminal tryptophan showed after 120 min a lower number of NPCs, which was not sensitive to importin β addition, indicating that in this condition interphasic NPC assembly did not occur.

 ©2012 European Molecular Biology Organization

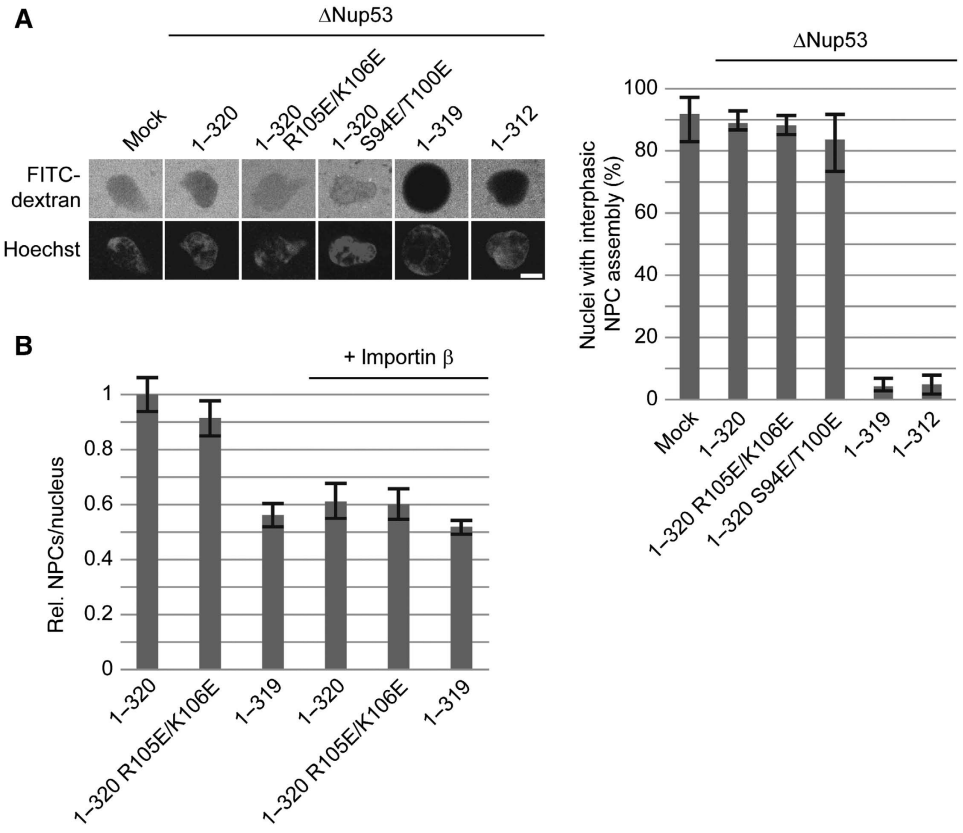

Figure 5 The C-terminal Nup53 membrane binding site is essential for interphasic nuclear pore complex (NPC) formation. (**A**) Nuclei were preassembled in mock or Nup53-depleted extracts supplemented with wild-type full-length protein (1–320), constructs with a mutated N-terminal membrane binding site (1–320 R105E/K106E, 1–320 S94E/T100E), or constructs lacking the C-terminal membrane interaction site (1–319, 1–312), respectively. After 90 min, the samples were supplemented with cytosol depleted of Nup53 and FG-containing nucleoporins. After 60 min, FITC-labelled 70-kDa dextran and Hoechst was added. Bar: 10 μm. The right panel shows the quantitation of three independent experiments with >300 randomly chosen chromatin substrates per sample. Error bars represent the range. (**B**) Nuclei were assembled in Nup53-depleted extracts supplemented with wild-type full-length protein (1–320), a construct with a mutated N-terminal membrane binding site (1–320 R105E/K106E), or a construct lacking the last C-terminal amino acid (1–319), respectively, for 120 min. Where indicated, *de novo* NPC assembly was blocked by the addition of 2 μM importin β after 50 min and nuclei were further incubated for 70 min. For each construct, total NPC numbers per nucleus identified by mAB414 immunofluorescence were quantified from 20 nuclei in 2 independent experiments and normalized to the wild-type full-length protein. Error bars represent the s.e. of the mean.

Nup53 can deform membranes

Many membrane binding proteins induce membrane deformation. Such a function is of special interest in the context of NPC formation as NPCs are integrated in the NE at sites where both nuclear membranes are deformed and fused to a pore. We therefore analysed the morphology of Nup53-bound liposomes using electron microcopy. As reported (Daumke *et al*, 2007), tubulation of liposomes is induced by the EH domain-containing protein EHD2 (Figure 6A). Interestingly, a Nup53 fragment containing both membrane binding sites (93–320) strongly induced liposome tubulation indicating a membrane deformation capability. A shorter fragment containing only the N-terminal membrane binding site and including the RRM domain (93–267) did not induce membrane tubulation, despite the fact that it was able to bind liposomes (Figure 3A). In contrast, a fragment comprising the RRM domain and the full C-terminus of Nup53 (130–320) strongly induced membrane tubulation indicating that the second, C-terminal membrane binding domain deforms membranes. Accordingly, fragments lacking the last eight residues (130–312), and therefore the second membrane binding site or only the last C-terminal tryptophan (130–319) did not cause membrane tubulation. Consistently, fragments mutated in the first, or N-terminal, membrane binding region of Nup53 (93–320 R105E/K106E and 93–320 S94E/T100E) induced membrane deformation. Efficient membrane binding of Nup53 depends not only on the individual membrane binding domains but also on dimerization (Figure 2C; Supplementary Figure S5). To determine the importance of the dimerization of Nup53 for membrane tubulation the RRM mutants of fragments that contained either both (93–320 RRM mutant) or only the C-terminal binding site (130–320 RRM mutant) were tested. Neither of the two fragments induced membrane tubulation emphasizing that membrane interaction is indeed required for this phenotype. The membrane binding fragment of Nup133 did not induce detectable tubulation, emphasizing that membrane binding alone does not account for membrane deformation.

Similar to Xenopus Nup53 both yeast isoforms—Nup53p and Nup59p—induced membrane tubulation (Figure 6B). This indicates that, in addition to membrane binding (Figure 1A), the membrane bending activity of Nup53 is conserved during evolution which suggests an important role for Nup53-induced membrane deformation in NPC formation and/or function.

©2012 European Molecular Biology Organization

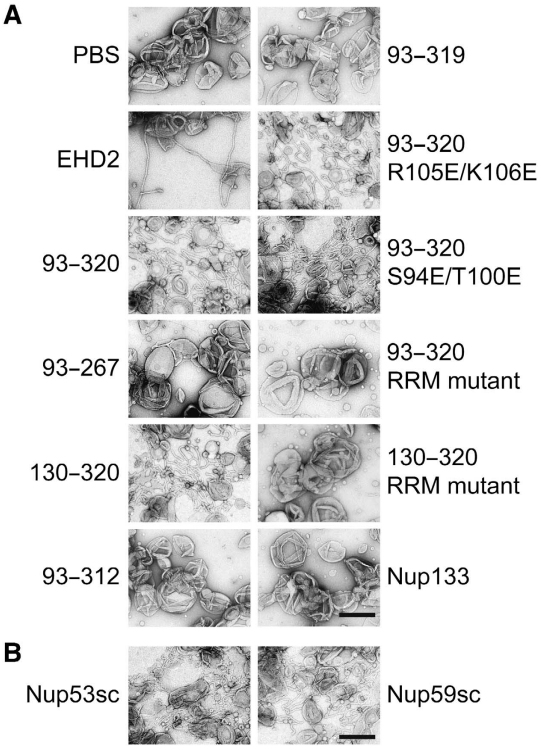

Figure 6 The C-terminus of Nup53 binds and deforms membranes. (**A**) Folch fraction I liposomes were incubated where indicated with 3 μM recombinant Nup53 fragments containing both (93–320), the N-terminal (93–267) or C-terminal (130–320) membrane binding sites including the RRM domain as well as fragments and mutants where the C-terminal (93–312, 93–319), the N-terminal (93–320 R105E/K106E, 93–320 S94E/T100E) membrane interaction site or the dimerization (93–320 RRM mutant and 130–320 RRM mutant) is compromised. The liposome deforming protein EHD2 (aa 1–543) and a fragment of Nup133 were used as positive and negative control, respectively. (**B**) 3 μM recombinant yeast Nup53 and Nup59 protein was incubated with liposomes and analysed. Bars: 400 nm.

Discussion

Here, we show that Nup53 binds membranes directly and independently of other proteins. We demonstrate that dimerization of the protein via its RRM domain is necessary for membrane interaction and identify two separate membrane binding regions within the protein. Binding of Nup53 to membranes is important for NPC assembly. Although either of the two membrane interaction regions is sufficient for postmitotic NPC formation, NPC assembly in interphase specifically requires the C-terminal membrane binding site, probably because of its capacity to induce membrane deformation.

Our results support the view that Nup53 is crucial for postmitotic NPC assembly in Xenopus egg extracts (Hawryluk-Gara *et al*, 2008). Depletion of Nup53 blocks NPC assembly and the formation of a closed NE. This phenotype is rescued by the addition of recombinant Nup53, confirming the specificity of the depletion (Hawryluk-Gara *et al*, 2008; Figures 2 and 4). In agreement with the cell-free data, RNAi-mediated depletion of Nup53 in HeLa cells results in severe nuclear morphology defects and reduced levels of Nup93, Nup205 and Nup155 at the nuclear rim, suggestive of defects in NPC assembly (Hawryluk-Gara *et al*, 2005). In *C. elegans*, RNAi knockdown of Nup53 as well as a deletion within the protein blocks postmitotic nuclear reformation and results in embryonic lethality (Galy *et al*, 2003; Rodenas *et al*, 2009), suggesting that Nup53 function is conserved in metazoa. Notably, Nup53 is found in all eukaryotic supergroups indicating that it is part of the NPC in the last common ancestor of eukaryotes (Neumann *et al*, 2010). However, its absence in some eukaryotic organisms shows that its loss can be compensated (DeGrasse *et al*, 2009; Neumann *et al*, 2010). Double deletion of both *S. cerevisiae* orthologues, Nup53p and Nup59p, is viable (Marelli *et al*, 1998; Onischenko *et al*, 2009). However, these strains exhibit growth defects and Nup53 becomes essential when interacting nucleoporins, including integral membrane proteins, are deleted (Marelli *et al*, 1998; Miao *et al*, 2006; Onischenko *et al*, 2009).

NPC assembly is a highly ordered process. In metazoa the NE and NPCs break down and reform during each round of mitosis. Postmitotic reassembly occurs on the decondensing chromatin. The earliest step involves the recruitment of the Nup107–160 subcomplex to the chromatin surface by MEL28/ELYS (Galy *et al*, 2006; Rasala *et al*, 2006; Franz *et al*, 2007), a DNA-binding protein that acts as a seeding point for NPC assembly. Membranes are subsequently recruited to chromatin causing an enrichment of NE/NPC-specific membrane proteins, including the transmembrane nucleoporins POM121 and NDC1 (Antonin *et al*, 2005; Mansfeld *et al*, 2006; Anderson *et al*, 2009). The order of these initial steps has been defined using both *in vitro* experiments and live-cell imaging (Dultz *et al*, 2008); however, less is known about the order of nucleoporin assembly following these events. MEL28 and Nup107 as well as POM121 and NDC1 containing membranes are detectable on the chromatin in Nup53-depleted nuclear assemblies (Figure 4D). The same pattern was seen in Nup93-depleted extracts (Sachdev *et al*, 2012). Our results suggest that Nup53, which is part of the Nup93 complex, is a key determinant for the recruitment of the other members of this complex. In the absence of Nup53, the chromatin recruitment of Nup155, Nup205, Nup188 and Nup93 was impaired (Figure 4D). Similarly, *C. elegans* Nup53 is necessary for the efficient accumulation of Nup155 and Nup58 but not Nup107 at the NE (Rodenas *et al*, 2009). This is also supported by live-cell imaging experiments in HeLa cells, which capture the recruitment of Nup58 slightly after Nup93 (Dultz *et al*, 2008). Accordingly, we have found that upon depletion of the two Nup93 containing subcomplexes, Nup93–Nup188 and Nup93–205, the two other members of the complex, Nup155 and Nup53, are still detectable, albeit at reduced levels on the assembling NPCs (Sachdev *et al*, 2012). Recruitment of the Nup62 complex to the chromatin template is prevented in the absence of both Nup53 (see lack of a Nup58 immunostaining, which is a constituent of the Nup62 complex, in Figure 4D) and Nup93 (Sachdev *et al*, 2012) consistent with the notion that Nup93 is a key determinant in recruiting the Nup62 complex during vertebrate NPC assembly at the end of mitosis (Sachdev *et al*, 2012). Taken together, these data suggest that after the binding of the Nup107–160 complex and nuclear membranes to the chromatin surface, Nup53 recruitment is the next decisive step in NPC assembly. Nup93 (Nup93–Nup188/Nup93–Nup205) binding and the subsequent recruitment of the Nup62 complex follow.

Nup53 interacts with a number of other nucleoporins, including NDC1, Nup155 and Nup93 (Lusk *et al*, 2002;

 ©2012 European Molecular Biology Organization

Hawryluk-Gara *et al*, 2005, 2008; Mansfeld *et al*, 2006; Sachdev *et al*, 2012) a feature that is conserved in yeast (Fahrenkrog *et al*, 2000; Onischenko *et al*, 2009; Amlacher *et al*, 2011). As previously reported (Hawryluk-Gara *et al*, 2008), the interaction of Nup53 with NDC1 is not necessary for postmitotic NPC assembly in Xenopus egg extracts (Figure 4A). A possible explanation might be that Nup53 can interact directly with membranes and that one of its two membrane binding regions is sufficient for postmitotic NPC formation. In addition, Nup53 interaction with other nucleoporins such as Nup155, which in turn binds POM121 (Mitchell *et al*, 2010; Yavuz *et al*, 2010) could be a possible mechanism linking Nup53 to the pore membrane which might compensate for the loss of the direct Nup53–NDC1 interaction.

The interaction of Nup53 with Nup155 is thought to be important for NPC assembly. A previous study found that after depleting Nup53 from Xenopus egg extracts, only fragments capable of binding to Nup155 allow for NPC formation (Hawryluk-Gara *et al*, 2008). However, in this case all fragments that rescued the NE/NPC assembly defect included the RRM domain and all fragments defective in NPC assembly and the Nup155 interaction lacked the intact RRM domain. Similarly, a deletion in *C. elegans* Nup53 blocked NE assembly also impaired the RRM domain (Rodenas *et al*, 2009). We demonstrate here that the RRM domain is important for Nup53 dimerization and in turn for membrane binding. Therefore, we currently cannot rule out that the primary cause for the previously described defects was a loss of the Nup53 membrane interaction.

Nup93 binds directly Nup53 (Hawryluk-Gara *et al*, 2005; Sachdev *et al*, 2012) and the interaction domain resides in the N-terminal half of Nup53 (Hawryluk-Gara *et al*, 2008). This interaction was previously considered to be dispensable for NPC assembly as a fragment lacking the N-terminal region as well as the C-terminal 26 amino acids replaced endogenous Nup53 in nuclear assemblies in Xenopus egg extracts (Hawryluk-Gara *et al*, 2008). This is quite surprising in the light of the results presented here, as this fragment also lacked both membrane binding regions identified in this study and does not allow for Nup93 recruitment which is an essential factor for postmitotic NPC assembly (Sachdev *et al*, 2012). Using a number of different Nup53 fragments that lacked the Nup93 binding region we were not able to replace endogenous Nup53 in NPC assembly (Supplementary Figure S6). Currently, we cannot rule out that this discrepancy is due to different Nup53 depletion efficiencies. In fact, we found that a small percentage of floated membrane preparations used in the nuclear assembly reactions contained minor amounts of Nup53, and we were careful to exclude these from our experiments.

Nup53 is also known as mitotic phosphoprotein of 44 kDa (Stukenberg *et al*, 1997). Indeed, Nup53 from mitotic extracts migrates significantly slower in SDS–PAGE compared to Nup53 from interphasic extracts (Supplementary Figure S3A). We identified a number of mitosis-specific phosphorylation sites on Nup53, of which a subset were consensus sites for CDK1. These findings are consistent with the fact that Nup53 has been identified as a CDK1 target in both yeast and humans (Lusk *et al*, 2007; Blethrow *et al*, 2008). The N-terminal membrane binding region of Nup53 is phosphorylated during mitosis. Phosphomimetic mutations and *in vitro* phosphorylation experiments suggest that CDK1-mediated phosphorylation renders this region incompetent for membrane interaction (Figure 3B). It is therefore possible that this mitotic phosphorylation weakens the interaction of Nup53 with the pore membrane to facilitate NPC disassembly during prophase.

Proteins without integral membrane regions can associate with cellular membranes by a variety of mechanisms (Cho and Stahelin, 2005). First, they can be covalently attached to a lipid moiety. However, we have no indication that Nup53 is modified in such a way. Second, peripheral membrane proteins are recruited to the lipid bilayer by specific protein–lipid interactions that involve binding to particular lipid head groups. In this regard, lipid arrays performed to date have not demonstrated an affinity of Nup53 for any specific lipid (unpublished observation). Furthermore, recombinant Nup53 binds to liposomes prepared from different lipid sources like pure DOPC (1,2-dioleoyl-*sn*-glycero-3-phosphocholine), a lipid mixture mimicking the ER/NE lipid composition (Franke *et al*, 1970; Supplementary Figure S7) or folch fraction I (unpublished observation). Third, some proteins are recruited to membranes via electrostatic interactions. As a fraction of the lipid head groups are negatively charged this involves positively charged clusters on the protein surface. Indeed, we found that the first membrane binding region of Nup53 contains such a cluster. Replacing these positive with negative residues as well as introducing negative charge by phosphorylation rendered this site incapable of membrane interaction (Figure 3A and B). Finally, peripheral membrane proteins can associate with lipid bilayers via hydrophobic regions. It has been suggested that the C-terminal region of Nup53 contains an amphipathic helix, which could serve as a hydrophobic module (Marelli *et al*, 2001; Patel and Rexach, 2008). In fact, the C-terminus of Nup53 contains a membrane binding region and deleting the last eight amino acids abolished its membrane interaction. Deletion of the C-terminal tryptophan only slightly reduced membrane binding of Nup53 in the full-length protein (Figure 3C), but inhibited interphasic NPC assembly (Figure 5) suggesting that this residue fulfills an important additional function. Indeed, the insertion of hydrophobic parts of a protein into a membrane is one of several mechanisms by which proteins can deform membranes (McMahon and Gallop, 2005). Our data suggest that the C-terminal membrane binding region and especially the last tryptophan of Nup53 fulfills this task (Figure 6A). Interestingly, *in vivo* intranuclear tubular membranes are induced upon overexpression of yeast Nup53p which is dependent on its C-terminus (Marelli *et al*, 2001). Thus, Nup53 might not only have an important function in binding to the pore membrane in turn promoting the recruitment of other nucleoporins, especially members of the Nup93 complex, but may additionally function to deform the NE membrane into a pore. In the latter instance, the insertion of the Nup53 C-terminus into the hydrophobic phase of the membrane would result in displacement of lipid head groups and reorientation of the hydrophobic lipid side chains, bending the lipid bilayer into a convex shape and inducing membrane curvature necessary to form and stabilize the pore (Antonin *et al*, 2008). The doughnut-like shape of the pore requires likewise stabilization of a concave curvature in the plane of the pore in addition to the convex curved membrane

©2012 European Molecular Biology Organization

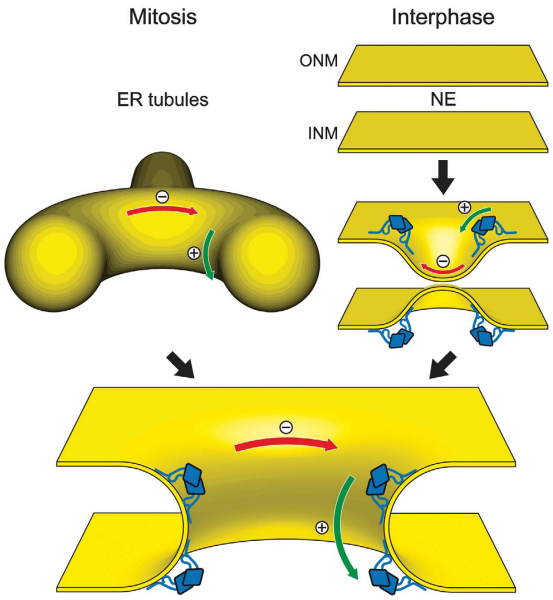

Figure 7 The role of Nup53 in NPC assembly. Schematic drawing of the postmitotic and interphasic modes of nuclear pore assembly focused on the membrane interacting function of Nup53. For the sake of clarity other membrane associated and integral proteins, including nucleoporins, participating in this process are omitted. Left pathway: after mitosis, outgrowing ER tubules (yellow) surround assembling NPCs providing negative/concave (red) and positive/convex (green) curvature which is stabilized by membrane binding Nup53 dimers (blue) for pore formation. Right pathway: in interphase, the intact nuclear envelope membranes (yellow) are deformed by the C-terminal membrane binding site of Nup53 introducing a convex membrane curvature for the approximation and following fusion of the two membranes leading to pore formation.

connection between outer and inner nuclear membrane (see Figure 7). This curvature might be induced and stabilized by a number of at least partially redundant mechanisms, such as formation of a coat-like structure by the Nup107–160 complex (Devos *et al*, 2004; Mans *et al*, 2004; Brohawn *et al*, 2008) or oligomerization of pore membrane proteins, although it is not clear how the different proteins contribute to the different modes of membrane bending. Similarly, in the context of the protein interaction network of an assembled NPC the N-terminal membrane binding region of Nup53, in addition to membrane interaction, might induce and/or stabilize curved membranes. Indeed, Nup53 is only functional when it dimerizes probably because this increases the avidity of the Nup53 membrane interaction. In addition, all the factors might also impose geometrical constrains to the membranes supporting a pore structure.

Although either one of the two membrane binding regions of Nup53 is sufficient for postmitotic NPC assembly and stability, the C-terminal site is specifically required for NPC assembly during interphase. It is a matter of debate whether NPC assembly during these different cell-cycle phases occurs by distinct mechanisms (Doucet *et al*, 2010; Dultz and Ellenberg, 2010; Lu *et al*, 2011). At the end of mitosis, NPC assembly occurs concomitantly with formation of a closed NE. It is possible that this mode of NPC formation does not require fusion between the outer and inner nuclear membrane to form a nuclear pore, in contrast to interphasic NPC assembly. Postmitotic pore assembly could rather arise by the enclosement of the assembling NPCs on the chromatin surface by an outgrowing ER network. In this scenario, Nup53 would stabilize the membrane curvature provided by the ER tubules rather than induce membrane deformation (see Figure 7, left pathway). The different requirements for Nup53 membrane binding regions in postmitotic and interphasic NPC assembly support the view of two different mechanistic pathways. A loss of the membrane deforming capability of Nup53 in postmitotic NPC assembly and NPC stability might be compensated by other factors such as the Nup107–160 complex or integral membrane proteins. However, during metazoan interphasic NPC assembly Nup53-mediated membrane deformation might be crucial for the initial approximation and/or fusion of both membrane layers (see Figure 7, right pathway). Interestingly, ER bending proteins of the reticulon family that induce convex membrane curvature (Hu *et al*, 2008) were shown to be important for NPC assembly into the intact NE both in yeast and in vertebrates (Dawson *et al*, 2009). Currently, it is unknown whether these proteins do also contribute to postmitotic NPC assembly. As their effect on ER membrane reorganization at the end of mitosis is a prerequisite for NE reformation (Anderson and Hetzer, 2008) it is difficult to separate these two functions. Finally, how the fusion of outer and inner nuclear membranes is achieved is largely unclear but our results suggest that Nup53, importantly its C-terminal membrane binding region, is critical for this process.

Materials and methods

Antibodies against POM121 and GP210 (Antonin *et al*, 2005), NDC1 (Mansfeld *et al*, 2006), Nup155 (Franz *et al*, 2005), MEL28/ELYS (Franz *et al*, 2007), Nup107 (Walther *et al*, 2003), Nup53 and Nup58 (Sachdev *et al*, 2012) as well as Nup188, Nup205, Nup98 and Nup53 (Theerthagiri *et al*, 2010) have been described. mAB414 and Nup88 antibodies were from Babco or BD Bioscience, respectively. For quantitation of Nup53 liposomes binding the antibody was affinity purified with a fragment comprising the RRM domain as this domain is included in all tested fragments (please see Supplementary Table S2 for list of all DNA constructs used in this study).

Nuclear assemblies

Nuclear assemblies and immunofluorescence (Theerthagiri *et al*, 2010), generation of affinity resins, sperm heads and floated membranes (Franz *et al*, 2005) as well as prelabelled membranes (Antonin *et al*, 2005) were done as described. Interphasic NPC assembly using dextran influx was monitored as described (Dawson *et al*, 2009) except that mock or Nup53-depleted extracts were incubated with 1.5 vol WGA-Agarose (Sigma) for 40 min. Counting of NPCs was performed on mAB414-labelled nuclei as described (Theerthagiri *et al*, 2010).

Protein expression and purification

Constructs for full-length Xenopus Nup53 and fragments, *S. cerevisiae* Nup53 and Nup59 were generated from a synthetic DNA optimized for codon usage in *E. coli* (Geneart, see Supplementary data) and cloned into a modified pET28a vector with a yeast SUMO solubility tag followed by a TEV site upstream of the Nup53 fragments. Proteins were expressed in *E. coli*, purified using Ni-agarose, His_6 and SUMO tags were cleaved by TEV protease, concentrated using VIVASPIN columns (Sartorius) and purified by gel filtration (Superdex200 10/300 GL or Superdex200 PC 3.2/30, GE Healthcare) either in PBS for liposome binding experiments or in sucrose buffer (Theerthagiri *et al*, 2010) for nuclear assemblies, respectively. Nup53 fragments aa 162–320 and aa 254–320 were purified by size exclusion chromatography without removal of the tags to retain stability. Fragments of Xenopus Nup98 (aa 676-863) as well as human Nup133 (aa 67–514) (Berke *et al*, 2004) were expressed from modified pET28a vectors with a His_6-NusA or

©2012 European Molecular Biology Organization

His_6 tag, which was cleaved of by thrombin or precision protease, respectively.

Liposome generation and flotation

E. coli polar lipid extract with 0.2 mol% 18:1–12:0 NBD-PE (1-oleoyl-2-{12-[(7-nitro-2-1,3-benzoxadiazol-4-yl)amino]dodecanoyl}-sn-glycero-3-phosphoethanolamine) (Avanti polar lipids) were dissolved in ethanol at 45°C. To form liposomes, the mixture was diluted 10-fold into PBS resulting in a final lipid concentration of 6.7 mg/ml while gently agitating. Liposomes were passed 21 × through Nuclepore Track-Etched Membranes (Whatman) with defined pore sizes (50, 100, 200, 400, 800 nm) at 45°C using the Avanti Mini-Extruder. To remove ethanol, liposomes were dialysed against PBS using Spectra/Por 2 dialysis tubing (MWCO 12-14 kDa). Liposome sizes were determined by light scattering using the AvidNano W130i. For quantitation of liposome binding, fluorescence intensity of the protein/liposome mixture and the top fraction was determined using a Molecular Imager VersaDoc MP 4000 Imaging System and ImageJ.

Folch fraction I lipids (Sigma) dissolved in chloroform were dried on a rotary evaporator and overnight under vacuum. PBS buffer was gently added to result in a final lipid concentration of 10 mg/ml. After 2 h of incubation at 37°C to allow spontaneous liposome formation the flask was agitated to dissolve residual lipids. After 10 cycles of freeze/thawing, liposomes were diluted 10-fold in PBS and extruded as described before.

Immunoprecipitation

Xenopus Nup53 as well as the RRM dimerization mutant (F172E/W203E) was cloned with N-terminal myc or HA tag, respectively, into a pSI vector (Promega). HeLa cells were transfected using Fugene 6 (Roche) following manufacturer's instructions, harvested 24 h post transfection and solubilized in 1% Triton X-100 in PBS supplemented with protease inhibitors (2 μg/ml leupeptin, 1 μg/ml pepstatin, 2 μg/ml aprotinin, 0.1 mg/ml AEBSF final concentration) for 10 min at 4°C. After centrifugation for 10 min at 15 000 *g* samples were diluted five-fold in PBS and employed for immunoprecipitation using α-myc or α-HA antibodies (Roche).

Miscellaneous

For *in vitro* phosphorylation, 3 μM proteins were incubated with 0.33 U/μl CDK1-CyclinB (NEB), 1 mM ATP, 10 mM $MgCl_2$ and 1 mM EDTA in PBS for 1 h at 30°C.

For liposome tubulation copper grids filmed with pioloform and carbon-coated were glow discharged before usage. Proteins were incubated with 1 mg/ml folch fraction I liposomes for 7 min on grids, washed with buffer (10 mM Hepes, 150 mM NaCl, 4.5 mM KCl) and stained with 2% UAc for 2 min and examined on a FEI Technai spirit 120 kV microscope.

Supplementary data

Supplementary data are available at *The EMBO Journal* Online (http://www.embojournal.org).

Acknowledgements

We thank M Flötenmeyer and S Würtenberger for help with the tubulation assay, B Uluvar for support in protein purification and M Lorenz for critical reading of the manuscript.

Author contributions: BV and WA designed and performed experiments and wrote the manuscript. AS quantified interphasic NPC assembly, RS and NE performed pull-down experiments, AMS performed the size determinations of the RRM domains. CS cloned constructs and prepared *Xenopus laevis* extracts. JM and BM performed mass spec analysis, UG performed measurements of different liposome sizes.

Conflict of interest

The authors declare that they have no conflict of interest.

References

Amlacher S, Sarges P, Flemming D, van Noort V, Kunze R, Devos DP, Arumugam M, Bork P, Hurt E (2011) Insight into structure and assembly of the nuclear pore complex by utilizing the genome of a eukaryotic thermophile. *Cell* **146:** 277–289

Anderson DJ, Hetzer MW (2008) Reshaping of the endoplasmic reticulum limits the rate for nuclear envelope formation. *J Cell Biol* **182:** 911–924

Anderson DJ, Vargas JD, Hsiao JP, Hetzer MW (2009) Recruitment of functionally distinct membrane proteins to chromatin mediates nuclear envelope formation *in vivo*. *J Cell Biol* **186:** 183–191

Antonin W, Ellenberg J, Dultz E (2008) Nuclear pore complex assembly through the cell cycle: regulation and membrane organization. *FEBS Lett* **582:** 2004–2016

Antonin W, Franz C, Haselmann U, Antony C, Mattaj IW (2005) The integral membrane nucleoporin pom121 functionally links nuclear pore complex assembly and nuclear envelope formation. *Mol Cell* **17:** 83–92

Berke IC, Boehmer T, Blobel G, Schwartz TU (2004) Structural and functional analysis of Nup133 domains reveals modular building blocks of the nuclear pore complex. *J Cell Biol* **167:** 591–597

Bilokapic S, Schwartz TU (2012) 3D ultrastructure of the nuclear pore complex. *Curr Opin Cell Biol* **24:** 86–91

Blethrow JD, Glavy JS, Morgan DO, Shokat KM (2008) Covalent capture of kinase-specific phosphopeptides reveals Cdk1-cyclin B substrates. *Proc Natl Acad Sci USA* **105:** 1442–1447

Brohawn SG, Leksa NC, Spear ED, Rajashankar KR, Schwartz TU (2008) Structural evidence for common ancestry of the nuclear pore complex and vesicle coats. *Science* **322:** 1369–1373

Cho W, Stahelin RV (2005) Membrane-protein interactions in cell signaling and membrane trafficking. *Annu Rev Biophys Biomol Struct* **34:** 119–151

Cronshaw JM, Krutchinsky AN, Zhang W, Chait BT, Matunis MJ (2002) Proteomic analysis of the mammalian nuclear pore complex. *J Cell Biol* **158:** 915–927

D'Angelo MA, Anderson DJ, Richard E, Hetzer MW (2006) Nuclear pores form de novo from both sides of the nuclear envelope. *Science* **312:** 440–443

Daumke O, Lundmark R, Vallis Y, Martens S, Butler PJ, McMahon HT (2007) Architectural and mechanistic insights into an EHD ATPase involved in membrane remodelling. *Nature* **449:** 923–927

Dawson TR, Lazarus MD, Hetzer MW, Wente SR (2009) ER membrane-bending proteins are necessary for de novo nuclear pore formation. *J Cell Biol* **184:** 659–675

DeGrasse JA, DuBois KN, Devos D, Siegel TN, Sali A, Field MC, Rout MP, Chait BT (2009) Evidence for a shared nuclear pore complex architecture that is conserved from the last common eukaryotic ancestor. *Mol Cell Proteomics* **8:** 2119–2130

Devos D, Dokudovskaya S, Alber F, Williams R, Chait BT, Sali A, Rout MP (2004) Components of coated vesicles and nuclear pore complexes share a common molecular architecture. *PLoS Biol* **2:** e380

Doucet CM, Hetzer MW (2010) Nuclear pore biogenesis into an intact nuclear envelope. *Chromosoma* **119:** 469–477

Doucet CM, Talamas JA, Hetzer MW (2010) Cell cycle-dependent differences in nuclear pore complex assembly in metazoa. *Cell* **141:** 1030–1041

Drin G, Casella JF, Gautier R, Boehmer T, Schwartz TU, Antonny B (2007) A general amphipathic alpha-helical motif for sensing membrane curvature. *Nat Struct Mol Biol* **14:** 138–146

Dultz E, Ellenberg J (2010) Live imaging of single nuclear pores reveals unique assembly kinetics and mechanism in interphase. *J Cell Biol* **191:** 15–22

Dultz E, Zanin E, Wurzenberger C, Braun M, Rabut G, Sironi L, Ellenberg J (2008) Systematic kinetic analysis of mitotic dis- and reassembly of the nuclear pore in living cells. *J Cell Biol* **180:** 857–865

Fahrenkrog B, Hubner W, Mandinova A, Pante N, Keller W, Aebi U (2000) The yeast nucleoporin Nup53p specifically interacts with

©2012 European Molecular Biology Organization

Nic96p and is directly involved in nuclear protein import. *Mol Biol Cell* **11:** 3885–3896

Field MC, Sali A, Rout MP (2011) Evolution: on a bender–BARs, ESCRTs, COPs, and finally getting your coat. *J Cell Biol* **193:** 963–972

Franke WW, Deumling B, Baerbelermen, Jarasch ED, Kleinig H (1970) Nuclear membranes from mammalian liver. I. Isolation procedure and general characterization. *J Cell Biol* **46:** 379–395

Franz C, Askjaer P, Antonin W, Iglesias CL, Haselmann U, Schelder M, de Marco A, Wilm M, Antony C, Mattaj IW (2005) Nup155 regulates nuclear envelope and nuclear pore complex formation in nematodes and vertebrates. *EMBO J* **24:** 3519–3531

Franz C, Walczak R, Yavuz S, Santarella R, Gentzel M, Askjaer P, Galy V, Hetzer M, Mattaj IW, Antonin W (2007) MEL-28/ELYS is required for the recruitment of nucleoporins to chromatin and postmitotic nuclear pore complex assembly. *EMBO Rep* **8:** 165–172

Galy V, Askjaer P, Franz C, López-Iglesias C, Mattaj IW (2006) MEL-28, a novel nuclear envelope and kinetochore protein essential for zygotic nuclear envelope assembly in C. elegans. *Curr Biol* **16:** 1748–1756

Galy V, Mattaj IW, Askjaer P (2003) Caenorhabditis elegans nucleoporins Nup93 and Nup205 determine the limit of nuclear pore complex size exclusion *in vivo*. *Mol Biol Cell* **14:** 5104–5115

Handa N, Kukimoto-Niino M, Akasaka R, Kishishita S, Murayama K, Terada T, Inoue M, Kigawa T, Kose S, Imamoto N, Tanaka A, Hayashizaki Y, Shirouzu M, Yokoyama S (2006) The crystal structure of mouse Nup35 reveals atypical RNP motifs and novel homodimerization of the RRM domain. *J Mol Biol* **363:** 114–124

Hawryluk-Gara LA, Platani M, Santarella R, Wozniak RW, Mattaj IW (2008) Nup53 is required for nuclear envelope and nuclear pore complex assembly. *Mol Biol Cell* **19:** 1753–1762

Hawryluk-Gara LA, Shibuya EK, Wozniak RW (2005) Vertebrate Nup53 interacts with the nuclear lamina and is required for the assembly of a Nup93-containing complex. *Mol Biol Cell* **16:** 2382–2394

Hoelz A, Debler EW, Blobel G (2011) The structure of the nuclear pore complex. *Annu Rev Biochem* **80:** 613–643

Hu J, Shibata Y, Voss C, Shemesh T, Li Z, Coughlin M, Kozlov MM, Rapoport TA, Prinz WA (2008) Membrane proteins of the endoplasmic reticulum induce high-curvature tubules. *Science* **319:** 1247–1250

Liu HL, De Souza CP, Osmani AH, Osmani SA (2009) The three fungal transmembrane nuclear pore complex proteins of Aspergillus nidulans are dispensable in the presence of an intact An-Nup84-120 complex. *Mol Biol Cell* **20:** 616–630

Lohka MJ (1998) Analysis of nuclear envelope assembly using extracts of Xenopus eggs. *Methods Cell Biol* **53:** 367–395

Lu L, Ladinsky MS, Kirchhausen T (2011) Formation of the postmitotic nuclear envelope from extended ER cisternae precedes nuclear pore assembly. *J Cell Biol* **194:** 425–440

Lusk CP, Makhnevych T, Marelli M, Aitchison JD, Wozniak RW (2002) Karyopherins in nuclear pore biogenesis: a role for Kap121p in the assembly of Nup53p into nuclear pore complexes. *J Cell Biol* **159:** 267–278

Lusk CP, Waller DD, Makhnevych T, Dienemann A, Whiteway M, Thomas DY, Wozniak RW (2007) Nup53p is a target of two mitotic kinases, Cdk1p and Hrr25p. *Traffic* **8:** 647–660

Mans BJ, Anantharaman V, Aravind L, Koonin EV (2004) Comparative genomics, evolution and origins of the nuclear envelope and nuclear pore complex. *Cell Cycle* **3:** 1612–1637

Mansfeld J, Guttinger S, Hawryluk-Gara LA, Pante N, Mall M, Galy V, Haselmann U, Muhlhausser P, Wozniak RW, Mattaj IW, Kutay U, Antonin W (2006) The conserved transmembrane nucleoporin NDC1 is required for nuclear pore complex assembly in vertebrate cells. *Mol Cell* **22:** 93–103

Marelli M, Aitchison JD, Wozniak RW (1998) Specific binding of the karyopherin Kap121p to a subunit of the nuclear pore complex containing Nup53p, Nup59p, and Nup170p. *J Cell Biol* **143:** 1813–1830

Marelli M, Lusk CP, Chan H, Aitchison JD, Wozniak RW (2001) A link between the synthesis of nucleoporins and the biogenesis of the nuclear envelope. *J Cell Biol* **153:** 709–724

McMahon HT, Gallop JL (2005) Membrane curvature and mechanisms of dynamic cell membrane remodelling. *Nature* **438:** 590–596

McMahon HT, Mills IG (2004) COP and clathrin-coated vesicle budding: different pathways, common approaches. *Curr Opin Cell Biol* **16:** 379–391

Miao M, Ryan KJ, Wente SR (2006) The integral membrane protein Pom34p functionally links nucleoporin subcomplexes. *Genetics* **172:** 1441–1457

Mitchell JM, Mansfeld J, Capitanio J, Kutay U, Wozniak RW (2010) Pom121 links two essential subcomplexes of the nuclear pore complex core to the membrane. *J Cell Biol* **191:** 505–521

Neumann N, Lundin D, Poole AM (2010) Comparative genomic evidence for a complete nuclear pore complex in the last eukaryotic common ancestor. *PLoS ONE* **5:** e13241

Onischenko E, Stanton LH, Madrid AS, Kieselbach T, Weis K (2009) Role of the Ndc1 interaction network in yeast nuclear pore complex assembly and maintenance. *J Cell Biol* **185:** 475–491

Onischenko E, Weis K (2011) Nuclear pore complex-a coat specifically tailored for the nuclear envelope. *Curr Opin Cell Biol* **23:** 293–301

Patel SS, Rexach MF (2008) Discovering novel interactions at the nuclear pore complex using bead halo: a rapid method for detecting molecular interactions of high and low affinity at equilibrium. *Mol Cell Proteomics* **7:** 121–131

Prufert K, Vogel A, Krohne G (2004) The lamin CxxM motif promotes nuclear membrane growth. *J Cell Sci* **117:** 6105–6116

Rasala BA, Orjalo AV, Shen Z, Briggs S, Forbes DJ (2006) ELYS is a dual nucleoporin/kinetochore protein required for nuclear pore assembly and proper cell division. *Proc Natl Acad Sci USA* **103:** 17801–17806

Rodenas E, Klerkx EP, Ayuso C, Audhya A, Askjaer P (2009) Early embryonic requirement for nucleoporin Nup35/NPP-19 in nuclear assembly. *Dev Biol* **327:** 399–409

Sachdev R, Sieverding C, Flotenmeyer M, Antonin W (2012) The C-terminal domain of Nup93 is essential for assembly of the structural backbone of nuclear pore complexes. *Mol Biol Cell* **23:** 740–749

Stavru F, Hulsmann BB, Spang A, Hartmann E, Cordes VC, Gorlich D (2006) NDC1: a crucial membrane-integral nucleoporin of metazoan nuclear pore complexes. *J Cell Biol* **173:** 509–519

Stukenberg PT, Lustig KD, McGarry TJ, King RW, Kuang J, Kirschner MW (1997) Systematic identification of mitotic phosphoproteins. *Curr Biol* **7:** 338–348

Theerthagiri G, Eisenhardt N, Schwarz H, Antonin W (2010) The nucleoporin Nup188 controls passage of membrane proteins across the nuclear pore complex. *J Cell Biol* **189:** 1129–1142

Walther TC, Alves A, Pickersgill H, Loiodice I, Hetzer M, Galy V, Hulsmann BB, Kocher T, Wilm M, Allen T, Mattaj IW, Doye V (2003) The conserved Nup107-160 complex is critical for nuclear pore complex assembly. *Cell* **113:** 195–206

Wente SR, Rout MP (2010) The nuclear pore complex and nuclear transport. *Cold Spring Harb Perspect Biol* **2:** a000562

West RR, Vaisberg EV, Ding R, Nurse P, McIntosh JR (1998) cut11(+): A gene required for cell cycle-dependent spindle pole body anchoring in the nuclear envelope and bipolar spindle formation in Schizosaccharomyces pombe. *Mol Biol Cell* **9:** 2839–2855

Winey M, Hoyt MA, Chan C, Goetsch L, Botstein D, Byers B (1993) NDC1: a nuclear periphery component required for yeast spindle pole body duplication. *J Cell Biol* **122:** 743–751

Yavuz S, Santarella-Mellwig R, Koch B, Jaedicke A, Mattaj IW, Antonin W (2010) NLS-mediated NPC functions of the nucleoporin Pom121. *FEBS Lett* **584:** 3292–3298

SOME RIGHTS RESERVED **_The EMBO Journal_ is published by Nature Publishing Group on behalf of European Molecular Biology Organization. This article is licensed under a Creative Commons Attribution-Noncommercial-Share Alike 3.0 Licence. [http://creativecommons.org/licenses/by-nc-sa/3.0/]**

 ©2012 European Molecular Biology Organization

Supplementary Information

Dimerization and direct membrane interaction of Nup53 contribute to nuclear pore complex assembly

Benjamin Vollmer[1], Allana Schooley[1], Ruchika Sachdev[1], Nathalie Eisenhardt[1], Anna Schneider[2], Cornelia Sieverding[1], Johannes Madlung[3], Uwe Gerken[4,5], Boris Macek[3], Wolfram Antonin[1,6]

[1] Friedrich Miescher Laboratory of the Max Planck Society, Spemannstraße 39, 72076 Tübingen, Germany

[2] Max Planck Institute for Developmental Biology, Spemannstraße 35, 72076 Tübingen, Germany

[3] Proteome Center Tübingen, University of Tübingen, 72076 Tübingen, Germany

[4] Institute of Microbiology, University of Hohenheim, Garbenstrasse 30, 70599 Stuttgart, Germany

[5] Present address: Lehrstuhl für Experimentalphysik IV, University of Bayreuth, Universitätsstrasse 30, 95447 Bayreuth

[6] author for correspondence: wolfram.antonin@tuebingen.mpg.de

Supplementary information contains:

Supplementary Figures S1–S7 & Table S1–S2

Supplementary Methods

Supplementary References

Supplementary Figure S1

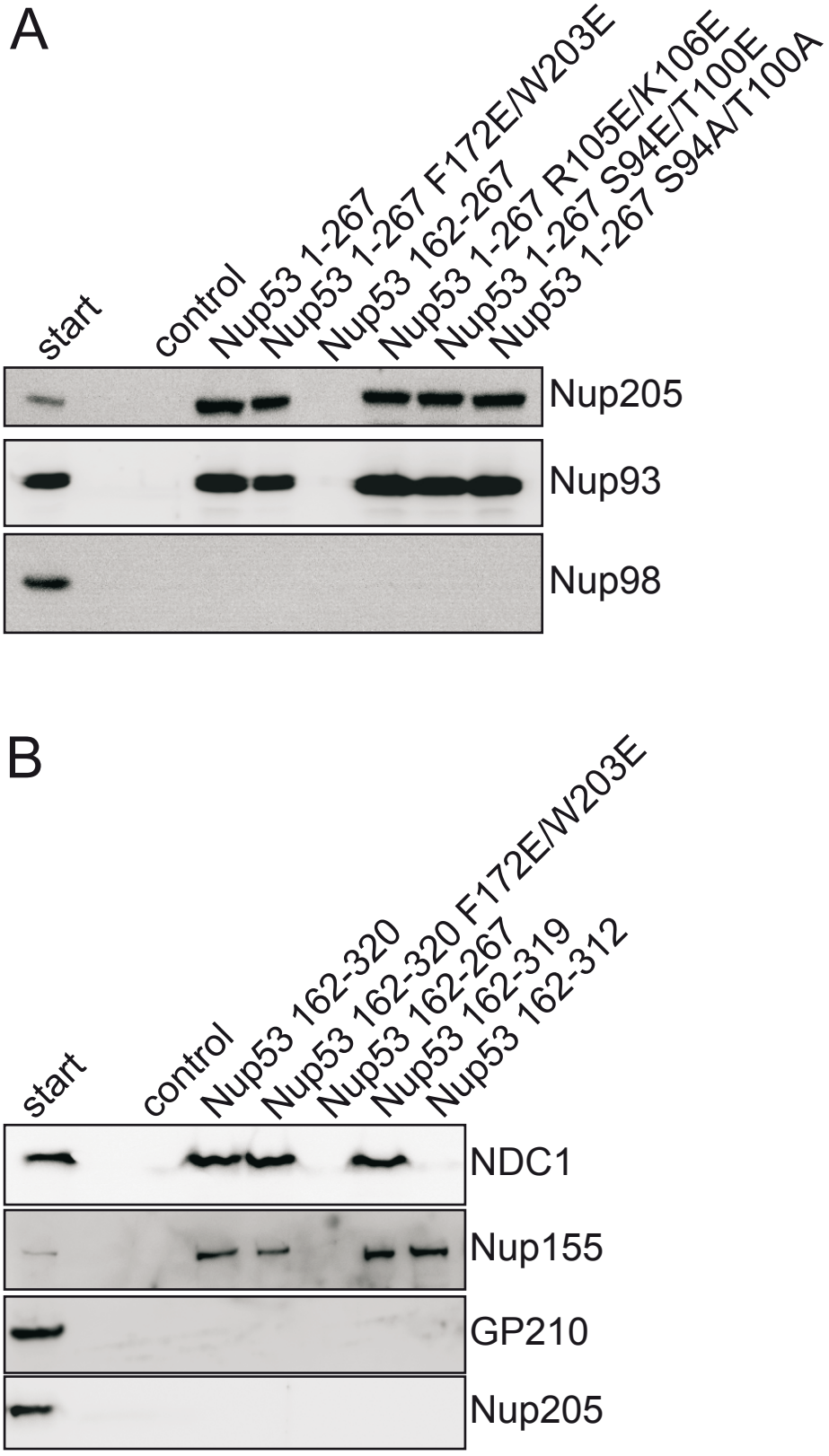

Figure S1

Nup53 has different binding sites for membrane and protein interaction.

(A) GST fusions of an N-terminal fragment of Xenopus Nup53 as well as Xenopus Nup98 (aa 487-634) (control) were incubated with cytosol from Xenopus egg extracts. Eluates were analyzed by western blotting with antibodies against the nucleoporins Nup205 and Nup93, known to bind this region, as well as Nup98 as a negative control. Please note that introducing amino acid changes causing the monomerization of Nup53 (F172E/W203E) also negatively influenced the interaction with Nup205 and Nup93. In contrast, mutations that inactivate the N-terminal membrane binding region (R105E/K106E and S94E/T100E) as well as the S94A/T100A control mutation did not interfere with Nup205 and Nup93 binding.

(B) GST fusions Xenopus Nup98 (aa 487-634) (control), the C-terminal fragment of Xenopus Nup53 (162-320), the RRM mutant (F172E/W203E) and C-terminal truncations were incubated with cytosol (for detection of Nup155 and Nup205) or Triton X-100 solubilized membranes (for NDC1 and GP210 detection) from Xenopus egg extracts. Eluates were analyzed by western blotting with antibodies against the nucleoporins Nup155 and NDC1, known to bind this region as well as Nup205 and GP210 as negative controls. Please note that mutation of the RRM domain (F172E/W203E) did not influence the interaction with NDC1 but results in a decreased binding to Nup155. The C-terminal truncations weakening the C-terminal membrane binding region (162-319 and 162-312) did not interfere with Nup155 binding and the 162-319 fragment was still able to interact with NDC1.

Supplementary Figure S2

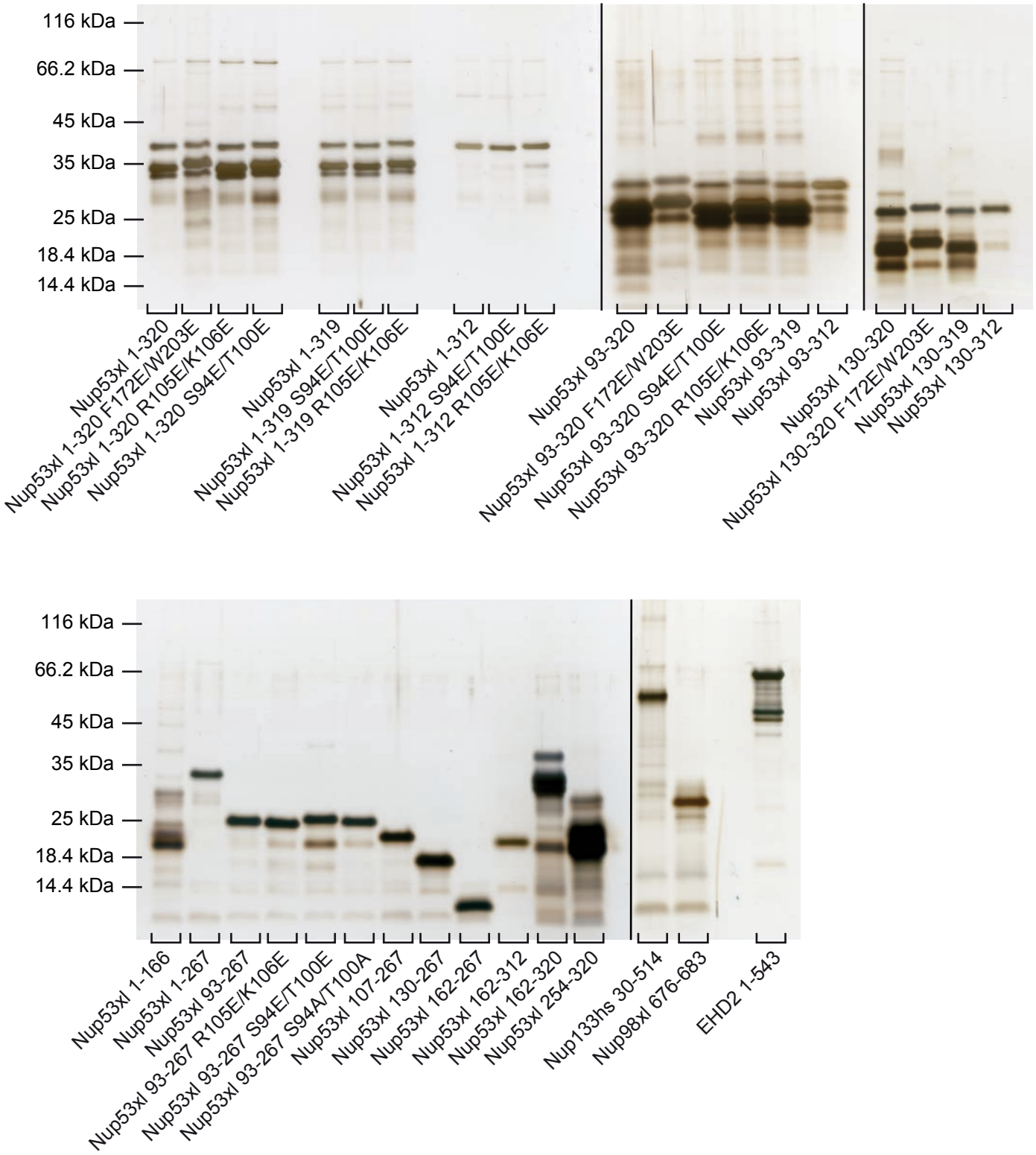

Figure S2

Proteins were separated on Tricine-SDS-PAGE Schägger gels (Schagger & von Jagow, 1987) followed by silver staining.

Supplementary Figure S3

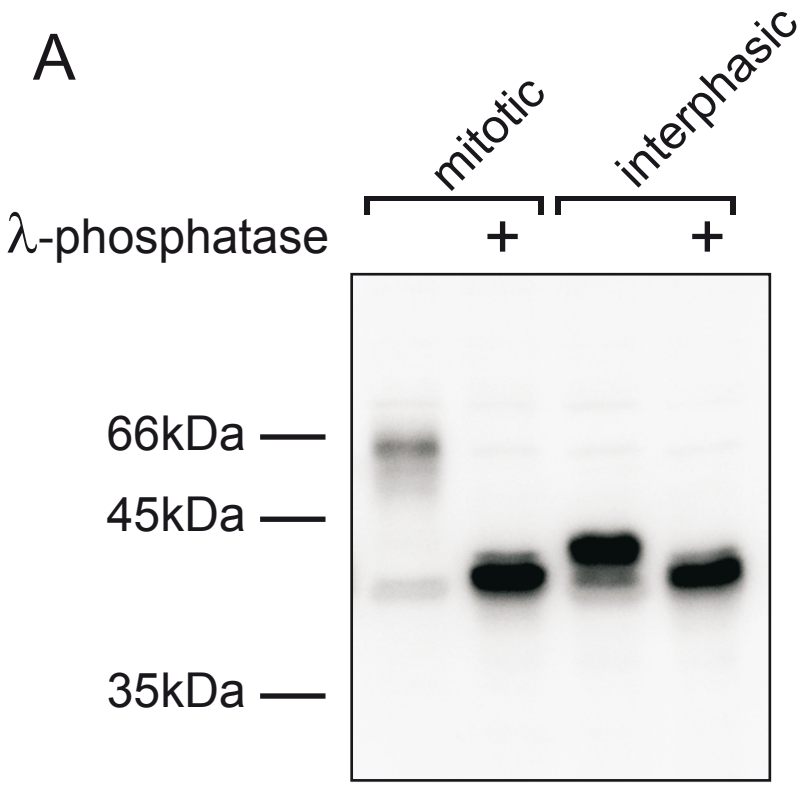

B

Protein IDs: gi_4584796;gi_148232142;gi_15987768;gi_nup53a;gi_nup53b;gi_32450351
Scannumber 8537
Source: 20101220_JM_CO_0221_R7_mitotic_01
Method: CID; ITMS

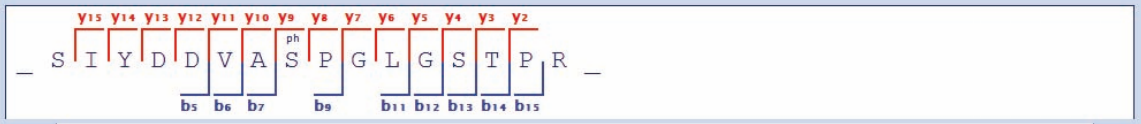

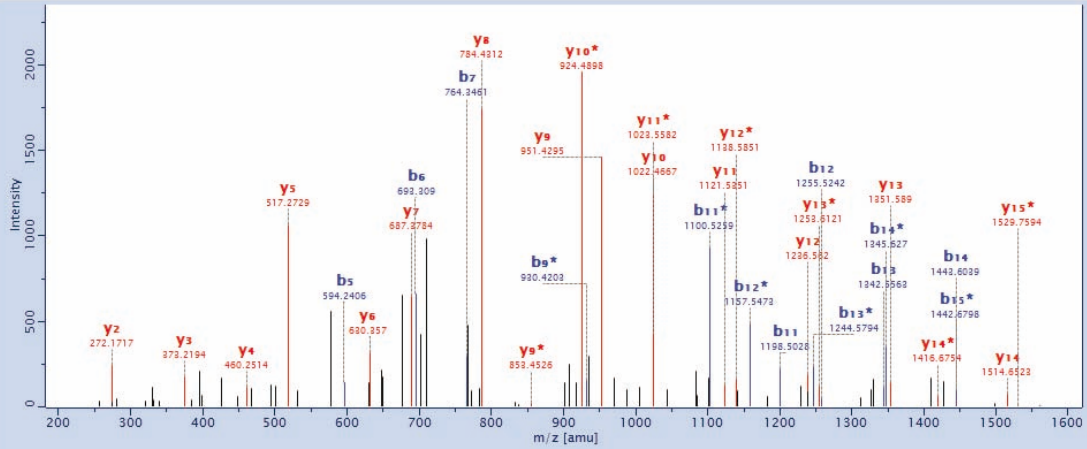

parent information

Mass:	1713.7611
m/z:	857.89
Charge:	2+
Mass Error [ppm]:	0.030899
PTM Score:	250.7
PEP:	7.5085E-41
Mascot Score:	100.54
Intensity:	13664197

general information

Annotation:	14 of 16 => 88 %
Intensity Coverage:	63 %
Protein Localisation:	89 ... 104

B-Ion					Y-Ion	
Δ Da	mass		seq		mass	Δ Da
NaN	88.0393049	1	S	16	NaN	NaN
NaN	201.1233689	2	I	15	1529.7594479	0.1181156
NaN	364.1866974	3	Y	14	1416.6753839	0.0124823
NaN	479.2136404	4	D	13	1253.6120554	0.0177054
0.310625	594.2405835	5	D	12	1138.5851123	0.0339649
0.1467521	693.3089974	6	V	11	1023.5581693	0.2597628
0.0844919	764.3461112	7	A	10	924.4897554	0.0853789
NaN	931.3444706	8	S	9	853.4526416	0.0651807
0.1978867	930.4203384	9	P	8	784.4311782	0.1097764
NaN	1085.4186981	10	G	7	687.3784143	0.0730627
0.1684698	1100.5258661	11	L	6	630.3569506	0.1070997
0.0851164	1157.5473299	12	G	5	517.2728866	0.1069351
0.0762814	1244.5793583	13	S	4	460.2514229	0.0053902
0.1205219	1345.6270367	14	T	3	373.2193945	0.0125464
0.1888518	1442.6798006	15	P	2	272.171716	0.0410398
NaN	NaN	16	R	1	175.1189522	NaN

Protein IDs: gi_4584796;gi_148232142;gi_15987768;gi_nup53a;gi_nup53b;gi_32450351
Scannumber 8673
Source: 20101126_CO_JM_0221WoAn_R5_IP_mitotic_01
Method: CID; ITMS

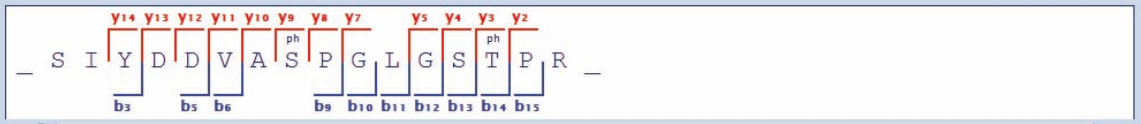

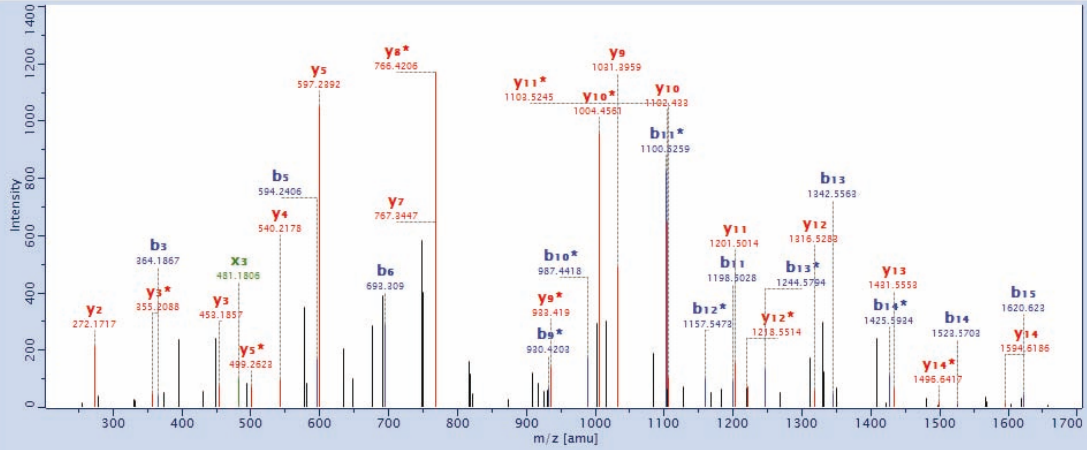

parent information

Mass:	1793.7274
m/z:	897.87
Charge:	2+
Mass Error [ppm]:	0.13197
PTM Score:	238.2
PEP:	8.3029E-53
Mascot Score:	51.05
Intensity:	18521420

general information

Annotation:	13 of 16 => 81 %
Intensity Coverage:	55 %
Protein Localisation:	89 ... 104

B-Ion					X-Ion		Y-Ion	
Δ Da	mass		seq		mass	Δ Da	mass	Δ Da
NaN	88.0393049	1	S	16	NaN	NaN	NaN	NaN
NaN	201.1233689	2	I	15	1733.6819395	NaN	1707.7026749	NaN
0.1353668	364.186697	3	Y	14	1620.5978755	NaN	1496.64171	0.2575771
NaN	479.2136404	4	D	13	1457.5345469	NaN	1431.55528	0.0981291
0.0384082	594.240583	5	D	12	1342.5076039	NaN	1218.55144	0.3596895
0.0780403	693.308997	6	V	11	1227.4806609	NaN	1103.5245	0.2493034
NaN	764.3461112	7	A	10	1128.412247	NaN	1004.45609	0.0672901
NaN	931.3444706	8	S	9	1057.3751332	NaN	933.418973	0.1262544
0.0214951	930.420338	9	P	8	890.3767738	NaN	766.420613	0.0788163
0.2336739	987.441802	10	G	7	793.3240099	NaN	767.344745	0.0776179
0.0236689	1100.52587	11	L	6	736.3025462	NaN	710.3232816	NaN
0.1385832	1157.54733	12	G	5	623.2184822	NaN	499.262322	0.0559618
0.0184452	1244.57936	13	S	4	566.1970185	NaN	540.217754	0.1073804
0.0542153	1425.59337	14	T	3	481.18064	0.1698237	355.20883	0.0389732
0.0871775	1620.62303	15	P	2	298.1509806	NaN	272.171716	0.0123227
NaN	NaN	16	R	1	201.0982167	NaN	175.1189522	NaN

Protein IDs: gi_4584796;gi_148232142;gi_15987768;gi_nup53a;gi_nup53b
Scannumber 5067
Source: 20101126_CO_JM_0221WoAn_R5_IP_mitotic_01
Method: CID; ITMS

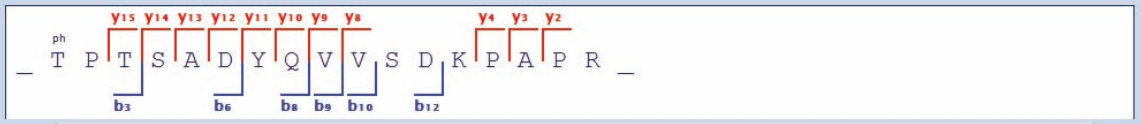

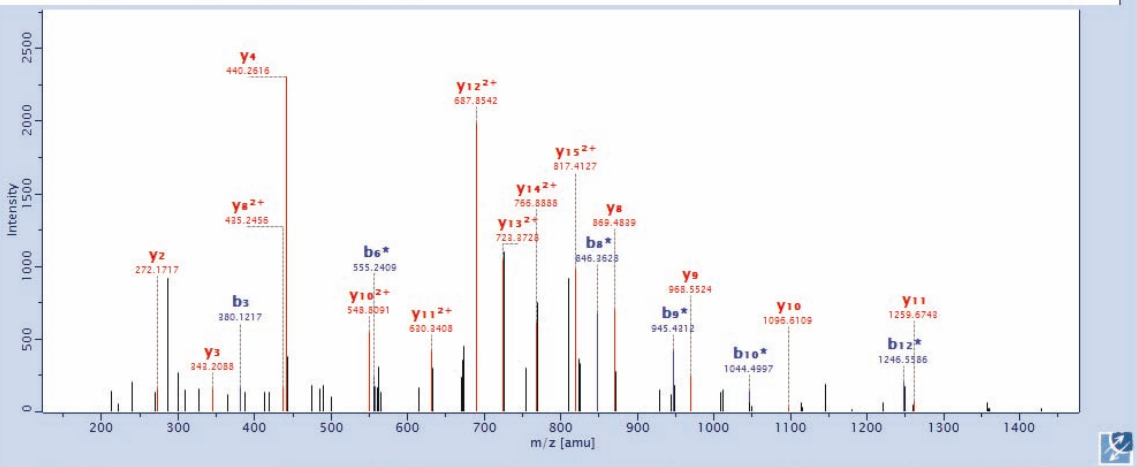

parent information

Mass:	1910.8775
m/z:	638.3
Charge:	3+
Mass Error [ppm]:	0.1223
PTM Score:	110.8
PEP:	5.3158E-06
Mascot Score:	37.4
Intensity:	1839497.9

general information

Annotation:	12 of 17 => 71 %
Intensity Coverage:	49 %
Protein Localisation:	288 ... 304

B-Ion					Y-Ion		Y-Ion²⁺	
Δ Da	mass		seq		mass	Δ Da	mass	Δ Da
NaN	182.0212859	1	T	17	NaN	NaN	NaN	NaN
NaN	279.0740498	2	P	16	1730.8707896	NaN	1730.8707896	NaN
0.0860354	**380.121728**	3	T	15	1633.8180257	NaN	**817.412651**	**0.3084793**
NaN	467.1537567	4	S	14	1532.7703472	NaN	**766.888812**	**0.0390804**
NaN	538.1908705	5	A	13	1445.7383188	NaN	**723.372798**	**0.0150096**
0.1898076	**555.240917**	6	D	12	1374.701205	NaN	**687.854241**	**0.315559**
NaN	816.281142	7	Y	11	**1259.67426**	**0.1249323**	**630.340769**	**0.0778099**
0.1566467	**846.362824**	8	Q	10	**1096.61093**	**0.0732137**	**548.809105**	**0.0020371**
0.0182254	**945.431237**	9	V	9	**968.552356**	**0.1522949**	968.552356	NaN
0.1110664	**1044.49965**	10	V	8	**869.483942**	**0.0255184**	**435.245609**	**0.0565758**
NaN	1229.5085758	11	S	7	770.4155281	NaN	770.4155281	NaN
0.2735886	**1246.55862**	12	D	6	683.3834997	NaN	683.3834997	NaN
NaN	1472.6304818	13	K	5	568.3565567	NaN	568.3565567	NaN
NaN	1569.6832457	14	P	4	**440.261594**	**0.0740997**	440.2615937	NaN
NaN	1640.7203595	15	A	3	**343.20883**	**0.0171794**	343.2088298	NaN
NaN	1737.7731233	16	P	2	**272.171716**	**0.1399295**	272.171716	NaN
NaN	NaN	17	R	1	175.1189522	NaN	175.1189522	NaN

Protein IDs: gi_4584796;gi_148232142;gi_15987768;gi_nup53a;gi_nup53b
Scannumber 5827
Source: 20101126_CO_JM_0221WoAn_R5_IP_mitotic_01
Method: CID; ITMS

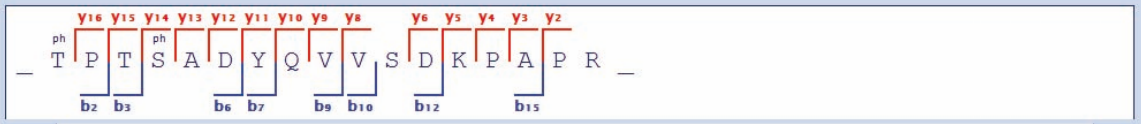

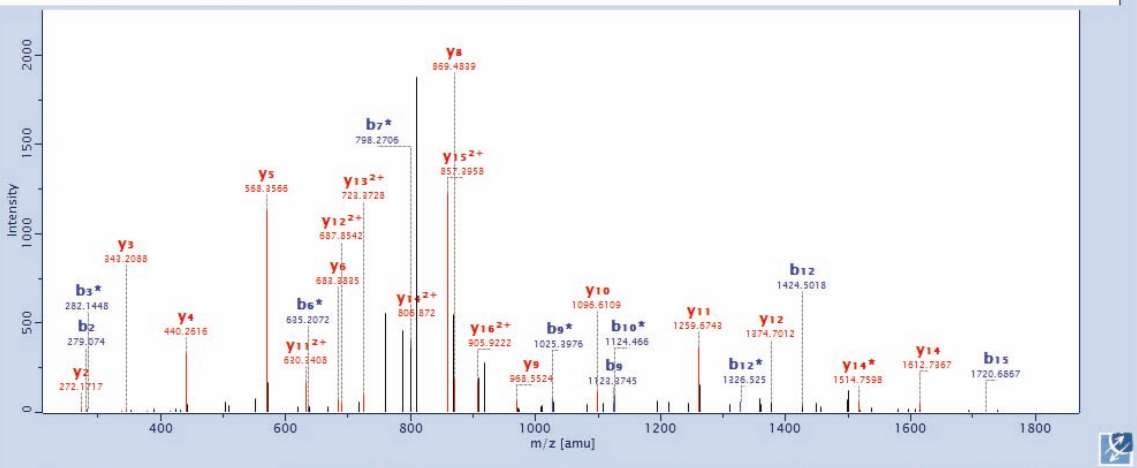

parent information

Mass:	1990.8439
m/z:	996.93
Charge:	2+
Mass Error [ppm]:	0.12316
PTM Score:	173.19
PEP:	3.1561E-23
Mascot Score:	52.53
Intensity:	723052.1

general information

Annotation:	14 of 17 => 82 %
Intensity Coverage:	46 %
Protein Localisation:	288 ... 304

B-Ion					Y-Ion		Y-Ion²⁺	
Δ Da	mass		seq		mass	Δ Da	mass	Δ Da
NaN	182.0212859	1	T	17	NaN	NaN	NaN	NaN
0.280595	**279.07405**	2	P	16	1810.8371206	NaN	**905.922199**	**0.03349**
0.2120625	**282.144832**	3	T	15	1713.7843567	NaN	**857.395817**	**0.1478846**
NaN	547.1200877	4	S	14	**1514.75978**	**0.204207**	**806.871977**	**0.2981887**
NaN	618.1572015	5	A	13	1445.7383188	NaN	**723.372798**	**0.4335988**
0.0729639	**635.207248**	6	D	12	**1374.70121**	**0.0788243**	**687.854241**	**0.1524731**
0.03962	**798.270577**	7	Y	11	**1259.67426**	**0.0252142**	**630.340769**	**0.1820579**
NaN	1024.3060505	8	Q	10	**1096.61093**	**0.1455363**	1096.6109335	NaN
0.0783546	**1025.39757**	9	V	9	**968.552356**	**0.0307739**	968.552356	NaN
0.1582852	**1124.46598**	10	V	8	**869.483942**	**0.1000423**	869.483942	NaN
NaN	1309.4749068	11	S	7	770.4155281	NaN	770.4155281	NaN
0.0591335	**1326.52495**	12	D	6	**683.3835**	**0.0513464**	683.3834997	NaN
NaN	1552.5968128	13	K	5	**568.356557**	**0.0124619**	568.3565567	NaN
NaN	1649.6495767	14	P	4	**440.261594**	**0.0915863**	440.2615937	NaN
0.2862099	**1720.68669**	15	A	3	**343.20883**	**0.1309529**	343.2088298	NaN
NaN	1817.7394543	16	P	2	**272.171716**	**0.0334842**	272.171716	NaN
NaN	NaN	17	R	1	175.1189522	NaN	175.1189522	NaN

Figure S3

(A) Nup53 is phosphorylated in interphase and mitosis

4 µl of mitotic (CSF arrested) or interphasic Xenopus egg extracts were diluted in 100 µl of phosphatase buffer (NEB) and incubated where indicated with 400 U λ-phosphatase for 30 min at 30°C. Samples were analyzed by 12% SDS-PAGE and Western blotting using the Xenopus Nup53 antibody. Please note the different shifting of mitotic and interphasic Nup53 after phosphatase treatment indicating that Nup53 is a phosphoprotein throughout the cell cycle but hyperphosphorylated during mitosis.

(B) Fragmentation mass spectra of Xenopus Nup53 peptides carrying mitotic specific phosphorylations

Supplementary Figure S4

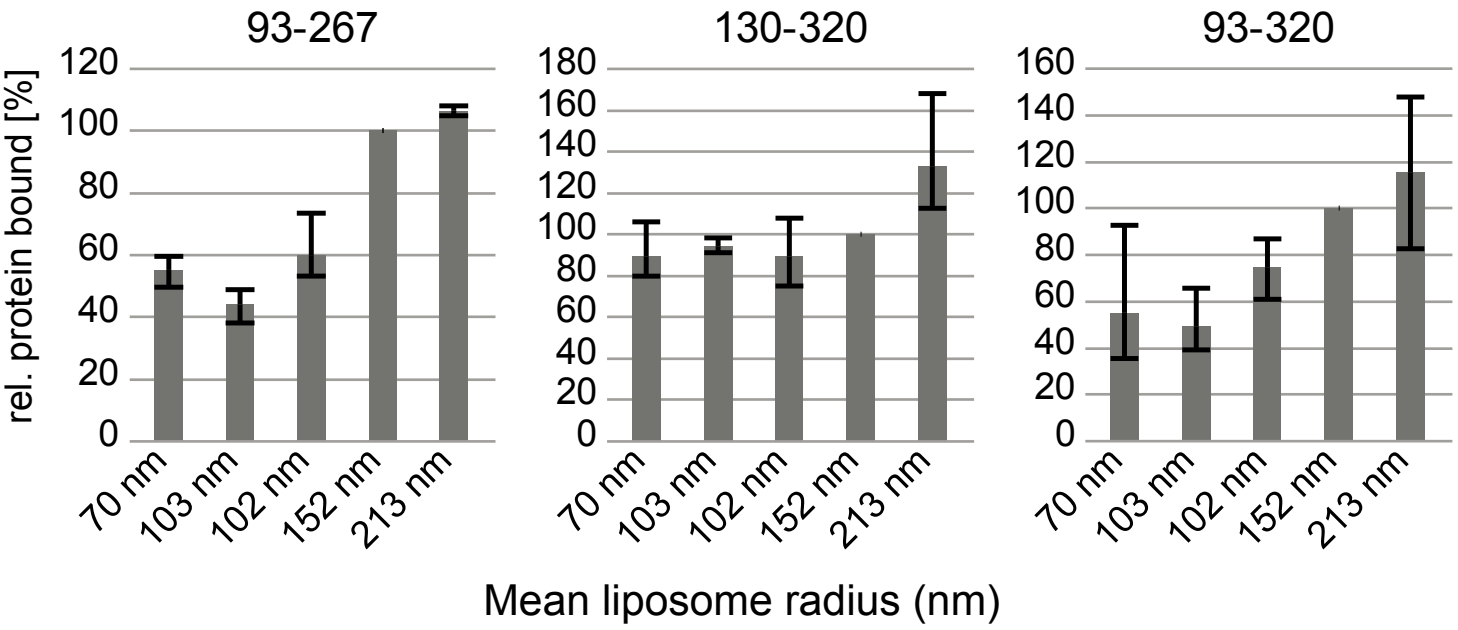

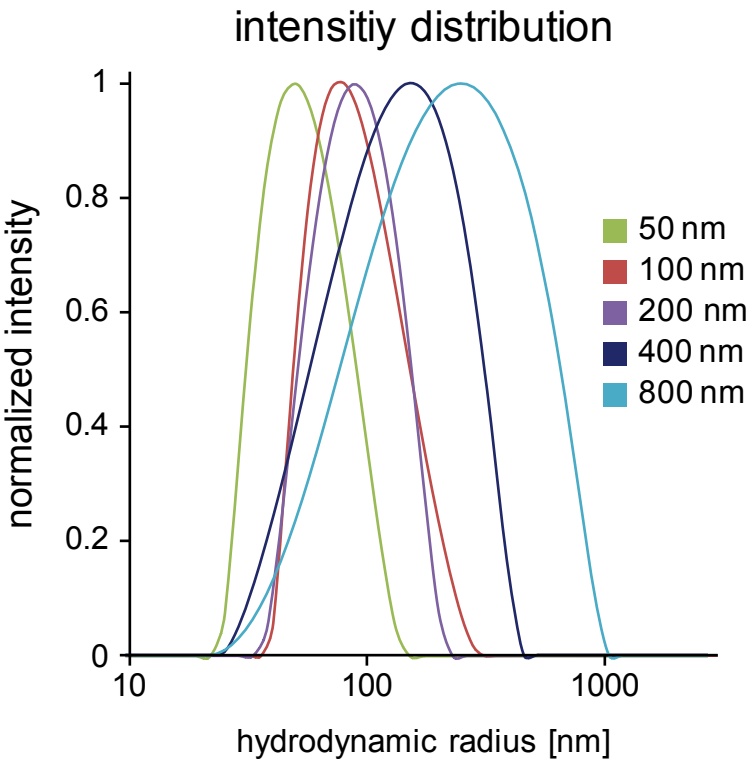

Figure S4

The two Nup53 membrane binding regions show different sensitivity to membrane curvature. Fragments comprising the N-terminal (93-267), C-terminal (130-320) or both (93-320) membrane binding sites, respectively, including the RRM domains were incubated with differently sized liposomes as indicated by the determined mean radii. Liposome binding was quantified as in Figure 2C. Whereas fragments which include the N-terminal membrane binding site (93-267 and 93-320) showed a significantly reduced binding to smaller liposome diameters and thus to higher membrane curvature this effect was not seen for the C-terminal membrane binding site (130-320). The averages of three independent experiments, normalized to the binding of the respective fragments to 150 nm liposomes, are shown. Error bars represent the range. Liposome radii were determined by light scattering after extrusion through membranes of different pore size as indicated for the different measurements. The lower panel shows one exemplary measurement done to determine the average radius of the respective preparation. Please note the rather similar average radii of liposomes prepared using 100 nm and 200 nm membranes.

Supplementary Figure S5

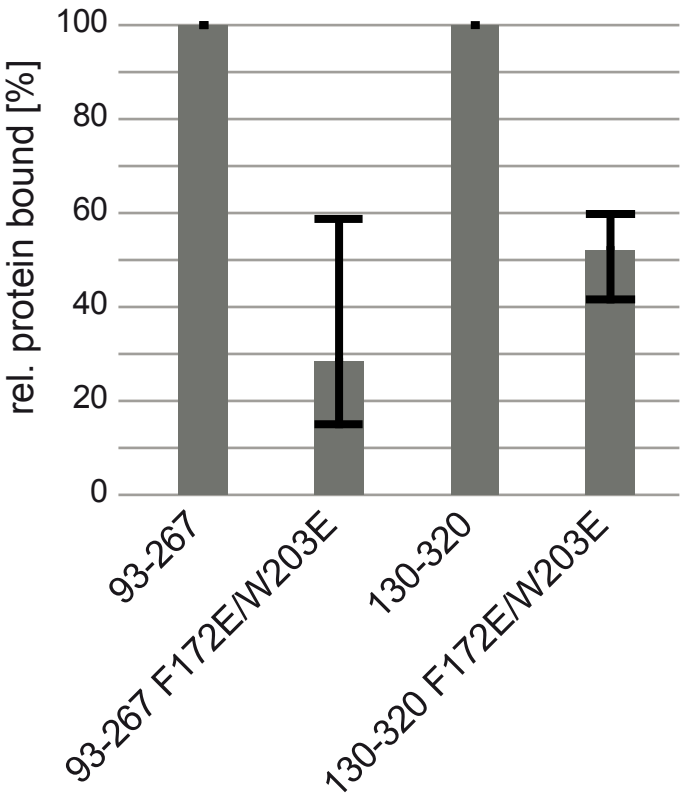

Figure S5

Both Nup53 membrane binding regions require dimerization by the RRM domain.

Nup53 fragments containing the first (93-267) or second (130-320) membrane binding region including the RRM domain were quantitatively assayed for liposome binding as in Figure 2C. Whereas fragments containing the wild type RRM domain bound to liposomes, introduction of two amino acid changes (F172E/W203E), which render the RRM domain incapable of dimerization, reduced liposome binding for both fragments. The averages of three independent experiments, normalized to liposome binding of the wild type protein, are shown. Error bars represent the range.

Supplementary Figure S6

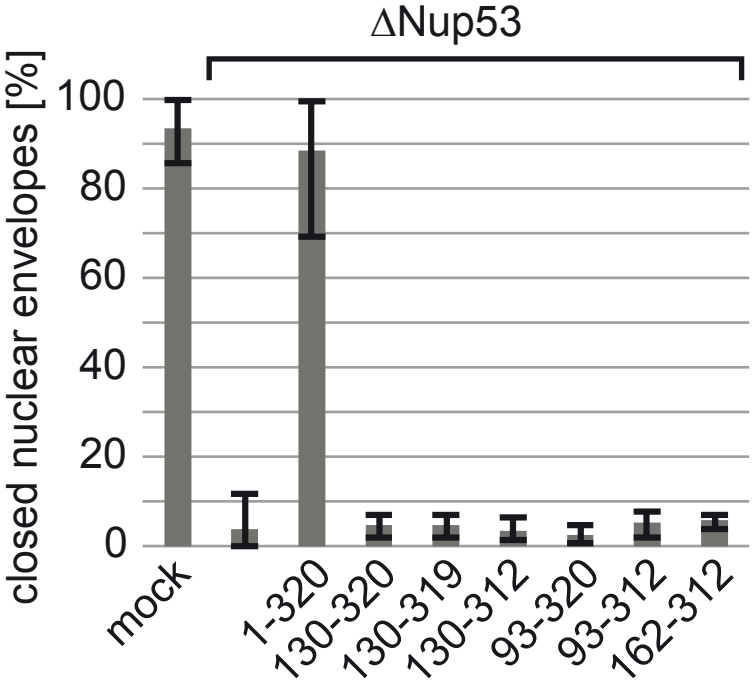

Figure S6

The interaction of Nup53 to Nup93 is necessary for nuclear envelope formation.

Nuclei were assembled in mock, Nup53 depleted extracts or Nup53 depleted extracts supplemented with wild type protein (1-320) or various fragments of Nup53 for 120 min, fixed with 2% PFA and 0.5% glutaraldehyde and analyzed for chromatin and membrane staining. Shown is the quantitation of chromatin substrates with a closed nuclear envelope as done in Figure 2F. Please note that all fragments lacking the N-terminal region of Nup53 necessary for Nup93 interaction (Figure S1A) and especially fragment 162-312 which has the ability to interact with Nup155 (Figure S1B) did not support nuclear envelope formation.

Supplementary Figure S7

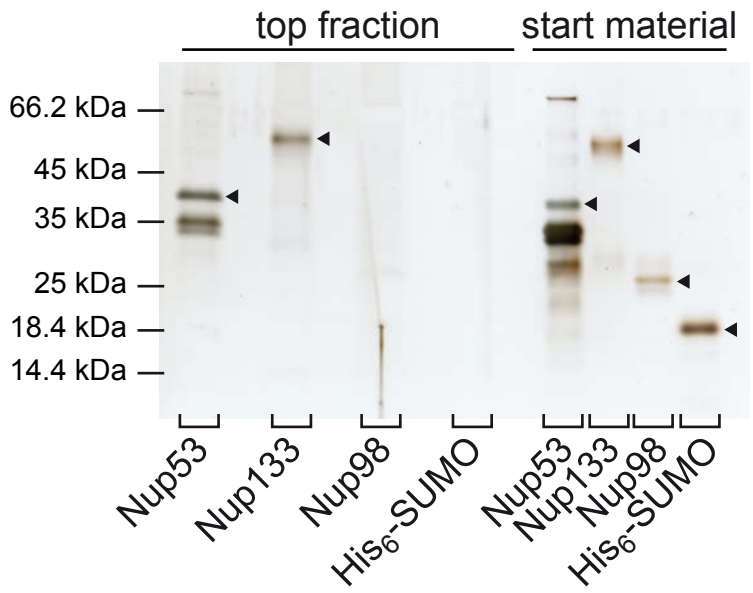

Figure S7

Recombinant Nup53 binds to liposomes mimicking the ER / nuclear envelope lipid composition

3 µM recombinant Xenopus Nup53 (Nup53) a fragment of Nup133 (aa 67-514) as positive control and Nup98 (aa 676-863) and His_6-tagged SUMO as negative controls, were incubated with 6 mg/ml fluorescently labeled liposomes prepared from a lipid mixture mimicking the ER/nuclear envelope lipid composition (see materials and methods). Flotation was done as described in Figure 1A.

Table S1: Peptides and phosphorylation sites identified in Xenopus Nup53 by mass spectrometric analysis

phosphopeptide	amino acid
PSAGAQFLPGFLLGDIPTPV**T**PQPR	T46
SPLH**S**GG**S**PPQPVLPTHK	S60, S64, S67
SPLHSGG**S**PPQPVLPTHK	S67
SIYDDVA**S**PGLGSTPR	S94
SIYDDVA**S**PGLGS**T**PR	S94, T100
MASFSVLHTPLSGAIPS**S**PAVFSPATIGQSR	S124
MASFSVLHTPLSGAIPSSPAVF**S**PATIGQSR	S131
V**S**TPSVSSVFTPPVK	S249
VS**T**PSVSSVFTPPVK	T250
VSTP**S**VSSVFTPPVK	S252
VSTP**S**VSSVF**T**PPVK	S252, T258
VSTPSVSSVF**T**PPVK	T258
SIRTPTQSVGTPR	S263
SIR**T**PTQSVGTPR	T266
SIRTPTQ**S**VGTPR	S270
TPTQSVG**T**PR	T273
TPTSADYQVVSDKPAPR	T288
TPT**S**ADYQVVSDKPAPR	T288, S291

Phosphorylation sites mapped in XenopusNup53 (genebank accession JQ747515) after immunoprecipitation from mitotic or interphase Xenopus egg extracts. Phosphorylation sites are indicated in red. Position T100, T288 and S291 were phosphorylated on Nup53 isolated from mitotic, but not interphasic extracts.

Table S2: DNA constructs used in this study

Constructs
pET28a SUMO Nup53xl 1-166
pET28a SUMO Nup53xl 1-267
pET28a SUMO Nup53xl 1-312
pET28a SUMO Nup53xl 1-312 S94E/T100E
pET28a SUMO Nup53xl 1-312 R105E/K106E
pET28a SUMO Nup53xl 1-319
pET28a SUMO Nup53xl 1-319 S94E/T100E
pET28a SUMO Nup53xl 1-319 R105E/K106E
pET28a SUMO Nup53xl 1-320
pET28a SUMO Nup53xl 1-320 S94E/T100E
pET28a SUMO Nup53xl 1-320 R105E/K106E
pET28a SUMO Nup53xl 1-320 F172E/W203E
pET28a SUMO Nup53xl 93-267
pET28a SUMO Nup53xl 93-267 S94A/T100A
pET28a SUMO Nup53xl 93-267 S94E/T100E
pET28a SUMO Nup53xl 93-267 R105E/K106E
pET28a SUMO Nup53xl 93-267 F172E/W203E
pET28a SUMO Nup53xl 93-312
pET28a SUMO Nup53xl 93-319
pET28a SUMO Nup53xl 93-320
pET28a SUMO Nup53xl 93-320 S94E/T100E
pET28a SUMO Nup53xl 93-320 R105E/K106E
pET28a SUMO Nup53xl 93-320 F172E/W203E
pET28a SUMO Nup53xl 107-267
pET28a SUMO Nup53xl 130-267
pET28a SUMO Nup53xl 130-312
pET28a SUMO Nup53xl 130-319
pET28a SUMO Nup53xl 130-320
pET28a SUMO Nup53xl 130-320 F172E/W203E
pET28a SUMO Nup53xl 162-267
pET28a SUMO Nup53xl 162-267 F172E/W203E
pET28a SUMO Nup53xl 162-312
pET28a SUMO Nup53xl 162-320
pET28a SUMO Nup53xl 254-320
pET28a SUMO Nup59sc 1-528
pET28a SUMO Nup53sc 1-475
pET28a PP Nup133hs 30-514
pET28a NusA Nup98xl 676-863
pET28a GST Nup53xl 1-267
pET28a GST Nup53xl 1-267 S94A/T100A
pET28a GST Nup53xl 1-267 S94E/T100E
pET28a GST Nup53xl 1-267 R105E/K106E
pET28a GST Nup53xl 1-267 F172E/W203E
pET28a GST Nup53xl 162-267
pET28a GST Nup53xl 162-312
pET28a GST Nup53xl 162-319
pET28a GST Nup53xl 162-320
pET28a GST Nup53xl 162-320 F172E/W203E
pET28a GST Nup98xl 487-634

Constructs
pSI HA Nup53xl
pSI HA Nup53xl F172E/W203E
pSI myc Nup53xl
pSI myc Nup53xl F172E/W203E

Supplementary Methods

Pulldown experiments

Fragments used for the GST pulldown experiments were cloned into a modified pET28a vector with GST tag followed by a recognition site for TEV protease and purified via the N-terminal His_6 tag. 60 µl GSH–Sepharose (GE Healthcare) were incubated with 300 µg of the respective bait proteins, washed and blocked with 5% BSA in PBS. Beads were incubated with cytosol from Xenopus egg extracts (diluted 1:1 with PBS, and cleared by centrifugation for 30 min at 100,000 rpm in a TLA110 rotor (Beckman Coulter) for 2 h and washed six times with PBS. Bound proteins were eluted by cleavage with TEV protease (0.5 mg/ml) for 1 h at RT and analyzed by SDS-PAGE and Western blotting. For detection of NDC1 and GP210, 5 mg of membranes from Xenopus egg extracts (Antonin et al, 2005) were solubilized in 5 ml 50 mM Phosphate buffer pH 7.4, 500 mM NaCl, 1% Triton X-100 and protease inhibitors (Roche), instead of cytosol and the first four washes with PBS were in the presence of 0.1% Triton X-100.

Mass Spectrometry

2 ml interphasic (Hartl et al, 1994) or (CSF arrested) mitotic (Murray, 1991) Xenopus egg extracts were diluted with 1.2 ml wash buffer (10 mM HEPES, 50 mM KCl, 2.5 mM $MgCl_2$ pH 7.4), cleared by centrifugation for 10 min at 100,000 rpm in a TLA110 rotor and incubated with 50 µl Protein A Sepharose (GE Healthcare), to which affinity purified Nup53 antibodies were bound and crosslinked with 10 mM dimethylpimelimidate (Pierce). After 1h incubation the sepharose was washed 10 times with wash buffer. Proteins were eluted with SDS sample buffer (without DTT) and separated by SDS-PAGE. Gel sections from 30-45 kDa were excised and proteins were in-gel digested by trypsin. The resulting peptide mixtures were measured on an LTQ-Orbitrap XL and processed by MaxQuant software as described (Borchert et al, 2010). Multistage activation was enabled in all MS measurements.

Generation of liposomes

A mixture of lipids resembling the ER/nuclear envelope composition (Franke et al, 1970) (60 mol % phosphatidylcholine, 19.8 mol % phosphatidylethanolamine, 10 mol % phosphatidylinositol, 5 mol % cholesterol, 2.5 mol % sphingomyelin, 2.5 mol % phosphatidylserine 0.2 mol % 18:1-12:0 NBD-PE all Avanti polar lipids) dissolved in chloroform were dried on a rotary evaporator and overnight under vacuum. PBS buffer was gently added to result in a final lipid concentration of 6 mg/ml. After 2 h of incubation at

37°C to allow spontaneous liposome formation the flask was agitated to dissolve residual lipids. After ten cycles of freeze/thawing liposomes were extruded as described before.

DNA sequence of Xenopus laevis Nup53 optimized for expression in E. coli

ATGATGGCAGCAGCATTTAGCATGGAACCGATGGGTGCAGAACCGATGGCACTG
GGTAGCCCGACCAGCCCGAAACCGAGTGCCGGTGCACAGTTTCTGCCTGGTTTTC
TGCTGGGTGATATTCCGACACCGGTTACACCGCAGCCTCGTCCGAGCCTGGGTAT
TATGGAAGTTCGTAGTCCGCTGCATAGCGGTGGTAGTCCTCCGCAGCCGGTTCTG
CCGACCCATAAAGATAAAAGCGGTGCACCTCCGGTTCGTAGCATTTATGATGATG
TTGCAAGTCCGGGTCTGGGTAGCACACCGCGTAATACCCGTAAAATGGCAAGCTT
TAGCGTTCTGCATACACCTCTGAGCGGTGCAATTCCGAGCAGTCCGGCAAGCAAT
GTTTTTAGTCCGGCAACCATTGGTCAGAGCCGTAAAACCACCCTGAGTCCGGCAC
AGATGGACCCGTTTTATACCCAGGGTGATGCACTGACCAGTGATGATCAGCTGGA
TGATACCTGGGTTACCGTTTTTGGTTTTCCGCAGGCAAGCGCAAGCTATATTCTGC
TGCAGTTTGCACAGTATGGCAATATTATTAAACATGTGATGAGCAATAATGGCAA
TTGGATGCATATTCAGTATCAGAGCAAACTGCAGGCACGTAAAGCACTGAGCAA
AGATGGTCGTATTTTTGGTGAAAGCATTATGATTGGTGTGAAACCGTGCATTGAT
AAAAGCGTTATGGAAGCAACCGAAAAAGTTAGCACCCCGAGCGTTAGCAGCGTT
TTTACACCTCCGGTTAAAAGCATTCGTACCCCGACCCAGAGCGTTGGTACACCGC
GTGCAGCAAGCATGCGTCCGCTGGCAGCAACCTATCGCACCCCGACCAGCGCAG
ATTATCAGGTTGTTAGCGATAAACCGGCACCGCGTAAAGATGAAAGCATTGTTAG
CAAAGCCATGGAATATATGTTTGGTTGGTGATAG

DNA sequence of Saccharomyces cerevisiae NUP53 optimized for expression in E. coli

ATGGCAGATCTGCAGAAACAAGAAAATTCAAGCCGTTTTACCAATGTTAGCGTTA
TTGCACCGGAAAGCCAGGGTCAGCATGAACAGCAGAAACAGCAAGAACAACAA
GAACAGCAGAAACAGCCGACAGGTCTGCTGAAAGGTCTGAATGGTTTTCCGAGC
GCACCGCAGCCGCTGTTTATGGAAGATCCTCCGAGCACCGTTAGCGGTGAACTGA
ATGATAATCCGGCATGGTTTAATAATCCGCGTAAACGTGCAATTCCGAATAGCAT
TATTAAACGTAGCAATGGTCAGAGCCTGAGTCCGGTTCGTAGCGATAGCGCAGAT
GTTCCGGCATTTAGCAATAGCAATGGCTTTAATAATGTGACCTTTGGCAGCAAAA
AAGATCCGCGTATTCTGAAAAATGTGAGCCCGAATGATAATAATAGCGCCAATA
ATAATGCCCATAGCAGCGATCTGGGCACCGTTGTTTTTGATAGCAATGAAGCACC
TCCGAAAACCAGCCTGGCAGATTGGCAGAAAGAAGATGGTATTTTTAGCAGCAA
AACCGATAATATTGAAGATCCGAATCTGAGCAGCAATATTACCTTTGATGGTAAA
CCGACCGCAACCCCGAGCCCGTTTCGTCCGCTGGAAAAAACCAGCCGTATTCTGA
ATTTTTTTGATAAAAATACCAAAACCACCCCGAATACCGCAAGCAGCGAAGCAA
GCGCAGGTAGCAAAGAAGGTGCAAGCACCAATTGGGATGATCATGCCATTATTA
TTTTTGGCTATCCGGAAACCATTGCCAATAGTATTATTTTTCATTTTGCCAATTTTG
GCGAAATTCTGGAAGATTTTCGCGTGATTAAAGATTTTAAAAAGCTGAACAGCAA
AAATAAAAGCAAAAGCCCGAGCCTGACCGCACAGAAATATCCGATTTATACCGG
TGATGGTTGGGTTAAACTGACCTATAAAAGCGAACTGAGCAAAAGCCGTGCACT
GCAAGAAAATGGCATTATTATGAATGGCACCCTGATTGGTTGCGTTAGCTATAGT
CCGGCAGCACTGAAACAGCTGGCAAGCCTGAAAAAAAGCGAAGAAATTATTAAT
AATAAAACCAGCAGCCAGACCAGCCTGAGCAGCAAAGATCTGAGCAATTATCGT
AAAACCGAAGGCATTTTTGAAAAAGCCAAAGCAAAAGCGGTGACCAGCAAAGTT
CGTAATGCCGAATTTAAAGTGAGCAAAAATAGCACCAGCTTTAAAAATCCGCGTC
GCCTGGAAATTAAAGATGGTCGTAGCCTGTTTCTGCGTAATCGTGGTAAAATTCA
TAGCGGTGTTCTGAGCAGCATTGAAAGCGATCTGAAAAAACGTGAACAGGCAAG
CAAAAGCAAAAAAAGCTGGCTGAATCGCCTGAATAATTGGCTGTTTGGTTGGAAT
GATCTGTAGTGA

DNA sequence of Saccharomyces cerevisiae NUP59 optimized for expression in E. coli

ATGTTTGGTATTCGCAGCGGCAATAATAATGGTGGTTTTACCAATCTGACCAGCC
AGGCACCGCAGACCACCCAGATGTTTCAGAGCCAGAGCCAGCTGCAGCCGCAGC
CGCAGCCTCAACCGCAGCAGCAGCAACAGCATCTGCAGTTTAATGGTAGCAGTG
ATGCAAGCAGCCTGCGTTTTGGTAATAGCCTGAGCAATACCGTGAATGCCAATAA
TTATAGCAGCAATATTGGCAATAACAGCATCAACAATAATAACATCAAAAATGG
CACCAATAACATTAGCCAGCATGGTCAGGGCAATAATCCGAGCTGGGTTAATAAT
CCGAAAAAACGTTTTACACCGCATACCGTTATTCGTCGTAAAACCACCAAACAGA
ATAGCAGCAGCGATATTAATCAGAATGATGATAGCAGCAGCATGAATGCAACCA
TGCGTAATTTTAGCAAACAGAATCAGGATAGCAAACATAATGAACGCAATAAAA
GCGCAGCCAATAATGATATTAATAGCCTGCTGAGCAACTTTAATGATATTCCTCC
GAGCGTTACCCTGCAGGATTGGCAGCGTGAAGATGAATTTGGTAGCATTCCGAGC
CTGACCACCCAGTTTGTTACCGATAAATATACCGCCAAAAAAACCAATCGCAGCG
CCTATGATAGCAAAAATACCCCGAATGTGTTTGATAAAGATAGCTATGTGCGCAT
TGCCAATATTGAACAGAATCATCTGGATAATAATTATAATACCGCAGAAACCAAT
AATAAAGTGCATGAAACCAGCAGCAAAAGCAGCAGCCTGAGCGCAATTATTGTT
TTTGGTTATCCGGAAAGCATTAGCAATGAACTGATTGAACATTTTAGCCATTTTGG
CCATATTATGGAAGATTTTCAGGTTCTGCGTCTGGGTCGTGGTATTAATCCGAATA
CCTTTCGCATTTTTCATAATCATGATACCGGCTGTGATGAAAATGATAGCACCGTG
AATAAAAGCATTACCCTGAAAGGTCGCAATAATGAAAGTAATAACAAAAAATAT
CCGATTTTTACAGGCGAAAGCTGGGTTAAACTGACCTATAATAGCCCGAGCAGCG
CACTGCGTGCACTGCAAGAAAATGGTACAATTTTTCGTGGTAGCCTGATTGGTTG
TATTCCGTATAGCAAAAATGCCGTTGAACAGCTGGCAGGTTGCAAAATTGATAAT
GTGGATGATATTGGCGAATTTAATGTGAGCATGTATCAGAATAGCAGTACCAGCA
GCACCAGCAATACCCCGAGTCCTCCGAATGTTATTATTACCGATGGCACCCTGCT
GCGCGAAGATGATAATACACCGGCAGGTCATGCAGGCAATCCGACCAATATTAG
CAGCCCGATTGTTGCAAATAGCCCGAATAAACGTCTGGATGTGATTGATGGTAAA
CTGCCGTTTATGCAGAATGCAGGTCCGAATAGCAATATTCCGAATCTGCTGCGTA
ATCTGGAAAGCAAAATGCGTCAGCAAGAAGCAAAATATCGTAATAATGAACCGG
CAGGCTTTACCCATAAACTGAGCAATTGGCTGTTTGGTTGGAATGATCTGTAGTG
A

Supplementary References

Antonin W, Franz C, Haselmann U, Antony C, Mattaj IW (2005) The integral membrane nucleoporin pom121 functionally links nuclear pore complex assembly and nuclear envelope formation. *Molecular cell* **17:** 83-92

Borchert N, Dieterich C, Krug K, Schutz W, Jung S, Nordheim A, Sommer RJ, Macek B (2010) Proteogenomics of Pristionchus pacificus reveals distinct proteome structure of nematode models. *Genome research* **20:** 837-846

Franke WW, Deumling B, Baerbelermen, Jarasch ED, Kleinig H (1970) Nuclear membranes from mammalian liver. I. Isolation procedure and general characterization. *The Journal of cell biology* **46:** 379-395

Hartl P, Olson E, Dang T, Forbes DJ (1994) Nuclear assembly with lambda DNA in fractionated Xenopus egg extracts: an unexpected role for glycogen in formation of a higher order chromatin intermediate. *The Journal of cell biology* **124:** 235-248

Murray AW (1991) Cell cycle extracts. *Methods in cell biology* **36:** 581-605

Schagger H, von Jagow G (1987) Tricine-sodium dodecyl sulfate-polyacrylamide gel electrophoresis for the separation of proteins in the range from 1 to 100 kDa. *Analytical biochemistry* **166:** 368-379

© 2014. Published by The Company of Biologists Ltd | Journal of Cell Science (2014) 127, 908–921 doi:10.1242/jcs.141739

RESEARCH ARTICLE

Interaction of Nup53 with Ndc1 and Nup155 is required for nuclear pore complex assembly

Nathalie Eisenhardt, Josef Redolfi and Wolfram Antonin*

ABSTRACT

Nuclear pore complexes (NPCs) are the gateways for nucleocytoplasmic exchange. The ordered assembly of these huge complexes from several hundred individual components into an intricate protein interaction network which deforms the two membranes of the nuclear envelope into a pore is only rudimentarily understood. Here, we show that the interaction between Nup53 and the integral pore membrane protein Ndc1 is essential for vertebrate NPC assembly. The Ndc1 binding site on Nup53 overlaps with a region that induces membrane bending and is specifically required to modulate this activity, suggesting that the membrane-deforming capability of Nup53 is adjusted during the NPC assembly process. We further demonstrate that the interaction of Nup53 and Nup155 has a crucial role in NPC formation as the main determinant of recruitment of Nup155 to the assembling pore. Overall, our results pinpoint the diversity of interaction modes accomplished by Nup53, highlighting this protein as an essential link between the pore membrane and the NPC, and as a crucial factor in the formation of the pore membrane.

KEY WORDS: Ndc1, Nuclear pore complex, Nup35, Nup53, Nup155

INTRODUCTION

The compartmentalization of eukaryotic cells entails the spatial organization of specialized functions in distinct membrane-bound organelles. The characteristic organelle of eukaryotes is the nucleus, which is enclosed by the double membrane of the nuclear envelope (NE). The NE forms a barrier that separates nuclear gene transcription from cytoplasmic protein synthesis, thereby ensuring accurate processing of the genetic information. Nuclear pore complexes (NPCs) intercept the NE at fusion sites of the two membranes and mediate the selective transport of macromolecules. In most eukaryotic cells, NPCs represent the largest protein complexes but contain only about 30 individual proteins, which are called nucleoporins (Nups), and are found in up to 32 copies per NPC (Cronshaw et al., 2002; Ori et al., 2013; Rout et al., 2000). They can be categorized into two groups: (1) scaffold nucleoporins, which form the NPC structural backbone and (2) barrier nucleoporins, which execute transport functions and exclude inert molecules from passage.

Friedrich Miescher Laboratory of the Max Planck Society, Spemannstr. 39, 72076 Tübingen, Germany.

*Author for correspondence (wolfram.antonin@tuebingen.mpg.de)

This is an Open Access article distributed under the terms of the Creative Commons Attribution License (http://creativecommons.org/licenses/by/3.0), which permits unrestricted use, distribution and reproduction in any medium provided that the original work is properly attributed.

Received 27 August 2013; Accepted 30 November 2013

The core NPC scaffold resides close to the pore membrane and is formed by two conserved subcomplexes, the Nup107–Nup160 complex and the Nup93 complex (Nup84 and Nic96 complexes in *S. cerevisiae*). Nucleoporins of these subcomplexes show structural similarities to vesicle coats (Brohawn et al., 2008; Devos et al., 2004; Mans et al., 2004) and might stabilize the highly curved pore membrane. The core scaffold is linked to the pore membrane through integral membrane proteins. So far, four membrane nucleoporins have been identified in different organisms: Pom34, Pom152, Pom33 and Ndc1 in yeast (Chadrin et al., 2010; Lau et al., 2004; Miao et al., 2006; Wozniak et al., 1994) and Gp210, Pom121 and Ndc1, which is the only one conserved as an integral pore membrane protein, in vertebrates (Gerace et al., 1982; Hallberg et al., 1993; Mans et al., 2004; Mansfeld et al., 2006; Stavru et al., 2006).

Ndc1 is crucial for NPC assembly in vertebrates and yeast (Madrid et al., 2006; Mansfeld et al., 2006; Stavru et al., 2006). It interacts with Nup53 (also referred to as Nup35), a member of the Nup93 complex, in metazoa and its two *S. cerevisiae* orthologs, Nup53 and Nup59 (Hawryluk-Gara et al., 2008; Mansfeld et al., 2006; Onischenko et al., 2009; Uetz et al., 2000; Vollmer et al., 2012). This interaction might link NPCs to the pore membrane. However, in some organisms Ndc1 is dispensable for NPC assembly or absent from the genome (DeGrasse et al., 2009; Liu et al., 2009; Mans et al., 2004; Neumann et al., 2010; Stavru et al., 2006). In vertebrates, the interaction between Ndc1 and Nup53 seems dispensable for NPC formation because Nup53 truncations lacking the Ndc1 binding region are functional in NPC assembly (Hawryluk-Gara et al., 2008; Vollmer et al., 2012). Hence, alternative interactions might connect the NPC with the pore membrane. Indeed, Nup53 and both of its yeast homologs can bind membranes directly (Patel and Rexach, 2008; Vollmer et al., 2012). In vertebrates, two independent membrane binding sites mediate the Nup53 interaction to the pore membrane and this feature is crucial for NPC assembly (Vollmer et al., 2012). Although either one of these membrane binding sites is sufficient for NPC assembly at the end of mitosis, they are not completely interchangeable because the C-terminal site deforms membranes and is exclusively required for NPC assembly during interphase.

In addition to its membrane-binding ability and its interaction with Ndc1, Nup53 is part of multiple protein–protein interactions within the Nup93–Nic96 complex. The metazoan protein, as well as its yeast counterparts Nup53 and Nup59, binds Nup155 (or its corresponding yeast proteins Nup157 and Nup170) and Nup93/Nic96 (Fahrenkrog et al., 2000; Hawryluk-Gara et al., 2005; Onischenko et al., 2009; Sachdev et al., 2012; Uetz et al., 2000; Vollmer et al., 2012). In a thermophilic fungus, additional direct interactions between Nup53 and Nup192, corresponding to Nup205 in metazoa, as well as Nup188 have been described (Amlacher et al., 2011). Nup53, Nup93 and Nup155 are each

Journal of Cell Science

Journal of Cell Science (2014) 127, 908–921 doi:10.1242/jcs.141739

essential for assembly of vertebrate NPCs and form a trimeric complex in which Nup93 stabilizes the interaction between Nup53 and Nup155 (Franz et al., 2005; Grandi et al., 1997; Hawryluk-Gara et al., 2008; Hawryluk-Gara et al., 2005; Krull et al., 2004; Mitchell et al., 2010; Sachdev et al., 2012; Vollmer et al., 2012). Additionally, Nup155 can interact with the transmembrane nucleoporins Ndc1 and Pom121 (Mitchell et al., 2010; Yavuz et al., 2010). Altogether, there seems to be a broad and at least partially redundant interaction network between the pore membrane including transmembrane nucleoporins and the Nup93 complex.

Here, we analyze the function of the different Nup53 interactions and their contribution to NPC assembly. By dissecting the direct membrane interaction of Nup53 and its ability to bind Ndc1, we find that the Ndc1–Nup53 interaction is indispensable for NPC formation. This interaction is not required for Nup53 recruitment to the NPC. Instead, Ndc1 is needed to modulate the membrane-deformation capability of Nup53 to promote NPC assembly. Similarly, we demonstrate that the direct binding of Nup53 to Nup155 is crucial for NPC assembly. This interaction localizes Nup155 to the nascent pore, a crucial step for downstream events in NPC biogenesis.

RESULTS

Ndc1 interacts directly with Nup53 through its N-terminal transmembrane regions

Xenopus Nup53 interacts directly with nuclear membranes and this membrane binding is crucial for NPC assembly (Vollmer et al., 2012). Nup53 is embedded in the complex protein–protein interaction network of the NPC, where different interactions might influence or regulate each other during NPC assembly or within the intact pore. In this respect, interaction of Nup53 with the integral pore membrane protein Ndc1 might be relevant for its membrane binding, but its functional importance is unknown. In *Xenopus laevis* the last eight amino acids of Nup53 are required for its interaction with Ndc1. This region also contains one of the two direct membrane binding sites. It is therefore important to determine whether these two features of Nup53 influence each other or act independently.

We reconstituted the interaction between *Xenopus* Nup53 and Ndc1 using recombinant proteins overexpressed in *E. coli*. Because Ndc1 is an integral membrane protein, it is important to maintain its membrane environment to preserve its functionality. To this end, a MISTIC tag (Roosild et al., 2005) was used to direct Ndc1 to the inner *E. coli* membrane. After harvesting the bacteria, membrane vesicles were generated and used as preys in GST pull-downs. The bait constructs comprised the C-terminal half of Nup53, including an RNA recognition motif (RRM) because this fragment interacts with Ndc1 (Vollmer et al., 2012 and supplementary material Fig. S1). In Nup53, the RRM domain acts as a dimerization domain and strengthens the interaction with other Nup93 complex members, including Nup93 and Nup155, and – most relevant here – is required for direct membrane binding (Handa et al., 2006; Vollmer et al., 2012). Hence, we used a dimerization mutant (F172E W203E, Nup53 162–320 RRM mutant, Fig. 1A) to discriminate protein–protein-mediated interactions from direct membrane binding of Nup53. Accordingly, *E.-coli*-derived membrane vesicles containing a fragment of the pore membrane protein Gp210 did not bind Nup53 above background levels (Fig. 1B). Inhibition of Nup53 dimerization does not affect Ndc1 interaction (Vollmer et al., 2012). Indeed, full-length Ndc1 eluted from the Nup53 bait, indicating a direct interaction.

Ndc1 consists of two parts: the N-terminal half comprises six predicted transmembrane helices and the C-terminal part is a conserved globular domain facing the nucleoplasmic side of the pore (Lau et al., 2006; Mansfeld et al., 2006; Stavru et al., 2006). To map the region required for the direct Nup53 interaction, we used membrane vesicles containing the N-terminal half of Ndc1 including all transmembrane helices (aa 1–301, Ndc1-N) or the C-terminal part starting from the last transmembrane helix including the globular C-terminal domain (aa 234–660, Ndc1-C, Fig. 1C). The Ndc1-N fragment bound Nup53 more strongly than the Ndc1-C fragment did (Fig. 1D). Further truncations of the transmembrane domain in which single transmembrane helices were sequentially deleted showed residual Nup53 binding (data not shown). This suggests that the Nup53 interaction surface is probably formed by multiple loops within the N-terminal region of Ndc1. Nup53 also interacted with the N-terminal half of Ndc1 in lysates of transfected HeLa cells (Fig. 1E). Here, full-length Ndc1 as well as Ndc1-N co-immunoprecipitated with Nup53. By contrast, Ndc1-C did not co-immunoprecipitate with Nup53. Accordingly, Nup53 co-immunoprecipitated with Ndc1 and Ndc1-N, but not Ndc1-C. Taken together, these data show that *Xenopus* Ndc1 and Nup53 interact directly and the N-terminal transmembrane domain of Ndc1 is necessary and sufficient for Nup53 binding.

The N- and the C-terminal halves of Ndc1 are required for NPC assembly

Having observed that the N-terminal half of Ndc1 mediates the interaction with Nup53, we tested whether this part is required for NPC assembly. For this, we used a cell-free system in which NPC assembly can be faithfully reconstituted. Incubation of cytosol and purified membranes from *Xenopus laevis* egg extracts with sperm heads gives rise to nuclei with closed NEs and functional NPCs (Gant and Wilson, 1997; Lohka and Masui, 1983; Wilson and Newport, 1988). Endogenous Ndc1 was specifically immunodepleted from the membrane fraction (Fig. 2A). This treatment did not affect other transmembrane proteins, including the pore membrane proteins Gp210 and Pom121. If mock-treated membranes and cytosol were used, a closed NE formed around the chromatin template, as indicated by membrane staining that had a smooth appearance (Fig. 2B,C). These nuclei contained NPCs as detected by the antibody mAB414, which acts as a read-out for NPC formation because it recognizes several nucleoporins that represent a major subfraction of the NPC. In the absence of Ndc1, a closed NE was not formed and mAB414 staining was markedly reduced, indicating a block in NE and NPC formation, consistent with a previous study (Mansfeld et al., 2006). Similar phenotypes have been observed upon depletion of other nucleoporins crucial for NPC assembly, including Pom121 (Antonin et al., 2005), Nup53 (Hawryluk-Gara et al., 2008; Vollmer et al., 2012), Nup93 (Grandi et al., 1997; Sachdev et al., 2012) and Nup155 (Franz et al., 2005). Upon depletion of Ndc1, Pom121 was still detected on the chromatin, showing that nuclear membrane recruitment to chromatin was not blocked in general (Fig. 2B,C). Re-addition of recombinant EGFP-tagged Ndc1 purified from *E. coli* and reconstituted into the Ndc1-depleted membranes rescued the phenotype at a concentration that was approximately endogenous. This demonstrates the specificity of the depletion and the functionality of the recombinant protein. Next, we replaced endogenous Ndc1 with EGFP-tagged Ndc1 fragments to investigate which region is required for NPC assembly. The Ndc1-N or the Ndc1-C fragments did not support NE and NPC formation, despite the fact that membrane vesicles containing the protein fragments were recruited to chromatin.

Journal of Cell Science

Journal of Cell Science (2014) 127, 908–921 doi:10.1242/jcs.141739

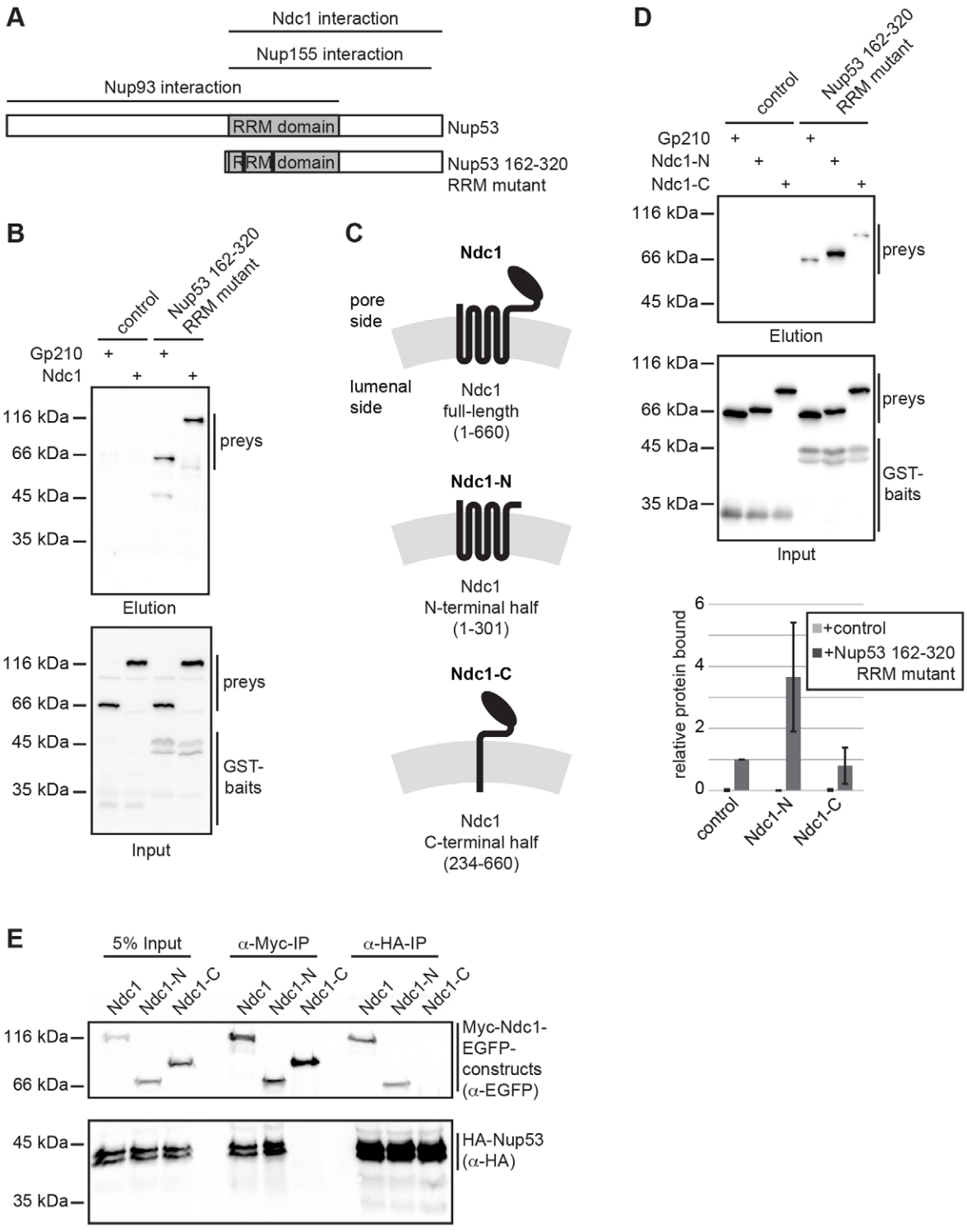

Fig. 1. The N-terminal portion of Ndc1 interacts directly with Nup53. (A) Schematic representation of *Xenopus* Nup53 and the Nup53 mutant fragment impaired for RRM-mediated dimerization and direct membrane binding. (B) GST fusions of the nucleoplasmic region of *Xenopus* Gp210 (control) or a Nup53 fragment comprising a mutated RRM domain decreasing direct membrane binding and the subsequent C-terminus (Nup53 162–320 RRM mutant) were incubated with *E.coli* lysates overexpressing the transmembrane region and the nucleoplasmic extension of *Xenopus* Gp210 or full-length Ndc1. Eluates and 3% of the input were analyzed by western blotting using a His_6 antibody. (C) Schematic representation of *Xenopus* Ndc1 (Ndc1), the N-terminal (Ndc1-N) and the C-terminal fragment (Ndc1-C) used. (D) Nup53 binding to the Ndc1-N and Ndc1-C fragments was analyzed as in B. The quantification shows the ratio of bait-bound protein to input of six independent experiments normalized to the binding of the lysate control to the Nup53 RRM mutant. Error bars show s.d. (E) HeLa cells were cotransfected with HA-tagged *Xenopus* Nup53 and full-length *Xenopus* Ndc1, the Ndc1-N or Ndc1-C fragment each fused with an N-terminal Myc and a C-terminal EGFP tag. Proteins were immunoprecipitated from cellular lysate with Myc or HA antibodies and analyzed by western blotting with indicated antibodies.

Journal of Cell Science (2014) 127, 908–921 doi:10.1242/jcs.141739

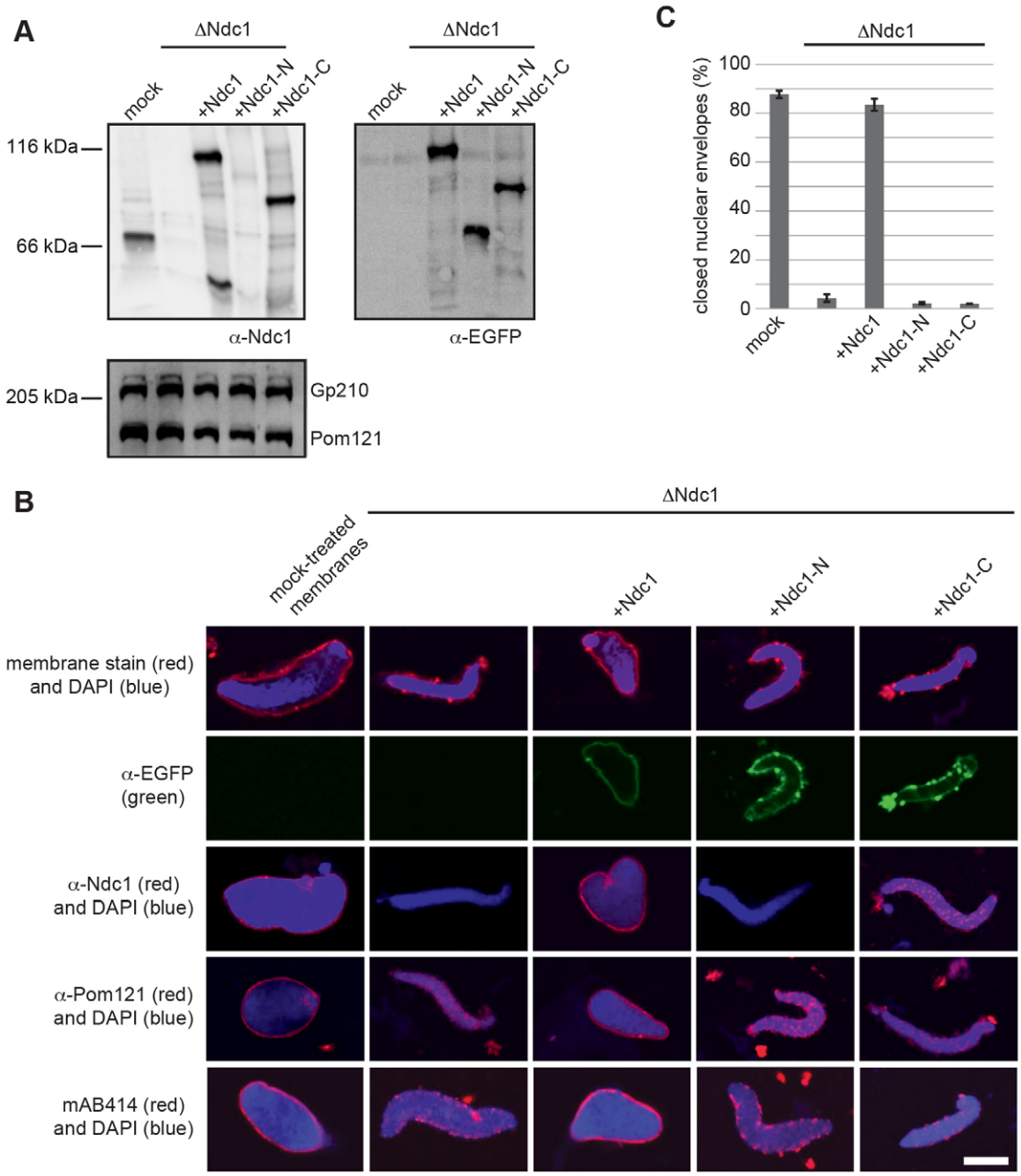

Fig. 2. Both the N-terminal and C-terminal halves of Ndc1 are required for NPC assembly. (A) Western blot analysis of mock-treated, Ndc1-depleted (ΔNdc1) or Ndc1-depleted and reconstituted membranes containing recombinant EGFP-tagged Ndc1, Ndc1-N or Ndc1-C fragments. Endogenous Ndc1, recombinant Ndc1 or Ndc1-C were detected by Ndc1 antibodies recognizing the C-terminus of the protein (left). The Ndc1-N construct, not recognized by this antibody, is detected – like all three recombinant Ndc1 proteins – by the EGFP antibody (right). Pom121 and Gp210 levels, detected with specific antibodies, were unaffected by the Ndc1 depletion and reconstitution (bottom panel). (B) Nuclei were assembled in cytosol and membranes from *Xenopus* egg extracts shown in A, and analyzed with indicated antibodies. Membranes were stained with $DiIC_{18}$ (red), DNA with DAPI (blue). Recombinant Ndc1 proteins were detected with EGFP antibodies (green), endogenous Ndc1, recombinant Ndc1 and the Ndc1-C fragment also with Ndc1 antibodies. Scale bar: 10 μm. (C) More than 300 nuclei of three independent experiments shown in B were quantified for the percentage of nuclei with closed NEs. Error bars show s.d.

This indicates that both parts of Ndc1 are required for NE and NPC assembly.

The N-terminal half of Ndc1 is dispensable for NPC assembly if Nup53 lacks its C-terminal membrane-binding side

One obvious explanation for the necessity of both parts of Ndc1 for NPC assembly could be that the N-terminus is required for Nup53 binding, whereas the C-terminal region executes some independent mandatory function. However, the Ndc1–Nup53 interaction is described as dispensable for *in vitro* NPC assembly because Nup53 truncations defective in this interaction could substitute for the endogenous protein (Hawryluk-Gara et al., 2008; Vollmer et al., 2012). To resolve this discrepancy, we performed double depletion and add-back experiments

Journal of Cell Science (2014) 127, 908–921 doi:10.1242/jcs.141739

manipulating Nup53 and Ndc1 from the egg extract cytosol and membranes, respectively. Nup53 was depleted without affecting the levels of other nucleoporins (Fig. 3A). In the absence of Nup53, formation of a closed NE was blocked (Fig. 3B,C, panels 1) as reported (Hawryluk-Gara et al., 2008; Vollmer et al., 2012). Re-addition of recombinant full-length Nup53 (Nup53 1–320) at endogenous levels (Fig. 3A) rescued this block when combined with mock-treated membranes containing endogenous Ndc1 (Fig. 3B,C panels 2). Also, a C-terminal truncation of Nup53 lacking the Ndc1 binding site (Nup53 1–312) restored NE formation together with mock-treated membranes (Fig. 3B,C, panels 3). These observations are in agreement with previous reports using untreated membranes (Hawryluk-Gara et al., 2008; Vollmer et al., 2012). If endogenous Ndc1 was depleted from the membranes, NPC formation was blocked in the presence of either Nup53 construct (Fig. 3B,C, panels 4,5). Re-addition of full-length Ndc1 in reconstituted membranes rescued NPC formation in combination with both Nup53 versions (Fig. 3B,C, panels 6,7). The Ndc1-N fragment could not replace endogenous Ndc1 in the presence of these Nup53 constructs (Fig. 3B,C, panels 8,9). This again suggests that the N-terminal half of Ndc1 is not sufficient for NE and NPC formation and that the C-terminal part is additionally required (see also Fig. 2B,C). The Ndc1-C fragment did not support formation of a closed NE in the presence of full-length Nup53 (Fig. 3B,C, panels 10). Surprisingly, in the presence of the Nup53 truncation impaired in the Ndc1 interaction (Nup53 1–312), the Ndc1-C fragment allowed NPC assembly (Fig. 3B,C, panels 11). This shows that the N-terminal half of Ndc1, which mediates Nup53 binding, is dispensable for NPC formation if Nup53 lacks the last eight amino acids.

Next, we analyzed the nuclei formed in the presence of the Ndc1-C fragment. In context of the Nup53 truncation defective in Ndc1 binding (Nup53 1–312), NPC formation is normal. All tested nucleoporins, including Nup53, localized properly to the NE (Fig. 3C, panel 11 and Fig. 3D) supporting the view that the N-terminal half of Ndc1 and thus the direct Ndc1–Nup53 interaction is not required to recruit Nup53 to reassembling NPCs. However, in the presence of full-length Nup53 (Nup53 1–320) Ndc1-C could not rescue NPC formation. Under these conditions Nup107, a nucleoporin that is recruited early to chromatin during NPC assembly, Pom121 and Gp210 were present on chromatin. Also, Nup53 and Nup155 were detected on chromatin but other Nup93 complex members, namely Nup93, Nup205 and Nup188, remained absent. This lack of recruitment of Nup93, Nup188 and Nup205 is similar to the Nup93-depletion phenotype (Sachdev et al., 2012), and suggests that Nup53 recruitment on its own cannot promote NPC assembly. Instead, the Ndc1–Nup53 interaction ensures the functionality of Nup53 in NE and NPC assembly.

The Ndc1 interaction and the C-terminal membrane-binding site of Nup53 can be separated

The previous experiments suggest that the Nup53–Ndc1 interaction is only dispensable when Nup53 lacks the last eight amino acids. This truncation not only abolishes the Ndc1 interaction, but also impairs membrane binding and deformation through the Nup53 C-terminus (Vollmer et al., 2012). Thus, the Ndc1–Nup53 interaction seems to be essential for NPC assembly if Nup53 can deform membranes. To test this, we generated a Nup53 construct that does not bind Ndc1 but retains all other features of the C-terminus. Because the Ndc1 interaction site and the C-terminal membrane binding site partially overlap (Vollmer et al., 2012), a stretch of eight amino acids upstream of the C-terminal membrane binding site (aa 275–282) was deleted. This deletion rendered Nup53 incompetent for Ndc1 interaction (Nup53 162–320 RRM mutant Δ275–282, Fig. 4A). To test for membrane binding, we inserted this deletion in a Nup53 fragment comprising the RRM domain and the C-terminal extension (aa 130–320). Because the N-terminal part of Nup53 contains another membrane-binding motif, this region was excluded. Similar to the control (Nup53 130–320), the deletion mutant (Nup53 130–320 Δ275–282) binds membranes directly when incubated with liposomes and floated through a sucrose cushion (Fig. 4B). By contrast, deletion of the last amino acid (Nup53 130–319) strongly reduced membrane binding (Vollmer et al., 2012). Similar to the wild-type fragment, the Nup53 deletion construct induced tubulation of liposomes (Fig. 4C). Notably, Nup155 binding, which also requires the C-terminal part of Nup53, remained unaffected by the deletion (supplementary material Fig. S2). Altogether, this shows that the Nup53 deletion construct is specifically impaired in its interaction with Ndc1, but its C-terminal membrane binding and deformation site remain intact.

Ndc1–Nup53 interaction is required for NPC assembly but can be bypassed if Nup53 lacks its C-terminus

After having identified a Nup53 version that was defective for the Ndc1 interaction but possessed a functional C-terminal membrane binding and bending site, we investigated the specific function of the Ndc1–Nup53 interaction in nuclear assembly. Endogenous Nup53 was depleted from the cytosol and replaced with different Nup53 versions (Fig. 5A) in the presence of untreated membranes containing endogenous Ndc1 (Fig. 5B). As before, Nup53 depletion blocked NE and NPC formation and this block was rescued by the wild-type protein (Nup53 1–320, Fig. 5C,D). However, the deletion construct (Nup53 1–320 Δ275–282) did not restore NE and NPC formation, demonstrating that the Ndc1–Nup53 interaction is necessary for NPC assembly. Interestingly, when the last amino acid of the deletion construct was removed (Nup53 1–319 Δ275–282), which impaired it for membrane interaction and deformation through the C-terminal membrane-binding site (Vollmer et al., 2012) (see also Fig. 4B,C), NE and NPC formation was rescued. By contrast, abolishing the membrane interaction through the N-terminal membrane-binding site of Nup53, which does not deform membranes, by exchange of a basic motif (Nup53 1–320 R105E K106E Δ275–282) (see Vollmer et al., 2012) did not rescue NE and NPC formation. This shows that the C-terminal membrane-binding site of Nup53 has to be specifically impaired to allow for NPC assembly if Nup53 is unable to interact with Ndc1 and that Ndc1 binding is required for NE and NPC formation if Nup53 can deform membranes.

All Nup53 constructs impaired in Ndc1 binding containing the N- or the C-terminal membrane-binding site localized to chromatin (Fig. 5C) showing that recruitment of Nup53 is independent of Ndc1. Accordingly, a Nup53 construct impaired in both membrane-binding sites and the Ndc1 interaction (Nup53 1–319 R105E K106E Δ275–282) was not detected on the chromatin and was defective in NPC and NE formation. This is consistent with previous findings whereby Nup53 membrane binding is the key determinant for its recruitment to the assembling NPC (Vollmer et al., 2012).

Altogether, these data indicate that Nup53 binding to Ndc1 is crucial for post-mitotic NPC assembly and only dispensable if

Journal of Cell Science

Journal of Cell Science (2014) 127, 908–921 doi:10.1242/jcs.141739

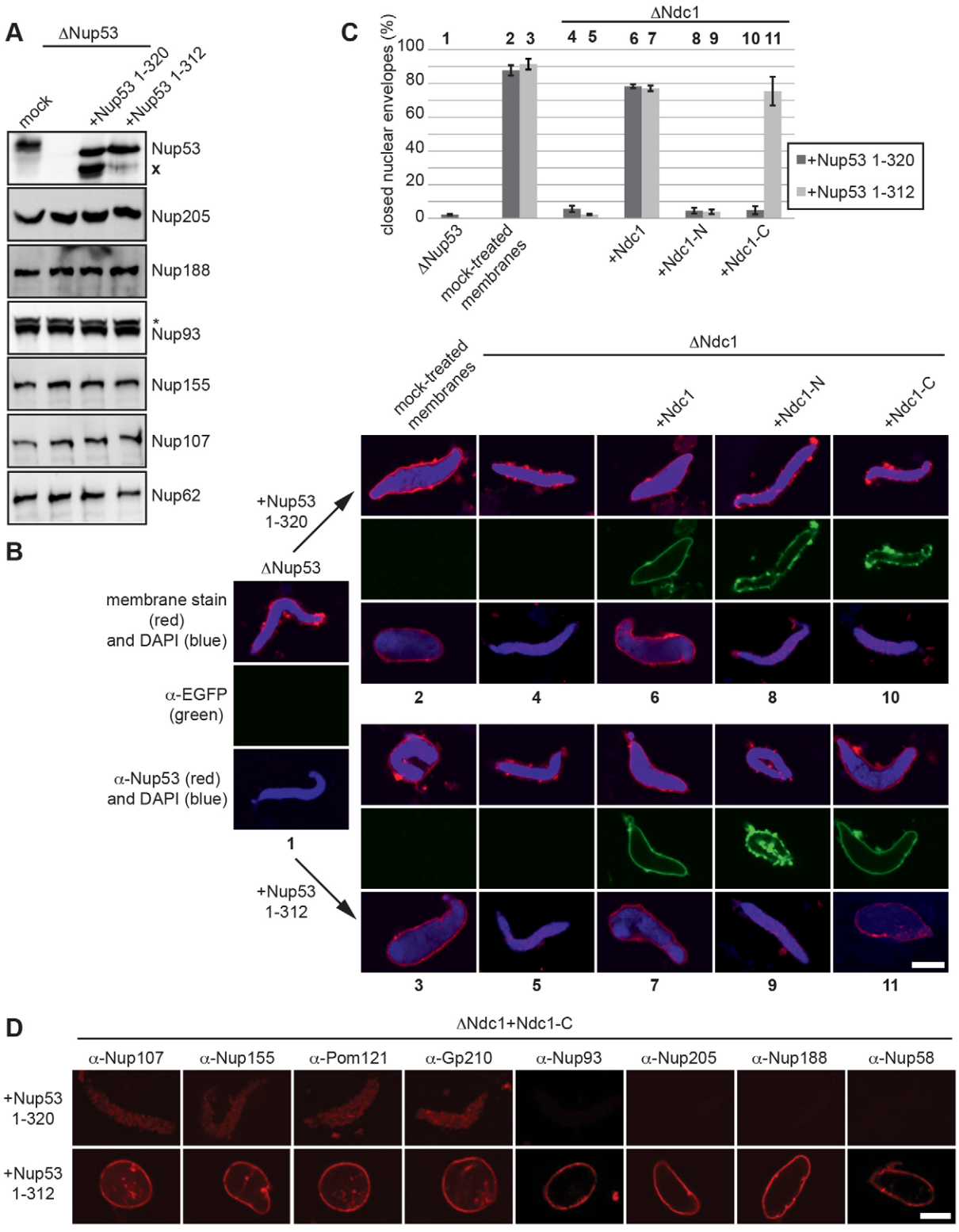

Fig. 3. Full-length Nup53 requires Ndc1 for NPC assembly. (A) Cytosol from *Xenopus* egg extracts was mock depleted, Nup53 depleted (ΔNup53) or Nup53 depleted and supplemented with full-length recombinant Nup53 (1–320) or a truncated version (1–312) lacking the final eight amino acids and analyzed with indicated antibodies. Note that endogenous Nup53 migrates slightly slower because of post-translational modifications absent in *E. coli*. Both, endogenous and recombinant Nup53 proteins are prone to C-terminal degradation (x). The Nup93 antibody recognizes a slightly slower-migrating crossreactivity (*). (B) Nuclei were assembled in Nup53-depleted cytosol (1) to which either recombinant full-length Nup53 (1–320, top panel) or a Nup53 fragment lacking the last eight amino acids (1–312, bottom panel) were added. The membranes were mock treated (2,3), depleted of endogenous Ndc1 (4,5) or Ndc1 depleted and reconstituted with either EGFP-tagged Ndc1 (6,7), Ndc1-N (8,9) or Ndc1-C (10,11). Membranes were stained with $DiIC_{18}$ (red), DNA with DAPI (blue). Nuclei were analyzed with antibodies against EGFP to detect recombinant Ndc1 proteins (green) and Nup53 antibodies. (C) Quantification of nuclei with a closed NE as in Fig. 2C. Bold numbers correspond to the experimental conditions in B. (D) Nuclei assembled as in B (10,11) were analyzed by immunofluorescence with indicated antibodies. Scale bars: 10 μm.

Journal of Cell Science

Journal of Cell Science (2014) 127, 908–921 doi:10.1242/jcs.141739

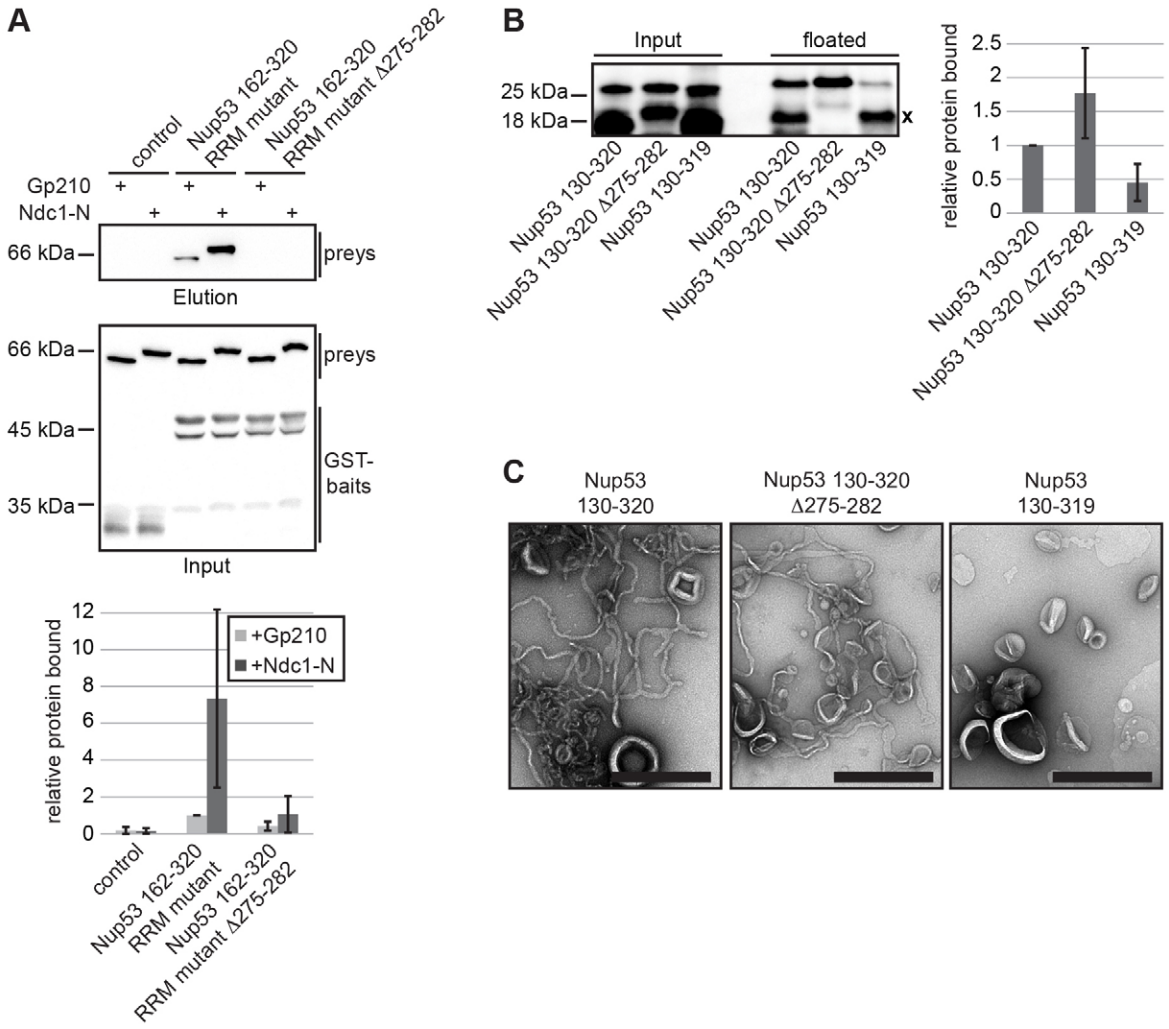

Fig. 4. Generation of a Nup53 mutant specifically impaired in Ndc1 binding. (A) GST pull-downs with the nucleoplasmic domain of Gp210 (control), a fragment of Nup53 comprising a mutated RRM domain and the C-terminus (Nup53 162–320 RRM mutant) or deleted of eight amino acids (Δ275–282) impairing the Ndc1 interaction and *E.coli* lysates as in Fig. 1B. Four independent experiments were quantified as in Fig. 1D (bottom). (B) A Nup53 fragment containing the C-terminal direct membrane binding site (130–320), the same construct with an additional deletion (Δ275–282) and a Nup53 construct deficient for membrane interaction (130–319) were tested in liposome flotation assays. 3% of the input and the floated fractions were analyzed by western blotting with Nup53 antibodies for membrane interaction. Nup53 degradations are indicated (x). Three independent experiments were quantified for membrane binding normalized to Nup53 130–320 (right). Error bars represent s.d. (C) Nup53 constructs from B were assayed for liposome tubulation by transmission electron microscopy after negative staining. Note the absence of tubules with Nup53 130–319. Scale bars: 500 nm.

Nup53 cannot deform membranes. Consistent with this, the N-terminal half of Ndc1, which provides the Nup53 interaction surface, is dispensable for NPC assembly if Nup53 lacks the membrane-deformation motif (Fig. 3B, panel 11, Fig. 3C,D). Hence, we conclude that Ndc1 modulates Nup53 membrane-deformation activity to allow for NPC assembly at the end of mitosis. Accordingly, we assumed that a Nup53 construct harboring a functional membrane deformation motif, which cannot be bound and regulated by Ndc1, might act as a dominant-negative version in NPC assembly. Indeed, if we added the Nup53 deletion construct defective for Ndc1 interaction (Nup53 1–320 Δ275–282) in excess to untreated nuclear assembly reactions (i.e. in the presence of endogenous Nup53 and Ndc1) NE and NPC formation was blocked (Fig. 5E). By contrast, a Nup53 construct that is unable to interact with Ndc1 but additionally is defective for membrane deformation did not show this effect (Nup53 1–319 Δ275–282). This experiment supports our hypothesis that the Ndc1–Nup53 interaction restrains the membrane-deformation capability of Nup53.

Nup53 interacts directly with Nup155

Nup53 combines different modes of interactions that are crucial for NPC assembly such as direct membrane binding and deformation, as well as interactions with other proteins within the NPC. We have demonstrated that the Ndc1 interaction is required to modulate the membrane-deformation ability and thus membrane binding through the C-terminus and Ndc1 interaction influence each other. Nup53 also interacts with Nup155 through its C-terminus (Amlacher et al., 2011; Hawryluk-Gara et al., 2008; Hawryluk-Gara et al., 2005; Marelli et al., 1998; Onischenko et al., 2009; Sachdev et al., 2012; Uetz et al., 2000; Vollmer et al., 2012). Similar to Ndc1 and Nup53, Nup155 is crucial for NPC assembly (Franz et al., 2005). Nup53 binding to Nup155 is thought to be essential for NPC assembly because

Journal of Cell Science (2014) 127, 908–921 doi:10.1242/jcs.141739

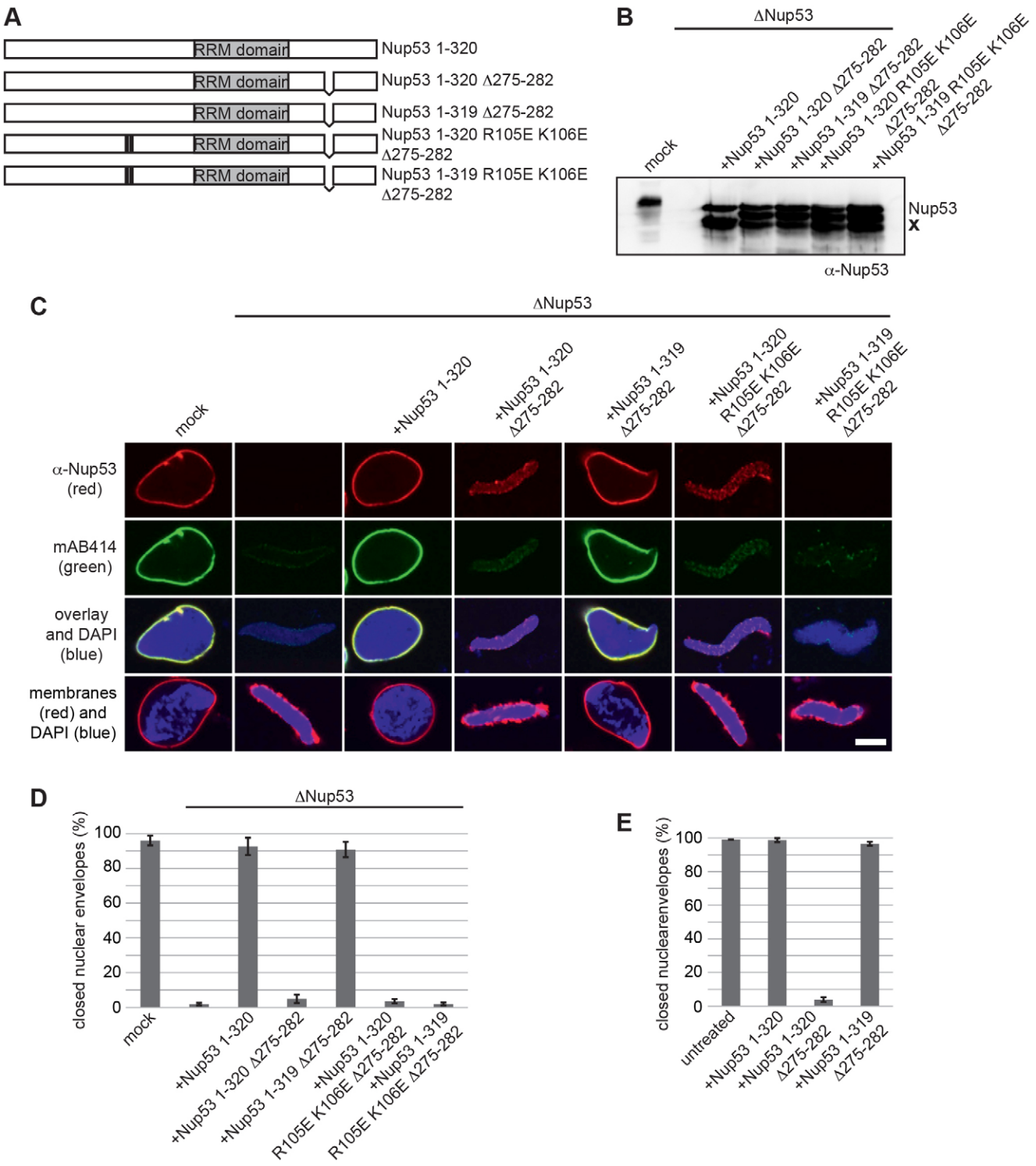

Fig. 5. Ndc1 functionally interacts with Nup53 membrane-bending activity. (A) Schematic representation of full-length *Xenopus* Nup53 (1–320) and the different mutants and fragments used. (B) *Xenopus* egg extracts were mock-treated, Nup53-depleted or Nup53-depleted and supplemented with recombinant wild-type Nup53 (1–320) or different constructs impaired for Ndc1 interaction (1–320 Δ275–282). Variants of the deletion construct deficient for membrane deformation (1–319 Δ275–282), membrane interaction through the N-terminal membrane binding site (1–320 R105E K106E Δ275–282) or both membrane interaction and deformation (1–319 R105E K106E Δ275–282) were included. Nup53 degradations are indicated (x). (C) Nuclei were assembled in mock, Nup53-depleted extracts or Nup53-depleted extracts supplemented with Nup53 constructs as in B. Nuclei were analyzed by immunofluorescence for Nup53 (red) or mAB414 (green). DNA was stained with DAPI (blue), membranes with $DiIC_{18}$ (red). Scale bar: 10 μm. (D) Quantification of nuclear assembly reactions from C performed as in Fig. 2C. (E) Recombinant full-length Nup53 (1–320), the Nup53 deletion construct impaired for Ndc1 interaction (1–320 Δ275–282) and a Nup53 construct impaired for Ndc1 interaction and defective in membrane deformation (1–319 Δ275–282) were added to untreated nuclear assembly reactions in 10-fold excess over endogenous Nup53 levels. More than 300 nuclei from three independent experiments were quantified. Error bars represent s.d.

Journal of Cell Science (2014) 127, 908–921 doi:10.1242/jcs.141739

Nup53 truncations lacking the Nup155 interaction site failed to replace the endogenous protein in nuclear assembly reactions (Hawryluk-Gara et al., 2008). However, these truncated versions also lacked the RRM domain that is required for Nup53 dimerization. This dimerization is necessary for binding of Nup53 to the membrane and, in turn, for NPC formation. Hence, it is unresolved whether the Nup53–Nup155 interaction is indeed essential for NPC formation and independent of other interactions of Nup53. To answer this, we separated the membrane binding and Nup155 interaction functions of Nup53 after mapping the Nup155 interaction site on Nup53 more precisely. Nup155 binds Nup53 upstream of Ndc1 (Vollmer et al., 2012). Therefore, we tested C-terminal truncations of Nup53 (Fig. 6A) in GST pull-downs. These constructs covered the RRM domain which might contribute to the interaction (Vollmer et al., 2012) and sections closer to the C-terminus. Nup53 truncations lacking the last eight (Nup53 162–312) or 25 amino acids (Nup53 162–295) bound Nup155 (Fig. 6B). Further C-terminal truncation up to amino acid 267 (Nup53 162–267) resulted in a loss of the interaction. If the RRM domain (aa 163–243 in the *Xenopus* protein) was absent, Nup53 failed to bind Nup155 (Fig. 6C) showing that the RRM domain of Nup53 is required but not sufficient for the Nup155 interaction. Thus, the RRM domain and an additional region (between aa 267–295) within the C-terminus of Nup53 form the Nup155 interaction surface.

Next, we generated a Nup53 point mutant to impair its interaction with Nup155. By exchanging the conserved lysine residue of position 262 to alanine, Nup53 binding to Nup155 was compromised both *in vitro* and *in vivo* without affecting the interaction with Ndc1 (Fig. 6D,E; supplementary material Fig. S3). Thus, the K262A mutation on Nup53 specifically affects Nup155 binding and provides a useful tool to study the role of the Nup53–Nup155 interaction in NPC assembly.

Nup53–Nup155 interaction is essential for NPC assembly

The Nup53 K262A point mutant was used in nuclear assemblies with Nup53-depleted egg extracts (1–320 K262A, Fig. 7A). As before, depletion of Nup53 blocked NE and NPC formation and wild-type Nup53 (Nup53 1–320) rescued this phenotype (Fig. 7B,C). By contrast, the Nup53 mutant deficient for the Nup155 interaction (1–320 K262A) did not support formation of a closed NE and NPCs. Interestingly, the Nup53 point mutant was recruited to the chromatin template, albeit at reduced levels. This indicates that localization of Nup53 to the reassembling NPC is independent of Nup155. By contrast, recruitment of Nup155 mainly depends on its interaction with Nup53 because Nup155 was hardly detectable on the chromatin in the presence of the mutant Nup53 construct (1–320 K262A). Other Nup93 complex members, including Nup93, Nup205 and Nup188 were absent from the chromatin if the Nup53 mutant was used (Fig. 7D). It is unlikely that this lack of recruitment was caused by disrupting the direct protein interaction between Nup53 and Nup93 because Nup93 binds to the N-terminal part of Nup53 (Amlacher et al., 2011; Fahrenkrog et al., 2000; Hawryluk-Gara et al., 2008; Vollmer et al., 2012), which was unaffected by the mutation, and rather indicates that the recruitment of Nup93 as well as of Nup188 and Nup205 requires a functional Nup53–Nup155 interaction. Similarly, Nup58, a member of the Nup62 complex, was not recruited because this requires the presence of Nup93 (Sachdev et al., 2012). Nup107, Ndc1, Pom121 and Gp210 were present on the chromatin but did not show smooth rim staining because no closed NE was formed. Therefore, the interactions of Nup155 with Ndc1 and Pom121 or the Nup107–Nup160 complex (Mitchell et al., 2010; Yavuz et al., 2010) are insufficient to locate Nup155 at the nuclear rim. These data show that binding of Nup53 to Nup155 is required for efficient recruitment of Nup155 to the assembling pore and is crucial for NPC assembly at the end of mitosis.

DISCUSSION

We have functionally analyzed the interactions of three essential nucleoporins in NPC assembly: Ndc1, Nup53 and Nup155. *Xenopus* Nup53 and Ndc1 interact directly. This interaction is mediated by the transmembrane regions of Ndc1 and the C-terminal part of Nup53. Our data indicate that this interaction is crucial for NPC reassembly at the end of mitosis and regulates the membrane-deformation capability of Nup53. Furthermore, our study reveals a crucial role for the direct interaction of Nup53 and Nup155 for NPC formation because abolishing this interaction by specific point mutation of Nup53 blocks NPC assembly.

Nup53 is a component of the Nup93 complex forming the inner ring of NPCs adjacent to the pore membrane (Alber et al., 2007; Brohawn et al., 2009). As a result of its many interactions, Nup53 acts as a connection point between the pore membrane and other nucleoporins. *Xenopus* Nup53 and the yeast counterparts bind membranes directly and this interaction in vertebrates is essential for NPC assembly (Patel and Rexach, 2008; Vollmer et al., 2012). Moreover, Nup53 interacts with the transmembrane nucleoporin Ndc1 (Hawryluk-Gara et al., 2008; Mansfeld et al., 2006; Onischenko et al., 2009; Uetz et al., 2000; Vollmer et al., 2012), as well as with Nup155 and Nup93, two other members of the Nup93 complex (Amlacher et al., 2011; Fahrenkrog et al., 2000; Hawryluk-Gara et al., 2005; Onischenko et al., 2009). In metazoa, Nup53 and Nup155 are both essential components of the Nup93 complex (Franz et al., 2005; Galy et al., 2003; Hawryluk-Gara et al., 2008; Hawryluk-Gara et al., 2005; Kiger et al., 1999; Mitchell et al., 2010; Ródenas et al., 2009; Vollmer et al., 2012). *S. cerevisiae* possesses two Nup53 orthologs, Nup53 and Nup59, and two Nup155 orthologs, Nup157 and Nup170. Double deletions of Nup53 and Nup59 in *S. cerevisiae* are viable (Marelli et al., 1998) but co-deletion of either one with Nup157 or Nup170 causes severe growth defects or lethality, respectively (Marelli et al., 1998). These observations suggest an important role of the Nup53–Nup155 interaction and, indeed, Nup155 binding to Nup53 is thought to be crucial for vertebrate NPC assembly (Hawryluk-Gara et al., 2008). However, the experiments defining the requirement of the vertebrate Nup53–Nup155 interaction used Nup53 constructs that not only lack the Nup155-interaction site but also the RRM domain, which is important for membrane binding. Also, a deletion in the gene encoding Nup53 in *C. elegans* that causes NPC defects (Ródenas et al., 2009) probably affects interaction with both the membrane and Nup155, because the major part of the RRM domain was absent from the protein product. By generating a Nup53 point mutant specifically impaired in Nup155 binding without modifying the RRM domain, we separated these two functions of Nup53 and show that the Nup53–Nup155 interaction is specifically required for NE and NPC assembly (Fig. 6,7).

Nup53 and Nup155 form a conserved trimeric complex with Nup93 in which Nup93 stabilizes the Nup53–Nup155 interaction (Amlacher et al., 2011; Sachdev et al., 2012). We found that Nup93 is absent from the chromatin in the context of the Nup53 point mutant deficient for Nup155 binding (Fig. 7D). This suggests that Nup53–Nup155 binding recruits Nup93 to the

Journal of Cell Science

Journal of Cell Science (2014) 127, 908–921 doi:10.1242/jcs.141739

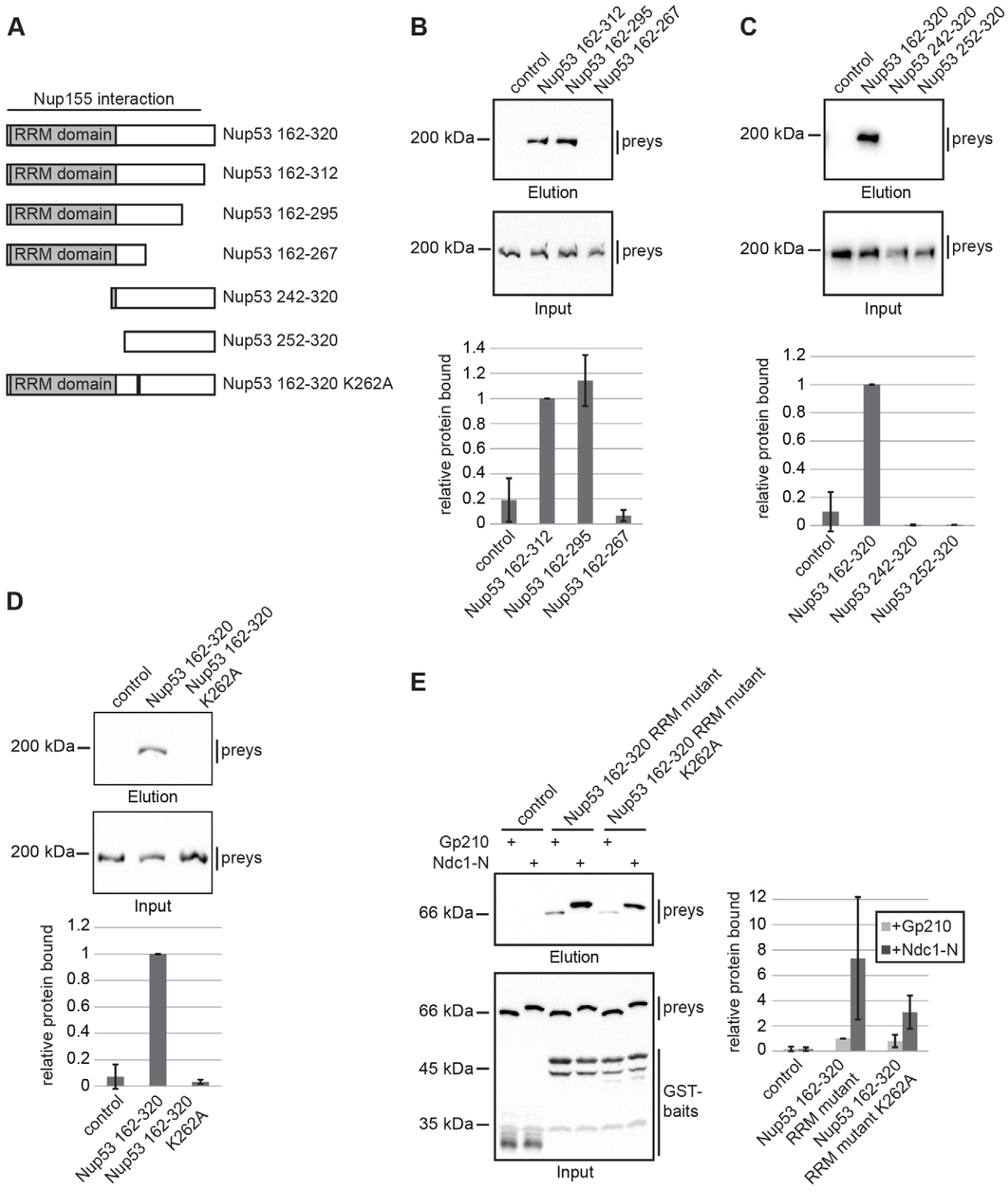

Fig. 6. Nup53 interacts with Nup155 through its C-terminal portion. (A) Schematic representation of *Xenopus* Nup53 constructs used. (B) GST pull-downs with the nucleoplasmic domain of *Xenopus* Gp210 (control) or fragments of *Xenopus* Nup53 comprising the RRM domain and parts of the C-terminus (Nup53 162–312, 162–295 and 162–267) and *E. coli* lysates overexpressing NusA-tagged *Xenopus* Nup155. Eluates and 3% of the input were analyzed using a His_6 antibody. Three independent experiments were quantified (bottom) for the bait-bound protein to input ratio normalized to Nup53 162–312. Error bars represent s.d. (C) GST pull-downs as in B, using Nup53 constructs comprising the RRM domain and the C-terminus (162–320) or lacking the RRM domain (242–320, 252–320). Three independent experiments were quantified and normalized to Nup53 162–320 as in B. (D) GST pull-downs as in B, using a Nup53 fragment comprising the RRM domain and the C-terminus (162–320) and a mutant impaired in the Nup155 interaction (162–320 K262A). (E) GST pull-downs with baits as in D and *E.coli* lysates as in Fig. 1B. Quantification was carried out as in Fig. 1D.

Journal of Cell Science (2014) 127, 908–921 doi:10.1242/jcs.141739

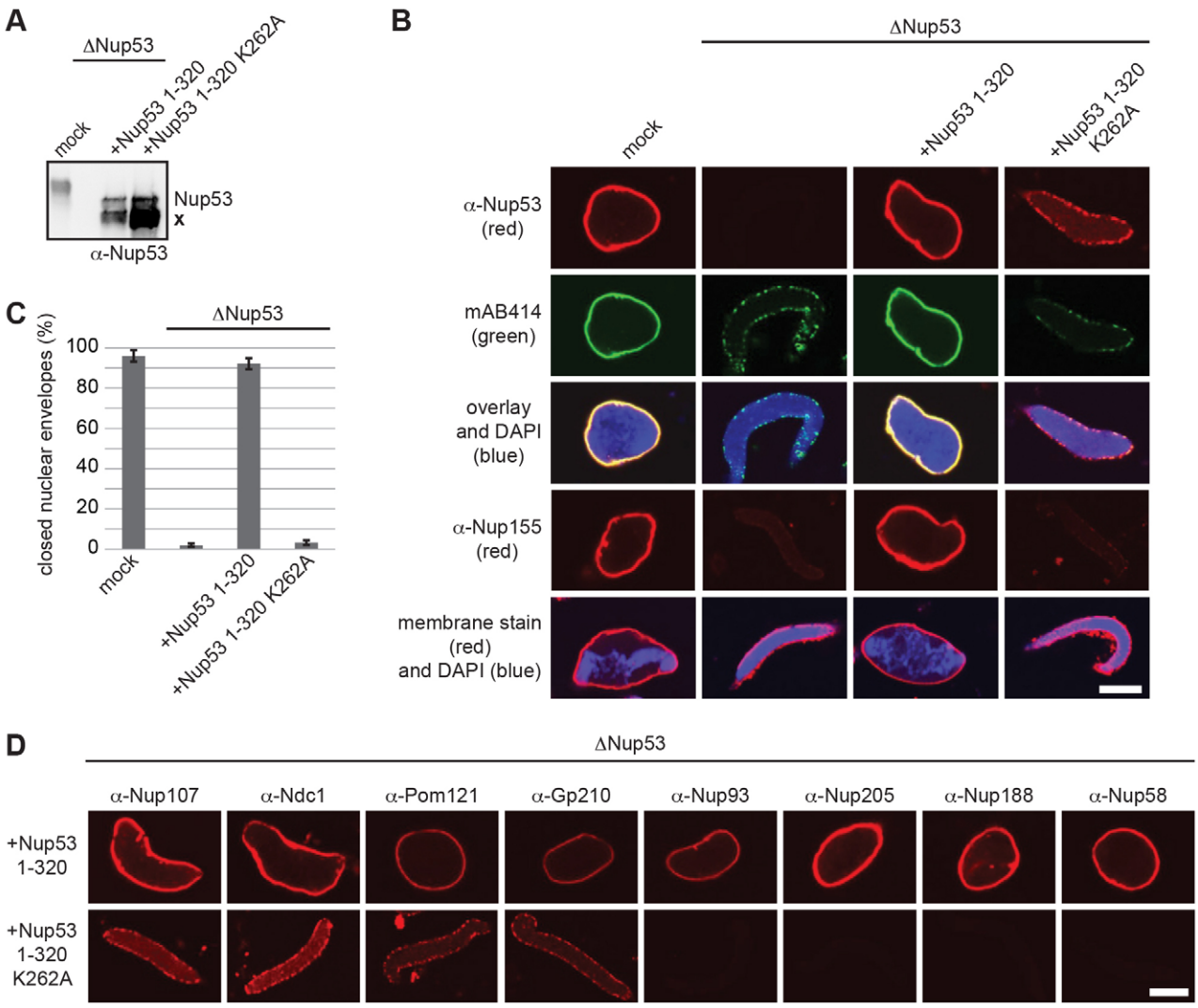

Fig. 7. The Nup53–Nup155 interaction is crucial for NPC assembly. (A) Cytosol from egg extracts was mock treated, Nup53 depleted or Nup53 depleted and supplemented with wild-type Nup53 (1–320) or a mutant impaired in the Nup155 interaction (1–320 K262A) and analyzed by western blotting. Nup53 degradations are indicated (x). (B) Nuclei were assembled in extracts from A and analyzed by immunofluorescence for Nup53 (red), mAB414 (green) or Nup155 (red). DNA was stained with DAPI (blue), membranes with $DiIC_{18}$ (red). (C) Quantification of nuclear assembly reactions from B, carried out as in Fig. 2C. (D) Nuclei assembled as in B, in the presence of full-length Nup53 (1–320) or the mutant deficient for the Nup155 interaction (1–320 K262A) were analyzed by immunofluorescence with the respective antibodies. Scale bars: 10 μm.

assembling NPC, which in turn recruits the Nup62 complex (Amlacher et al., 2011; Grandi et al., 1995; Sachdev et al., 2012). Interestingly, Nup53, Nup155 and Nup93 are identified in all eukaryotic super-groups (Neumann et al., 2010) and could have been present in the last common eukaryotic ancestor. Altogether, this implicates an essential, evolutionary conserved role of the three proteins and their interaction in NPC assembly and function.

Ndc1 is a crucial factor for NPC assembly both in metazoa (Mansfeld et al., 2006; Stavru et al., 2006) and yeast (Madrid et al., 2006). In *S. cerevisiae*, it binds directly both Nup53 orthologs, Nup53 and Nup59 (Onischenko et al., 2009). Our data demonstrate that this direct interaction is evolutionarily conserved (Fig. 1) and important for NPC assembly (Fig. 5). Upon separation of the Ndc1–Nup53 interaction from the Nup53 C-terminal membrane binding and deformation activity, we determined the specific requirement of the Nup53–Ndc1 interplay during NPC formation. This revises previous observations, suggesting a redundant role of this interaction in NPC assembly (Hawryluk-Gara et al., 2008; Vollmer et al., 2012). We show that the Ndc1 interaction is specifically required if Nup53 can deform membranes (Fig. 5). The Ndc1 transmembrane domain, which contains the Nup53 binding site, becomes dispensable if endogenous Nup53 is replaced by a Nup53 truncation that is defective in membrane deformation (Fig. 3). Our finding that the N-terminal part of Ndc1 is the Nup53 interaction surface (Fig. 1) is surprising at first glance because the C-terminal part of Ndc1 is much better conserved and exposed to the NPC (Lau et al., 2006; Mansfeld et al., 2006; Stavru et al., 2006). This region serves as an interaction platform for two other nucleoporins, Aladin and Nup155 (Kind et al., 2009; Mitchell et al., 2010; Yamazumi et al., 2009). The N-terminal half of Ndc1 comprises the six predicted transmembrane helices embedded in the pore membrane and interacts with the C-terminus of Nup53, which in turn is required for membrane deformation. Similarly, yeast Nup53 and Nup59

Journal of Cell Science

Journal of Cell Science (2014) 127, 908–921 doi:10.1242/jcs.141739

both interact with Ndc1 through their C-terminal ends (Onischenko et al., 2009). These regions are predicted to fold into amphipathic α-helices and might also deform membranes (Marelli et al., 2001; Patel and Rexach, 2008; Vollmer et al., 2012). Thus, the Ndc1–Nup53 interaction could take place within the lipid bilayer and membrane integration of the Nup53 binding site might hence be required. Our data highlight the fact that the Ndc1–Nup53 interaction is only required for post-mitotic NPC assembly if Nup53 can deform membranes (Figs 3,5). This membrane deformation activity of the Nup53 C-terminus is dispensable for NPC formation at the end of mitosis but essential if NPCs integrate into the closed NE during interphase (Vollmer et al., 2012). We propose that Nup53 membrane deformation activity needs to be counteracted or fine-tuned and this requires Ndc1 binding. During NPC formation, both at the end of mitosis and in interphase, nuclear membranes might initially show high positive curvature at local sites of pore formation. However, during the process of NPC formation these highly curved membranes have to convert into the specific structure of the nuclear pore (Fig. 8). This final membrane shape is characterized by the coexistence of a positive and a negative curvature. Because the negative curvature could energetically balance the positive curvature (Terasaki et al., 2013), the final pore membrane structure might be passively adopted and might not require active membrane deformation as induced by Nup53. In this regard, Ndc1 might be the crucial factor regulating the membrane-deformation activity of Nup53 in the NPC.

A similar regulation of membrane-deforming activity was reported for reticulons, which are ER-tubulating proteins that associate with highly curved membranes (Hu et al., 2008; Voeltz et al., 2006). These proteins are displaced from the reforming NE at the end of mitosis. In human cells, overexpression of reticulons delays re-formation of the NE and a reduction in reticulons accelerates it (Anderson and Hetzer, 2008). Hence, it might be generally important to attenuate membrane deformation during re-formation of the NE and NPCs. This could be achieved by the removal of tubulating proteins or regulation by other proteins. How this happens mechanistically for the Ndc1–Nup53 interaction can only be speculated. Ndc1 might deform the pore membrane in the opposite way as a result of its shape or by oligomerization, which then obliterates the membrane curvature induced by Nup53 (Fig. 8A). Alternatively, Ndc1 binding could induce a conformational change in Nup53, resulting in a rearrangement of its C-terminus, which might then be buried inside the protein or the interaction surfaces (Fig. 8B).

Surprisingly, Ndc1 is not found in all eukaryotes (DeGrasse et al., 2009; Neumann et al., 2010) and is dispensable in the fungus *Aspergillus nidulans* (Liu et al., 2009). *A. nidulans* also lacks any obvious Nup53 ortholog, which is in agreement with our observation that the Ndc1–Nup53 interaction is only essential if Nup53 can deform membranes. Some organisms contain a Nup53 but no Ndc1 ortholog (Neumann et al., 2010). In these organisms Nup53 might be regulated by other proteins or their Nup53 orthologs could lack the membrane-deformation ability. Indeed, Ndc1 is absent from all *Amoebozoa* tested (Neumann et al., 2010) and their Nup53 proteins show only little sequence homology to the yeast or metazoan proteins in their C-termini, suggesting that they might not be able to deform membranes. Overall, it seems that not only is the direct Ndc1–Nup53 interaction conserved, but the function of this complex in controlling the membrane-deformation activity of Nup53 is also maintained.

The analyses of the different Nup53 interactions reveal its diverse functions in NPC assembly and elucidate the step-wise process of re-formation of the metazoan NPC at the end of mitosis (for a review, see Schooley et al., 2012). NPC reassembly starts on the decondensing chromatin by DNA binding of the nucleoporin Mel28/ELYS, which in turn recruits the Nup107–Nup160 complex (Franz et al., 2007; Galy et al., 2006; Gillespie et al., 2007; Rasala et al., 2006). Subsequently, NE precursor membranes bind to the NPC assembly sites, including the integral pore membrane proteins Ndc1 and Pom121 (Antonin et al., 2005; Mansfeld et al., 2006; Rasala et al., 2008). Pom121 was detected on the chromatin templates in the absence of Ndc1 (Fig. 2). This suggests that recruitment of Ndc1 and Pom121 can occur independently and supports the previously observed redundancy in the membrane recruitment step. Next, the Nup93 complex is localized to the nascent pore. This step is initiated by the recruitment of Nup53 for which its membrane interaction is crucial (Vollmer et al., 2012). Nup53 recruitment is independent of the Ndc1 interaction because Nup53 is also localized to assembling NPCs if both proteins cannot interact or if Ndc1 is depleted (Figs 3,5). The Nup155 recruitment and subsequent establishment of the Nup53–Nup155 interaction is the next decisive step in NPC assembly. In Nup53-depleted extracts or if Nup53 is defective in binding Nup155, staining for Nup155 on the chromatin is strongly decreased and other members of the Nup93 complex as well as the Nup62 complex are not detectable (Fig. 7 and Hawryluk-Gara et al., 2008; Vollmer et al., 2012). Consistently, knockdown of Nup53 by siRNA in HeLa cells

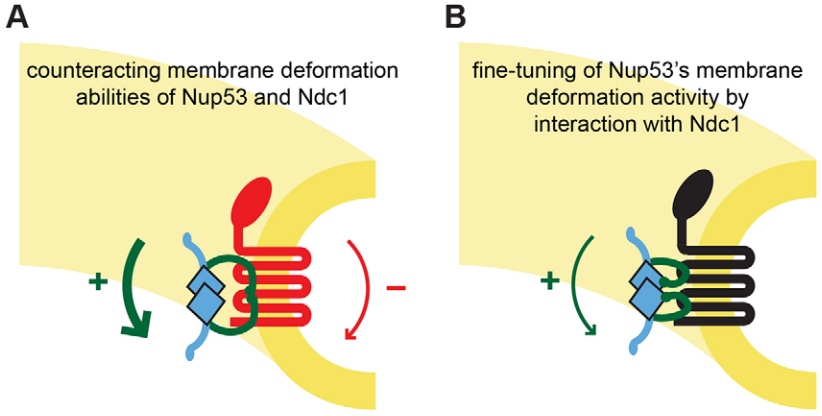

Fig. 8. Regulation of Nup53 membrane deformation by Ndc1. In the pore membrane, positive membrane curving (green arrow) by the Nup53 C-terminus (green) might be partially antagonized by negative curvature (red arrow) induced by Ndc1 (red, A). Alternatively, Ndc1 (black) might attenuate the membrane-deformation activity of Nup53 (green) by direct binding (B). For the sake of simplicity, other membrane-curving factors as the Nup107–Nup160 complex and reticulons are omitted.

decreases the levels of Nup155 at the nuclear rim, as well as of Nup93 and Nup205 (Hawryluk-Gara et al., 2005), and in *C. elegans*, localization of Nup155 requires Nup53 (Ródenas et al., 2009). Together, this indicates that recruitment of Nup155 predominantly depends on the presence of Nup53, despite the fact that it also interacts with Ndc1 and Pom121. If Nup53 and Nup155 are present in an intact complex, NPC assembly proceeds further, probably by recruiting Nup93 and subsequently, the Nup62 complex (Sachdev et al., 2012). Eventually, further components of the nuclear basket and cytoplasmic filaments are recruited by yet ill-defined steps, completing the process of NPC assembly at the end of mitosis and yielding fully assembled functional NPCs.

MATERIALS AND METHODS

Antibodies against Ndc1 (Mansfeld et al., 2006), Pom121 and Gp210 (Antonin et al., 2005), Nup53, Nup188 and Nup205 (Theerthagiri et al., 2010), Nup93 and Nup58 (Sachdev et al., 2012), Nup155 (Franz et al., 2005) and Nup107 (Walther et al., 2003) have been described previously. MAB414 was obtained from BAbCO (Richmond, CA), antibodies against EGFP, His_6, Myc and HA were from Roche (Mannheim, Germany), Alexa Fluor 488 goat anti-rabbit IgG, Cy3 goat anti -mouse IgG and 1,1′-Dioctadecyl-3,3,3′,3′-tetramethylindocarbocyanine perchlorate ($DiIC_{18}$) were from Invitrogen (Eugene, OR).

Protein expression and purification

Constructs are listed as supplementary material Table S1. Nup53 constructs were generated from a synthetic DNA optimized for *E. coli* codon usage (Vollmer et al., 2012). For pull-down reactions, Nup53 fragments were cloned into a pET28a vector (EMD, Darmstadt, Germany) with an N-terminal GST tag and a TEV-protease recognition site upstream of the Nup53 fragments, or have been described previously (Vollmer et al., 2012). The nucleoplasmic domain of *Xenopus* Gp210 (Antonin et al., 2005) was cloned into the same modified vector. Proteins were expressed in *E. coli* BL21de3 and purified using an N-terminal His_6 tag with Ni-NTA agarose (Qiagen, Hilden, Germany).

For nuclear assembly, liposome flotation or tubulation Nup53 fragments were cloned into a pET28a vector with a yeast SUMO tag (SMT3) and a TEV-protease recognition site upstream of the protein fragments. His_6 and SUMO tags were cleaved off after purification from *E. coli*; the proteins were concentrated using Vivaspin 500 (Sartorius, Goettingen, Germany) and purified by gel filtration, either in PBS for liposome flotation and tubulation or in sucrose buffer for nuclear assembly. The Nup53 deletion constructs impaired in Ndc1 interaction were generated by replacing the eight amino acids of positions 275–282 (RAASMRPL) with the linker sequence GGSGSGGS and cloned into the respective vectors for pull-down, flotation, liposome tubulation and NPC assembly experiments.

To express integral membrane proteins, *Xenopus* Ndc1, the respective Ndc1 fragments or the Gp210 fragment comprising the transmembrane region and the nucleoplasmic part were cloned into a pET28a vector with an N-terminal Mistic (membrane-integrating sequence for translation of integral membrane protein constructs) sequence to enhance expression at the *E. coli* membrane (Roosild et al., 2005; Theerthagiri et al., 2010) followed by an EGFP tag upstream of the respective protein and a C-terminal His_6 tag. Proteins were expressed in *E. coli* and used as lysate in pull-downs or further purified in the presence of 1% (w/v) cetyltrimethylammoniumbromide (Calbiochem, Darmstadt, Germany) using Ni-NTA agarose and dialyzed against sucrose buffer (Theerthagiri et al., 2010).

Pull-down experiments

E. coli lysates overexpressing the transmembrane nucleoporin constructs were adjusted with lysates from *E. coli* transformed with empty vector to equal protein concentrations and incubated with 1.5 µM of GST baits in a final volume of 800 µl. For Fig. 1B, 0.5 µM GST baits were incubated in 2 ml of the respective *E. coli* lysates. After 1 hour, 9 µl of magnetic glutathione beads (Pierce, Rockford, IL) were added for another hour, washed six times with 20 mM Tris-HCl, pH 7.5 and 150 mM NaCl and eluted in 30 µl total volume by TEV protease cleavage (0.5 mg/ml) for 1 hour at 25°C. For pull-downs with recombinant Nup155, 1.5 µM of respective GST baits were incubated with *E. coli* lysates overexpressing NusA-fused full-length Nup155 (Sachdev et al., 2012). Pull-downs with *Xenopus*-derived cytosol and membranes were performed as described previously (Vollmer et al., 2012).

Immunoprecipitation

Full-length *Xenopus* Ndc1, the respective fragments or full-length *Xenopus* Nup155 were cloned with an N-terminal Myc tag into pEGFP-N1 (Clontech, Saint-Germain-en-Laye, France) containing a C-terminal EGFP-tag. HA-tagged *Xenopus* Nup53 has been described previously (Vollmer et al., 2012) and the K262A point mutation was introduced in this construct. Transfection of HeLa cells and immunoprecipitation were carried out as described (Vollmer et al., 2012).

Other methods

Nuclear assembly and immunofluorescence (Antonin et al., 2005; Theerthagiri et al., 2010), generation of affinity resins, sperm heads and floated membranes (Franz et al., 2005) as well as prelabelled membranes (Antonin et al., 2005) were all carried out as described previously. For add-back of recombinant Ndc1 constructs, purified proteins were reconstituted into solubilized membranes (Mansfeld et al., 2006). For testing dominant-negative effects in nuclear assembly, recombinant proteins were added to untreated *Xenopus* egg extracts at the beginning of the reaction. Liposome flotation and tubulation were done as described previously (Vollmer et al., 2012).

Acknowledgements

We thank U. Kutay for discussion of unpublished data, S. Astrinidis, C. Sieverding and T. Strittmatter for technical support, and M. Lorenz, R. Sachdev, K. Schellhaus, A. Schooley and B. Vollmer for critical reading of the manuscript.

Author contributions

N.E. and W.A. designed and performed experiments and wrote the manuscript. J.R. developed the methods to express and purify transmembrane nucleoporins from *E. coli*.

Competing interests

The authors declare no competing interest.

Funding

The work was funded by the Max Planck Society.

Supplementary material

Supplementary material available online at
http://jcs.biologists.org/lookup/suppl/doi:10.1242/jcs.141739/-/DC1

References

Alber, F., Dokudovskaya, S., Veenhoff, L. M., Zhang, W., Kipper, J., Devos, D., Suprapto, A., Karni-Schmidt, O., Williams, R., Chait, B. T. et al. (2007). The molecular architecture of the nuclear pore complex. *Nature* **450**, 695-701.

Amlacher, S., Sarges, P., Flemming, D., van Noort, V., Kunze, R., Devos, D. P., Arumugam, M., Bork, P. and Hurt, E. (2011). Insight into structure and assembly of the nuclear pore complex by utilizing the genome of a eukaryotic thermophile. *Cell* **146**, 277-289.

Anderson, D. J. and Hetzer, M. W. (2008). Reshaping of the endoplasmic reticulum limits the rate for nuclear envelope formation. *J. Cell Biol.* **182**, 911-924.

Antonin, W., Franz, C., Haselmann, U., Antony, C. and Mattaj, I. W. (2005). The integral membrane nucleoporin pom121 functionally links nuclear pore complex assembly and nuclear envelope formation. *Mol. Cell* **17**, 83-92.

Brohawn, S. G., Leksa, N. C., Spear, E. D., Rajashankar, K. R. and Schwartz, T. U. (2008). Structural evidence for common ancestry of the nuclear pore complex and vesicle coats. *Science* **322**, 1369-1373.

Brohawn, S. G., Partridge, J. R., Whittle, J. R. and Schwartz, T. U. (2009). The nuclear pore complex has entered the atomic age. *Structure* **17**, 1156-1168.

Chadrin, A., Hess, B., San Roman, M., Gatti, X., Lombard, B., Loew, D., Barral, Y., Palancade, B. and Doye, V. (2010). Pom33, a novel transmembrane nucleoporin required for proper nuclear pore complex distribution. *J. Cell Biol.* **189**, 795-811.

Journal of Cell Science

Cronshaw, J. M., Krutchinsky, A. N., Zhang, W., Chait, B. T. and Matunis, M. J. (2002). Proteomic analysis of the mammalian nuclear pore complex. *J. Cell Biol.* **158**, 915-927.
DeGrasse, J. A., DuBois, K. N., Devos, D., Siegel, T. N., Sali, A., Field, M. C., Rout, M. P. and Chait, B. T. (2009). Evidence for a shared nuclear pore complex architecture that is conserved from the last common eukaryotic ancestor. *Molecular & Cellular Proteomics* **8**, 2119-2130.
Devos, D., Dokudovskaya, S., Alber, F., Williams, R., Chait, B. T., Sali, A. and Rout, M. P. (2004). Components of coated vesicles and nuclear pore complexes share a common molecular architecture. *PLoS Biol.* **2**, e380.
Fahrenkrog, B., Hübner, W., Mandinova, A., Panté, N., Keller, W. and Aebi, U. (2000). The yeast nucleoporin Nup53p specifically interacts with Nic96p and is directly involved in nuclear protein import. *Mol. Biol. Cell* **11**, 3885-3896.
Franz, C., Askjaer, P., Antonin, W., Iglesias, C. L., Haselmann, U., Schelder, M., de Marco, A., Wilm, M., Antony, C. and Mattaj, I. W. (2005). Nup155 regulates nuclear envelope and nuclear pore complex formation in nematodes and vertebrates. *EMBO J.* **24**, 3519-3531.
Franz, C., Walczak, R., Yavuz, S., Santarella, R., Gentzel, M., Askjaer, P., Galy, V., Hetzer, M., Mattaj, I. W. and Antonin, W. (2007). MEL-28/ELYS is required for the recruitment of nucleoporins to chromatin and postmitotic nuclear pore complex assembly. *EMBO Rep.* **8**, 165-172.
Galy, V., Mattaj, I. W. and Askjaer, P. (2003). Caenorhabditis elegans nucleoporins Nup93 and Nup205 determine the limit of nuclear pore complex size exclusion in vivo. *Mol. Biol. Cell* **14**, 5104-5115.
Galy, V., Askjaer, P., Franz, C., López-Iglesias, C. and Mattaj, I. W. (2006). MEL-28, a novel nuclear envelope and kinetochore protein essential for zygotic nuclear envelope assembly in C. elegans. *Curr. Biol.* **16**, 1748-1756.
Gant, T. M. and Wilson, K. L. (1997). Nuclear assembly. *Annu. Rev. Cell Dev. Biol.* **13**, 669-695.
Gerace, L., Ottaviano, Y. and Kondor-Koch, C. (1982). Identification of a major polypeptide of the nuclear pore complex. *J. Cell Biol.* **95**, 826-837.
Gillespie, P. J., Khoudoli, G. A., Stewart, G., Swedlow, J. R. and Blow, J. J. (2007). ELYS/MEL-28 chromatin association coordinates nuclear pore complex assembly and replication licensing. *Curr. Biol.* **17**, 1657-1662.
Grandi, P., Schlaich, N., Tekotte, H. and Hurt, E. C. (1995). Functional interaction of Nic96p with a core nucleoporin complex consisting of Nsp1p, Nup49p and a novel protein Nup57p. *EMBO J.* **14**, 76-87.
Grandi, P., Dang, T., Pané, N., Shevchenko, A., Mann, M., Forbes, D. and Hurt, E. (1997). Nup93, a vertebrate homologue of yeast Nic96p, forms a complex with a novel 205-kDa protein and is required for correct nuclear pore assembly. *Mol. Biol. Cell* **8**, 2017-2038.
Hallberg, E., Wozniak, R. W. and Blobel, G. (1993). An integral membrane protein of the pore membrane domain of the nuclear envelope contains a nucleoporin-like region. *J. Cell Biol.* **122**, 513-521.
Handa, N., Kukimoto-Niino, M., Akasaka, R., Kishishita, S., Murayama, K., Terada, T., Inoue, M., Kigawa, T., Kose, S., Imamoto, N. et al. (2006). The crystal structure of mouse Nup35 reveals atypical RNP motifs and novel homodimerization of the RRM domain. *J. Mol. Biol.* **363**, 114-124.
Hawryluk-Gara, L. A., Shibuya, E. K. and Wozniak, R. W. (2005). Vertebrate Nup53 interacts with the nuclear lamina and is required for the assembly of a Nup93-containing complex. *Mol. Biol. Cell* **16**, 2382-2394.
Hawryluk-Gara, L. A., Platani, M., Santarella, R., Wozniak, R. W. and Mattaj, I. W. (2008). Nup53 is required for nuclear envelope and nuclear pore complex assembly. *Mol. Biol. Cell* **19**, 1753-1762.
Hu, J., Shibata, Y., Voss, C., Shemesh, T., Li, Z., Coughlin, M., Kozlov, M. M., Rapoport, T. A. and Prinz, W. A. (2008). Membrane proteins of the endoplasmic reticulum induce high-curvature tubules. *Science* **319**, 1247-1250.
Kiger, A. A., Gigliotti, S. and Fuller, M. T. (1999). Developmental genetics of the essential Drosophila nucleoporin nup154: allelic differences due to an outward-directed promoter in the P-element 3′ end. *Genetics* **153**, 799-812.
Kind, B., Koehler, K., Lorenz, M. and Huebner, A. (2009). The nuclear pore complex protein ALADIN is anchored via NDC1 but not via POM121 and GP210 in the nuclear envelope. *Biochem. Biophys. Res. Commun.* **390**, 205-210.
Krull, S., Thyberg, J., Björkroth, B., Rackwitz, H. R. and Cordes, V. C. (2004). Nucleoporins as components of the nuclear pore complex core structure and Tpr as the architectural element of the nuclear basket. *Mol. Biol. Cell* **15**, 4261-4277.
Lau, C. K., Giddings, T. H., Jr and Winey, M. (2004). A novel allele of Saccharomyces cerevisiae NDC1 reveals a potential role for the spindle pole body component Ndc1p in nuclear pore assembly. *Eukaryot. Cell* **3**, 447-458.
Lau, C. K., Delmar, V. A. and Forbes, D. J. (2006). Topology of yeast Ndc1p: predictions for the human NDC1/NET3 homologue. *Anat. Rec. A Discov. Mol. Cell. Evol. Biol.* **288A**, 681-694.
Liu, H. L., De Souza, C. P., Osmani, A. H. and Osmani, S. A. (2009). The three fungal transmembrane nuclear pore complex proteins of Aspergillus nidulans are dispensable in the presence of an intact An-Nup84-120 complex. *Mol. Biol. Cell* **20**, 616-630.
Lohka, M. J. and Masui, Y. (1983). Formation in vitro of sperm pronuclei and mitotic chromosomes induced by amphibian ooplasmic components. *Science* **220**, 719-721.
Madrid, A. S., Mancuso, J., Cande, W. Z. and Weis, K. (2006). The role of the integral membrane nucleoporins Ndc1p and Pom152p in nuclear pore complex assembly and function. *J. Cell Biol.* **173**, 361-371.
Mans, B. J., Anantharaman, V., Aravind, L. and Koonin, E. V. (2004). Comparative genomics, evolution and origins of the nuclear envelope and nuclear pore complex. *Cell Cycle* **3**, 1625-1650.
Mansfeld, J., Güttinger, S., Hawryluk-Gara, L. A., Panté, N., Mall, M., Galy, V., Haselmann, U., Mühlhäusser, P., Wozniak, R. W., Mattaj, I. W. et al. (2006). The conserved transmembrane nucleoporin NDC1 is required for nuclear pore complex assembly in vertebrate cells. *Mol. Cell* **22**, 93-103.
Marelli, M., Aitchison, J. D. and Wozniak, R. W. (1998). Specific binding of the karyopherin Kap121p to a subunit of the nuclear pore complex containing Nup53p, Nup59p, and Nup170p. *J. Cell Biol.* **143**, 1813-1830.
Marelli, M., Lusk, C. P., Chan, H., Aitchison, J. D. and Wozniak, R. W. (2001). A link between the synthesis of nucleoporins and the biogenesis of the nuclear envelope. *J. Cell Biol.* **153**, 709-724.
Miao, M., Ryan, K. J. and Wente, S. R. (2006). The integral membrane protein Pom34p functionally links nucleoporin subcomplexes. *Genetics* **172**, 1441-1457.
Mitchell, J. M., Mansfeld, J., Capitanio, J., Kutay, U. and Wozniak, R. W. (2010). Pom121 links two essential subcomplexes of the nuclear pore complex core to the membrane. *J. Cell Biol.* **191**, 505-521.
Neumann, N., Lundin, D. and Poole, A. M. (2010). Comparative genomic evidence for a complete nuclear pore complex in the last eukaryotic common ancestor. *PLoS ONE* **5**, e13241.
Onischenko, E., Stanton, L. H., Madrid, A. S., Kieselbach, T. and Weis, K. (2009). Role of the Ndc1 interaction network in yeast nuclear pore complex assembly and maintenance. *J. Cell Biol.* **185**, 475-491.
Ori, A., Banterle, N., Iskar, M., Andrés-Pons, A., Escher, C., Khanh Bui, H., Sparks, L., Solis-Mezarino, V., Rinner, O., Bork, P. et al. (2013). Cell type-specific nuclear pores: a case in point for context-dependent stoichiometry of molecular machines. *Mol. Syst. Biol.* **9**, 648.
Patel, S. S. and Rexach, M. F. (2008). Discovering novel interactions at the nuclear pore complex using bead halo: a rapid method for detecting molecular interactions of high and low affinity at equilibrium. *Molecular & Cellular Proteomics* **7**, 121-131.
Rasala, B. A., Orjalo, A. V., Shen, Z., Briggs, S. and Forbes, D. J. (2006). ELYS is a dual nucleoporin/kinetochore protein required for nuclear pore assembly and proper cell division. *Proc. Natl. Acad. Sci. USA* **103**, 17801-17806.
Rasala, B. A., Ramos, C., Harel, A. and Forbes, D. J. (2008). Capture of AT-rich chromatin by ELYS recruits POM121 and NDC1 to initiate nuclear pore assembly. *Mol. Biol. Cell* **19**, 3982-3996.
Ródenas, E., Klerkx, E. P., Ayuso, C., Audhya, A. and Askjaer, P. (2009). Early embryonic requirement for nucleoporin Nup35/NPP-19 in nuclear assembly. *Dev. Biol.* **327**, 399-409.
Roosild, T. P., Greenwald, J., Vega, M., Castronovo, S., Riek, R. and Choe, S. (2005). NMR structure of Mistic, a membrane-integrating protein for membrane protein expression. *Science* **307**, 1317-1321.
Rout, M. P., Aitchison, J. D., Suprapto, A., Hjertaas, K., Zhao, Y. and Chait, B. T. (2000). The yeast nuclear pore complex: composition, architecture, and transport mechanism. *J. Cell Biol.* **148**, 635-651.
Sachdev, R., Sieverding, C., Flötenmeyer, M. and Antonin, W. (2012). The C-terminal domain of Nup93 is essential for assembly of the structural backbone of nuclear pore complexes. *Mol. Biol. Cell* **23**, 740-749.
Schooley, A., Vollmer, B. and Antonin, W. (2012). Building a nuclear envelope at the end of mitosis: coordinating membrane reorganization, nuclear pore complex assembly, and chromatin de-condensation. *Chromosoma* **121**, 539-554.
Stavru, F., Hülsmann, B. B., Spang, A., Hartmann, E., Cordes, V. C. and Görlich, D. (2006). NDC1: a crucial membrane-integral nucleoporin of metazoan nuclear pore complexes. *J. Cell Biol.* **173**, 509-519.
Terasaki, M., Shemesh, T., Kasthuri, N., Klemm, R. W., Schalek, R., Hayworth, K. J., Hand, A. R., Yankova, M., Huber, G., Lichtman, J. W. et al. (2013). Stacked endoplasmic reticulum sheets are connected by helicoidal membrane motifs. *Cell* **154**, 285-296.
Theerthagiri, G., Eisenhardt, N., Schwarz, H. and Antonin, W. (2010). The nucleoporin Nup188 controls passage of membrane proteins across the nuclear pore complex. *J. Cell Biol.* **189**, 1129-1142.
Uetz, P., Giot, L., Cagney, G., Mansfield, T. A., Judson, R. S., Knight, J. R., Lockshon, D., Narayan, V., Srinivasan, M., Pochart, P. et al. (2000). A comprehensive analysis of protein-protein interactions in Saccharomyces cerevisiae. *Nature* **403**, 623-627.
Voeltz, G. K., Prinz, W. A., Shibata, Y., Rist, J. M. and Rapoport, T. A. (2006). A class of membrane proteins shaping the tubular endoplasmic reticulum. *Cell* **124**, 573-586.
Vollmer, B., Schooley, A., Sachdev, R., Eisenhardt, N., Schneider, A. M., Sieverding, C., Madlung, J., Gerken, U., Macek, B. and Antonin, W. (2012). Dimerization and direct membrane interaction of Nup53 contribute to nuclear pore complex assembly. *EMBO J.* **31**, 4072-4084.
Walther, T. C., Alves, A., Pickersgill, H., Loïodice, I., Hetzer, M., Galy, V., Hülsmann, B. B., Köcher, T., Wilm, M., Allen, T. et al. (2003). The conserved Nup107-160 complex is critical for nuclear pore complex assembly. *Cell* **113**, 195-206.
Wilson, K. L. and Newport, J. (1988). A trypsin-sensitive receptor on membrane vesicles is required for nuclear envelope formation in vitro. *J. Cell Biol.* **107**, 57-68.
Wozniak, R. W., Blobel, G. and Rout, M. P. (1994). POM152 is an integral protein of the pore membrane domain of the yeast nuclear envelope. *J. Cell Biol.* **125**, 31-42.
Yamazumi, Y., Kamiya, A., Nishida, A., Nishihara, A., Iemura, S., Natsume, T. and Akiyama, T. (2009). The transmembrane nucleoporin NDC1 is required for targeting of ALADIN to nuclear pore complexes. *Biochem. Biophys. Res. Commun.* **389**, 100-104.
Yavuz, S., Santarella-Mellwig, R., Koch, B., Jaedicke, A., Mattaj, I. W. and Antonin, W. (2010). NLS-mediated NPC functions of the nucleoporin Pom121. *FEBS Lett.* **584**, 3292-3298.

FIGURE S1

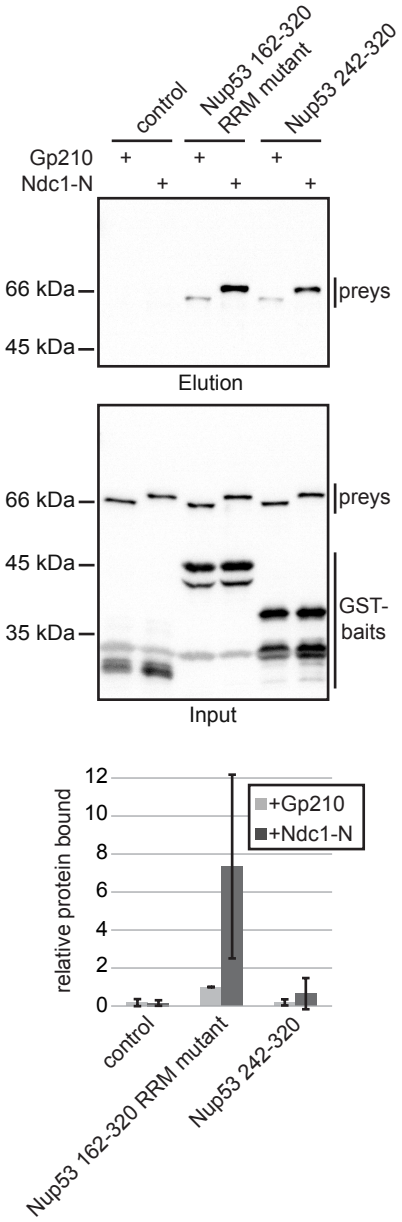
control
Nup53 162-320 RRM mutant
Nup53 242-320
Gp210 + + +
Ndc1-N + + +
66 kDa
45 kDa
preys
Elution
66 kDa
45 kDa
35 kDa
preys
GST-baits
Input
relative protein bound
12
10
8
6
4
2
0
+Gp210
+Ndc1-N
control
Nup53 162-320 RRM mutant
Nup53 242-320

FIGURE S2

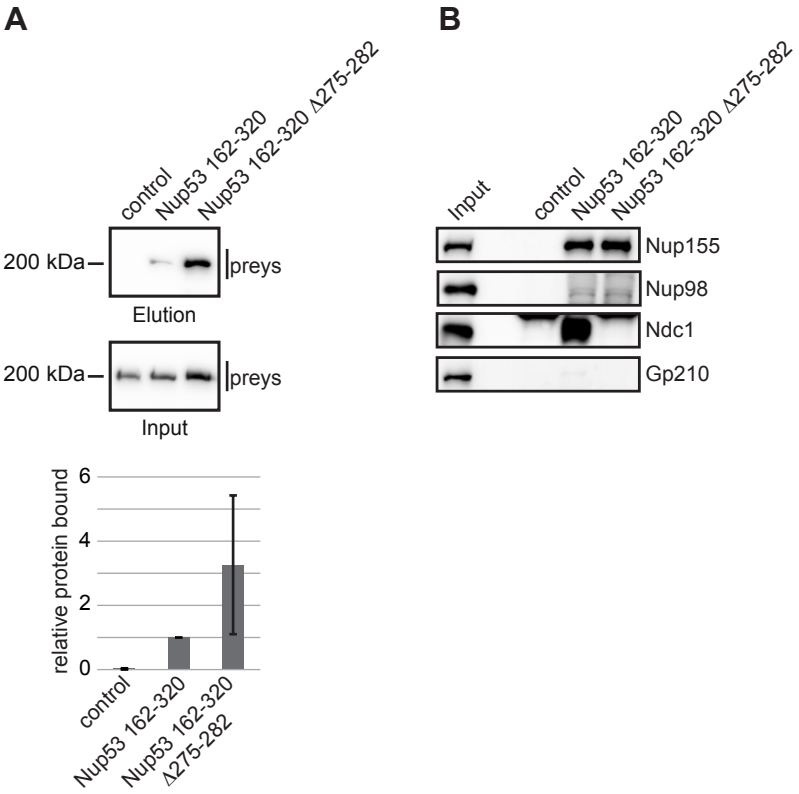
A
control
Nup53 162-320
Nup53 162-320 Δ275-282
200 kDa
preys
Elution
200 kDa
preys
Input
relative protein bound
6
4
2
0
control
Nup53 162-320
Nup53 162-320 Δ275-282
B
Input
control
Nup53 162-320
Nup53 162-320 Δ275-282
Nup155
Nup98
Ndc1
Gp210

FIGURE S3

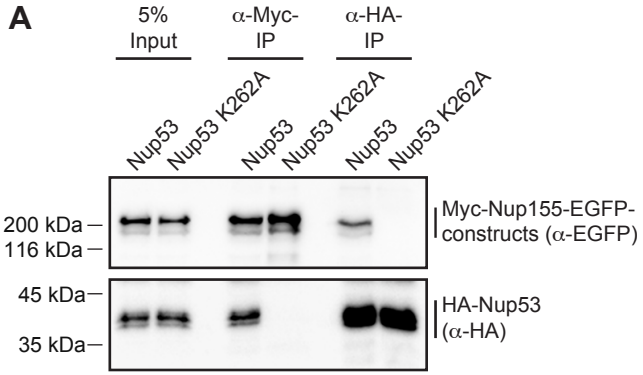
A
5% Input
α-Myc-IP
α-HA-IP
Nup53
Nup53 K262A
Nup53
Nup53 K262A
Nup53
Nup53 K262A
200 kDa
116 kDa
45 kDa
35 kDa
Myc-Nup155-EGFP-constructs (α-EGFP)
HA-Nup53 (α-HA)

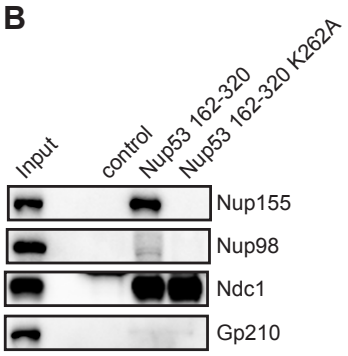
B
Input
control
Nup53 162-320
Nup53 162-320 K262A
Nup155
Nup98
Ndc1
Gp210

Supplementary figure legends

Figure S1 The Nup53 RRM domain contributes to the Nup53-Ndc1 interaction

GST-fusions of the nucleoplasmic part of *Xenopus* Gp210 (control), fragments of *Xenopus* Nup53 comprising a mutated RRM domain to decrease direct membrane binding and the subsequent C-terminus (Nup53 162-320 RRM mutant) or a shorter construct lacking the RRM domain (Nup53 242-320) were incubated with *E. coli* lysates overexpressing the transmembrane region and the nucleoplasmic extension of *Xenopus* Gp210 or the N-terminal part of *Xenopus* Ndc1 (Ndc1-N) that interacts with Nup53. Eluates and 3% of the input were analyzed by western blotting using a His_6-antibody. The quantification shows the ratio of bait-bound protein to input of six independent experiments normalized to the binding of control lysate to the Nup53 RRM mutant. Error bars represent s.d.

Figure S2 The Nup53 deletion construct impaired for the Ndc1 interaction binds Nup155

(**A**) GST-pulldown experiments using GST-fusions with the nucleoplasmic domain of *Xenopus* Gp210 (control), with a fragment of *Xenopus* Nup53 comprising the RRM domain and the subsequent C-terminus (Nup53 162-320) or with a Nup53 fragment impaired in Ndc1 interaction due to a deletion of eight amino acids (Δ275-282) and *E. coli* lysates overexpressing NusA-tagged *Xenopus* Nup155. Eluates and 3% of the input were analyzed by western blotting using a His_6-antibody. Three independent experiments were quantified (lower panel) for the bait-bound protein to input ratio normalized to Nup53 162-320, which was used as positive control. Error bars represent s.d.

(**B**) The same GST-fusions as in (**A**) were incubated with cytosol or Triton X-100 solublized membranes derived from *Xenopus laevis* egg extracts. 5% of input and eluates were analyzed by western blotting with the indicated antibodies. Nup98 served as negative control in the cytosolic fraction and Gp210 in the membrane fraction.

Figure S3 The point mutation K262A in Nup53 specifically impairs the Nup155 interaction

(**A**) HeLa cells were co-transfected with wildtype *Xenopus* Nup53 or the point mutant K262A of Nup53 tagged with HA and *Xenopus* Nup155 fused with an N-terminal Myc- and a C-terminal EGFP-tag. Proteins were immunoprecipitated from cellular lysate with Myc- or HA-antibodies and analyzed by western blotting using HA-antibodies to detect Nup53 and EGFP-antibodies for Nup155.

(**B**) GST-fusions of the nucleoplasmic domain of Gp210 (control), the C-terminal fragment of *Xenopus* Nup53 comprising the RRM domain and the subsequent C-terminus (162-320) and the corresponding fragment carrying the K262A-point mutation impairing the Nup155 interaction were incubated with cytosol or Triton X-100 solublized membranes derived from *Xenopus laevis* egg extracts. 5% of input and eluates were analyzed by western blotting with the respective antibodies. Nup98 was used as negative control for the cytosolic fraction and Gp210 for the membranes.

Table S1. Recombinant protein constructs used in this study

Construct	Reference
pET28a MISTIC Ndc1xl 1-660	this study
pET28a MISTIC Gp210xl TMR+NPD	this study
pET28a MISTIC Ndc1xl 1-301	this study
pET28a MISTIC Ndc1xl 234-660	this study
pET28a MISTIC EGFP Ndc1xl 1-660	this study
pET28a MISTIC EGFP Ndc1xl 1-301	this study
pET28a MISTIC EGFP Ndc1xl 234-660	this study
pET28a GST Nup53xl 162-320 F172E W203	Vollmer et al, 2012
pET28a GST Gp210xl NPD	Sachdev et al, 2012
pET28a GST Nup53xl 162-320 F172E W203 Δ275-282	this study
pET28a GST Nup53xl 162-312	Vollmer et al, 2012
pET28a GST Nup53xl 162-295	this study
pET28a GST Nup53xl 162-267	Vollmer et al, 2012
pET28a GST Nup53xl 242-320	this study
pET28a GST Nup53xl 252-320	this study
pET28a SUMO Nup53xl 1-320	Vollmer et al, 2012
pET28a SUMO Nup53xl 1-312	Vollmer et al, 2012
pET28a SUMO Nup53xl 130-320	Vollmer et al, 2012
pET28a SUMO Nup53xl 130-320 Δ275-282	this study
pET28a SUMO Nup53xl 130-319	Vollmer et al, 2012
pET28a SUMO Nup53xl 1-320 Δ275-282	this study
pET28a SUMO Nup53xl 1-319 Δ275-282	this study
pET28a SUMO Nup53xl 1-320 R105E K106E Δ275-282	this study
pET28a SUMO Nup53xl 1-319 R105E K106E Δ275-282	this study
pET28a SUMO Nup53xl 1-320 K262A	this study
pET28a NusA Nup155xl	Sachdev et al, 2012
pEGFP-N1 MYC Ndc1xl 1-660	this study
pEGFP-N1 MYC Ndc1xl 1-301	this study
pEGFP-N1 MYC Ndc1xl 234-660	this study
pEGFP-N1 MYC Nup155xl	this study
pSI HA Nup53xl	Vollmer et al, 2012
pSI HA Nup53xl K262A	this study

Pre-print version of submitted manuscript.
Final manuscript will be published in Methods in Cell Biol. 2014;122:193-218. doi: 10.1016/B978-0-12-417160-2.00009-6.

Xenopus in vitro assays to analyze the function of transmembrane nucleoporins and targeting of inner nuclear membrane proteins

Nathalie Eisenhardt, Allana Schooley and Wolfram Antonin*

Friedrich Miescher Laboratory of the Max Planck Society, Spemannstrasse 39, 72076 Tübingen, Germany

* author for correspondence

Abstract (100-150 words)

Xenopus egg extracts have been widely used to study cell cycle regulation and to analyze mitotic or nuclear processes on a biochemical level. Most instrumental, proteins of interest can be immunodepleted by specific antibodies. However, this approach has been restricted to non-membrane proteins, which limits its versatility especially when studying membrane dependent processes such as nuclear envelope reformation at the end of mitosis or nuclear pore complex assembly. We describe here the methods developed and used in our laboratory to specifically remove transmembrane proteins from endogenous membranes and to insert recombinant integral membrane proteins into endogenous membranes. The latter procedure is important for re-addition of a depleted protein in rescue experiments but also for introducing artificial membrane proteins such as reporters to investigate the passage of inner nuclear membrane proteins through nuclear pore complexes.

Keywords:

Cell free assay, immunodepletion, integral membrane protein, membrane reconstitution, nuclear envelope, nuclear pore complex, nuclear reformation, nuclear transport, proteoliposomes, Xenopus egg extracts

Introduction

Cell free extracts derived from frog eggs (Lohka & Masui, 1983) have widely been used to study cell cycle regulation as well as many mitotic and nuclear processes since their development and first use thirty years ago. Although eggs from other sources such as *Rana pipiens* (Lohka & Masui, 1983) or *Xenopus tropicalis* (Brown, Blower, Maresca, Grammer, Harland, & Heald, 2007) can be employed, the use of *Xenopus laevis* eggs is most popular because these frogs are relatively easily maintained in a laboratory environment and they provide plentiful eggs with little seasonal variation in yield and quality.

In the absence of intact cells, *Xenopus laevis* egg extracts recapitulate complicated cellular reactions in a test tube such as chromatin condensation (de la Barre, Robert-Nicoud, & Dimitrov, 1999), spindle assembly (Maresca & Heald, 2006), nuclear breakdown and reformation (Galy, Antonin, Jaedicke, Sachse, Santarella, Haselmann, & Mattaj, 2008; Lohka, 1998), nucleocytoplasmic transport (Chan & Forbes, 2006) or DNA replication (Gillespie, Gambus, & Blow, 2012). Since these egg extracts can be prepared at different stages of the cell cycle, which are easily interconvertible, cell cycle dependent processes can also be studied (Murray, 1991). Most importantly, a single defined step in a complex series of processes such as the metazoan cell cycle can be isolated and investigated in molecular detail with this system. To identify key factors involved in various distinct processes of interest, convenient biochemical manipulations of the extracts are possible. In this regard, the opportunity to easily remove proteins of interest from these extracts by specific antibodies is most instrumental. For example, the importance of individual nuclear pore complex (NPC) proteins, nucleoporins, for NPC assembly and function has been defined in this way (see Chapter 8 in this Volume). This “biochemical knockout”

strategy is highly efficient to deplete proteins of interest below a detection limit. In contrast to RNAi, gene deletion or morpholino experiments, this method is naturally not limited by the viability of cells and organisms. As assays can be tailored to monitor a single process of interest, this also avoids complications due to secondary effects upon protein depletion, which might occur in other stages of the cell cycle or during development. However, this approach has been majorly restricted to non-membrane proteins, which limits its versatility especially when studying membrane dependent processes such as nuclear envelope or NPC formation.

In this chapter we describe the methods developed and employed in our lab to immunodeplete specific integral membrane proteins of the NPC from *Xenopus* membranes. Removing integral membrane proteins from *Xenopus* membranes is technically challenging as this procedure includes membrane solubilization and a final reconstitution of the depleted membranes besides the specific immunodepletion (Figure 2A). However, the method is in our eyes superior to antibody (IgG or Fab) inhibition experiments classically used to study the function of integral membrane proteins, which are often ill-defined especially with regard to the precise molecular inhibiting effect of the antibody. Preferably, immunodepletion of a given protein should be followed by an “addback experiment”, in which a recombinant version of the depleted factor is re-added to revert the observed depletion phenotype, thereby demonstrating the point specificity of the depletion. Such addback experiments are also feasible for transmembrane proteins (Figure 2B and C). Here we outline the procedures of the expression of eukaryotic transmembrane proteins in *E. coli*, their purification and their reconstitution in *Xenopus* membranes. Moreover, recombinant modified transmembrane proteins can be added to endogenous *Xenopus* membranes to analyze the passage of integral membrane proteins through the NPC *in vitro* (Figure 3). As nuclear transport has mainly been studied for soluble proteins

in the past, the mechanisms of NPC passage of transmembrane proteins are only emerging (for review see Antonin, Ungricht, & Kutay, 2011; Lusk, Blobel, & King, 2007). The assay we describe here provides a powerful tool to study NPC passage of integral membrane proteins in *Xenopus* egg extracts in a quantitative and time resolved manner. By combining it with immunodepletion approaches, integral membrane protein transport through NPCs can not only be studied under wildtype conditions but also in the absence of specific factors including distinct NPC proteins.

I. Preparation of *Xenopus* egg extract cytosol and membranes

1. Preparation of interphasic egg extracts

Xenopus eggs are arrested in the second metaphase of meiosis. Addition of calcium ionophore, which mimics the calcium influx generated during fertilization, activates these unfertilized eggs to enter the first interphase. Cell cycle progression into the first mitosis requires the translation of a single protein, cyclin B (Murray & Kirschner, 1989). To arrest the extracts in interphase, cyclin B synthesis is prevented by the translation inhibitor cycloheximide. We use a protocol for interphasic egg extract preparation adapted from Newmeyer & Wilson, 1991.

For editors; PLEASE INSERT FIGURE 1 HERE

A. Materials and equipment

- 240 IU/ml pregnant mare serum gonadotropin (PMSG, available as Intergonan, Intervet)
- 1000 IU/ml human chorionic gonadotropin (HCG, available as Ovogest, Intervet)
- Beckman L-60 Ultracentrifuge, SW55 Ti swinging bucket rotor and ultra-clear tubes (or equivalents)
- Beckman Optima TLX Ultracentrifuge, TLA 120.2 rotor and tubes (or equivalent system)
- Häreus-Multifuge 1-LR-Centrifuge (or equivalent)
- 5ml Syringes, 27G 3/4” and 16G 1½” needles
- large orifice tip (MBP® 1000G Pipet Tips, Molecular BioProducts)

B. Buffers and solutions

- MMR buffer: 100 mM NaCl, 2 mM KCl, 5 mM Hepes, 0.1 mM EDTA pH 8.0, 1 mM $MgCl_2$, 2 mM $CaCl_2$. Prepare a 20x stock solution in deionized water and autoclave, adjust pH to 8.0 with 5 M KOH. 1x MMR is freshly prepared before use by dilution in deionized water and re-adjustment of the pH to 8.0 with 5 M KOH.
- Dejellying buffer: 2% cystein in 0.25x MMR buffer, pH 7.8. This buffer should be prepared freshly and kept at 4-8°C. To save time, pre-cool the water.
- Calcium ionophore A23187: 2 mg/ml in ethanol
- Protease inhibitor mix (PI): 10 mg/ml AEBSF (4-(2-Aminoethyl)-benzensulfonylfluoride), 0.2 mg/ml leupeptin, 0.1 mg/ml pepstatin, 0.2 mg/ml aprotinin in deionized water. Store in aliquots at -20ºC.
- Dithiothreitol (DTT): 1 M in deionized water
- Cycloheximide: 20 mg/ml in ethanol
- Cytochalasin B: 10 mg/ml in DMSO
- Sucrose buffer: 250 mM sucrose, 50 mM KCl, 2.5 mM $MgCl_2$, 10 mM Hepes pH 7.5, 1 mM DTT (freshly added), 1:100 PI. Keep at 4°C.
- Dilution buffer: 50 mM KCl, 2.5 mM $MgCl_2$, 10 mM Hepes pH 7.5, 1 mM DTT (freshly added), 1:100 PI. Keep at 4°C.

C. Method

Note: For frog maintenance see Sive, Grainger, & Harland, 2000.

1. Prime frogs to ovulate by injecting 60 U PMSG into their dorsal lymph sac three to ten days before the experiment (5 ml Syringes, 27G 3/4” needles).
2. On the day before the experiment, inject frogs with 250 U HCG in their dorsal lymph sac (5 ml Syringes, 27G 3/4” needles) and place them in individual laying tanks containing 2 l of 1x MMR buffer for 16-18 h at 18°C.

3. Collect high quality eggs by pooling the good batches and wash them several times with 1x MMR buffer. Good eggs will be individually laid, uniform in size, and pigmented with clearly defined animal and vegetal hemispheres. Eggs laid in clumps or strings or white eggs should be excluded. It is important to carefully sort the eggs at this early step and throughout the procedure as the presence of a few “bad eggs” can quickly spoil the rest.

Note: For detailed description of “good” versus “bad” eggs see Gillespie et al., 2012.

4. Dejelly eggs in cold dejellying buffer for 10 min. Change buffer once and swirl continuously. Eggs become closely packed during this step.
5. Rinse eggs 4 times with 1x MMR buffer. This washing must be done gently, as the eggs are now fragile, and taking care not to expose the eggs to air.
6. Activate eggs in 100 ml 1x MMR buffer by adding 8 µl of the calcium ionophore A23187 for 10 min or until activation becomes visible (animal cap contraction), whichever comes first.
7. Rinse eggs carefully 4 times with 1x MMR buffer and once again carefully to keep them from being exposed to air.
8. Incubate eggs for 20 min at room temperature.
9. Replace the MMR buffer with cold sucrose buffer by washing twice. All subsequent steps must be carried out on ice.
10. Carefully place the eggs in SW55 tubes containing 50 µl sucrose buffer, 50 µl PI, 5 µl 1M DTT, 12.5 µl cycloheximide, and 2.5 µl cytochalasin B using a wide-mouthed (cut) transfer pipette. Remove excess buffer and refill the tubes until they are completely full.

11. Pack eggs by centrifugation at 400 rpm (approx. $3xg_{av}$) for 60 s in Häreus-Multifuge 1-LR-centrifuge. Remove excess liquid along with white eggs that have now floated to the top.
12. Crush the eggs by centrifugation at 15.000 rpm ($21,000xg_{av}$) for 20 min in a SW55 Ti rotor at 4°C (Figure 1).
13. Remove the (pale yellow) low speed extracts between the bright yellow yolk on top and dark broken eggs at the bottom using a syringe (16G 1½" needle). From one full SW55 tube, expect approximately 2.5 ml of low speed extract.
14. Add 10 µl PI, 1 µl 1M DTT, 2.5 µl cycloheximide and 0.5 µl cytochalasin B per ml of low speed extract. Mix well and load into fresh SW55 tubes. Spin for 40 min at 45.000 rpm ($190,000xg_{av}$) in a SW55 Ti rotor at 4°C.
15. Remove the (pale yellow) cytosolic phase between the white lipids on the top and the dark pellet containing pigments using a syringe (16G 1½" needle). From one full SW55 tube, expect approximately 3-4 ml of extract.
16. Dilute the extract with 0.3 ml of dilution buffer per 1 ml of cytosolic extract, mix well and load into fresh SW55 tubes for a final round of centrifugation. Spin for 40 min at 45.000 rpm ($190,000xg_{av}$) in a SW55 Ti rotor at 4°C.
17. Carefully remove the cytosol between the white lipids on the top and membranes, mitochondria and pigments at the bottom using a pipette. It is important to avoid contamination from the white lipids as they can hinder the *in vitro* nuclear assembly reaction. The membranes obtained at this step can be further purified using the protocols described in section **I, 2**.
18. Cytosol is cleared from residual membranes by two rounds of centrifugation for 12 min each at 100.000 rpm ($360,000xg_{av}$) in a TLA120.2 rotor at 4°C and used directly in the nuclear assembly reactions (section **IV**).

2. Preparation of *Xenopus* membranes

Nuclear envelope assembly in high-speed fractionated egg extracts requires the presence of both the cytosolic and membrane fractions (Sheehan, Mills, Sleeman, Laskey, & Blow, 1988; Vigers & Lohka, 1991; Wilson & Newport, 1988). Although it is possible to employ the crude membrane fraction to this end, this fraction contains cytosolic contaminations. At least after depletion of proteins from egg extract cytosol, a purified membrane fraction should be used. Crude membranes are mostly used in biochemical applications, such as membrane protein depletion and reconstitution, due to their high concentration. We describe here the preparation of both the crude membranes, adapted from Pfaller, Smythe, & Newport, 1991, and floatation purified membranes, adapted from Wilson & Newport, 1988.

A. Materials and equipment

- Tissue grinders: One 30 ml douncer with loose pestel and one 7 ml douncer with tight pestel (Wheaton, Millville, USA)
- Beckman L-60 Ultracentrifuge, SW40 Ti swinging bucket rotor and ultra-clear tubes (or equivalent system)
- Beckman Optima TLX Ultracentrifuge, TLA 100.4 rotor and tubes (or equivalent system)

B. Buffers and solutions

- Protease inhibitor mix (PI), DTT and sucrose buffer are described in section **I,1**.
- 2.1 M sucrose buffer: 2.1 M sucrose, 50 mM KCl, 2.5 mM $MgCl_2$, 10 mM Hepes pH 7.5, 1 mM DTT (freshly added), 1:100 PI. Keep at 4°C.
- Sucrose cushions: 1400 mM, 1300 mM, 1100 mM, 900 mM and 700 mM sucrose. Prepare sucrose cushions by mixing sucrose buffer from section **I,1**

and 2.1 M sucrose buffer in appropriate ratios to obtain the according sucrose concentration.

C. Method

Our protocols for the preparation of crude and floated membranes start with the generation of high-speed interphasic egg extract outlined in section **I,1** (Figure 1).

Preparation of crude membranes:

1. Membranes are isolated immediately following the final centrifugation step of high-speed extract preparation (step 17 in section **I,1**). At this point, they are easily distinguishable as a slightly viscous pale yellow layer located above the darkly colored mitochondria and pigments. Following removal of the egg cytosol, membranes are extracted with a syringe. From a full SW55 tube, expect approximately 1-1.5 ml of membrane suspension. Dilute the pooled membranes in 10 volumes of sucrose buffer and homogenize with two strokes of the loose pestel in a 30 ml glass douncer.
2. Transfer the homogenized membranes to SW40 tubes and spin for 20 min at 15.000 rpm (28,000xg_{av}) in a SW40 Ti rotor at 4°C.
3. After removing the supernatant, resuspend the membrane pellet in sucrose buffer. Homogenize the membrane suspension with five strokes of the tight pestel in a 7 ml glass douncer.
4. Adjust the final volume of the membrane suspension to 50% of the cytosol volume with sucrose buffer. Aliquot, snap freeze, and store in liquid nitrogen.

Preparation of floatation purified membranes:

1. As for the crude membrane preparation, the yellow membrane layer is extracted immediately following the final centrifugation step of the high-speed extract preparation using a syringe.
2. Mix membranes with four volumes of cold 2.1 M sucrose. Homogenize membranes with two strokes of the loose pestel in a 30 ml douncer.
3. Place 5 ml of homogenized membranes in SW40 tubes and overlay sequentially with 1.4 ml of each of the five sucrose cushions starting from 1400 mM to 700 mM sucrose. Finish the step gradient with 0.2 ml of sucrose buffer.
4. Membranes are separated by centrifugation for 4 h at 38.000 rpm (180,000xg_{av}) in an SW40 Ti rotor at 4°C.
5. Following centrifugation, carefully isolate the upper three membrane phases. Dilute the pooled membrane fractions with 3 volumes of sucrose buffer and spin for 30 min at 100.000 rpm (420.000xg_{av}) in a TLA100.4 rotor at 4°C.
6. After removing the supernatant, resuspend the membrane pellet in sucrose buffer. Homogenize the membrane suspension with five strokes of the tight pestel in a 7 ml glass douncer. Take care that the membranes are completely resuspended.
7. Adjust the final volume of the floated membranes to 50% of the volume of the cytosol. Aliquot, snap freeze, and store in liquid nitrogen.

II. Protein expression

1. Expression and purification of integral membrane proteins in *E. coli*

For addback reactions after depletion of soluble as well as transmembrane proteins natively purified proteins from *Xenopus* membranes (Antonin, Franz, Haselmann,

Antony, & Mattaj, 2005) but also recombinant proteins might be employed (Eisenhardt, Redolfi, & Antonin, 2013; Mansfeld, Guttinger, Hawryluk-Gara, Pante, Mall, Galy, Haselmann, Muhlhausser, Wozniak, Mattaj, Kutay, & Antonin, 2006). Wherever possible, recombinant proteins are preferable as this obviates the co-purification and co-addition of other *Xenopus* proteins.

Expression of eukaryotic transmembrane proteins can be achieved in several systems such as yeast, insect cells or mammalian cell lines. We have good experience with *E. coli* as expression system when fusing the protein of interest to the Mistic sequence from *B. subtilis* in a pET28a vector for expression in *E. coli* (Eisenhardt et al., 2013; Theerthagiri, Eisenhardt, Schwarz, & Antonin, 2010). The Mistic sequence directs the integral membrane protein to the inner *E. coli* membrane (Roosild, Greenwald, Vega, Castronovo, Riek, & Choe, 2005) and can be fused either N- or C-terminal of the protein sequence. For most proteins, expression in a BL21de3 strain works well but it might be worth testing other expression strains as expression efficiency in different strains varies for different proteins.

A. Materials and equipment

- 2 l glass flasks (Duran, Roth, Germany)
- Bacterial shaker
- French press (e.g. EmulsiFlex-C3 from Avestin, Germany, or equivalent system)
- Sorvall centrifuge and rotors (or equivalent system)
- Rotating wheel
- Cheese cloth (Ypsifix® 8cm/4m, Holthaus Medical, Germany)
- Ni-NTA Agarose (Qiagen, Germany)
- 20 ml plastic chromatography columns (Econo-Pac® disposable chromatography columns, Bio-Rad, Germany)

B. Buffers and solutions

- LB medium: 1% peptone (w/v), 0.5% yeast extract (w/v) and 0.5% NaCl (w/v), adjust pH to 7.0 with 10 N NaOH, autoclave.
- Kanamycin: 25 mg/ml in water.
- 1 M $MgSO_4$: 24.65 g $MgSO_4x7H_2O$ in water, autoclave.
- 20x NPS (NPS = 100 mM PO_4, 25 mM SO_4, 50 mM NH_4, 100 mM Na, 50 mM K): 0.5 M $(NH_4)_2SO_4$, 1 M KH_2PO_4 and 1 M Na_2HPO_4. pH of 20x NPS in water should be ~6.75, autoclave.
- 50x 5052: 25% glycerol (v/v), 0.25% glucose (w/v) and 2% alpha-lactose (w/v) in water, autoclave.
- Ni-wash buffer: 20 mM TRIS pH7.4, 500 mM NaCl and 30 mM Imidazole, autoclave.
- $MgCl_2$: 1 M stock in water, autoclave.
- Phenylmethanesulfonylfluoride (PMSF): 0.2 M in ethanol (Applichem, Germany)
- Deoxyribonuclease I (DNase I): 10 U/µl in PBS (bovine pancreas, ≥ 60.000 Dornase units/mg dry weight, Merck KGaA, Germany)
- Ni-elution buffer: 20 mM TRIS pH 7.4, 500 mM NaCl, 400 mM Imidazole, 10% glycerol (v/v).
- EDTA: 500 mM stock, dissolved in deionized water, pH 8.0, autoclave.
- Sucrose buffer as in section **I,1**.
- Cetyltrimethylammonium Bromide (CTAB, Calbiochem, Germany)

C. Method

1. Grow primary culture overnight in LB medium with Kanamycin 1:1000 at 37°C in a bacterial shaker.

2. Inoculate large scale expression cultures from overnight culture 1:100. Supplement the LB medium with 1 mM $MgSO_4$, 1x 5052, 1x NPS and Kanamycin 1:1000 (in this order). Fill at maximum 500 ml culture in 2 l flasks.
3. Grow cultures at 37ºC and 300 rpm until OD_{600}=1.5 in a bacterial shaker.
4. Shift to expression temperature and shake at 300 rpm for 12-20h (OD_{600} should be at least 5 before harvesting).

Notes: Induction in LB medium with IPTG is an alternative. However, as bacteria can be grown in much higher density in autoinduction medium the yield per expression volume is much higher. In our hands, autoinduction works fine for most of the tested proteins.

Best expression temperature needs to be determined experimentally.

5. Harvest cultures for 15 min at 4.500 g and 4°C in Sorvall centrifuge (or equivalent system).
6. Resuspend bacterial pellet obtained from 1 l culture in 150-200 ml cold Ni-wash buffer and add 1 ml of 0.2 M PMSF. All following steps should be done on ice or in the cold and using cold buffers.
7. Break bacteria by a French press or equivalently.
8. Add 2 mM $MgCl_2$, 450 ml of 10 U/µl DnaseI in PBS and 2 ml of 0.2 M PMSF per 1 l of expression culture to the lysate and incubate 10 min on ice.
9. Freeze lysate at -20°C or proceed immediately. Spin lysate for 20 min at 28.000 g and 4°C in Sorvall centrifuge.
10. Resuspend pellets at room temperature in 10 ml Ni-wash buffer + 1% CTAB and add 2 ml of 0.2 M PMSF per 1 l expression culture. Add Ni-wash buffer + 1% CTAB to a total volume of 320 ml per 1 l expression culture and rotate for 45 min at room temperature on a rotating wheel to solubilize the bacterial

membranes. All following steps, in which CTAB is present, should be done at room temperature as CTAB precipitates in the cold.

11. Spin for 15 min at 20°C and 15.000 g to remove unsolubilized membranes in Sorvall centrifuge and filter the supernatant through a cheese cloth.
12. Add 500 µl Ni-NTA Agarose beads to the supernatant derived from 1 l expression culture for 2 h at room temperature. Rotate samples on a rotating wheel.

Note: The amount of Ni-NTA Agarose beads depends on the expression yield and has to be determined for each construct.

13. Collect Ni-NTA Agarose beads in a 20 ml plastic chromatography column. Wash beads 2-3 times with one column volume of Ni-wash buffer + 0.1% CTAB.
14. Close column and elute the protein of interest from the beads with 500 µl Ni-elution buffer + 1% CTAB for 5 min at room temperature. Collect eluate and elute beads again with 250 µl Ni-elution buffer + 1% CTAB for 5 min. Pool both eluates.

Note: The volume of Ni-elution buffer depends on the protein concentration and the Agarose beads volume. Elution works best with 50% slurry of Agarose beads or more diluted. A third elution might be done if a lot of protein remains on the Agarose beads. Analyze beads for elution efficiency if you purify the protein the first time.

15. Dialyze eluates to sucrose buffer + 1 mM EDTA for 1h at 4°C and again over night with fresh buffer.

Note: Dependent on the later use of the protein, the dialysis buffer can be altered. For addback in nuclear assembly assays (section **IV, 1**) sucrose buffer is recommended.

16. Determine protein concentration by SDS-PAGE, aliquot and freeze in liquid nitrogen. Store protein aliquots at -80°C for later use.

Note: Traces of CTAB are still present in the protein sample and might interfere with most methods of protein concentration determination. It is best to judge the protein concentration by comparing the band on a protein gel to a known concentration of BSA.

2. Expression and purification of NusA-TEV

TEV protease for nuclear assembly reactions to measure the transport of inner nuclear membrane proteins through nuclear pore complexes (section **IV,4**) is fused to NusA to increase its size above the size exclusion limit of nuclear pore complexes, cloned into a pET28a expression vector and transformed into BL21de3 bacteria for expression.

A. Materials and equipment

- Chromatography columns (Econo-Column® Chromatography Column, 5.0 x 20 cm, Bio-Rad, Germany)
- Other material as in section **II,1**.

B. Buffers and solutions

- As in section **II,1**.

C. Method

1. Inoculate 4 ml of an overnight culture of transformed bacteria (grown in LB medium with 25 µg/ml Kanamycin) in 400 ml auto-induction medium (LB supplemented as in section **II,1**). Fill in 2 l glass flasks and grow at 37ºC at 300 rpm in bacterial shaker.
2. Shift culture to expression temperature of 25°C when OD_{600}=1.5.

3. After 14-20 h at 25°C, OD_{600} should be at least 5. Harvest bacteria by centrifugation for 15 min at 4.500 g in a cold rotor at 4°C in a Sorvall centrifuge.
4. Resuspend pellet in 10 ml cold Ni-wash buffer, fill up to at least 100 ml and add 1 ml of 0.2 M PMSF. All following steps should be done keeping the proteins on ice or in the cold and using cold buffers.
5. Break bacteria in Emulsiflex, French press or equivalent system.
6. Add 1 mM $MgCl_2$, 200 µl of 10 U/µl DnaseI in PBS and 1 ml of 0.2 M PMSF and incubate 10 min on ice.
7. Spin 15 min at 22.000 g in a rotor at 4°C. Spin again if supernatant is not cleared sufficiently. Filter supernatant through cheese cloth.
8. Apply 1.6 ml of 50% slurry of Ni-NTA Agarose to the supernatant and incubate for 2 h at 4°C on a rotating wheel.
9. Apply Agarose beads to chromatography column. If all agarose is collected in the column wash with 100 ml cold Ni-wash buffer.
10. Elute the His_6-NusA-TEV protein with 4 ml Ni-elution buffer
11. Dialyze eluate to sucrose buffer, determine protein concentration and store aliquots at -80°C. We usually obtain 20 mg of protein from 400 ml autoinduction culture.

III. Biochemical Procedures

1. Generation of antibody beads

Depletion of soluble or membrane integral proteins from *Xenopus* egg extracts is achieved by passage of the cytosol or solubilized membrane fraction, respectively, over a bead material with crosslinked antibodies. Because of the high abundance of

many nucleoporins these antibody beads should provide a high capacity and we therefore prefer Protein A-Sepharose over magnetic Protein A-beads.

A. Materials and equipment

- Protein A-Sepharose (GE Healthcare, Sweden)
- Rabbit IgG (Calbiochem, Germany)
- Häreus-Multifuge 1-LR-Centrifuge (or equivalent)
- Dimethylpimelimidate (DMP, store solid and dry at 4°C; Pierce, Thermo Fisher Scientific, Bonn, Germany)
- Rotating wheel (or equivalent)
- BSA (Fraction V, Calbiochem, Germany)
- Sodium azide (NaN_3)

B. Buffers and solutions

- Phosphate buffer saline (PBS): 2.7 mM KCl, 137 mM NaCl, 10 mM $Na_2HPO_4 \cdot 2H_2O$, 2 mM KH_2PO_4. Prepare a 10x stock solution, adjust to pH 7.4 with 10 N NaOH and autoclave. Dilute to 1x PBS freshly before use.
- Coupling buffer: 200 mM $NaHCO_3$, 100 mM NaCl, pH 9.3.
- Blocking buffer: 0.1 M ethanolamine pH 8.2.
- Buffer A: 100 mM sodiumacetate, 500 mM NaCl pH 4.2.
- Buffer B: 100 mM $NaHCO_3$, 500 mM NaCl, pH 8.3.
- Protease inhibitor mix (PI) as in section **I,1**.

C. Method

1. Incubate 4 mg of affinity purified antibody with 1 ml Protein A-Sepharose (50% slurry) in PBS for 4-16 h at 4°C on a rotating wheel. For control beads use rabbit IgGs at approximately the same concentration.

2. Wash beads twice with coupling buffer by spinning beads down for 2 min at 3000 rpm and 4°C in a Häreus-Multifuge 1-LR-Centrifuge. Remove supernatant and add fresh buffer.
3. Crosslink antibodies and Protein A-Sepharose beads in 10 mM DMP in coupling buffer for 20 min at room temperature on a rotating wheel.
4. Wash beads once with coupling buffer (spin as in step 2) and crosslink again in 10 mM DMP in coupling buffer for 20 min at room temperature on a rotating wheel.
5. Wash beads once with blocking buffer (spin as in step 2) and rotate for 1 h in blocking buffer at room temperature.
6. Wash beads alternating twice with buffer A and B (spin as in step 2).
7. Block beads in 3% BSA in PBS supplemented with PI (1:1000) for 1 h at 4°C on a rotating wheel.
8. Store beads as a 50% slurry in 3% BSA in PBS supplemented with PI (1:1000) and 0.05% NaN_3 at 4°C.

2. Preparation of G50-chromatography columns

For reconstitution of membranes after depletion (section **III,3**) or generation of proteoliposomes (section **III,4**) detergent is removed by gelfiltration with Sephadex G50-columns. To avoid major protein and lipid loss during column passage the gelfiltration column is pre-blocked with BSA and a lipid mixture.

A. Materials and equipment

- G50 gel filtration medium (Sephadex G-50 Fine, GE Healthcare, Sweden)
- glass chromatography column (Econo-Column®, 0.5 x 20 cm, Bio-Rad, Germany)

- Polyethylene tubing (or equivalent)
- BSA
- n-Octyl-β-D-glucopyranoside (Calbiochem, Germany) or equivalent detergent

B. Buffers and solutions

- Lipid mix: 3 mg/ml cholesterol (ovine wool, >98), 3 mg/ml L-α-phosphatidylserine (sodium salt, brain, porcine), 3 mg/ml L-α-phosphatidylinositol (sodium salt, liver, bovine), 6 mg/ml L-α-phosphatidylethanolamine (egg, chicken), 15 mg/ml L-α-phosphatidylcholine (egg, chicken; all from Avanti Polar Lipids, USA) in 10% n-Octyl-β-D-glucopyranoside
- $DiIC_{18}$: 1 mg/ml 1,1'-Dioctadecyl-3,3,3',3'-Tetramethylindocarbocyanine Perchlorate in DMSO ('DiI', $DiIC_{18}$(3), crystalline; Life Technologies GmbH, Germany)
- Sucrose buffer as in section **I,1** and PBS as in section **III,1**.

C. Method

1. Swell G50 beads in sucrose buffer for 10 min at room temperature.
2. Remove bottom and top lids from the chromatography column and fill column with swollen G50 beads. Let beads settle by gravity. Add more beads carefully until the glass cylinder of the column is nearly filled (leave about 0.5 cm space at the top). The upper edge of the bead layer should remain visible.

Note: Avoid air bubbles in the column. Be careful that columns don't run dry.

3. Fill column with sucrose buffer, put top lid on and connect the lid to a buffer reservoir via tubing.
4. Wash column with sucrose buffer from the reservoir by letting the buffer pass by gravity flow.

5. To block the column, take top lid off, carefully remove excess buffer and add 100 µl of 1 mg/ml BSA in sucrose buffer directly onto the bead layer. Let the solution enter the beads, then fill the column immediately but carefully with buffer, put top lid back on and wash the column as in step 4.
6. Block column again with 20 µl lipid mix diluted 1:5 with PBS in 100 µl total volume as in step 5.

Note: Lipid mix can be altered as well as the detergent used to dissolve the lipids. A relatively high CMC (critical micelle concentration) value of the detergent and small aggregation number is important to ensure its removal by gelfiltration.

7. Wash column with sucrose buffer for 30 min as in step 4.
8. Close bottom lid of the column. To store your columns for longer term, add 0.1% NaN_3 to the sucrose buffer.

Note: For long term storage of the columns, let some buffer pass from time to time.

3. Depletion of transmembrane proteins from *Xenopus* membranes

To specifically deplete transmembrane proteins, *Xenopus* membranes are solubilized by detergent and the protein of interest is immunodepleted by passage of the solubilized membrane fraction over an antibody column (Figure 2A). Detergent removal from the solubilized and depleted membrane fraction reconstitutes the membranes. An efficient way for detergent removal is passage of a gel filtration column (Allen, Romans, Kercret, & Segrest, 1980) under the pre-condition that the detergent has a relative high CMC (critical micelle concentration) value, which defines the concentration of the free detergent in solution in contrast to its micellar form, and a not small aggregation number.

For addback experiments the purified integral membrane protein (see section **II,1**) is added to the solubilized and depleted membrane fraction and co-reconstituted by passage of the gelfiltration column.

For editors; PLEASE INSERT FIGURE 2 HERE

A. Materials and equipment

- n-Octyl-β-D-glucopyranoside or equivalent detergent as in section **III,2**.
- Beckman Optima TLX Ultracentrifuge, TLA 100 rotor and tubes (or equivalent system)
- Mobicol columns (Mobicol "classic" with 1 closed screw cap and plug and 35 µm pore size filters, MoBiTec GmbH, Germany)
- cooled tabletop microcentrifuge
- Crude membranes, antibody beads and G50-chromatography columns described in sections **I,2**, **III,1** and **III,2**.

B. Buffers and solutions

- Sucrose buffer, lipid mix and $DiIC_{18}$ as in sections **I,1** and **III,2**.

C. Method

1. Solubilize 20 µl of crude membranes (for preparation see section **I,2**) in sucrose buffer with 1% n-Octyl-β-D-glucopyranoside for 10 min at 4°C.

Notes: Frozen membrane aliquots can be used.

Ensure proper membrane solubilization with marker proteins by Western blotting.

If necessary other detergents (with relative high CMC values and small aggregation numbers to allow for their removal afterwards) might be used such as CHAPS.

Use high quality detergent, some batches of n-Octyl-β-D-glucopyranoside need to be purified before use by passage over a mixed bead resin (e.g. AG501-X8 from Bio-Rad, Germany)

2. Clear by centrifugation for 10 min at 200.000 g and 4°C in a TLA100 rotor and take supernatant.
3. Equilibrate 40 µl of antibody beads (50% slurry, prepared as described in section **III,1**) in a Mobicol column with sucrose buffer immediately before use, spin dry by centrifugation for 30 s at 5000 g and 4°C in a cooled tabletop microcentrifuge. Apply supernatant of step 2 to dried beads and incubate for 30 min at 4°C on a rotating wheel.

Note: Optimal bead to solubilized membranes ratio needs to be determined. However, the given conditions work for most of the proteins we tested.

4. Elute unbound supernatant (spin as in step 3) and incubate a second time as in step 3 with fresh antibody beads.
5. Elute unbound supernatant and add 20 µl lipid mix and 0.2 µl of 1 mg/ml $DiIC_{18}$ in DMSO. For add-back experiments, add your protein of interest in approximately endogenous concentration together with the lipid mix to the eluate.

Notes: The optimal amount of re-added protein needs to be determined. In our hands, for most add-back attempts achieving endogenous protein levels works fine (Figure 2B).

If necessary one can avoid the use of a fluorescent dye and reconstituted membranes are collected blindly. For this, a test run in which one can follow the reconstituted fraction with a marker (e.g. a fluorescent dye) is performed and the number of drops counted until the reconstituted membrane fraction runs out of the column.

6. Reconstitute membranes by detergent removal by passing the sample over a G50-chromatography column (prepared as described in section **III,2**) equilibrated to sucrose buffer. Remove excess of buffer and load the samples directly on the bead layer. Fill the column with buffer as soon as the sample has entered the beads. Collect the membrane containing fraction (approximately 400µl or 8-9 drops), which appears pink due to addition of $DiIC_{18}$.
7. Pellet reconstituted membranes by centrifugation for 30 min at 200.000 g in a TLA100 rotor.
8. Resuspend membrane pellet in 20 µl sucrose buffer. Reconstituted membranes are now ready to use in the nuclear assembly reaction (section **IV, 1**).

4. Reconstitution of recombinant integral membrane proteins in proteoliposomes

For purification, integral membrane proteins are detergent solubilized from membranes. At the end of the purification process, the detergent is removed to maintain the proper functionality of the integral membrane protein by reconstitution in proteoliposomes, which can be used as a tool for functional studies as in section **IV**.

A. Materials and equipment

- Beckman Optima TLX Ultracentrifuge, TLA 120.2 rotor and tubes (or equivalent system)
- G50-chromatography columns described in section **III,2**.

B. Buffers and solutions

- PBS, lipid mix, $DiIC_{18}$ and sucrose buffer as in sections **I,1**, **III,1** and **III,2**.

C. Method

1. Prepare pre-blocked G50-columns as described in section **III,2** but use PBS instead of sucrose buffer.
2. Apply a mix consisting of 20 µl lipid mix, 5 µl purified protein (conc. < 1mg/ml), 50 µl PBS and 0.5 µl $DiIC_{18}$ (1 mg/ml in DMSO) directly onto the bead layer.
3. Fill column with buffer as soon as the lipid mixture has entered the column. Collect $DiIC_{18}$-labelled fraction (approximately 8-9 drops or 400µl) containing reconstituted proteoliposomes.

Note: Alternatively, another fluorescent membrane dye or fluorescently labeled lipids can be used.

4. Pellet proteoliposomes in PBS in a TLA120.2 rotor for 30 min at 100.000 rpm (360,000xg_{av}) and 4°C. Resuspend pellet in 20 µl sucrose buffer.
5. Wash column after use with buffer and store it as described in section **III,2**.

Note: If you don't want to use a fluorescent dye, proteoliposomes can be collected blindly (compare Notes for section **III,3**). Column can be reused but upper bead layers (~ 1 cm) have to be exchanged from time to time. After renewal of the upper bead layer, block column with BSA and lipids before next use as described in section **III,2**.

IV. Nuclear assembly reactions

1. Nuclear assembly reactions using depleted and reconstituted membranes

In vitro assembled nuclei can be reconstituted using cytosol and membranes from egg extracts combined with chromatin of demembranated sperm. Preparation of demembranated sperm is described in Murray, 1991, see also Bernis et al., chapter 8 in this volume. For depletion experiments of transmembrane nucleoporins,

endogenous membranes are replaced by a depleted membrane fraction prepared as described in section **III,3**.

A. Materials and equipment

- Vectashield 1000 (Vector Laboratories, Burlingame, USA)
- Round glass coverslips (12 mm diameter, Menzel, Braunschweig, Germany)
- 6 ml flat bottom tubes (Greiner, Germany)
- large orifice tip (MBP® 200G/1000G Pipet Tips, Molecular BioProducts)
- Häreus-Multifuge 1-LR-Centrifuge
- Nail polish/coverslip sealant
- 24-well-plates (Greiner, Germany)

B. Buffers and solutions

- Energy mix: 50 mM ATP, 50 mM GTP, 500 mM creatine phosphate and 10 mg/ml creatine kinase in sucrose buffer. The energy mixture can be prepared and stored as single use aliquots at -80°C.
- Glycogen: 0.2 g/ml in sucrose buffer (oyster glycogen, USB, Amersham)
- 0.1% Poly-L-Lysine solution in water (Sigma-Aldrich, USA)
- Sucrose cushion: 30% sucrose in PBS
- 4',6-diamidino-2-phenylindole (DAPI): 10 mg/ml in water, store in small aliquots in the dark at -20°C.
- Membrane fixative: 2% Paraformaldehyde, 0.5% Glutaraldehyde (Sigma-Aldrich, USA) in 80 mM Pipes pH 6.8, 1 mM $MgCl_2$, 150 mM sucrose. Add 1 µg/ml DAPI prior to use.
- IF fixative: 2% Paraformaldehyde in 80 mM Pipes pH 6.8, 1 mM $MgCl_2$, 150 mM sucrose.
- PBS, sucrose buffer and $DiIC_{18}$ see sections **I,1**, **III,1** and **III,2**.

C. Method

1. Add 0.6 µl of demembranated sperm chromatin (from stock of 3000 sperm heads/µl to reach a final concentration of ~ 100 sperm heads/µl) to 20 µl of freshly prepared membrane free cytosol (described in section **I,1**) and mix carefully with a large orifice tip. Incubate for 10 min at 20°C to allow for sperm chromatin decondensation.

Note: In contrast to most nuclear assembly reactions, for which frozen aliquots of egg extract cytosol are used, this assay is very sensitive to the quality of the cytosol and we only use freshly prepared extracts.

2. Add 0.5 µl energy mix, 0.5 µl glycogen and 4.4 µl of reconstituted membranes (described in section **III,3**) and mix carefully with a large orifice tip. Incubate for 110 min at 20°C.

Note: Include control samples, in which membranes are replaced by sucrose buffer, to confirm that cytosol is membrane free.

3. For visualization of membranes: Add 0.2 µl of 0.1 mg/ml $DiIC_{18}$ (dissolved in DMSO) 5 min before the end of incubation and mix carefully.
4. Fix samples for 20 min on ice either in 0.5 ml membrane fixative (for $DiIC_{18}$ membrane staining) or in 0.5 ml IF fixative (for immunofluorescence).
5. Load fixed nuclei onto a 0.8 ml sucrose cushion in the flat-bottomed tubes containing poly-L-Lysine coated coverslips. Transfer nuclei onto the coverslips by spinning at 3500 rpm ($250xg_{av}$) for 15 min at 4°C in a Häreus-Multifuge 1-LR-Centrifuge.

Note: Coverslips are coated by covering them with a 0.1% Poly-L-Lysine solution for 5 min, washed once with water and dried.

6. For visualization of membranes: Wash coverslips once with deionized water and mount them on a 2 µl drop of Vectashield 1000. Seal coverslips with nail polish. Be careful that the coverslips do not dry-out.

   For immunofluorescence staining: Place coverslips in 24-well-plates, wash once and store in PBS. Continue with “Immunofluorescence of nuclear assembly reactions” in section **IV,2**.

2. Immunofluorescence of nuclear assembly reactions

The membrane staining of nuclei prepared in nuclear assembly reactions (section **IV,1**) visualizes the formation of a closed nuclear envelope around the reconstituted nuclei. The incorporation of NPCs into the nuclear envelope can be examined by immunofluorescence (Figure 2C). By using specific antibodies against individual nucleoporins, NPC composition can be investigated. This is especially useful after immunodepletion of nucleoporins to assay the impact of these individual NPC components on NPC formation.

A. Materials and equipment

- Fluorescently labeled secondary antibody (e.g. from Life Technologies GmbH, Germany)
- Vectashield 1000, nail polish or coverslip sealant and 24-well-plates as in section **IV,1**.

B. Buffers and solutions

- PBS and DAPI stock solution as in sections **III,1** and **IV,1**.
- 50 mM NH_4Cl in PBS.
- Blocking buffer: 3% BSA in PBS + 0.1% Triton X-100 (Carl Roth GmbH + Co. KG, Karlsruhe, Germany).

C. Method

1. Carefully remove PBS and quench samples for 5 min with 50 mM NH_4Cl in PBS. Although the samples are fixed, the nuclei and particularly the nuclear envelope are very fragile to small breaks. All washes and buffer exchanges should be done carefully. It is also important that the coverslips do not dry out.
2. Incubate coverslips in blocking buffer for 30 min.
3. Incubate coverslips upside down on top of a drop of approximately 70 µl of primary antibody dilution in blocking buffer in a humidity chamber for 2 h. The user should determine optimal antibody dilutions.

Note: Rabbit sera produced in our lab are generally diluted 1:100, while purified antibodies but also the widely used monoclonal antibody mAB414 can often be diluted to 1:1000 or 1:2000.

4. Wash coverslips 3 times for 2 min with PBS + 0.1% Triton X-100 in the 24-well-plate.
5. Incubate coverslips with 250 µl of fluorescently labeled secondary antibodies (usually diluted 1:2000 in blocking buffer) for 1 h in 24-well-plates in the dark.
6. Wash coverslips 3 times for 2 min with PBS + 0.1% Triton X-100. Avoid longer light exposure.
7. Incubate coverslips for 10 min in PBS + DAPI (1:2000) in the dark.
8. Wash coverslips once with water and mount them on a 1 µl drop of Vectashield 1000. Seal coverslips with nail polish. Keep coverslips in the dark and store at 4°C.

3. Transmission electron microscopy of nuclear assembly reactions

For ultrastructural analysis of the assembled nuclei, samples are prepared for transmission electron microscopy. Nuclear membranes and nuclear pore complexes

are easily detectable due to the use of osmium tetroxide for contrast enhancement of membranes. The protocol is adapted from (Macaulay & Forbes, 1996) including an re-isolation of fixed *in vitro* assembled nuclei on the surface of a coverslip before embedding. In this way, most nuclei are concentrated in a relative small volume and easily identified in a limited number of ultrathin sections.

A. Materials and equipment

- 24-well-plate as in section **IV,1**.
- Epon/Araldite kit (EMS, Hatfield, USA)
- dissecting microscope
- needle
- jigsaw

B. Buffers and solutions

- Fix buffer: 25 mM HEPES pH7.5, 25 mM PIPES, 1 mM EGTA, 50 mM KCl, 2 mM MgAc, 5% sucrose.
- Cacodylate buffer: 100 mM cacodylate dissolved in deionized water, pH 7.2.
- 1% Osmium tetroxide (OsO_4): dissolved in cacodylate buffer (w/v).
- 1.5% Potassium hexacyanidoferrate (II) ($K_4[Fe(CN)_6] \times 3H_2O$): dissolved in cacodylate buffer.
- 1% Uranyl acetate: dissolved in deionized water, keep in the dark at 4°C.
- Epon/araldite-mixture: for 26.5 ml of resin use 7.75 g Epon 812 Procure, 5.55 g Araldite 502 and 15.25 g DDSA. After thorough mixing, add 490 µl DMP-30.

C. Method

1. After centrifugation of the assembly reactions on poly-L-Lysine coated coverslips (see section **IV,1**), place coverslips in a 24-well-plate.
2. Wash coverslips once with fix buffer.
3. Fix coverslips for 1 h on ice in fix buffer with 1% Glutaraldehyde (v/v).

4. Postfix samples for 2 h on ice in fix buffer with 2.5% Glutaraldehyde (v/v).
5. Wash once with ice-cold Cacodylate buffer.
6. Incubate samples for 40 min on ice in 1% OsO_4 and 1.5% K_4[Fe(Orso, Pendin, Liu, Tosetto, Moss, Faust, Micaroni, Egorova, Martinuzzi, McNew, & Daga)$_6$] (Orso et al.).
7. Wash coverslips with deionized water.
8. Incubate for 1 h with 1% uranyl acetate at 4°C in the dark.
9. Wash coverslips with water.
10. Dehydrate samples in a graded ethanol series of 30%, 50%, 90% and 2x 100% ethanol each for 10 min.
11. Resin infiltration: 50% Epon/Araldite in Ethanol, 2 x 100% Epon/Araldite each 30 min.
12. After resin infiltration, remove the coverslips from the 24-well-plate and place them on a resin filled lid of a 1.5 ml Eppendorf cup, sample side facing down.

Note: Avoid capturing any air bubbles.

13. Resin curing at 60°C for 48 h.
14. Remove the glass coverslips from the cured resin-embedded samples by submerging them in liquid nitrogen.

Note: This step has to be repeated several times until every bit of glass is removed from the sample surface. More often than not, remaining glass shards have to be carefully pried from the resin surface with a fine tungsten needle under the dissecting microscope. Wear personal protective equipment while working with liquid nitrogen and glass.

15. Find and mark out areas with nuclear assemblies under the dissecting microscope with a fine needle.
16. Cut out the areas of interest with a fine jigsaw.

17. Prepare ultrathin sections parallel to the sample surface.

4. Nuclear assembly reactions measuring transport of inner nuclear membrane proteins through nuclear pore complexes

Nuclei assembled *in vitro* in *Xenopus* egg extracts can be used both, to study nuclear import of soluble cargos (for a detailed method description see Chan & Forbes, 2006) as well as to analyze transport of inner nuclear membrane proteins through nuclear pore complexes. For the latter use, integral membrane protein reporters are expressed and purified from *E. coli* (see section **II,1**) and reconstituted in proteoliposomes (see section **III,4**). These proteoliposomes are added to a nuclear assembly reaction at time points when the nuclear envelope is already closed around the chromatin. Proteoliposomes readily fuse with the endoplasmic reticulum and the reporter is immediately distributed throughout the membranes of the endoplasmic reticulum including the outer nuclear membrane.

Nuclear pore complex passage of the reporter to the inner nuclear membrane is monitored by its protection from a protease added to the cytoplasm (Figure 3). We have best experience with a TEV (tobacco etch virus) protease fused to the large bacterial protein NusA, which increases the size of the protease-fusion protein to at least 90 kDa thereby preventing its diffusion through the NPC (Figure 3B). Consequently, reporter proteins contain a TEV protease recognition site followed by a domain, which is cleaved off upon TEV protease activity (Figure 3A). The latter domain is usually an EGFP-tag in our assay, as this allows to follow cleavage both by light microscopy (Figure 3C) and western blotting (Figure 3D). We have good experience with reporter constructs containing EGFP-tag and TEV cleavage site N-terminally fused to BC08, a INM protein with a single C-terminal transmembrane region (Ulbert et al., 2006) or the first transmembrane region of LBR (lamin B

receptor), which is sufficient for INM targeting (Soullam & Worman, 1995). But also multispanning INM proteins such as full-length LBR or nurim work as reporters.

For editors; PLEASE INSERT FIGURE 3 HERE

A. Materials and equipment

- EGFP-antibody (cat. no. 11814460001, Roche, Germany)

B. Buffers and solutions

- SDS-sample buffer: 0.19M TRIS pH 6.8, 30% sucrose (w/v), 0.9% SDS (w/v), 0.1% Bromphenolblue (w/v), 0.1M DTT.
- Energy mix, glycogen and IF fixative as in section **IV,1**.

C. Method

1. Incubate 45 µl of freshly prepared membrane free cytosol (preparation described in section **I,1**) with 2.5 µl sperm heads (3000 sperm heads/µl) for 10 min at 20°C to allow for sperm decondensation.
2. Add 1 µl energy mix, 1 µl glycogen and 2.5 µl of floatation purified membranes (preparation described in section **I,2**) and incubate for 50 min at 20°C.
3. Add 5µl of resuspended proteoliposomes (prepared as described in section **II,4**) and mix carefully, incubate at 20°C.
4. Take out 10 µl from the sample each after 0, 5, 10, 15 and 30 min after proteoliposome addition and add 1µl of 5 µg/µl TEV protease for 5 min at 20°C to each. Stop cleavage reaction by adding 5 µl SDS-sample buffer and immediate heating for 5 min at 95°C.
5. Analyze time course of cleavage reaction by western blotting with an EGFP-antibody. Alternatively, the loss of EGFP signal can be monitored by

immunofluorescence. For this, stop TEV cleavage reaction by fixation in IF fixative and proceed with immunofluorescence as described in section **IV,2**.

Conclusion

Xenopus egg extracts provide a powerful cell-free tool to study nuclear assembly and functions. Since their first use more than 30 years ago (Lohka & Masui, 1983) they have been employed in a variety of assays focusing on different aspects of nuclear organization, dynamics and functions. Accordingly, slight variations in the protocols for preparing such extracts exist (e.g. see Chapter 8 for a modified egg extract preparation protocol).

Immunodepletion of soluble proteins is a key advantage of the *Xenopus* egg extract system. It facilitates analysis of the function of specific proteins in definite aspects of nuclear dynamics, such as nuclear pore complex assembly. By employing the methods described here, the technical repertoire is expanded to include integral membrane proteins. These methods have already been applied to analyze the function of transmembrane nucleoporins or the passage of membrane proteins through the pore but they are certainly not limited to these questions. In the future, they could be used to study the functional interaction of transmembrane proteins with chromatin or membrane fusion reactions mediated by transmembrane proteins to name just two examples.

References

Allen, T. M., Romans, A. Y., Kercret, H., & Segrest, J. P. (1980). Detergent removal during membrane reconstitution. *Biochim Biophys Acta, 601*(2), 328-342.

Antonin, W., Franz, C., Haselmann, U., Antony, C., & Mattaj, I. W. (2005). The integral membrane nucleoporin pom121 functionally links nuclear pore complex assembly and nuclear envelope formation. *Mol Cell, 17*(1), 83-92.

Antonin, W., Ungricht, R., & Kutay, U. (2011). Traversing the NPC along the pore membrane: Targeting of membrane proteins to the INM. *Nucleus, 2*(2), 87-91. doi: 10.4161/nucl.2.2.14637

Brown, K. S., Blower, M. D., Maresca, T. J., Grammer, T. C., Harland, R. M., & Heald, R. (2007). Xenopus tropicalis egg extracts provide insight into scaling of the mitotic spindle. *J Cell Biol, 176*(6), 765-770. doi: 10.1083/jcb.200610043

Chan, R. C., & Forbes, D. I. (2006). In vitro study of nuclear assembly and nuclear import using Xenopus egg extracts. *Methods Mol Biol, 322*, 289-300.

de la Barre, A. E., Robert-Nicoud, M., & Dimitrov, S. (1999). Assembly of mitotic chromosomes in Xenopus egg extract. *Methods Mol Biol, 119*, 219-229. doi: 10.1385/1-59259-681-9:219

Eisenhardt, N., Redolfi, J., & Antonin, W. (2013). *Nup53 interaction with Ndc1 and Nup155 are required for nuclear pore complex assembly*. J Cell Sci.

Galy, V., Antonin, W., Jaedicke, A., Sachse, M., Santarella, R., Haselmann, U. (2008). A role for gp210 in mitotic nuclear-envelope breakdown. *J Cell Sci, 121*(Pt 3), 317-328.

Gillespie, P. J., Gambus, A., & Blow, J. J. (2012). Preparation and use of Xenopus egg extracts to study DNA replication and chromatin associated proteins. *Methods, 57*(2), 203-213. doi: 10.1016/j.ymeth.2012.03.029

Lohka, M. J. (1998). Analysis of nuclear envelope assembly using extracts of Xenopus eggs. *Methods Cell Biol, 53*, 367-395.

Lohka, M. J., & Masui, Y. (1983). Formation in vitro of sperm pronuclei and mitotic chromosomes induced by amphibian ooplasmic components. *Science, 220*(4598), 719-721.

Lusk, C. P., Blobel, G., & King, M. C. (2007). Highway to the inner nuclear membrane: rules for the road. *Nat Rev Mol Cell Biol, 8*(5), 414-420. doi: nrm2165 [pii]

10.1038/nrm2165

Macaulay, C., & Forbes, D. J. (1996). Assembly of the nuclear pore: biochemically distinct steps revealed with NEM, GTP gamma S, and BAPTA. *J Cell Biol, 132*(1-2), 5-20.

Mansfeld, J., Guttinger, S., Hawryluk-Gara, L. A., Pante, N., Mall, M., Galy, V. (2006). The conserved transmembrane nucleoporin NDC1 is required for nuclear pore complex assembly in vertebrate cells. *Mol Cell, 22*(1), 93-103.

Maresca, T. J., & Heald, R. (2006). Methods for studying spindle assembly and chromosome condensation in Xenopus egg extracts. *Methods in molecular biology, 322*, 459-474.

Murray, A. W. (1991). Cell cycle extracts. *Methods Cell Biol, 36*, 581-605.

Murray, A. W., & Kirschner, M. W. (1989). Cyclin synthesis drives the early embryonic cell cycle. *Nature, 339*(6222), 275-280. doi: 10.1038/339275a0

Newmeyer, D. D., & Wilson, K. L. (1991). Egg extracts for nuclear import and nuclear assembly reactions. *Methods Cell Biol, 36*, 607-634.

Orso, G., Pendin, D., Liu, S., Tosetto, J., Moss, T. J., Faust, J. E. (2009). Homotypic fusion of ER membranes requires the dynamin-like GTPase atlastin. *Nature, 460*(7258), 978-983. doi: 10.1038/nature08280

Pfaller, R., Smythe, C., & Newport, J. W. (1991). Assembly/disassembly of the nuclear envelope membrane: cell cycle-dependent binding of nuclear membrane vesicles to chromatin in vitro. *Cell, 65*(2), 209-217.

Roosild, T. P., Greenwald, J., Vega, M., Castronovo, S., Riek, R., & Choe, S. (2005). NMR structure of Mistic, a membrane-integrating protein for membrane protein expression. *Science, 307*(5713), 1317-1321. doi: 10.1126/science.1106392

Sheehan, M. A., Mills, A. D., Sleeman, A. M., Laskey, R. A., & Blow, J. J. (1988). Steps in the assembly of replication-competent nuclei in a cell-free system from Xenopus eggs. *J Cell Biol, 106*(1), 1-12.

Sive, H. L., Grainger, R. M., & Harland, R. M. (2000). Early Development of Xenopus laevis - a laboratory manual. *Cold Spring Harbor Laboratory Press*.

Soullam, B., & Worman, H. J. (1995). Signals and structural features involved in integral membrane protein targeting to the inner nuclear membrane. *J Cell Biol, 130*(1), 15-27.

Theerthagiri, G., Eisenhardt, N., Schwarz, H., & Antonin, W. (2010). The nucleoporin Nup188 controls passage of membrane proteins across the nuclear pore complex. *J Cell Biol, 189*(7), 1129-1142. doi: 10.1083/jcb.200912045

Vigers, G. P., & Lohka, M. J. (1991). A distinct vesicle population targets membranes and pore complexes to the nuclear envelope in Xenopus eggs. *J Cell Biol, 112*(4), 545-556.

Wilson, K. L., & Newport, J. (1988). A trypsin-sensitive receptor on membrane vesicles is required for nuclear envelope formation in vitro. *J Cell Biol, 107*(1), 57-68.

Figure legends

Figure 1 Schematic overview of cytosol and membrane preparation from *Xenopus* eggs.

Activated *Xenopus laevis* eggs are crushed by centrifugation to obtain the cellular content as low speed extracts. These low speed extracts are further separated into a cytosol and a membrane fraction. After separating both fractions, residual membrane components are removed from the cytosol by two additional high speed centrifugation steps. The membranes can either be purified in a crude preparation by dilution and centrifugation or further fractionated by floatation through a sucrose step gradient. Floated membrane fractions, for example fractions 1-3 are pooled, and purified by a final dilution and centrifugation step.

Figure 2 Depletion and functional add-back of membrane proteins.

A: Schematic illustration of immunodepletion of transmembrane proteins from *Xenopus* membranes. Membranes are solubilized with a detergent and the target membrane protein is depleted from the solubilized membrane fraction by specific antibody beads. Finally, the depleted membranes are reconstituted by detergent removal.

B: Western Blot analysis of *Xenopus* membranes, which were mock-depleted, immunodepleted of endogenous NDC1 or NDC1-depleted and substituted with recombinant EGFP-NDC1 expressed in *E. coli* (addback). Endogenous and recombinant NDC1 are detected by NDC1-antibodies, the recombinant protein also by EGFP-antibodies. The NDC1-depletion does not affect levels of other integral membrane proteins including the transmembrane nucleoporins GP210 and POM121.

C: Immunofluorescence of nuclear assembly reactions with *Xenopus* cytosol and membranes from B. Recombinant EGFP-NDC1 is faithfully integrated into the

nuclear membranes as detected by NDC1- and EGFP-antibodies. NDC1 depletion blocks NPC formation (ΔNDC1). This phenotype is rescued by the addition of recombinant EGFP-NDC1 (addback) as indicated by the presence of Nup58, a nucleoporin located in the inner part of the NPC. DNA is stained with DAPI. Bar: 10 µm.

Figure 3 Analysis of inner nuclear membrane protein passage through nuclear pore complexes (modified after Theerthagiri et al., 2010).

A: Schematic illustration of an inner nuclear membrane (INM) protein reporter. The reporter protein is fused to an N-terminal EGFP-tag followed by a TEV-protease recognition site.

B: The reporter construct reconstituted in proteoliposomes is added to nuclear assembly reactions when the nuclear envelope is already closed. The reporter is immediately distributed throughout the membranes of the endoplasmic reticulum (ER), including the outer nuclear membrane (ONM). To monitor its transport through nuclear pore complexes, a NusA-fused TEV protease is added, which is excluded from NPC passage due to its size. The reporter protein is accessible for cleavage of the EGFP-tag by the TEV-protease if present in the membranes of the ER or ONM, whereas in the inner nuclear membrane (INM) the reporter constructs are protease protected.

C: Immunofluorescence of the assay described in B. The reporter construct is visualized by EGFP-antibodies and can be detected in the ER and ONM at 0 min. 30 min after addition, the reporter construct is enriched in the INM, where it is protease protected from NusA-TEV due to size exclusion of nuclear pore complexes. If the TEV protease construct is actively imported into the nucleus due to a nuclear

localization (NLS)-site, the EGFP-tag of the reported is cleaved off, also when residing in the INM after 30 min. DNA is stained with DAPI. Bar: 10 µm.

D: Western Blot analysis of isolated nuclei from the experiment in C at different time points using the EGFP-antibody. Cleavage of the reporter by TEV-protease results in the appearance of a band of free EGFP (around 25 kDa) which is absent if the reporter is protease protected due to transport to the INM, which occurs approximately 15min after addition of the reporter construct.

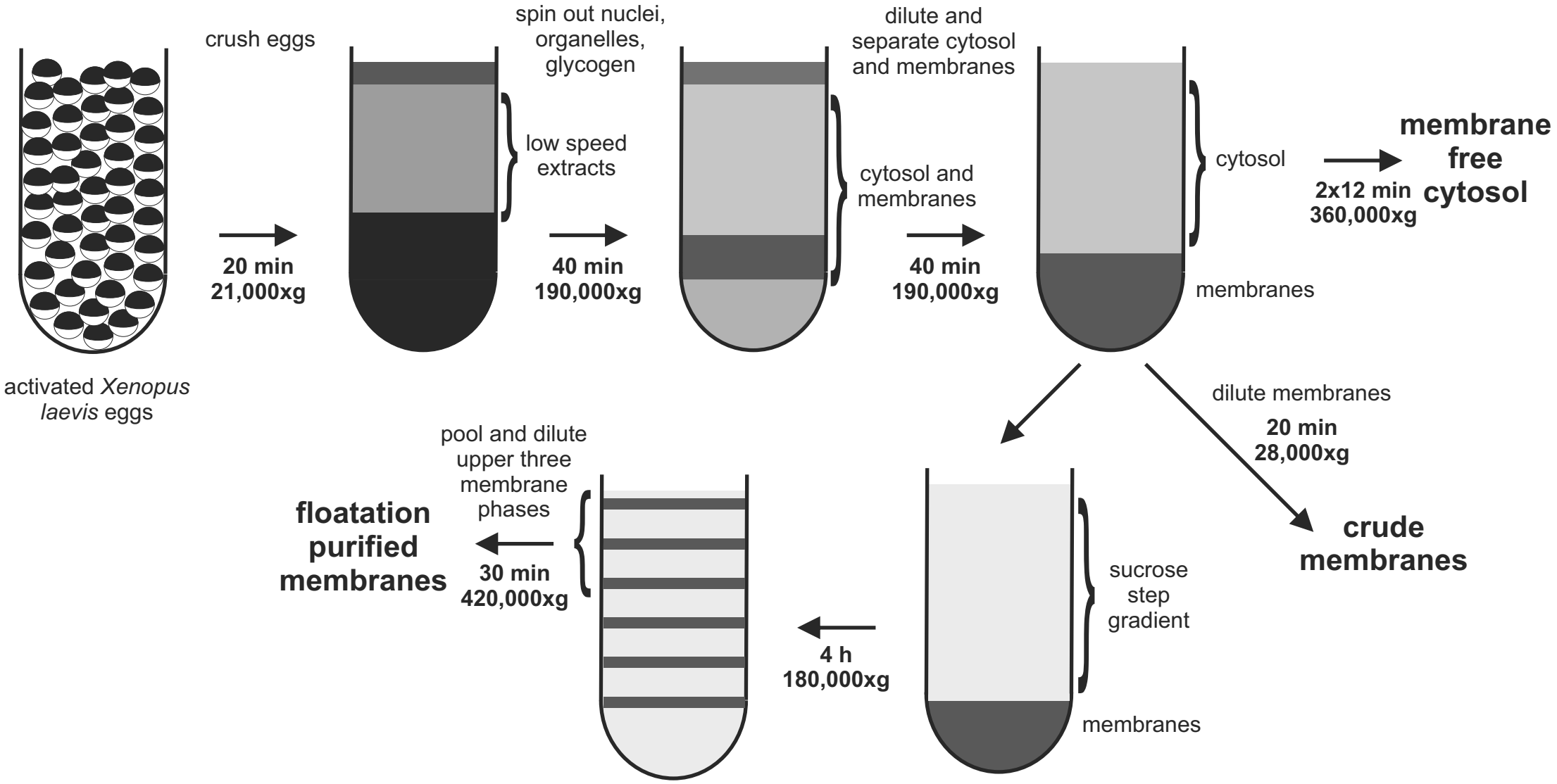
activated *Xenopus laevis* eggs
crush eggs
20 min
21,000xg
low speed extracts
spin out nuclei, organelles, glycogen
40 min
190,000xg
cytosol and membranes
dilute and separate cytosol and membranes
40 min
190,000xg
cytosol
membranes
2x12 min
360,000xg
membrane free cytosol
dilute membranes
20 min
28,000xg
crude membranes
sucrose step gradient
membranes
4 h
180,000xg
pool and dilute upper three membrane phases
30 min
420,000xg
floatation purified membranes

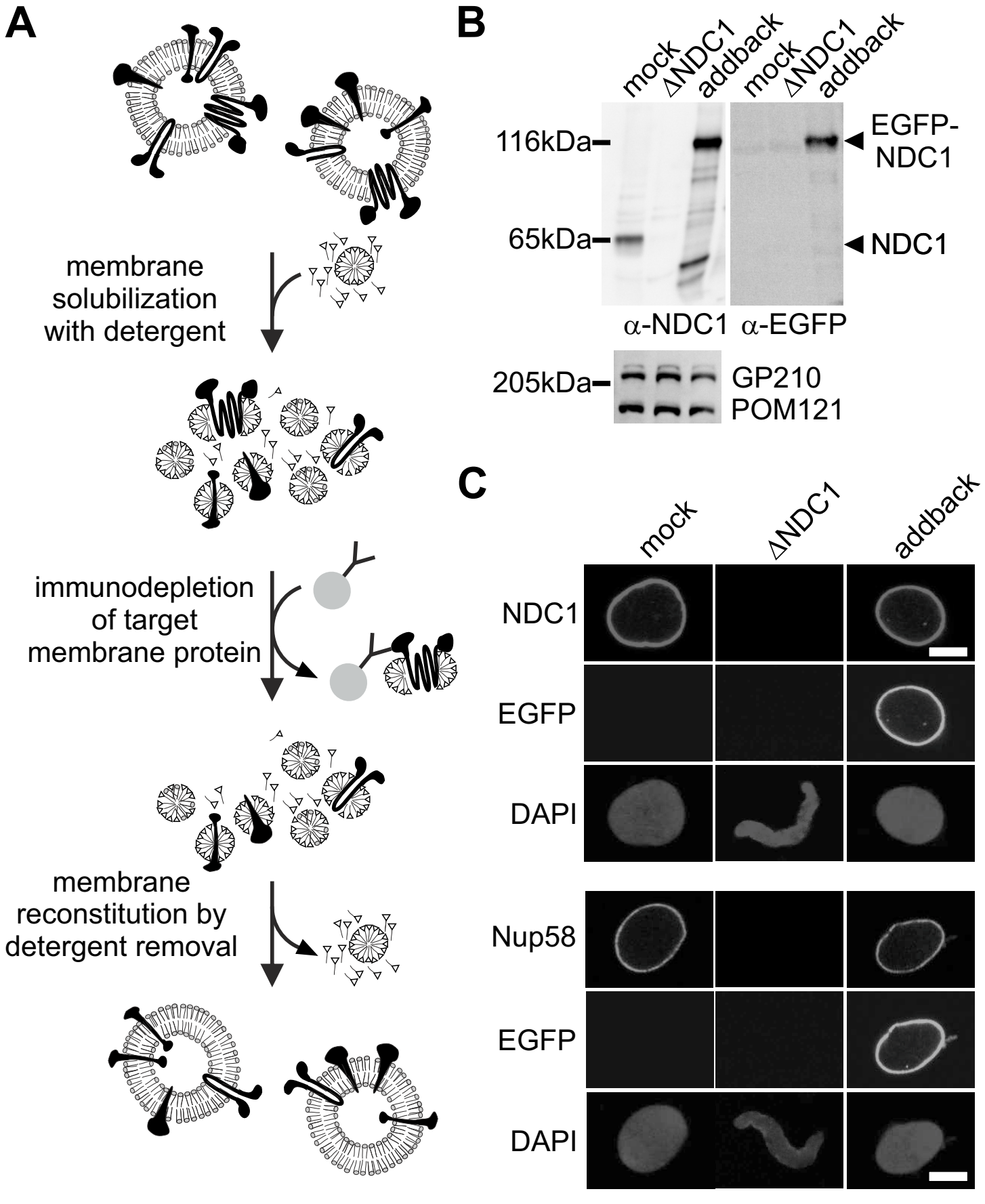
A
membrane solubilization with detergent
immunodepletion of target membrane protein
membrane reconstitution by detergent removal
B
mock
ΔNDC1
addback
mock
ΔNDC1
addback
116kDa
65kDa
EGFP-NDC1
NDC1
α-NDC1
α-EGFP
205kDa
GP210
POM121
C
mock
ΔNDC1
addback
NDC1
EGFP
DAPI
Nup58
EGFP
DAPI

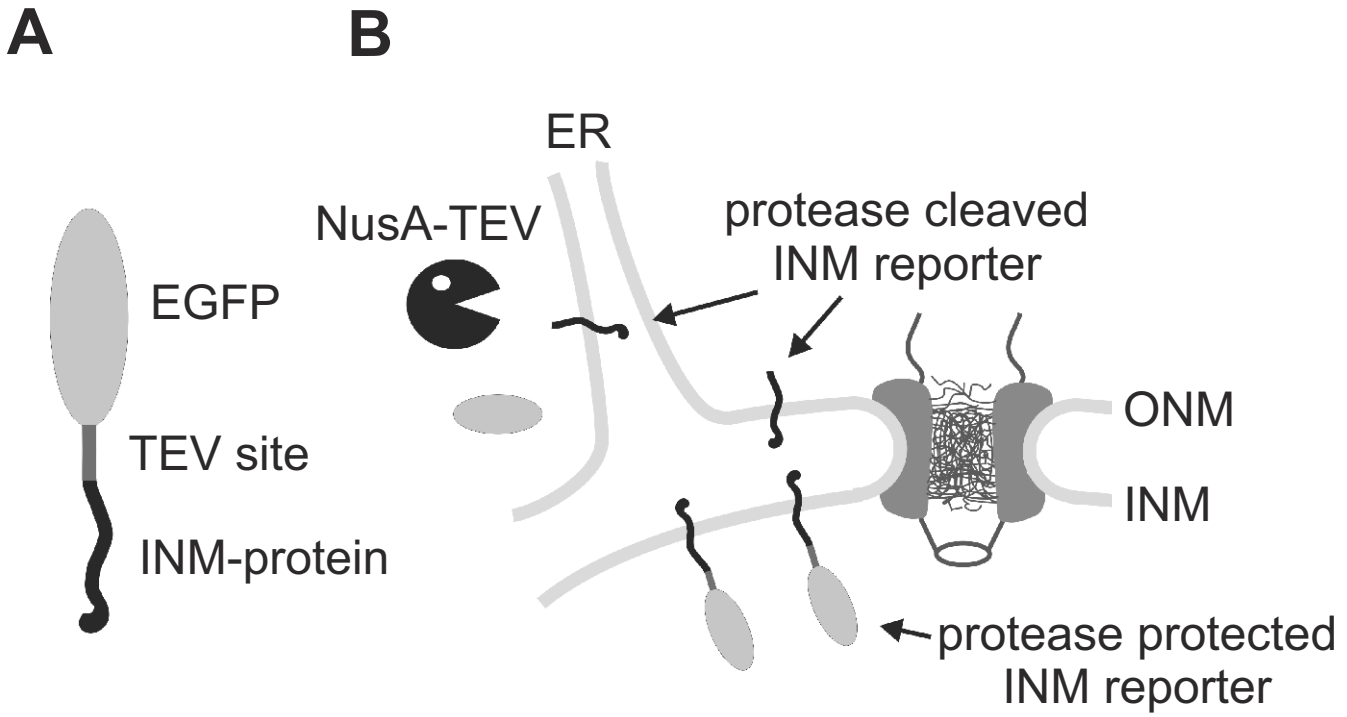
A
B
EGFP
TEV site
INM-protein
ER
NusA-TEV
protease cleaved
INM reporter
ONM
INM
protease protected
INM reporter

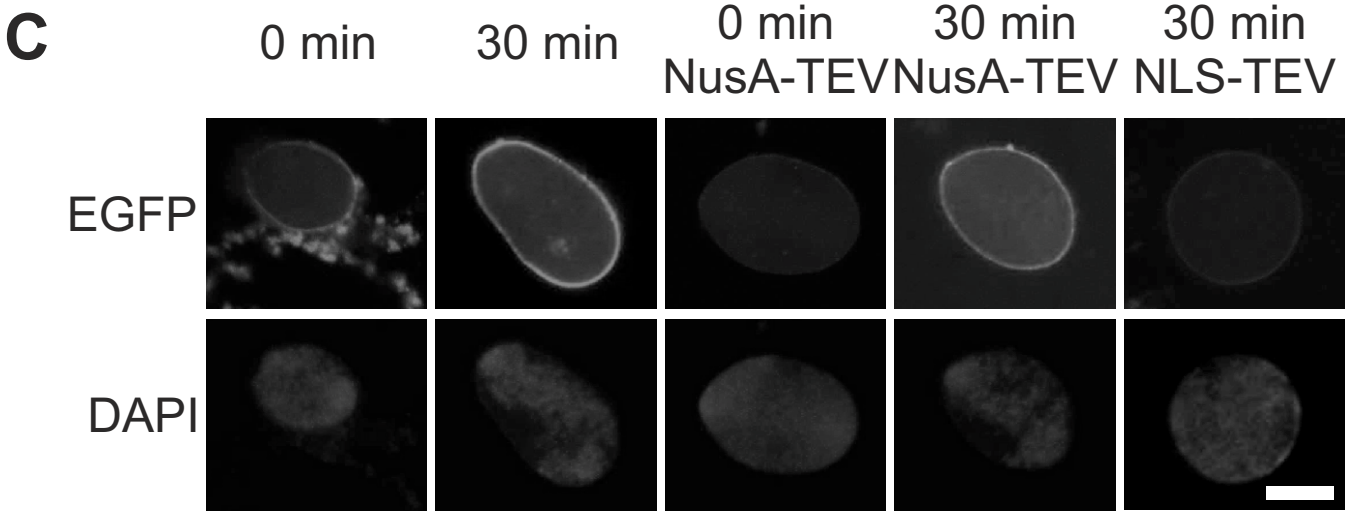
C
0 min
30 min
0 min
NusA-TEV
30 min
NusA-TEV
30 min
NLS-TEV
EGFP
DAPI

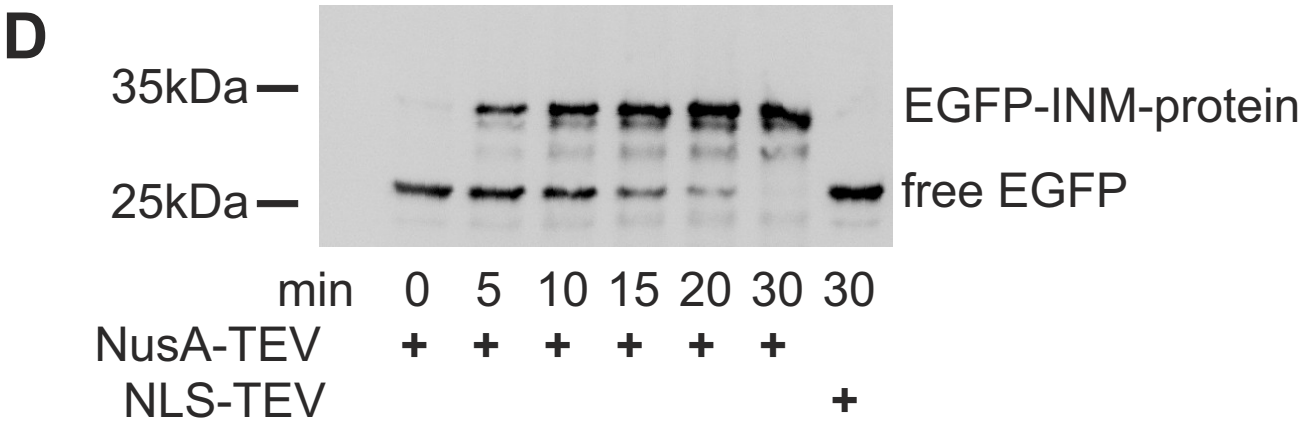
D
35kDa
25kDa
EGFP-INM-protein
free EGFP
min 0 5 10 15 20 30 30
NusA-TEV + + + + + +
NLS-TEV +

Published June 21, 2010

The nucleoporin Nup188 controls passage of membrane proteins across the nuclear pore complex

Gandhi Theerthagiri,[1] Nathalie Eisenhardt,[1] Heinz Schwarz,[2] and Wolfram Antonin[1]

[1]Friedrich Miescher Laboratory of the Max Planck Society and [2]Max Planck Institute for Developmental Biology, Max Planck Campus Tübingen, 72076 Tübingen, Germany

All transport across the nuclear envelope (NE) is mediated by nuclear pore complexes (NPCs). Despite their enormous size, ~60 MD in vertebrates, they are comprised of only ~30 distinct proteins (nucleoporins or Nups), many of which form subcomplexes that act as building blocks for NPC assembly. One of these evolutionarily conserved subcomplexes, the Nup93 complex, is a major structural component linking the NPC to the membranes of the NE. Using in vitro nuclear assembly assays, we show that two components of the Nup93 complex, Nup188 and Nup205, are dispensable for NPC formation. However, nuclei lacking Nup188 increase in size by several fold compared with wild type. We demonstrate that this phenotype is caused by an accelerated translocation of integral membrane proteins through NPCs, suggesting that Nup188 confines the passage of membrane proteins and is thus crucial for the homeostasis of the different nuclear membranes.

Introduction

The defining attribute of eukaryotes is the compartmentalization of genetic material inside the cell's nucleus. The physical boundary of the nuclear envelope (NE) has allowed eukaryotic cells to separate transcription and translation both spatially and temporally to achieve a level of regulatory complexity unprecedented in prokaryotes. Two lipid bilayers form the NE, the outer nuclear membrane (ONM) and the inner nuclear membrane (INM; for review see Hetzer et al., 2005). The ONM is continuous with the ER and is thought to have a rather similar protein composition (Mattaj, 2004; Lusk et al., 2007). The INM is characterized by a set of integral membrane proteins, although little is currently known as to how this specific protein composition is established and maintained (Mattaj, 2004; Zuleger et al., 2008).

Nuclear pore complexes (NPCs) are incorporated into the NE at sites where the INM and the ONM are fused. They function as gatekeepers of the nucleus, performing the essential cellular role of mediating an enormous exchange of proteins, nucleic acids, and other factors between the nucleoplasm and the cytoplasm. Transport of soluble factors has attracted much interest in previous decades: ions and small metabolites can diffuse through the NPCs; however, molecules >2.5 nm in radius (Mohr et al., 2009) are actively translocated by a large family of transport receptors (for reviews see Weis, 2003; Cook et al., 2007).

In addition to soluble cargoes, membrane-anchored proteins must also reach the nuclear interior. In the interphasic cell, passage through the NPC via the facing pore membrane is the most likely mechanism by which this could occur (Ohba et al., 2004). Transmembrane proteins of the NE are thought to be synthesized in the ER. They might reach the ONM and the cytoplasmic portion of the NPC by diffusion, although the existence of a directed transport mechanism cannot currently be ruled out. As INM proteins pass along the pore membrane, both transmembrane segments and hydrophilic domains encounter elements of the NPC. A recent study in mammalian cells has demonstrated that transport of integral membrane proteins to the INM is energy dependent (Ohba et al., 2004), and in budding yeast, INM targeting has been found to require transport receptors (King et al., 2006).

NPCs are huge assemblies of ~45 MD in budding yeast and 60 MD in vertebrates (for review see Brohawn et al., 2008). They are formed by about 30 different nuclear pore proteins

Correspondence to Wolfram Antonin: wolfram.antonin@tuebingen.mpg.de

Abbreviations used in this paper: INM, inner nuclear membrane; LBR, lamin B receptor; MISTIC, membrane-integrating sequence for translation of integral membrane protein constructs; NE, nuclear envelope; NPC, nuclear pore complex; ONM, outer nuclear membrane; TEV, tobacco etch virus.

© 2010 Theerthagiri et al. This article is distributed under the terms of an Attribution–Noncommercial–Share Alike–No Mirror Sites license for the first six months after the publication date (see http://www.rupress.org/terms). After six months it is available under a Creative Commons License (Attribution–Noncommercial–Share Alike 3.0 Unported license, as described at http://creativecommons.org/licenses/by-nc-sa/3.0/).

Supplemental Material can be found at:
http://jcb.rupress.org/content/suppl/2010/06/16/jcb.200912045.DC1.html

The Rockefeller University Press $30.00
J. Cell Biol. Vol. 189 No. 7 1129–1142
www.jcb.org/cgi/doi/10.1083/jcb.200912045

THE JOURNAL OF CELL BIOLOGY

Downloaded from jcb.rupress.org on December 5, 2013

Published June 21, 2010

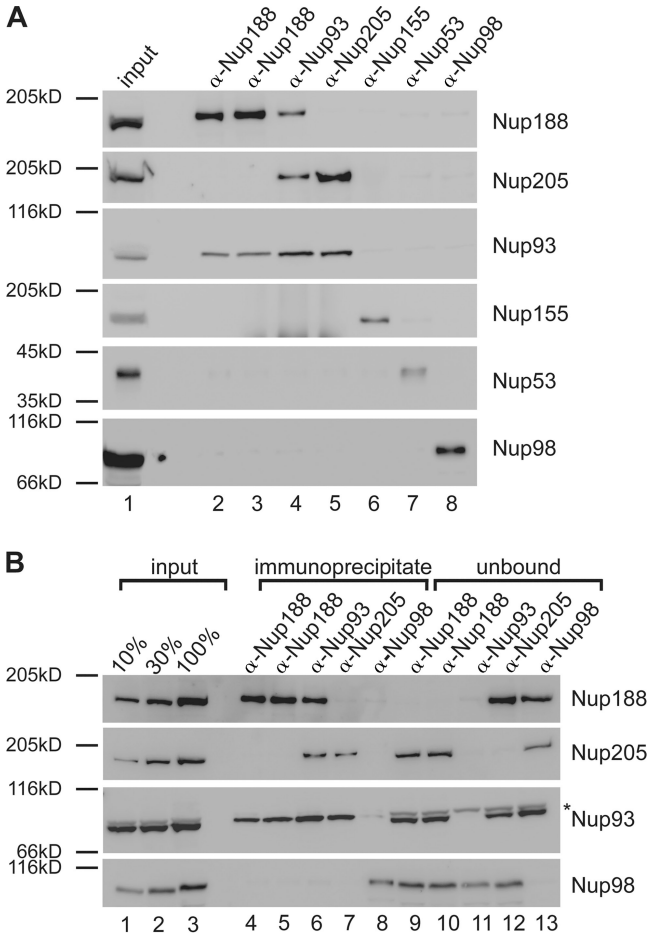

Figure 1. **Nup93 forms two distinct complexes.** (A) Immunoprecipitations were performed from *Xenopus* egg cytosol with antibodies against Nup188 (two antibodies raised in different rabbits), Nup93, Nup205, Nup155, and Nup53 and, as a control, Nup98. The indicated proteins were identified by Western blotting with the respective antisera. 10% of starting material (input) was loaded on the left. (B) Quantitative immunoprecipitations were performed from limited amounts of *Xenopus* egg cytosol with antibodies against Nup188, Nup93, and Nup205 and, as a control, Nup98. Immunoprecipitates and unbound material as well as 10, 30, and 100% of the starting material (input) were analyzed by Western blotting. The Nup93 antibody also recognized a cross-reactivity (asterisk) in the starting and unbound material migrating slightly slower.

referred to as nucleoporins or Nups. Although most, if not all, nucleoporins have now been identified, it is not understood how the individual nucleoporins interact to form this large complex (Antonin et al., 2008; D'Angelo and Hetzer, 2008).

The majority of nucleoporins are organized in discrete subcomplexes each present in multiple copies in the NPC. The best characterized of these is the heptameric Nup84 complex in yeast and the vertebrate counterpart, the nonameric Nup107–Nup160 complex, which is essential for NPC assembly and one of the major structural components of the pore (Fabre and Hurt, 1997; Boehmer et al., 2003; Galy et al., 2003; Harel et al., 2003; Walther et al., 2003). The second major structural unit of the NPC is the Nup93 subcomplex in vertebrates or the Nic96 complex in yeast. In vertebrates, it is comprised of five nucleoporins: Nup205, Nup188, Nup155, Nup93, and Nup53. Both Nup155 and Nup53 have been found to be essential for NE and NPC assembly (Franz et al., 2005; Hawryluk-Gara et al., 2008), and loss of the two budding yeast Nup155 homologues Nup170p and Nup157p blocks NPC assembly (Makio et al., 2009). Interestingly, Nup170p and Nup157p bind to Nup53p and Nup59p, which in turn associate, like the corresponding Nup53 in vertebrates, with the transmembrane nucleoporin Ndc1p (Mansfeld et al., 2006; Onischenko et al., 2007), potentially anchoring the NPC in the membrane of the NE. In vertebrates, the three remaining nucleoporins Nup205, Nup188, and Nup93 are thought to exist in a complex (Meier et al., 1995). Immunodepletion of Nup93 from *Xenopus laevis* extracts followed by in vitro nuclear assembly reactions resulted in nuclei with reduced NPC staining, which suggests that NPC formation is impaired in the absence of Nup93 (Zabel et al., 1996). Similarly, the budding yeast Nup93 homologue Nic96p is required for NPC formation and interacts with both Nup188p and Nup192 (Nehrbass et al., 1996; Zabel et al., 1996; Gomez-Ospina et al., 2000), which in metazoans correspond to Nup188 and Nup205, respectively.

In this study, we characterize vertebrate Nup188 and Nup205. We show that both interact with Nup93 but not with each other and form two distinct complexes that can be functionally distinguished. Depletion of the Nup188–Nup93 complex from *Xenopus* egg extracts produces in vitro assembled nuclei that increase several fold in size compared with control nuclei and that contain NPCs, which allow an elevated flow of INM proteins across the pore membrane. This suggests that Nup188–Nup93 can restrict the passage of membrane proteins from the ONM to the INM and is thus an important factor in the establishment of these two membrane subcompartments of the NE.

Results

Nup93 is part of two different complexes

To understand the protein interaction network of the Nup93 complex, we performed immunoprecipitations using antibodies against each of the five members of the complex from the cytosol of *Xenopus* egg extracts (Fig. 1 A). Antibodies against Nup53 and Nup155 precipitated the respective antigens but not major proportions of other members of the Nup93 complex (Fig. 1 A, lane 6 and 7), as observed previously (Franz et al., 2005; Hawryluk-Gara et al., 2008). Unexpectedly, the three remaining members of the complex did not form a trimeric complex: antibodies against Nup188 from two different rabbits coprecipitated Nup93 but not Nup205 (Fig. 1 A, lane 2 and 3), and antibodies against Nup205 precipitated Nup93 but not Nup188 (Fig. 1 A, lane 5). Consistent with this, antibodies against Nup93 coprecipitated both Nup188 and Nup205 (Fig. 1 A, lane 4). As a negative control, no interactions were seen between Nup98 and Nup205, Nup188, Nup155, Nup93 or Nup53.

To exclude the possibility that the lack of interaction is caused by precipitating only a subpopulation of Nup188 or Nup205, we performed the experiment in a quantitative manner (Fig. 1 B). Even when all Nup188 was immunoprecipitated and therefore removed from the unbound (Fig. 1 B, lane 9 and 10), Nup205 was not detected in the precipitate (Fig. 1 B, lane 4 and 5) and vice versa (Fig. 1 B, lane 7 and 12). Both Nup188 and Nup205 immunoprecipitated ~45% of Nup93 (Fig. S1).

Downloaded from jcb.rupress.org on December 5, 2013

Published June 21, 2010

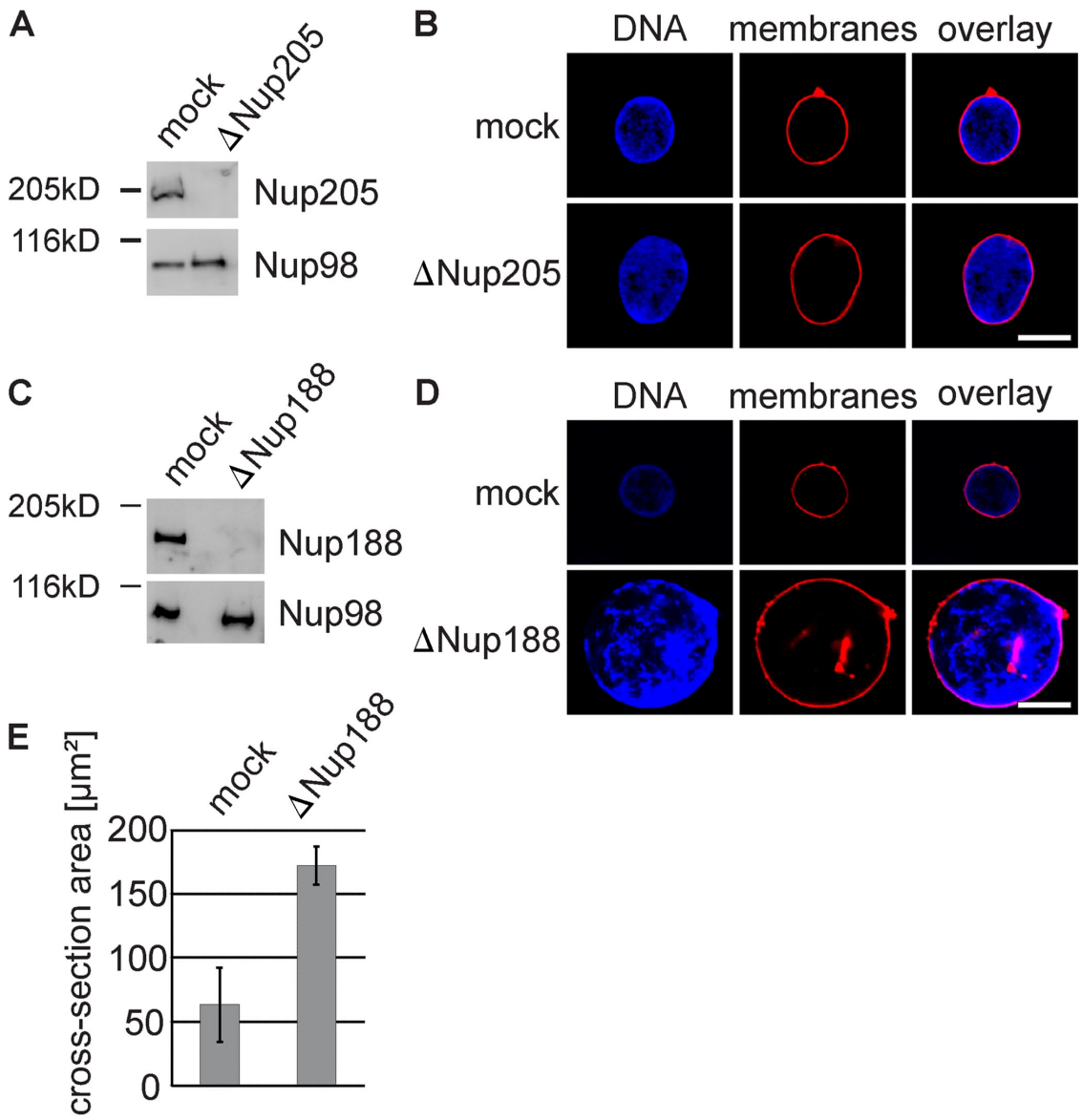

Figure 2. **Removal of Nup188–Nup93 enlarges nuclei.** (A and C) Western blot analysis of mock- and Nup205–Nup93 (A)- or Nup188–Nup93 (C)-depleted extracts. (B and D) Nuclei were assembled in mock- and Nup205–Nup93 (B)- or Nup188–Nup93 (D)-depleted extracts for 90 min, fixed with 4% PFA and 0.5% glutaraldehyde, and analyzed for chromatin and membrane staining (blue, DAPI; red, DiIC18). (E) Quantitation of the cross-sectional area of mock- and Nup188–Nup93-depleted nuclei of experiments performed as in D. More than 100 randomly chosen chromatin substrates were counted per reaction. The mean of three independent experiments is shown, and error bars represent the total variation. Bars, 20 μm.

These data indicate that Nup93 forms two distinct complexes in *Xenopus* egg extracts of approximate equal abundance, one with Nup188 and one with Nup205.

Nuclei lacking Nup188–Nup93 enlarge in size

To understand the functional significance of the two Nup93 complexes for NPC assembly and function, we depleted them separately from *Xenopus* egg extracts using antibodies specific for Nup205 or Nup188. Extracts were efficiently depleted of the respective Nup93 complexes, as determined by Western blotting (Fig. 2, A and C) and immunofluorescence (Fig. 3 A and Fig. S2 A). Nuclei formed in extracts depleted of the Nup205–Nup93 complex for 90 min were normal in appearance, as visualized by the membrane and chromatin stain (Fig. 2 B), and contained NPCs (Fig. S2 A), as determined by mAb414 staining, which recognizes FG repeat–containing nucleoporins, and with Nup93, Nup188, Nup53, and Nup155, the other members of the Nup93 complex (Fig. S2 B). In contrast, nuclei lacking Nup188–Nup93 were much larger than control nuclei (Fig. 2, D and E). These nuclei also contained NPCs (Fig. 3 A), as shown by mAb414 immunofluorescence. We found threefold more NPCs on Nup188–Nup93-depleted (18,480 ± 4,224 NPCs per nucleus) compared with control nuclei (6,137 ± 1,080; see Fig. 7 B). However, the NPC density per membrane area remained approximately constant (8.5 ± 1.2 NPCs/μm^2 in Nup188–Nup93 vs. 9.1 ± 1.2 NPCs/μm^2 in mock depletion). The NPCs contained Nup93 as well as Nup205, Nup53, and Nup155 (Fig. 3 B). Except for their increased size, Nup188–Nup93-depleted nuclei did not exhibit morphological alterations of the nuclear

Downloaded from jcb.rupress.org on December 5, 2013

Published June 21, 2010

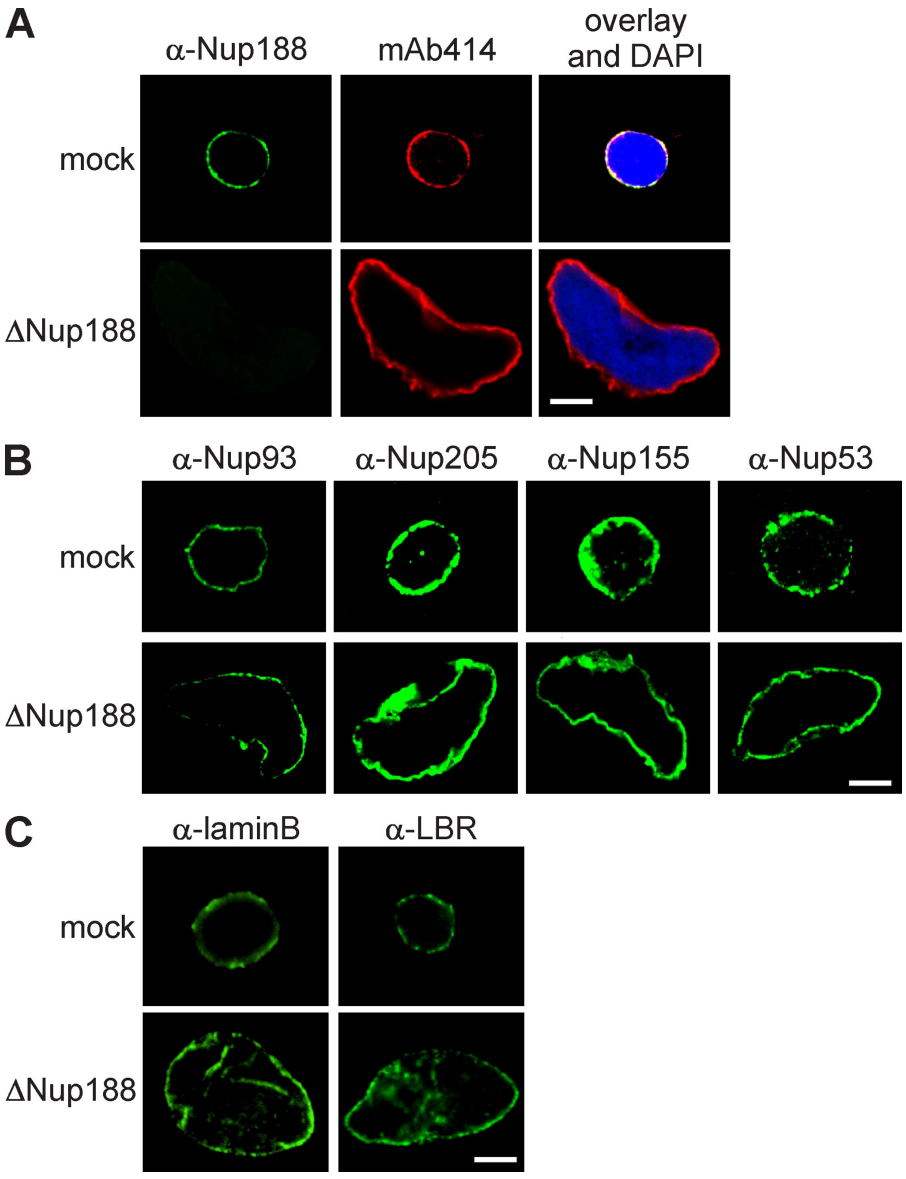

Figure 3. **Nup188–Nup93-depleted nuclei contain NPCs and INM proteins.** (A) Nuclei were assembled in mock- or Nup188–Nup93-depleted extracts for 90 min, fixed with 4% PFA, and analyzed with Nup188-specific antibodies (green) or the monoclonal antibody mAb414, which recognizes FG-repeat nucleoporins (red). Chromatin is stained with DAPI. (B and C) Samples were prepared as in A and analyzed by immunofluorescence with the indicated antibodies. Bars, 20 µm.

membranes or NPCs (Fig. S2 C), as determined by transmission electron microscopy. Also, marker proteins like B-type lamins and lamin B receptor (LBR) localized to the INM (Fig. 3 C). In a time course, chromatin substrates in mock- and Nup188–Nup93-depleted extracts were undistinguishable until a closed NE was formed at 50 min, after which Nup188–Nup93-depleted nuclei grew rapidly in size (Fig. S3). It should be noted that control nuclei also grow after having formed a closed NE as long as reentry into mitosis is blocked; however, they do this at a significantly slower rate.

Nup188–Nup93-depleted nuclei have normal nuclear functions

Given that Nup188–Nup93-depleted nuclei grow to an increased size after a closed NE is formed, we sought to determine which nuclear function is responsible for the observed phenotype. Upon nuclear assembly in *Xenopus* egg extracts, DNA can undergo one round of replication. Replication licensing ensures that replication happens exactly once during each round of the cell cycle (Blow and Sleeman, 1990). We wanted to know whether Nup188–Nup93 depletion impairs replication licensing, causing more than one round of DNA replication, which would in turn lead to increased DNA content in the nuclei. To test this idea, we assembled nuclei in mock- and Nup188–Nup93-depleted extracts in the presence of 16 µM of the DNA polymerase inhibitor aphidicolin. These conditions blocked DNA replication, as confirmed by the failure of DNA to incorporate fluorescently labeled nucleotides (Fig. 4 A). When DNA replication was blocked, the size of Nup188–Nup93-depleted nuclei still enlarged, indicating that the volume increase is not caused by a higher DNA content.

NPCs constitute a diffusion barrier between the cytoplasm and the nucleoplasm for substances >30 kD (Mohr et al., 2009), which can be translocated only by signal-mediated transport. We were wondering whether depletion of Nup188–Nup93 would impair this diffusion barrier, causing an uncontrolled accumulation of material in the nucleus and in turn lead to the observed size increase. Indeed, the yeast homologue Nup188p

Downloaded from jcb.rupress.org on December 5, 2013

Published June 21, 2010

was shown to be important for the diffusion barrier (Shulga et al., 2000). To test the integrity of the diffusion barrier of the NPC, we added fluorescently labeled dextrans of different but defined sizes to in vitro assembled nuclei that were lacking either Nup205 or Nup188 (Fig. 4 B). Both, Nup205–Nup93- and Nup188–Nup93-depleted nuclei were still able to exclude 70-kD dextrans, indicating that the diffusion barrier in these nuclei was intact. Smaller sized 10-kD dextrans could diffuse through the NPC as expected. As a control for an impaired diffusion barrier, nuclei depleted for Nup98 did not exclude the 70-kD dextran. These data indicate that a malfunction of the diffusion barrier of the NPC is unlikely to cause the enlargement of Nup188–Nup93-depleted nuclei.

NPCs mediate signal-dependent import and export across the NE. To check whether these functions are affected by Nup188–Nup93 depletion, we first tested nuclear accumulation of substrates containing an importin α/β– or transportin-based import signal, respectively. Both substrates were fused to an N-terminal EGFP linked to a tobacco etch virus (TEV) protease recognition site. They were added to a nuclear assembly reaction at 50 min, when an NE had formed and Nup188–Nup93- and mock-depleted nuclei were of similar size with approximately the same NPC content (2,737 ± 1,160 NPCs per nucleus in mock-depleted nuclei vs. 2,739 ± 1,437 in Nup188–Nup93-depleted nuclei; see Fig. 7 B). At the indicated time points, a TEV protease fused to a bacterial protein (NusA) was added. NusA increased the size of the protease fusion protein to 90 kD, which prevented its diffusion through the NPC. Nuclear import of the substrates rendered them protease protected and they could thus be quantified by Western blotting. Import kinetics were unchanged upon Nup188–Nup93 depletion for both substrates (Fig. 4 C).

To check for nuclear export, we used an EGFP-fused shuttling substrate with a nuclear import and export signal. The substrate did not accumulate in the nucleus both in mock- and Nup188–Nup93-depleted nuclei, indicating that nuclear export was not impaired (Fig. 4 D). To verify the function of the shuttling substrate, we added leptomycin B, which blocks crm1-mediated nuclear export (Fornerod et al., 1997). As expected, under these conditions, the shuttling substrate accumulated in the nucleus. Interestingly, leptomycin B–treated control nuclei did not increase in size, showing that a block in nuclear export does not phenocopy Nup188–Nup93 depletion. These data show that nuclei lacking Nup188–Nup93 have unchanged nuclear transport capabilities for the tested proteins. Together with the fact that the Nup188–Nup93-depleted nuclei replicate their DNA and grow, both processes requiring nuclear import, it is unlikely that an impairment of nuclear transport of soluble cargoes causes the observed nuclear growth phenotype upon Nup188–Nup93 depletion.

Xenopus egg extracts are largely transcriptionally inactive. Thus, an accumulation of mRNA in the nucleus is unlikely to cause nuclear enlargement. Coherent with this, addition of the transcriptional inhibitors 5,6-dichloro-1-β-D-ribobenzimidazole or actinomycin D did not block nuclear growth of Nup188–Nup93-depleted nuclei (unpublished data).

Nup188–Nup93 restricts transport of membrane proteins through the NPC

Having established that both diffusion and active transport of soluble substrates is unlikely to account for the increase in nuclear size upon Nup188–Nup93 depletion, we focused on the transport of membrane components. As described in the section Nuclei lacking Nup188–Nup93 enlarge in size, nuclei assembled in *Xenopus* egg extracts did enlarge upon further incubation provided that reentry into mitosis was prevented. However, this nuclear growth was much slower in untreated or mock-depleted extracts compared with the Nup188–Nup93-depleted nuclei (Fig. S3 and not depicted). We reasoned that as nuclear growth requires expansion of the NE, it must also involve an acquisition of nuclear membrane components. As the ER is continuous with the ONM, it is easy to envision how membrane components (both lipids and proteins) can be delivered to the ONM. The INM and ONM are connected by the membrane facing the NPC, the pore membrane. Thus, if the INM expands, membrane components need to pass through the NPC via the pore membrane. We speculated that pore membrane passage could limit and restrict nuclear growth and that this restriction might be attenuated upon Nup188–Nup93 depletion. To investigate this, we developed an assay to follow the transport of integral membrane proteins to the INM. BC08, an INM protein with a single C-terminal transmembrane region (Ulbert et al., 2006), was fused to an N-terminal EGFP followed by a recognition site for the TEV protease. The fusion protein was expressed and purified in *Escherichia coli* and reconstituted into liposomes. Liposomes were then added to a nuclear assembly reaction at time points when the NE had already formed around chromatin and under conditions in which they readily fused with the ER (Fig. 5, A and B). The reporter was distributed immediately throughout the membranes of the ER, including the NE, as observed by immunofluorescence (Fig. 5 B). After 30 min, the reporter was enriched at the NE. To distinguish between INM and ONM (including bulk ER) localization, we added the TEV protease fused to NusA, which prevents its diffusion through the NPC. Initially, the reporter was protease sensitive, indicating that it was localized to the ER and the ONM. However, after 30 min, the reporter was protease protected, which is indicative of INM localization. At the same time point, a TEV protease coupled to an NLS-bearing peptide (which is therefore localized to the interior of the nucleus) was able to cleave the reporter. This confirms that the reporter remains cleavable when it is accessible to the protease, and therefore, it is localization to INM that renders it protease protected in this assay. Cleavage of the reporter and its protease protection can be also followed by Western blotting over time, which indicates that about half of the reporter was protease protected after 10 min (Fig. 5 C).

Having established a functional assay for INM translocation, we asked whether the increased size of Nup188–Nup93-depleted nuclei is the result of accelerated membrane delivery to the INM. Nuclei were assembled in Nup188–Nup93- or mock-depleted extracts for 50 min, at which point the NE was closed but the nuclei had not increased in size (Fig. S3, 50-min time points). Liposomes containing the reporter were then added,

Downloaded from jcb.rupress.org on December 5, 2013

Published June 21, 2010

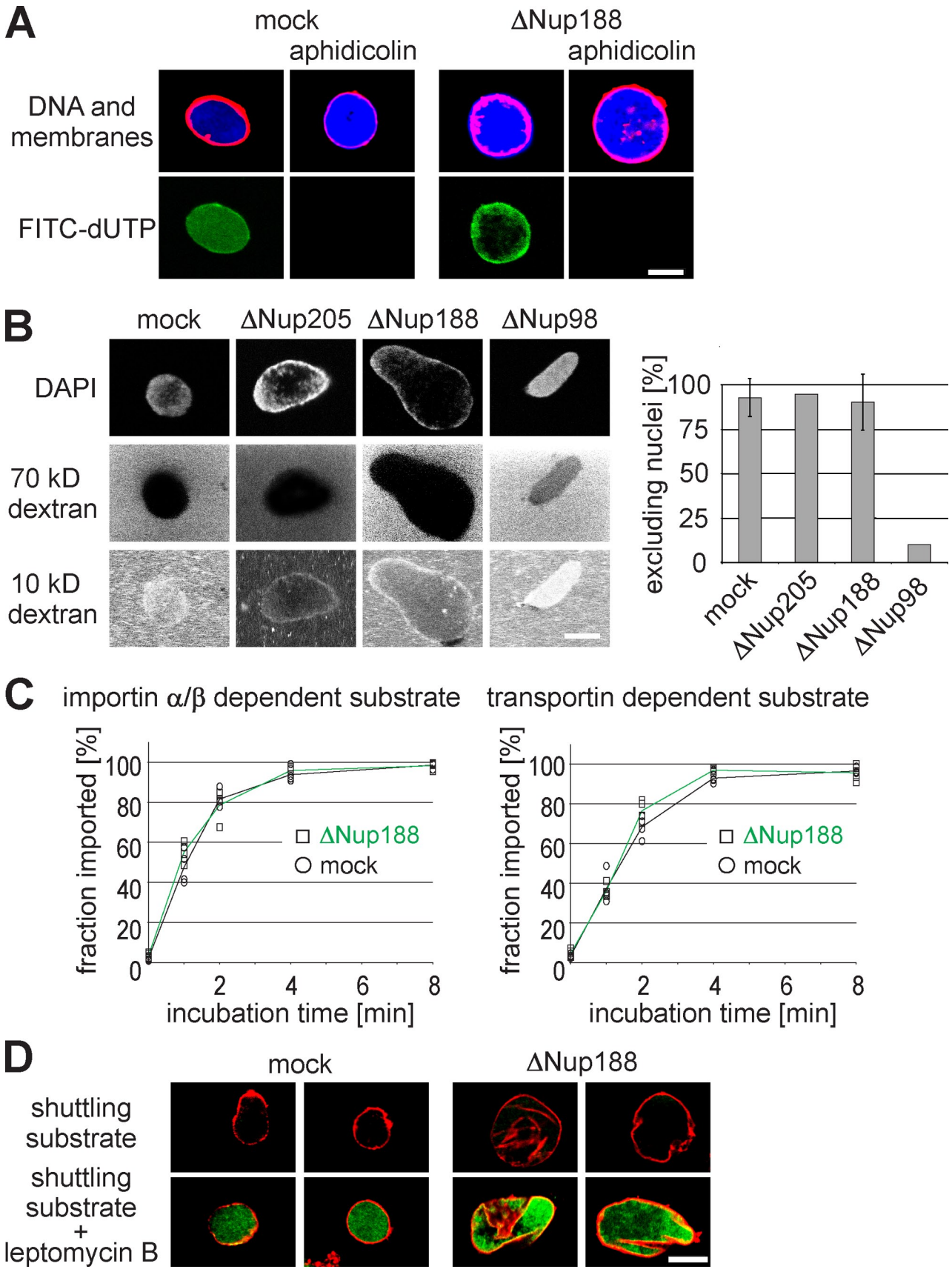

Figure 4. **Nuclear functions are unaffected by Nup188–Nup93 depletion.** (A) Nuclei were assembled in mock- or Nup188–Nup93-depleted extracts. After 50 min, fluorescently labeled dUTP (green in overlay) and, where indicated, aphidicolin were added. After 90 min, replication was analyzed by confocal microscopy. Membranes were stained with DiIC18 (red), and chromatin was stained with DAPI (blue). (B) Nuclei were assembled in mock-,

Downloaded from jcb.rupress.org on December 5, 2013

Published June 21, 2010

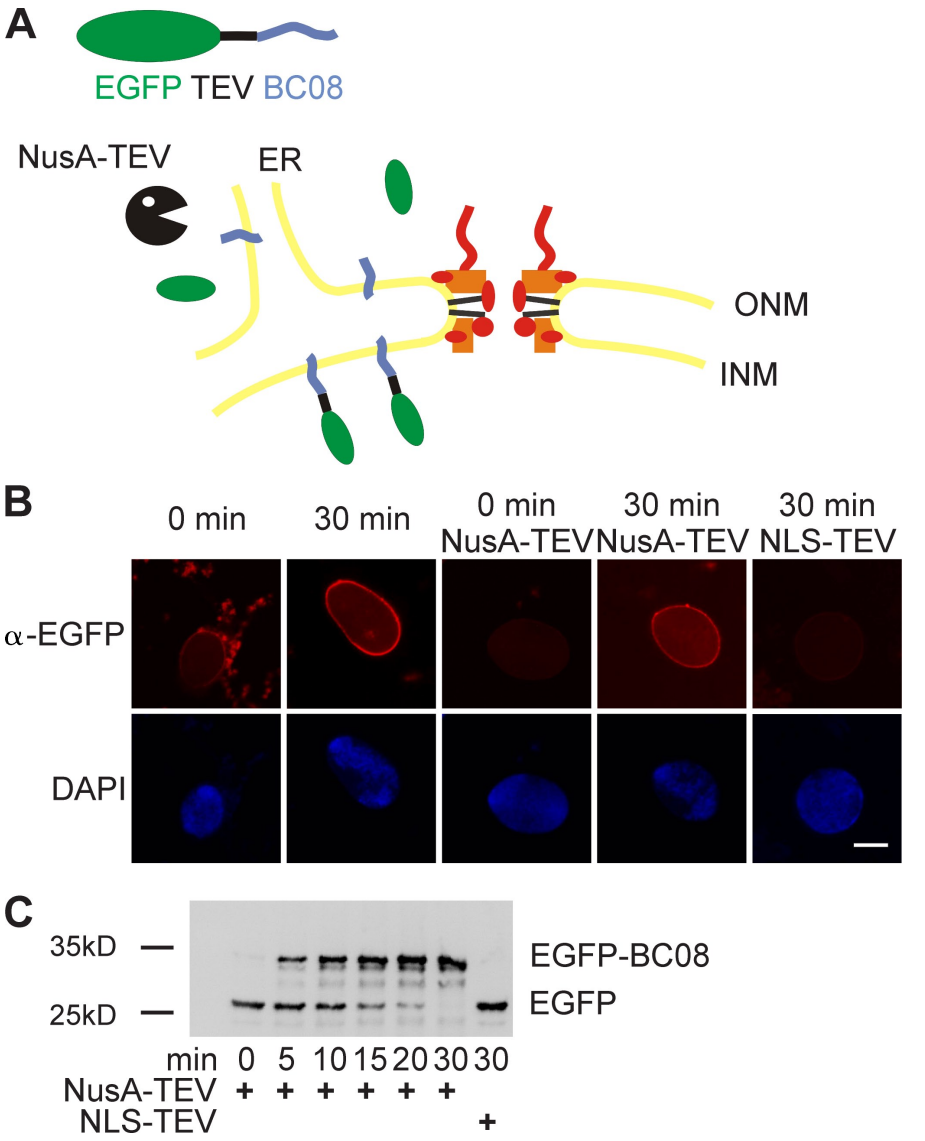

Figure 5. **An assay for the transport of membrane proteins to the INM.** (A) Schematic representation of the assay. The transmembrane-containing INM protein BC08 is fused to an EGFP domain followed by a recognition site for the TEV protease (top). The fusion protein is reconstituted into liposomes that rapidly fuse with the ER and ONM in the nuclear assembly reaction. INM localization of the reporter can be distinguished from ONM and ER localization by the reporter's protection from TEV protease fused with a large NusA domain to prevent its diffusion through the NPC. (B) Nuclei were assembled in *Xenopus* egg extracts. After 50 min, i.e., when a closed NE had formed, proteoliposomes containing the reporter were added. At the indicated time points, buffer, NusA-fused TEV protease, or TEV protease linked to NLS peptides was added. Protease cleavage was stopped after 5 min by fixation, and samples were processed for immunofluorescence and analyzed by confocal microscopy. α-EGFP immunofluorescence is shown in red, and DAPI is shown in blue. (C) Reactions were performed as in B. Protease cleavage was stopped by the addition of SDS sample buffer and boiling. Protease protection of the reporter was analyzed by Western blotting with the position of the uncleaved (EGFP-BC08) and the cleaved reporter with only the EGFP visible indicated. Bar, 20 µm.

and protease protection followed over time. In Nup188–Nup93-depleted nuclei, ∼50% of the reporter was protease protected after 5 min, significantly earlier than in control-treated nuclei (Fig. 6, A and B). Similar results were obtained when a reporter containing the first transmembrane region of the LBR, sufficient for INM targeting (Soullam and Worman, 1995), was used (Fig. S4 A). To confirm that the effect of Nup188–Nup93 depletion was specific, an addback experiment was performed. *Xenopus* Nup93 and mouse Nup188 were cotranslated in vitro (Fig. S4 B) and added to mock- or Nup188–Nup93-depleted extracts. Nuclei assembled in these extracts grew to a similar size as mock-treated extracts (Fig. 6 C and Fig. S4 C) and, importantly, did not show accelerated delivery of the BC08 and LBR reporter to the INM (Fig. 6 B and Fig. S4 A). As the antibody against *Xenopus* Nup188 does not detect the mammalian orthologue by immunofluorescence, nuclei assembled in Nup188–Nup93-depleted extracts supplemented with the recombinant proteins were isolated, and incorporation of recombinant Nup188–Nup93 into the nuclei was confirmed by Western blotting (Fig. 6 D). Notably, addition of neither Nup188 nor Nup93 alone rescued the observed phenotypes, indicating that the complex of Nup188 and Nup93 is indeed required (unpublished data).

Nup205–Nup93-, Nup188–Nup93-, and Nup98-depleted extracts. After 90 min, fluorescently labeled 2-MD (not depicted), 70-kD (middle), and 10-kD (bottom) dextrans were added. DNA was stained with DAPI, and samples were analyzed by confocal microscopy. For quantitation, only nuclei with an intact NE (as judged by the exclusion of 2-MD dextrans; >95% of nuclei in each sample) were analyzed. For mock- and Nup188–Nup93-depleted samples, seven independent experiments were analyzed (error bars show the standard deviation), and for Nup205–Nup93- and Nup98-depleted samples, two independent experiments were analyzed. (C) Nuclei were assembled as in A. After 50 min, i.e., when a closed NE had formed, importin α/β– or transportin-dependent reporter substrates containing a TEV cleavage site were added. To assay the nuclear import kinetics of the reporter, NusA-fused TEV protease was added at the indicated time points. Protease cleavage was stopped after 1 min by the addition of SDS sample buffer and boiling. Lines mark the mean of four independent experiments. (D) Nuclei were assembled as in A, and an EGFP-fused shuttling substrate was added. Nuclear export function was inhibited by the addition of 300 nM leptomycin B. Nuclei were isolated and analyzed by confocal microscopy. Membranes are stained with DiIC18 (red). Bars, 20 µm.

Downloaded from jcb.rupress.org on December 5, 2013

Published June 21, 2010

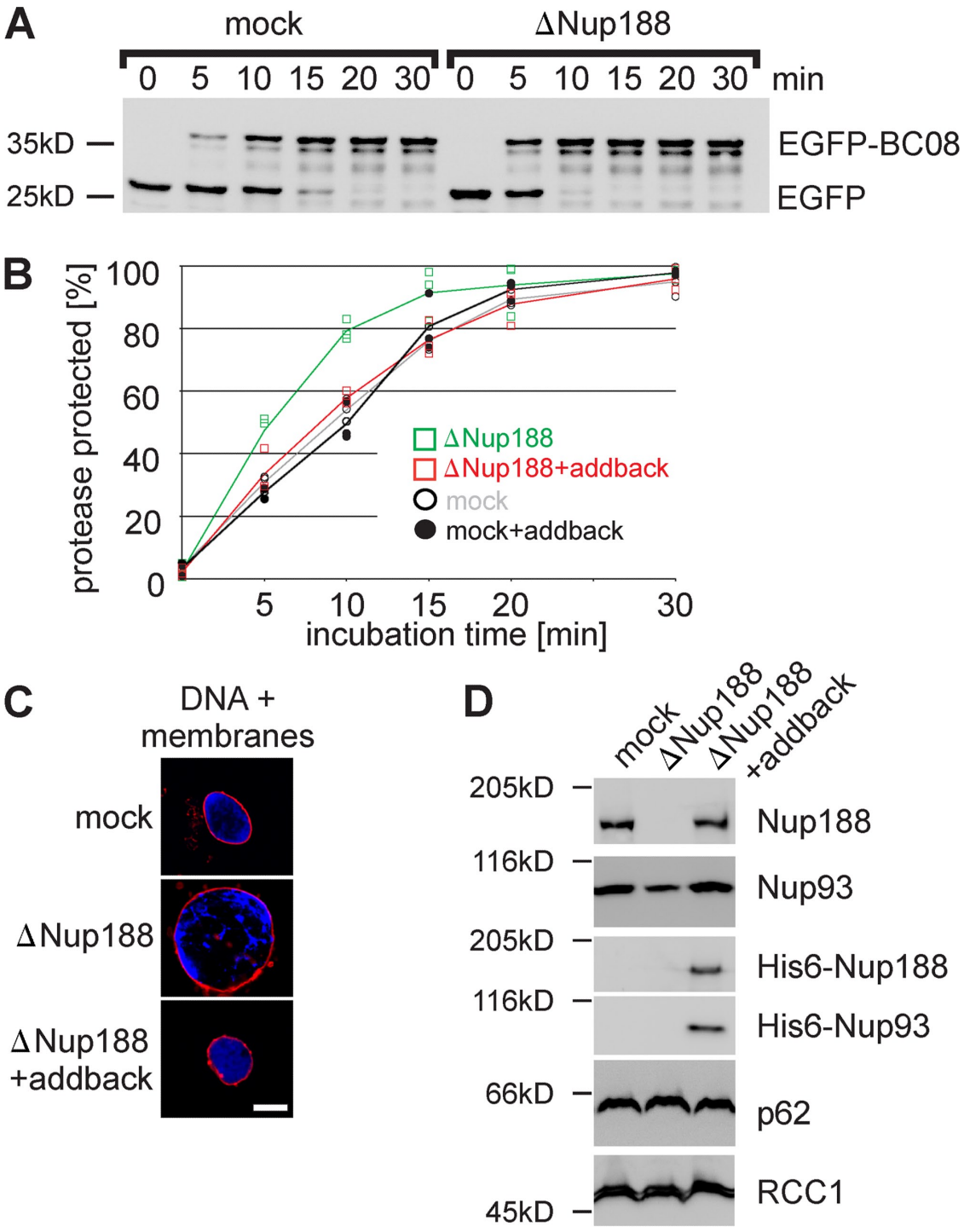

Figure 6. **Nup188–Nup93 depletion causes a faster delivery of integral membrane proteins to the INM.** (A) Nuclei were assembled in mock- or Nup188–Nup93-depleted *Xenopus* egg extracts and analyzed by Western blotting. Positions of the uncleaved (EGFP-BC08) and the cleaved (EGFP) reporter are indicated. (B) Quantification from three independent experiments performed as in A. Squares are from Nup188–Nup93-depleted samples (green without and red with the addition of in vitro translated Nup188–Nup93 [addback]), and circles are from mock-treated samples. Lines mark the mean of three independent experiments. (C) The addition of recombinant Nup188–Nup93 rescues the Nup188–Nup93 depletion phenotype. Nuclei were assembled for 120 min in mock- or Nup188–Nup93-depleted extracts without or with the addition of in vitro translated Nup188–Nup93 (addback), fixed with 4% PFA and 0.5% glutaraldehyde, and analyzed for chromatin and membrane staining (blue, DAPI; red, DiIC18). (D) In vitro translated Nup188–Nup93 is incorporated into in vitro assembled nuclei. Nuclei were assembled for 1 h to ensure approximately equal NPC numbers per nucleus, isolated, and analyzed by Western blotting. In vitro translated Nup188 and Nup93 could be also detected using an anti-His6 antibody (third and fourth row). The nucleoporin p62 was detected with mAb414, and the chromatin-binding protein RCC1 serves as a control for equal loading of nuclei. Bar, 20 µm.

Downloaded from jcb.rupress.org on December 5, 2013

Published June 21, 2010

Collectively, these data indicate that both the increase in nuclear size and the accelerated targeting of integral membrane proteins to the INM are specific for Nup188–Nup93 depletion. Interestingly, nuclei depleted for Nup205–Nup93 showed the same rate of INM targeting of the two reporters as mock controls (Fig. S4 D), which is consistent with the fact that they do not show the nuclear growth phenotype.

As INM proteins reached the nuclear interior significantly faster in Nup188–Nup93-depleted nuclei compared with controls, we wondered whether the effect was specific to proteins destined for the INM or whether the segregation of the INM from the ONM and connected ER was lost in the absence of Nup188–Nup93. To test this idea, we replaced the INM reporter with bona fide ER membrane proteins: SPC18, a membrane-spanning subunit of the signal peptidase complex, or a C-terminal fragment (including the transmembrane region) of the ER-localized chaperone protein calnexin. Both reporters were sensitive to TEV protease cleavage even after 60 min, indicating that they were not localized to the INM (Fig. S5 A). Notably, the cytoplasmic domains for the SPC18 (31 kD)- and calnexin (41 kD)-based reporters fall within the size range of the nucleoplasmic regions of the BC08 and LBR reporters described in the preceding experiments. Therefore, Nup188–Nup93-depleted NPCs continue to act as a diffusion barrier preventing uncontrolled intermixing of INM and ONM (and ER) components.

The nucleoplasmic domains of most INM proteins are limited in size to ~40 kD. It has been shown that increasing this size to 47 kD prevents membrane protein targeting to the INM (Ohba et al., 2004). We tested whether depletion of Nup188–Nup93 would impair the stringency of this size limit. For this, the size of the BC08 reporter was increased to 94 kD and 64 kD by fusing an additional NusA or GST moiety, respectively (Fig. S5 B). In all cases, the reporter did not target to the INM, both in mock- and Nup188–Nup93-depleted nuclei.

Up to now, we have demonstrated that upon Nup188–Nup93 depletion, the passage of INM proteins through the pore is enhanced and that the transfer of membrane components could be rate limiting for nuclear growth. Two possible scenarios can be envisioned. Nup188–Nup93 could restrict the passage of transmembrane or membrane proteins through the pore. Depletion of Nup188–Nup93 might abrogate this restriction, causing an increased flow of membrane components through the pore, leading to an enlargement of the NE in which more NPCs can integrate (Fig. 7 A, top route). Alternatively, Nup188–Nup93 depletion could facilitate NPC formation, giving rise to more NPCs with an overall increased total transport capacity (Fig. 7 A, bottom route). In this scenario, the increase in NE area would be a secondary effect. To distinguish the two possibilities, we blocked de novo NPC assembly into intact NEs by an excess of importin β (D'Angelo et al., 2006), which inhibits the Nup107–Nup160 complex, an essential early component for NPC formation (Harel et al., 2003; Walther et al., 2003; Rasala et al., 2006; Franz et al., 2007). When 2 µM importin β was added to mock- and Nup188–Nup93-depleted extracts after 50 min, i.e., when a closed NE with intact NPCs was formed, the NPC number did not increase in the next 70 min (Fig. 7 B, green bars). Despite approximately the same number of NPCs at the time of importin β addition and a subsequent block in de novo NPC assembly, Nup188–Nup93-depleted nuclei grew within the next 70 min significantly faster than mock-depleted nuclei so that the NPC density at the end of the incubation time was more decreased in Nup188–Nup93-depleted compared with mock-depleted nuclei (2.8 NPCs/µm^2 NE membrane vs. 5.2 NPCs/µm^2; Fig. 7 B, red bars). These data indicate that the accelerated growth of the nuclei and the nuclear membrane expansion upon Nup188–Nup93 depletion cannot only be attributed to an increased NPC number. Importantly, in Nup188–Nup93-depleted nuclei treated with importin β, the EGFP-BC08 reporter was still protease protected significantly earlier than in mock-treated nuclei (Fig. 7 C). Therefore, we could rule out that an increased NPC number was the primary cause of the enhanced translocation of the reporter to the INM. Collectively, this demonstrates that Nup188–Nup93 depletion results in increased passage of proteins destined for the INM across the NPC. This suggests that Nup188–Nup93 is a crucial component within the NPC that restricts the flux of integral membrane proteins and likely other membrane components along the pore membrane.

Discussion

In this study, we have shown that the nucleoporin Nup93 is part of two distinct complexes. It interacts either with Nup205 or -188. Unexpectedly, nuclei depleted of Nup188–Nup93 grew to enormous sizes, a phenotype previously not observed upon depletion of a nucleoporin. Integral membrane proteins and probably other membrane components are delivered faster to the INM upon Nup188–Nup93 depletion. We suggest that this causes rapid expansion of the NE as a primary effect and in turn facilitates increased integration of NPCs. The higher NPC number would have a higher overall transport rate both for soluble cargoes and membrane components, which would then further augment the nuclear growth effect.

Transport of soluble cargo via the NPC has been intensely studied in previous decades (for reviews see Weis, 2003; Cook et al., 2007). However, transmembrane proteins must also access the INM, where several of them bind lamin and/or chromatin. Little is currently known about how transmembrane proteins are delivered to the INM of the interphasic nucleus (Zuleger et al., 2008). Although a scenario can be envisioned in which the ONM and INM periodically fuse to provide transient connections allowing diffusional exchange between these membrane domains, there is at present no evidence supporting this. Alternatively, membrane vesicle budding from the ONM into the perinuclear lumen and subsequent fusion with the INM could also explain how membrane proteins are delivered to the INM. However, aside from the observation that the reverse process occurs during herpesvirus egress from the nucleus (Mettenleiter et al., 2009), there is little proof for this model. A more likely scenario involves transmembrane protein transit from the ONM to the INM via the NPC along the plane of the pore membrane. Indeed, antibodies to the transmembrane nucleoporin gp210 as well as WGA, a lectin which cross-links several nucleoporins, are both able to block the movement of integral membrane

Downloaded from jcb.rupress.org on December 5, 2013

Published June 21, 2010

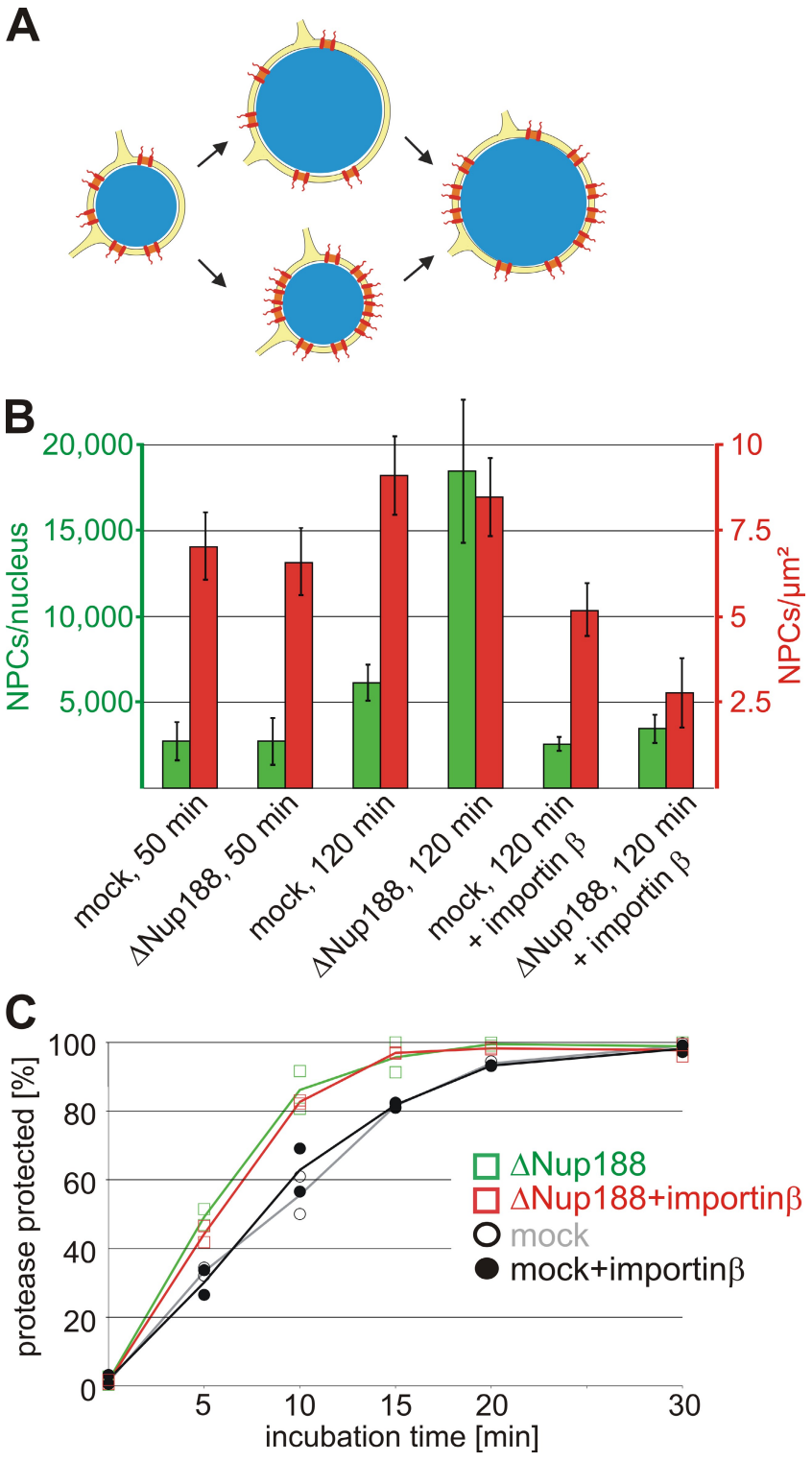

Figure 7. **The nuclear growth phenotype and the faster INM targeting are independent of the increased NPC number upon Nup188–Nup93 depletion.** (A) Two possible scenarios for the relationship of the nuclear membrane expansion and the increase in NPC numbers upon Nup188–Nup93 depletion. In the top route, Nup188–Nup93 depletion causes a faster growth of the NE, which in turn allows more NPCs (red) to be integrated. In the bottom route, NPC assembly increases on Nup188–Nup93-depleted nuclei. The resulting higher total transport capacity of these allows accelerated nuclear volume and envelope expansion. (B) Nuclei were assembled in mock- and Nup188–Nup93-depleted extracts for 50 min and 120 min. Where indicated, de novo NPC assembly was blocked by the addition of 2 µM importin β after 50 min, i.e., after a closed NE had formed, and nuclei were further incubated for 70 min. NPC numbers per nucleus (green bars) and NPC density (red bars) were quantified. (C) Nuclei were assembled in mock- and Nup188–Nup93-depleted extracts for 50 min. Then, where indicated, de novo NPC assembly was blocked by the addition of 2 µM importin β. INM targeting of the reporter was analyzed as in Fig. 6. Squares are from Nup188–Nup93-depleted samples, and circles from mock-treated samples. Lines mark the mean of two independent experiments.

proteins from the ONM to the INM, most likely by sterically occluding the passageways (Ohba et al., 2004). In yeast, deletion of Nup170, one of the Nup155 homologues, causes delocalization of two integral membrane proteins, Heh1p and Heh2p, from the INM (King et al., 2006). Together with the fact that delivery of Heh1p and Heh2p to the INM requires classical transport receptors (importin α and β), these data argue strongly in favor of NPC involvement in the movement of integral membrane proteins from the ONM to the INM. Indeed, when depleting the Nup107–Nup160 complex, which leads to the formation of nuclei without NPCs (Harel et al., 2003; Walther et al., 2003), no INM targeting of the reporter constructs was observed (Fig. S5 C).

In this study, we show that Nup188–Nup93 restricts the passage of integral membrane proteins from the ONM to the INM. Although proteins destined to the INM reach these sites faster in Nup188–Nup93-depleted nuclei, bona fide ER proteins

Downloaded from jcb.rupress.org on December 5, 2013

Published June 21, 2010

are not mislocalized to the INM. In yeast, depletion of Nup188p or the integral membrane nucleoporin Pom152p was found to reduce INM localization of the ubiquitin ligase Doa10p (Deng and Hochstrasser, 2006). Normally, the majority of cellular Doa10p resides in the ER, although it is also found at the INM, where it drives the degradation of intranuclear targets. During excessive nuclear membrane proliferation, Doa10p is enriched at the INM. Under these conditions, deletion of Nup188 causes the redistribution of Doa10p to the ER, probably via enhanced passage through the NPC.

Nucleoporins containing FG-repeat domains contribute to the transport properties of the NPC by establishing a permeability barrier and promoting transport receptor–mediated NPC passage. They are mainly localized to the interior center of the NPC (Rout et al., 2000; Alber et al., 2007). In contrast, Nup188p and Nup170p do not contain FG repeats and are found comparatively more proximal to the pore membrane. Interestingly, depletion of Nup188–Nup93 did not reduce mAb414 staining, which recognizes FG-containing nucleoporins (Fig. 3 A), and did not destroy the diffusion barrier of the NPC or affect nuclear import and export of soluble reporter cargoes (Fig. 4). This suggests that the transport of soluble and membrane proteins requires distinct features within the NPC and uses different pathways within the pore.

It has been proposed that NPCs accommodate not only a large central channel for active and transport receptor–mediated import and export but also eight peripheral channels that mediate passive exchange of metabolites and ions (Hinshaw and Milligan, 2003; Kramer et al., 2007; Naim et al., 2007). Although recent cryoelectron tomography of NPCs from *Dictyostelium discoideum* confirmed the existence of peripheral channels ∼9 nm in diameter (Beck et al., 2007), the idea of separate passageways for soluble factors is in contrast to the prevailing model in which FG-repeat domains form a common barrier for both facilitated and passive exchange (Ribbeck and Görlich, 2001; Rout and Aitchison, 2001). Passive diffusion is sensitive to many of the same ligands and inhibitors that target active transport across the NE. This argues strongly for a single permeability barrier for soluble molecules passing through the NPC either by active transport or passive diffusion (Mohr et al., 2009). Alternatively, the peripheral channels could be important for membrane proteins passing the NPC (Powell and Burke, 1990; Zuleger et al., 2008). Although the nucleoplasmic domains of most INM proteins are limited in size to ∼40 kD and therefore might be small enough to fit in the cavities of the channels, we propose that structural rearrangements within the NPC are necessary to allow for integral membrane passage without disrupting the diffusion barrier. Depletion of Nup188–Nup93 may enhance conformational flexibility within the NPC, resulting in the increased passage of membrane proteins through the NPC that we have observed in this study without affecting the size limit for these proteins.

The metazoan Nup93 complex and the corresponding Nic96 complex in yeast is one of the major building blocks of the NPC. However, compared with the well-characterized Nup107–Nup160 complex, which can be purified from *Xenopus* egg extracts (Vasu et al., 2001; Walther et al., 2003), the association of Nup93 complex components is remarkably less stable. Nup155 and Nup53 can be precipitated mainly as individual proteins, as observed previously (Franz et al., 2005; Hawryluk-Gara et al., 2008). Additionally, Nup205, Nup188, and Nup93 do not exist in a single complex in *Xenopus* egg extracts as previously suggested (Meier et al., 1995). Formerly, immunoprecipitations were performed using antibodies against Nup93, which, as we have shown, actually precipitates two different Nup93-containing complexes. However, the Nup188–Nup93 and the Nup205–Nup93 interactions seem to be rather stable. Interestingly, in the add-back experiment, we could only restore the phenotype if Nup188 and Nup93 were coexpressed and added despite the fact that after Nup188–Nup93 depletion, ∼50% of Nup93 remains in the extracts (most in a complex with Nup205 and a smaller proportion not bound to Nup205; Fig. 1 and Fig. S1), suggesting that Nup93 cannot exchange between the different complexes under the given conditions.

Whereas depletion of Nup155 and Nup53 from *Xenopus* egg extracts prevents NPC and NE formation (Franz et al., 2005; Hawryluk-Gara et al., 2008), extracts depleted of Nup205–Nup93 or Nup188–Nup93 assemble nuclei with seemingly intact NPCs and a closed NE. Currently, we cannot exclude the possibility that the Nup188–Nup93 and Nup205–Nup93 complexes have partially redundant functions during NPC formation. Double depletion of both complexes (with antibodies against Nup205 and Nup188) followed by nuclear assembly reactions was for technical reasons unfeasible, requiring, in total, four rounds of incubation of extracts with antibody beads. Interestingly, depletion of Nup93-containing complexes from *Xenopus* egg extracts with α-Nup93 antibodies blocked NPC assembly (Grandi et al., 1997; unpublished data). However, we cannot exclude the possibility that Nup93 is of functional importance outside of its role in the Nup188–Nup93 and Nup205–Nup93 complexes. Indeed, a subfraction of 5–10% of Nup93 has been shown to interact with the FG repeat–containing nucleoporin p62 (Zabel et al., 1996), as does the yeast homologue Nic96p with Nsp1p (Zabel et al., 1996). This could be a subpopulation distinct from the Nup188–Nup93 and Nup205–Nup93 complexes. Notably, we found that ∼5% of Nup93 cannot be depleted with a combination of antibodies against Nup205 and Nup188 (Fig. S1)

Depletion of neither Nup188–Nup93 nor Nup205–Nup93 impaired the exclusion limit of the NPCs for inert substances (Fig. 4 B). For Nup205–Nup93, this was particularly unexpected as depletion of *Caenorhabditis elegans* Nup205 by RNAi causes failure of nuclear exclusion of 70-kD dextrans (Galy et al., 2003). Interestingly, up to now, no *C. elegans* Nup188 orthologue has been identified. It is possible that the Nup205–Nup93 and Nup188–Nup93 complexes in *Xenopus* have partially redundant functions in establishing the exclusion limit of NPCs. Because of the absence of Nup188 in *C. elegans*, Nup205–Nup93 could still accommodate this function, which is lost upon Nup205 depletion.

In summary, our work establishes that members of the Nup93 complex, which is regarded as one of the structural building blocks of the NPC, can be depleted without blocking NPC formation. Intriguingly, Nup188–Nup93 is rather important for controlling the passage of transmembrane proteins and

Downloaded from jcb.rupress.org on December 5, 2013

Published June 21, 2010

probably other membrane components through the NPC. Thus, in addition to regulating the composition of the nucleoplasm by restricting access of soluble factors to the nuclear interior, NPCs are also important in the establishment of the two membrane subcompartments of the NE.

Materials and methods

Materials

An EST containing the C-terminal region of *Xenopus* Nup188 (GenBank/EMBL/DDBJ accession number BQ725804) was identified by BLAST search using the mouse sequence as bait. ESTs for *Xenopus* Nup98, Nup205, BC08, LBR, and mouse Nup188 were under GenBank/EMBL/DDBJ accession numbers CF286969, CA986989, BC082226, BC124994, BG861579, respectively. *Xenopus* Nup53, NPM2, calnexin, and SPC18 were amplified from a *Xenopus* cDNA.

Leptomycin B and aphidicolin were obtained from Enzo Life Sciences, Inc., and DiIC18 (1,1′-dioctadecyl-3,3,3′,3′-tetramethylindocarbocyanine perchlorate), fluorescently labeled dextrans, and secondary antibodies (Alexa Fluor 488 goat α-rabbit IgG and Cy3 goat α-mouse IgG) were obtained from Invitrogen. Detergents were purchased from EMD, and lipids were purchased from Avanti Polar Lipids, Inc.

Antibodies

For the generation of antibodies, a fragment of *Xenopus* Nup188 corresponding to aa 1573–1731 of the mouse sequence and a fragment of Nup98 (aa 1–185) were expressed as GST fusion proteins and purified using glutathione Sepharose (GE Healthcare). Fragments of *Xenopus* Nup53 (aa 78–310) and LBR (aa 47–216) were cloned into pET28a (EMD), expressed as a His6-tagged fusion, and purified using Ni–nitrilotriacetic acid agarose (QIAGEN). A fragment of *Xenopus* Nup205 (aa 1–283) was fused to NusA as a solubility tag, cloned into pET28a, and expressed as a His6-tagged fusion. Recombinant proteins were dialyzed to PBS and injected into rabbits for antibody production.

Antibodies against Nup155 and RCC1 (Franz et al., 2005) as well as Nup160 and Nup93 (Franz et al., 2007) have been described previously. mAb414 was obtained from Babco, anti–lamin B (X223) was obtained from ImmuQuest, and anti-EGFP and anti-His6 were obtained from Roche.

DNA replication, dextran exclusion, and nuclear transport function

For testing DNA replication, nuclear assembly reactions were incubated with 43.5 µM fluorescein-12-dUTP and, where indicated, 16 µM aphidicolin. Samples were fixed and processed for microscopy as described previously (Franz et al., 2005). All fluorescence microscopy images were recorded on the confocal microscope (FV1000; Olympus; equipped with a photomultiplier [model R7862; Hamamatsu]) with 405-, 488-, and 559-nm laser lines and a 60× NA 1.35 oil immersion objective lens using the Fluoview software (Olympus) at room temperature using Vectashield (Vector Laboratories) as a mounting medium.

For the size exclusion assay, nuclei were assembled for 90 min, at which point 10 µg/ml of 10-kD dextran labeled with Texas red, 30 µg/ml of 70-kD dextran labeled with fluorescein, and 40 µg/ml of 2-MD dextran labeled with tetramethylrhodamine were added. The samples were incubated for 5 min and analyzed by confocal microscopy without fixation and mounting, but otherwise as in the previous paragraph.

TEV protease was fused to a NusA domain, cloned into pET28a, and expressed and purified as a His6-tagged fusion. TEV protease without a NusA domain was expressed and purified as a His6-tagged fusion and cross-linked to NLS peptides as described previously (Vasu et al., 2001).

To test importin α/β– or transportin-dependent nuclear import function, full-length NPM2 (nucleoplasmin) or Nplc-M9-M10 (from Englmeier et al. [1999]), respectively, was fused to an N-terminal EGFP, followed by a TEV recognition site, and cloned into a modified pET28a vector, allowing purification via a C-terminal His6 tag. After Ni–nitrilotriacetic acid chromatography, all substrates were further purified by size exclusion chromatography on a Sepharose 200 column (GE Healthcare). 50-µl nuclear assembly reactions were assembled in the volume ratio as described previously (Franz et al., 2005). 50 min after the addition of membranes, 1 µg of the respective reporter was added. At the indicated time points, 10 µl of the samples was added to 1 µl of 5 µg/µl NusA-TEV protease and incubated for 1 min at 20°C. TEV cleavage was stopped by the addition of SDS sample buffer and immediate incubation at 95°C for 5 min, followed by SDS-PAGE and Western blotting.

For testing nuclear export function, a reporter as well as a control substrate, Nplc-M9-NES and Nplc-M9-M10, respectively (from Englmeier et al. [1999]) were fused to an N-terminal EGFP, cloned into pET28a, and purified as in the previous paragraph. 0.1 mg/ml of the export reporters was added to a nuclear assembly reaction, incubated for 90 min, fixed, and processed for microscopy.

For generation of reporter constructs for INM targeting, full-length BC08, a part of the N terminus of LBR including the first transmembrane region (aa 146–258), and full-length SPC18 (all from *Xenopus*) were fused to an N-terminal MISTIC (membrane-integrating sequence for translation of integral membrane protein constructs) fragment (Roosild et al., 2005), followed by a thrombin cleavage site, an EGFP domain, and a TEV protease cleavage site, and cloned into a modified pET28a vector, allowing purification via a C-terminal His6 tag. For the calnexin reporter construct, the C-terminal region including the transmembrane region of calnexin (aa 485–608) was placed 3′ of the MISTIC fragment and 5′ of the TEV cleavage site and the EGFP domain and integrated into the modified pET28a vector with a C-terminal His6 tag. For the INM targeting constructs with increased nucleoplasmatic sizes, a NusA or GST domain was inserted 5′ of the EGFP moiety in the reporter constructs.

Proteins were expressed in *E. coli* BL21de3, purified in the presence of 1% (wt/vol) cetyltrimethylammonium bromide on magnetic Ni-loaded agarose beads (EMD), and dialyzed for 16 h against PBS containing 1 mM EDTA. The MISTIC fragments were cleaved off using thrombin, and the reporters were reconstituted into liposomes. For this, ∼10 µg of protein was mixed with 20 µl of a lipid mix containing 3 mg/ml cholesterol, 3 mg/ml Na-phosphatidylserine, 3 mg/ml Na-phosphatidylinositol, 6 mg/ml phosphatidylethanolamine, 15 mg/ml phosphatidylcholine (all solubilized in 10% octylglucopyranoside), and 2 µl of 1 mg/ml DiIC18 in DMSO. Detergent was removed by passing the sample over a G-50 column equilibrated in sucrose buffer (10 mM Hepes, 250 mM sucrose, 50 mM KCl, and 2.5 mM $MgCl_2$, pH 7.5). The proteoliposome-containing fraction (identified by the color of the dye) was collected, and the liposomes were pelleted by centrifugation for 30 min at 200,000 *g*. The pellets were resuspended in 40 µl of sucrose buffer. Proteins were correctly oriented within the liposomes with the EGFP unit facing the exterior as judged by their sensitivity to TEV protease cleavage.

45 µl of cytosol supplemented with 1 µl of 20 mg/ml glycogen and 1 µl of energy mix (50 mM ATP, 500 mM creatine phosphate, and 10 mg/ml creatine kinase) was incubated with 7,500 sperm heads as chromatin template. 50 min after the addition of 2.5 µl of membranes, 5 µl of resuspended proteoliposomes was added. At the indicated time points, 10 µl of the samples was added to 1 µl of 5 µg/µl NusA-TEV protease in sucrose buffer and incubated for 5 min at 20°C. The cleavage reaction was stopped by fixation with 4% PFA and processed for microscopy as described previously (Franz et al., 2005). For Western blot analysis, TEV cleavage was stopped by the addition of SDS sample buffer and immediate incubation at 95°C for 5 min, followed by SDS-PAGE and Western blotting.

In vitro translation

For the in vitro translation, we generated a modified pET28a vector containing a stem loop–forming sequence derived from the 5′ untranslated region of gene 10 of the T7 bacteriophage (5′-AGGGAGACCACAACGGUUUCCCU-3′) 5′ of the in vitro transcribed/translated gene. This is known to enhance in vitro transcription (O'Connor and Dahlberg, 2001). As DNA templates, full-length mouse Nup188 and *Xenopus* Nup93 were cloned into this vector and used in the PURExpress in vitro synthesis kit (New England Biolabs, Inc.) according to the manufacturer's instructions, extending the incubation time to 4 h.

Miscellaneous

Generation of affinity resins for protein depletion, preparation of sperm heads and floated membranes, nuclear assembly reactions, and transmission electron microscopy were performed as described previously (Franz et al., 2005) except that tannic acid was omitted to increase the visibility of NPCs. For depletions, high speed extracts were incubated twice with a 1:1 bead to cytosol ratio for 40 min (Franz et al., 2007). Prelabeled membranes were prepared as in Antonin et al. [2005] using DiIC18, and immunoprecipitations were performed as in Franz et al. [2007]. NPCs from at least 50 nuclei from three independent experiments were counted (D'Angelo et al., 2006) using the Imaris 6.1.5 software (Bitplane AG) for 3D reconstruction. In vitro assembled nuclei were isolated as in Baur et al. (2007).

Online supplemental material

Fig. S1 shows the quantification of the relative amounts of the different Nup93 complexes. Fig. S2 shows immunofluorescences of nuclei lacking

Downloaded from jcb.rupress.org on December 5, 2013

Published June 21, 2010

Nup205–Nup93 as well as transmission electron images of mock- and Nup188–Nup93-depleted nuclei. Fig. S3 shows the time course of nuclear assembly in mock- and Nup188–Nup93-depleted extracts. Fig. S4 shows INM targeting assays on nuclei lacking Nup188–Nup93 and Nup205–Nup93 and additional data of the addback experiments. Fig. S5 provides supporting experiments characterizing the INM targeting assay. Online supplemental material is available at http://www.jcb.org/cgi/content/full/jcb.200912045/DC1.

We thank Josef Redolfi and Cornelia Sieverding for excellent technical support, Virgilio Failla for help with NPC quantification, and Elisa Izaurralde, Adriana Magalska, Ruchika Sachdev, Allana Schooley, and Benjamin Vollmer for critical reading of the manuscript.

Submitted: 8 December 2009
Accepted: 26 May 2010

References

Alber, F., S. Dokudovskaya, L.M. Veenhoff, W. Zhang, J. Kipper, D. Devos, A. Suprapto, O. Karni-Schmidt, R. Williams, B.T. Chait, et al. 2007. Determining the architectures of macromolecular assemblies. *Nature*. 450:683–694. doi:10.1038/nature06404

Antonin, W., C. Franz, U. Haselmann, C. Antony, and I.W. Mattaj. 2005. The integral membrane nucleoporin pom121 functionally links nuclear pore complex assembly and nuclear envelope formation. *Mol. Cell*. 17:83–92. doi:10.1016/j.molcel.2004.12.010

Antonin, W., J. Ellenberg, and E. Dultz. 2008. Nuclear pore complex assembly through the cell cycle: regulation and membrane organization. *FEBS Lett.* 582:2004–2016. doi:10.1016/j.febslet.2008.02.067

Baur, T., K. Ramadan, A. Schlundt, J. Kartenbeck, and H.H. Meyer. 2007. NSF- and SNARE-mediated membrane fusion is required for nuclear envelope formation and completion of nuclear pore complex assembly in *Xenopus laevis* egg extracts. *J. Cell Sci.* 120:2895–2903. doi:10.1242/jcs.010181

Beck, M., V. Lucić, F. Förster, W. Baumeister, and O. Medalia. 2007. Snapshots of nuclear pore complexes in action captured by cryo-electron tomography. *Nature*. 449:611–615. doi:10.1038/nature06170

Blow, J.J., and A.M. Sleeman. 1990. Replication of purified DNA in *Xenopus* egg extract is dependent on nuclear assembly. *J. Cell Sci.* 95:383–391.

Boehmer, T., J. Enninga, S. Dales, G. Blobel, and H. Zhong. 2003. Depletion of a single nucleoporin, Nup107, prevents the assembly of a subset of nucleoporins into the nuclear pore complex. *Proc. Natl. Acad. Sci. USA*. 100:981–985. doi:10.1073/pnas.252749899

Brohawn, S.G., N.C. Leksa, E.D. Spear, K.R. Rajashankar, and T.U. Schwartz. 2008. Structural evidence for common ancestry of the nuclear pore complex and vesicle coats. *Science*. 322:1369–1373. doi:10.1126/science.1165886

Cook, A., F. Bono, M. Jinek, and E. Conti. 2007. Structural biology of nucleocytoplasmic transport. *Annu. Rev. Biochem.* 76:647–671. doi:10.1146/annurev.biochem.76.052705.161529

D'Angelo, M.A., and M.W. Hetzer. 2008. Structure, dynamics and function of nuclear pore complexes. *Trends Cell Biol.* 18:456–466. doi:10.1016/j.tcb.2008.07.009

D'Angelo, M.A., D.J. Anderson, E. Richard, and M.W. Hetzer. 2006. Nuclear pores form de novo from both sides of the nuclear envelope. *Science*. 312:440–443. doi:10.1126/science.1124196

Deng, M., and M. Hochstrasser. 2006. Spatially regulated ubiquitin ligation by an ER/nuclear membrane ligase. *Nature*. 443:827–831. doi:10.1038/nature05170

Englmeier, L., J.C. Olivo, and I.W. Mattaj. 1999. Receptor-mediated substrate translocation through the nuclear pore complex without nucleotide triphosphate hydrolysis. *Curr. Biol.* 9:30–41. doi:10.1016/S0960-9822(99)80044-X

Fabre, E., and E. Hurt. 1997. Yeast genetics to dissect the nuclear pore complex and nucleocytoplasmic trafficking. *Annu. Rev. Genet.* 31:277–313. doi:10.1146/annurev.genet.31.1.277

Fornerod, M., M. Ohno, M. Yoshida, and I.W. Mattaj. 1997. CRM1 is an export receptor for leucine-rich nuclear export signals. *Cell*. 90:1051–1060. doi:10.1016/S0092-8674(00)80371-2

Franz, C., P. Askjaer, W. Antonin, C.L. Iglesias, U. Haselmann, M. Schelder, A. de Marco, M. Wilm, C. Antony, and I.W. Mattaj. 2005. Nup155 regulates nuclear envelope and nuclear pore complex formation in nematodes and vertebrates. *EMBO J.* 24:3519–3531. doi:10.1038/sj.emboj.7600825

Franz, C., R. Walczak, S. Yavuz, R. Santarella, M. Gentzel, P. Askjaer, V. Galy, M. Hetzer, I.W. Mattaj, and W. Antonin. 2007. MEL-28/ELYS is required for the recruitment of nucleoporins to chromatin and postmitotic nuclear pore complex assembly. *EMBO Rep.* 8:165–172. doi:10.1038/sj.embor.7400889

Galy, V., I.W. Mattaj, and P. Askjaer. 2003. *Caenorhabditis elegans* nucleoporins Nup93 and Nup205 determine the limit of nuclear pore complex size exclusion in vivo. *Mol. Biol. Cell*. 14:5104–5115. doi:10.1091/mbc.E03-04-0237

Gomez-Ospina, N., G. Morgan, T.H. Giddings Jr., B. Kosova, E. Hurt, and M. Winey. 2000. Yeast nuclear pore complex assembly defects determined by nuclear envelope reconstruction. *J. Struct. Biol.* 132:1–5. doi:10.1006/jsbi.2000.4305

Grandi, P., T. Dang, N. Pané, A. Shevchenko, M. Mann, D. Forbes, and E. Hurt. 1997. Nup93, a vertebrate homologue of yeast Nic96p, forms a complex with a novel 205-kDa protein and is required for correct nuclear pore assembly. *Mol. Biol. Cell*. 8:2017–2038.

Harel, A., A.V. Orjalo, T. Vincent, A. Lachish-Zalait, S. Vasu, S. Shah, E. Zimmerman, M. Elbaum, and D.J. Forbes. 2003. Removal of a single pore subcomplex results in vertebrate nuclei devoid of nuclear pores. *Mol. Cell*. 11:853–864. doi:10.1016/S1097-2765(03)00116-3

Hawryluk-Gara, L.A., M. Platani, R. Santarella, R.W. Wozniak, and I.W. Mattaj. 2008. Nup53 is required for nuclear envelope and nuclear pore complex assembly. *Mol. Biol. Cell*. 19:1753–1762. doi:10.1091/mbc.E07-08-0820

Hetzer, M.W., T.C. Walther, and I.W. Mattaj. 2005. Pushing the envelope: structure, function, and dynamics of the nuclear periphery. *Annu. Rev. Cell Dev. Biol.* 21:347–380. doi:10.1146/annurev.cellbio.21.090704.151152

Hinshaw, J.E., and R.A. Milligan. 2003. Nuclear pore complexes exceeding eightfold rotational symmetry. *J. Struct. Biol.* 141:259–268. doi:10.1016/S1047-8477(02)00626-3

King, M.C., C.P. Lusk, and G. Blobel. 2006. Karyopherin-mediated import of integral inner nuclear membrane proteins. *Nature*. 442:1003–1007. doi:10.1038/nature05075

Kramer, A., Y. Ludwig, V. Shahin, and H. Oberleithner. 2007. A pathway separate from the central channel through the nuclear pore complex for inorganic ions and small macromolecules. *J. Biol. Chem.* 282:31437–31443. doi:10.1074/jbc.M703720200

Lusk, C.P., G. Blobel, and M.C. King. 2007. Highway to the inner nuclear membrane: rules for the road. *Nat. Rev. Mol. Cell Biol.* 8:414–420. doi:10.1038/nrm2165

Makio, T., L.H. Stanton, C.C. Lin, D.S. Goldfarb, K. Weis, and R.W. Wozniak. 2009. The nucleoporins Nup170p and Nup157p are essential for nuclear pore complex assembly. *J. Cell Biol.* 185:459–473. doi:10.1083/jcb.200810029

Mansfeld, J., S. Güttinger, L.A. Hawryluk-Gara, N. Panté, M. Mall, V. Galy, U. Haselmann, P. Mühlhäusser, R.W. Wozniak, I.W. Mattaj, et al. 2006. The conserved transmembrane nucleoporin NDC1 is required for nuclear pore complex assembly in vertebrate cells. *Mol. Cell*. 22:93–103. doi:10.1016/j.molcel.2006.02.015

Mattaj, I.W. 2004. Sorting out the nuclear envelope from the endoplasmic reticulum. *Nat. Rev. Mol. Cell Biol.* 5:65–69. doi:10.1038/nrm1263

Meier, E., B.R. Miller, and D.J. Forbes. 1995. Nuclear pore complex assembly studied with a biochemical assay for annulate lamellae formation. *J. Cell Biol.* 129:1459–1472. doi:10.1083/jcb.129.6.1459

Mettenleiter, T.C., B.G. Klupp, and H. Granzow. 2009. Herpesvirus assembly: an update. *Virus Res.* 143:222–234. doi:10.1016/j.virusres.2009.03.018

Mohr, D., S. Frey, T. Fischer, T. Güttler, and D. Görlich. 2009. Characterisation of the passive permeability barrier of nuclear pore complexes. *EMBO J.* 28:2541–2553. doi:10.1038/emboj.2009.200

Naim, B., V. Brumfeld, R. Kapon, V. Kiss, R. Nevo, and Z. Reich. 2007. Passive and facilitated transport in nuclear pore complexes is largely uncoupled. *J. Biol. Chem.* 282:3881–3888. doi:10.1074/jbc.M608329200

Nehrbass, U., M.P. Rout, S. Maguire, G. Blobel, and R.W. Wozniak. 1996. The yeast nucleoporin Nup188p interacts genetically and physically with the core structures of the nuclear pore complex. *J. Cell Biol.* 133:1153–1162. doi:10.1083/jcb.133.6.1153

O'Connor, M., and A.E. Dahlberg. 2001. Enhancement of translation by the epsilon element is independent of the sequence of the 460 region of 16S rRNA. *Nucleic Acids Res.* 29:1420–1425. doi:10.1093/nar/29.7.1420

Ohba, T., E.C. Schirmer, T. Nishimoto, and L. Gerace. 2004. Energy- and temperature-dependent transport of integral proteins to the inner nuclear membrane via the nuclear pore. *J. Cell Biol.* 167:1051–1062. doi:10.1083/jcb.200409149

Onischenko, E.A., E. Crafoord, and E. Hallberg. 2007. Phosphomimetic mutation of the mitotically phosphorylated serine 1880 compromises the interaction of the transmembrane nucleoporin gp210 with the nuclear pore complex. *Exp. Cell Res.* 313:2744–2751. doi:10.1016/j.yexcr.2007.05.011

Powell, L., and B. Burke. 1990. Internuclear exchange of an inner nuclear membrane protein (p55) in heterokaryons: in vivo evidence for the

Downloaded from jcb.rupress.org on December 5, 2013

Published June 21, 2010

interaction of p55 with the nuclear lamina. *J. Cell Biol.* 111:2225–2234. doi:10.1083/jcb.111.6.2225

Rasala, B.A., A.V. Orjalo, Z. Shen, S. Briggs, and D.J. Forbes. 2006. ELYS is a dual nucleoporin/kinetochore protein required for nuclear pore assembly and proper cell division. *Proc. Natl. Acad. Sci. USA*. 103:17801–17806. doi:10.1073/pnas.0608484103

Ribbeck, K., and D. Görlich. 2001. Kinetic analysis of translocation through nuclear pore complexes. *EMBO J.* 20:1320–1330. doi:10.1093/emboj/20.6.1320

Roosild, T.P., J. Greenwald, M. Vega, S. Castronovo, R. Riek, and S. Choe. 2005. NMR structure of Mistic, a membrane-integrating protein for membrane protein expression. *Science*. 307:1317–1321. doi:10.1126/science.1106392

Rout, M.P., and J.D. Aitchison. 2001. The nuclear pore complex as a transport machine. *J. Biol. Chem.* 276:16593–16596. doi:10.1074/jbc.R100015200

Rout, M.P., J.D. Aitchison, A. Suprapto, K. Hjertaas, Y. Zhao, and B.T. Chait. 2000. The yeast nuclear pore complex: composition, architecture, and transport mechanism. *J. Cell Biol.* 148:635–651. doi:10.1083/jcb.148.4.635

Shulga, N., N. Mosammaparast, R. Wozniak, and D.S. Goldfarb. 2000. Yeast nucleoporins involved in passive nuclear envelope permeability. *J. Cell Biol.* 149:1027–1038. doi:10.1083/jcb.149.5.1027

Soullam, B., and H.J. Worman. 1995. Signals and structural features involved in integral membrane protein targeting to the inner nuclear membrane. *J. Cell Biol.* 130:15–27. doi:10.1083/jcb.130.1.15

Ulbert, S., M. Platani, S. Boue, and I.W. Mattaj. 2006. Direct membrane protein-DNA interactions required early in nuclear envelope assembly. *J. Cell Biol.* 173:469–476. doi:10.1083/jcb.200512078

Vasu, S., S. Shah, A. Orjalo, M. Park, W.H. Fischer, and D.J. Forbes. 2001. Novel vertebrate nucleoporins Nup133 and Nup160 play a role in mRNA export. *J. Cell Biol.* 155:339–354. doi:10.1083/jcb.200108007

Walther, T.C., A. Alves, H. Pickersgill, I. Loïodice, M. Hetzer, V. Galy, B.B. Hülsmann, T. Köcher, M. Wilm, T. Allen, et al. 2003. The conserved Nup107-160 complex is critical for nuclear pore complex assembly. *Cell*. 113:195–206. doi:10.1016/S0092-8674(03)00235-6

Weis, K. 2003. Regulating access to the genome: nucleocytoplasmic transport throughout the cell cycle. *Cell*. 112:441–451. doi:10.1016/S0092-8674(03)00082-5

Zabel, U., V. Doye, H. Tekotte, R. Wepf, P. Grandi, and E.C. Hurt. 1996. Nic96p is required for nuclear pore formation and functionally interacts with a novel nucleoporin, Nup188p. *J. Cell Biol.* 133:1141–1152. doi:10.1083/jcb.133.6.1141

Zuleger, N., N. Korfali, and E.C. Schirmer. 2008. Inner nuclear membrane protein transport is mediated by multiple mechanisms. *Biochem. Soc. Trans.* 36:1373–1377. doi:10.1042/BST0361373

Downloaded from jcb.rupress.org on December 5, 2013

Theerthagiri et al., http://www.jcb.org/cgi/content/full/jcb.200912045/DC1

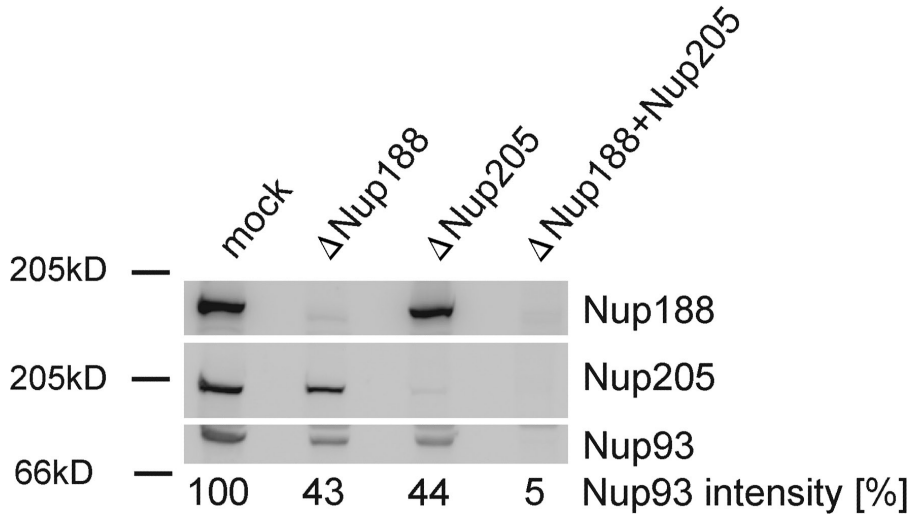

Figure S1. **Quantitation of the different Nup93-containing complexes.** Extracts were passed over a control IgG (mock), α-Nup188, α-Nup205, or a mixed α-Nup188/α-Nup205 matrix. Unbound material was analyzed by Western blotting, and the Nup93 signal was quantified and normalized to the mock control.

THE JOURNAL OF CELL BIOLOGY

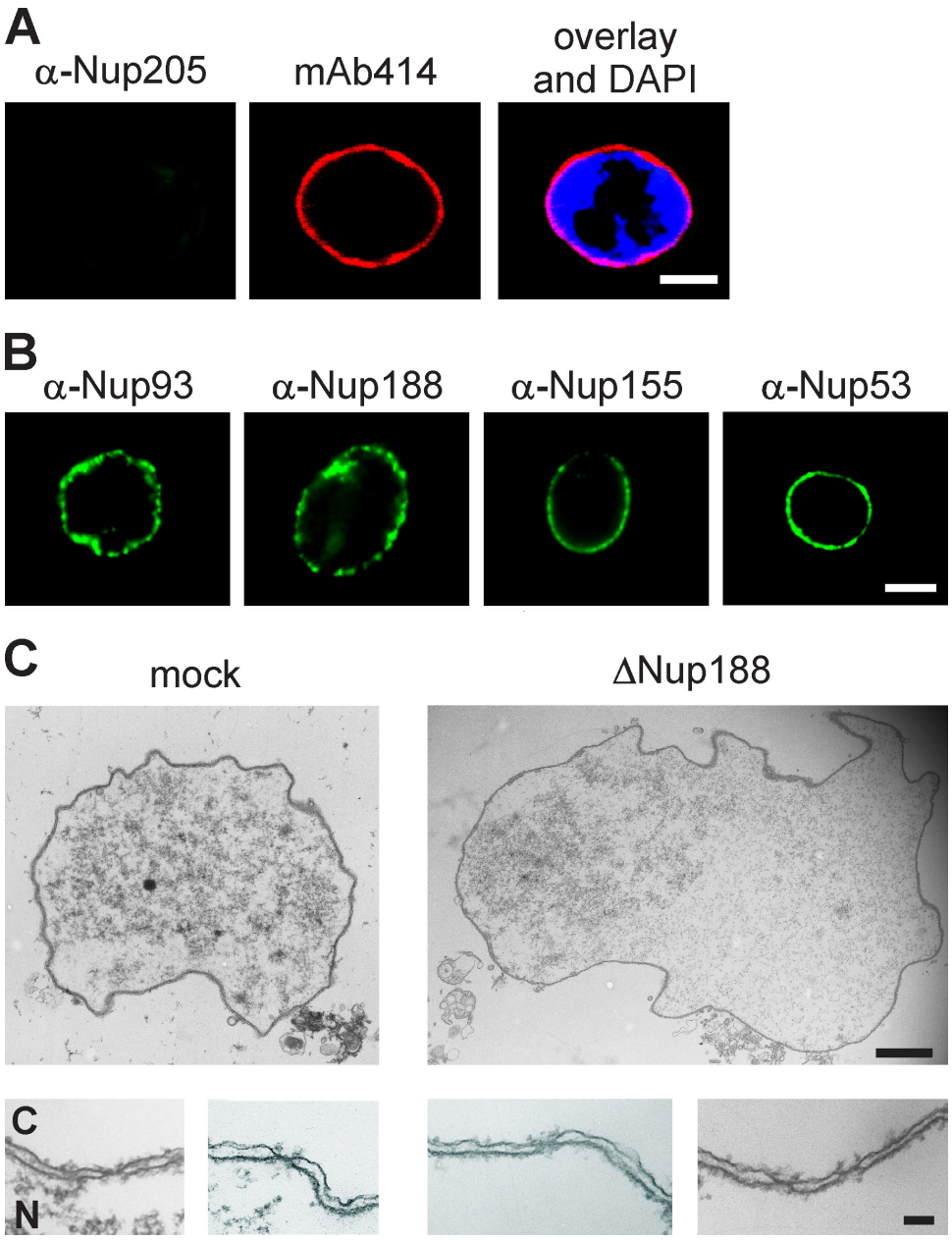

Figure S2. **Immunofluorescences of nuclei lacking Nup205–Nup93 and transmission electron images of mock- and Nup188–Nup93-depleted nuclei.** (A) Nup205–Nup93-depleted nuclei contain NPCs. Nuclei were assembled in Nup205–Nup93-depleted extracts for 90 min, fixed with 4% PFA, and analyzed with Nup205-specific antibodies (green) and the monoclonal antibody mAb414 (red). Chromatin is stained with DAPI. (B) Nup205–Nup93-depleted nuclei contain all other nucleoporins of the subcomplex. Samples were prepared as in A and analyzed by immunofluorescence with the indicated antibodies. (C) Electron microscopy analysis of Nup188–Nup93-depleted nuclei transmission electron microscopy analysis of nuclei assembled in mock- and Nup188–Nup93-depleted extracts. C indicates the cytoplasmic site, and N indicates the nucleoplasmic site of the NE. Bars: (A and B) 20 µm; (C, top) 1 µm; (C, bottom) 100 nm.

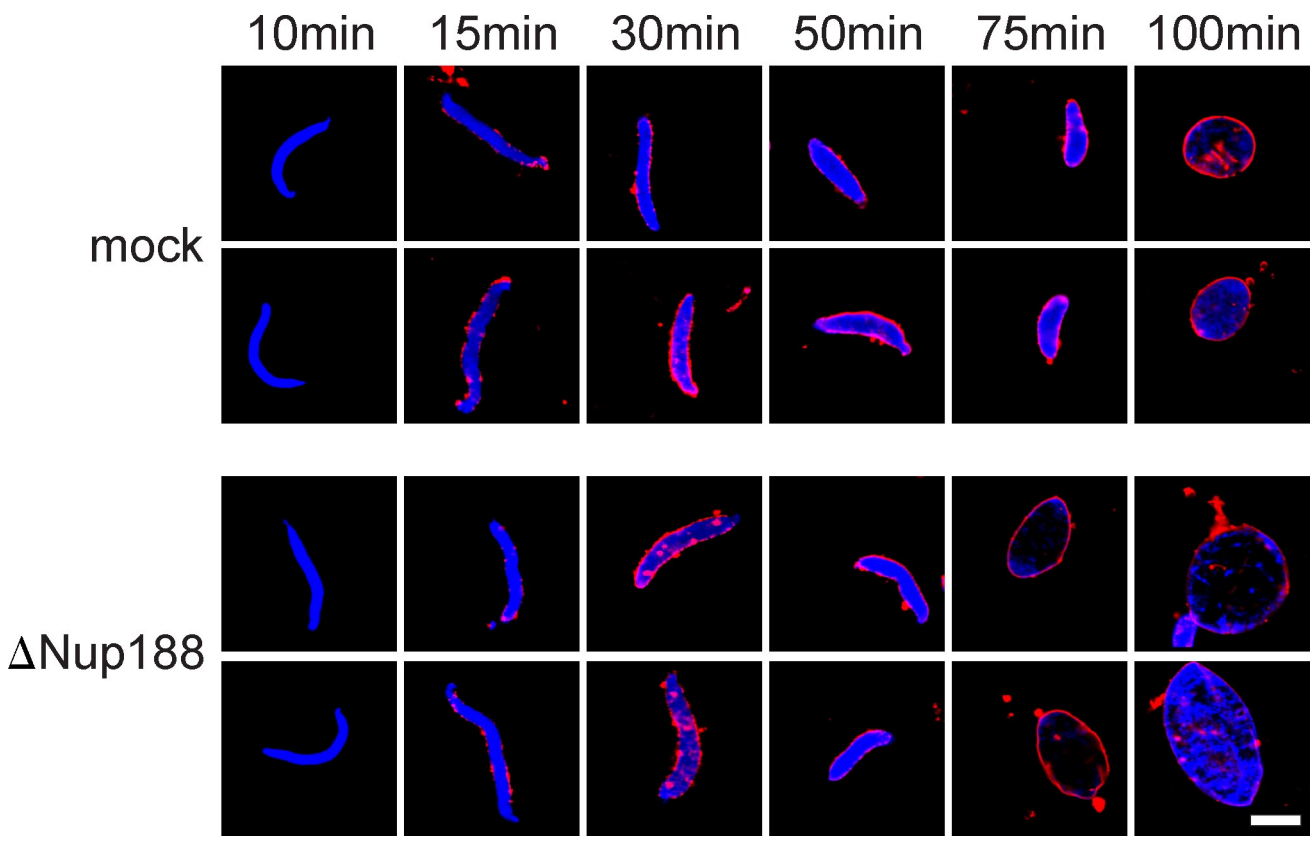

Figure S3. **Time course of nuclear assembly in mock- and Nup188–Nup93-depleted extracts.** Nup188–Nup93-depleted nuclei grow faster after NE closure. Demembranated sperm chromatin was incubated in mock- or Nup188–Nup93-depleted *Xenopus* egg extracts for 10 min. At this time, DiIC18-prelabeled membranes (red in overlay) were added to the reaction. Reactions were stopped at the indicated time points by fixation with 4% PFA and 0.5% glutaraldehyde, chromatin was stained with DAPI (blue), and the samples were analyzed by confocal microscopy. Bar, 20 µm.

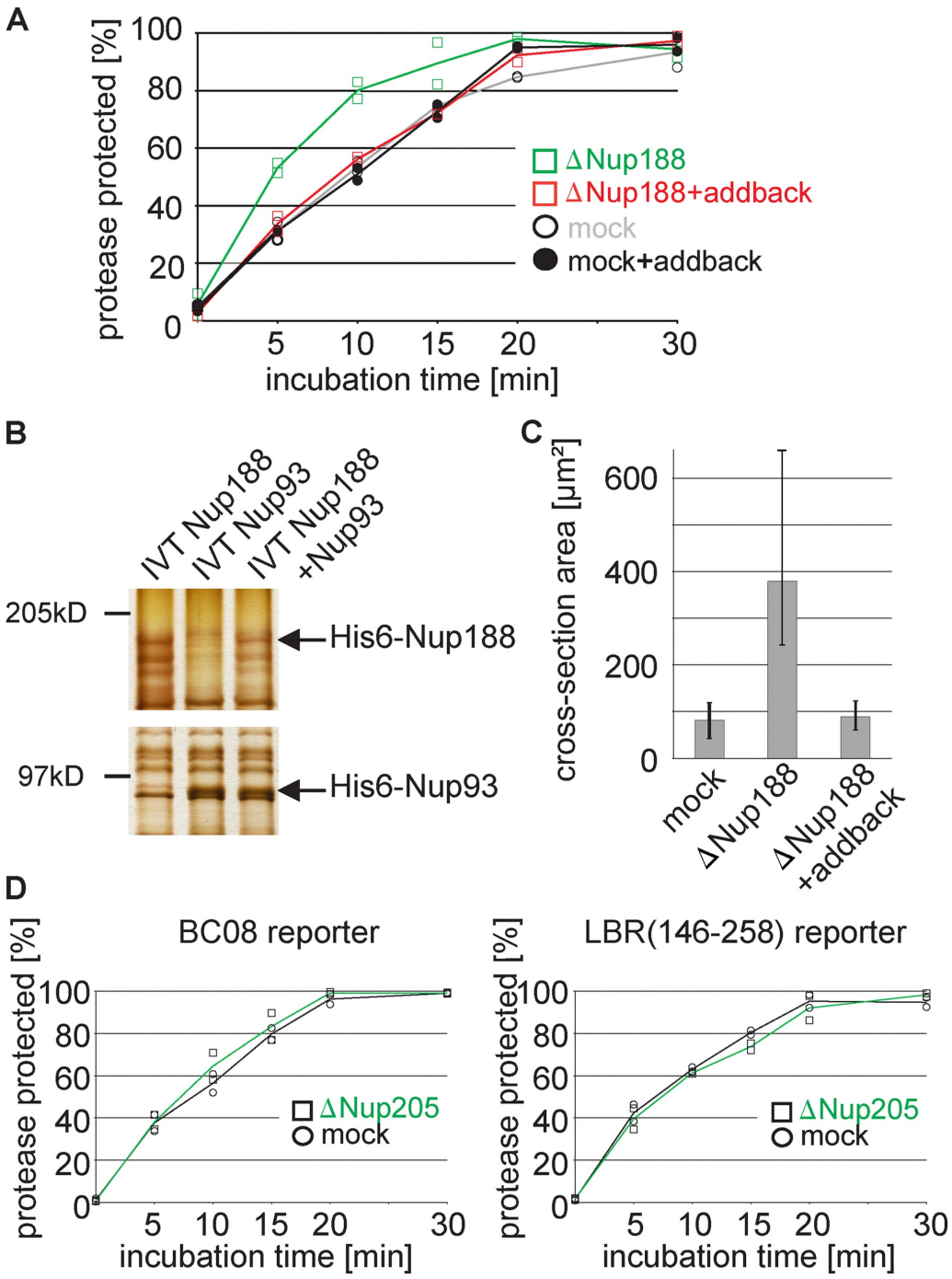

Figure S4. **INM targeting assays on nuclei lacking Nup188–Nup93 and Nup205–Nup93 and additional data of the addback experiments.** (A) Nup188–Nup93 depletion causes a faster delivery of an LBR reporter to the INM. Quantification of INM targeting of an LBR-based transport substrate. Squares are from Nup188–Nup93-depleted samples (green without and red with addition of in vitro translated Nup188–Nup93 [addback]), and circles are from mock-treated samples. Lines mark the mean of two independent experiments. (B) Analysis of the recombinant Nup188–Nup93 used in the addback experiments. In vitro translated (IVT) products of Nup188 alone, Nup93 alone, and combined Nup188–Nup93 were analyzed by SDS-PAGE (8%) and silver stained. Positions of full-length recombinant Nup188 and Nup93 are indicated. (C) The addback restores normal nuclear size in Nup188–Nup93-depleted nuclei. Quantitation of the cross-sectional area of nuclei assembled for 120 min in mock- or Nup188–Nup93– depleted extracts or Nup188–Nup93-depleted extracts supplemented with in vitro translated Nup188–Nup93 (addback). More than 30 randomly chosen chromatin substrates were counted per reaction. The mean of three independent experiments is shown, and error bars represent the total variation. (D) Nup205–Nup93-depleted nuclei show normal INM targeting. Quantification of INM targeting of the BC08- and LBR-based transport substrate from two independent experiments in Nup205–Nup93-depleted nuclei (squares and green line for mean) and mock-depleted nuclei (circles and black line for mean).

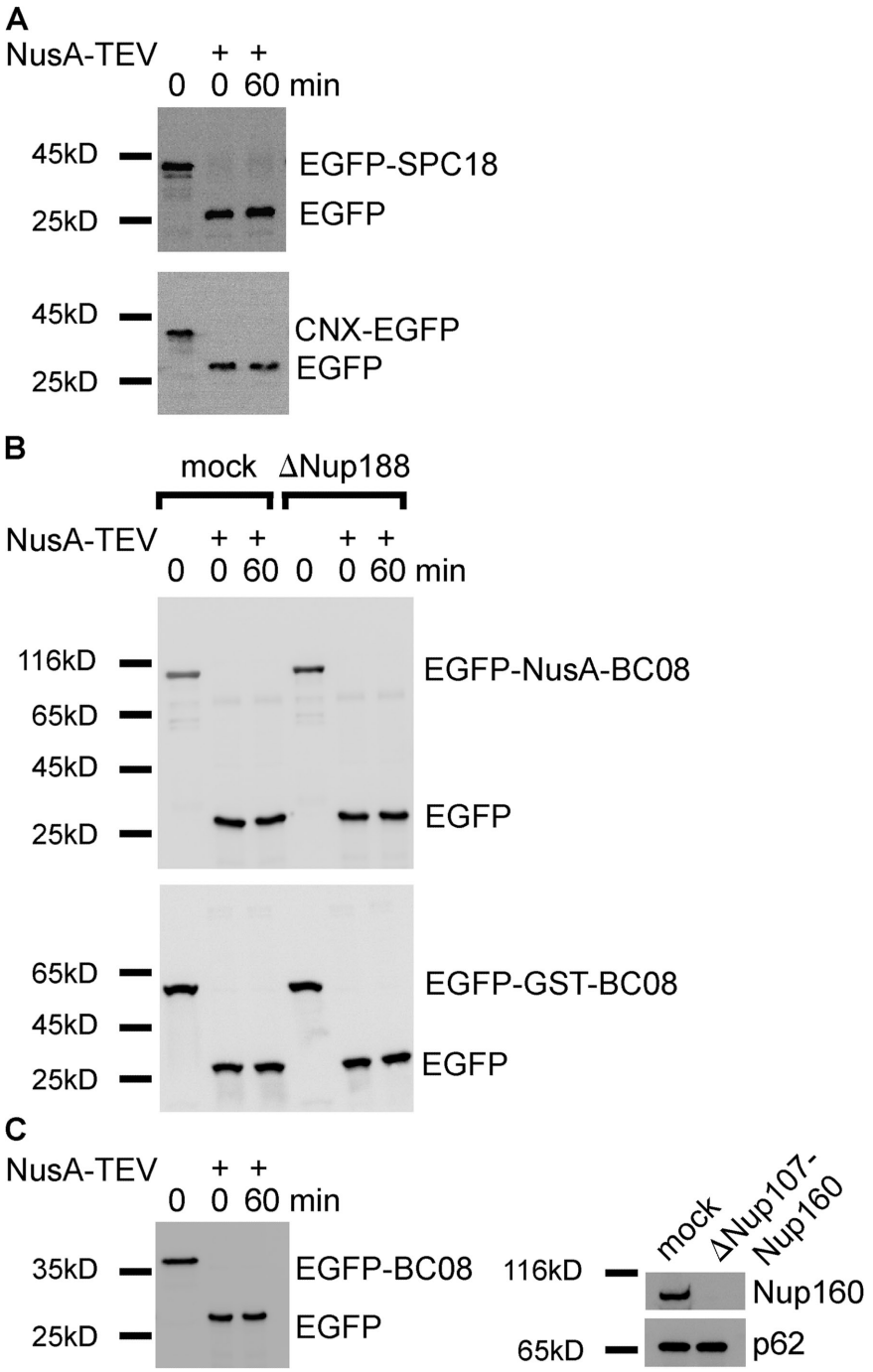

Figure S5. **Supporting experiments characterizing the INM targeting assay.** (A) ER proteins are not mistargeted in Nup188–Nup93-depleted nuclei. Two reporters based on bona fide ER membrane proteins (the signal peptidase subunit SPC18 [top] or a fragment of the transmembrane region and C-terminal part of the ER chaperon calnexin [CNX; bottom]) were used in Nup188–Nup93-depleted extracts. Where indicated, after 0 or 60 min, NusA-TEV protease was added, and samples analyzed by Western blotting. Protease protection was not detected even after 60 min, indicating that substrates did not localize to the INM. (B) Nup188–Nup93-depleted NPCs show normal size exclusion limits for targeting of INM proteins. The nucleoplasmic domain of the BC08 reporter was increased to 94 or 64 kD and used in mock- or Nup188–Nup93-depleted extracts. Where indicated, after 0 or 60 min, NusA-TEV protease was added, and samples were analyzed by Western blotting. Protease protection was not detected even after 60 min, indicating that substrates did not localize to the INM. (C) Nup107–Nup160-depleted nuclei show no INM targeting. The EGFP-BC08 reporter was used in Nup107–Nup160-depleted extracts (Walther et al., 2003). Where indicated, after 0 or 60 min, NusA-TEV protease was added, and samples were analyzed by Western blotting (left). Protease protection was not detected even after 60 min, indicating that substrates did not localize to the INM. Removal of Nup160 upon Nup107–Nup160 depletion is shown on the right. The nucleoporin p62 detected with the antibody mAb414 serves as a loading control.

Reference

Walther, T.C., A. Alves, H. Pickersgill, I. Loïodice, M. Hetzer, V. Galy, B.B. Hülsmann, T. Köcher, M. Wilm, T. Allen, et al. 2003. The conserved Nup107-160 complex is critical for nuclear pore complex assembly. *Cell*. 113:195–206. doi:10.1016/S0092-8674(03)00235-6

The EMBO Journal (2012) 31, 4072–4084 | © 2012 European Molecular Biology Organization | Some Rights Reserved 0261-4189/12
www.embojournal.org

THE EMBO JOURNAL

EMBO open

Dimerization and direct membrane interaction of Nup53 contribute to nuclear pore complex assembly

Benjamin Vollmer[1], Allana Schooley[1], Ruchika Sachdev[1], Nathalie Eisenhardt[1], Anna M Schneider[2], Cornelia Sieverding[1], Johannes Madlung[3], Uwe Gerken[4,5], Boris Macek[3] and Wolfram Antonin[1,*]

[1]Friedrich Miescher Laboratory of the Max Planck Society, Tübingen, Germany, [2]Max Planck Institute for Developmental Biology, Department of Biochemistry, Tübingen, Germany, [3]Proteome Center Tübingen, University of Tübingen, Tübingen, Germany and [4]Institute of Microbiology, University of Hohenheim, Stuttgart, Germany

Nuclear pore complexes (NPCs) fuse the two membranes of the nuclear envelope (NE) to a pore, connecting cytoplasm and nucleoplasm and allowing exchange of macromolecules between these compartments. Most NPC proteins do not contain integral membrane domains and thus it is largely unclear how NPCs are embedded and anchored in the NE. Here, we show that the evolutionary conserved nuclear pore protein Nup53 binds independently of other proteins to membranes, a property that is crucial for NPC assembly and conserved between yeast and vertebrates. The vertebrate protein comprises two membrane binding sites, of which the C-terminal domain has membrane deforming capabilities, and is specifically required for *de novo* NPC assembly and insertion into the intact NE during interphase. Dimerization of Nup53 contributes to its membrane interaction and is crucial for its function in NPC assembly.

The EMBO Journal (2012) **31,** 4072–4084. doi:10.1038/emboj.2012.256; Published online 7 September 2012
Subject Categories: membranes & transport; cell & tissue architecture
Keywords: nuclear envelope formation; nuclear pore complex assembly; nuclear membrane; Nup35; Nup53

Introduction

The defining feature of the eukaryotic cell is the compartmentalization of genetic material inside the nucleus. The spatial and temporal separation of transcription and translation has enabled eukaryotes to achieve a level of regulatory complexity that is unprecedented in prokaryotes. This is accomplished by the nuclear envelope (NE), which serves as the physical barrier between the cytoplasm and the nucleoplasm. Nuclear pore complexes (NPCs) are the exclusive gateways in the NE allowing diffusion of small substances and regulated trafficking of macromolecules up to a size of 15 nm for ribosomal subunits or even 50 nm for Balbiani ring particles (for review, see Wente and Rout, 2010; Hoelz *et al*, 2011; Bilokapic and Schwartz, 2012). NPCs form large pores in the NE, having a diameter of ~130 nm. Unlike other transport channels, NPCs span two lipid bilayers, at sites where the outer and inner membranes of the NE are fused. Therefore, NPCs are assumed to play an important role in deforming these membranes to form a pore as well as in stabilizing this highly curved pore membrane (Antonin *et al*, 2008).

Given the structural complexity and extraordinary transport capabilities of NPCs, it is quite surprising that these huge macromolecular assemblies of 40–60 MDa are only composed of ~30 different proteins. These nucleoporins (Nups) can be roughly categorized into those forming the structure of the pore and those mediating transport through the NPC. The latter class is characterized by a high number of FG repeats. Two evolutionary conserved subcomplexes form the major part of the structural scaffold. The Nup107–160 complex in metazoa, or the corresponding Nup84 complex in yeast, is the best characterized of these owing to an extensive set of genetic, biochemical and structural data. Computational and structural analyses suggest that this complex is related to vesicle coats (Devos *et al*, 2004; Mans *et al*, 2004; Brohawn *et al*, 2008). It is possible that these proteins form a coat-like assembly stabilizing the curved pore membrane of the NPC, which is analogous to clathrin or COPI and II during vesicle formation (Field *et al*, 2011; Onischenko and Weis, 2011). Notably, neither clathrin nor COP coats interact directly with the lipid bilayers. They are rather linked to the deformed membrane via adaptor and integral proteins (McMahon and Mills, 2004). Although three integral membrane proteins are known in the vertebrate NPC, it is unclear how a possible link between the Nup107–160 complex and the membrane is established.

The second major structural and evolutionarily conserved subcomplex of the NPC is the metazoan Nup93 complex, Nic96 in yeast, which might serve as a link to the pore membrane. In vertebrates, it is composed of five nucleoporins: Nup205, Nup188, Nup155, Nup93 and Nup53. Nup53, also referred to as Nup35 (Cronshaw *et al*, 2002), interacts with Nup93 and Nup155 (Hawryluk-Gara *et al*, 2005), corresponding to Nup170 and Nic96 in yeast (Marelli *et al*, 1998; Fahrenkrog *et al*, 2000). Nup155, Nup93 and Nup53 are each indispensable for NPC formation in vertebrates (Franz *et al*, 2005; Hawryluk-Gara *et al*, 2008; Mitchell *et al*, 2010; Sachdev *et al*, 2012). Interestingly, Nup53 and its corresponding yeast homologues Nup53p and Nup59p interact with the transmembrane nucleoporin NDC1, thereby potentially linking the NPC to the pore membrane (Mansfeld *et al*, 2006; Onischenko *et al*, 2009). Although NDC1 is essential in both vertebrates and yeast (Winey *et al*, 1993; West *et al*, 1998; Mansfeld *et al*, 2006; Stavru *et al*, 2006) it is not found in all eukaryotes (Mans *et al*, 2004; DeGrasse *et al*, 2009; Neumann *et al*, 2010), suggesting that in

*Corresponding author. Friedrich Miescher Laboratory of the Max Planck Society, Spemannstraße 39, Tübingen 72076, Germany.
Tel.: +49 70 7160 1836; Fax: +49 70 7160 1801;
E-mail: wolfram.antonin@tuebingen.mpg.de
[5]Present address: Lehrstuhl für Experimentalphysik IV, University of Bayreuth, Universitätsstrasse 30, 95447 Bayreuth, Germany

Received: 16 April 2012; accepted: 21 August 2012; published online: 7 September 2012

 ©2012 European Molecular Biology Organization

some organisms NPCs can form in the absence of a Nup53–NDC1 interaction. Indeed, *Aspergillus nidulans* is viable in the absence of all three known transmembrane nucleoporins (Liu *et al*, 2009). This suggests that there are alternative modes of interaction between the nucleoporins and the pore membrane.

Here, we show that Nup53 binds membranes directly and independently of other proteins. It possesses two membrane interaction regions, which are important for NPC assembly. Although either site is sufficient for NPC assembly at the end of mitosis, the C-terminal membrane binding site of Nup53 is specifically required for NPC assembly during interphase, probably because of its membrane deforming capabilities.

Results

Nup53 is a membrane binding protein

Overexpression of Nup53 in yeast causes expansion of the NE (Marelli *et al*, 2001). Similar membrane proliferation phenotypes have been observed upon overexpression of nuclear membrane binding proteins, such as lamin B (Prufert *et al*, 2004). Yeast Nup53 contains a C-terminal region predicted to form an amphipathic helix (Marelli *et al*, 2001; Patel and Rexach, 2008), which could serve as a membrane binding module. However, Nup53 interacts with the integral pore membrane protein NDC1 in both yeast and metazoa (Mansfeld *et al*, 2006; Onischenko *et al*, 2009) and thus might be linked to the membrane via this interaction. We therefore tested whether Nup53 is able to interact with membranes independently of other proteins.

To assay for membrane binding, we generated liposomes with an average radius of ~150 nm. These liposomes were incubated with different, recombinantly expressed nucleoporins and floated through sucrose cushions. Liposome binding proteins were recovered after centrifugation from the top fraction (Figure 1A). A Nup133 membrane binding fragment (Drin *et al*, 2007) was used as a positive control and found in the liposome containing top fraction (Figure 1A). Similarly, Xenopus Nup53 was found in the top fraction, indicating membrane interaction. In contrast, a fragment of the FG repeat-containing nucleoporin Nup98 did not bind liposomes. Thus, Xenopus Nup53 binds directly to

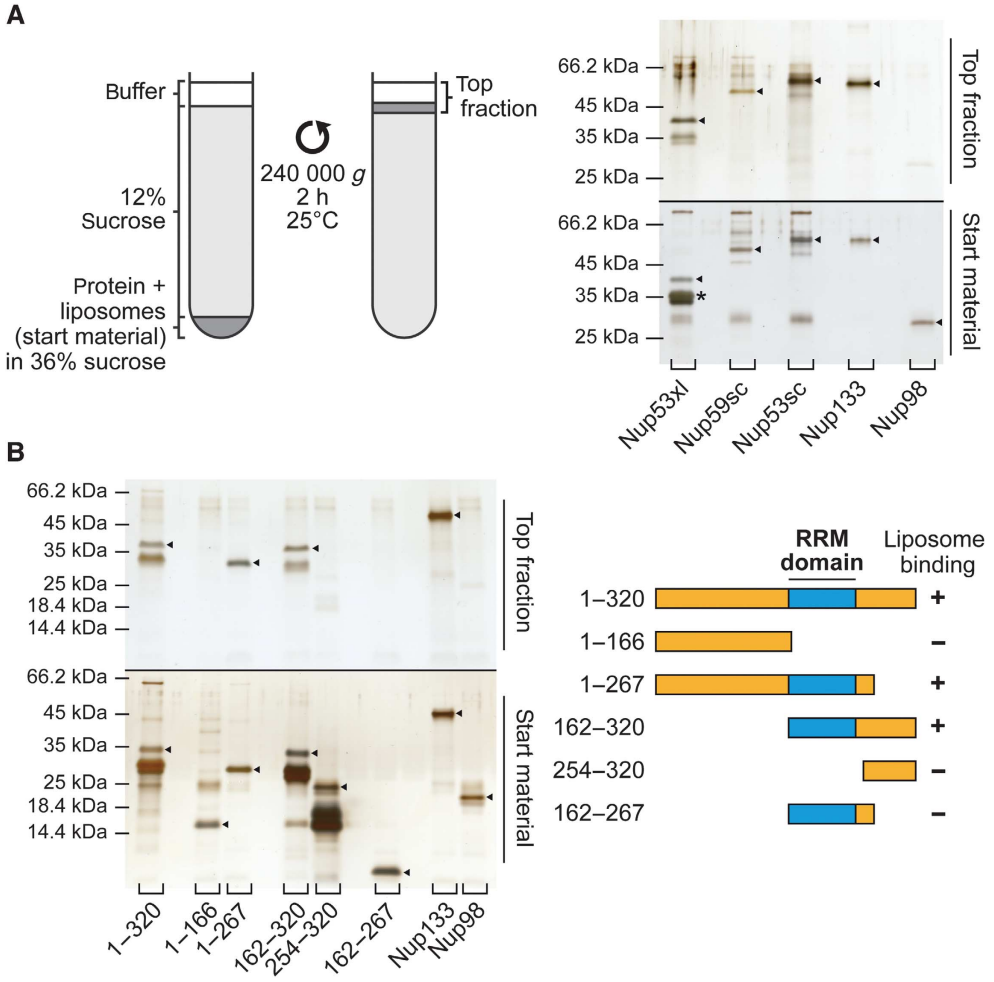

Figure 1 Nup53 directly binds membranes. (**A**) 3 μM recombinant Xenopus Nup53 (Nup53xl), the two yeast orthologues Nup59sc and Nup53sc as well as fragments of Nup133 and Nup98 as positive and negative controls, respectively, were incubated with 6 mg/ml fluorescently labelled liposomes prepared from *E. coli* polar lipids and floated through a sucrose gradient as indicated on the left. Top fractions of the gradient, as well as 3% of the starting material, were analysed by SDS–PAGE and silver staining. Please note that Nup53 is sensitive to C-terminal degradation (*) and that the full-length protein significantly enriched in the liposome bound fraction. (**B**) Full-length (1–320) and different fragments of Xenopus Nup53 as well as fragments of Nup133 and Nup98 were analysed for liposome binding as in (**A**). Only fragments comprising the RRM domain (indicated in blue in the schematic representation) bound liposomes.

©2012 European Molecular Biology Organization

membranes independently of other interacting proteins. To determine whether this feature is conserved during evolution, we tested the two yeast homologues Nup53p and Nup59p, which both bound liposomes (Figure 1A).

We next sought to define the regions of Xenopus Nup53 important for its membrane interaction. Nup53 can be roughly divided into three parts: the N-terminus (amino acid (aa) 1–166), a middle region (aa 166–267) comprising a conserved RNA recognition motif (RRM) domain and the C-terminus (aa 267–320) (Figure 1B). We generated different N- and C-terminal truncations of Nup53 and tested them for liposome binding (Figure 1B). While full-length Nup53 (aa 1–320) bound to liposomes, the N-terminal region of the protein (aa 1–166) showed no binding. Extending this fragment by 100 aa to include the RRM domain rendered the protein capable of membrane binding (aa 1–267). The C-terminal half of Nup53 (aa 162–320), which included the RRM domain, also interacted with liposomes. However, a fragment consisting of only the C-terminal region of Nup53 but lacking the RRM domain (aa 254–320) could not bind liposomes. Surprisingly, a fragment comprising only the RRM domain (aa 162–267) did not bind liposomes showing that the RRM domain is necessary but not sufficient for Nup53 membrane binding.

Nup53 dimerization is necessary for membrane binding and NPC formation

As the RRM domain is crucial for Nup53 membrane interaction we investigated the function of this domain. The crystal structure of the mouse domain suggests that it acts as a dimerization rather than an RNA binding module (Handa *et al*, 2006). We designed a mutant of this domain by exchanging two amino acids (F172E/W203E) in the dimerization surface. Size exclusion chromatography in combination with multi-angle laser light scattering revealed that the resulting fragment was monomeric (Figure 2A).

To confirm that the dimerization occurs also *in vivo*, we performed co-transfection experiments in HeLa cells using HA- and myc-tagged Xenopus Nup53. Either α-HA or α-myc antibodies immunoprecipitated both HA- and myc-tagged wild-type Nup53 indicating that the proteins formed a complex (Figure 2B, lanes 5 and 10). If cells were transfected with either construct separately before they were mixed for protein extraction, then no co-immunoprecipitation was observed (Figure 2B, lanes 9 and 14) demonstrating that complex formation cannot occur under the conditions of the immunoprecipitation. Co-transfections of RRM mutants as well as RRM mutants and wild-type protein did not result in complex formation (Figure 2B, lanes 6–8 and 11–13) indicating that the F172E/W203E exchange inhibited dimerization/oligomerization.

Next, we tested the effect of these mutations on membrane binding. In the context of the full-length protein, these mutations decreased liposome binding by 70% (Figure 2C) suggesting that the dimerization of Nup53 is important for its membrane interaction.

As Nup53 is essential for postmitotic NPC formation (Hawryluk-Gara *et al*, 2008) we examined the relevance of Nup53 membrane binding for this. We employed *Xenopus laevis* egg extracts to study nuclear reformation *in vitro* (Lohka, 1998). With antibodies against Nup53 we depleted the endogenous protein without co-depletion of other nucleoporins including the other members of the Nup93 complex: Nup93, Nup155, Nup205 and Nup188 (Figure 2D). These depleted extracts were incubated with sperm heads serving as chromatin template. In the absence of Nup53, NPC formation was blocked (Figure 2E) as reported (Hawryluk-Gara *et al*, 2008). This was indicated by the absence of immunofluorescent signal on the chromatin surface for mab414, an antibody recognizing several nucleoporins that represent a major subfraction of the NPC. Addition of recombinantly expressed wild-type Nup53 to the depleted extracts at levels similar to the endogenous protein (Figure 2D) restored NPC formation. The recombinant protein was integrated into NPCs as indicated by immunostaining with a Nup53 antibody. In contrast, the dimerization and membrane binding defective Nup53 mutant (1–320 F172E/W203E) was unable to substitute for the endogenous protein in NPC formation (Figure 2E).

Individual depletion of several nucleoporins essential for NPC assembly from Xenopus egg extracts also blocks formation of a closed NE. These nucleoporins include POM121, NDC1, Nup155, Nup93 (Antonin *et al*, 2005; Franz *et al*, 2005; Mansfeld *et al*, 2006; Sachdev *et al*, 2012) and Nup53 (Hawryluk-Gara *et al*, 2008). Upon Nup53 depletion, membrane vesicles bound to the chromatin surface but did not fuse to form a closed NE (Figure 2F; Hawryluk-Gara *et al*, 2008). This phenotype was rescued by the wild-type Nup53 protein, but not by the dimerization defective mutant. Together with the liposome-binding assay, this suggests that Nup53 membrane binding could be important for NPC assembly and formation of a closed NE. However, we cannot exclude that the RRM mutant also affects interaction of Nup53 with other nucleoporins. Indeed, in GST pull-down assays we observed a slight reduction of Nup93, Nup205 and Nup155 binding to Nup53 in the context of the RRM mutant as compared to the wild-type protein (Supplementary Figure S1A). In contrast, NDC1 binding to Nup53 was unaffected by the dimerization mutant (Supplementary Figure S1B).

Nup53 possesses two membrane binding regions

These results reveal a crucial role for Nup53 dimerization via its RRM domain in NE reformation. However, the RRM domain alone did not bind to membranes. We tested different Nup53 truncations for liposome binding to map the membrane interaction sites (Figure 3A; Supplementary Figure S2 shows the purity of all recombinant proteins used in the different liposome experiments). An N-terminal fragment of Nup53 including the RRM domain (aa 1–267) bound to liposomes with only a slightly decreased binding efficiency, 83% of the levels of the full-length protein. Further truncations from the N-terminus revealed a minimal membrane binding region between aa 93 and 107 as indicated by a four-fold decrease in liposome binding upon removal of these 15 amino acids. This region comprises a patch of basic residues, which as in other membrane binding proteins might be important for the interaction with negatively charged lipids. Indeed, changing two residues to negatively charged residues (R105E/K106E) abolished membrane binding (Figure 3A, 83% reduction as compared to the 93–267 fragment).

Interestingly, the N-terminal membrane binding region of Nup53 contains one of two regions that were differentially phosphorylated depending on the cell-cycle stage (Supplementary Figure S3; Supplementary Table S1). Two

 ©2012 European Molecular Biology Organization

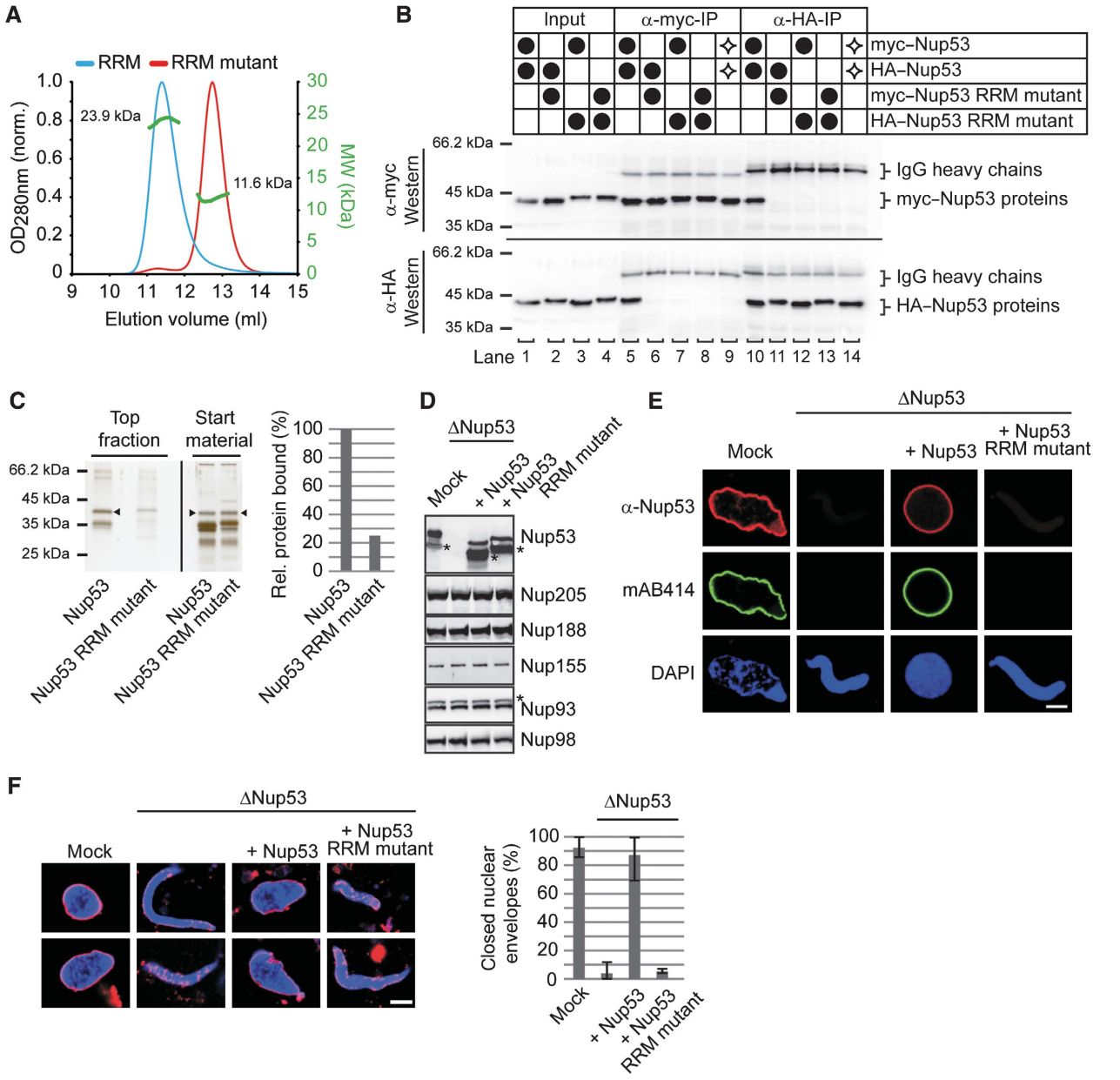

Figure 2 Dimerization of the RRM domain is essential for Nup53 membrane binding and nuclear pore complex formation. (**A**) Size exclusion chromatography on a Superdex75 10/300 GL column followed by multi-angle static laser light scattering of the Xenopus Nup53 RRM domain and the F172E/W203E mutant, which rendered the domain monomeric. The green dots relate to the secondary axis and show the molecular weight of the eluting particles. (**B**) HeLa cells were co-transfected with myc- and HA-tagged Xenopus Nup53 wild-type protein and/or dimerization mutant as indicated (●). Proteins were immunoprecipitated from cell lysates with α-myc or α-HA antibodies, and analysed by western blotting. Ten per cent of the start materials are loaded as input. To exclude complex formation after cell lysis, extracts from single transfected myc–Nup53 and HA–Nup53 cell batches were mixed and processed for immunoprecipitation (✧). Under these conditions, no co-precipitation was observed. (**C**) Full-length Xenopus Nup53 and the respective F172E/W203E mutant (RRM mutant) were analysed for liposome binding as in Figure 1. The right panel shows the quantitation of liposome binding analysed by western blotting and normalized to the levels of the wild-type protein (one out of two independent experiments). (**D**) Western blot analysis of mock, Nup53-depleted (ΔNup53) and Nup53-depleted extracts supplemented with recombinant wild-type protein (Nup53) or the dimerization mutant (Nup53 RRM mutant), respectively. Recombinant proteins were added to approximate endogenous Nup53 levels (judged by the full-length protein, please note for both endogenous and recombinant Nup53 proteins C-terminal degradation products (*)). The recombinant Nup53 migrated slightly faster than the endogenous protein due to absence of eukaryotic post-translational modifications. The Nup93 antibody recognizes a slightly slower migrating cross-reactivity by western blotting (*). (**E**) Nuclei were assembled in mock, Nup53-depleted extracts or Nup53-depleted extracts supplemented with wild-type protein (Nup53) or the dimerization mutant for 120 min, fixed with 4% PFA and analysed with Nup53 antibodies (red) and mAb414 (green). Chromatin was stained with DAPI. Bar: 10 μm. (**F**) Nuclei were assembled as in (**E**), fixed with 2% PFA and 0.5% glutaraldehyde and analysed for chromatin (blue: DAPI) and membrane staining (red: DiIC18, bar: 10 μm). Right panel shows the quantitation of chromatin substrates with a closed nuclear envelope (averages of three independent experiments with >300 randomly chosen chromatin substrates per sample, error bars represent the range).

amino acids identified, Serine 94 and Threonine 100, are phosphorylated during mitosis, most likely by cdk 1 as they possess a consensus site for this kinase (Blethrow *et al*, 2008). To investigate the impact of this modification on membrane binding, we generated mutants mimicking the phosphorylated (S94E/T100E) and the unphosphorylated

©2012 European Molecular Biology Organization

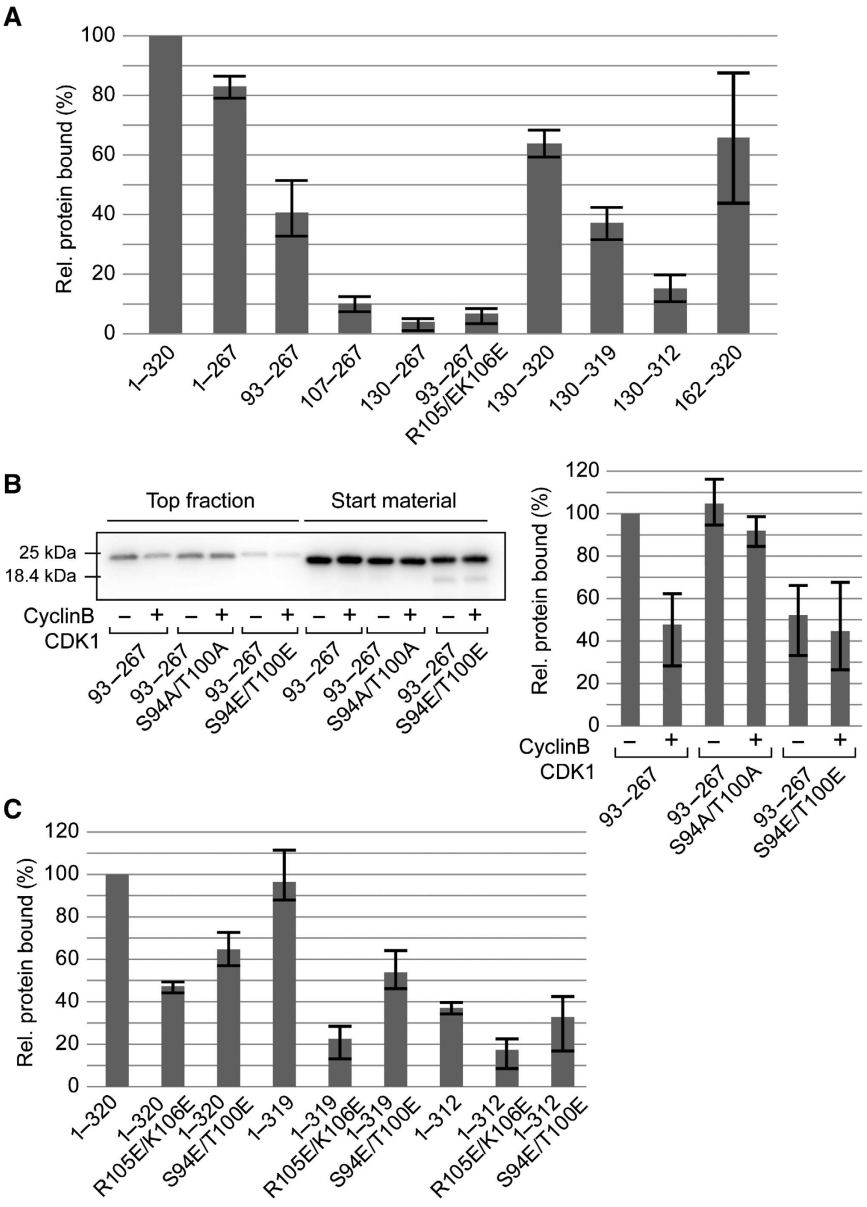

Figure 3 Nup53 possesses two independent membrane binding regions. (**A**) Full-length protein (1–320) and different fragments of Xenopus Nup53 were quantitatively analysed for liposome binding as in Figure 2B (normalized to the full-length protein, three independent experiments). (**B**) A fragment comprising the first membrane binding region and the RRM domain (93–267) as well as a phosphomimetic (93–267 S94E/T100E) and a non-phosphorylatable mutant (93–267 S94A/T100A) was treated with CyclinB/CDK1. Samples were tested for liposome binding as in Figure 1A and analysed by western blotting (left panel) and quantified (right panel: two independent experiments, normalized to liposome binding of wild-type fragment without CDK1 pretreatment). (**C**) Mutants/truncations affecting the N- (1–320 R105E/K106E, 1–320 S94E/T100E), the C-terminal (1–319, 1–312) as well as both (1–319 R105E/K106E, 1–319 S94E/T100E, 1–312 R105E/K106E, 1–312 S94E/T100E) membrane binding sites of Nup53 were quantitatively assayed for liposome binding in the context of full-length protein (normalized to wild-type protein (1–320), average of three independent experiments, error bars represent the range).

(S94A/T100A) state of the protein. The phosphomimetic mutant was impaired in liposome binding (Figure 3B, reduced by 50% compared to the 93–267 fragment) while the S94A/T100A control bound to liposomes with efficiency comparable to the wild type. Furthermore, *in vitro* phosphorylation by CyclinB/CDK1 reduced liposome binding of the wild-type protein by 50%, levels similar to the phosphomimetic mutant (S94E/T100E), but did not affect the S94A/T100A mutant, suggesting that mitotic phosphorylation regulates the membrane binding of Nup53.

The C-terminal part of Nup53 also interacts with membranes, an activity that requires the presence of the RRM domain (Figure 1B). Fragments comprising both regions showed efficient binding to liposomes (aa 130–320 and 162–320) (Figure 3A). The second membrane binding region was mapped to the absolute C-terminus of Nup53 as deletion of the last amino acid reduced liposome binding by 42% (aa 130–319) and removal of the last eight amino acids abolished liposome binding (aa 130–312).

These data suggest that Nup53 possesses two independent membrane binding sites. Consistently, in the context of the full-length protein mutations in the N-terminal site (R105E/K106E as well as S94E/T100E) reduced liposome binding by 50 and 40% (Figure 3C). Deletion of the

 ©2012 European Molecular Biology Organization

C-terminal amino acid had a less prominent effect, but removal of the last eight amino acids reduced liposome binding by 60%. The combination of mutations and truncations affecting both binding sites showed an additive effect supporting the view that each site is individually capable of membrane binding. Our data also suggest that the N-terminal membrane interaction is mediated via a pair of basic amino acids. The N-terminal binding site is additionally dependent on membrane curvature, the fragment binding less efficiently to more highly curved membranes (Supplementary Figure S4). Conversely, the C-terminal membrane binding site is less sensitive to membrane curvature and seems to largely depend on the last amino acid, a hydrophobic tryptophan. This could indicate that the two membrane interaction sites operate via different binding mechanisms. In both cases, the dimerization of Nup53 via the RRM domain is important: mutations in the individual membrane binding fragments (93–267 F172E/W203E and 130–320 F172E/W203E) rendering the RRM domain monomeric reduced their membrane interaction (Supplementary Figure S5).

Nup53 membrane binding is necessary for NPC formation

The Nup53 mutant defective in RRM dimerization, which showed reduced membrane binding, was unable to substitute for the endogenous protein in nuclear assembly (Figure 2). We therefore analysed the contribution of each of the membrane interaction sites to NPC assembly by substituting endogenous Nup53 with constructs defective in the N-terminal membrane interaction site, lacking the C-terminal membrane interaction site, or comprising a combination of both deficient sites (Figure 4A). Surprisingly, mutants of the N-terminal membrane binding site (1–320 R105E/K106E and 1–320 S94E/T100E) supported NPC formation as indicated by mAB414 staining (Figure 4A). They also supported formation of a closed NE (Figure 4A and B). Correspondingly, mutations in the N-terminal binding region did not alter the NE localization of any other nucleoporins (Figure 4D). These nucleoporins include members of the Nup93 complex (Nup93, Nup188, Nup205 and Nup155) as well as the transmembrane nucleoporins NDC1 and POM121. Accordingly, interactions of these mutants with Nup93 and Nup205, which bind the N-terminal part of Nup53 (Fahrenkrog *et al*, 2000; Hawryluk-Gara *et al*, 2008), were unaffected as shown by GST pull downs (Supplementary Figure S1A).

The fragment lacking the C-terminal tryptophan (1–319) also supported NPC assembly and formation of a closed NE. Deletion of this tryptophan did not interfere with Nup53 binding to NDC1 or Nup155 (Supplementary Figure S1B), two binding partners interacting with the C-terminal region. The truncation lacking the last eight C-terminal amino acids (1–312) also allowed for NPC assembly and formation of a closed NE. All tested nucleoporins were located at the NE in these nuclei (Figure 4D). Notably, this truncation did not bind to NDC1 (Supplementary Figure S1B), supporting the view that the Nup53–NDC1 interaction is not required for postmitotic NPC formation (Hawryluk-Gara *et al*, 2008). These observations suggest that a single Nup53 membrane binding region is sufficient for NPC assembly at the end of mitosis.

In contrast to the Nup53 mutants and truncations that abrogate one membrane binding region, mutants affecting both membrane binding sites (1–319 R105E/K106E, 1–319 S94E/T100E, 1–312 R105E/K106E and 1–312 S94E/T100E) did not support NPC assembly and NE reformation (Figure 4A). Under these conditions, MEL28 (also referred to as ELYS) as well as Nup107, which both bind early to chromatin during the NPC assembly process (Galy *et al*, 2006; Rasala *et al*, 2006; Franz *et al*, 2007), as well as the transmembrane nucleoporins, NDC1 and POM121, were detected on the chromatin (Figure 4D). In contrast, Nup205, Nup188, Nup155 and Nup93 were not recruited. However, this lack of recruitment as well as the block in NPC assembly is unlikely to be caused by disrupting Nup53 binding to these interaction partners as the mutations introduced did not affect binding to Nup93, Nup205 and Nup155 in GST pull downs (Supplementary Figure S1A). It is also unlikely that the loss of the Nup53–NDC1 interaction caused this phenotype as the Nup53 fragment 1–312 still allowed for postmitotic NPC assembly but was not able to bind NDC1 (Supplementary Figure S1B). Nup58 representing an FG-containing nucleoporin of the central channel as well as the peripheral nucleoporin Nup88 was also absent on chromatin in the presence of a Nup53 construct that lacked both membrane binding regions (1–312 R105E/K106E) (Figure 4D). These data support the conclusion that the direct Nup53 membrane interaction is important for postmitotic NPC formation.

Interphasic NPC assembly requires the C-terminal membrane binding site of Nup53

Metazoan NPC assembly occurs in two different stages of the cell cycle: at the end of mitosis when NPCs assemble concomitantly with the reforming NE and during interphase when new NPCs are assembled and integrated into the intact NE (Antonin *et al*, 2008; Doucet and Hetzer, 2010). Recent data suggest that there are different requirements for these two possible modes of NPC assembly (Doucet *et al*, 2010). The *in vitro* nuclear assemblies described up to now reflect the situation at the end of mitosis. We therefore assayed whether the mutants that support postmitotic NPC assembly also support NPC formation during interphase. In an experimental set-up developed by the Hetzer laboratory (Dawson *et al*, 2009), nuclei with newly integrated NPCs can be visualized by an influx of dextrans when nucleoporins forming the permeability barrier of newly formed NPCs are depleted. Under these conditions, mutants defective in the N-terminal membrane binding site of Nup53 (1–320 R105E/K106E and 1–320 S94E/T100E) supported interphasic NPC formation (Figure 5A). Conversely, Nup53 truncations affecting the C-terminal membrane binding site did not substitute for the wild-type protein in this mode of NPC assembly. This indicates that, in contrast to postmitotic NPC assembly where both membrane binding regions individually support NPC formation, only the C-terminal membrane binding site of Nup53 is required for interphasic NPC formation.

Interestingly, the Nup53 truncation lacking the C-terminal tryptophan (1–319) did not support interphasic NPC assembly in the dextran influx assay despite the fact that membrane interaction is only slightly reduced (Figure 3C). We confirmed these findings in an independent assay directly counting NPCs identified by mAB414 immunostaining (D'Angelo *et al*, 2006; Theerthagiri *et al*, 2010). NPC numbers were determined on nuclei where NPCs assembled in the postmitotic and interphasic mode and nuclei where interphasic

©2012 European Molecular Biology Organization

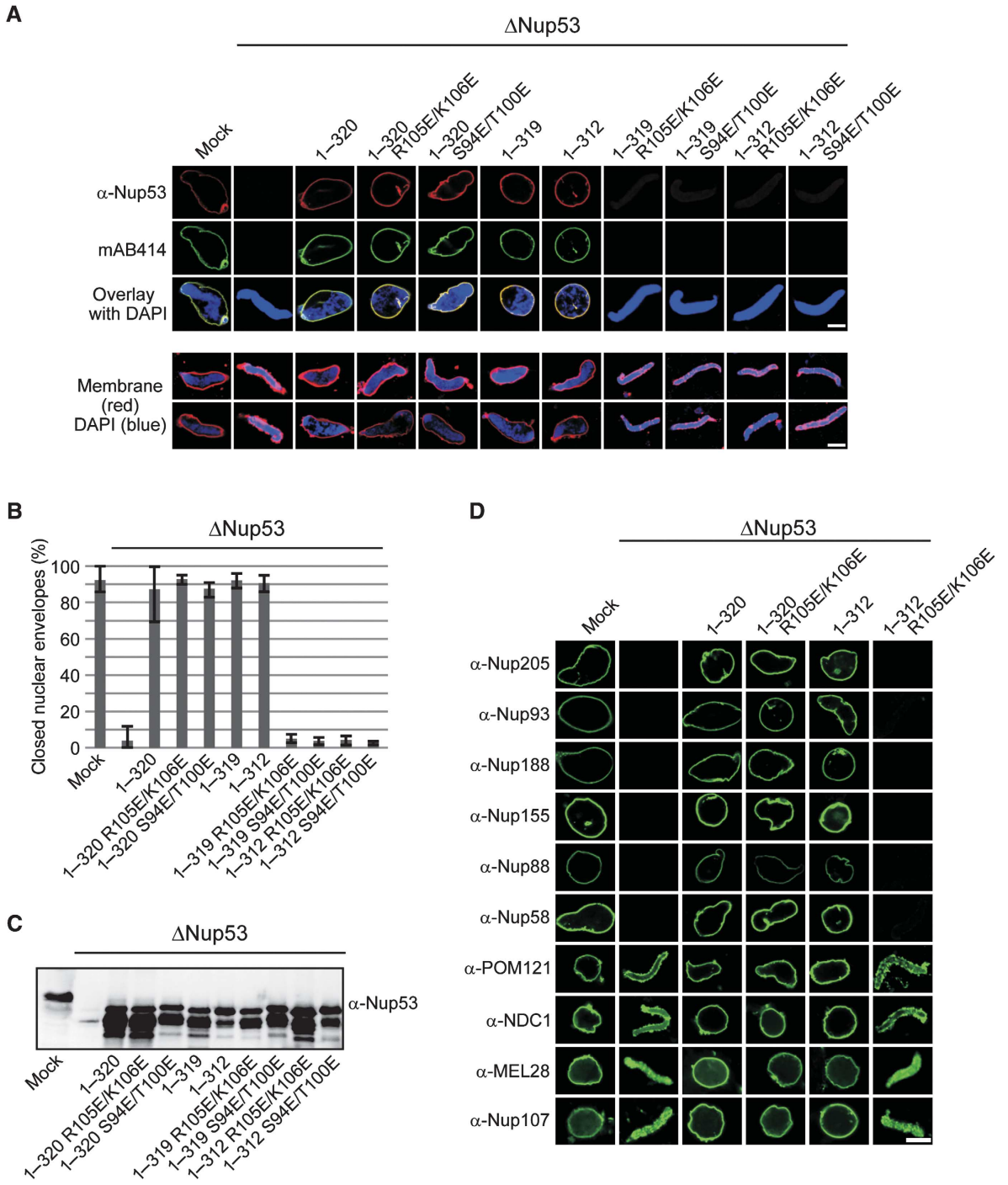

Figure 4 Either of the two membrane binding regions of Nup53 is sufficient for postmitotic NPC assembly. (**A**) Nuclei were assembled in mock, Nup53-depleted extracts or Nup53-depleted extracts supplemented with wild-type Nup53 (1–320), constructs featuring mutations in the N-terminal membrane binding site (1–320 R105E/K106E, 1–320 S94E/T100E), constructs lacking the C-terminal membrane binding site (1–319, 1–312) or both (1–319 R105E/K106E, 1–319 S94E/T100E, 1–312 R105E/K106E, 1–312 S94E/T100E), respectively. Samples were fixed after 120 min with 4% PFA and analysed with Nup53 antibodies (red) and mAb414 (green, upper panel) or with 2% PFA and 0.5% glutaraldehyde and analysed for chromatin (blue: DAPI) and membrane staining (red: DiIC18, lower panel). Bars: 10 μm. (**B**) Quantitation of chromatin substrates with a closed NE was done as in Figure 2F. (**C**) Western blot analysis of extracts used in (**A**) showing the re-addition of the recombinant proteins to approximately endogenous Nup53 levels. (**D**) Nuclei were assembled as in (**A**), fixed with 4% PFA and analysed with respective antibodies. Bar: 10 μm.

NPC formation was specifically blocked by addition of 2 μM importin β (D'Angelo *et al*, 2006; Theerthagiri *et al*, 2010). The NPC numbers of nuclei assembled for 120 min in the presence of recombinant wild-type Nup53 as well as the Nup53 mutant defective in the N-terminal membrane binding site (1–320 R105E/K106E) were reduced by importin β addition after 50 min, i.e., when a closed NE with intact NPC was formed (Figure 5B). In contrast, the Nup53 truncation lacking the C-terminal tryptophan showed after 120 min a lower number of NPCs, which was not sensitive to importin β addition, indicating that in this condition interphasic NPC assembly did not occur.

 ©2012 European Molecular Biology Organization

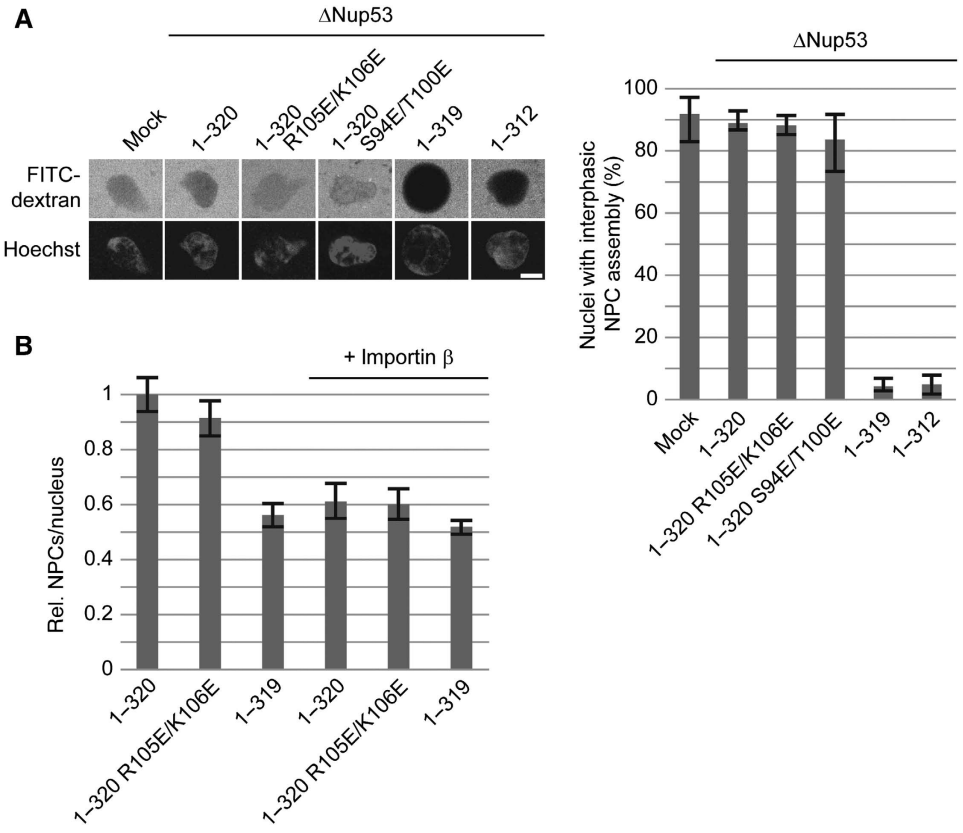

Figure 5 The C-terminal Nup53 membrane binding site is essential for interphasic nuclear pore complex (NPC) formation. (**A**) Nuclei were preassembled in mock or Nup53-depleted extracts supplemented with wild-type full-length protein (1–320), constructs with a mutated N-terminal membrane binding site (1–320 R105E/K106E, 1–320 S94E/T100E), or constructs lacking the C-terminal membrane interaction site (1–319, 1–312), respectively. After 90 min, the samples were supplemented with cytosol depleted of Nup53 and FG-containing nucleoporins. After 60 min, FITC-labelled 70-kDa dextran and Hoechst was added. Bar: 10 μm. The right panel shows the quantitation of three independent experiments with >300 randomly chosen chromatin substrates per sample. Error bars represent the range. (**B**) Nuclei were assembled in Nup53-depleted extracts supplemented with wild-type full-length protein (1–320), a construct with a mutated N-terminal membrane binding site (1–320 R105E/K106E), or a construct lacking the last C-terminal amino acid (1–319), respectively, for 120 min. Where indicated, *de novo* NPC assembly was blocked by the addition of 2 μM importin β after 50 min and nuclei were further incubated for 70 min. For each construct, total NPC numbers per nucleus identified by mAB414 immunofluorescence were quantified from 20 nuclei in 2 independent experiments and normalized to the wild-type full-length protein. Error bars represent the s.e. of the mean.

Nup53 can deform membranes

Many membrane binding proteins induce membrane deformation. Such a function is of special interest in the context of NPC formation as NPCs are integrated in the NE at sites where both nuclear membranes are deformed and fused to a pore. We therefore analysed the morphology of Nup53-bound liposomes using electron microcopy. As reported (Daumke *et al*, 2007), tubulation of liposomes is induced by the EH domain-containing protein EHD2 (Figure 6A). Interestingly, a Nup53 fragment containing both membrane binding sites (93–320) strongly induced liposome tubulation indicating a membrane deformation capability. A shorter fragment containing only the N-terminal membrane binding site and including the RRM domain (93–267) did not induce membrane tubulation, despite the fact that it was able to bind liposomes (Figure 3A). In contrast, a fragment comprising the RRM domain and the full C-terminus of Nup53 (130–320) strongly induced membrane tubulation indicating that the second, C-terminal membrane binding domain deforms membranes. Accordingly, fragments lacking the last eight residues (130–312), and therefore the second membrane binding site or only the last C-terminal tryptophan (130–319) did not cause membrane tubulation. Consistently, fragments mutated in the first, or N-terminal, membrane binding region of Nup53 (93–320 R105E/K106E and 93–320 S94E/T100E) induced membrane deformation. Efficient membrane binding of Nup53 depends not only on the individual membrane binding domains but also on dimerization (Figure 2C; Supplementary Figure S5). To determine the importance of the dimerization of Nup53 for membrane tubulation the RRM mutants of fragments that contained either both (93–320 RRM mutant) or only the C-terminal binding site (130–320 RRM mutant) were tested. Neither of the two fragments induced membrane tubulation emphasizing that membrane interaction is indeed required for this phenotype. The membrane binding fragment of Nup133 did not induce detectable tubulation, emphasizing that membrane binding alone does not account for membrane deformation.

Similar to Xenopus Nup53 both yeast isoforms—Nup53p and Nup59p—induced membrane tubulation (Figure 6B). This indicates that, in addition to membrane binding (Figure 1A), the membrane bending activity of Nup53 is conserved during evolution which suggests an important role for Nup53-induced membrane deformation in NPC formation and/or function.

©2012 European Molecular Biology Organization

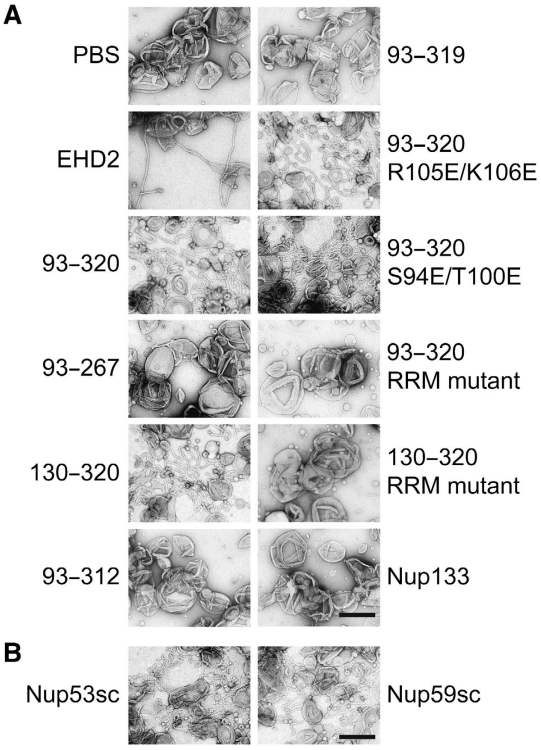

Figure 6 The C-terminus of Nup53 binds and deforms membranes. (**A**) Folch fraction I liposomes were incubated where indicated with 3 μM recombinant Nup53 fragments containing both (93–320), the N-terminal (93–267) or C-terminal (130–320) membrane binding sites including the RRM domain as well as fragments and mutants where the C-terminal (93–312, 93–319), the N-terminal (93–320 R105E/K106E, 93–320 S94E/T100E) membrane interaction site or the dimerization (93–320 RRM mutant and 130–320 RRM mutant) is compromised. The liposome deforming protein EHD2 (aa 1–543) and a fragment of Nup133 were used as positive and negative control, respectively. (**B**) 3 μM recombinant yeast Nup53 and Nup59 protein was incubated with liposomes and analysed. Bars: 400 nm.

Discussion

Here, we show that Nup53 binds membranes directly and independently of other proteins. We demonstrate that dimerization of the protein via its RRM domain is necessary for membrane interaction and identify two separate membrane binding regions within the protein. Binding of Nup53 to membranes is important for NPC assembly. Although either of the two membrane interaction regions is sufficient for postmitotic NPC formation, NPC assembly in interphase specifically requires the C-terminal membrane binding site, probably because of its capacity to induce membrane deformation.

Our results support the view that Nup53 is crucial for postmitotic NPC assembly in Xenopus egg extracts (Hawryluk-Gara *et al*, 2008). Depletion of Nup53 blocks NPC assembly and the formation of a closed NE. This phenotype is rescued by the addition of recombinant Nup53, confirming the specificity of the depletion (Hawryluk-Gara *et al*, 2008; Figures 2 and 4). In agreement with the cell-free data, RNAi-mediated depletion of Nup53 in HeLa cells results in severe nuclear morphology defects and reduced levels of Nup93, Nup205 and Nup155 at the nuclear rim, suggestive of defects in NPC assembly (Hawryluk-Gara *et al*, 2005). In *C. elegans*, RNAi knockdown of Nup53 as well as a deletion within the protein blocks postmitotic nuclear reformation and results in embryonic lethality (Galy *et al*, 2003; Rodenas *et al*, 2009), suggesting that Nup53 function is conserved in metazoa. Notably, Nup53 is found in all eukaryotic supergroups indicating that it is part of the NPC in the last common ancestor of eukaryotes (Neumann *et al*, 2010). However, its absence in some eukaryotic organisms shows that its loss can be compensated (DeGrasse *et al*, 2009; Neumann *et al*, 2010). Double deletion of both *S. cerevisiae* orthologues, Nup53p and Nup59p, is viable (Marelli *et al*, 1998; Onischenko *et al*, 2009). However, these strains exhibit growth defects and Nup53 becomes essential when interacting nucleoporins, including integral membrane proteins, are deleted (Marelli *et al*, 1998; Miao *et al*, 2006; Onischenko *et al*, 2009).

NPC assembly is a highly ordered process. In metazoa the NE and NPCs break down and reform during each round of mitosis. Postmitotic reassembly occurs on the decondensing chromatin. The earliest step involves the recruitment of the Nup107–160 subcomplex to the chromatin surface by MEL28/ELYS (Galy *et al*, 2006; Rasala *et al*, 2006; Franz *et al*, 2007), a DNA-binding protein that acts as a seeding point for NPC assembly. Membranes are subsequently recruited to chromatin causing an enrichment of NE/NPC-specific membrane proteins, including the transmembrane nucleoporins POM121 and NDC1 (Antonin *et al*, 2005; Mansfeld *et al*, 2006; Anderson *et al*, 2009). The order of these initial steps has been defined using both *in vitro* experiments and live-cell imaging (Dultz *et al*, 2008); however, less is known about the order of nucleoporin assembly following these events. MEL28 and Nup107 as well as POM121 and NDC1 containing membranes are detectable on the chromatin in Nup53-depleted nuclear assemblies (Figure 4D). The same pattern was seen in Nup93-depleted extracts (Sachdev *et al*, 2012). Our results suggest that Nup53, which is part of the Nup93 complex, is a key determinant for the recruitment of the other members of this complex. In the absence of Nup53, the chromatin recruitment of Nup155, Nup205, Nup188 and Nup93 was impaired (Figure 4D). Similarly, *C. elegans* Nup53 is necessary for the efficient accumulation of Nup155 and Nup58 but not Nup107 at the NE (Rodenas *et al*, 2009). This is also supported by live-cell imaging experiments in HeLa cells, which capture the recruitment of Nup58 slightly after Nup93 (Dultz *et al*, 2008). Accordingly, we have found that upon depletion of the two Nup93 containing subcomplexes, Nup93–Nup188 and Nup93–205, the two other members of the complex, Nup155 and Nup53, are still detectable, albeit at reduced levels on the assembling NPCs (Sachdev *et al*, 2012). Recruitment of the Nup62 complex to the chromatin template is prevented in the absence of both Nup53 (see lack of a Nup58 immunostaining, which is a constituent of the Nup62 complex, in Figure 4D) and Nup93 (Sachdev *et al*, 2012) consistent with the notion that Nup93 is a key determinant in recruiting the Nup62 complex during vertebrate NPC assembly at the end of mitosis (Sachdev *et al*, 2012). Taken together, these data suggest that after the binding of the Nup107–160 complex and nuclear membranes to the chromatin surface, Nup53 recruitment is the next decisive step in NPC assembly. Nup93 (Nup93–Nup188/Nup93–Nup205) binding and the subsequent recruitment of the Nup62 complex follow.

Nup53 interacts with a number of other nucleoporins, including NDC1, Nup155 and Nup93 (Lusk *et al*, 2002;

 ©2012 European Molecular Biology Organization

Hawryluk-Gara *et al*, 2005, 2008; Mansfeld *et al*, 2006; Sachdev *et al*, 2012) a feature that is conserved in yeast (Fahrenkrog *et al*, 2000; Onischenko *et al*, 2009; Amlacher *et al*, 2011). As previously reported (Hawryluk-Gara *et al*, 2008), the interaction of Nup53 with NDC1 is not necessary for postmitotic NPC assembly in Xenopus egg extracts (Figure 4A). A possible explanation might be that Nup53 can interact directly with membranes and that one of its two membrane binding regions is sufficient for postmitotic NPC formation. In addition, Nup53 interaction with other nucleoporins such as Nup155, which in turn binds POM121 (Mitchell *et al*, 2010; Yavuz *et al*, 2010) could be a possible mechanism linking Nup53 to the pore membrane which might compensate for the loss of the direct Nup53–NDC1 interaction.

The interaction of Nup53 with Nup155 is thought to be important for NPC assembly. A previous study found that after depleting Nup53 from Xenopus egg extracts, only fragments capable of binding to Nup155 allow for NPC formation (Hawryluk-Gara *et al*, 2008). However, in this case all fragments that rescued the NE/NPC assembly defect included the RRM domain and all fragments defective in NPC assembly and the Nup155 interaction lacked the intact RRM domain. Similarly, a deletion in *C. elegans* Nup53 blocked NE assembly also impaired the RRM domain (Rodenas *et al*, 2009). We demonstrate here that the RRM domain is important for Nup53 dimerization and in turn for membrane binding. Therefore, we currently cannot rule out that the primary cause for the previously described defects was a loss of the Nup53 membrane interaction.

Nup93 binds directly Nup53 (Hawryluk-Gara *et al*, 2005; Sachdev *et al*, 2012) and the interaction domain resides in the N-terminal half of Nup53 (Hawryluk-Gara *et al*, 2008). This interaction was previously considered to be dispensable for NPC assembly as a fragment lacking the N-terminal region as well as the C-terminal 26 amino acids replaced endogenous Nup53 in nuclear assemblies in Xenopus egg extracts (Hawryluk-Gara *et al*, 2008). This is quite surprising in the light of the results presented here, as this fragment also lacked both membrane binding regions identified in this study and does not allow for Nup93 recruitment which is an essential factor for postmitotic NPC assembly (Sachdev *et al*, 2012). Using a number of different Nup53 fragments that lacked the Nup93 binding region we were not able to replace endogenous Nup53 in NPC assembly (Supplementary Figure S6). Currently, we cannot rule out that this discrepancy is due to different Nup53 depletion efficiencies. In fact, we found that a small percentage of floated membrane preparations used in the nuclear assembly reactions contained minor amounts of Nup53, and we were careful to exclude these from our experiments.

Nup53 is also known as mitotic phosphoprotein of 44 kDa (Stukenberg *et al*, 1997). Indeed, Nup53 from mitotic extracts migrates significantly slower in SDS–PAGE compared to Nup53 from interphasic extracts (Supplementary Figure S3A). We identified a number of mitosis-specific phosphorylation sites on Nup53, of which a subset were consensus sites for CDK1. These findings are consistent with the fact that Nup53 has been identified as a CDK1 target in both yeast and humans (Lusk *et al*, 2007; Blethrow *et al*, 2008). The N-terminal membrane binding region of Nup53 is phosphorylated during mitosis. Phosphomimetic mutations and *in vitro* phosphorylation experiments suggest that CDK1-mediated phosphorylation renders this region incompetent for membrane interaction (Figure 3B). It is therefore possible that this mitotic phosphorylation weakens the interaction of Nup53 with the pore membrane to facilitate NPC disassembly during prophase.

Proteins without integral membrane regions can associate with cellular membranes by a variety of mechanisms (Cho and Stahelin, 2005). First, they can be covalently attached to a lipid moiety. However, we have no indication that Nup53 is modified in such a way. Second, peripheral membrane proteins are recruited to the lipid bilayer by specific protein–lipid interactions that involve binding to particular lipid head groups. In this regard, lipid arrays performed to date have not demonstrated an affinity of Nup53 for any specific lipid (unpublished observation). Furthermore, recombinant Nup53 binds to liposomes prepared from different lipid sources like pure DOPC (1,2-dioleoyl-*sn*-glycero-3-phosphocholine), a lipid mixture mimicking the ER/NE lipid composition (Franke *et al*, 1970; Supplementary Figure S7) or folch fraction I (unpublished observation). Third, some proteins are recruited to membranes via electrostatic interactions. As a fraction of the lipid head groups are negatively charged this involves positively charged clusters on the protein surface. Indeed, we found that the first membrane binding region of Nup53 contains such a cluster. Replacing these positive with negative residues as well as introducing negative charge by phosphorylation rendered this site incapable of membrane interaction (Figure 3A and B). Finally, peripheral membrane proteins can associate with lipid bilayers via hydrophobic regions. It has been suggested that the C-terminal region of Nup53 contains an amphipathic helix, which could serve as a hydrophobic module (Marelli *et al*, 2001; Patel and Rexach, 2008). In fact, the C-terminus of Nup53 contains a membrane binding region and deleting the last eight amino acids abolished its membrane interaction. Deletion of the C-terminal tryptophan only slightly reduced membrane binding of Nup53 in the full-length protein (Figure 3C), but inhibited interphasic NPC assembly (Figure 5) suggesting that this residue fulfills an important additional function. Indeed, the insertion of hydrophobic parts of a protein into a membrane is one of several mechanisms by which proteins can deform membranes (McMahon and Gallop, 2005). Our data suggest that the C-terminal membrane binding region and especially the last tryptophan of Nup53 fulfills this task (Figure 6A). Interestingly, *in vivo* intranuclear tubular membranes are induced upon overexpression of yeast Nup53p which is dependent on its C-terminus (Marelli *et al*, 2001). Thus, Nup53 might not only have an important function in binding to the pore membrane in turn promoting the recruitment of other nucleoporins, especially members of the Nup93 complex, but may additionally function to deform the NE membrane into a pore. In the latter instance, the insertion of the Nup53 C-terminus into the hydrophobic phase of the membrane would result in displacement of lipid head groups and reorientation of the hydrophobic lipid side chains, bending the lipid bilayer into a convex shape and inducing membrane curvature necessary to form and stabilize the pore (Antonin *et al*, 2008). The doughnut-like shape of the pore requires likewise stabilization of a concave curvature in the plane of the pore in addition to the convex curved membrane

©2012 European Molecular Biology Organization

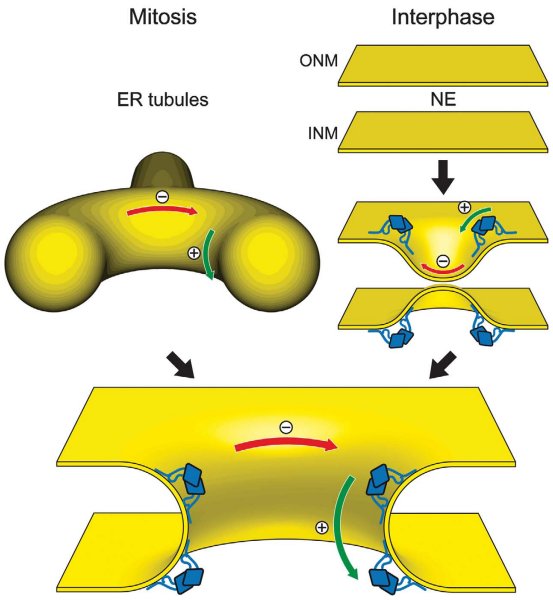

Figure 7 The role of Nup53 in NPC assembly. Schematic drawing of the postmitotic and interphasic modes of nuclear pore assembly focused on the membrane interacting function of Nup53. For the sake of clarity other membrane associated and integral proteins, including nucleoporins, participating in this process are omitted. Left pathway: after mitosis, outgrowing ER tubules (yellow) surround assembling NPCs providing negative/concave (red) and positive/convex (green) curvature which is stabilized by membrane binding Nup53 dimers (blue) for pore formation. Right pathway: in interphase, the intact nuclear envelope membranes (yellow) are deformed by the C-terminal membrane binding site of Nup53 introducing a convex membrane curvature for the approximation and following fusion of the two membranes leading to pore formation.

connection between outer and inner nuclear membrane (see Figure 7). This curvature might be induced and stabilized by a number of at least partially redundant mechanisms, such as formation of a coat-like structure by the Nup107–160 complex (Devos *et al*, 2004; Mans *et al*, 2004; Brohawn *et al*, 2008) or oligomerization of pore membrane proteins, although it is not clear how the different proteins contribute to the different modes of membrane bending. Similarly, in the context of the protein interaction network of an assembled NPC the N-terminal membrane binding region of Nup53, in addition to membrane interaction, might induce and/or stabilize curved membranes. Indeed, Nup53 is only functional when it dimerizes probably because this increases the avidity of the Nup53 membrane interaction. In addition, all the factors might also impose geometrical constrains to the membranes supporting a pore structure.

Although either one of the two membrane binding regions of Nup53 is sufficient for postmitotic NPC assembly and stability, the C-terminal site is specifically required for NPC assembly during interphase. It is a matter of debate whether NPC assembly during these different cell-cycle phases occurs by distinct mechanisms (Doucet *et al*, 2010; Dultz and Ellenberg, 2010; Lu *et al*, 2011). At the end of mitosis, NPC assembly occurs concomitantly with formation of a closed NE. It is possible that this mode of NPC formation does not require fusion between the outer and inner nuclear membrane to form a nuclear pore, in contrast to interphasic NPC assembly. Postmitotic pore assembly could rather arise by the enclosement of the assembling NPCs on the chromatin surface by an outgrowing ER network. In this scenario, Nup53 would stabilize the membrane curvature provided by the ER tubules rather than induce membrane deformation (see Figure 7, left pathway). The different requirements for Nup53 membrane binding regions in postmitotic and interphasic NPC assembly support the view of two different mechanistic pathways. A loss of the membrane deforming capability of Nup53 in postmitotic NPC assembly and NPC stability might be compensated by other factors such as the Nup107–160 complex or integral membrane proteins. However, during metazoan interphasic NPC assembly Nup53-mediated membrane deformation might be crucial for the initial approximation and/or fusion of both membrane layers (see Figure 7, right pathway). Interestingly, ER bending proteins of the reticulon family that induce convex membrane curvature (Hu *et al*, 2008) were shown to be important for NPC assembly into the intact NE both in yeast and in vertebrates (Dawson *et al*, 2009). Currently, it is unknown whether these proteins do also contribute to postmitotic NPC assembly. As their effect on ER membrane reorganization at the end of mitosis is a prerequisite for NE reformation (Anderson and Hetzer, 2008) it is difficult to separate these two functions. Finally, how the fusion of outer and inner nuclear membranes is achieved is largely unclear but our results suggest that Nup53, importantly its C-terminal membrane binding region, is critical for this process.

Materials and methods

Antibodies against POM121 and GP210 (Antonin *et al*, 2005), NDC1 (Mansfeld *et al*, 2006), Nup155 (Franz *et al*, 2005), MEL28/ELYS (Franz *et al*, 2007), Nup107 (Walther *et al*, 2003), Nup53 and Nup58 (Sachdev *et al*, 2012) as well as Nup188, Nup205, Nup98 and Nup53 (Theerthagiri *et al*, 2010) have been described. mAB414 and Nup88 antibodies were from Babco or BD Bioscience, respectively. For quantitation of Nup53 liposomes binding the antibody was affinity purified with a fragment comprising the RRM domain as this domain is included in all tested fragments (please see Supplementary Table S2 for list of all DNA constructs used in this study).

Nuclear assemblies

Nuclear assemblies and immunofluorescence (Theerthagiri *et al*, 2010), generation of affinity resins, sperm heads and floated membranes (Franz *et al*, 2005) as well as prelabelled membranes (Antonin *et al*, 2005) were done as described. Interphasic NPC assembly using dextran influx was monitored as described (Dawson *et al*, 2009) except that mock or Nup53-depleted extracts were incubated with 1.5 vol WGA-Agarose (Sigma) for 40 min. Counting of NPCs was performed on mAB414-labelled nuclei as described (Theerthagiri *et al*, 2010).

Protein expression and purification

Constructs for full-length Xenopus Nup53 and fragments, *S. cerevisiae* Nup53 and Nup59 were generated from a synthetic DNA optimized for codon usage in *E. coli* (Geneart, see Supplementary data) and cloned into a modified pET28a vector with a yeast SUMO solubility tag followed by a TEV site upstream of the Nup53 fragments. Proteins were expressed in *E. coli*, purified using Ni-agarose, His_6 and SUMO tags were cleaved by TEV protease, concentrated using VIVASPIN columns (Sartorius) and purified by gel filtration (Superdex200 10/300 GL or Superdex200 PC 3.2/30, GE Healthcare) either in PBS for liposome binding experiments or in sucrose buffer (Theerthagiri *et al*, 2010) for nuclear assemblies, respectively. Nup53 fragments aa 162–320 and aa 254–320 were purified by size exclusion chromatography without removal of the tags to retain stability. Fragments of Xenopus Nup98 (aa 676-863) as well as human Nup133 (aa 67–514) (Berke *et al*, 2004) were expressed from modified pET28a vectors with a His_6-NusA or

©2012 European Molecular Biology Organization

His_6 tag, which was cleaved of by thrombin or precision protease, respectively.

Liposome generation and flotation

E. coli polar lipid extract with 0.2 mol% 18:1–12:0 NBD-PE (1-oleoyl-2-{12-[(7-nitro-2-1,3-benzoxadiazol-4-yl)amino]dodecanoyl}-sn-glycero-3-phosphoethanolamine) (Avanti polar lipids) were dissolved in ethanol at 45°C. To form liposomes, the mixture was diluted 10-fold into PBS resulting in a final lipid concentration of 6.7 mg/ml while gently agitating. Liposomes were passed 21 × through Nuclepore Track-Etched Membranes (Whatman) with defined pore sizes (50, 100, 200, 400, 800 nm) at 45°C using the Avanti Mini-Extruder. To remove ethanol, liposomes were dialysed against PBS using Spectra/Por 2 dialysis tubing (MWCO 12-14 kDa). Liposome sizes were determined by light scattering using the AvidNano W130i. For quantitation of liposome binding, fluorescence intensity of the protein/liposome mixture and the top fraction was determined using a Molecular Imager VersaDoc MP 4000 Imaging System and ImageJ.

Folch fraction I lipids (Sigma) dissolved in chloroform were dried on a rotary evaporator and overnight under vacuum. PBS buffer was gently added to result in a final lipid concentration of 10 mg/ml. After 2 h of incubation at 37°C to allow spontaneous liposome formation the flask was agitated to dissolve residual lipids. After 10 cycles of freeze/thawing, liposomes were diluted 10-fold in PBS and extruded as described before.

Immunoprecipitation

Xenopus Nup53 as well as the RRM dimerization mutant (F172E/W203E) was cloned with N-terminal myc or HA tag, respectively, into a pSI vector (Promega). HeLa cells were transfected using Fugene 6 (Roche) following manufacturer's instructions, harvested 24 h post transfection and solubilized in 1% Triton X-100 in PBS supplemented with protease inhibitors (2 μg/ml leupeptin, 1 μg/ml pepstatin, 2 μg/ml aprotinin, 0.1 mg/ml AEBSF final concentration) for 10 min at 4°C. After centrifugation for 10 min at 15 000 *g* samples were diluted five-fold in PBS and employed for immunoprecipitation using α-myc or α-HA antibodies (Roche).

Miscellaneous

For *in vitro* phosphorylation, 3 μM proteins were incubated with 0.33 U/μl CDK1-CyclinB (NEB), 1 mM ATP, 10 mM $MgCl_2$ and 1 mM EDTA in PBS for 1 h at 30°C.

For liposome tubulation copper grids filmed with pioloform and carbon-coated were glow discharged before usage. Proteins were incubated with 1 mg/ml folch fraction I liposomes for 7 min on grids, washed with buffer (10 mM Hepes, 150 mM NaCl, 4.5 mM KCl) and stained with 2% UAc for 2 min and examined on a FEI Technai spirit 120 kV microscope.

Supplementary data

Supplementary data are available at *The EMBO Journal* Online (http://www.embojournal.org).

Acknowledgements

We thank M Flötenmeyer and S Würtenberger for help with the tubulation assay, B Uluvar for support in protein purification and M Lorenz for critical reading of the manuscript.

Author contributions: BV and WA designed and performed experiments and wrote the manuscript. AS quantified interphasic NPC assembly, RS and NE performed pull-down experiments, AMS performed the size determinations of the RRM domains. CS cloned constructs and prepared *Xenopus laevis* extracts. JM and BM performed mass spec analysis, UG performed measurements of different liposome sizes.

Conflict of interest

The authors declare that they have no conflict of interest.

References

Amlacher S, Sarges P, Flemming D, van Noort V, Kunze R, Devos DP, Arumugam M, Bork P, Hurt E (2011) Insight into structure and assembly of the nuclear pore complex by utilizing the genome of a eukaryotic thermophile. *Cell* **146:** 277–289

Anderson DJ, Hetzer MW (2008) Reshaping of the endoplasmic reticulum limits the rate for nuclear envelope formation. *J Cell Biol* **182:** 911–924

Anderson DJ, Vargas JD, Hsiao JP, Hetzer MW (2009) Recruitment of functionally distinct membrane proteins to chromatin mediates nuclear envelope formation *in vivo*. *J Cell Biol* **186:** 183–191

Antonin W, Ellenberg J, Dultz E (2008) Nuclear pore complex assembly through the cell cycle: regulation and membrane organization. *FEBS Lett* **582:** 2004–2016

Antonin W, Franz C, Haselmann U, Antony C, Mattaj IW (2005) The integral membrane nucleoporin pom121 functionally links nuclear pore complex assembly and nuclear envelope formation. *Mol Cell* **17:** 83–92

Berke IC, Boehmer T, Blobel G, Schwartz TU (2004) Structural and functional analysis of Nup133 domains reveals modular building blocks of the nuclear pore complex. *J Cell Biol* **167:** 591–597

Bilokapic S, Schwartz TU (2012) 3D ultrastructure of the nuclear pore complex. *Curr Opin Cell Biol* **24:** 86–91

Blethrow JD, Glavy JS, Morgan DO, Shokat KM (2008) Covalent capture of kinase-specific phosphopeptides reveals Cdk1-cyclin B substrates. *Proc Natl Acad Sci USA* **105:** 1442–1447

Brohawn SG, Leksa NC, Spear ED, Rajashankar KR, Schwartz TU (2008) Structural evidence for common ancestry of the nuclear pore complex and vesicle coats. *Science* **322:** 1369–1373

Cho W, Stahelin RV (2005) Membrane-protein interactions in cell signaling and membrane trafficking. *Annu Rev Biophys Biomol Struct* **34:** 119–151

Cronshaw JM, Krutchinsky AN, Zhang W, Chait BT, Matunis MJ (2002) Proteomic analysis of the mammalian nuclear pore complex. *J Cell Biol* **158:** 915–927

D'Angelo MA, Anderson DJ, Richard E, Hetzer MW (2006) Nuclear pores form de novo from both sides of the nuclear envelope. *Science* **312:** 440–443

Daumke O, Lundmark R, Vallis Y, Martens S, Butler PJ, McMahon HT (2007) Architectural and mechanistic insights into an EHD ATPase involved in membrane remodelling. *Nature* **449:** 923–927

Dawson TR, Lazarus MD, Hetzer MW, Wente SR (2009) ER membrane-bending proteins are necessary for de novo nuclear pore formation. *J Cell Biol* **184:** 659–675

DeGrasse JA, DuBois KN, Devos D, Siegel TN, Sali A, Field MC, Rout MP, Chait BT (2009) Evidence for a shared nuclear pore complex architecture that is conserved from the last common eukaryotic ancestor. *Mol Cell Proteomics* **8:** 2119–2130

Devos D, Dokudovskaya S, Alber F, Williams R, Chait BT, Sali A, Rout MP (2004) Components of coated vesicles and nuclear pore complexes share a common molecular architecture. *PLoS Biol* **2:** e380

Doucet CM, Hetzer MW (2010) Nuclear pore biogenesis into an intact nuclear envelope. *Chromosoma* **119:** 469–477

Doucet CM, Talamas JA, Hetzer MW (2010) Cell cycle-dependent differences in nuclear pore complex assembly in metazoa. *Cell* **141:** 1030–1041

Drin G, Casella JF, Gautier R, Boehmer T, Schwartz TU, Antonny B (2007) A general amphipathic alpha-helical motif for sensing membrane curvature. *Nat Struct Mol Biol* **14:** 138–146

Dultz E, Ellenberg J (2010) Live imaging of single nuclear pores reveals unique assembly kinetics and mechanism in interphase. *J Cell Biol* **191:** 15–22

Dultz E, Zanin E, Wurzenberger C, Braun M, Rabut G, Sironi L, Ellenberg J (2008) Systematic kinetic analysis of mitotic dis- and reassembly of the nuclear pore in living cells. *J Cell Biol* **180:** 857–865

Fahrenkrog B, Hubner W, Mandinova A, Pante N, Keller W, Aebi U (2000) The yeast nucleoporin Nup53p specifically interacts with

©2012 European Molecular Biology Organization

Nic96p and is directly involved in nuclear protein import. *Mol Biol Cell* **11:** 3885–3896

Field MC, Sali A, Rout MP (2011) Evolution: on a bender–BARs, ESCRTs, COPs, and finally getting your coat. *J Cell Biol* **193:** 963–972

Franke WW, Deumling B, Baerbelermen, Jarasch ED, Kleinig H (1970) Nuclear membranes from mammalian liver. I. Isolation procedure and general characterization. *J Cell Biol* **46:** 379–395

Franz C, Askjaer P, Antonin W, Iglesias CL, Haselmann U, Schelder M, de Marco A, Wilm M, Antony C, Mattaj IW (2005) Nup155 regulates nuclear envelope and nuclear pore complex formation in nematodes and vertebrates. *EMBO J* **24:** 3519–3531

Franz C, Walczak R, Yavuz S, Santarella R, Gentzel M, Askjaer P, Galy V, Hetzer M, Mattaj IW, Antonin W (2007) MEL-28/ELYS is required for the recruitment of nucleoporins to chromatin and postmitotic nuclear pore complex assembly. *EMBO Rep* **8:** 165–172

Galy V, Askjaer P, Franz C, López-Iglesias C, Mattaj IW (2006) MEL-28, a novel nuclear envelope and kinetochore protein essential for zygotic nuclear envelope assembly in C. elegans. *Curr Biol* **16:** 1748–1756

Galy V, Mattaj IW, Askjaer P (2003) Caenorhabditis elegans nucleoporins Nup93 and Nup205 determine the limit of nuclear pore complex size exclusion *in vivo*. *Mol Biol Cell* **14:** 5104–5115

Handa N, Kukimoto-Niino M, Akasaka R, Kishishita S, Murayama K, Terada T, Inoue M, Kigawa T, Kose S, Imamoto N, Tanaka A, Hayashizaki Y, Shirouzu M, Yokoyama S (2006) The crystal structure of mouse Nup35 reveals atypical RNP motifs and novel homodimerization of the RRM domain. *J Mol Biol* **363:** 114–124

Hawryluk-Gara LA, Platani M, Santarella R, Wozniak RW, Mattaj IW (2008) Nup53 is required for nuclear envelope and nuclear pore complex assembly. *Mol Biol Cell* **19:** 1753–1762

Hawryluk-Gara LA, Shibuya EK, Wozniak RW (2005) Vertebrate Nup53 interacts with the nuclear lamina and is required for the assembly of a Nup93-containing complex. *Mol Biol Cell* **16:** 2382–2394

Hoelz A, Debler EW, Blobel G (2011) The structure of the nuclear pore complex. *Annu Rev Biochem* **80:** 613–643

Hu J, Shibata Y, Voss C, Shemesh T, Li Z, Coughlin M, Kozlov MM, Rapoport TA, Prinz WA (2008) Membrane proteins of the endoplasmic reticulum induce high-curvature tubules. *Science* **319:** 1247–1250

Liu HL, De Souza CP, Osmani AH, Osmani SA (2009) The three fungal transmembrane nuclear pore complex proteins of Aspergillus nidulans are dispensable in the presence of an intact An-Nup84-120 complex. *Mol Biol Cell* **20:** 616–630

Lohka MJ (1998) Analysis of nuclear envelope assembly using extracts of Xenopus eggs. *Methods Cell Biol* **53:** 367–395

Lu L, Ladinsky MS, Kirchhausen T (2011) Formation of the postmitotic nuclear envelope from extended ER cisternae precedes nuclear pore assembly. *J Cell Biol* **194:** 425–440

Lusk CP, Makhnevych T, Marelli M, Aitchison JD, Wozniak RW (2002) Karyopherins in nuclear pore biogenesis: a role for Kap121p in the assembly of Nup53p into nuclear pore complexes. *J Cell Biol* **159:** 267–278

Lusk CP, Waller DD, Makhnevych T, Dienemann A, Whiteway M, Thomas DY, Wozniak RW (2007) Nup53p is a target of two mitotic kinases, Cdk1p and Hrr25p. *Traffic* **8:** 647–660

Mans BJ, Anantharaman V, Aravind L, Koonin EV (2004) Comparative genomics, evolution and origins of the nuclear envelope and nuclear pore complex. *Cell Cycle* **3:** 1612–1637

Mansfeld J, Guttinger S, Hawryluk-Gara LA, Pante N, Mall M, Galy V, Haselmann U, Muhlhausser P, Wozniak RW, Mattaj IW, Kutay U, Antonin W (2006) The conserved transmembrane nucleoporin NDC1 is required for nuclear pore complex assembly in vertebrate cells. *Mol Cell* **22:** 93–103

Marelli M, Aitchison JD, Wozniak RW (1998) Specific binding of the karyopherin Kap121p to a subunit of the nuclear pore complex containing Nup53p, Nup59p, and Nup170p. *J Cell Biol* **143:** 1813–1830

Marelli M, Lusk CP, Chan H, Aitchison JD, Wozniak RW (2001) A link between the synthesis of nucleoporins and the biogenesis of the nuclear envelope. *J Cell Biol* **153:** 709–724

McMahon HT, Gallop JL (2005) Membrane curvature and mechanisms of dynamic cell membrane remodelling. *Nature* **438:** 590–596

McMahon HT, Mills IG (2004) COP and clathrin-coated vesicle budding: different pathways, common approaches. *Curr Opin Cell Biol* **16:** 379–391

Miao M, Ryan KJ, Wente SR (2006) The integral membrane protein Pom34p functionally links nucleoporin subcomplexes. *Genetics* **172:** 1441–1457

Mitchell JM, Mansfeld J, Capitanio J, Kutay U, Wozniak RW (2010) Pom121 links two essential subcomplexes of the nuclear pore complex core to the membrane. *J Cell Biol* **191:** 505–521

Neumann N, Lundin D, Poole AM (2010) Comparative genomic evidence for a complete nuclear pore complex in the last eukaryotic common ancestor. *PLoS ONE* **5:** e13241

Onischenko E, Stanton LH, Madrid AS, Kieselbach T, Weis K (2009) Role of the Ndc1 interaction network in yeast nuclear pore complex assembly and maintenance. *J Cell Biol* **185:** 475–491

Onischenko E, Weis K (2011) Nuclear pore complex-a coat specifically tailored for the nuclear envelope. *Curr Opin Cell Biol* **23:** 293–301

Patel SS, Rexach MF (2008) Discovering novel interactions at the nuclear pore complex using bead halo: a rapid method for detecting molecular interactions of high and low affinity at equilibrium. *Mol Cell Proteomics* **7:** 121–131

Prufert K, Vogel A, Krohne G (2004) The lamin CxxM motif promotes nuclear membrane growth. *J Cell Sci* **117:** 6105–6116

Rasala BA, Orjalo AV, Shen Z, Briggs S, Forbes DJ (2006) ELYS is a dual nucleoporin/kinetochore protein required for nuclear pore assembly and proper cell division. *Proc Natl Acad Sci USA* **103:** 17801–17806

Rodenas E, Klerkx EP, Ayuso C, Audhya A, Askjaer P (2009) Early embryonic requirement for nucleoporin Nup35/NPP-19 in nuclear assembly. *Dev Biol* **327:** 399–409

Sachdev R, Sieverding C, Flotenmeyer M, Antonin W (2012) The C-terminal domain of Nup93 is essential for assembly of the structural backbone of nuclear pore complexes. *Mol Biol Cell* **23:** 740–749

Stavru F, Hulsmann BB, Spang A, Hartmann E, Cordes VC, Gorlich D (2006) NDC1: a crucial membrane-integral nucleoporin of metazoan nuclear pore complexes. *J Cell Biol* **173:** 509–519

Stukenberg PT, Lustig KD, McGarry TJ, King RW, Kuang J, Kirschner MW (1997) Systematic identification of mitotic phosphoproteins. *Curr Biol* **7:** 338–348

Theerthagiri G, Eisenhardt N, Schwarz H, Antonin W (2010) The nucleoporin Nup188 controls passage of membrane proteins across the nuclear pore complex. *J Cell Biol* **189:** 1129–1142

Walther TC, Alves A, Pickersgill H, Loiodice I, Hetzer M, Galy V, Hulsmann BB, Kocher T, Wilm M, Allen T, Mattaj IW, Doye V (2003) The conserved Nup107-160 complex is critical for nuclear pore complex assembly. *Cell* **113:** 195–206

Wente SR, Rout MP (2010) The nuclear pore complex and nuclear transport. *Cold Spring Harb Perspect Biol* **2:** a000562

West RR, Vaisberg EV, Ding R, Nurse P, McIntosh JR (1998) cut11(+): A gene required for cell cycle-dependent spindle pole body anchoring in the nuclear envelope and bipolar spindle formation in Schizosaccharomyces pombe. *Mol Biol Cell* **9:** 2839–2855

Winey M, Hoyt MA, Chan C, Goetsch L, Botstein D, Byers B (1993) NDC1: a nuclear periphery component required for yeast spindle pole body duplication. *J Cell Biol* **122:** 743–751

Yavuz S, Santarella-Mellwig R, Koch B, Jaedicke A, Mattaj IW, Antonin W (2010) NLS-mediated NPC functions of the nucleoporin Pom121. *FEBS Lett* **584:** 3292–3298

SOME RIGHTS RESERVED **_The EMBO Journal_ is published by Nature Publishing Group on behalf of European Molecular Biology Organization. This article is licensed under a Creative Commons Attribution-Noncommercial-Share Alike 3.0 Licence. [http://creativecommons.org/licenses/by-nc-sa/3.0/]**

 ©2012 European Molecular Biology Organization

Supplementary Information

Dimerization and direct membrane interaction of Nup53 contribute to nuclear pore complex assembly

Benjamin Vollmer[1], Allana Schooley[1], Ruchika Sachdev[1], Nathalie Eisenhardt[1], Anna Schneider[2], Cornelia Sieverding[1], Johannes Madlung[3], Uwe Gerken[4,5], Boris Macek[3], Wolfram Antonin[1,6]

[1] Friedrich Miescher Laboratory of the Max Planck Society, Spemannstraße 39, 72076 Tübingen, Germany

[2] Max Planck Institute for Developmental Biology, Spemannstraße 35, 72076 Tübingen, Germany

[3] Proteome Center Tübingen, University of Tübingen, 72076 Tübingen, Germany

[4] Institute of Microbiology, University of Hohenheim, Garbenstrasse 30, 70599 Stuttgart, Germany

[5] Present address: Lehrstuhl für Experimentalphysik IV, University of Bayreuth, Universitätsstrasse 30, 95447 Bayreuth

[6] author for correspondence: wolfram.antonin@tuebingen.mpg.de

Supplementary information contains:

Supplementary Figures S1–S7 & Table S1–S2

Supplementary Methods

Supplementary References

Supplementary Figure S1

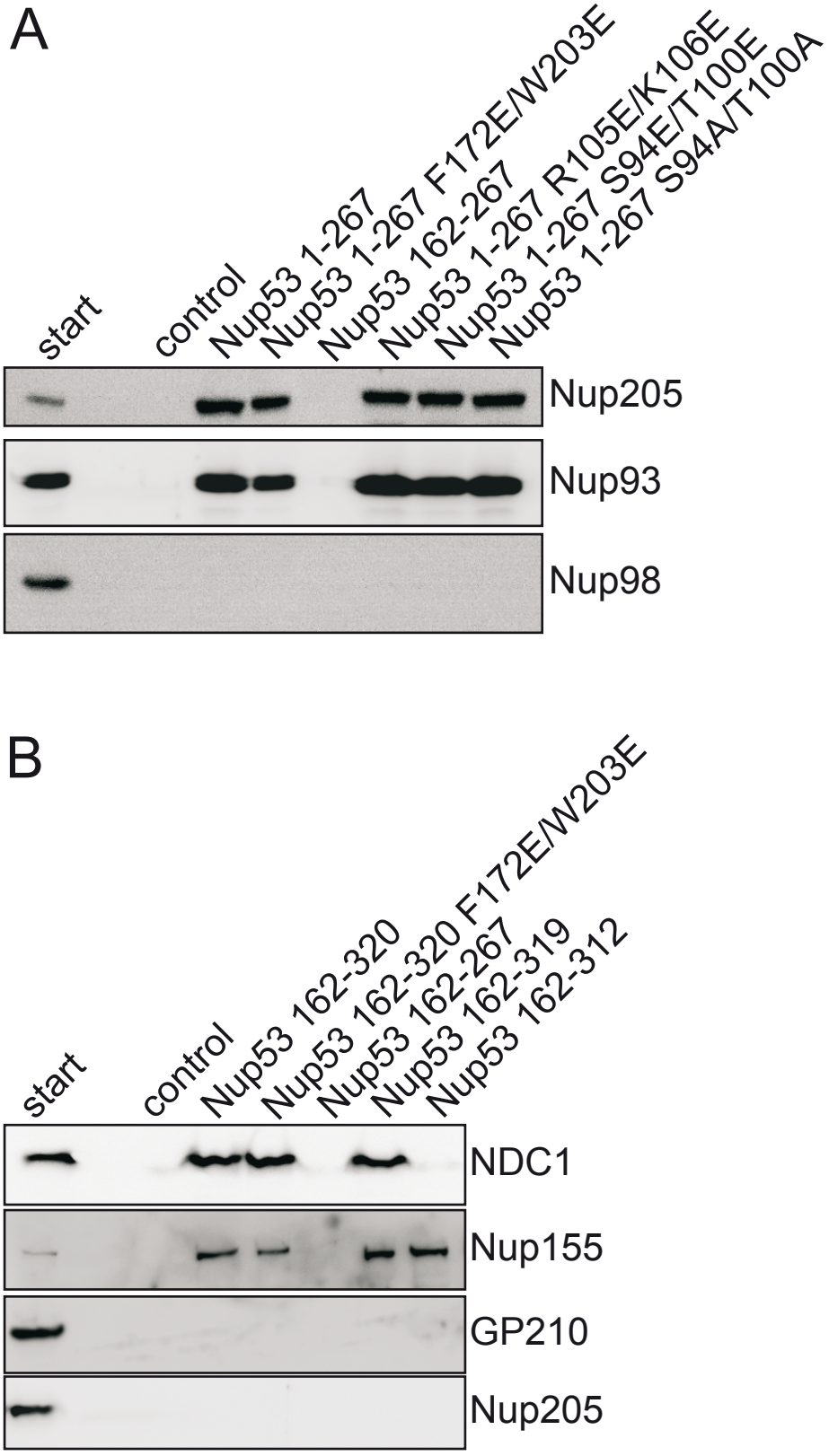

Figure S1

Nup53 has different binding sites for membrane and protein interaction.

(A) GST fusions of an N-terminal fragment of Xenopus Nup53 as well as Xenopus Nup98 (aa 487-634) (control) were incubated with cytosol from Xenopus egg extracts. Eluates were analyzed by western blotting with antibodies against the nucleoporins Nup205 and Nup93, known to bind this region, as well as Nup98 as a negative control. Please note that introducing amino acid changes causing the monomerization of Nup53 (F172E/W203E) also negatively influenced the interaction with Nup205 and Nup93. In contrast, mutations that inactivate the N-terminal membrane binding region (R105E/K106E and S94E/T100E) as well as the S94A/T100A control mutation did not interfere with Nup205 and Nup93 binding.

(B) GST fusions Xenopus Nup98 (aa 487-634) (control), the C-terminal fragment of Xenopus Nup53 (162-320), the RRM mutant (F172E/W203E) and C-terminal truncations were incubated with cytosol (for detection of Nup155 and Nup205) or Triton X-100 solubilized membranes (for NDC1 and GP210 detection) from Xenopus egg extracts. Eluates were analyzed by western blotting with antibodies against the nucleoporins Nup155 and NDC1, known to bind this region as well as Nup205 and GP210 as negative controls. Please note that mutation of the RRM domain (F172E/W203E) did not influence the interaction with NDC1 but results in a decreased binding to Nup155. The C-terminal truncations weakening the C-terminal membrane binding region (162-319 and 162-312) did not interfere with Nup155 binding and the 162-319 fragment was still able to interact with NDC1.

Supplementary Figure S2

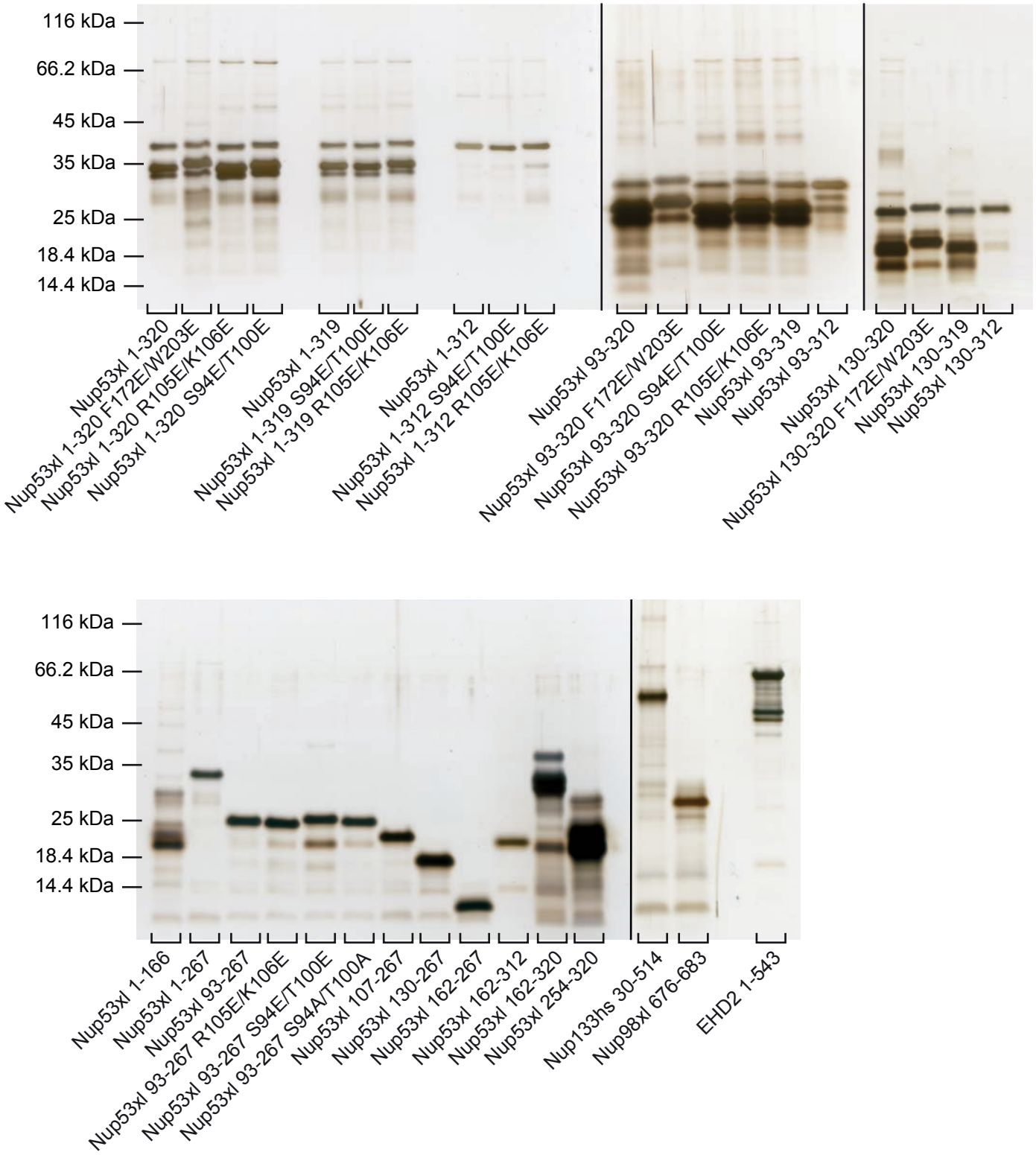

Figure S2

Proteins were separated on Tricine-SDS-PAGE Schägger gels (Schagger & von Jagow, 1987) followed by silver staining.

Supplementary Figure S3

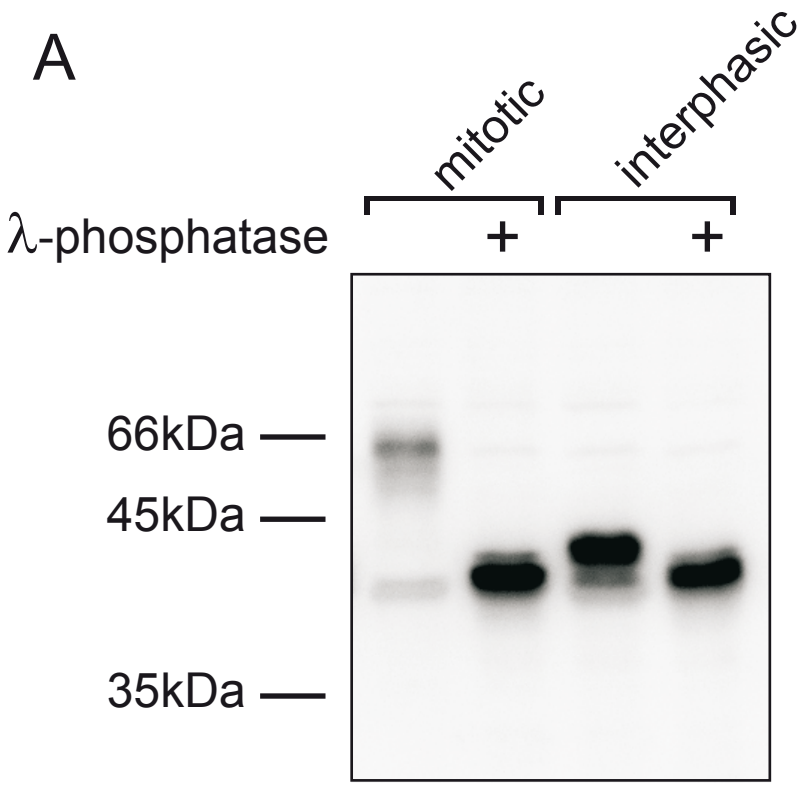

B

Protein IDs: gi_4584796;gi_148232142;gi_15987768;gi_nup53a;gi_nup53b;gi_32450351
Scannumber 8537
Source: 20101220_JM_CO_0221_R7_mitotic_01
Method: CID; ITMS

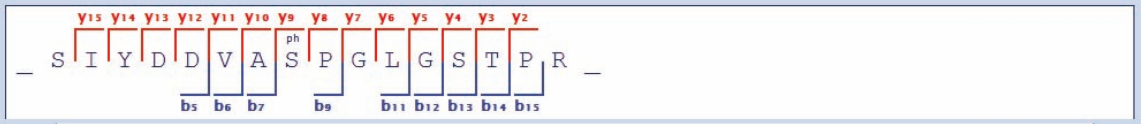

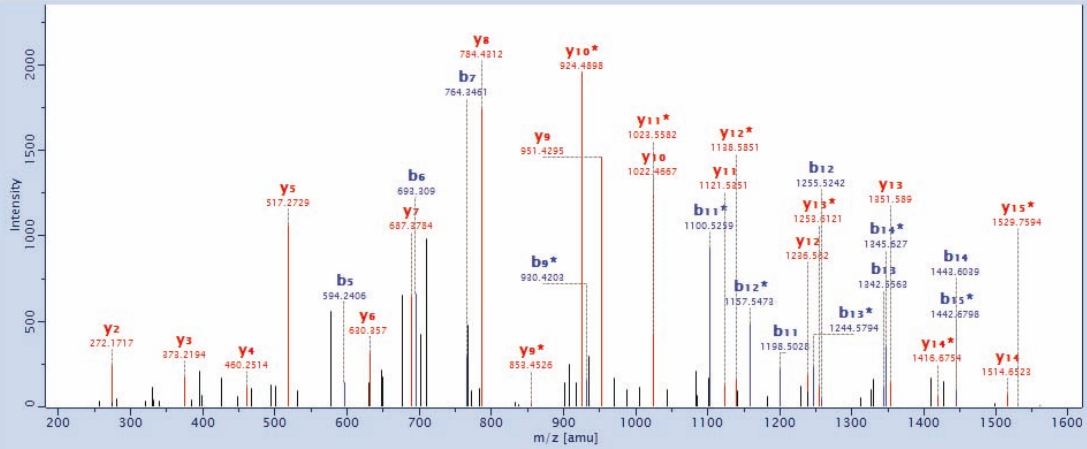

parent information

Mass:	1713.7611
m/z:	857.89
Charge:	2+
Mass Error [ppm]:	0.030899
PTM Score:	250.7
PEP:	7.5085E-41
Mascot Score:	100.54
Intensity:	13664197

general information

Annotation:	14 of 16 => 88 %
Intensity Coverage:	63 %
Protein Localisation:	89 ... 104

B-Ion					Y-Ion	
Δ Da	mass		seq		mass	Δ Da
NaN	88.0393049	1	S	16	NaN	NaN
NaN	201.1233689	2	I	15	1529.7594479	0.1181156
NaN	364.1866974	3	Y	14	1416.6753839	0.0124823
NaN	479.2136404	4	D	13	1253.6120554	0.0177054
0.310625	594.2405835	5	D	12	1138.5851123	0.0339649
0.1467521	693.3089974	6	V	11	1023.5581693	0.2597628
0.0844919	764.3461112	7	A	10	924.4897554	0.0853789
NaN	931.3444706	8	S	9	853.4526416	0.0651807
0.1978867	930.4203384	9	P	8	784.4311782	0.1097764
NaN	1085.4186981	10	G	7	687.3784143	0.0730627
0.1684698	1100.5258661	11	L	6	630.3569506	0.1070997
0.0851164	1157.5473299	12	G	5	517.2728866	0.1069351
0.0762814	1244.5793583	13	S	4	460.2514229	0.0053902
0.1205219	1345.6270367	14	T	3	373.2193945	0.0125464
0.1888518	1442.6798006	15	P	2	272.171716	0.0410398
NaN	NaN	16	R	1	175.1189522	NaN

Protein IDs: gi_4584796;gi_148232142;gi_15987768;gi_nup53a;gi_nup53b;gi_32450351
Scannumber 8673
Source: 20101126_CO_JM_0221WoAn_R5_IP_mitotic_01
Method: CID; ITMS

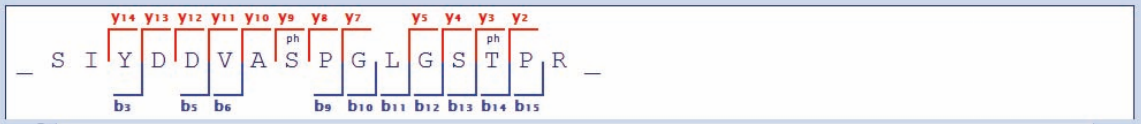

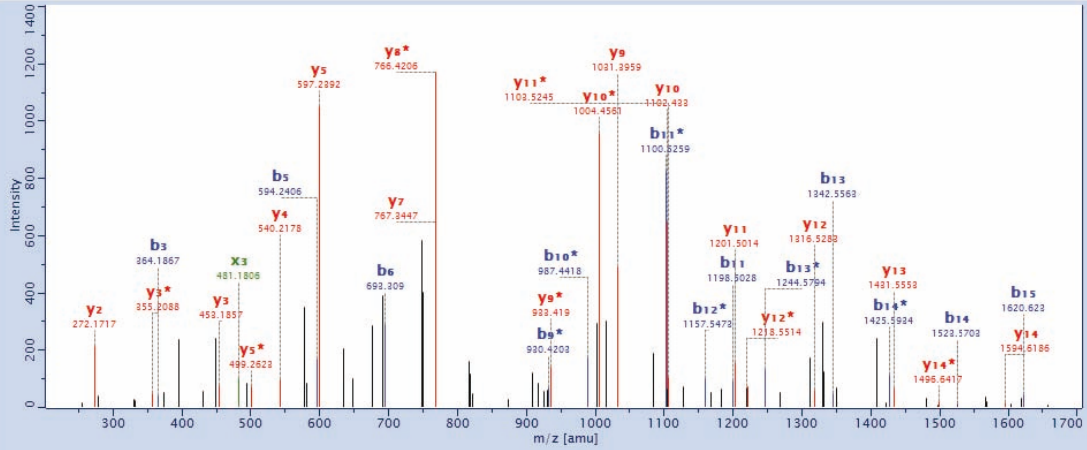

parent information

Mass:	1793.7274
m/z:	897.87
Charge:	2+
Mass Error [ppm]:	0.13197
PTM Score:	238.2
PEP:	8.3029E-53
Mascot Score:	51.05
Intensity:	18521420

general information

Annotation:	13 of 16 => 81 %
Intensity Coverage:	55 %
Protein Localisation:	89 ... 104

B-Ion					X-Ion		Y-Ion	
Δ Da	mass		seq		mass	Δ Da	mass	Δ Da
NaN	88.0393049	1	S	16	NaN	NaN	NaN	NaN
NaN	201.1233689	2	I	15	1733.6819395	NaN	1707.7026749	NaN
0.1353668	364.186697	3	Y	14	1620.5978755	NaN	1496.64171	0.2575771
NaN	479.2136404	4	D	13	1457.5345469	NaN	1431.55528	0.0981291
0.0384082	594.240583	5	D	12	1342.5076039	NaN	1218.55144	0.3596895
0.0780403	693.308997	6	V	11	1227.4806609	NaN	1103.5245	0.2493034
NaN	764.3461112	7	A	10	1128.412247	NaN	1004.45609	0.0672901
NaN	931.3444706	8	S	9	1057.3751332	NaN	933.418973	0.1262544
0.0214951	930.420338	9	P	8	890.3767738	NaN	766.420613	0.0788163
0.2336739	987.441802	10	G	7	793.3240099	NaN	767.344745	0.0776179
0.0236689	1100.52587	11	L	6	736.3025462	NaN	710.3232816	NaN
0.1385832	1157.54733	12	G	5	623.2184822	NaN	499.262322	0.0559618
0.0184452	1244.57936	13	S	4	566.1970185	NaN	540.217754	0.1073804
0.0542153	1425.59337	14	T	3	481.18064	0.1698237	355.20883	0.0389732
0.0871775	1620.62303	15	P	2	298.1509806	NaN	272.171716	0.0123227
NaN	NaN	16	R	1	201.0982167	NaN	175.1189522	NaN

Protein IDs: gi_4584796;gi_148232142;gi_15987768;gi_nup53a;gi_nup53b
Scannumber 5067
Source: 20101126_CO_JM_0221WoAn_R5_IP_mitotic_01
Method: CID; ITMS

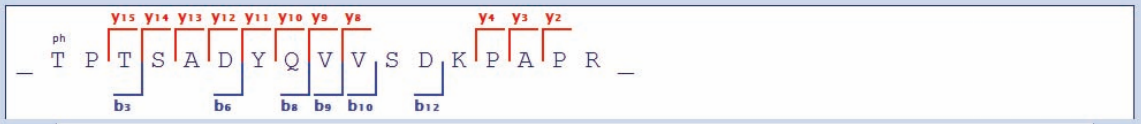

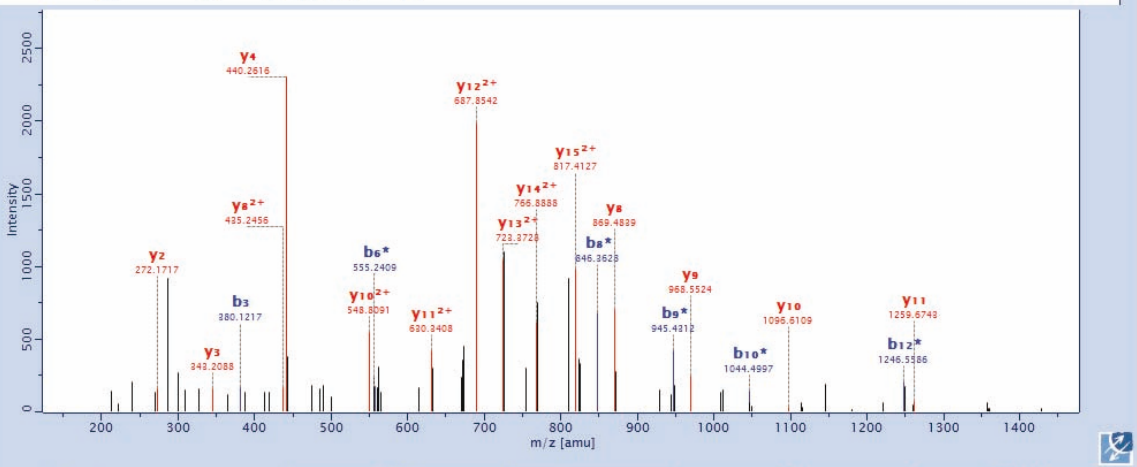

parent information

Mass:	1910.8775
m/z:	638.3
Charge:	3+
Mass Error [ppm]:	0.1223
PTM Score:	110.8
PEP:	5.3158E-06
Mascot Score:	37.4
Intensity:	1839497.9

general information

Annotation:	12 of 17 => 71 %
Intensity Coverage:	49 %
Protein Localisation:	288 ... 304

B-Ion					Y-Ion		Y-Ion²⁺	
Δ Da	mass		seq		mass	Δ Da	mass	Δ Da
NaN	182.0212859	1	T	17	NaN	NaN	NaN	NaN
NaN	279.0740498	2	P	16	1730.8707896	NaN	1730.8707896	NaN
0.0860354	**380.121728**	3	T	15	1633.8180257	NaN	**817.412651**	**0.3084793**
NaN	467.1537567	4	S	14	1532.7703472	NaN	**766.888812**	**0.0390804**
NaN	538.1908705	5	A	13	1445.7383188	NaN	**723.372798**	**0.0150096**
0.1898076	**555.240917**	6	D	12	1374.701205	NaN	**687.854241**	**0.315559**
NaN	816.281142	7	Y	11	**1259.67426**	**0.1249323**	**630.340769**	**0.0778099**
0.1566467	**846.362824**	8	Q	10	**1096.61093**	**0.0732137**	**548.809105**	**0.0020371**
0.0182254	**945.431237**	9	V	9	**968.552356**	**0.1522949**	968.552356	NaN
0.1110664	**1044.49965**	10	V	8	**869.483942**	**0.0255184**	**435.245609**	**0.0565758**
NaN	1229.5085758	11	S	7	770.4155281	NaN	770.4155281	NaN
0.2735886	**1246.55862**	12	D	6	683.3834997	NaN	683.3834997	NaN
NaN	1472.6304818	13	K	5	568.3565567	NaN	568.3565567	NaN
NaN	1569.6832457	14	P	4	**440.261594**	**0.0740997**	440.2615937	NaN
NaN	1640.7203595	15	A	3	**343.20883**	**0.0171794**	343.2088298	NaN
NaN	1737.7731233	16	P	2	**272.171716**	**0.1399295**	272.171716	NaN
NaN	NaN	17	R	1	175.1189522	NaN	175.1189522	NaN

Protein IDs: gi_4584796;gi_148232142;gi_15987768;gi_nup53a;gi_nup53b
Scannumber 5827
Source: 20101126_CO_JM_0221WoAn_R5_IP_mitotic_01
Method: CID; ITMS

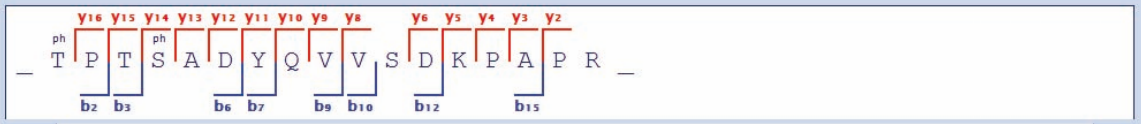

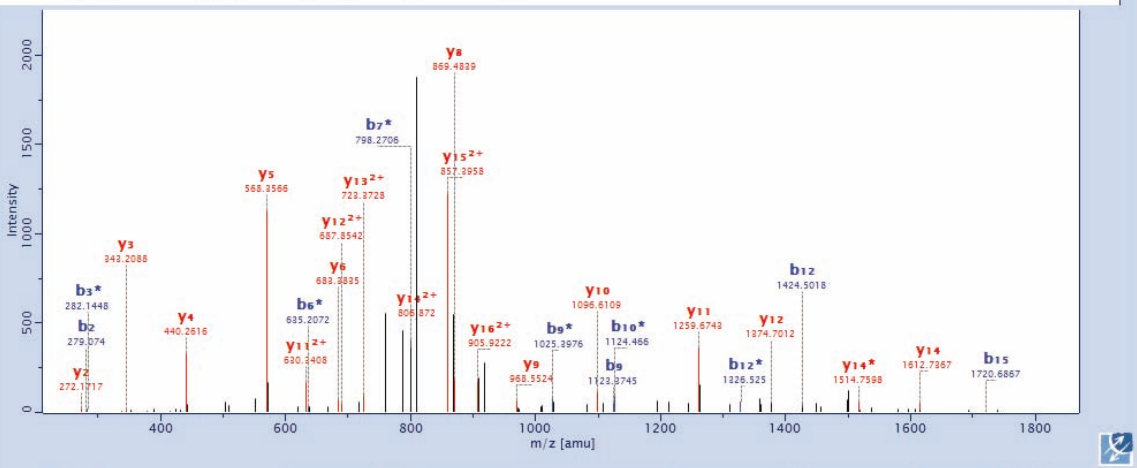

parent information

Mass:	1990.8439
m/z:	996.93
Charge:	2+
Mass Error [ppm]:	0.12316
PTM Score:	173.19
PEP:	3.1561E-23
Mascot Score:	52.53
Intensity:	723052.1

general information

Annotation:	14 of 17 => 82 %
Intensity Coverage:	46 %
Protein Localisation:	288 ... 304

B-Ion					Y-Ion		Y-Ion²⁺	
Δ Da	mass		seq		mass	Δ Da	mass	Δ Da
NaN	182.0212859	1	T	17	NaN	NaN	NaN	NaN
0.280595	**279.07405**	2	P	16	1810.8371206	NaN	**905.922199**	**0.03349**
0.2120625	**282.144832**	3	T	15	1713.7843567	NaN	**857.395817**	**0.1478846**
NaN	547.1200877	4	S	14	**1514.75978**	**0.204207**	**806.871977**	**0.2981887**
NaN	618.1572015	5	A	13	1445.7383188	NaN	**723.372798**	**0.4335988**
0.0729639	**635.207248**	6	D	12	**1374.70121**	**0.0788243**	**687.854241**	**0.1524731**
0.03962	**798.270577**	7	Y	11	**1259.67426**	**0.0252142**	**630.340769**	**0.1820579**
NaN	1024.3060505	8	Q	10	**1096.61093**	**0.1455363**	1096.6109335	NaN
0.0783546	**1025.39757**	9	V	9	**968.552356**	**0.0307739**	968.552356	NaN
0.1582852	**1124.46598**	10	V	8	**869.483942**	**0.1000423**	869.483942	NaN
NaN	1309.4749068	11	S	7	770.4155281	NaN	770.4155281	NaN
0.0591335	**1326.52495**	12	D	6	**683.3835**	**0.0513464**	683.3834997	NaN
NaN	1552.5968128	13	K	5	**568.356557**	**0.0124619**	568.3565567	NaN
NaN	1649.6495767	14	P	4	**440.261594**	**0.0915863**	440.2615937	NaN
0.2862099	**1720.68669**	15	A	3	**343.20883**	**0.1309529**	343.2088298	NaN
NaN	1817.7394543	16	P	2	**272.171716**	**0.0334842**	272.171716	NaN
NaN	NaN	17	R	1	175.1189522	NaN	175.1189522	NaN

Figure S3

(A) Nup53 is phosphorylated in interphase and mitosis

4 µl of mitotic (CSF arrested) or interphasic Xenopus egg extracts were diluted in 100 µl of phosphatase buffer (NEB) and incubated where indicated with 400 U λ-phosphatase for 30 min at 30°C. Samples were analyzed by 12% SDS-PAGE and Western blotting using the Xenopus Nup53 antibody. Please note the different shifting of mitotic and interphasic Nup53 after phosphatase treatment indicating that Nup53 is a phosphoprotein throughout the cell cycle but hyperphosphorylated during mitosis.

(B) Fragmentation mass spectra of Xenopus Nup53 peptides carrying mitotic specific phosphorylations

Supplementary Figure S4

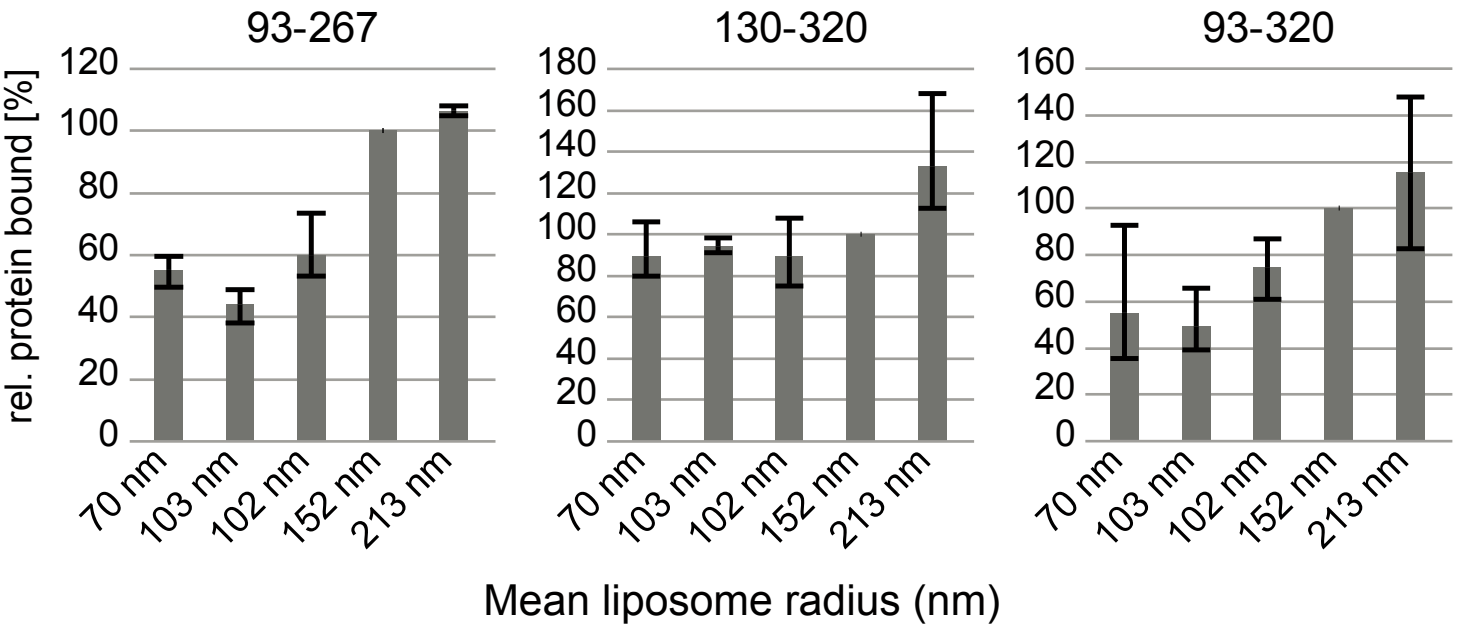

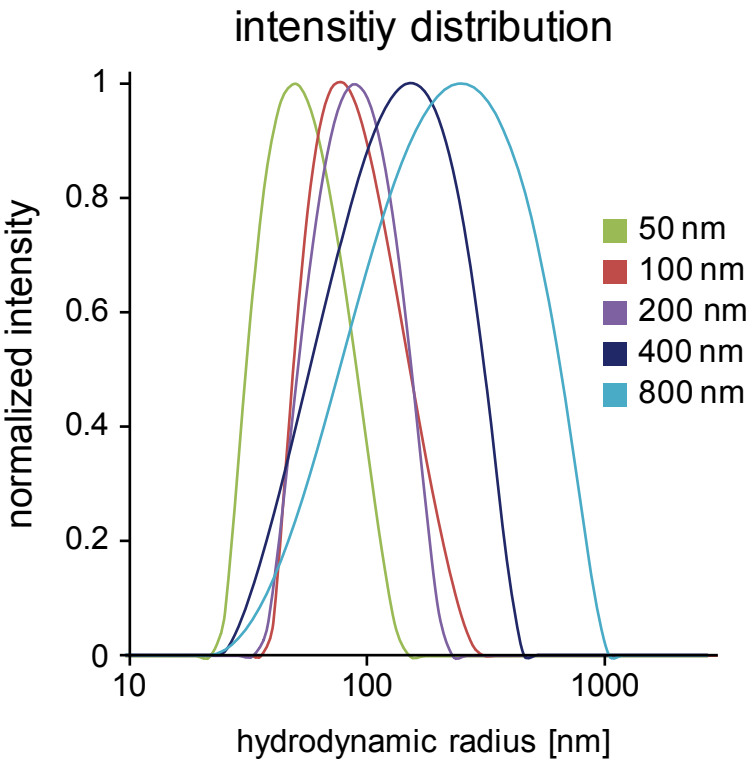

Figure S4

The two Nup53 membrane binding regions show different sensitivity to membrane curvature. Fragments comprising the N-terminal (93-267), C-terminal (130-320) or both (93-320) membrane binding sites, respectively, including the RRM domains were incubated with differently sized liposomes as indicated by the determined mean radii. Liposome binding was quantified as in Figure 2C. Whereas fragments which include the N-terminal membrane binding site (93-267 and 93-320) showed a significantly reduced binding to smaller liposome diameters and thus to higher membrane curvature this effect was not seen for the C-terminal membrane binding site (130-320). The averages of three independent experiments, normalized to the binding of the respective fragments to 150 nm liposomes, are shown. Error bars represent the range. Liposome radii were determined by light scattering after extrusion through membranes of different pore size as indicated for the different measurements. The lower panel shows one exemplary measurement done to determine the average radius of the respective preparation. Please note the rather similar average radii of liposomes prepared using 100 nm and 200 nm membranes.

Supplementary Figure S5

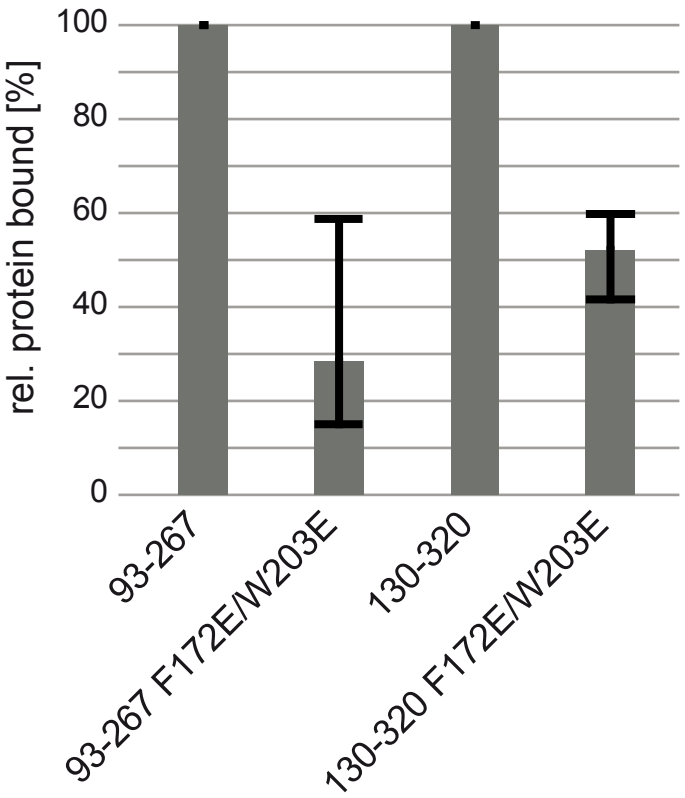

Figure S5

Both Nup53 membrane binding regions require dimerization by the RRM domain.

Nup53 fragments containing the first (93-267) or second (130-320) membrane binding region including the RRM domain were quantitatively assayed for liposome binding as in Figure 2C. Whereas fragments containing the wild type RRM domain bound to liposomes, introduction of two amino acid changes (F172E/W203E), which render the RRM domain incapable of dimerization, reduced liposome binding for both fragments. The averages of three independent experiments, normalized to liposome binding of the wild type protein, are shown. Error bars represent the range.

Supplementary Figure S6

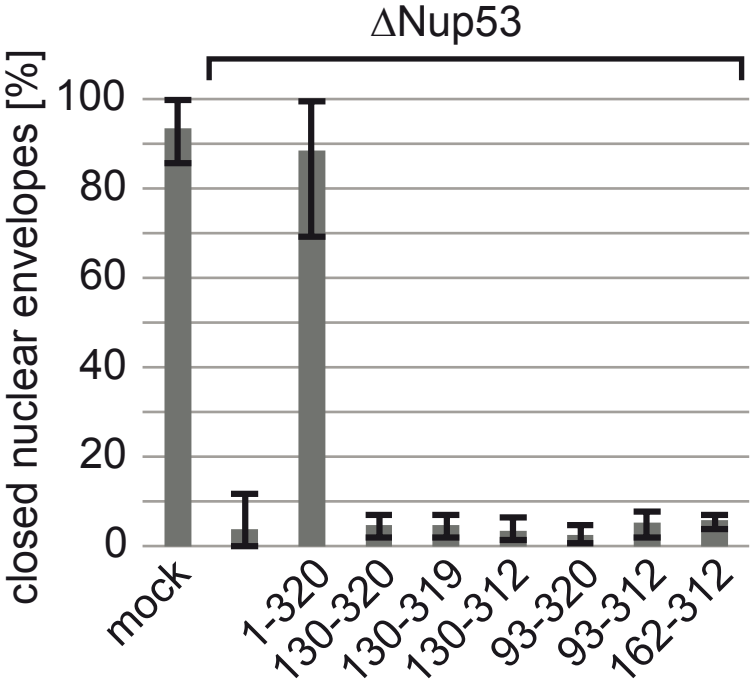

Figure S6

The interaction of Nup53 to Nup93 is necessary for nuclear envelope formation.

Nuclei were assembled in mock, Nup53 depleted extracts or Nup53 depleted extracts supplemented with wild type protein (1-320) or various fragments of Nup53 for 120 min, fixed with 2% PFA and 0.5% glutaraldehyde and analyzed for chromatin and membrane staining. Shown is the quantitation of chromatin substrates with a closed nuclear envelope as done in Figure 2F. Please note that all fragments lacking the N-terminal region of Nup53 necessary for Nup93 interaction (Figure S1A) and especially fragment 162-312 which has the ability to interact with Nup155 (Figure S1B) did not support nuclear envelope formation.

Supplementary Figure S7

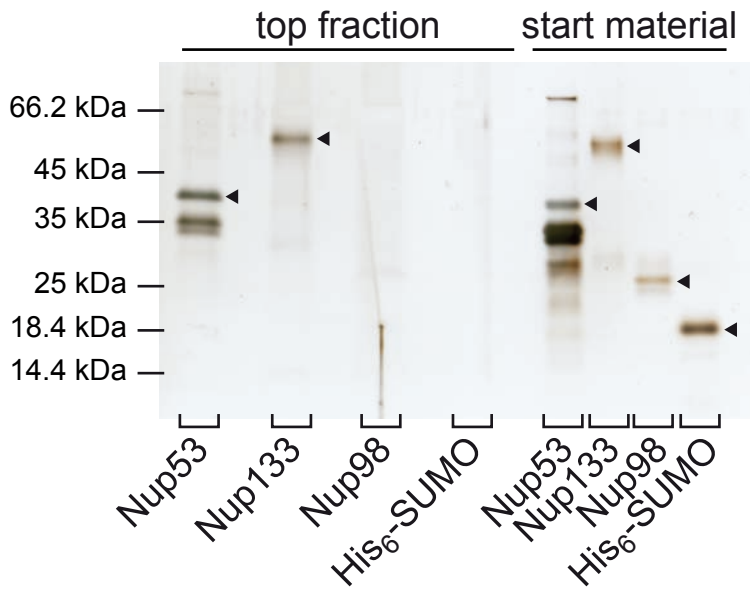

Figure S7

Recombinant Nup53 binds to liposomes mimicking the ER / nuclear envelope lipid composition

3 µM recombinant Xenopus Nup53 (Nup53) a fragment of Nup133 (aa 67-514) as positive control and Nup98 (aa 676-863) and His_6-tagged SUMO as negative controls, were incubated with 6 mg/ml fluorescently labeled liposomes prepared from a lipid mixture mimicking the ER/nuclear envelope lipid composition (see materials and methods). Flotation was done as described in Figure 1A.

Table S1: Peptides and phosphorylation sites identified in Xenopus Nup53 by mass spectrometric analysis

phosphopeptide	amino acid
PSAGAQFLPGFLLGDIPTPV**T**PQPR	T46
SPLH**S**GG**S**PPQPVLPTHK	S60, S64, S67
SPLHSGG**S**PPQPVLPTHK	S67
SIYDDVA**S**PGLGSTPR	S94
SIYDDVA**S**PGLGS**T**PR	S94, T100
MASFSVLHTPLSGAIPS**S**PAVFSPATIGQSR	S124
MASFSVLHTPLSGAIPSSPAVF**S**PATIGQSR	S131
V**S**TPSVSSVFTPPVK	S249
VS**T**PSVSSVFTPPVK	T250
VSTP**S**VSSVFTPPVK	S252
VSTP**S**VSSVF**T**PPVK	S252, T258
VSTPSVSSVF**T**PPVK	T258
SIRTPTQSVGTPR	S263
SIR**T**PTQSVGTPR	T266
SIRTPTQ**S**VGTPR	S270
TPTQSVG**T**PR	T273
TPTSADYQVVSDKPAPR	T288
TPT**S**ADYQVVSDKPAPR	T288, S291

Phosphorylation sites mapped in XenopusNup53 (genebank accession JQ747515) after immunoprecipitation from mitotic or interphase Xenopus egg extracts. Phosphorylation sites are indicated in red. Position T100, T288 and S291 were phosphorylated on Nup53 isolated from mitotic, but not interphasic extracts.

Table S2: DNA constructs used in this study

Constructs
pET28a SUMO Nup53xl 1-166
pET28a SUMO Nup53xl 1-267
pET28a SUMO Nup53xl 1-312
pET28a SUMO Nup53xl 1-312 S94E/T100E
pET28a SUMO Nup53xl 1-312 R105E/K106E
pET28a SUMO Nup53xl 1-319
pET28a SUMO Nup53xl 1-319 S94E/T100E
pET28a SUMO Nup53xl 1-319 R105E/K106E
pET28a SUMO Nup53xl 1-320
pET28a SUMO Nup53xl 1-320 S94E/T100E
pET28a SUMO Nup53xl 1-320 R105E/K106E
pET28a SUMO Nup53xl 1-320 F172E/W203E
pET28a SUMO Nup53xl 93-267
pET28a SUMO Nup53xl 93-267 S94A/T100A
pET28a SUMO Nup53xl 93-267 S94E/T100E
pET28a SUMO Nup53xl 93-267 R105E/K106E
pET28a SUMO Nup53xl 93-267 F172E/W203E
pET28a SUMO Nup53xl 93-312
pET28a SUMO Nup53xl 93-319
pET28a SUMO Nup53xl 93-320
pET28a SUMO Nup53xl 93-320 S94E/T100E
pET28a SUMO Nup53xl 93-320 R105E/K106E
pET28a SUMO Nup53xl 93-320 F172E/W203E
pET28a SUMO Nup53xl 107-267
pET28a SUMO Nup53xl 130-267
pET28a SUMO Nup53xl 130-312
pET28a SUMO Nup53xl 130-319
pET28a SUMO Nup53xl 130-320
pET28a SUMO Nup53xl 130-320 F172E/W203E
pET28a SUMO Nup53xl 162-267
pET28a SUMO Nup53xl 162-267 F172E/W203E
pET28a SUMO Nup53xl 162-312
pET28a SUMO Nup53xl 162-320
pET28a SUMO Nup53xl 254-320
pET28a SUMO Nup59sc 1-528
pET28a SUMO Nup53sc 1-475
pET28a PP Nup133hs 30-514
pET28a NusA Nup98xl 676-863
pET28a GST Nup53xl 1-267
pET28a GST Nup53xl 1-267 S94A/T100A
pET28a GST Nup53xl 1-267 S94E/T100E
pET28a GST Nup53xl 1-267 R105E/K106E
pET28a GST Nup53xl 1-267 F172E/W203E
pET28a GST Nup53xl 162-267
pET28a GST Nup53xl 162-312
pET28a GST Nup53xl 162-319
pET28a GST Nup53xl 162-320
pET28a GST Nup53xl 162-320 F172E/W203E
pET28a GST Nup98xl 487-634

Constructs
pSI HA Nup53xl
pSI HA Nup53xl F172E/W203E
pSI myc Nup53xl
pSI myc Nup53xl F172E/W203E

Supplementary Methods

Pulldown experiments

Fragments used for the GST pulldown experiments were cloned into a modified pET28a vector with GST tag followed by a recognition site for TEV protease and purified via the N-terminal His_6 tag. 60 µl GSH–Sepharose (GE Healthcare) were incubated with 300 µg of the respective bait proteins, washed and blocked with 5% BSA in PBS. Beads were incubated with cytosol from Xenopus egg extracts (diluted 1:1 with PBS, and cleared by centrifugation for 30 min at 100,000 rpm in a TLA110 rotor (Beckman Coulter) for 2 h and washed six times with PBS. Bound proteins were eluted by cleavage with TEV protease (0.5 mg/ml) for 1 h at RT and analyzed by SDS-PAGE and Western blotting. For detection of NDC1 and GP210, 5 mg of membranes from Xenopus egg extracts (Antonin et al, 2005) were solubilized in 5 ml 50 mM Phosphate buffer pH 7.4, 500 mM NaCl, 1% Triton X-100 and protease inhibitors (Roche), instead of cytosol and the first four washes with PBS were in the presence of 0.1% Triton X-100.

Mass Spectrometry

2 ml interphasic (Hartl et al, 1994) or (CSF arrested) mitotic (Murray, 1991) Xenopus egg extracts were diluted with 1.2 ml wash buffer (10 mM HEPES, 50 mM KCl, 2.5 mM $MgCl_2$ pH 7.4), cleared by centrifugation for 10 min at 100,000 rpm in a TLA110 rotor and incubated with 50 µl Protein A Sepharose (GE Healthcare), to which affinity purified Nup53 antibodies were bound and crosslinked with 10 mM dimethylpimelimidate (Pierce). After 1h incubation the sepharose was washed 10 times with wash buffer. Proteins were eluted with SDS sample buffer (without DTT) and separated by SDS-PAGE. Gel sections from 30-45 kDa were excised and proteins were in-gel digested by trypsin. The resulting peptide mixtures were measured on an LTQ-Orbitrap XL and processed by MaxQuant software as described (Borchert et al, 2010). Multistage activation was enabled in all MS measurements.

Generation of liposomes

A mixture of lipids resembling the ER/nuclear envelope composition (Franke et al, 1970) (60 mol % phosphatidylcholine, 19.8 mol % phosphatidylethanolamine, 10 mol % phosphatidylinositol, 5 mol % cholesterol, 2.5 mol % sphingomyelin, 2.5 mol % phosphatidylserine 0.2 mol % 18:1-12:0 NBD-PE all Avanti polar lipids) dissolved in chloroform were dried on a rotary evaporator and overnight under vacuum. PBS buffer was gently added to result in a final lipid concentration of 6 mg/ml. After 2 h of incubation at

37°C to allow spontaneous liposome formation the flask was agitated to dissolve residual lipids. After ten cycles of freeze/thawing liposomes were extruded as described before.

DNA sequence of Xenopus laevis Nup53 optimized for expression in E. coli

ATGATGGCAGCAGCATTTAGCATGGAACCGATGGGTGCAGAACCGATGGCACTG
GGTAGCCCGACCAGCCCGAAACCGAGTGCCGGTGCACAGTTTCTGCCTGGTTTTC
TGCTGGGTGATATTCCGACACCGGTTACACCGCAGCCTCGTCCGAGCCTGGGTAT
TATGGAAGTTCGTAGTCCGCTGCATAGCGGTGGTAGTCCTCCGCAGCCGGTTCTG
CCGACCCATAAAGATAAAAGCGGTGCACCTCCGGTTCGTAGCATTTATGATGATG
TTGCAAGTCCGGGTCTGGGTAGCACACCGCGTAATACCCGTAAAATGGCAAGCTT
TAGCGTTCTGCATACACCTCTGAGCGGTGCAATTCCGAGCAGTCCGGCAAGCAAT
GTTTTTAGTCCGGCAACCATTGGTCAGAGCCGTAAAACCACCCTGAGTCCGGCAC
AGATGGACCCGTTTTATACCCAGGGTGATGCACTGACCAGTGATGATCAGCTGGA
TGATACCTGGGTTACCGTTTTTGGTTTTCCGCAGGCAAGCGCAAGCTATATTCTGC
TGCAGTTTGCACAGTATGGCAATATTATTAAACATGTGATGAGCAATAATGGCAA
TTGGATGCATATTCAGTATCAGAGCAAACTGCAGGCACGTAAAGCACTGAGCAA
AGATGGTCGTATTTTTGGTGAAAGCATTATGATTGGTGTGAAACCGTGCATTGAT
AAAAGCGTTATGGAAGCAACCGAAAAAGTTAGCACCCCGAGCGTTAGCAGCGTT
TTTACACCTCCGGTTAAAAGCATTCGTACCCCGACCCAGAGCGTTGGTACACCGC
GTGCAGCAAGCATGCGTCCGCTGGCAGCAACCTATCGCACCCCGACCAGCGCAG
ATTATCAGGTTGTTAGCGATAAACCGGCACCGCGTAAAGATGAAAGCATTGTTAG
CAAAGCCATGGAATATATGTTTGGTTGGTGATAG

DNA sequence of Saccharomyces cerevisiae NUP53 optimized for expression in E. coli

ATGGCAGATCTGCAGAAACAAGAAAATTCAAGCCGTTTTACCAATGTTAGCGTTA
TTGCACCGGAAAGCCAGGGTCAGCATGAACAGCAGAAACAGCAAGAACAACAA
GAACAGCAGAAACAGCCGACAGGTCTGCTGAAAGGTCTGAATGGTTTTCCGAGC
GCACCGCAGCCGCTGTTTATGGAAGATCCTCCGAGCACCGTTAGCGGTGAACTGA
ATGATAATCCGGCATGGTTTAATAATCCGCGTAAACGTGCAATTCCGAATAGCAT
TATTAAACGTAGCAATGGTCAGAGCCTGAGTCCGGTTCGTAGCGATAGCGCAGAT
GTTCCGGCATTTAGCAATAGCAATGGCTTTAATAATGTGACCTTTGGCAGCAAAA
AAGATCCGCGTATTCTGAAAAATGTGAGCCCGAATGATAATAATAGCGCCAATA
ATAATGCCCATAGCAGCGATCTGGGCACCGTTGTTTTTGATAGCAATGAAGCACC
TCCGAAAACCAGCCTGGCAGATTGGCAGAAAGAAGATGGTATTTTTAGCAGCAA
AACCGATAATATTGAAGATCCGAATCTGAGCAGCAATATTACCTTTGATGGTAAA
CCGACCGCAACCCCGAGCCCGTTTCGTCCGCTGGAAAAAACCAGCCGTATTCTGA
ATTTTTTTGATAAAAATACCAAAACCACCCCGAATACCGCAAGCAGCGAAGCAA
GCGCAGGTAGCAAAGAAGGTGCAAGCACCAATTGGGATGATCATGCCATTATTA
TTTTTGGCTATCCGGAAACCATTGCCAATAGTATTATTTTTCATTTTGCCAATTTTG
GCGAAATTCTGGAAGATTTTCGCGTGATTAAAGATTTTAAAAAGCTGAACAGCAA
AAATAAAAGCAAAAGCCCGAGCCTGACCGCACAGAAATATCCGATTTATACCGG
TGATGGTTGGGTTAAACTGACCTATAAAAGCGAACTGAGCAAAAGCCGTGCACT
GCAAGAAAATGGCATTATTATGAATGGCACCCTGATTGGTTGCGTTAGCTATAGT
CCGGCAGCACTGAAACAGCTGGCAAGCCTGAAAAAAAGCGAAGAAATTATTAAT
AATAAAACCAGCAGCCAGACCAGCCTGAGCAGCAAAGATCTGAGCAATTATCGT
AAAACCGAAGGCATTTTTGAAAAAGCCAAAGCAAAAGCGGTGACCAGCAAAGTT
CGTAATGCCGAATTTAAAGTGAGCAAAAATAGCACCAGCTTTAAAAATCCGCGTC
GCCTGGAAATTAAAGATGGTCGTAGCCTGTTTCTGCGTAATCGTGGTAAAATTCA
TAGCGGTGTTCTGAGCAGCATTGAAAGCGATCTGAAAAAACGTGAACAGGCAAG
CAAAAGCAAAAAAAGCTGGCTGAATCGCCTGAATAATTGGCTGTTTGGTTGGAAT
GATCTGTAGTGA

DNA sequence of Saccharomyces cerevisiae NUP59 optimized for expression in E. coli

ATGTTTGGTATTCGCAGCGGCAATAATAATGGTGGTTTTACCAATCTGACCAGCC
AGGCACCGCAGACCACCCAGATGTTTCAGAGCCAGAGCCAGCTGCAGCCGCAGC
CGCAGCCTCAACCGCAGCAGCAGCAACAGCATCTGCAGTTTAATGGTAGCAGTG
ATGCAAGCAGCCTGCGTTTTGGTAATAGCCTGAGCAATACCGTGAATGCCAATAA
TTATAGCAGCAATATTGGCAATAACAGCATCAACAATAATAACATCAAAAATGG
CACCAATAACATTAGCCAGCATGGTCAGGGCAATAATCCGAGCTGGGTTAATAAT
CCGAAAAAACGTTTTACACCGCATACCGTTATTCGTCGTAAAACCACCAAACAGA
ATAGCAGCAGCGATATTAATCAGAATGATGATAGCAGCAGCATGAATGCAACCA
TGCGTAATTTTAGCAAACAGAATCAGGATAGCAAACATAATGAACGCAATAAAA
GCGCAGCCAATAATGATATTAATAGCCTGCTGAGCAACTTTAATGATATTCCTCC
GAGCGTTACCCTGCAGGATTGGCAGCGTGAAGATGAATTTGGTAGCATTCCGAGC
CTGACCACCCAGTTTGTTACCGATAAATATACCGCCAAAAAAACCAATCGCAGCG
CCTATGATAGCAAAAATACCCCGAATGTGTTTGATAAAGATAGCTATGTGCGCAT
TGCCAATATTGAACAGAATCATCTGGATAATAATTATAATACCGCAGAAACCAAT
AATAAAGTGCATGAAACCAGCAGCAAAAGCAGCAGCCTGAGCGCAATTATTGTT
TTTGGTTATCCGGAAAGCATTAGCAATGAACTGATTGAACATTTTAGCCATTTTGG
CCATATTATGGAAGATTTTCAGGTTCTGCGTCTGGGTCGTGGTATTAATCCGAATA
CCTTTCGCATTTTTCATAATCATGATACCGGCTGTGATGAAAATGATAGCACCGTG
AATAAAAGCATTACCCTGAAAGGTCGCAATAATGAAAGTAATAACAAAAAATAT
CCGATTTTTACAGGCGAAAGCTGGGTTAAACTGACCTATAATAGCCCGAGCAGCG
CACTGCGTGCACTGCAAGAAAATGGTACAATTTTTCGTGGTAGCCTGATTGGTTG
TATTCCGTATAGCAAAAATGCCGTTGAACAGCTGGCAGGTTGCAAAATTGATAAT
GTGGATGATATTGGCGAATTTAATGTGAGCATGTATCAGAATAGCAGTACCAGCA
GCACCAGCAATACCCCGAGTCCTCCGAATGTTATTATTACCGATGGCACCCTGCT
GCGCGAAGATGATAATACACCGGCAGGTCATGCAGGCAATCCGACCAATATTAG
CAGCCCGATTGTTGCAAATAGCCCGAATAAACGTCTGGATGTGATTGATGGTAAA
CTGCCGTTTATGCAGAATGCAGGTCCGAATAGCAATATTCCGAATCTGCTGCGTA
ATCTGGAAAGCAAAATGCGTCAGCAAGAAGCAAAATATCGTAATAATGAACCGG
CAGGCTTTACCCATAAACTGAGCAATTGGCTGTTTGGTTGGAATGATCTGTAGTG
A

Supplementary References

Antonin W, Franz C, Haselmann U, Antony C, Mattaj IW (2005) The integral membrane nucleoporin pom121 functionally links nuclear pore complex assembly and nuclear envelope formation. *Molecular cell* **17:** 83-92

Borchert N, Dieterich C, Krug K, Schutz W, Jung S, Nordheim A, Sommer RJ, Macek B (2010) Proteogenomics of Pristionchus pacificus reveals distinct proteome structure of nematode models. *Genome research* **20:** 837-846

Franke WW, Deumling B, Baerbelermen, Jarasch ED, Kleinig H (1970) Nuclear membranes from mammalian liver. I. Isolation procedure and general characterization. *The Journal of cell biology* **46:** 379-395

Hartl P, Olson E, Dang T, Forbes DJ (1994) Nuclear assembly with lambda DNA in fractionated Xenopus egg extracts: an unexpected role for glycogen in formation of a higher order chromatin intermediate. *The Journal of cell biology* **124:** 235-248

Murray AW (1991) Cell cycle extracts. *Methods in cell biology* **36:** 581-605

Schagger H, von Jagow G (1987) Tricine-sodium dodecyl sulfate-polyacrylamide gel electrophoresis for the separation of proteins in the range from 1 to 100 kDa. *Analytical biochemistry* **166:** 368-379

© 2014. Published by The Company of Biologists Ltd | Journal of Cell Science (2014) 127, 908–921 doi:10.1242/jcs.141739

RESEARCH ARTICLE

Interaction of Nup53 with Ndc1 and Nup155 is required for nuclear pore complex assembly

Nathalie Eisenhardt, Josef Redolfi and Wolfram Antonin*

ABSTRACT

Nuclear pore complexes (NPCs) are the gateways for nucleocytoplasmic exchange. The ordered assembly of these huge complexes from several hundred individual components into an intricate protein interaction network which deforms the two membranes of the nuclear envelope into a pore is only rudimentarily understood. Here, we show that the interaction between Nup53 and the integral pore membrane protein Ndc1 is essential for vertebrate NPC assembly. The Ndc1 binding site on Nup53 overlaps with a region that induces membrane bending and is specifically required to modulate this activity, suggesting that the membrane-deforming capability of Nup53 is adjusted during the NPC assembly process. We further demonstrate that the interaction of Nup53 and Nup155 has a crucial role in NPC formation as the main determinant of recruitment of Nup155 to the assembling pore. Overall, our results pinpoint the diversity of interaction modes accomplished by Nup53, highlighting this protein as an essential link between the pore membrane and the NPC, and as a crucial factor in the formation of the pore membrane.

KEY WORDS: Ndc1, Nuclear pore complex, Nup35, Nup53, Nup155

INTRODUCTION

The compartmentalization of eukaryotic cells entails the spatial organization of specialized functions in distinct membrane-bound organelles. The characteristic organelle of eukaryotes is the nucleus, which is enclosed by the double membrane of the nuclear envelope (NE). The NE forms a barrier that separates nuclear gene transcription from cytoplasmic protein synthesis, thereby ensuring accurate processing of the genetic information. Nuclear pore complexes (NPCs) intercept the NE at fusion sites of the two membranes and mediate the selective transport of macromolecules. In most eukaryotic cells, NPCs represent the largest protein complexes but contain only about 30 individual proteins, which are called nucleoporins (Nups), and are found in up to 32 copies per NPC (Cronshaw et al., 2002; Ori et al., 2013; Rout et al., 2000). They can be categorized into two groups: (1) scaffold nucleoporins, which form the NPC structural backbone and (2) barrier nucleoporins, which execute transport functions and exclude inert molecules from passage.

Friedrich Miescher Laboratory of the Max Planck Society, Spemannstr. 39, 72076 Tübingen, Germany.

*Author for correspondence (wolfram.antonin@tuebingen.mpg.de)

This is an Open Access article distributed under the terms of the Creative Commons Attribution License (http://creativecommons.org/licenses/by/3.0), which permits unrestricted use, distribution and reproduction in any medium provided that the original work is properly attributed.

Received 27 August 2013; Accepted 30 November 2013

The core NPC scaffold resides close to the pore membrane and is formed by two conserved subcomplexes, the Nup107–Nup160 complex and the Nup93 complex (Nup84 and Nic96 complexes in *S. cerevisiae*). Nucleoporins of these subcomplexes show structural similarities to vesicle coats (Brohawn et al., 2008; Devos et al., 2004; Mans et al., 2004) and might stabilize the highly curved pore membrane. The core scaffold is linked to the pore membrane through integral membrane proteins. So far, four membrane nucleoporins have been identified in different organisms: Pom34, Pom152, Pom33 and Ndc1 in yeast (Chadrin et al., 2010; Lau et al., 2004; Miao et al., 2006; Wozniak et al., 1994) and Gp210, Pom121 and Ndc1, which is the only one conserved as an integral pore membrane protein, in vertebrates (Gerace et al., 1982; Hallberg et al., 1993; Mans et al., 2004; Mansfeld et al., 2006; Stavru et al., 2006).

Ndc1 is crucial for NPC assembly in vertebrates and yeast (Madrid et al., 2006; Mansfeld et al., 2006; Stavru et al., 2006). It interacts with Nup53 (also referred to as Nup35), a member of the Nup93 complex, in metazoa and its two *S. cerevisiae* orthologs, Nup53 and Nup59 (Hawryluk-Gara et al., 2008; Mansfeld et al., 2006; Onischenko et al., 2009; Uetz et al., 2000; Vollmer et al., 2012). This interaction might link NPCs to the pore membrane. However, in some organisms Ndc1 is dispensable for NPC assembly or absent from the genome (DeGrasse et al., 2009; Liu et al., 2009; Mans et al., 2004; Neumann et al., 2010; Stavru et al., 2006). In vertebrates, the interaction between Ndc1 and Nup53 seems dispensable for NPC formation because Nup53 truncations lacking the Ndc1 binding region are functional in NPC assembly (Hawryluk-Gara et al., 2008; Vollmer et al., 2012). Hence, alternative interactions might connect the NPC with the pore membrane. Indeed, Nup53 and both of its yeast homologs can bind membranes directly (Patel and Rexach, 2008; Vollmer et al., 2012). In vertebrates, two independent membrane binding sites mediate the Nup53 interaction to the pore membrane and this feature is crucial for NPC assembly (Vollmer et al., 2012). Although either one of these membrane binding sites is sufficient for NPC assembly at the end of mitosis, they are not completely interchangeable because the C-terminal site deforms membranes and is exclusively required for NPC assembly during interphase.

In addition to its membrane-binding ability and its interaction with Ndc1, Nup53 is part of multiple protein–protein interactions within the Nup93–Nic96 complex. The metazoan protein, as well as its yeast counterparts Nup53 and Nup59, binds Nup155 (or its corresponding yeast proteins Nup157 and Nup170) and Nup93/Nic96 (Fahrenkrog et al., 2000; Hawryluk-Gara et al., 2005; Onischenko et al., 2009; Sachdev et al., 2012; Uetz et al., 2000; Vollmer et al., 2012). In a thermophilic fungus, additional direct interactions between Nup53 and Nup192, corresponding to Nup205 in metazoa, as well as Nup188 have been described (Amlacher et al., 2011). Nup53, Nup93 and Nup155 are each

Journal of Cell Science

Journal of Cell Science (2014) 127, 908–921 doi:10.1242/jcs.141739

essential for assembly of vertebrate NPCs and form a trimeric complex in which Nup93 stabilizes the interaction between Nup53 and Nup155 (Franz et al., 2005; Grandi et al., 1997; Hawryluk-Gara et al., 2008; Hawryluk-Gara et al., 2005; Krull et al., 2004; Mitchell et al., 2010; Sachdev et al., 2012; Vollmer et al., 2012). Additionally, Nup155 can interact with the transmembrane nucleoporins Ndc1 and Pom121 (Mitchell et al., 2010; Yavuz et al., 2010). Altogether, there seems to be a broad and at least partially redundant interaction network between the pore membrane including transmembrane nucleoporins and the Nup93 complex.

Here, we analyze the function of the different Nup53 interactions and their contribution to NPC assembly. By dissecting the direct membrane interaction of Nup53 and its ability to bind Ndc1, we find that the Ndc1–Nup53 interaction is indispensable for NPC formation. This interaction is not required for Nup53 recruitment to the NPC. Instead, Ndc1 is needed to modulate the membrane-deformation capability of Nup53 to promote NPC assembly. Similarly, we demonstrate that the direct binding of Nup53 to Nup155 is crucial for NPC assembly. This interaction localizes Nup155 to the nascent pore, a crucial step for downstream events in NPC biogenesis.

RESULTS

Ndc1 interacts directly with Nup53 through its N-terminal transmembrane regions

Xenopus Nup53 interacts directly with nuclear membranes and this membrane binding is crucial for NPC assembly (Vollmer et al., 2012). Nup53 is embedded in the complex protein–protein interaction network of the NPC, where different interactions might influence or regulate each other during NPC assembly or within the intact pore. In this respect, interaction of Nup53 with the integral pore membrane protein Ndc1 might be relevant for its membrane binding, but its functional importance is unknown. In *Xenopus laevis* the last eight amino acids of Nup53 are required for its interaction with Ndc1. This region also contains one of the two direct membrane binding sites. It is therefore important to determine whether these two features of Nup53 influence each other or act independently.

We reconstituted the interaction between *Xenopus* Nup53 and Ndc1 using recombinant proteins overexpressed in *E. coli*. Because Ndc1 is an integral membrane protein, it is important to maintain its membrane environment to preserve its functionality. To this end, a MISTIC tag (Roosild et al., 2005) was used to direct Ndc1 to the inner *E. coli* membrane. After harvesting the bacteria, membrane vesicles were generated and used as preys in GST pull-downs. The bait constructs comprised the C-terminal half of Nup53, including an RNA recognition motif (RRM) because this fragment interacts with Ndc1 (Vollmer et al., 2012 and supplementary material Fig. S1). In Nup53, the RRM domain acts as a dimerization domain and strengthens the interaction with other Nup93 complex members, including Nup93 and Nup155, and – most relevant here – is required for direct membrane binding (Handa et al., 2006; Vollmer et al., 2012). Hence, we used a dimerization mutant (F172E W203E, Nup53 162–320 RRM mutant, Fig. 1A) to discriminate protein–protein-mediated interactions from direct membrane binding of Nup53. Accordingly, *E.-coli*-derived membrane vesicles containing a fragment of the pore membrane protein Gp210 did not bind Nup53 above background levels (Fig. 1B). Inhibition of Nup53 dimerization does not affect Ndc1 interaction (Vollmer et al., 2012). Indeed, full-length Ndc1 eluted from the Nup53 bait, indicating a direct interaction.

Ndc1 consists of two parts: the N-terminal half comprises six predicted transmembrane helices and the C-terminal part is a conserved globular domain facing the nucleoplasmic side of the pore (Lau et al., 2006; Mansfeld et al., 2006; Stavru et al., 2006). To map the region required for the direct Nup53 interaction, we used membrane vesicles containing the N-terminal half of Ndc1 including all transmembrane helices (aa 1–301, Ndc1-N) or the C-terminal part starting from the last transmembrane helix including the globular C-terminal domain (aa 234–660, Ndc1-C, Fig. 1C). The Ndc1-N fragment bound Nup53 more strongly than the Ndc1-C fragment did (Fig. 1D). Further truncations of the transmembrane domain in which single transmembrane helices were sequentially deleted showed residual Nup53 binding (data not shown). This suggests that the Nup53 interaction surface is probably formed by multiple loops within the N-terminal region of Ndc1. Nup53 also interacted with the N-terminal half of Ndc1 in lysates of transfected HeLa cells (Fig. 1E). Here, full-length Ndc1 as well as Ndc1-N co-immunoprecipitated with Nup53. By contrast, Ndc1-C did not co-immunoprecipitate with Nup53. Accordingly, Nup53 co-immunoprecipitated with Ndc1 and Ndc1-N, but not Ndc1-C. Taken together, these data show that *Xenopus* Ndc1 and Nup53 interact directly and the N-terminal transmembrane domain of Ndc1 is necessary and sufficient for Nup53 binding.

The N- and the C-terminal halves of Ndc1 are required for NPC assembly

Having observed that the N-terminal half of Ndc1 mediates the interaction with Nup53, we tested whether this part is required for NPC assembly. For this, we used a cell-free system in which NPC assembly can be faithfully reconstituted. Incubation of cytosol and purified membranes from *Xenopus laevis* egg extracts with sperm heads gives rise to nuclei with closed NEs and functional NPCs (Gant and Wilson, 1997; Lohka and Masui, 1983; Wilson and Newport, 1988). Endogenous Ndc1 was specifically immunodepleted from the membrane fraction (Fig. 2A). This treatment did not affect other transmembrane proteins, including the pore membrane proteins Gp210 and Pom121. If mock-treated membranes and cytosol were used, a closed NE formed around the chromatin template, as indicated by membrane staining that had a smooth appearance (Fig. 2B,C). These nuclei contained NPCs as detected by the antibody mAB414, which acts as a read-out for NPC formation because it recognizes several nucleoporins that represent a major subfraction of the NPC. In the absence of Ndc1, a closed NE was not formed and mAB414 staining was markedly reduced, indicating a block in NE and NPC formation, consistent with a previous study (Mansfeld et al., 2006). Similar phenotypes have been observed upon depletion of other nucleoporins crucial for NPC assembly, including Pom121 (Antonin et al., 2005), Nup53 (Hawryluk-Gara et al., 2008; Vollmer et al., 2012), Nup93 (Grandi et al., 1997; Sachdev et al., 2012) and Nup155 (Franz et al., 2005). Upon depletion of Ndc1, Pom121 was still detected on the chromatin, showing that nuclear membrane recruitment to chromatin was not blocked in general (Fig. 2B,C). Re-addition of recombinant EGFP-tagged Ndc1 purified from *E. coli* and reconstituted into the Ndc1-depleted membranes rescued the phenotype at a concentration that was approximately endogenous. This demonstrates the specificity of the depletion and the functionality of the recombinant protein. Next, we replaced endogenous Ndc1 with EGFP-tagged Ndc1 fragments to investigate which region is required for NPC assembly. The Ndc1-N or the Ndc1-C fragments did not support NE and NPC formation, despite the fact that membrane vesicles containing the protein fragments were recruited to chromatin.

Journal of Cell Science

Journal of Cell Science (2014) 127, 908–921 doi:10.1242/jcs.141739

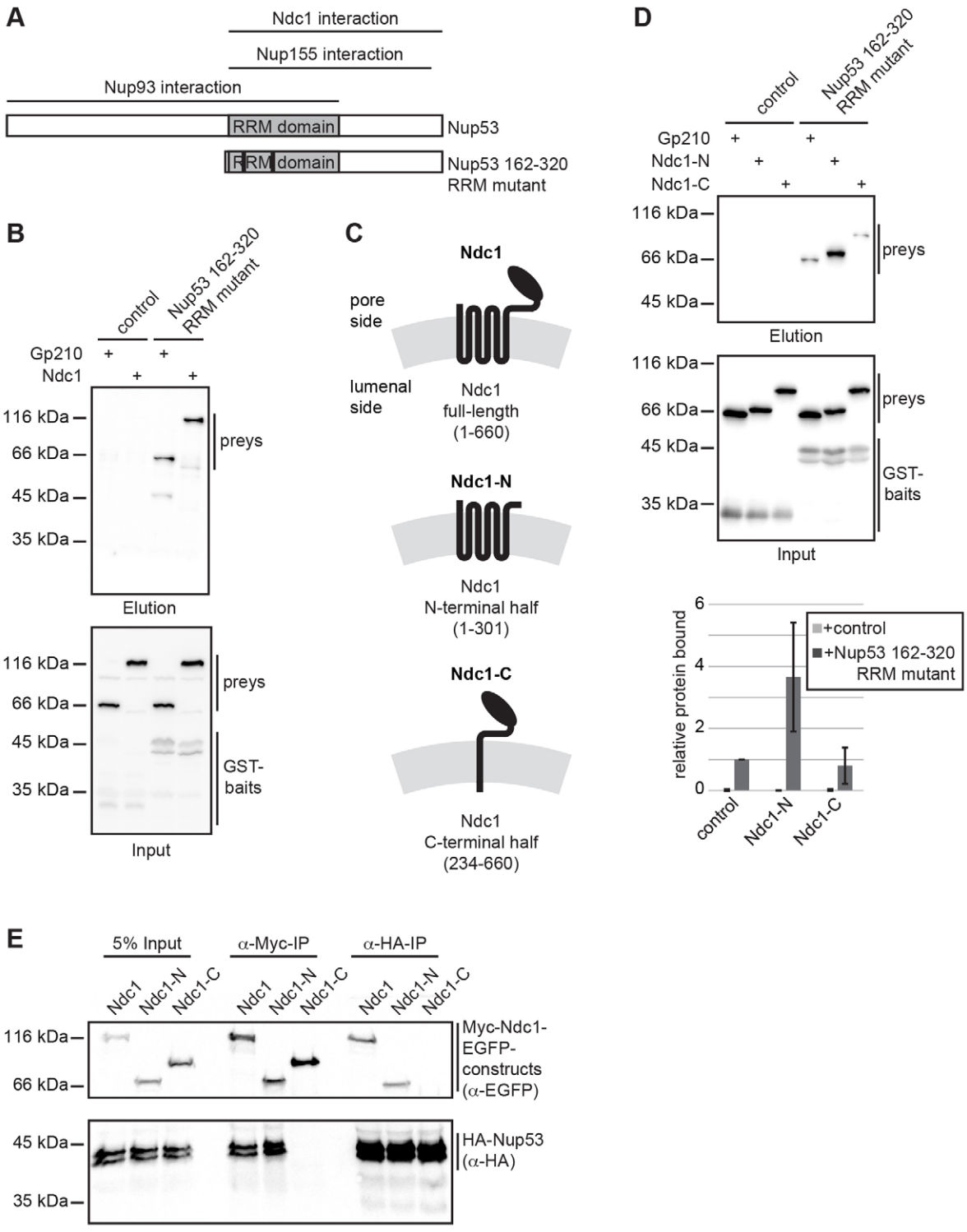

Fig. 1. The N-terminal portion of Ndc1 interacts directly with Nup53. (A) Schematic representation of *Xenopus* Nup53 and the Nup53 mutant fragment impaired for RRM-mediated dimerization and direct membrane binding. (B) GST fusions of the nucleoplasmic region of *Xenopus* Gp210 (control) or a Nup53 fragment comprising a mutated RRM domain decreasing direct membrane binding and the subsequent C-terminus (Nup53 162–320 RRM mutant) were incubated with *E.coli* lysates overexpressing the transmembrane region and the nucleoplasmic extension of *Xenopus* Gp210 or full-length Ndc1. Eluates and 3% of the input were analyzed by western blotting using a His_6 antibody. (C) Schematic representation of *Xenopus* Ndc1 (Ndc1), the N-terminal (Ndc1-N) and the C-terminal fragment (Ndc1-C) used. (D) Nup53 binding to the Ndc1-N and Ndc1-C fragments was analyzed as in B. The quantification shows the ratio of bait-bound protein to input of six independent experiments normalized to the binding of the lysate control to the Nup53 RRM mutant. Error bars show s.d. (E) HeLa cells were cotransfected with HA-tagged *Xenopus* Nup53 and full-length *Xenopus* Ndc1, the Ndc1-N or Ndc1-C fragment each fused with an N-terminal Myc and a C-terminal EGFP tag. Proteins were immunoprecipitated from cellular lysate with Myc or HA antibodies and analyzed by western blotting with indicated antibodies.

Journal of Cell Science (2014) 127, 908–921 doi:10.1242/jcs.141739

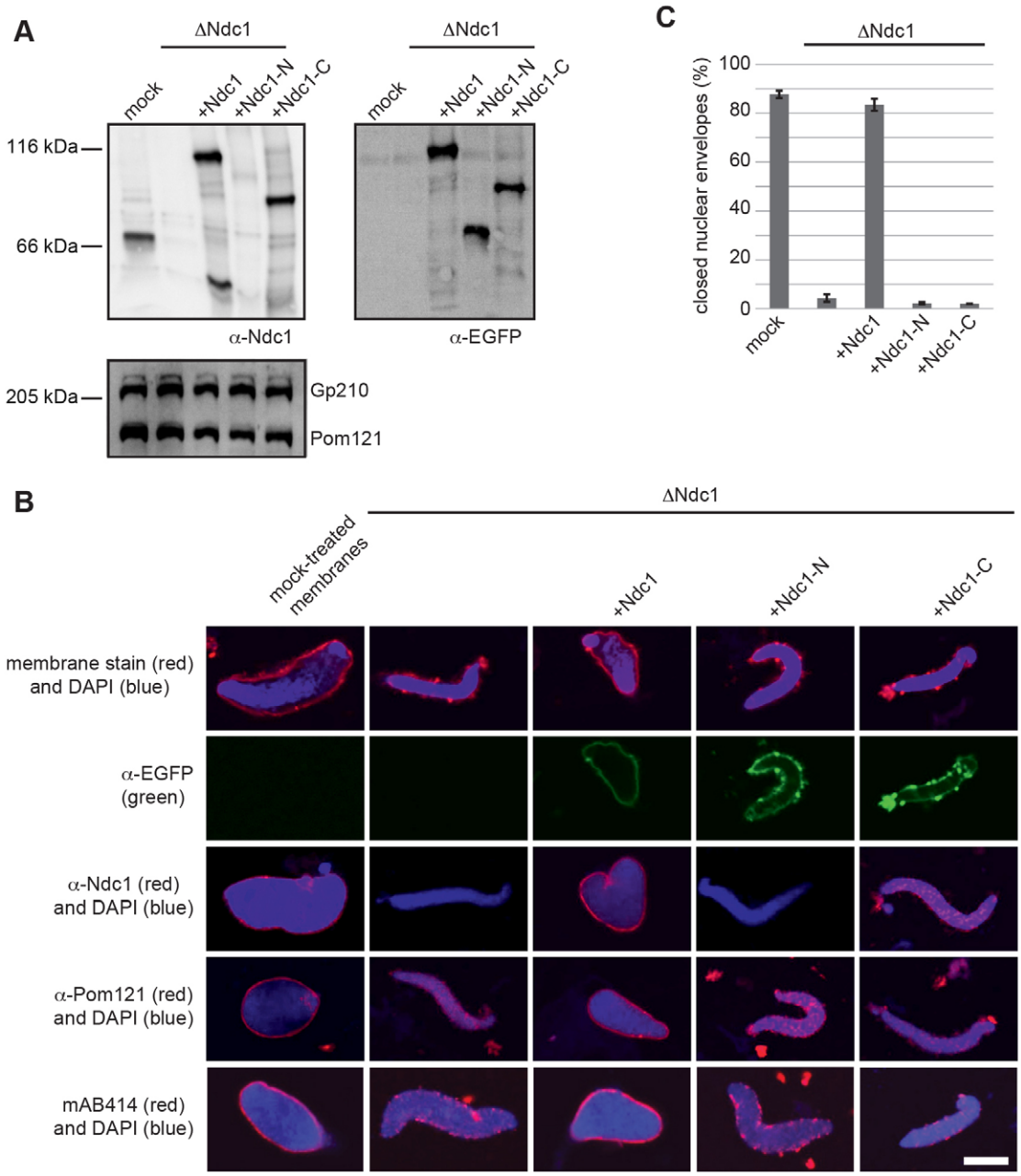

Fig. 2. Both the N-terminal and C-terminal halves of Ndc1 are required for NPC assembly. (A) Western blot analysis of mock-treated, Ndc1-depleted (ΔNdc1) or Ndc1-depleted and reconstituted membranes containing recombinant EGFP-tagged Ndc1, Ndc1-N or Ndc1-C fragments. Endogenous Ndc1, recombinant Ndc1 or Ndc1-C were detected by Ndc1 antibodies recognizing the C-terminus of the protein (left). The Ndc1-N construct, not recognized by this antibody, is detected – like all three recombinant Ndc1 proteins – by the EGFP antibody (right). Pom121 and Gp210 levels, detected with specific antibodies, were unaffected by the Ndc1 depletion and reconstitution (bottom panel). (B) Nuclei were assembled in cytosol and membranes from *Xenopus* egg extracts shown in A, and analyzed with indicated antibodies. Membranes were stained with $DiIC_{18}$ (red), DNA with DAPI (blue). Recombinant Ndc1 proteins were detected with EGFP antibodies (green), endogenous Ndc1, recombinant Ndc1 and the Ndc1-C fragment also with Ndc1 antibodies. Scale bar: 10 μm. (C) More than 300 nuclei of three independent experiments shown in B were quantified for the percentage of nuclei with closed NEs. Error bars show s.d.

This indicates that both parts of Ndc1 are required for NE and NPC assembly.

The N-terminal half of Ndc1 is dispensable for NPC assembly if Nup53 lacks its C-terminal membrane-binding side

One obvious explanation for the necessity of both parts of Ndc1 for NPC assembly could be that the N-terminus is required for Nup53 binding, whereas the C-terminal region executes some independent mandatory function. However, the Ndc1–Nup53 interaction is described as dispensable for *in vitro* NPC assembly because Nup53 truncations defective in this interaction could substitute for the endogenous protein (Hawryluk-Gara et al., 2008; Vollmer et al., 2012). To resolve this discrepancy, we performed double depletion and add-back experiments

Journal of Cell Science (2014) 127, 908–921 doi:10.1242/jcs.141739

manipulating Nup53 and Ndc1 from the egg extract cytosol and membranes, respectively. Nup53 was depleted without affecting the levels of other nucleoporins (Fig. 3A). In the absence of Nup53, formation of a closed NE was blocked (Fig. 3B,C, panels 1) as reported (Hawryluk-Gara et al., 2008; Vollmer et al., 2012). Re-addition of recombinant full-length Nup53 (Nup53 1–320) at endogenous levels (Fig. 3A) rescued this block when combined with mock-treated membranes containing endogenous Ndc1 (Fig. 3B,C panels 2). Also, a C-terminal truncation of Nup53 lacking the Ndc1 binding site (Nup53 1–312) restored NE formation together with mock-treated membranes (Fig. 3B,C, panels 3). These observations are in agreement with previous reports using untreated membranes (Hawryluk-Gara et al., 2008; Vollmer et al., 2012). If endogenous Ndc1 was depleted from the membranes, NPC formation was blocked in the presence of either Nup53 construct (Fig. 3B,C, panels 4,5). Re-addition of full-length Ndc1 in reconstituted membranes rescued NPC formation in combination with both Nup53 versions (Fig. 3B,C, panels 6,7). The Ndc1-N fragment could not replace endogenous Ndc1 in the presence of these Nup53 constructs (Fig. 3B,C, panels 8,9). This again suggests that the N-terminal half of Ndc1 is not sufficient for NE and NPC formation and that the C-terminal part is additionally required (see also Fig. 2B,C). The Ndc1-C fragment did not support formation of a closed NE in the presence of full-length Nup53 (Fig. 3B,C, panels 10). Surprisingly, in the presence of the Nup53 truncation impaired in the Ndc1 interaction (Nup53 1–312), the Ndc1-C fragment allowed NPC assembly (Fig. 3B,C, panels 11). This shows that the N-terminal half of Ndc1, which mediates Nup53 binding, is dispensable for NPC formation if Nup53 lacks the last eight amino acids.

Next, we analyzed the nuclei formed in the presence of the Ndc1-C fragment. In context of the Nup53 truncation defective in Ndc1 binding (Nup53 1–312), NPC formation is normal. All tested nucleoporins, including Nup53, localized properly to the NE (Fig. 3C, panel 11 and Fig. 3D) supporting the view that the N-terminal half of Ndc1 and thus the direct Ndc1–Nup53 interaction is not required to recruit Nup53 to reassembling NPCs. However, in the presence of full-length Nup53 (Nup53 1–320) Ndc1-C could not rescue NPC formation. Under these conditions Nup107, a nucleoporin that is recruited early to chromatin during NPC assembly, Pom121 and Gp210 were present on chromatin. Also, Nup53 and Nup155 were detected on chromatin but other Nup93 complex members, namely Nup93, Nup205 and Nup188, remained absent. This lack of recruitment of Nup93, Nup188 and Nup205 is similar to the Nup93-depletion phenotype (Sachdev et al., 2012), and suggests that Nup53 recruitment on its own cannot promote NPC assembly. Instead, the Ndc1–Nup53 interaction ensures the functionality of Nup53 in NE and NPC assembly.

The Ndc1 interaction and the C-terminal membrane-binding site of Nup53 can be separated

The previous experiments suggest that the Nup53–Ndc1 interaction is only dispensable when Nup53 lacks the last eight amino acids. This truncation not only abolishes the Ndc1 interaction, but also impairs membrane binding and deformation through the Nup53 C-terminus (Vollmer et al., 2012). Thus, the Ndc1–Nup53 interaction seems to be essential for NPC assembly if Nup53 can deform membranes. To test this, we generated a Nup53 construct that does not bind Ndc1 but retains all other features of the C-terminus. Because the Ndc1 interaction site and the C-terminal membrane binding site partially overlap (Vollmer et al., 2012), a stretch of eight amino acids upstream of the C-terminal membrane binding site (aa 275–282) was deleted. This deletion rendered Nup53 incompetent for Ndc1 interaction (Nup53 162–320 RRM mutant Δ275–282, Fig. 4A). To test for membrane binding, we inserted this deletion in a Nup53 fragment comprising the RRM domain and the C-terminal extension (aa 130–320). Because the N-terminal part of Nup53 contains another membrane-binding motif, this region was excluded. Similar to the control (Nup53 130–320), the deletion mutant (Nup53 130–320 Δ275–282) binds membranes directly when incubated with liposomes and floated through a sucrose cushion (Fig. 4B). By contrast, deletion of the last amino acid (Nup53 130–319) strongly reduced membrane binding (Vollmer et al., 2012). Similar to the wild-type fragment, the Nup53 deletion construct induced tubulation of liposomes (Fig. 4C). Notably, Nup155 binding, which also requires the C-terminal part of Nup53, remained unaffected by the deletion (supplementary material Fig. S2). Altogether, this shows that the Nup53 deletion construct is specifically impaired in its interaction with Ndc1, but its C-terminal membrane binding and deformation site remain intact.

Ndc1–Nup53 interaction is required for NPC assembly but can be bypassed if Nup53 lacks its C-terminus

After having identified a Nup53 version that was defective for the Ndc1 interaction but possessed a functional C-terminal membrane binding and bending site, we investigated the specific function of the Ndc1–Nup53 interaction in nuclear assembly. Endogenous Nup53 was depleted from the cytosol and replaced with different Nup53 versions (Fig. 5A) in the presence of untreated membranes containing endogenous Ndc1 (Fig. 5B). As before, Nup53 depletion blocked NE and NPC formation and this block was rescued by the wild-type protein (Nup53 1–320, Fig. 5C,D). However, the deletion construct (Nup53 1–320 Δ275–282) did not restore NE and NPC formation, demonstrating that the Ndc1–Nup53 interaction is necessary for NPC assembly. Interestingly, when the last amino acid of the deletion construct was removed (Nup53 1–319 Δ275–282), which impaired it for membrane interaction and deformation through the C-terminal membrane-binding site (Vollmer et al., 2012) (see also Fig. 4B,C), NE and NPC formation was rescued. By contrast, abolishing the membrane interaction through the N-terminal membrane-binding site of Nup53, which does not deform membranes, by exchange of a basic motif (Nup53 1–320 R105E K106E Δ275–282) (see Vollmer et al., 2012) did not rescue NE and NPC formation. This shows that the C-terminal membrane-binding site of Nup53 has to be specifically impaired to allow for NPC assembly if Nup53 is unable to interact with Ndc1 and that Ndc1 binding is required for NE and NPC formation if Nup53 can deform membranes.

All Nup53 constructs impaired in Ndc1 binding containing the N- or the C-terminal membrane-binding site localized to chromatin (Fig. 5C) showing that recruitment of Nup53 is independent of Ndc1. Accordingly, a Nup53 construct impaired in both membrane-binding sites and the Ndc1 interaction (Nup53 1–319 R105E K106E Δ275–282) was not detected on the chromatin and was defective in NPC and NE formation. This is consistent with previous findings whereby Nup53 membrane binding is the key determinant for its recruitment to the assembling NPC (Vollmer et al., 2012).

Altogether, these data indicate that Nup53 binding to Ndc1 is crucial for post-mitotic NPC assembly and only dispensable if

Journal of Cell Science

Journal of Cell Science (2014) 127, 908–921 doi:10.1242/jcs.141739

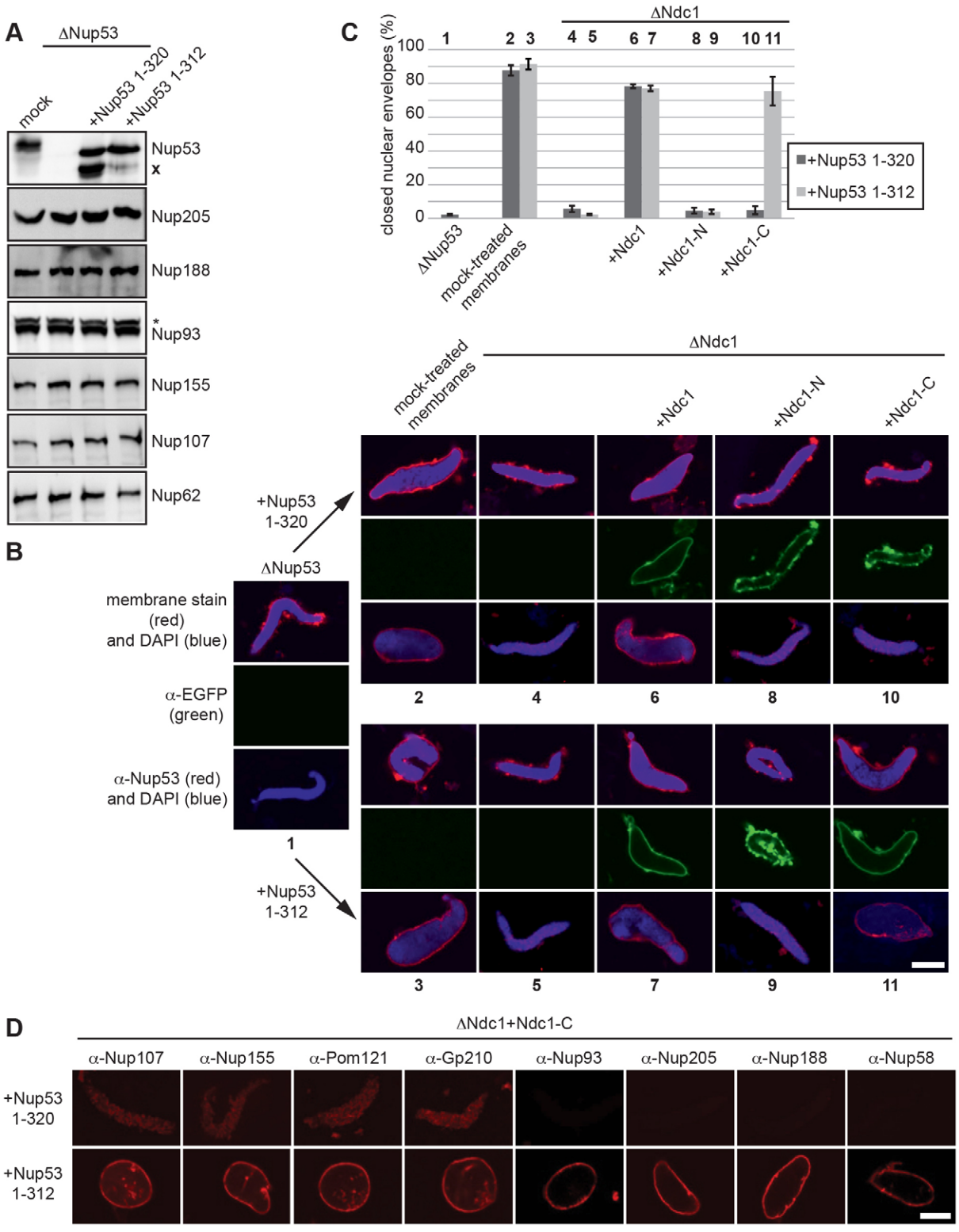

Fig. 3. Full-length Nup53 requires Ndc1 for NPC assembly. (A) Cytosol from *Xenopus* egg extracts was mock depleted, Nup53 depleted (ΔNup53) or Nup53 depleted and supplemented with full-length recombinant Nup53 (1–320) or a truncated version (1–312) lacking the final eight amino acids and analyzed with indicated antibodies. Note that endogenous Nup53 migrates slightly slower because of post-translational modifications absent in *E. coli*. Both, endogenous and recombinant Nup53 proteins are prone to C-terminal degradation (x). The Nup93 antibody recognizes a slightly slower-migrating crossreactivity (*). (B) Nuclei were assembled in Nup53-depleted cytosol (1) to which either recombinant full-length Nup53 (1–320, top panel) or a Nup53 fragment lacking the last eight amino acids (1–312, bottom panel) were added. The membranes were mock treated (2,3), depleted of endogenous Ndc1 (4,5) or Ndc1 depleted and reconstituted with either EGFP-tagged Ndc1 (6,7), Ndc1-N (8,9) or Ndc1-C (10,11). Membranes were stained with $DiIC_{18}$ (red), DNA with DAPI (blue). Nuclei were analyzed with antibodies against EGFP to detect recombinant Ndc1 proteins (green) and Nup53 antibodies. (C) Quantification of nuclei with a closed NE as in Fig. 2C. Bold numbers correspond to the experimental conditions in B. (D) Nuclei assembled as in B (10,11) were analyzed by immunofluorescence with indicated antibodies. Scale bars: 10 μm.

Journal of Cell Science

Journal of Cell Science (2014) 127, 908–921 doi:10.1242/jcs.141739

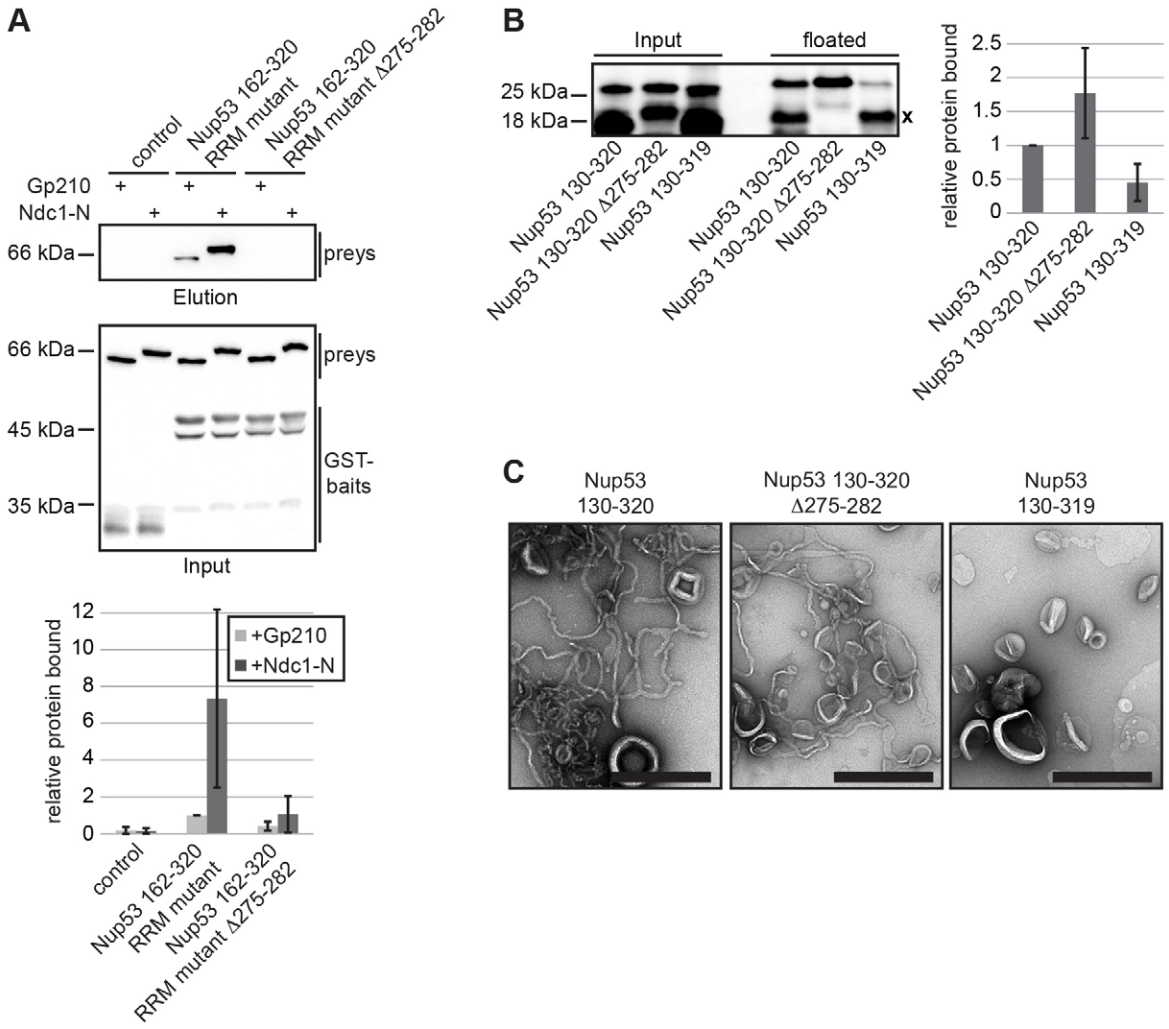

Fig. 4. Generation of a Nup53 mutant specifically impaired in Ndc1 binding. (A) GST pull-downs with the nucleoplasmic domain of Gp210 (control), a fragment of Nup53 comprising a mutated RRM domain and the C-terminus (Nup53 162–320 RRM mutant) or deleted of eight amino acids (Δ275–282) impairing the Ndc1 interaction and *E.coli* lysates as in Fig. 1B. Four independent experiments were quantified as in Fig. 1D (bottom). (B) A Nup53 fragment containing the C-terminal direct membrane binding site (130–320), the same construct with an additional deletion (Δ275–282) and a Nup53 construct deficient for membrane interaction (130–319) were tested in liposome flotation assays. 3% of the input and the floated fractions were analyzed by western blotting with Nup53 antibodies for membrane interaction. Nup53 degradations are indicated (x). Three independent experiments were quantified for membrane binding normalized to Nup53 130–320 (right). Error bars represent s.d. (C) Nup53 constructs from B were assayed for liposome tubulation by transmission electron microscopy after negative staining. Note the absence of tubules with Nup53 130–319. Scale bars: 500 nm.

Nup53 cannot deform membranes. Consistent with this, the N-terminal half of Ndc1, which provides the Nup53 interaction surface, is dispensable for NPC assembly if Nup53 lacks the membrane-deformation motif (Fig. 3B, panel 11, Fig. 3C,D). Hence, we conclude that Ndc1 modulates Nup53 membrane-deformation activity to allow for NPC assembly at the end of mitosis. Accordingly, we assumed that a Nup53 construct harboring a functional membrane deformation motif, which cannot be bound and regulated by Ndc1, might act as a dominant-negative version in NPC assembly. Indeed, if we added the Nup53 deletion construct defective for Ndc1 interaction (Nup53 1–320 Δ275–282) in excess to untreated nuclear assembly reactions (i.e. in the presence of endogenous Nup53 and Ndc1) NE and NPC formation was blocked (Fig. 5E). By contrast, a Nup53 construct that is unable to interact with Ndc1 but additionally is defective for membrane deformation did not show this effect (Nup53 1–319 Δ275–282). This experiment supports our hypothesis that the Ndc1–Nup53 interaction restrains the membrane-deformation capability of Nup53.

Nup53 interacts directly with Nup155

Nup53 combines different modes of interactions that are crucial for NPC assembly such as direct membrane binding and deformation, as well as interactions with other proteins within the NPC. We have demonstrated that the Ndc1 interaction is required to modulate the membrane-deformation ability and thus membrane binding through the C-terminus and Ndc1 interaction influence each other. Nup53 also interacts with Nup155 through its C-terminus (Amlacher et al., 2011; Hawryluk-Gara et al., 2008; Hawryluk-Gara et al., 2005; Marelli et al., 1998; Onischenko et al., 2009; Sachdev et al., 2012; Uetz et al., 2000; Vollmer et al., 2012). Similar to Ndc1 and Nup53, Nup155 is crucial for NPC assembly (Franz et al., 2005). Nup53 binding to Nup155 is thought to be essential for NPC assembly because

Journal of Cell Science (2014) 127, 908–921 doi:10.1242/jcs.141739

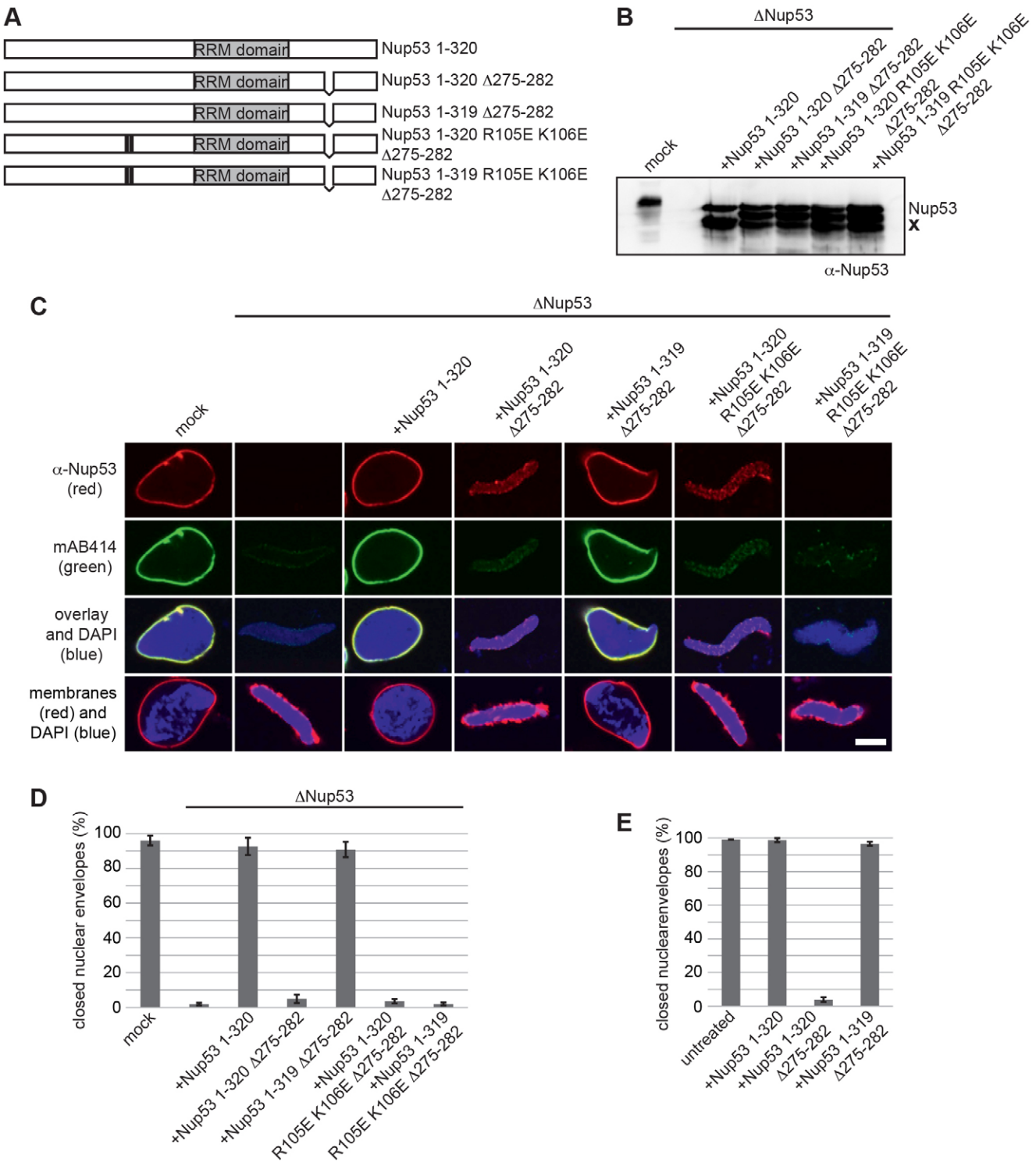

Fig. 5. Ndc1 functionally interacts with Nup53 membrane-bending activity. (A) Schematic representation of full-length *Xenopus* Nup53 (1–320) and the different mutants and fragments used. (B) *Xenopus* egg extracts were mock-treated, Nup53-depleted or Nup53-depleted and supplemented with recombinant wild-type Nup53 (1–320) or different constructs impaired for Ndc1 interaction (1–320 Δ275–282). Variants of the deletion construct deficient for membrane deformation (1–319 Δ275–282), membrane interaction through the N-terminal membrane binding site (1–320 R105E K106E Δ275–282) or both membrane interaction and deformation (1–319 R105E K106E Δ275–282) were included. Nup53 degradations are indicated (x). (C) Nuclei were assembled in mock, Nup53-depleted extracts or Nup53-depleted extracts supplemented with Nup53 constructs as in B. Nuclei were analyzed by immunofluorescence for Nup53 (red) or mAB414 (green). DNA was stained with DAPI (blue), membranes with $DiIC_{18}$ (red). Scale bar: 10 μm. (D) Quantification of nuclear assembly reactions from C performed as in Fig. 2C. (E) Recombinant full-length Nup53 (1–320), the Nup53 deletion construct impaired for Ndc1 interaction (1–320 Δ275–282) and a Nup53 construct impaired for Ndc1 interaction and defective in membrane deformation (1–319 Δ275–282) were added to untreated nuclear assembly reactions in 10-fold excess over endogenous Nup53 levels. More than 300 nuclei from three independent experiments were quantified. Error bars represent s.d.

Journal of Cell Science (2014) 127, 908–921 doi:10.1242/jcs.141739

Nup53 truncations lacking the Nup155 interaction site failed to replace the endogenous protein in nuclear assembly reactions (Hawryluk-Gara et al., 2008). However, these truncated versions also lacked the RRM domain that is required for Nup53 dimerization. This dimerization is necessary for binding of Nup53 to the membrane and, in turn, for NPC formation. Hence, it is unresolved whether the Nup53–Nup155 interaction is indeed essential for NPC formation and independent of other interactions of Nup53. To answer this, we separated the membrane binding and Nup155 interaction functions of Nup53 after mapping the Nup155 interaction site on Nup53 more precisely. Nup155 binds Nup53 upstream of Ndc1 (Vollmer et al., 2012). Therefore, we tested C-terminal truncations of Nup53 (Fig. 6A) in GST pull-downs. These constructs covered the RRM domain which might contribute to the interaction (Vollmer et al., 2012) and sections closer to the C-terminus. Nup53 truncations lacking the last eight (Nup53 162–312) or 25 amino acids (Nup53 162–295) bound Nup155 (Fig. 6B). Further C-terminal truncation up to amino acid 267 (Nup53 162–267) resulted in a loss of the interaction. If the RRM domain (aa 163–243 in the *Xenopus* protein) was absent, Nup53 failed to bind Nup155 (Fig. 6C) showing that the RRM domain of Nup53 is required but not sufficient for the Nup155 interaction. Thus, the RRM domain and an additional region (between aa 267–295) within the C-terminus of Nup53 form the Nup155 interaction surface.

Next, we generated a Nup53 point mutant to impair its interaction with Nup155. By exchanging the conserved lysine residue of position 262 to alanine, Nup53 binding to Nup155 was compromised both *in vitro* and *in vivo* without affecting the interaction with Ndc1 (Fig. 6D,E; supplementary material Fig. S3). Thus, the K262A mutation on Nup53 specifically affects Nup155 binding and provides a useful tool to study the role of the Nup53–Nup155 interaction in NPC assembly.

Nup53–Nup155 interaction is essential for NPC assembly

The Nup53 K262A point mutant was used in nuclear assemblies with Nup53-depleted egg extracts (1–320 K262A, Fig. 7A). As before, depletion of Nup53 blocked NE and NPC formation and wild-type Nup53 (Nup53 1–320) rescued this phenotype (Fig. 7B,C). By contrast, the Nup53 mutant deficient for the Nup155 interaction (1–320 K262A) did not support formation of a closed NE and NPCs. Interestingly, the Nup53 point mutant was recruited to the chromatin template, albeit at reduced levels. This indicates that localization of Nup53 to the reassembling NPC is independent of Nup155. By contrast, recruitment of Nup155 mainly depends on its interaction with Nup53 because Nup155 was hardly detectable on the chromatin in the presence of the mutant Nup53 construct (1–320 K262A). Other Nup93 complex members, including Nup93, Nup205 and Nup188 were absent from the chromatin if the Nup53 mutant was used (Fig. 7D). It is unlikely that this lack of recruitment was caused by disrupting the direct protein interaction between Nup53 and Nup93 because Nup93 binds to the N-terminal part of Nup53 (Amlacher et al., 2011; Fahrenkrog et al., 2000; Hawryluk-Gara et al., 2008; Vollmer et al., 2012), which was unaffected by the mutation, and rather indicates that the recruitment of Nup93 as well as of Nup188 and Nup205 requires a functional Nup53–Nup155 interaction. Similarly, Nup58, a member of the Nup62 complex, was not recruited because this requires the presence of Nup93 (Sachdev et al., 2012). Nup107, Ndc1, Pom121 and Gp210 were present on the chromatin but did not show smooth rim staining because no closed NE was formed. Therefore, the interactions of Nup155 with Ndc1 and Pom121 or the Nup107–Nup160 complex (Mitchell et al., 2010; Yavuz et al., 2010) are insufficient to locate Nup155 at the nuclear rim. These data show that binding of Nup53 to Nup155 is required for efficient recruitment of Nup155 to the assembling pore and is crucial for NPC assembly at the end of mitosis.

DISCUSSION

We have functionally analyzed the interactions of three essential nucleoporins in NPC assembly: Ndc1, Nup53 and Nup155. *Xenopus* Nup53 and Ndc1 interact directly. This interaction is mediated by the transmembrane regions of Ndc1 and the C-terminal part of Nup53. Our data indicate that this interaction is crucial for NPC reassembly at the end of mitosis and regulates the membrane-deformation capability of Nup53. Furthermore, our study reveals a crucial role for the direct interaction of Nup53 and Nup155 for NPC formation because abolishing this interaction by specific point mutation of Nup53 blocks NPC assembly.

Nup53 is a component of the Nup93 complex forming the inner ring of NPCs adjacent to the pore membrane (Alber et al., 2007; Brohawn et al., 2009). As a result of its many interactions, Nup53 acts as a connection point between the pore membrane and other nucleoporins. *Xenopus* Nup53 and the yeast counterparts bind membranes directly and this interaction in vertebrates is essential for NPC assembly (Patel and Rexach, 2008; Vollmer et al., 2012). Moreover, Nup53 interacts with the transmembrane nucleoporin Ndc1 (Hawryluk-Gara et al., 2008; Mansfeld et al., 2006; Onischenko et al., 2009; Uetz et al., 2000; Vollmer et al., 2012), as well as with Nup155 and Nup93, two other members of the Nup93 complex (Amlacher et al., 2011; Fahrenkrog et al., 2000; Hawryluk-Gara et al., 2005; Onischenko et al., 2009). In metazoa, Nup53 and Nup155 are both essential components of the Nup93 complex (Franz et al., 2005; Galy et al., 2003; Hawryluk-Gara et al., 2008; Hawryluk-Gara et al., 2005; Kiger et al., 1999; Mitchell et al., 2010; Ródenas et al., 2009; Vollmer et al., 2012). *S. cerevisiae* possesses two Nup53 orthologs, Nup53 and Nup59, and two Nup155 orthologs, Nup157 and Nup170. Double deletions of Nup53 and Nup59 in *S. cerevisiae* are viable (Marelli et al., 1998) but co-deletion of either one with Nup157 or Nup170 causes severe growth defects or lethality, respectively (Marelli et al., 1998). These observations suggest an important role of the Nup53–Nup155 interaction and, indeed, Nup155 binding to Nup53 is thought to be crucial for vertebrate NPC assembly (Hawryluk-Gara et al., 2008). However, the experiments defining the requirement of the vertebrate Nup53–Nup155 interaction used Nup53 constructs that not only lack the Nup155-interaction site but also the RRM domain, which is important for membrane binding. Also, a deletion in the gene encoding Nup53 in *C. elegans* that causes NPC defects (Ródenas et al., 2009) probably affects interaction with both the membrane and Nup155, because the major part of the RRM domain was absent from the protein product. By generating a Nup53 point mutant specifically impaired in Nup155 binding without modifying the RRM domain, we separated these two functions of Nup53 and show that the Nup53–Nup155 interaction is specifically required for NE and NPC assembly (Fig. 6,7).

Nup53 and Nup155 form a conserved trimeric complex with Nup93 in which Nup93 stabilizes the Nup53–Nup155 interaction (Amlacher et al., 2011; Sachdev et al., 2012). We found that Nup93 is absent from the chromatin in the context of the Nup53 point mutant deficient for Nup155 binding (Fig. 7D). This suggests that Nup53–Nup155 binding recruits Nup93 to the

Journal of Cell Science

Journal of Cell Science (2014) 127, 908–921 doi:10.1242/jcs.141739

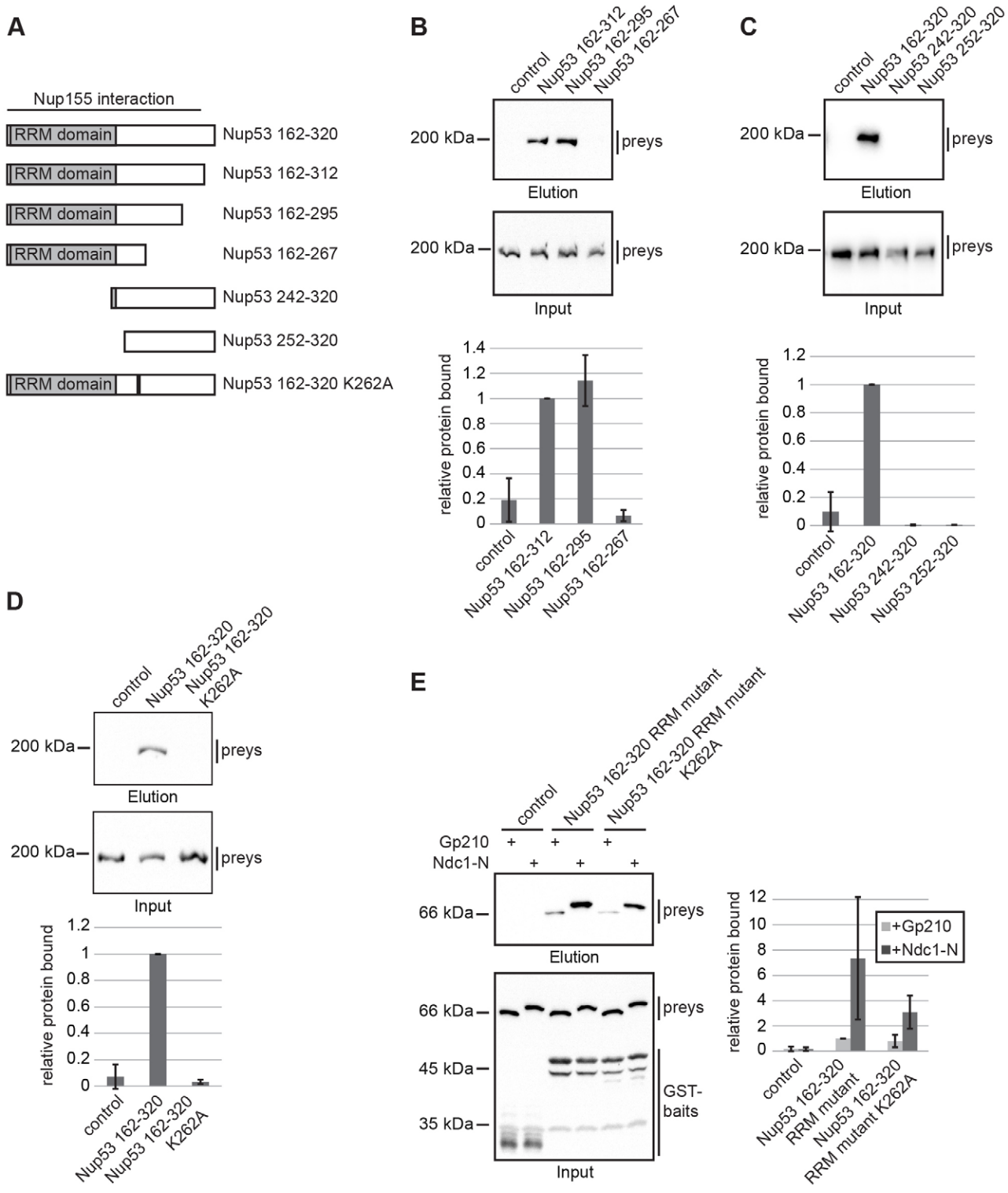

Fig. 6. Nup53 interacts with Nup155 through its C-terminal portion. (A) Schematic representation of *Xenopus* Nup53 constructs used. (B) GST pull-downs with the nucleoplasmic domain of *Xenopus* Gp210 (control) or fragments of *Xenopus* Nup53 comprising the RRM domain and parts of the C-terminus (Nup53 162–312, 162–295 and 162–267) and *E. coli* lysates overexpressing NusA-tagged *Xenopus* Nup155. Eluates and 3% of the input were analyzed using a His_6 antibody. Three independent experiments were quantified (bottom) for the bait-bound protein to input ratio normalized to Nup53 162–312. Error bars represent s.d. (C) GST pull-downs as in B, using Nup53 constructs comprising the RRM domain and the C-terminus (162–320) or lacking the RRM domain (242–320, 252–320). Three independent experiments were quantified and normalized to Nup53 162–320 as in B. (D) GST pull-downs as in B, using a Nup53 fragment comprising the RRM domain and the C-terminus (162–320) and a mutant impaired in the Nup155 interaction (162–320 K262A). (E) GST pull-downs with baits as in D and *E.coli* lysates as in Fig. 1B. Quantification was carried out as in Fig. 1D.

Journal of Cell Science (2014) 127, 908–921 doi:10.1242/jcs.141739

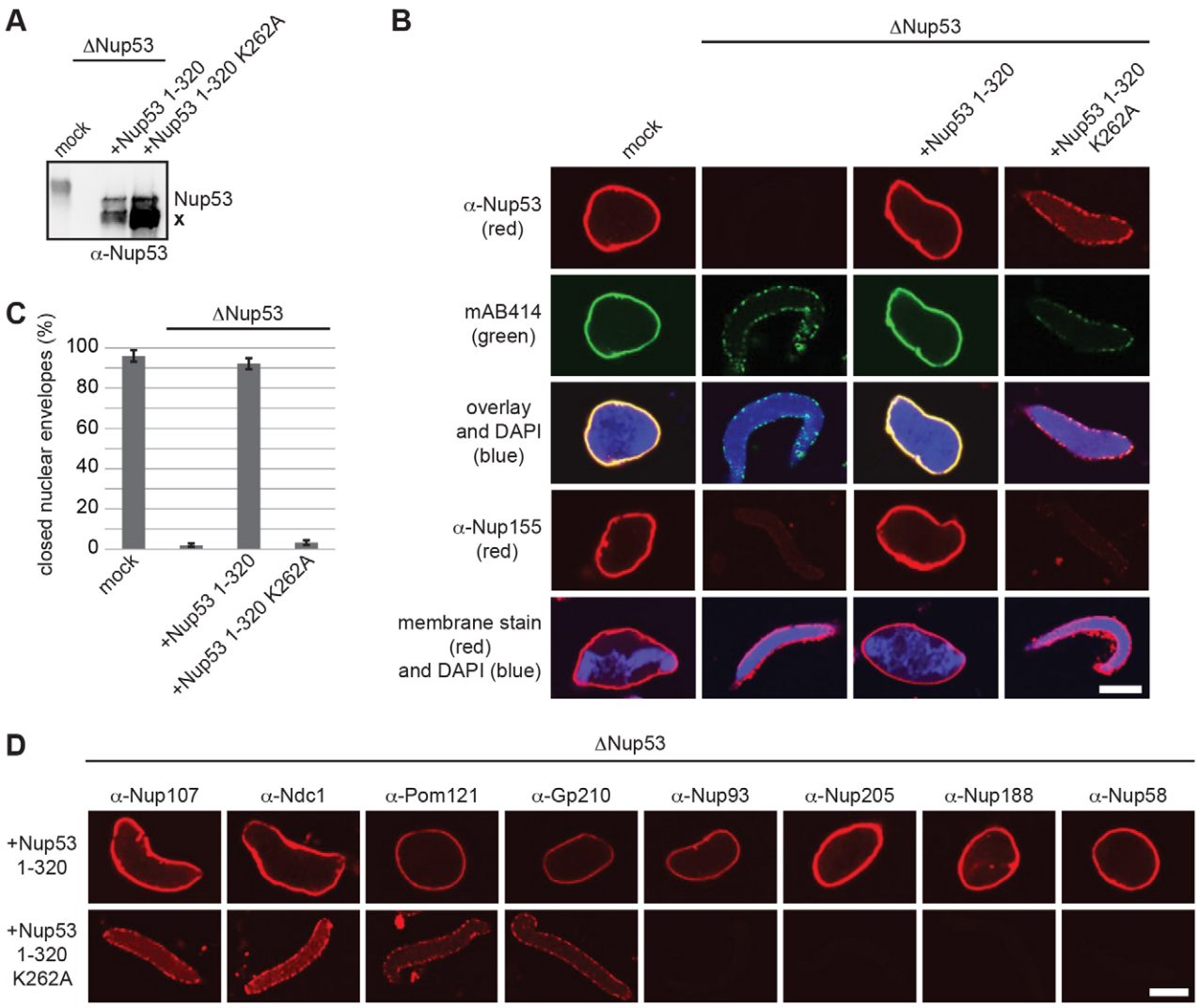

Fig. 7. The Nup53–Nup155 interaction is crucial for NPC assembly. (A) Cytosol from egg extracts was mock treated, Nup53 depleted or Nup53 depleted and supplemented with wild-type Nup53 (1–320) or a mutant impaired in the Nup155 interaction (1–320 K262A) and analyzed by western blotting. Nup53 degradations are indicated (x). (B) Nuclei were assembled in extracts from A and analyzed by immunofluorescence for Nup53 (red), mAB414 (green) or Nup155 (red). DNA was stained with DAPI (blue), membranes with $DiIC_{18}$ (red). (C) Quantification of nuclear assembly reactions from B, carried out as in Fig. 2C. (D) Nuclei assembled as in B, in the presence of full-length Nup53 (1–320) or the mutant deficient for the Nup155 interaction (1–320 K262A) were analyzed by immunofluorescence with the respective antibodies. Scale bars: 10 μm.

assembling NPC, which in turn recruits the Nup62 complex (Amlacher et al., 2011; Grandi et al., 1995; Sachdev et al., 2012). Interestingly, Nup53, Nup155 and Nup93 are identified in all eukaryotic super-groups (Neumann et al., 2010) and could have been present in the last common eukaryotic ancestor. Altogether, this implicates an essential, evolutionary conserved role of the three proteins and their interaction in NPC assembly and function.

Ndc1 is a crucial factor for NPC assembly both in metazoa (Mansfeld et al., 2006; Stavru et al., 2006) and yeast (Madrid et al., 2006). In *S. cerevisiae*, it binds directly both Nup53 orthologs, Nup53 and Nup59 (Onischenko et al., 2009). Our data demonstrate that this direct interaction is evolutionarily conserved (Fig. 1) and important for NPC assembly (Fig. 5). Upon separation of the Ndc1–Nup53 interaction from the Nup53 C-terminal membrane binding and deformation activity, we determined the specific requirement of the Nup53–Ndc1 interplay during NPC formation. This revises previous observations, suggesting a redundant role of this interaction in NPC assembly (Hawryluk-Gara et al., 2008; Vollmer et al., 2012). We show that the Ndc1 interaction is specifically required if Nup53 can deform membranes (Fig. 5). The Ndc1 transmembrane domain, which contains the Nup53 binding site, becomes dispensable if endogenous Nup53 is replaced by a Nup53 truncation that is defective in membrane deformation (Fig. 3). Our finding that the N-terminal part of Ndc1 is the Nup53 interaction surface (Fig. 1) is surprising at first glance because the C-terminal part of Ndc1 is much better conserved and exposed to the NPC (Lau et al., 2006; Mansfeld et al., 2006; Stavru et al., 2006). This region serves as an interaction platform for two other nucleoporins, Aladin and Nup155 (Kind et al., 2009; Mitchell et al., 2010; Yamazumi et al., 2009). The N-terminal half of Ndc1 comprises the six predicted transmembrane helices embedded in the pore membrane and interacts with the C-terminus of Nup53, which in turn is required for membrane deformation. Similarly, yeast Nup53 and Nup59

Journal of Cell Science

Journal of Cell Science (2014) 127, 908–921 doi:10.1242/jcs.141739

both interact with Ndc1 through their C-terminal ends (Onischenko et al., 2009). These regions are predicted to fold into amphipathic α-helices and might also deform membranes (Marelli et al., 2001; Patel and Rexach, 2008; Vollmer et al., 2012). Thus, the Ndc1–Nup53 interaction could take place within the lipid bilayer and membrane integration of the Nup53 binding site might hence be required. Our data highlight the fact that the Ndc1–Nup53 interaction is only required for post-mitotic NPC assembly if Nup53 can deform membranes (Figs 3,5). This membrane deformation activity of the Nup53 C-terminus is dispensable for NPC formation at the end of mitosis but essential if NPCs integrate into the closed NE during interphase (Vollmer et al., 2012). We propose that Nup53 membrane deformation activity needs to be counteracted or fine-tuned and this requires Ndc1 binding. During NPC formation, both at the end of mitosis and in interphase, nuclear membranes might initially show high positive curvature at local sites of pore formation. However, during the process of NPC formation these highly curved membranes have to convert into the specific structure of the nuclear pore (Fig. 8). This final membrane shape is characterized by the coexistence of a positive and a negative curvature. Because the negative curvature could energetically balance the positive curvature (Terasaki et al., 2013), the final pore membrane structure might be passively adopted and might not require active membrane deformation as induced by Nup53. In this regard, Ndc1 might be the crucial factor regulating the membrane-deformation activity of Nup53 in the NPC.

A similar regulation of membrane-deforming activity was reported for reticulons, which are ER-tubulating proteins that associate with highly curved membranes (Hu et al., 2008; Voeltz et al., 2006). These proteins are displaced from the reforming NE at the end of mitosis. In human cells, overexpression of reticulons delays re-formation of the NE and a reduction in reticulons accelerates it (Anderson and Hetzer, 2008). Hence, it might be generally important to attenuate membrane deformation during re-formation of the NE and NPCs. This could be achieved by the removal of tubulating proteins or regulation by other proteins. How this happens mechanistically for the Ndc1–Nup53 interaction can only be speculated. Ndc1 might deform the pore membrane in the opposite way as a result of its shape or by oligomerization, which then obliterates the membrane curvature induced by Nup53 (Fig. 8A). Alternatively, Ndc1 binding could induce a conformational change in Nup53, resulting in a rearrangement of its C-terminus, which might then be buried inside the protein or the interaction surfaces (Fig. 8B).

Surprisingly, Ndc1 is not found in all eukaryotes (DeGrasse et al., 2009; Neumann et al., 2010) and is dispensable in the fungus *Aspergillus nidulans* (Liu et al., 2009). *A. nidulans* also lacks any obvious Nup53 ortholog, which is in agreement with our observation that the Ndc1–Nup53 interaction is only essential if Nup53 can deform membranes. Some organisms contain a Nup53 but no Ndc1 ortholog (Neumann et al., 2010). In these organisms Nup53 might be regulated by other proteins or their Nup53 orthologs could lack the membrane-deformation ability. Indeed, Ndc1 is absent from all *Amoebozoa* tested (Neumann et al., 2010) and their Nup53 proteins show only little sequence homology to the yeast or metazoan proteins in their C-termini, suggesting that they might not be able to deform membranes. Overall, it seems that not only is the direct Ndc1–Nup53 interaction conserved, but the function of this complex in controlling the membrane-deformation activity of Nup53 is also maintained.

The analyses of the different Nup53 interactions reveal its diverse functions in NPC assembly and elucidate the step-wise process of re-formation of the metazoan NPC at the end of mitosis (for a review, see Schooley et al., 2012). NPC reassembly starts on the decondensing chromatin by DNA binding of the nucleoporin Mel28/ELYS, which in turn recruits the Nup107–Nup160 complex (Franz et al., 2007; Galy et al., 2006; Gillespie et al., 2007; Rasala et al., 2006). Subsequently, NE precursor membranes bind to the NPC assembly sites, including the integral pore membrane proteins Ndc1 and Pom121 (Antonin et al., 2005; Mansfeld et al., 2006; Rasala et al., 2008). Pom121 was detected on the chromatin templates in the absence of Ndc1 (Fig. 2). This suggests that recruitment of Ndc1 and Pom121 can occur independently and supports the previously observed redundancy in the membrane recruitment step. Next, the Nup93 complex is localized to the nascent pore. This step is initiated by the recruitment of Nup53 for which its membrane interaction is crucial (Vollmer et al., 2012). Nup53 recruitment is independent of the Ndc1 interaction because Nup53 is also localized to assembling NPCs if both proteins cannot interact or if Ndc1 is depleted (Figs 3,5). The Nup155 recruitment and subsequent establishment of the Nup53–Nup155 interaction is the next decisive step in NPC assembly. In Nup53-depleted extracts or if Nup53 is defective in binding Nup155, staining for Nup155 on the chromatin is strongly decreased and other members of the Nup93 complex as well as the Nup62 complex are not detectable (Fig. 7 and Hawryluk-Gara et al., 2008; Vollmer et al., 2012). Consistently, knockdown of Nup53 by siRNA in HeLa cells

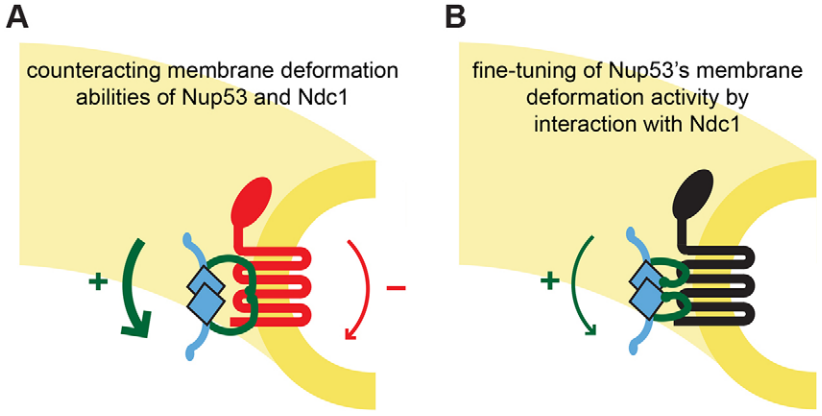

Fig. 8. Regulation of Nup53 membrane deformation by Ndc1. In the pore membrane, positive membrane curving (green arrow) by the Nup53 C-terminus (green) might be partially antagonized by negative curvature (red arrow) induced by Ndc1 (red, A). Alternatively, Ndc1 (black) might attenuate the membrane-deformation activity of Nup53 (green) by direct binding (B). For the sake of simplicity, other membrane-curving factors as the Nup107–Nup160 complex and reticulons are omitted.

decreases the levels of Nup155 at the nuclear rim, as well as of Nup93 and Nup205 (Hawryluk-Gara et al., 2005), and in *C. elegans*, localization of Nup155 requires Nup53 (Ródenas et al., 2009). Together, this indicates that recruitment of Nup155 predominantly depends on the presence of Nup53, despite the fact that it also interacts with Ndc1 and Pom121. If Nup53 and Nup155 are present in an intact complex, NPC assembly proceeds further, probably by recruiting Nup93 and subsequently, the Nup62 complex (Sachdev et al., 2012). Eventually, further components of the nuclear basket and cytoplasmic filaments are recruited by yet ill-defined steps, completing the process of NPC assembly at the end of mitosis and yielding fully assembled functional NPCs.

MATERIALS AND METHODS

Antibodies against Ndc1 (Mansfeld et al., 2006), Pom121 and Gp210 (Antonin et al., 2005), Nup53, Nup188 and Nup205 (Theerthagiri et al., 2010), Nup93 and Nup58 (Sachdev et al., 2012), Nup155 (Franz et al., 2005) and Nup107 (Walther et al., 2003) have been described previously. MAB414 was obtained from BAbCO (Richmond, CA), antibodies against EGFP, His_6, Myc and HA were from Roche (Mannheim, Germany), Alexa Fluor 488 goat anti-rabbit IgG, Cy3 goat anti -mouse IgG and 1,1′-Dioctadecyl-3,3,3′,3′-tetramethylindocarbocyanine perchlorate ($DiIC_{18}$) were from Invitrogen (Eugene, OR).

Protein expression and purification

Constructs are listed as supplementary material Table S1. Nup53 constructs were generated from a synthetic DNA optimized for *E. coli* codon usage (Vollmer et al., 2012). For pull-down reactions, Nup53 fragments were cloned into a pET28a vector (EMD, Darmstadt, Germany) with an N-terminal GST tag and a TEV-protease recognition site upstream of the Nup53 fragments, or have been described previously (Vollmer et al., 2012). The nucleoplasmic domain of *Xenopus* Gp210 (Antonin et al., 2005) was cloned into the same modified vector. Proteins were expressed in *E. coli* BL21de3 and purified using an N-terminal His_6 tag with Ni-NTA agarose (Qiagen, Hilden, Germany).

For nuclear assembly, liposome flotation or tubulation Nup53 fragments were cloned into a pET28a vector with a yeast SUMO tag (SMT3) and a TEV-protease recognition site upstream of the protein fragments. His_6 and SUMO tags were cleaved off after purification from *E. coli*; the proteins were concentrated using Vivaspin 500 (Sartorius, Goettingen, Germany) and purified by gel filtration, either in PBS for liposome flotation and tubulation or in sucrose buffer for nuclear assembly. The Nup53 deletion constructs impaired in Ndc1 interaction were generated by replacing the eight amino acids of positions 275–282 (RAASMRPL) with the linker sequence GGSGSGGS and cloned into the respective vectors for pull-down, flotation, liposome tubulation and NPC assembly experiments.

To express integral membrane proteins, *Xenopus* Ndc1, the respective Ndc1 fragments or the Gp210 fragment comprising the transmembrane region and the nucleoplasmic part were cloned into a pET28a vector with an N-terminal Mistic (membrane-integrating sequence for translation of integral membrane protein constructs) sequence to enhance expression at the *E. coli* membrane (Roosild et al., 2005; Theerthagiri et al., 2010) followed by an EGFP tag upstream of the respective protein and a C-terminal His_6 tag. Proteins were expressed in *E. coli* and used as lysate in pull-downs or further purified in the presence of 1% (w/v) cetyltrimethylammoniumbromide (Calbiochem, Darmstadt, Germany) using Ni-NTA agarose and dialyzed against sucrose buffer (Theerthagiri et al., 2010).

Pull-down experiments

E. coli lysates overexpressing the transmembrane nucleoporin constructs were adjusted with lysates from *E. coli* transformed with empty vector to equal protein concentrations and incubated with 1.5 µM of GST baits in a final volume of 800 µl. For Fig. 1B, 0.5 µM GST baits were incubated in 2 ml of the respective *E. coli* lysates. After 1 hour, 9 µl of magnetic glutathione beads (Pierce, Rockford, IL) were added for another hour, washed six times with 20 mM Tris-HCl, pH 7.5 and 150 mM NaCl and eluted in 30 µl total volume by TEV protease cleavage (0.5 mg/ml) for 1 hour at 25°C. For pull-downs with recombinant Nup155, 1.5 µM of respective GST baits were incubated with *E. coli* lysates overexpressing NusA-fused full-length Nup155 (Sachdev et al., 2012). Pull-downs with *Xenopus*-derived cytosol and membranes were performed as described previously (Vollmer et al., 2012).

Immunoprecipitation

Full-length *Xenopus* Ndc1, the respective fragments or full-length *Xenopus* Nup155 were cloned with an N-terminal Myc tag into pEGFP-N1 (Clontech, Saint-Germain-en-Laye, France) containing a C-terminal EGFP-tag. HA-tagged *Xenopus* Nup53 has been described previously (Vollmer et al., 2012) and the K262A point mutation was introduced in this construct. Transfection of HeLa cells and immunoprecipitation were carried out as described (Vollmer et al., 2012).

Other methods

Nuclear assembly and immunofluorescence (Antonin et al., 2005; Theerthagiri et al., 2010), generation of affinity resins, sperm heads and floated membranes (Franz et al., 2005) as well as prelabelled membranes (Antonin et al., 2005) were all carried out as described previously. For add-back of recombinant Ndc1 constructs, purified proteins were reconstituted into solubilized membranes (Mansfeld et al., 2006). For testing dominant-negative effects in nuclear assembly, recombinant proteins were added to untreated *Xenopus* egg extracts at the beginning of the reaction. Liposome flotation and tubulation were done as described previously (Vollmer et al., 2012).

Acknowledgements

We thank U. Kutay for discussion of unpublished data, S. Astrinidis, C. Sieverding and T. Strittmatter for technical support, and M. Lorenz, R. Sachdev, K. Schellhaus, A. Schooley and B. Vollmer for critical reading of the manuscript.

Author contributions

N.E. and W.A. designed and performed experiments and wrote the manuscript. J.R. developed the methods to express and purify transmembrane nucleoporins from *E. coli*.

Competing interests

The authors declare no competing interest.

Funding

The work was funded by the Max Planck Society.

Supplementary material

Supplementary material available online at
http://jcs.biologists.org/lookup/suppl/doi:10.1242/jcs.141739/-/DC1

References

Alber, F., Dokudovskaya, S., Veenhoff, L. M., Zhang, W., Kipper, J., Devos, D., Suprapto, A., Karni-Schmidt, O., Williams, R., Chait, B. T. et al. (2007). The molecular architecture of the nuclear pore complex. *Nature* **450**, 695-701.

Amlacher, S., Sarges, P., Flemming, D., van Noort, V., Kunze, R., Devos, D. P., Arumugam, M., Bork, P. and Hurt, E. (2011). Insight into structure and assembly of the nuclear pore complex by utilizing the genome of a eukaryotic thermophile. *Cell* **146**, 277-289.

Anderson, D. J. and Hetzer, M. W. (2008). Reshaping of the endoplasmic reticulum limits the rate for nuclear envelope formation. *J. Cell Biol.* **182**, 911-924.

Antonin, W., Franz, C., Haselmann, U., Antony, C. and Mattaj, I. W. (2005). The integral membrane nucleoporin pom121 functionally links nuclear pore complex assembly and nuclear envelope formation. *Mol. Cell* **17**, 83-92.

Brohawn, S. G., Leksa, N. C., Spear, E. D., Rajashankar, K. R. and Schwartz, T. U. (2008). Structural evidence for common ancestry of the nuclear pore complex and vesicle coats. *Science* **322**, 1369-1373.

Brohawn, S. G., Partridge, J. R., Whittle, J. R. and Schwartz, T. U. (2009). The nuclear pore complex has entered the atomic age. *Structure* **17**, 1156-1168.

Chadrin, A., Hess, B., San Roman, M., Gatti, X., Lombard, B., Loew, D., Barral, Y., Palancade, B. and Doye, V. (2010). Pom33, a novel transmembrane nucleoporin required for proper nuclear pore complex distribution. *J. Cell Biol.* **189**, 795-811.

Journal of Cell Science

Cronshaw, J. M., Krutchinsky, A. N., Zhang, W., Chait, B. T. and Matunis, M. J. (2002). Proteomic analysis of the mammalian nuclear pore complex. *J. Cell Biol.* **158**, 915-927.
DeGrasse, J. A., DuBois, K. N., Devos, D., Siegel, T. N., Sali, A., Field, M. C., Rout, M. P. and Chait, B. T. (2009). Evidence for a shared nuclear pore complex architecture that is conserved from the last common eukaryotic ancestor. *Molecular & Cellular Proteomics* **8**, 2119-2130.
Devos, D., Dokudovskaya, S., Alber, F., Williams, R., Chait, B. T., Sali, A. and Rout, M. P. (2004). Components of coated vesicles and nuclear pore complexes share a common molecular architecture. *PLoS Biol.* **2**, e380.
Fahrenkrog, B., Hübner, W., Mandinova, A., Panté, N., Keller, W. and Aebi, U. (2000). The yeast nucleoporin Nup53p specifically interacts with Nic96p and is directly involved in nuclear protein import. *Mol. Biol. Cell* **11**, 3885-3896.
Franz, C., Askjaer, P., Antonin, W., Iglesias, C. L., Haselmann, U., Schelder, M., de Marco, A., Wilm, M., Antony, C. and Mattaj, I. W. (2005). Nup155 regulates nuclear envelope and nuclear pore complex formation in nematodes and vertebrates. *EMBO J.* **24**, 3519-3531.
Franz, C., Walczak, R., Yavuz, S., Santarella, R., Gentzel, M., Askjaer, P., Galy, V., Hetzer, M., Mattaj, I. W. and Antonin, W. (2007). MEL-28/ELYS is required for the recruitment of nucleoporins to chromatin and postmitotic nuclear pore complex assembly. *EMBO Rep.* **8**, 165-172.
Galy, V., Mattaj, I. W. and Askjaer, P. (2003). Caenorhabditis elegans nucleoporins Nup93 and Nup205 determine the limit of nuclear pore complex size exclusion in vivo. *Mol. Biol. Cell* **14**, 5104-5115.
Galy, V., Askjaer, P., Franz, C., López-Iglesias, C. and Mattaj, I. W. (2006). MEL-28, a novel nuclear envelope and kinetochore protein essential for zygotic nuclear envelope assembly in C. elegans. *Curr. Biol.* **16**, 1748-1756.
Gant, T. M. and Wilson, K. L. (1997). Nuclear assembly. *Annu. Rev. Cell Dev. Biol.* **13**, 669-695.
Gerace, L., Ottaviano, Y. and Kondor-Koch, C. (1982). Identification of a major polypeptide of the nuclear pore complex. *J. Cell Biol.* **95**, 826-837.
Gillespie, P. J., Khoudoli, G. A., Stewart, G., Swedlow, J. R. and Blow, J. J. (2007). ELYS/MEL-28 chromatin association coordinates nuclear pore complex assembly and replication licensing. *Curr. Biol.* **17**, 1657-1662.
Grandi, P., Schlaich, N., Tekotte, H. and Hurt, E. C. (1995). Functional interaction of Nic96p with a core nucleoporin complex consisting of Nsp1p, Nup49p and a novel protein Nup57p. *EMBO J.* **14**, 76-87.
Grandi, P., Dang, T., Pané, N., Shevchenko, A., Mann, M., Forbes, D. and Hurt, E. (1997). Nup93, a vertebrate homologue of yeast Nic96p, forms a complex with a novel 205-kDa protein and is required for correct nuclear pore assembly. *Mol. Biol. Cell* **8**, 2017-2038.
Hallberg, E., Wozniak, R. W. and Blobel, G. (1993). An integral membrane protein of the pore membrane domain of the nuclear envelope contains a nucleoporin-like region. *J. Cell Biol.* **122**, 513-521.
Handa, N., Kukimoto-Niino, M., Akasaka, R., Kishishita, S., Murayama, K., Terada, T., Inoue, M., Kigawa, T., Kose, S., Imamoto, N. et al. (2006). The crystal structure of mouse Nup35 reveals atypical RNP motifs and novel homodimerization of the RRM domain. *J. Mol. Biol.* **363**, 114-124.
Hawryluk-Gara, L. A., Shibuya, E. K. and Wozniak, R. W. (2005). Vertebrate Nup53 interacts with the nuclear lamina and is required for the assembly of a Nup93-containing complex. *Mol. Biol. Cell* **16**, 2382-2394.
Hawryluk-Gara, L. A., Platani, M., Santarella, R., Wozniak, R. W. and Mattaj, I. W. (2008). Nup53 is required for nuclear envelope and nuclear pore complex assembly. *Mol. Biol. Cell* **19**, 1753-1762.
Hu, J., Shibata, Y., Voss, C., Shemesh, T., Li, Z., Coughlin, M., Kozlov, M. M., Rapoport, T. A. and Prinz, W. A. (2008). Membrane proteins of the endoplasmic reticulum induce high-curvature tubules. *Science* **319**, 1247-1250.
Kiger, A. A., Gigliotti, S. and Fuller, M. T. (1999). Developmental genetics of the essential Drosophila nucleoporin nup154: allelic differences due to an outward-directed promoter in the P-element 3′ end. *Genetics* **153**, 799-812.
Kind, B., Koehler, K., Lorenz, M. and Huebner, A. (2009). The nuclear pore complex protein ALADIN is anchored via NDC1 but not via POM121 and GP210 in the nuclear envelope. *Biochem. Biophys. Res. Commun.* **390**, 205-210.
Krull, S., Thyberg, J., Björkroth, B., Rackwitz, H. R. and Cordes, V. C. (2004). Nucleoporins as components of the nuclear pore complex core structure and Tpr as the architectural element of the nuclear basket. *Mol. Biol. Cell* **15**, 4261-4277.
Lau, C. K., Giddings, T. H., Jr and Winey, M. (2004). A novel allele of Saccharomyces cerevisiae NDC1 reveals a potential role for the spindle pole body component Ndc1p in nuclear pore assembly. *Eukaryot. Cell* **3**, 447-458.
Lau, C. K., Delmar, V. A. and Forbes, D. J. (2006). Topology of yeast Ndc1p: predictions for the human NDC1/NET3 homologue. *Anat. Rec. A Discov. Mol. Cell. Evol. Biol.* **288A**, 681-694.
Liu, H. L., De Souza, C. P., Osmani, A. H. and Osmani, S. A. (2009). The three fungal transmembrane nuclear pore complex proteins of Aspergillus nidulans are dispensable in the presence of an intact An-Nup84-120 complex. *Mol. Biol. Cell* **20**, 616-630.
Lohka, M. J. and Masui, Y. (1983). Formation in vitro of sperm pronuclei and mitotic chromosomes induced by amphibian ooplasmic components. *Science* **220**, 719-721.
Madrid, A. S., Mancuso, J., Cande, W. Z. and Weis, K. (2006). The role of the integral membrane nucleoporins Ndc1p and Pom152p in nuclear pore complex assembly and function. *J. Cell Biol.* **173**, 361-371.
Mans, B. J., Anantharaman, V., Aravind, L. and Koonin, E. V. (2004). Comparative genomics, evolution and origins of the nuclear envelope and nuclear pore complex. *Cell Cycle* **3**, 1625-1650.
Mansfeld, J., Güttinger, S., Hawryluk-Gara, L. A., Panté, N., Mall, M., Galy, V., Haselmann, U., Mühlhäusser, P., Wozniak, R. W., Mattaj, I. W. et al. (2006). The conserved transmembrane nucleoporin NDC1 is required for nuclear pore complex assembly in vertebrate cells. *Mol. Cell* **22**, 93-103.
Marelli, M., Aitchison, J. D. and Wozniak, R. W. (1998). Specific binding of the karyopherin Kap121p to a subunit of the nuclear pore complex containing Nup53p, Nup59p, and Nup170p. *J. Cell Biol.* **143**, 1813-1830.
Marelli, M., Lusk, C. P., Chan, H., Aitchison, J. D. and Wozniak, R. W. (2001). A link between the synthesis of nucleoporins and the biogenesis of the nuclear envelope. *J. Cell Biol.* **153**, 709-724.
Miao, M., Ryan, K. J. and Wente, S. R. (2006). The integral membrane protein Pom34p functionally links nucleoporin subcomplexes. *Genetics* **172**, 1441-1457.
Mitchell, J. M., Mansfeld, J., Capitanio, J., Kutay, U. and Wozniak, R. W. (2010). Pom121 links two essential subcomplexes of the nuclear pore complex core to the membrane. *J. Cell Biol.* **191**, 505-521.
Neumann, N., Lundin, D. and Poole, A. M. (2010). Comparative genomic evidence for a complete nuclear pore complex in the last eukaryotic common ancestor. *PLoS ONE* **5**, e13241.
Onischenko, E., Stanton, L. H., Madrid, A. S., Kieselbach, T. and Weis, K. (2009). Role of the Ndc1 interaction network in yeast nuclear pore complex assembly and maintenance. *J. Cell Biol.* **185**, 475-491.
Ori, A., Banterle, N., Iskar, M., Andrés-Pons, A., Escher, C., Khanh Bui, H., Sparks, L., Solis-Mezarino, V., Rinner, O., Bork, P. et al. (2013). Cell type-specific nuclear pores: a case in point for context-dependent stoichiometry of molecular machines. *Mol. Syst. Biol.* **9**, 648.
Patel, S. S. and Rexach, M. F. (2008). Discovering novel interactions at the nuclear pore complex using bead halo: a rapid method for detecting molecular interactions of high and low affinity at equilibrium. *Molecular & Cellular Proteomics* **7**, 121-131.
Rasala, B. A., Orjalo, A. V., Shen, Z., Briggs, S. and Forbes, D. J. (2006). ELYS is a dual nucleoporin/kinetochore protein required for nuclear pore assembly and proper cell division. *Proc. Natl. Acad. Sci. USA* **103**, 17801-17806.
Rasala, B. A., Ramos, C., Harel, A. and Forbes, D. J. (2008). Capture of AT-rich chromatin by ELYS recruits POM121 and NDC1 to initiate nuclear pore assembly. *Mol. Biol. Cell* **19**, 3982-3996.
Ródenas, E., Klerkx, E. P., Ayuso, C., Audhya, A. and Askjaer, P. (2009). Early embryonic requirement for nucleoporin Nup35/NPP-19 in nuclear assembly. *Dev. Biol.* **327**, 399-409.
Roosild, T. P., Greenwald, J., Vega, M., Castronovo, S., Riek, R. and Choe, S. (2005). NMR structure of Mistic, a membrane-integrating protein for membrane protein expression. *Science* **307**, 1317-1321.
Rout, M. P., Aitchison, J. D., Suprapto, A., Hjertaas, K., Zhao, Y. and Chait, B. T. (2000). The yeast nuclear pore complex: composition, architecture, and transport mechanism. *J. Cell Biol.* **148**, 635-651.
Sachdev, R., Sieverding, C., Flötenmeyer, M. and Antonin, W. (2012). The C-terminal domain of Nup93 is essential for assembly of the structural backbone of nuclear pore complexes. *Mol. Biol. Cell* **23**, 740-749.
Schooley, A., Vollmer, B. and Antonin, W. (2012). Building a nuclear envelope at the end of mitosis: coordinating membrane reorganization, nuclear pore complex assembly, and chromatin de-condensation. *Chromosoma* **121**, 539-554.
Stavru, F., Hülsmann, B. B., Spang, A., Hartmann, E., Cordes, V. C. and Görlich, D. (2006). NDC1: a crucial membrane-integral nucleoporin of metazoan nuclear pore complexes. *J. Cell Biol.* **173**, 509-519.
Terasaki, M., Shemesh, T., Kasthuri, N., Klemm, R. W., Schalek, R., Hayworth, K. J., Hand, A. R., Yankova, M., Huber, G., Lichtman, J. W. et al. (2013). Stacked endoplasmic reticulum sheets are connected by helicoidal membrane motifs. *Cell* **154**, 285-296.
Theerthagiri, G., Eisenhardt, N., Schwarz, H. and Antonin, W. (2010). The nucleoporin Nup188 controls passage of membrane proteins across the nuclear pore complex. *J. Cell Biol.* **189**, 1129-1142.
Uetz, P., Giot, L., Cagney, G., Mansfield, T. A., Judson, R. S., Knight, J. R., Lockshon, D., Narayan, V., Srinivasan, M., Pochart, P. et al. (2000). A comprehensive analysis of protein-protein interactions in Saccharomyces cerevisiae. *Nature* **403**, 623-627.
Voeltz, G. K., Prinz, W. A., Shibata, Y., Rist, J. M. and Rapoport, T. A. (2006). A class of membrane proteins shaping the tubular endoplasmic reticulum. *Cell* **124**, 573-586.
Vollmer, B., Schooley, A., Sachdev, R., Eisenhardt, N., Schneider, A. M., Sieverding, C., Madlung, J., Gerken, U., Macek, B. and Antonin, W. (2012). Dimerization and direct membrane interaction of Nup53 contribute to nuclear pore complex assembly. *EMBO J.* **31**, 4072-4084.
Walther, T. C., Alves, A., Pickersgill, H., Loïodice, I., Hetzer, M., Galy, V., Hülsmann, B. B., Köcher, T., Wilm, M., Allen, T. et al. (2003). The conserved Nup107-160 complex is critical for nuclear pore complex assembly. *Cell* **113**, 195-206.
Wilson, K. L. and Newport, J. (1988). A trypsin-sensitive receptor on membrane vesicles is required for nuclear envelope formation in vitro. *J. Cell Biol.* **107**, 57-68.
Wozniak, R. W., Blobel, G. and Rout, M. P. (1994). POM152 is an integral protein of the pore membrane domain of the yeast nuclear envelope. *J. Cell Biol.* **125**, 31-42.
Yamazumi, Y., Kamiya, A., Nishida, A., Nishihara, A., Iemura, S., Natsume, T. and Akiyama, T. (2009). The transmembrane nucleoporin NDC1 is required for targeting of ALADIN to nuclear pore complexes. *Biochem. Biophys. Res. Commun.* **389**, 100-104.
Yavuz, S., Santarella-Mellwig, R., Koch, B., Jaedicke, A., Mattaj, I. W. and Antonin, W. (2010). NLS-mediated NPC functions of the nucleoporin Pom121. *FEBS Lett.* **584**, 3292-3298.

FIGURE S1

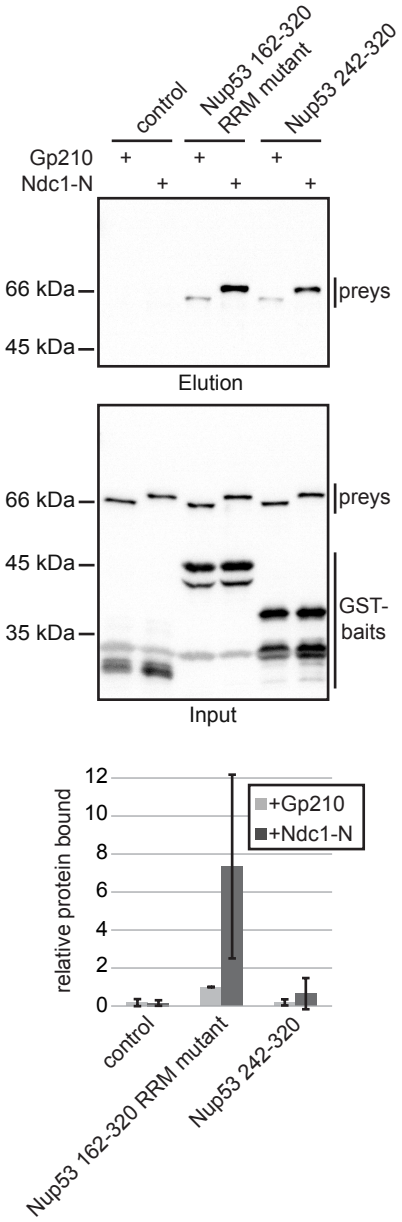
control
Nup53 162-320 RRM mutant
Nup53 242-320
Gp210 + + +
Ndc1-N + + +
66 kDa
45 kDa
preys
Elution
66 kDa
45 kDa
35 kDa
preys
GST-baits
Input
relative protein bound
12
10
8
6
4
2
0
+Gp210
+Ndc1-N
control
Nup53 162-320 RRM mutant
Nup53 242-320

FIGURE S2

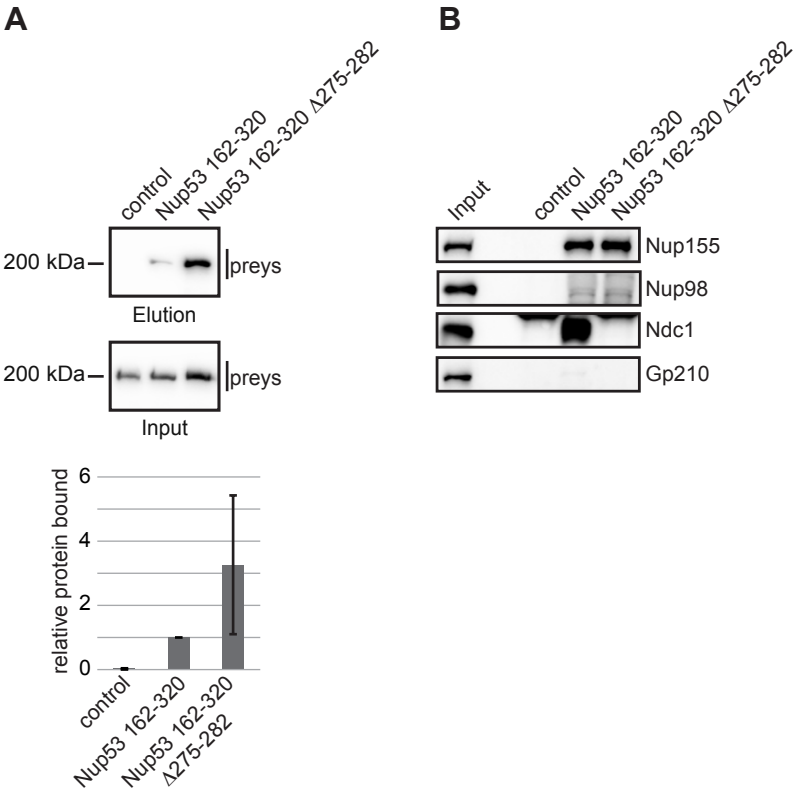
A
control
Nup53 162-320
Nup53 162-320 Δ275-282
200 kDa
preys
Elution
200 kDa
preys
Input
relative protein bound
6
4
2
0
control
Nup53 162-320
Nup53 162-320 Δ275-282
B
Input
control
Nup53 162-320
Nup53 162-320 Δ275-282
Nup155
Nup98
Ndc1
Gp210

FIGURE S3

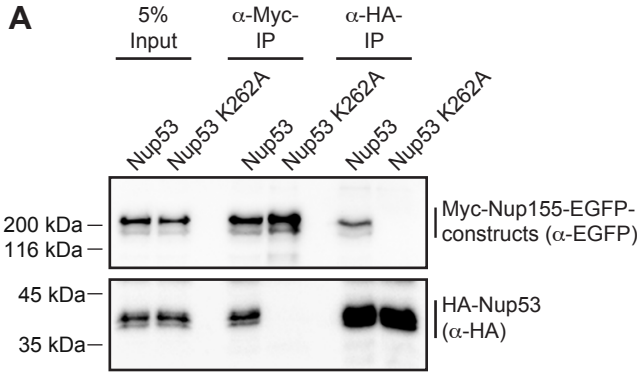
A
5% Input
α-Myc-IP
α-HA-IP
Nup53
Nup53 K262A
Nup53
Nup53 K262A
Nup53
Nup53 K262A
200 kDa
116 kDa
45 kDa
35 kDa
Myc-Nup155-EGFP-constructs (α-EGFP)
HA-Nup53 (α-HA)

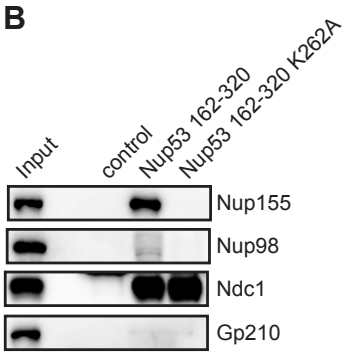
B
Input
control
Nup53 162-320
Nup53 162-320 K262A
Nup155
Nup98
Ndc1
Gp210

Supplementary figure legends

Figure S1 The Nup53 RRM domain contributes to the Nup53-Ndc1 interaction

GST-fusions of the nucleoplasmic part of *Xenopus* Gp210 (control), fragments of *Xenopus* Nup53 comprising a mutated RRM domain to decrease direct membrane binding and the subsequent C-terminus (Nup53 162-320 RRM mutant) or a shorter construct lacking the RRM domain (Nup53 242-320) were incubated with *E. coli* lysates overexpressing the transmembrane region and the nucleoplasmic extension of *Xenopus* Gp210 or the N-terminal part of *Xenopus* Ndc1 (Ndc1-N) that interacts with Nup53. Eluates and 3% of the input were analyzed by western blotting using a His_6-antibody. The quantification shows the ratio of bait-bound protein to input of six independent experiments normalized to the binding of control lysate to the Nup53 RRM mutant. Error bars represent s.d.

Figure S2 The Nup53 deletion construct impaired for the Ndc1 interaction binds Nup155

(**A**) GST-pulldown experiments using GST-fusions with the nucleoplasmic domain of *Xenopus* Gp210 (control), with a fragment of *Xenopus* Nup53 comprising the RRM domain and the subsequent C-terminus (Nup53 162-320) or with a Nup53 fragment impaired in Ndc1 interaction due to a deletion of eight amino acids (Δ275-282) and *E. coli* lysates overexpressing NusA-tagged *Xenopus* Nup155. Eluates and 3% of the input were analyzed by western blotting using a His_6-antibody. Three independent experiments were quantified (lower panel) for the bait-bound protein to input ratio normalized to Nup53 162-320, which was used as positive control. Error bars represent s.d.

(**B**) The same GST-fusions as in (**A**) were incubated with cytosol or Triton X-100 solublized membranes derived from *Xenopus laevis* egg extracts. 5% of input and eluates were analyzed by western blotting with the indicated antibodies. Nup98 served as negative control in the cytosolic fraction and Gp210 in the membrane fraction.

Figure S3 The point mutation K262A in Nup53 specifically impairs the Nup155 interaction

(**A**) HeLa cells were co-transfected with wildtype *Xenopus* Nup53 or the point mutant K262A of Nup53 tagged with HA and *Xenopus* Nup155 fused with an N-terminal Myc- and a C-terminal EGFP-tag. Proteins were immunoprecipitated from cellular lysate with Myc- or HA-antibodies and analyzed by western blotting using HA-antibodies to detect Nup53 and EGFP-antibodies for Nup155.

(**B**) GST-fusions of the nucleoplasmic domain of Gp210 (control), the C-terminal fragment of *Xenopus* Nup53 comprising the RRM domain and the subsequent C-terminus (162-320) and the corresponding fragment carrying the K262A-point mutation impairing the Nup155 interaction were incubated with cytosol or Triton X-100 solublized membranes derived from *Xenopus laevis* egg extracts. 5% of input and eluates were analyzed by western blotting with the respective antibodies. Nup98 was used as negative control for the cytosolic fraction and Gp210 for the membranes.

Table S1. Recombinant protein constructs used in this study

Construct	Reference
pET28a MISTIC Ndc1xl 1-660	this study
pET28a MISTIC Gp210xl TMR+NPD	this study
pET28a MISTIC Ndc1xl 1-301	this study
pET28a MISTIC Ndc1xl 234-660	this study
pET28a MISTIC EGFP Ndc1xl 1-660	this study
pET28a MISTIC EGFP Ndc1xl 1-301	this study
pET28a MISTIC EGFP Ndc1xl 234-660	this study
pET28a GST Nup53xl 162-320 F172E W203	Vollmer et al, 2012
pET28a GST Gp210xl NPD	Sachdev et al, 2012
pET28a GST Nup53xl 162-320 F172E W203 Δ275-282	this study
pET28a GST Nup53xl 162-312	Vollmer et al, 2012
pET28a GST Nup53xl 162-295	this study
pET28a GST Nup53xl 162-267	Vollmer et al, 2012
pET28a GST Nup53xl 242-320	this study
pET28a GST Nup53xl 252-320	this study
pET28a SUMO Nup53xl 1-320	Vollmer et al, 2012
pET28a SUMO Nup53xl 1-312	Vollmer et al, 2012
pET28a SUMO Nup53xl 130-320	Vollmer et al, 2012
pET28a SUMO Nup53xl 130-320 Δ275-282	this study
pET28a SUMO Nup53xl 130-319	Vollmer et al, 2012
pET28a SUMO Nup53xl 1-320 Δ275-282	this study
pET28a SUMO Nup53xl 1-319 Δ275-282	this study
pET28a SUMO Nup53xl 1-320 R105E K106E Δ275-282	this study
pET28a SUMO Nup53xl 1-319 R105E K106E Δ275-282	this study
pET28a SUMO Nup53xl 1-320 K262A	this study
pET28a NusA Nup155xl	Sachdev et al, 2012
pEGFP-N1 MYC Ndc1xl 1-660	this study
pEGFP-N1 MYC Ndc1xl 1-301	this study
pEGFP-N1 MYC Ndc1xl 234-660	this study
pEGFP-N1 MYC Nup155xl	this study
pSI HA Nup53xl	Vollmer et al, 2012
pSI HA Nup53xl K262A	this study

Pre-print version of submitted manuscript.
Final manuscript will be published in Methods in Cell Biol. 2014;122:193-218. doi: 10.1016/B978-0-12-417160-2.00009-6.

Xenopus in vitro assays to analyze the function of transmembrane nucleoporins and targeting of inner nuclear membrane proteins

Nathalie Eisenhardt, Allana Schooley and Wolfram Antonin*

Friedrich Miescher Laboratory of the Max Planck Society, Spemannstrasse 39, 72076 Tübingen, Germany

* author for correspondence

Abstract (100-150 words)

Xenopus egg extracts have been widely used to study cell cycle regulation and to analyze mitotic or nuclear processes on a biochemical level. Most instrumental, proteins of interest can be immunodepleted by specific antibodies. However, this approach has been restricted to non-membrane proteins, which limits its versatility especially when studying membrane dependent processes such as nuclear envelope reformation at the end of mitosis or nuclear pore complex assembly. We describe here the methods developed and used in our laboratory to specifically remove transmembrane proteins from endogenous membranes and to insert recombinant integral membrane proteins into endogenous membranes. The latter procedure is important for re-addition of a depleted protein in rescue experiments but also for introducing artificial membrane proteins such as reporters to investigate the passage of inner nuclear membrane proteins through nuclear pore complexes.

Keywords:

Cell free assay, immunodepletion, integral membrane protein, membrane reconstitution, nuclear envelope, nuclear pore complex, nuclear reformation, nuclear transport, proteoliposomes, Xenopus egg extracts

Introduction

Cell free extracts derived from frog eggs (Lohka & Masui, 1983) have widely been used to study cell cycle regulation as well as many mitotic and nuclear processes since their development and first use thirty years ago. Although eggs from other sources such as *Rana pipiens* (Lohka & Masui, 1983) or *Xenopus tropicalis* (Brown, Blower, Maresca, Grammer, Harland, & Heald, 2007) can be employed, the use of *Xenopus laevis* eggs is most popular because these frogs are relatively easily maintained in a laboratory environment and they provide plentiful eggs with little seasonal variation in yield and quality.

In the absence of intact cells, *Xenopus laevis* egg extracts recapitulate complicated cellular reactions in a test tube such as chromatin condensation (de la Barre, Robert-Nicoud, & Dimitrov, 1999), spindle assembly (Maresca & Heald, 2006), nuclear breakdown and reformation (Galy, Antonin, Jaedicke, Sachse, Santarella, Haselmann, & Mattaj, 2008; Lohka, 1998), nucleocytoplasmic transport (Chan & Forbes, 2006) or DNA replication (Gillespie, Gambus, & Blow, 2012). Since these egg extracts can be prepared at different stages of the cell cycle, which are easily interconvertible, cell cycle dependent processes can also be studied (Murray, 1991). Most importantly, a single defined step in a complex series of processes such as the metazoan cell cycle can be isolated and investigated in molecular detail with this system. To identify key factors involved in various distinct processes of interest, convenient biochemical manipulations of the extracts are possible. In this regard, the opportunity to easily remove proteins of interest from these extracts by specific antibodies is most instrumental. For example, the importance of individual nuclear pore complex (NPC) proteins, nucleoporins, for NPC assembly and function has been defined in this way (see Chapter 8 in this Volume). This “biochemical knockout”

strategy is highly efficient to deplete proteins of interest below a detection limit. In contrast to RNAi, gene deletion or morpholino experiments, this method is naturally not limited by the viability of cells and organisms. As assays can be tailored to monitor a single process of interest, this also avoids complications due to secondary effects upon protein depletion, which might occur in other stages of the cell cycle or during development. However, this approach has been majorly restricted to non-membrane proteins, which limits its versatility especially when studying membrane dependent processes such as nuclear envelope or NPC formation.

In this chapter we describe the methods developed and employed in our lab to immunodeplete specific integral membrane proteins of the NPC from *Xenopus* membranes. Removing integral membrane proteins from *Xenopus* membranes is technically challenging as this procedure includes membrane solubilization and a final reconstitution of the depleted membranes besides the specific immunodepletion (Figure 2A). However, the method is in our eyes superior to antibody (IgG or Fab) inhibition experiments classically used to study the function of integral membrane proteins, which are often ill-defined especially with regard to the precise molecular inhibiting effect of the antibody. Preferably, immunodepletion of a given protein should be followed by an “addback experiment”, in which a recombinant version of the depleted factor is re-added to revert the observed depletion phenotype, thereby demonstrating the point specificity of the depletion. Such addback experiments are also feasible for transmembrane proteins (Figure 2B and C). Here we outline the procedures of the expression of eukaryotic transmembrane proteins in *E. coli*, their purification and their reconstitution in *Xenopus* membranes. Moreover, recombinant modified transmembrane proteins can be added to endogenous *Xenopus* membranes to analyze the passage of integral membrane proteins through the NPC *in vitro* (Figure 3). As nuclear transport has mainly been studied for soluble proteins

in the past, the mechanisms of NPC passage of transmembrane proteins are only emerging (for review see Antonin, Ungricht, & Kutay, 2011; Lusk, Blobel, & King, 2007). The assay we describe here provides a powerful tool to study NPC passage of integral membrane proteins in *Xenopus* egg extracts in a quantitative and time resolved manner. By combining it with immunodepletion approaches, integral membrane protein transport through NPCs can not only be studied under wildtype conditions but also in the absence of specific factors including distinct NPC proteins.

I. Preparation of *Xenopus* egg extract cytosol and membranes

1. Preparation of interphasic egg extracts

Xenopus eggs are arrested in the second metaphase of meiosis. Addition of calcium ionophore, which mimics the calcium influx generated during fertilization, activates these unfertilized eggs to enter the first interphase. Cell cycle progression into the first mitosis requires the translation of a single protein, cyclin B (Murray & Kirschner, 1989). To arrest the extracts in interphase, cyclin B synthesis is prevented by the translation inhibitor cycloheximide. We use a protocol for interphasic egg extract preparation adapted from Newmeyer & Wilson, 1991.

For editors; PLEASE INSERT FIGURE 1 HERE

A. Materials and equipment

- 240 IU/ml pregnant mare serum gonadotropin (PMSG, available as Intergonan, Intervet)
- 1000 IU/ml human chorionic gonadotropin (HCG, available as Ovogest, Intervet)
- Beckman L-60 Ultracentrifuge, SW55 Ti swinging bucket rotor and ultra-clear tubes (or equivalents)
- Beckman Optima TLX Ultracentrifuge, TLA 120.2 rotor and tubes (or equivalent system)
- Häreus-Multifuge 1-LR-Centrifuge (or equivalent)
- 5ml Syringes, 27G 3/4” and 16G 1½” needles
- large orifice tip (MBP® 1000G Pipet Tips, Molecular BioProducts)

B. Buffers and solutions

- MMR buffer: 100 mM NaCl, 2 mM KCl, 5 mM Hepes, 0.1 mM EDTA pH 8.0, 1 mM $MgCl_2$, 2 mM $CaCl_2$. Prepare a 20x stock solution in deionized water and autoclave, adjust pH to 8.0 with 5 M KOH. 1x MMR is freshly prepared before use by dilution in deionized water and re-adjustment of the pH to 8.0 with 5 M KOH.
- Dejellying buffer: 2% cystein in 0.25x MMR buffer, pH 7.8. This buffer should be prepared freshly and kept at 4-8°C. To save time, pre-cool the water.
- Calcium ionophore A23187: 2 mg/ml in ethanol
- Protease inhibitor mix (PI): 10 mg/ml AEBSF (4-(2-Aminoethyl)-benzensulfonylfluoride), 0.2 mg/ml leupeptin, 0.1 mg/ml pepstatin, 0.2 mg/ml aprotinin in deionized water. Store in aliquots at -20ºC.
- Dithiothreitol (DTT): 1 M in deionized water
- Cycloheximide: 20 mg/ml in ethanol
- Cytochalasin B: 10 mg/ml in DMSO
- Sucrose buffer: 250 mM sucrose, 50 mM KCl, 2.5 mM $MgCl_2$, 10 mM Hepes pH 7.5, 1 mM DTT (freshly added), 1:100 PI. Keep at 4°C.
- Dilution buffer: 50 mM KCl, 2.5 mM $MgCl_2$, 10 mM Hepes pH 7.5, 1 mM DTT (freshly added), 1:100 PI. Keep at 4°C.

C. Method

Note: For frog maintenance see Sive, Grainger, & Harland, 2000.

1. Prime frogs to ovulate by injecting 60 U PMSG into their dorsal lymph sac three to ten days before the experiment (5 ml Syringes, 27G 3/4” needles).
2. On the day before the experiment, inject frogs with 250 U HCG in their dorsal lymph sac (5 ml Syringes, 27G 3/4” needles) and place them in individual laying tanks containing 2 l of 1x MMR buffer for 16-18 h at 18°C.

3. Collect high quality eggs by pooling the good batches and wash them several times with 1x MMR buffer. Good eggs will be individually laid, uniform in size, and pigmented with clearly defined animal and vegetal hemispheres. Eggs laid in clumps or strings or white eggs should be excluded. It is important to carefully sort the eggs at this early step and throughout the procedure as the presence of a few “bad eggs” can quickly spoil the rest.

Note: For detailed description of “good” versus “bad” eggs see Gillespie et al., 2012.

4. Dejelly eggs in cold dejellying buffer for 10 min. Change buffer once and swirl continuously. Eggs become closely packed during this step.
5. Rinse eggs 4 times with 1x MMR buffer. This washing must be done gently, as the eggs are now fragile, and taking care not to expose the eggs to air.
6. Activate eggs in 100 ml 1x MMR buffer by adding 8 µl of the calcium ionophore A23187 for 10 min or until activation becomes visible (animal cap contraction), whichever comes first.
7. Rinse eggs carefully 4 times with 1x MMR buffer and once again carefully to keep them from being exposed to air.
8. Incubate eggs for 20 min at room temperature.
9. Replace the MMR buffer with cold sucrose buffer by washing twice. All subsequent steps must be carried out on ice.
10. Carefully place the eggs in SW55 tubes containing 50 µl sucrose buffer, 50 µl PI, 5 µl 1M DTT, 12.5 µl cycloheximide, and 2.5 µl cytochalasin B using a wide-mouthed (cut) transfer pipette. Remove excess buffer and refill the tubes until they are completely full.

11. Pack eggs by centrifugation at 400 rpm (approx. $3xg_{av}$) for 60 s in Häreus-Multifuge 1-LR-centrifuge. Remove excess liquid along with white eggs that have now floated to the top.
12. Crush the eggs by centrifugation at 15.000 rpm ($21,000xg_{av}$) for 20 min in a SW55 Ti rotor at 4°C (Figure 1).
13. Remove the (pale yellow) low speed extracts between the bright yellow yolk on top and dark broken eggs at the bottom using a syringe (16G 1½" needle). From one full SW55 tube, expect approximately 2.5 ml of low speed extract.
14. Add 10 µl PI, 1 µl 1M DTT, 2.5 µl cycloheximide and 0.5 µl cytochalasin B per ml of low speed extract. Mix well and load into fresh SW55 tubes. Spin for 40 min at 45.000 rpm ($190,000xg_{av}$) in a SW55 Ti rotor at 4°C.
15. Remove the (pale yellow) cytosolic phase between the white lipids on the top and the dark pellet containing pigments using a syringe (16G 1½" needle). From one full SW55 tube, expect approximately 3-4 ml of extract.
16. Dilute the extract with 0.3 ml of dilution buffer per 1 ml of cytosolic extract, mix well and load into fresh SW55 tubes for a final round of centrifugation. Spin for 40 min at 45.000 rpm ($190,000xg_{av}$) in a SW55 Ti rotor at 4°C.
17. Carefully remove the cytosol between the white lipids on the top and membranes, mitochondria and pigments at the bottom using a pipette. It is important to avoid contamination from the white lipids as they can hinder the *in vitro* nuclear assembly reaction. The membranes obtained at this step can be further purified using the protocols described in section **I, 2**.
18. Cytosol is cleared from residual membranes by two rounds of centrifugation for 12 min each at 100.000 rpm ($360,000xg_{av}$) in a TLA120.2 rotor at 4°C and used directly in the nuclear assembly reactions (section **IV**).

2. Preparation of *Xenopus* membranes

Nuclear envelope assembly in high-speed fractionated egg extracts requires the presence of both the cytosolic and membrane fractions (Sheehan, Mills, Sleeman, Laskey, & Blow, 1988; Vigers & Lohka, 1991; Wilson & Newport, 1988). Although it is possible to employ the crude membrane fraction to this end, this fraction contains cytosolic contaminations. At least after depletion of proteins from egg extract cytosol, a purified membrane fraction should be used. Crude membranes are mostly used in biochemical applications, such as membrane protein depletion and reconstitution, due to their high concentration. We describe here the preparation of both the crude membranes, adapted from Pfaller, Smythe, & Newport, 1991, and floatation purified membranes, adapted from Wilson & Newport, 1988.

A. Materials and equipment

- Tissue grinders: One 30 ml douncer with loose pestel and one 7 ml douncer with tight pestel (Wheaton, Millville, USA)
- Beckman L-60 Ultracentrifuge, SW40 Ti swinging bucket rotor and ultra-clear tubes (or equivalent system)
- Beckman Optima TLX Ultracentrifuge, TLA 100.4 rotor and tubes (or equivalent system)

B. Buffers and solutions

- Protease inhibitor mix (PI), DTT and sucrose buffer are described in section **I,1**.
- 2.1 M sucrose buffer: 2.1 M sucrose, 50 mM KCl, 2.5 mM $MgCl_2$, 10 mM Hepes pH 7.5, 1 mM DTT (freshly added), 1:100 PI. Keep at 4°C.
- Sucrose cushions: 1400 mM, 1300 mM, 1100 mM, 900 mM and 700 mM sucrose. Prepare sucrose cushions by mixing sucrose buffer from section **I,1**

and 2.1 M sucrose buffer in appropriate ratios to obtain the according sucrose concentration.

C. Method

Our protocols for the preparation of crude and floated membranes start with the generation of high-speed interphasic egg extract outlined in section **I,1** (Figure 1).

Preparation of crude membranes:

1. Membranes are isolated immediately following the final centrifugation step of high-speed extract preparation (step 17 in section **I,1**). At this point, they are easily distinguishable as a slightly viscous pale yellow layer located above the darkly colored mitochondria and pigments. Following removal of the egg cytosol, membranes are extracted with a syringe. From a full SW55 tube, expect approximately 1-1.5 ml of membrane suspension. Dilute the pooled membranes in 10 volumes of sucrose buffer and homogenize with two strokes of the loose pestel in a 30 ml glass douncer.
2. Transfer the homogenized membranes to SW40 tubes and spin for 20 min at 15.000 rpm (28,000xg_{av}) in a SW40 Ti rotor at 4°C.
3. After removing the supernatant, resuspend the membrane pellet in sucrose buffer. Homogenize the membrane suspension with five strokes of the tight pestel in a 7 ml glass douncer.
4. Adjust the final volume of the membrane suspension to 50% of the cytosol volume with sucrose buffer. Aliquot, snap freeze, and store in liquid nitrogen.

Preparation of floatation purified membranes:

1. As for the crude membrane preparation, the yellow membrane layer is extracted immediately following the final centrifugation step of the high-speed extract preparation using a syringe.
2. Mix membranes with four volumes of cold 2.1 M sucrose. Homogenize membranes with two strokes of the loose pestel in a 30 ml douncer.
3. Place 5 ml of homogenized membranes in SW40 tubes and overlay sequentially with 1.4 ml of each of the five sucrose cushions starting from 1400 mM to 700 mM sucrose. Finish the step gradient with 0.2 ml of sucrose buffer.
4. Membranes are separated by centrifugation for 4 h at 38.000 rpm (180,000xg_{av}) in an SW40 Ti rotor at 4°C.
5. Following centrifugation, carefully isolate the upper three membrane phases. Dilute the pooled membrane fractions with 3 volumes of sucrose buffer and spin for 30 min at 100.000 rpm (420.000xg_{av}) in a TLA100.4 rotor at 4°C.
6. After removing the supernatant, resuspend the membrane pellet in sucrose buffer. Homogenize the membrane suspension with five strokes of the tight pestel in a 7 ml glass douncer. Take care that the membranes are completely resuspended.
7. Adjust the final volume of the floated membranes to 50% of the volume of the cytosol. Aliquot, snap freeze, and store in liquid nitrogen.

II. Protein expression

1. Expression and purification of integral membrane proteins in *E. coli*

For addback reactions after depletion of soluble as well as transmembrane proteins natively purified proteins from *Xenopus* membranes (Antonin, Franz, Haselmann,

Antony, & Mattaj, 2005) but also recombinant proteins might be employed (Eisenhardt, Redolfi, & Antonin, 2013; Mansfeld, Guttinger, Hawryluk-Gara, Pante, Mall, Galy, Haselmann, Muhlhausser, Wozniak, Mattaj, Kutay, & Antonin, 2006). Wherever possible, recombinant proteins are preferable as this obviates the co-purification and co-addition of other *Xenopus* proteins.

Expression of eukaryotic transmembrane proteins can be achieved in several systems such as yeast, insect cells or mammalian cell lines. We have good experience with *E. coli* as expression system when fusing the protein of interest to the Mistic sequence from *B. subtilis* in a pET28a vector for expression in *E. coli* (Eisenhardt et al., 2013; Theerthagiri, Eisenhardt, Schwarz, & Antonin, 2010). The Mistic sequence directs the integral membrane protein to the inner *E. coli* membrane (Roosild, Greenwald, Vega, Castronovo, Riek, & Choe, 2005) and can be fused either N- or C-terminal of the protein sequence. For most proteins, expression in a BL21de3 strain works well but it might be worth testing other expression strains as expression efficiency in different strains varies for different proteins.

A. Materials and equipment

- 2 l glass flasks (Duran, Roth, Germany)
- Bacterial shaker
- French press (e.g. EmulsiFlex-C3 from Avestin, Germany, or equivalent system)
- Sorvall centrifuge and rotors (or equivalent system)
- Rotating wheel
- Cheese cloth (Ypsifix® 8cm/4m, Holthaus Medical, Germany)
- Ni-NTA Agarose (Qiagen, Germany)
- 20 ml plastic chromatography columns (Econo-Pac® disposable chromatography columns, Bio-Rad, Germany)

B. Buffers and solutions

- LB medium: 1% peptone (w/v), 0.5% yeast extract (w/v) and 0.5% NaCl (w/v), adjust pH to 7.0 with 10 N NaOH, autoclave.
- Kanamycin: 25 mg/ml in water.
- 1 M $MgSO_4$: 24.65 g $MgSO_4x7H_2O$ in water, autoclave.
- 20x NPS (NPS = 100 mM PO_4, 25 mM SO_4, 50 mM NH_4, 100 mM Na, 50 mM K): 0.5 M $(NH_4)_2SO_4$, 1 M KH_2PO_4 and 1 M Na_2HPO_4. pH of 20x NPS in water should be ~6.75, autoclave.
- 50x 5052: 25% glycerol (v/v), 0.25% glucose (w/v) and 2% alpha-lactose (w/v) in water, autoclave.
- Ni-wash buffer: 20 mM TRIS pH7.4, 500 mM NaCl and 30 mM Imidazole, autoclave.
- $MgCl_2$: 1 M stock in water, autoclave.
- Phenylmethanesulfonylfluoride (PMSF): 0.2 M in ethanol (Applichem, Germany)
- Deoxyribonuclease I (DNase I): 10 U/µl in PBS (bovine pancreas, ≥ 60.000 Dornase units/mg dry weight, Merck KGaA, Germany)
- Ni-elution buffer: 20 mM TRIS pH 7.4, 500 mM NaCl, 400 mM Imidazole, 10% glycerol (v/v).
- EDTA: 500 mM stock, dissolved in deionized water, pH 8.0, autoclave.
- Sucrose buffer as in section **I,1**.
- Cetyltrimethylammonium Bromide (CTAB, Calbiochem, Germany)

C. Method

1. Grow primary culture overnight in LB medium with Kanamycin 1:1000 at 37°C in a bacterial shaker.

2. Inoculate large scale expression cultures from overnight culture 1:100. Supplement the LB medium with 1 mM $MgSO_4$, 1x 5052, 1x NPS and Kanamycin 1:1000 (in this order). Fill at maximum 500 ml culture in 2 l flasks.
3. Grow cultures at 37ºC and 300 rpm until OD_{600}=1.5 in a bacterial shaker.
4. Shift to expression temperature and shake at 300 rpm for 12-20h (OD_{600} should be at least 5 before harvesting).

Notes: Induction in LB medium with IPTG is an alternative. However, as bacteria can be grown in much higher density in autoinduction medium the yield per expression volume is much higher. In our hands, autoinduction works fine for most of the tested proteins.

Best expression temperature needs to be determined experimentally.

5. Harvest cultures for 15 min at 4.500 g and 4°C in Sorvall centrifuge (or equivalent system).
6. Resuspend bacterial pellet obtained from 1 l culture in 150-200 ml cold Ni-wash buffer and add 1 ml of 0.2 M PMSF. All following steps should be done on ice or in the cold and using cold buffers.
7. Break bacteria by a French press or equivalently.
8. Add 2 mM $MgCl_2$, 450 ml of 10 U/µl DnaseI in PBS and 2 ml of 0.2 M PMSF per 1 l of expression culture to the lysate and incubate 10 min on ice.
9. Freeze lysate at -20°C or proceed immediately. Spin lysate for 20 min at 28.000 g and 4°C in Sorvall centrifuge.
10. Resuspend pellets at room temperature in 10 ml Ni-wash buffer + 1% CTAB and add 2 ml of 0.2 M PMSF per 1 l expression culture. Add Ni-wash buffer + 1% CTAB to a total volume of 320 ml per 1 l expression culture and rotate for 45 min at room temperature on a rotating wheel to solubilize the bacterial

membranes. All following steps, in which CTAB is present, should be done at room temperature as CTAB precipitates in the cold.

11. Spin for 15 min at 20°C and 15.000 g to remove unsolubilized membranes in Sorvall centrifuge and filter the supernatant through a cheese cloth.
12. Add 500 µl Ni-NTA Agarose beads to the supernatant derived from 1 l expression culture for 2 h at room temperature. Rotate samples on a rotating wheel.

Note: The amount of Ni-NTA Agarose beads depends on the expression yield and has to be determined for each construct.

13. Collect Ni-NTA Agarose beads in a 20 ml plastic chromatography column. Wash beads 2-3 times with one column volume of Ni-wash buffer + 0.1% CTAB.
14. Close column and elute the protein of interest from the beads with 500 µl Ni-elution buffer + 1% CTAB for 5 min at room temperature. Collect eluate and elute beads again with 250 µl Ni-elution buffer + 1% CTAB for 5 min. Pool both eluates.

Note: The volume of Ni-elution buffer depends on the protein concentration and the Agarose beads volume. Elution works best with 50% slurry of Agarose beads or more diluted. A third elution might be done if a lot of protein remains on the Agarose beads. Analyze beads for elution efficiency if you purify the protein the first time.

15. Dialyze eluates to sucrose buffer + 1 mM EDTA for 1h at 4°C and again over night with fresh buffer.

Note: Dependent on the later use of the protein, the dialysis buffer can be altered. For addback in nuclear assembly assays (section **IV, 1**) sucrose buffer is recommended.

16. Determine protein concentration by SDS-PAGE, aliquot and freeze in liquid nitrogen. Store protein aliquots at -80°C for later use.

Note: Traces of CTAB are still present in the protein sample and might interfere with most methods of protein concentration determination. It is best to judge the protein concentration by comparing the band on a protein gel to a known concentration of BSA.

2. Expression and purification of NusA-TEV

TEV protease for nuclear assembly reactions to measure the transport of inner nuclear membrane proteins through nuclear pore complexes (section **IV,4**) is fused to NusA to increase its size above the size exclusion limit of nuclear pore complexes, cloned into a pET28a expression vector and transformed into BL21de3 bacteria for expression.

A. Materials and equipment

- Chromatography columns (Econo-Column® Chromatography Column, 5.0 x 20 cm, Bio-Rad, Germany)
- Other material as in section **II,1**.

B. Buffers and solutions

- As in section **II,1**.

C. Method

1. Inoculate 4 ml of an overnight culture of transformed bacteria (grown in LB medium with 25 µg/ml Kanamycin) in 400 ml auto-induction medium (LB supplemented as in section **II,1**). Fill in 2 l glass flasks and grow at 37ºC at 300 rpm in bacterial shaker.
2. Shift culture to expression temperature of 25°C when OD_{600}=1.5.

3. After 14-20 h at 25°C, OD_{600} should be at least 5. Harvest bacteria by centrifugation for 15 min at 4.500 g in a cold rotor at 4°C in a Sorvall centrifuge.
4. Resuspend pellet in 10 ml cold Ni-wash buffer, fill up to at least 100 ml and add 1 ml of 0.2 M PMSF. All following steps should be done keeping the proteins on ice or in the cold and using cold buffers.
5. Break bacteria in Emulsiflex, French press or equivalent system.
6. Add 1 mM $MgCl_2$, 200 µl of 10 U/µl DnaseI in PBS and 1 ml of 0.2 M PMSF and incubate 10 min on ice.
7. Spin 15 min at 22.000 g in a rotor at 4°C. Spin again if supernatant is not cleared sufficiently. Filter supernatant through cheese cloth.
8. Apply 1.6 ml of 50% slurry of Ni-NTA Agarose to the supernatant and incubate for 2 h at 4°C on a rotating wheel.
9. Apply Agarose beads to chromatography column. If all agarose is collected in the column wash with 100 ml cold Ni-wash buffer.
10. Elute the His_6-NusA-TEV protein with 4 ml Ni-elution buffer
11. Dialyze eluate to sucrose buffer, determine protein concentration and store aliquots at -80°C. We usually obtain 20 mg of protein from 400 ml autoinduction culture.

III. Biochemical Procedures

1. Generation of antibody beads

Depletion of soluble or membrane integral proteins from *Xenopus* egg extracts is achieved by passage of the cytosol or solubilized membrane fraction, respectively, over a bead material with crosslinked antibodies. Because of the high abundance of

many nucleoporins these antibody beads should provide a high capacity and we therefore prefer Protein A-Sepharose over magnetic Protein A-beads.

A. Materials and equipment

- Protein A-Sepharose (GE Healthcare, Sweden)
- Rabbit IgG (Calbiochem, Germany)
- Häreus-Multifuge 1-LR-Centrifuge (or equivalent)
- Dimethylpimelimidate (DMP, store solid and dry at 4°C; Pierce, Thermo Fisher Scientific, Bonn, Germany)
- Rotating wheel (or equivalent)
- BSA (Fraction V, Calbiochem, Germany)
- Sodium azide (NaN_3)

B. Buffers and solutions

- Phosphate buffer saline (PBS): 2.7 mM KCl, 137 mM NaCl, 10 mM $Na_2HPO_4 \cdot 2H_2O$, 2 mM KH_2PO_4. Prepare a 10x stock solution, adjust to pH 7.4 with 10 N NaOH and autoclave. Dilute to 1x PBS freshly before use.
- Coupling buffer: 200 mM $NaHCO_3$, 100 mM NaCl, pH 9.3.
- Blocking buffer: 0.1 M ethanolamine pH 8.2.
- Buffer A: 100 mM sodiumacetate, 500 mM NaCl pH 4.2.
- Buffer B: 100 mM $NaHCO_3$, 500 mM NaCl, pH 8.3.
- Protease inhibitor mix (PI) as in section **I,1**.

C. Method

1. Incubate 4 mg of affinity purified antibody with 1 ml Protein A-Sepharose (50% slurry) in PBS for 4-16 h at 4°C on a rotating wheel. For control beads use rabbit IgGs at approximately the same concentration.

2. Wash beads twice with coupling buffer by spinning beads down for 2 min at 3000 rpm and 4°C in a Häreus-Multifuge 1-LR-Centrifuge. Remove supernatant and add fresh buffer.
3. Crosslink antibodies and Protein A-Sepharose beads in 10 mM DMP in coupling buffer for 20 min at room temperature on a rotating wheel.
4. Wash beads once with coupling buffer (spin as in step 2) and crosslink again in 10 mM DMP in coupling buffer for 20 min at room temperature on a rotating wheel.
5. Wash beads once with blocking buffer (spin as in step 2) and rotate for 1 h in blocking buffer at room temperature.
6. Wash beads alternating twice with buffer A and B (spin as in step 2).
7. Block beads in 3% BSA in PBS supplemented with PI (1:1000) for 1 h at 4°C on a rotating wheel.
8. Store beads as a 50% slurry in 3% BSA in PBS supplemented with PI (1:1000) and 0.05% NaN_3 at 4°C.

2. Preparation of G50-chromatography columns

For reconstitution of membranes after depletion (section **III,3**) or generation of proteoliposomes (section **III,4**) detergent is removed by gelfiltration with Sephadex G50-columns. To avoid major protein and lipid loss during column passage the gelfiltration column is pre-blocked with BSA and a lipid mixture.

A. Materials and equipment

- G50 gel filtration medium (Sephadex G-50 Fine, GE Healthcare, Sweden)
- glass chromatography column (Econo-Column®, 0.5 x 20 cm, Bio-Rad, Germany)

- Polyethylene tubing (or equivalent)
- BSA
- n-Octyl-β-D-glucopyranoside (Calbiochem, Germany) or equivalent detergent

B. Buffers and solutions

- Lipid mix: 3 mg/ml cholesterol (ovine wool, >98), 3 mg/ml L-α-phosphatidylserine (sodium salt, brain, porcine), 3 mg/ml L-α-phosphatidylinositol (sodium salt, liver, bovine), 6 mg/ml L-α-phosphatidylethanolamine (egg, chicken), 15 mg/ml L-α-phosphatidylcholine (egg, chicken; all from Avanti Polar Lipids, USA) in 10% n-Octyl-β-D-glucopyranoside
- $DiIC_{18}$: 1 mg/ml 1,1'-Dioctadecyl-3,3,3',3'-Tetramethylindocarbocyanine Perchlorate in DMSO ('DiI', $DiIC_{18}$(3), crystalline; Life Technologies GmbH, Germany)
- Sucrose buffer as in section **I,1** and PBS as in section **III,1**.

C. Method

1. Swell G50 beads in sucrose buffer for 10 min at room temperature.
2. Remove bottom and top lids from the chromatography column and fill column with swollen G50 beads. Let beads settle by gravity. Add more beads carefully until the glass cylinder of the column is nearly filled (leave about 0.5 cm space at the top). The upper edge of the bead layer should remain visible.

Note: Avoid air bubbles in the column. Be careful that columns don't run dry.

3. Fill column with sucrose buffer, put top lid on and connect the lid to a buffer reservoir via tubing.
4. Wash column with sucrose buffer from the reservoir by letting the buffer pass by gravity flow.

5. To block the column, take top lid off, carefully remove excess buffer and add 100 µl of 1 mg/ml BSA in sucrose buffer directly onto the bead layer. Let the solution enter the beads, then fill the column immediately but carefully with buffer, put top lid back on and wash the column as in step 4.
6. Block column again with 20 µl lipid mix diluted 1:5 with PBS in 100 µl total volume as in step 5.

Note: Lipid mix can be altered as well as the detergent used to dissolve the lipids. A relatively high CMC (critical micelle concentration) value of the detergent and small aggregation number is important to ensure its removal by gelfiltration.

7. Wash column with sucrose buffer for 30 min as in step 4.
8. Close bottom lid of the column. To store your columns for longer term, add 0.1% NaN_3 to the sucrose buffer.

Note: For long term storage of the columns, let some buffer pass from time to time.

3. Depletion of transmembrane proteins from *Xenopus* membranes

To specifically deplete transmembrane proteins, *Xenopus* membranes are solubilized by detergent and the protein of interest is immunodepleted by passage of the solubilized membrane fraction over an antibody column (Figure 2A). Detergent removal from the solubilized and depleted membrane fraction reconstitutes the membranes. An efficient way for detergent removal is passage of a gel filtration column (Allen, Romans, Kercret, & Segrest, 1980) under the pre-condition that the detergent has a relative high CMC (critical micelle concentration) value, which defines the concentration of the free detergent in solution in contrast to its micellar form, and a not small aggregation number.

For addback experiments the purified integral membrane protein (see section **II,1**) is added to the solubilized and depleted membrane fraction and co-reconstituted by passage of the gelfiltration column.

For editors; PLEASE INSERT FIGURE 2 HERE

A. Materials and equipment

- n-Octyl-β-D-glucopyranoside or equivalent detergent as in section **III,2**.
- Beckman Optima TLX Ultracentrifuge, TLA 100 rotor and tubes (or equivalent system)
- Mobicol columns (Mobicol "classic" with 1 closed screw cap and plug and 35 µm pore size filters, MoBiTec GmbH, Germany)
- cooled tabletop microcentrifuge
- Crude membranes, antibody beads and G50-chromatography columns described in sections **I,2**, **III,1** and **III,2**.

B. Buffers and solutions

- Sucrose buffer, lipid mix and $DiIC_{18}$ as in sections **I,1** and **III,2**.

C. Method

1. Solubilize 20 µl of crude membranes (for preparation see section **I,2**) in sucrose buffer with 1% n-Octyl-β-D-glucopyranoside for 10 min at 4°C.

Notes: Frozen membrane aliquots can be used.

Ensure proper membrane solubilization with marker proteins by Western blotting.

If necessary other detergents (with relative high CMC values and small aggregation numbers to allow for their removal afterwards) might be used such as CHAPS.

Use high quality detergent, some batches of n-Octyl-β-D-glucopyranoside need to be purified before use by passage over a mixed bead resin (e.g. AG501-X8 from Bio-Rad, Germany)

2. Clear by centrifugation for 10 min at 200.000 g and 4°C in a TLA100 rotor and take supernatant.
3. Equilibrate 40 µl of antibody beads (50% slurry, prepared as described in section **III,1**) in a Mobicol column with sucrose buffer immediately before use, spin dry by centrifugation for 30 s at 5000 g and 4°C in a cooled tabletop microcentrifuge. Apply supernatant of step 2 to dried beads and incubate for 30 min at 4°C on a rotating wheel.

Note: Optimal bead to solubilized membranes ratio needs to be determined. However, the given conditions work for most of the proteins we tested.

4. Elute unbound supernatant (spin as in step 3) and incubate a second time as in step 3 with fresh antibody beads.
5. Elute unbound supernatant and add 20 µl lipid mix and 0.2 µl of 1 mg/ml $DiIC_{18}$ in DMSO. For add-back experiments, add your protein of interest in approximately endogenous concentration together with the lipid mix to the eluate.

Notes: The optimal amount of re-added protein needs to be determined. In our hands, for most add-back attempts achieving endogenous protein levels works fine (Figure 2B).

If necessary one can avoid the use of a fluorescent dye and reconstituted membranes are collected blindly. For this, a test run in which one can follow the reconstituted fraction with a marker (e.g. a fluorescent dye) is performed and the number of drops counted until the reconstituted membrane fraction runs out of the column.

6. Reconstitute membranes by detergent removal by passing the sample over a G50-chromatography column (prepared as described in section **III,2**) equilibrated to sucrose buffer. Remove excess of buffer and load the samples directly on the bead layer. Fill the column with buffer as soon as the sample has entered the beads. Collect the membrane containing fraction (approximately 400µl or 8-9 drops), which appears pink due to addition of $DiIC_{18}$.
7. Pellet reconstituted membranes by centrifugation for 30 min at 200.000 g in a TLA100 rotor.
8. Resuspend membrane pellet in 20 µl sucrose buffer. Reconstituted membranes are now ready to use in the nuclear assembly reaction (section **IV, 1**).

4. Reconstitution of recombinant integral membrane proteins in proteoliposomes

For purification, integral membrane proteins are detergent solubilized from membranes. At the end of the purification process, the detergent is removed to maintain the proper functionality of the integral membrane protein by reconstitution in proteoliposomes, which can be used as a tool for functional studies as in section **IV**.

A. Materials and equipment

- Beckman Optima TLX Ultracentrifuge, TLA 120.2 rotor and tubes (or equivalent system)
- G50-chromatography columns described in section **III,2**.

B. Buffers and solutions

- PBS, lipid mix, $DiIC_{18}$ and sucrose buffer as in sections **I,1**, **III,1** and **III,2**.

C. Method

1. Prepare pre-blocked G50-columns as described in section **III,2** but use PBS instead of sucrose buffer.
2. Apply a mix consisting of 20 µl lipid mix, 5 µl purified protein (conc. < 1mg/ml), 50 µl PBS and 0.5 µl $DiIC_{18}$ (1 mg/ml in DMSO) directly onto the bead layer.
3. Fill column with buffer as soon as the lipid mixture has entered the column. Collect $DiIC_{18}$-labelled fraction (approximately 8-9 drops or 400µl) containing reconstituted proteoliposomes.

Note: Alternatively, another fluorescent membrane dye or fluorescently labeled lipids can be used.

4. Pellet proteoliposomes in PBS in a TLA120.2 rotor for 30 min at 100.000 rpm (360,000xg_{av}) and 4°C. Resuspend pellet in 20 µl sucrose buffer.
5. Wash column after use with buffer and store it as described in section **III,2**.

Note: If you don't want to use a fluorescent dye, proteoliposomes can be collected blindly (compare Notes for section **III,3**). Column can be reused but upper bead layers (~ 1 cm) have to be exchanged from time to time. After renewal of the upper bead layer, block column with BSA and lipids before next use as described in section **III,2**.

IV. Nuclear assembly reactions

1. Nuclear assembly reactions using depleted and reconstituted membranes

In vitro assembled nuclei can be reconstituted using cytosol and membranes from egg extracts combined with chromatin of demembranated sperm. Preparation of demembranated sperm is described in Murray, 1991, see also Bernis et al., chapter 8 in this volume. For depletion experiments of transmembrane nucleoporins,

endogenous membranes are replaced by a depleted membrane fraction prepared as described in section **III,3**.

A. Materials and equipment

- Vectashield 1000 (Vector Laboratories, Burlingame, USA)
- Round glass coverslips (12 mm diameter, Menzel, Braunschweig, Germany)
- 6 ml flat bottom tubes (Greiner, Germany)
- large orifice tip (MBP® 200G/1000G Pipet Tips, Molecular BioProducts)
- Häreus-Multifuge 1-LR-Centrifuge
- Nail polish/coverslip sealant
- 24-well-plates (Greiner, Germany)

B. Buffers and solutions

- Energy mix: 50 mM ATP, 50 mM GTP, 500 mM creatine phosphate and 10 mg/ml creatine kinase in sucrose buffer. The energy mixture can be prepared and stored as single use aliquots at -80°C.
- Glycogen: 0.2 g/ml in sucrose buffer (oyster glycogen, USB, Amersham)
- 0.1% Poly-L-Lysine solution in water (Sigma-Aldrich, USA)
- Sucrose cushion: 30% sucrose in PBS
- 4',6-diamidino-2-phenylindole (DAPI): 10 mg/ml in water, store in small aliquots in the dark at -20°C.
- Membrane fixative: 2% Paraformaldehyde, 0.5% Glutaraldehyde (Sigma-Aldrich, USA) in 80 mM Pipes pH 6.8, 1 mM $MgCl_2$, 150 mM sucrose. Add 1 µg/ml DAPI prior to use.
- IF fixative: 2% Paraformaldehyde in 80 mM Pipes pH 6.8, 1 mM $MgCl_2$, 150 mM sucrose.
- PBS, sucrose buffer and $DiIC_{18}$ see sections **I,1**, **III,1** and **III,2**.

C. Method

1. Add 0.6 µl of demembranated sperm chromatin (from stock of 3000 sperm heads/µl to reach a final concentration of ~ 100 sperm heads/µl) to 20 µl of freshly prepared membrane free cytosol (described in section **I,1**) and mix carefully with a large orifice tip. Incubate for 10 min at 20°C to allow for sperm chromatin decondensation.

Note: In contrast to most nuclear assembly reactions, for which frozen aliquots of egg extract cytosol are used, this assay is very sensitive to the quality of the cytosol and we only use freshly prepared extracts.

2. Add 0.5 µl energy mix, 0.5 µl glycogen and 4.4 µl of reconstituted membranes (described in section **III,3**) and mix carefully with a large orifice tip. Incubate for 110 min at 20°C.

Note: Include control samples, in which membranes are replaced by sucrose buffer, to confirm that cytosol is membrane free.

3. For visualization of membranes: Add 0.2 µl of 0.1 mg/ml $DiIC_{18}$ (dissolved in DMSO) 5 min before the end of incubation and mix carefully.
4. Fix samples for 20 min on ice either in 0.5 ml membrane fixative (for $DiIC_{18}$ membrane staining) or in 0.5 ml IF fixative (for immunofluorescence).
5. Load fixed nuclei onto a 0.8 ml sucrose cushion in the flat-bottomed tubes containing poly-L-Lysine coated coverslips. Transfer nuclei onto the coverslips by spinning at 3500 rpm ($250xg_{av}$) for 15 min at 4°C in a Häreus-Multifuge 1-LR-Centrifuge.

Note: Coverslips are coated by covering them with a 0.1% Poly-L-Lysine solution for 5 min, washed once with water and dried.

6. For visualization of membranes: Wash coverslips once with deionized water and mount them on a 2 µl drop of Vectashield 1000. Seal coverslips with nail polish. Be careful that the coverslips do not dry-out.

   For immunofluorescence staining: Place coverslips in 24-well-plates, wash once and store in PBS. Continue with “Immunofluorescence of nuclear assembly reactions” in section **IV,2**.

2. Immunofluorescence of nuclear assembly reactions

The membrane staining of nuclei prepared in nuclear assembly reactions (section **IV,1**) visualizes the formation of a closed nuclear envelope around the reconstituted nuclei. The incorporation of NPCs into the nuclear envelope can be examined by immunofluorescence (Figure 2C). By using specific antibodies against individual nucleoporins, NPC composition can be investigated. This is especially useful after immunodepletion of nucleoporins to assay the impact of these individual NPC components on NPC formation.

A. Materials and equipment

- Fluorescently labeled secondary antibody (e.g. from Life Technologies GmbH, Germany)
- Vectashield 1000, nail polish or coverslip sealant and 24-well-plates as in section **IV,1**.

B. Buffers and solutions

- PBS and DAPI stock solution as in sections **III,1** and **IV,1**.
- 50 mM NH_4Cl in PBS.
- Blocking buffer: 3% BSA in PBS + 0.1% Triton X-100 (Carl Roth GmbH + Co. KG, Karlsruhe, Germany).

C. Method

1. Carefully remove PBS and quench samples for 5 min with 50 mM NH_4Cl in PBS. Although the samples are fixed, the nuclei and particularly the nuclear envelope are very fragile to small breaks. All washes and buffer exchanges should be done carefully. It is also important that the coverslips do not dry out.
2. Incubate coverslips in blocking buffer for 30 min.
3. Incubate coverslips upside down on top of a drop of approximately 70 µl of primary antibody dilution in blocking buffer in a humidity chamber for 2 h. The user should determine optimal antibody dilutions.

Note: Rabbit sera produced in our lab are generally diluted 1:100, while purified antibodies but also the widely used monoclonal antibody mAB414 can often be diluted to 1:1000 or 1:2000.

4. Wash coverslips 3 times for 2 min with PBS + 0.1% Triton X-100 in the 24-well-plate.
5. Incubate coverslips with 250 µl of fluorescently labeled secondary antibodies (usually diluted 1:2000 in blocking buffer) for 1 h in 24-well-plates in the dark.
6. Wash coverslips 3 times for 2 min with PBS + 0.1% Triton X-100. Avoid longer light exposure.
7. Incubate coverslips for 10 min in PBS + DAPI (1:2000) in the dark.
8. Wash coverslips once with water and mount them on a 1 µl drop of Vectashield 1000. Seal coverslips with nail polish. Keep coverslips in the dark and store at 4°C.

3. Transmission electron microscopy of nuclear assembly reactions

For ultrastructural analysis of the assembled nuclei, samples are prepared for transmission electron microscopy. Nuclear membranes and nuclear pore complexes

are easily detectable due to the use of osmium tetroxide for contrast enhancement of membranes. The protocol is adapted from (Macaulay & Forbes, 1996) including an re-isolation of fixed *in vitro* assembled nuclei on the surface of a coverslip before embedding. In this way, most nuclei are concentrated in a relative small volume and easily identified in a limited number of ultrathin sections.

A. Materials and equipment

- 24-well-plate as in section **IV,1**.
- Epon/Araldite kit (EMS, Hatfield, USA)
- dissecting microscope
- needle
- jigsaw

B. Buffers and solutions

- Fix buffer: 25 mM HEPES pH7.5, 25 mM PIPES, 1 mM EGTA, 50 mM KCl, 2 mM MgAc, 5% sucrose.
- Cacodylate buffer: 100 mM cacodylate dissolved in deionized water, pH 7.2.
- 1% Osmium tetroxide (OsO_4): dissolved in cacodylate buffer (w/v).
- 1.5% Potassium hexacyanidoferrate (II) ($K_4[Fe(CN)_6] \times 3H_2O$): dissolved in cacodylate buffer.
- 1% Uranyl acetate: dissolved in deionized water, keep in the dark at 4°C.
- Epon/araldite-mixture: for 26.5 ml of resin use 7.75 g Epon 812 Procure, 5.55 g Araldite 502 and 15.25 g DDSA. After thorough mixing, add 490 µl DMP-30.

C. Method

1. After centrifugation of the assembly reactions on poly-L-Lysine coated coverslips (see section **IV,1**), place coverslips in a 24-well-plate.
2. Wash coverslips once with fix buffer.
3. Fix coverslips for 1 h on ice in fix buffer with 1% Glutaraldehyde (v/v).

4. Postfix samples for 2 h on ice in fix buffer with 2.5% Glutaraldehyde (v/v).
5. Wash once with ice-cold Cacodylate buffer.
6. Incubate samples for 40 min on ice in 1% OsO_4 and 1.5% K_4[Fe(Orso, Pendin, Liu, Tosetto, Moss, Faust, Micaroni, Egorova, Martinuzzi, McNew, & Daga)$_6$] (Orso et al.).
7. Wash coverslips with deionized water.
8. Incubate for 1 h with 1% uranyl acetate at 4°C in the dark.
9. Wash coverslips with water.
10. Dehydrate samples in a graded ethanol series of 30%, 50%, 90% and 2x 100% ethanol each for 10 min.
11. Resin infiltration: 50% Epon/Araldite in Ethanol, 2 x 100% Epon/Araldite each 30 min.
12. After resin infiltration, remove the coverslips from the 24-well-plate and place them on a resin filled lid of a 1.5 ml Eppendorf cup, sample side facing down.

Note: Avoid capturing any air bubbles.

13. Resin curing at 60°C for 48 h.
14. Remove the glass coverslips from the cured resin-embedded samples by submerging them in liquid nitrogen.

Note: This step has to be repeated several times until every bit of glass is removed from the sample surface. More often than not, remaining glass shards have to be carefully pried from the resin surface with a fine tungsten needle under the dissecting microscope. Wear personal protective equipment while working with liquid nitrogen and glass.

15. Find and mark out areas with nuclear assemblies under the dissecting microscope with a fine needle.
16. Cut out the areas of interest with a fine jigsaw.

17. Prepare ultrathin sections parallel to the sample surface.

4. Nuclear assembly reactions measuring transport of inner nuclear membrane proteins through nuclear pore complexes

Nuclei assembled *in vitro* in *Xenopus* egg extracts can be used both, to study nuclear import of soluble cargos (for a detailed method description see Chan & Forbes, 2006) as well as to analyze transport of inner nuclear membrane proteins through nuclear pore complexes. For the latter use, integral membrane protein reporters are expressed and purified from *E. coli* (see section **II,1**) and reconstituted in proteoliposomes (see section **III,4**). These proteoliposomes are added to a nuclear assembly reaction at time points when the nuclear envelope is already closed around the chromatin. Proteoliposomes readily fuse with the endoplasmic reticulum and the reporter is immediately distributed throughout the membranes of the endoplasmic reticulum including the outer nuclear membrane.

Nuclear pore complex passage of the reporter to the inner nuclear membrane is monitored by its protection from a protease added to the cytoplasm (Figure 3). We have best experience with a TEV (tobacco etch virus) protease fused to the large bacterial protein NusA, which increases the size of the protease-fusion protein to at least 90 kDa thereby preventing its diffusion through the NPC (Figure 3B). Consequently, reporter proteins contain a TEV protease recognition site followed by a domain, which is cleaved off upon TEV protease activity (Figure 3A). The latter domain is usually an EGFP-tag in our assay, as this allows to follow cleavage both by light microscopy (Figure 3C) and western blotting (Figure 3D). We have good experience with reporter constructs containing EGFP-tag and TEV cleavage site N-terminally fused to BC08, a INM protein with a single C-terminal transmembrane region (Ulbert et al., 2006) or the first transmembrane region of LBR (lamin B

receptor), which is sufficient for INM targeting (Soullam & Worman, 1995). But also multispanning INM proteins such as full-length LBR or nurim work as reporters.

For editors; PLEASE INSERT FIGURE 3 HERE

A. Materials and equipment

- EGFP-antibody (cat. no. 11814460001, Roche, Germany)

B. Buffers and solutions

- SDS-sample buffer: 0.19M TRIS pH 6.8, 30% sucrose (w/v), 0.9% SDS (w/v), 0.1% Bromphenolblue (w/v), 0.1M DTT.
- Energy mix, glycogen and IF fixative as in section **IV,1**.

C. Method

1. Incubate 45 µl of freshly prepared membrane free cytosol (preparation described in section **I,1**) with 2.5 µl sperm heads (3000 sperm heads/µl) for 10 min at 20°C to allow for sperm decondensation.
2. Add 1 µl energy mix, 1 µl glycogen and 2.5 µl of floatation purified membranes (preparation described in section **I,2**) and incubate for 50 min at 20°C.
3. Add 5µl of resuspended proteoliposomes (prepared as described in section **II,4**) and mix carefully, incubate at 20°C.
4. Take out 10 µl from the sample each after 0, 5, 10, 15 and 30 min after proteoliposome addition and add 1µl of 5 µg/µl TEV protease for 5 min at 20°C to each. Stop cleavage reaction by adding 5 µl SDS-sample buffer and immediate heating for 5 min at 95°C.
5. Analyze time course of cleavage reaction by western blotting with an EGFP-antibody. Alternatively, the loss of EGFP signal can be monitored by

immunofluorescence. For this, stop TEV cleavage reaction by fixation in IF fixative and proceed with immunofluorescence as described in section **IV,2**.

Conclusion

Xenopus egg extracts provide a powerful cell-free tool to study nuclear assembly and functions. Since their first use more than 30 years ago (Lohka & Masui, 1983) they have been employed in a variety of assays focusing on different aspects of nuclear organization, dynamics and functions. Accordingly, slight variations in the protocols for preparing such extracts exist (e.g. see Chapter 8 for a modified egg extract preparation protocol).

Immunodepletion of soluble proteins is a key advantage of the *Xenopus* egg extract system. It facilitates analysis of the function of specific proteins in definite aspects of nuclear dynamics, such as nuclear pore complex assembly. By employing the methods described here, the technical repertoire is expanded to include integral membrane proteins. These methods have already been applied to analyze the function of transmembrane nucleoporins or the passage of membrane proteins through the pore but they are certainly not limited to these questions. In the future, they could be used to study the functional interaction of transmembrane proteins with chromatin or membrane fusion reactions mediated by transmembrane proteins to name just two examples.

References

Allen, T. M., Romans, A. Y., Kercret, H., & Segrest, J. P. (1980). Detergent removal during membrane reconstitution. *Biochim Biophys Acta, 601*(2), 328-342.

Antonin, W., Franz, C., Haselmann, U., Antony, C., & Mattaj, I. W. (2005). The integral membrane nucleoporin pom121 functionally links nuclear pore complex assembly and nuclear envelope formation. *Mol Cell, 17*(1), 83-92.

Antonin, W., Ungricht, R., & Kutay, U. (2011). Traversing the NPC along the pore membrane: Targeting of membrane proteins to the INM. *Nucleus, 2*(2), 87-91. doi: 10.4161/nucl.2.2.14637

Brown, K. S., Blower, M. D., Maresca, T. J., Grammer, T. C., Harland, R. M., & Heald, R. (2007). Xenopus tropicalis egg extracts provide insight into scaling of the mitotic spindle. *J Cell Biol, 176*(6), 765-770. doi: 10.1083/jcb.200610043

Chan, R. C., & Forbes, D. I. (2006). In vitro study of nuclear assembly and nuclear import using Xenopus egg extracts. *Methods Mol Biol, 322*, 289-300.

de la Barre, A. E., Robert-Nicoud, M., & Dimitrov, S. (1999). Assembly of mitotic chromosomes in Xenopus egg extract. *Methods Mol Biol, 119*, 219-229. doi: 10.1385/1-59259-681-9:219

Eisenhardt, N., Redolfi, J., & Antonin, W. (2013). *Nup53 interaction with Ndc1 and Nup155 are required for nuclear pore complex assembly*. J Cell Sci.

Galy, V., Antonin, W., Jaedicke, A., Sachse, M., Santarella, R., Haselmann, U. (2008). A role for gp210 in mitotic nuclear-envelope breakdown. *J Cell Sci, 121*(Pt 3), 317-328.

Gillespie, P. J., Gambus, A., & Blow, J. J. (2012). Preparation and use of Xenopus egg extracts to study DNA replication and chromatin associated proteins. *Methods, 57*(2), 203-213. doi: 10.1016/j.ymeth.2012.03.029

Lohka, M. J. (1998). Analysis of nuclear envelope assembly using extracts of Xenopus eggs. *Methods Cell Biol, 53*, 367-395.

Lohka, M. J., & Masui, Y. (1983). Formation in vitro of sperm pronuclei and mitotic chromosomes induced by amphibian ooplasmic components. *Science, 220*(4598), 719-721.

Lusk, C. P., Blobel, G., & King, M. C. (2007). Highway to the inner nuclear membrane: rules for the road. *Nat Rev Mol Cell Biol, 8*(5), 414-420. doi: nrm2165 [pii]

10.1038/nrm2165

Macaulay, C., & Forbes, D. J. (1996). Assembly of the nuclear pore: biochemically distinct steps revealed with NEM, GTP gamma S, and BAPTA. *J Cell Biol, 132*(1-2), 5-20.

Mansfeld, J., Guttinger, S., Hawryluk-Gara, L. A., Pante, N., Mall, M., Galy, V. (2006). The conserved transmembrane nucleoporin NDC1 is required for nuclear pore complex assembly in vertebrate cells. *Mol Cell, 22*(1), 93-103.

Maresca, T. J., & Heald, R. (2006). Methods for studying spindle assembly and chromosome condensation in Xenopus egg extracts. *Methods in molecular biology, 322*, 459-474.

Murray, A. W. (1991). Cell cycle extracts. *Methods Cell Biol, 36*, 581-605.

Murray, A. W., & Kirschner, M. W. (1989). Cyclin synthesis drives the early embryonic cell cycle. *Nature, 339*(6222), 275-280. doi: 10.1038/339275a0

Newmeyer, D. D., & Wilson, K. L. (1991). Egg extracts for nuclear import and nuclear assembly reactions. *Methods Cell Biol, 36*, 607-634.

Orso, G., Pendin, D., Liu, S., Tosetto, J., Moss, T. J., Faust, J. E. (2009). Homotypic fusion of ER membranes requires the dynamin-like GTPase atlastin. *Nature, 460*(7258), 978-983. doi: 10.1038/nature08280

Pfaller, R., Smythe, C., & Newport, J. W. (1991). Assembly/disassembly of the nuclear envelope membrane: cell cycle-dependent binding of nuclear membrane vesicles to chromatin in vitro. *Cell, 65*(2), 209-217.

Roosild, T. P., Greenwald, J., Vega, M., Castronovo, S., Riek, R., & Choe, S. (2005). NMR structure of Mistic, a membrane-integrating protein for membrane protein expression. *Science, 307*(5713), 1317-1321. doi: 10.1126/science.1106392

Sheehan, M. A., Mills, A. D., Sleeman, A. M., Laskey, R. A., & Blow, J. J. (1988). Steps in the assembly of replication-competent nuclei in a cell-free system from Xenopus eggs. *J Cell Biol, 106*(1), 1-12.

Sive, H. L., Grainger, R. M., & Harland, R. M. (2000). Early Development of Xenopus laevis - a laboratory manual. *Cold Spring Harbor Laboratory Press*.

Soullam, B., & Worman, H. J. (1995). Signals and structural features involved in integral membrane protein targeting to the inner nuclear membrane. *J Cell Biol, 130*(1), 15-27.

Theerthagiri, G., Eisenhardt, N., Schwarz, H., & Antonin, W. (2010). The nucleoporin Nup188 controls passage of membrane proteins across the nuclear pore complex. *J Cell Biol, 189*(7), 1129-1142. doi: 10.1083/jcb.200912045

Vigers, G. P., & Lohka, M. J. (1991). A distinct vesicle population targets membranes and pore complexes to the nuclear envelope in Xenopus eggs. *J Cell Biol, 112*(4), 545-556.

Wilson, K. L., & Newport, J. (1988). A trypsin-sensitive receptor on membrane vesicles is required for nuclear envelope formation in vitro. *J Cell Biol, 107*(1), 57-68.

Figure legends

Figure 1 Schematic overview of cytosol and membrane preparation from *Xenopus* eggs.

Activated *Xenopus laevis* eggs are crushed by centrifugation to obtain the cellular content as low speed extracts. These low speed extracts are further separated into a cytosol and a membrane fraction. After separating both fractions, residual membrane components are removed from the cytosol by two additional high speed centrifugation steps. The membranes can either be purified in a crude preparation by dilution and centrifugation or further fractionated by floatation through a sucrose step gradient. Floated membrane fractions, for example fractions 1-3 are pooled, and purified by a final dilution and centrifugation step.

Figure 2 Depletion and functional add-back of membrane proteins.

A: Schematic illustration of immunodepletion of transmembrane proteins from *Xenopus* membranes. Membranes are solubilized with a detergent and the target membrane protein is depleted from the solubilized membrane fraction by specific antibody beads. Finally, the depleted membranes are reconstituted by detergent removal.

B: Western Blot analysis of *Xenopus* membranes, which were mock-depleted, immunodepleted of endogenous NDC1 or NDC1-depleted and substituted with recombinant EGFP-NDC1 expressed in *E. coli* (addback). Endogenous and recombinant NDC1 are detected by NDC1-antibodies, the recombinant protein also by EGFP-antibodies. The NDC1-depletion does not affect levels of other integral membrane proteins including the transmembrane nucleoporins GP210 and POM121.

C: Immunofluorescence of nuclear assembly reactions with *Xenopus* cytosol and membranes from B. Recombinant EGFP-NDC1 is faithfully integrated into the

nuclear membranes as detected by NDC1- and EGFP-antibodies. NDC1 depletion blocks NPC formation (ΔNDC1). This phenotype is rescued by the addition of recombinant EGFP-NDC1 (addback) as indicated by the presence of Nup58, a nucleoporin located in the inner part of the NPC. DNA is stained with DAPI. Bar: 10 µm.

Figure 3 Analysis of inner nuclear membrane protein passage through nuclear pore complexes (modified after Theerthagiri et al., 2010).

A: Schematic illustration of an inner nuclear membrane (INM) protein reporter. The reporter protein is fused to an N-terminal EGFP-tag followed by a TEV-protease recognition site.

B: The reporter construct reconstituted in proteoliposomes is added to nuclear assembly reactions when the nuclear envelope is already closed. The reporter is immediately distributed throughout the membranes of the endoplasmic reticulum (ER), including the outer nuclear membrane (ONM). To monitor its transport through nuclear pore complexes, a NusA-fused TEV protease is added, which is excluded from NPC passage due to its size. The reporter protein is accessible for cleavage of the EGFP-tag by the TEV-protease if present in the membranes of the ER or ONM, whereas in the inner nuclear membrane (INM) the reporter constructs are protease protected.

C: Immunofluorescence of the assay described in B. The reporter construct is visualized by EGFP-antibodies and can be detected in the ER and ONM at 0 min. 30 min after addition, the reporter construct is enriched in the INM, where it is protease protected from NusA-TEV due to size exclusion of nuclear pore complexes. If the TEV protease construct is actively imported into the nucleus due to a nuclear

localization (NLS)-site, the EGFP-tag of the reported is cleaved off, also when residing in the INM after 30 min. DNA is stained with DAPI. Bar: 10 µm.

D: Western Blot analysis of isolated nuclei from the experiment in C at different time points using the EGFP-antibody. Cleavage of the reporter by TEV-protease results in the appearance of a band of free EGFP (around 25 kDa) which is absent if the reporter is protease protected due to transport to the INM, which occurs approximately 15min after addition of the reporter construct.

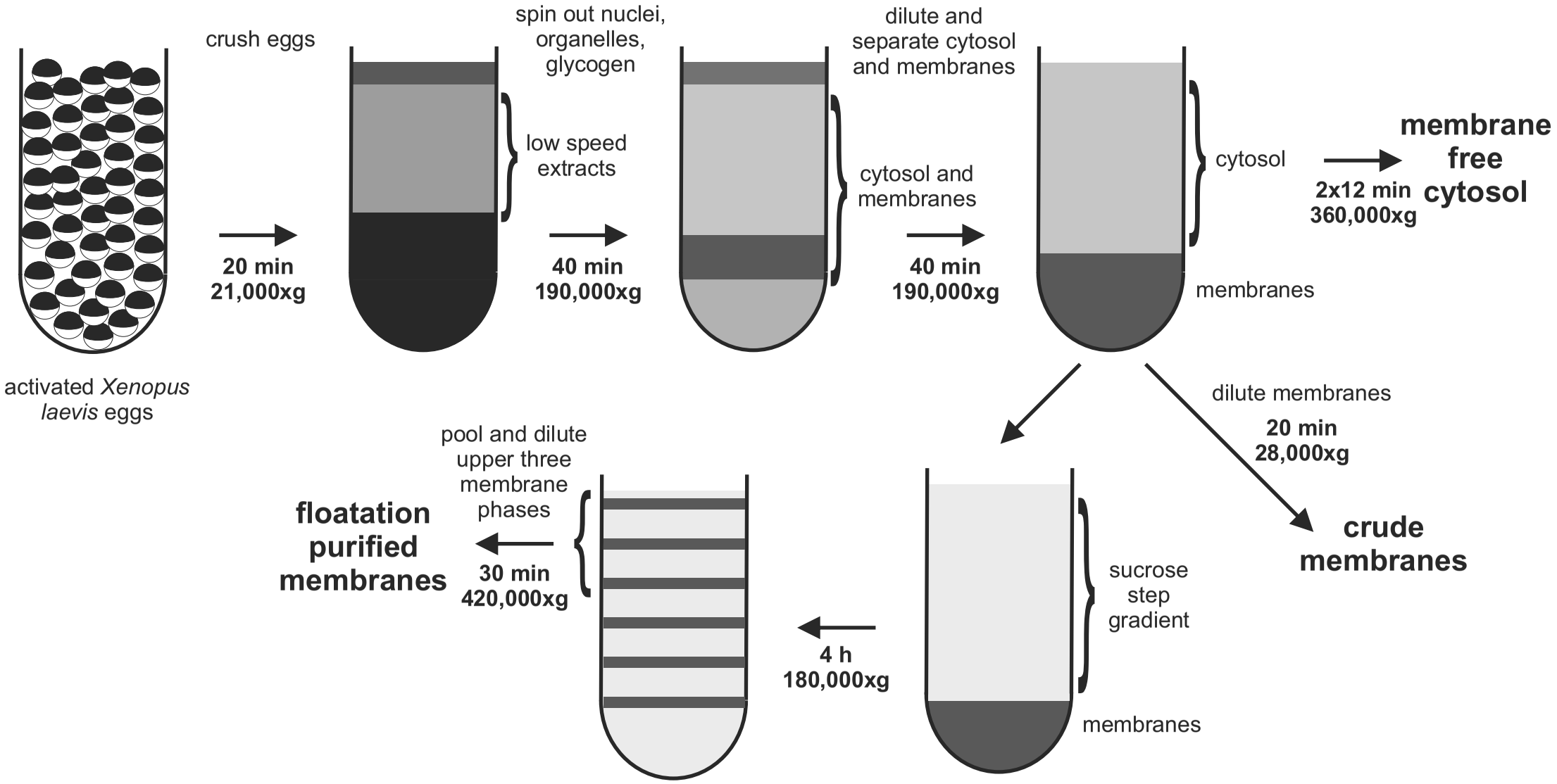
activated *Xenopus laevis* eggs
crush eggs
20 min
21,000xg
low speed extracts
spin out nuclei, organelles, glycogen
40 min
190,000xg
cytosol and membranes
dilute and separate cytosol and membranes
40 min
190,000xg
cytosol
membranes
2x12 min
360,000xg
membrane free cytosol
dilute membranes
20 min
28,000xg
crude membranes
sucrose step gradient
membranes
4 h
180,000xg
pool and dilute upper three membrane phases
30 min
420,000xg
floatation purified membranes

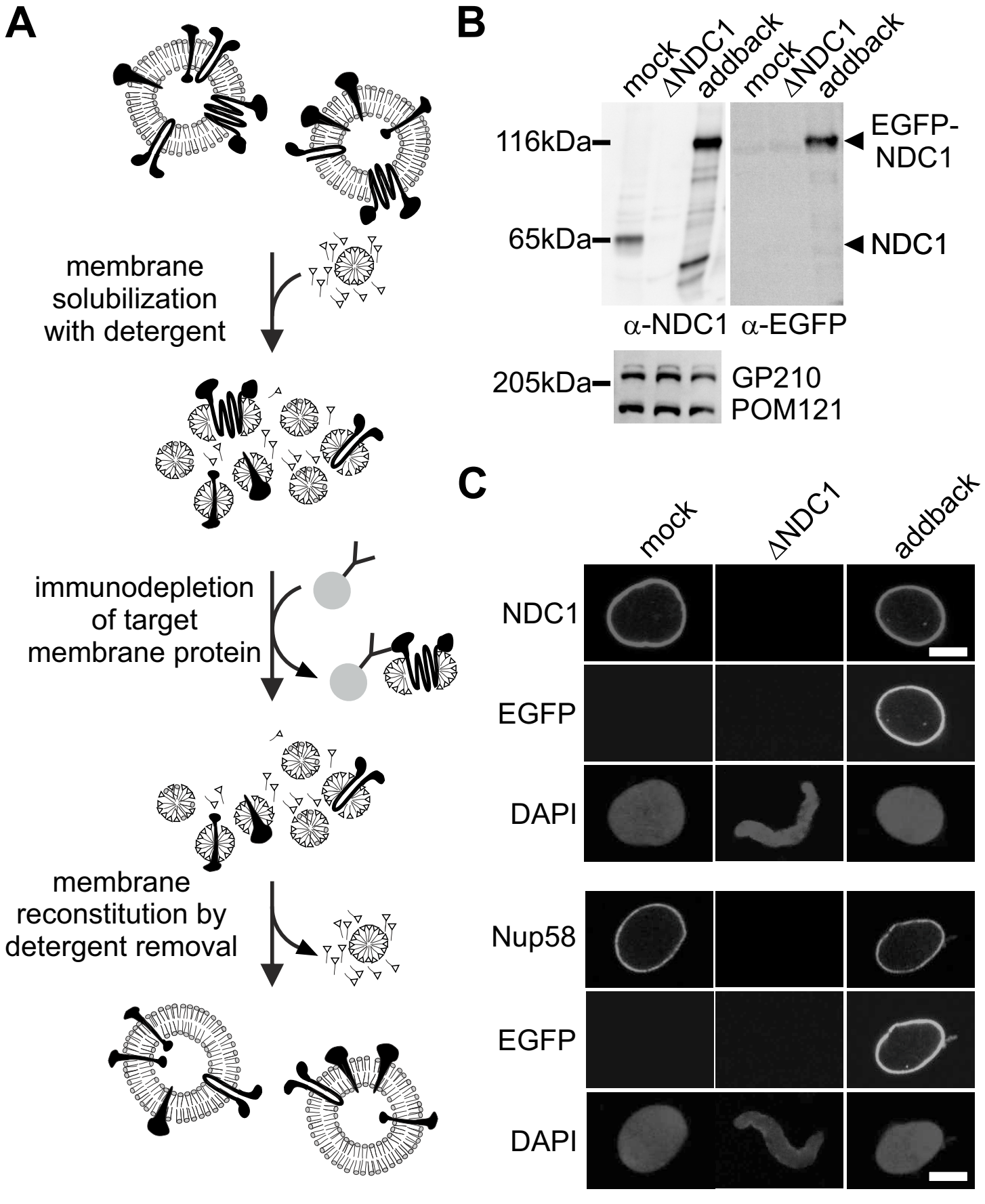
A
membrane solubilization with detergent
immunodepletion of target membrane protein
membrane reconstitution by detergent removal
B
mock
ΔNDC1
addback
mock
ΔNDC1
addback
116kDa
65kDa
EGFP-NDC1
NDC1
α-NDC1
α-EGFP
205kDa
GP210
POM121
C
mock
ΔNDC1
addback
NDC1
EGFP
DAPI
Nup58
EGFP
DAPI

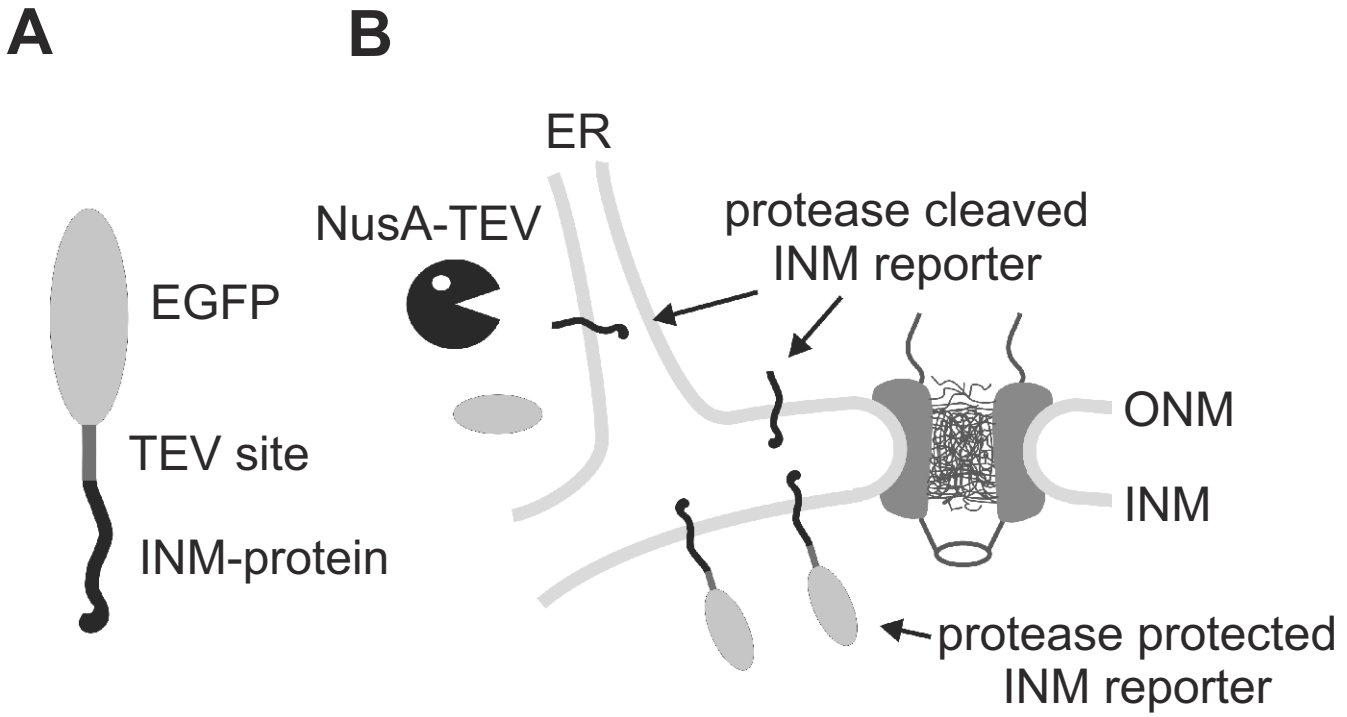
A
B
EGFP
TEV site
INM-protein
ER
NusA-TEV
protease cleaved
INM reporter
ONM
INM
protease protected
INM reporter

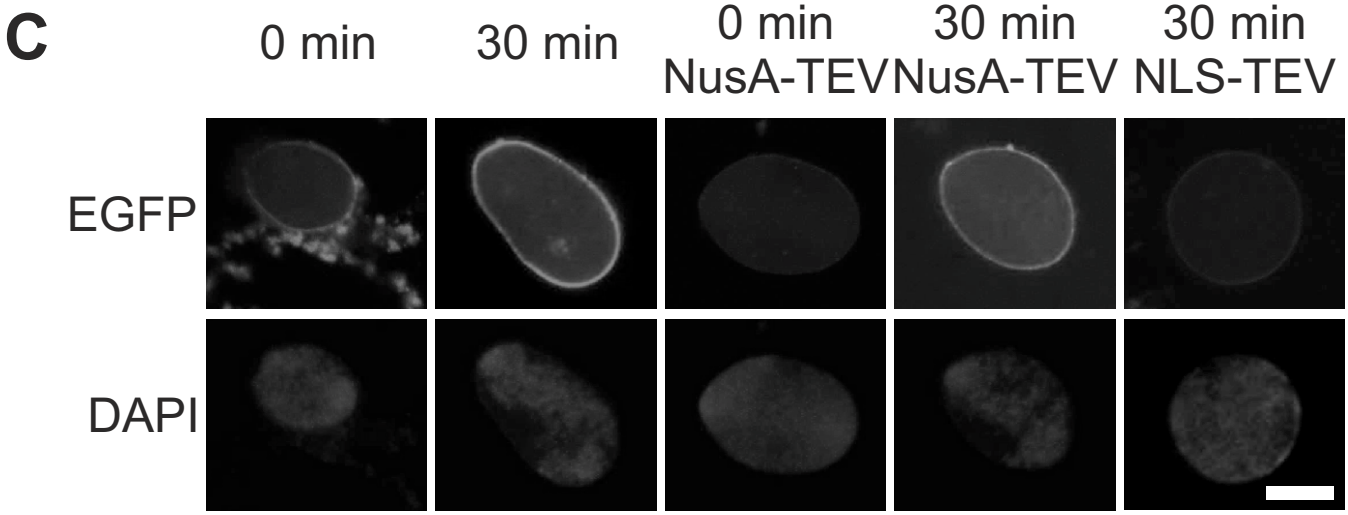
C
0 min
30 min
0 min
NusA-TEV
30 min
NusA-TEV
30 min
NLS-TEV
EGFP
DAPI

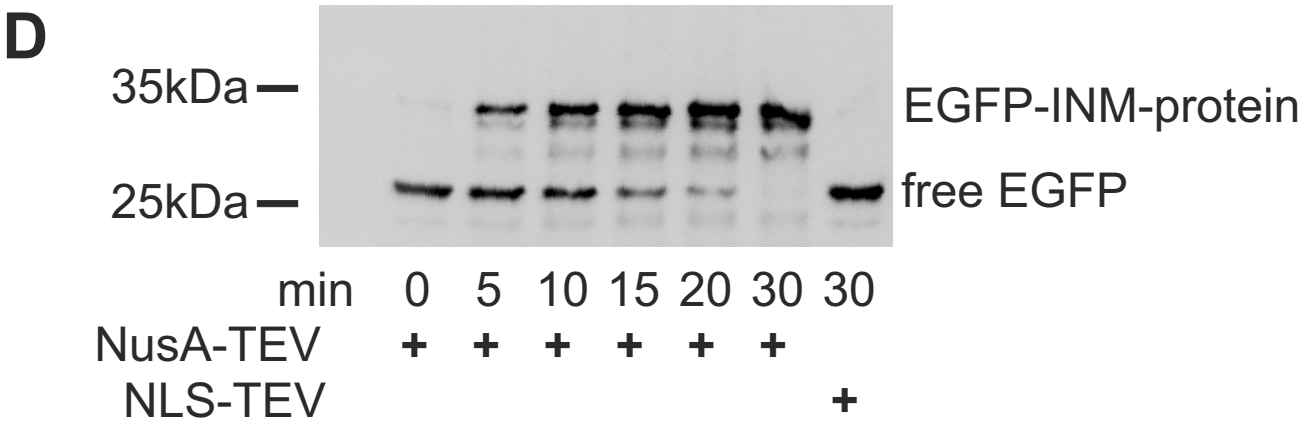
D
35kDa
25kDa
EGFP-INM-protein
free EGFP
min 0 5 10 15 20 30 30
NusA-TEV + + + + + +
NLS-TEV +